GEOLOGICAL SURVEY OF CANADA
COMMISSION GÉOLOGIQUE DU CANADA

PAPER
ÉTUDE 82-1B

CURRENT RESEARCH
PART B

RECHERCHES EN COURS
PARTIE B

Canada

1982

Notice to Librarians and Indexers

The Geological Survey's thrice-yearly *Current Research* series contains many reports comparable in scope and subject matter to those appearing in scientific journals and other serials. All contributions to the Scientific and Technical Report section of *Current Research* include an abstract and bibliographic citation. It is hoped that these will assist you in cataloguing and indexing these reports and that this will result in a still wider dissemination of the results of the Geological Survey's research activities.

Avis aux bibliothécaires et préparateurs d'index

La série Recherches en cours *de la Commission géologique paraît trois fois par année; elle contient plusieurs rapports dont la portée et la nature sont comparable à ceux qui paraissent dans les revues scientifiques et autres périodiques. Tous les articles publiés dans la section des rapports scientifiques et techniques de la publication* Recherches en cours *sont accompagnés d'un résumé et d'une bibliographie, ce qui vous permettra, nous l'espérons, de cataloguer et d'indexer ces rapports, d'où une meilleure diffusion des résultats de recherche de la Commission géologique.*

Technical editing and compilation
Rédaction et compilation techniques
R.L. Christie
H. Dumych
P.J. Griffin
L. Machan
W.C. Morgan
L.E. Vincent

Production editing and layout
Préparation et mise en page
Leona R. Mahoney
Debby Busby

Typed and checked by
Dactylographie et vérification
Jacinthe Caron
Susan Gagnon
Janet Gilliland
Shirley Kostiew
Janet Legere

GEOLOGICAL SURVEY
PAPER 82-1B

COMMISSION GÉOLOGIQUE
ÉTUDE 82-1B

CURRENT RESEARCH
PART B

RECHERCHES EN COURS
PARTIE B

1982

Available in Canada through

authorized bookstore agents
and other bookstores

or by mail from

Canadian Government Publishing Centre
Supply and Services Canada
Hull, Québec, Canada K1A 0S9

and from

Geological Survey of Canada
601 Booth Street
Ottawa, Canada K1A 0E8

A deposit copy of this publication is also available
for reference in public libraries across Canada

Cat. No. M44-82/1BE Canada: $8.00
ISBN 0-660-11169-1 Other countries: $9.60

Price subject to change without notice

Geological Survey of Canada – *Commission géologique du Canada*

R.A. PRICE
Director General
Directeur général

J.G. FYLES
Chief Geologist
Géologue en chef

M.J. KEEN
Director, Atlantic Geoscience Centre, Dartmouth, Nova Scotia
Directeur du Centre géoscientifique de l'Atlantique, Dartmouth (Nouvelle-Ecosse)

J.A. MAXWELL
Director, Central Laboratories and Technical Services Division
Directeur de la Division des laboratoires centraux et des services techniques

R.G. BLACKADAR
Director, Geological Information Division
Directeur de la Division de l'information géologique

W.W. NASSICHUK
Director, Institute of Sedimentary and Petroleum Geology, Calgary, Alberta
Directeur de l'Institut de géologie sédimentaire et pétrolière, Calgary (Alberta)

J.C. McGLYNN
Director, Precambrian Geology Division
Directeur/par int. de la Division de la géologie du Précambrien

A.G. DARNLEY
Director, Resource Geophysics and Geochemistry Division
Directeur de la Division de la géophysique et de la géochimie appliquées

J.S. SCOTT
Director, Terrain Sciences Division
Directeur de la Division de la science des terrains

G.B. LEECH
Director, Economic Geology Division
Directeur de la Division de la géologie économique

R.B. CAMPBELL
Director, Cordilleran Geology Division, Vancouver, British Columbia
Directeur de la Division de la géologie de la Cordillère, Vancouver (Colombie-Britannique)

Separates

A limited number of separates of the papers that appear in this volume are available by direct request to the individual authors. The addresses of the Geological Survey of Canada offices follow:

601 Booth Street,
OTTAWA, Ontario
K1A 0E8

Institute of Sedimentary and Petroleum Geology,
3303-33rd Street N.W.,
CALGARY, Alberta
T2L 2A7

Cordilleran Geology Division
100 West Pender Street,
VANCOUVER, B.C.
V6B 1R8

Atlantic Geoscience Centre,
Bedford Institute of Oceanography,
P.O. Box 1006,
DARTMOUTH, N.S.
B2Y 4A2

When no location accompanies an author's name in the title of a paper, the Ottawa address should be used.

Tirés à part

On peut obtenir un nombre limité de "tirés à part" des articles qui paraissent dans cette publication en s'adressant directement à chaque auteur. Les adresses des différents bureaux de la Commission géologique du Canada sont les suivantes:

601, rue Booth
OTTAWA, Ontario
K1A 0E8

Institut de géologie sédimentaire et pétrolière
3303-33rd, St. N.W.,
CALGARY, Alberta
T2L 2A7

Division de la géologie de la Cordillère
100 West Pender Street
VANCOUVER, Colombie-Britannique
V6B 1R8

Centre géoscientifique de l'Atlantique
Institut océanographique de Bedford
B.P. 1006
DARTMOUTH, Nouvelle-Ecosse
B2Y 4A2

Lorsque l'adresse de l'auteur ne figure pas sous le titre d'un document, on doit alors utiliser l'adresse d'Ottawa.

SCIENTIFIC AND TECHNICAL REPORTS
RAPPORTS SCIENTIFIQUES ET TECHNIQUES

QUATERNARY GEOLOGY/GÉOLOGIE DU QUATERNAIRE

REGIONAL GEOLOGY/GÉOLOGIE RÉGIONALE

Appalachian Region/Région des Appalaches

Cordilleran Region/Région de la Cordillère

Precambrian Shield/Bouclier précambrien

SCIENTIFIC AND TECHNICAL NOTES
NOTES SCIENTIFIQUES ET TECHNIQUES

DISCUSSIONS AND COMMUNICATIONS
DISCUSSIONS ET COMMUNICATIONS

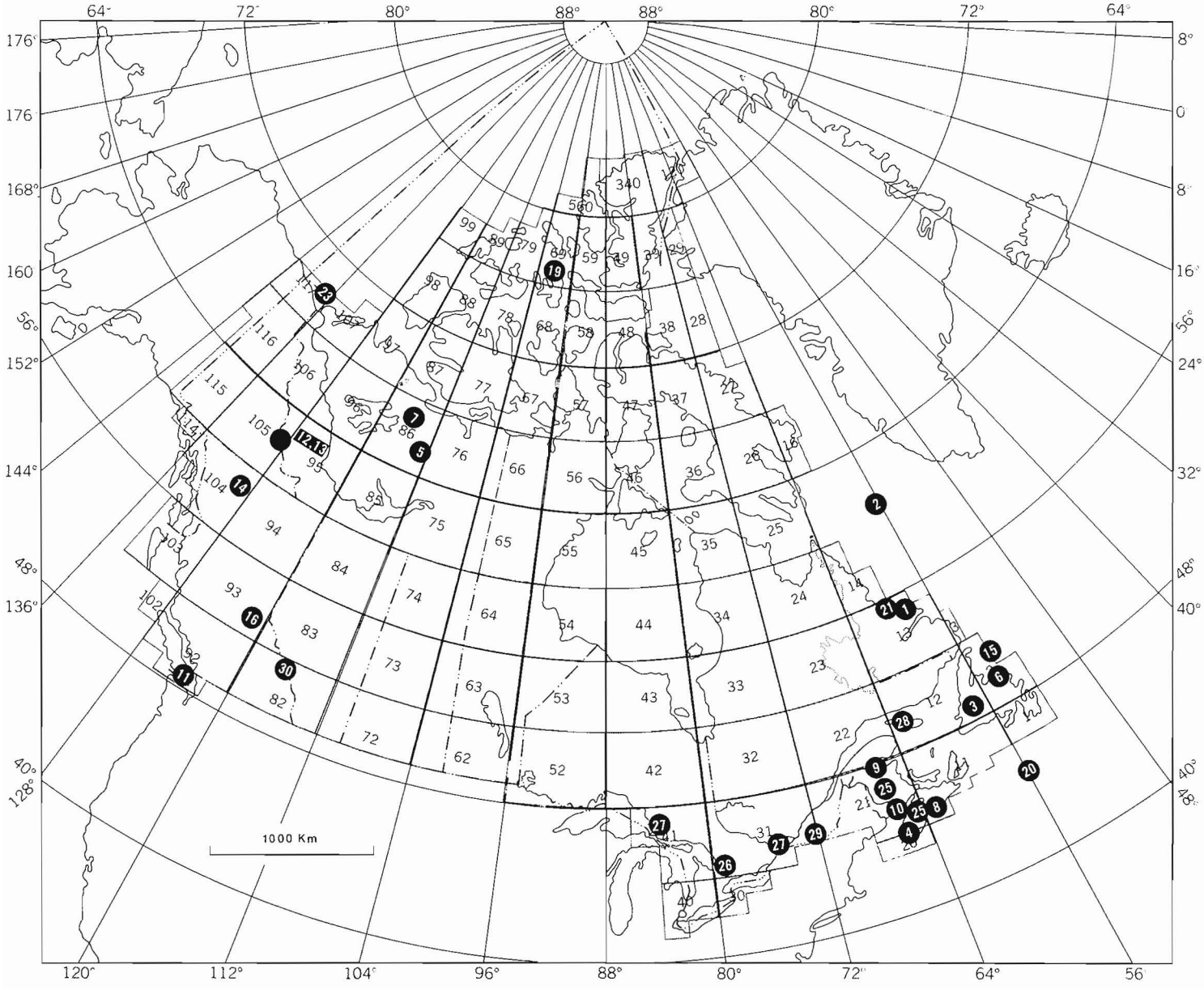
64°
72°
80°
88°
88°
80°
72°
64°
176°
176
168°
160
56°
152°
144°
48°
136°
40°
128°
8°
0
8°
16°
56°
24°
32°
48°
40°
48°
120°
112°
104°
96°
88°
80°
72°
64°
56
1000 Km
12,13

1. # LATE QUATERNARY LITHOSTRATIGRAPHY AND SEDIMENTATION, KAIPOKOK BAY, LABRADOR

E.M.R. Research Agreement 147/4/79

Nikolos Kontopoulos[1] and David J.W. Piper
Atlantic Geoscience Centre, Dartmouth

Kontopoulos, Nikolos and Piper, David J.W., Late Quaternary stratigraphy and sedimentation, Kaipokok Bay, Labrador; in Current Research, Part B, Geological Survey of Canada, Paper 82-1B, p. 1-6, 1982.

Abstract

Forty kilometres of Huntec high resolution seismic profiles and four piston cores have been studied from Kaipokok Bay, Labrador. Sedimentary and acoustic facies have been correlated. Proglacial gravels, sands and muds fill basin floors, generally resting on bedrock but locally on till. These are overlain by more widespread proglacial muds that drape over topographic highs. Small scale cyclic sedimentation of proglacial sands and muds may be a result of shifting of stream discharge points, either beneath the edge of a floating ice shelf, or on a subaerial outwash delta. Flocculation leads to mineralogic segegation of illite in proximal environments and non-clay rock flour in distal environments. Late Holocene muds rest with an erosional unconformity on the proglacial sediments. They have accumulated as marine energy has been increasingly damped at the sill as sea level has fallen.

Introduction

Kaipokok Bay is a 50 km long fiord on the Labrador coast at 55°N (Fig. 1.1). Its greatest depth is about 135 m, and it is divided by shallow sills into several basins. The sill at the mouth has a maximum depth of about 30 m. It is cut into Precambrian rocks of the Archaean Hopedale Gneiss and lower Proterozoic Aillik Group (mostly metasediments) (Gandhi et al., 1969). Kaipokok Bay lies just north of Makkovik Bay. The marine geology of the latter area was recently investigated in detail (Piper and Iuliucci, 1978; Barrie, 1979, 1980; Barrie and Piper, 1982); the rocks in both areas have similar stratigraphic characteristics.

This work is based on 40 km of Huntec deep tow seismic (DTS) system high resolution reflection profile and a simultaneous air gun profile, and four piston cores collected by R.H. Fillon on **CSS Hudson** cruise 79-019.

Methods

Cores were split in their liners, X-radiographed, and the split core face described. Textural analysis was by standard sieve and pipette techniques. Clay mineralogy was determined by X-ray diffraction of the less than two micron fraction (separated by settling techniques). Mineral abundance was quantified by the method of Barrie (1980), similar to that used by Piper and Slatt (1977).

Seismic Reflection Profiles

In the Huntec DTS records, four main acoustic facies can be distinguished on the basis of distribution and reflector character:

Basal Unit, with a highly irregular surface (acoustic facies 1). In most places, this is probably bedrock, but locally it may consist of till up to 50 ms thick, since exceptionally isolated coherent reflectors are visible at greater depth on the air gun profile.

Highly stratified basin fill (acoustic facies 2). This is restricted to deep basins and increases in maximum thickness from 20 ms (about 20 m) upbay (Fig. 1.2c) to 40 ms downbay (Fig. 1.2a). Pockets of strata between reflectors in some places gently pinch and swell, but often thin only slightly at the edge of the basin (Fig. 1.2a). Laterally some reflectors die out or grade into thicker strata lacking coherent internal reflectors near the basin margin (Fig. 1.2a). In shallower basins, stratification is less pronounced and more widely spaced (Fig. 1.2c).

An acoustic facies with faint internal reflectors that in most places blankets irregular basement topography (acoustic facies 3). It is generally 5-10 ms thick in the upper bay and a little thinner downbay. Locally it appears laterally equivalent to acoustic facies 2 (e.g. Fig. 1.2b) but in many places clearly overlies facies 2 (Fig. 1.2c). This appears to be equivalent to Barrie's (1979) "conformable cover unit."

Acoustically transparent sediment (acoustic facies 4) that rests with a pronounced unconformity on facies 1 to 3 (Fig. 1.2a,c). This is generally thickest in basins (although in Fig. 1.2c it is thickest in a gentle basin flank), ranging from 5 ms downbay to more than 10 ms upbay. This is probably equivalent to Barrie's (1979) "upper basin fill unit."

Sediment Facies in Cores

Eight sedimentary facies are distinguished by visual examination of split core surfaces (Fig. 1.3). These facies have been further characterized by X-radiography, textural and petrologic analyses.

Olive mud (facies A)

This facies occurs only in core 39 at the northeast, seaward end of the bay. It is generally olive grey 5Y3/2 in colour, contains rare fine gravel clasts and scattered sandy patches. Mollusc shell fragments are scattered through the sediment, and dark (?pyrite) mottles are seen. Bioturbation is visible in X-radiographs, and the reaction with hydrogen peroxide suggest a high organic carbon content. Texturally the sediment is silty clay with 5-25 per cent sand (Fig. 1.4, 1.5). Pennate diatoms are more abundant than centric forms. At the base of this facies, at 135 cm in core 39, is a 15 cm thick bed of slightly gravelly sandy mud (Fig. 1.5, analysis 2).

[1] Geological Laboratory, University of Patras, Patras, Greece

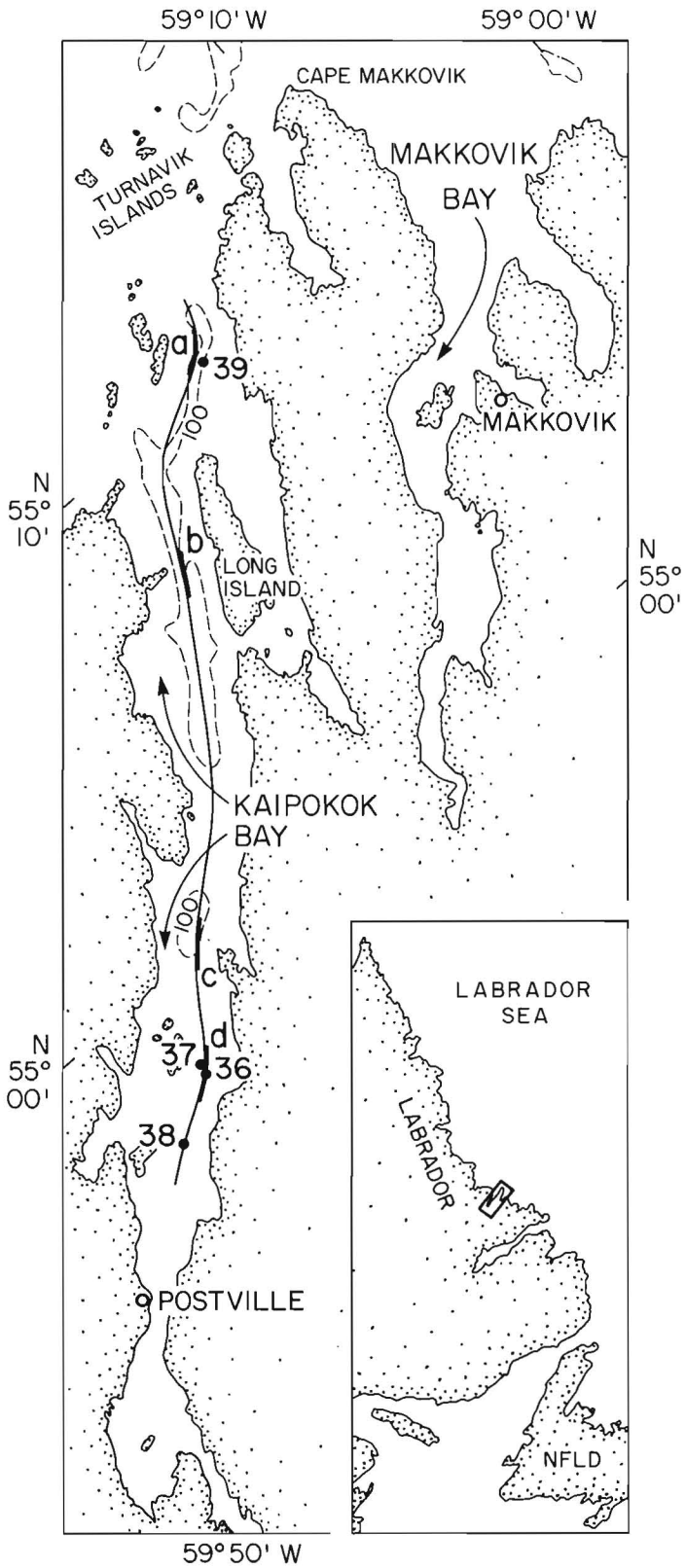

Figure 1.1. *General bathymetric map of Kaipokok and Makkovik bays, showing location of cores (36-39) and seismic reflection profile. a-d are profile segments illustrated in Figure 1.2.*

Dark yellowish-brown mud (facies B)

Facies B is found at the top of cores 36 to 38. It is generally 10YR4/2 in colour, and contains rare shell fragments and rare pyritic mottles. It is more clayey than facies A (Fig. 1.4), and scattered granules and pebbles are common (Fig. 1.5, analysis 3). Bioturbation is visible in X-radiographs and no primary lamination is seen. Centric diatoms are more common than in facies A. This facies appears to be a facies equivalent of A in the shallower upbay cores and the exchange with open shelf water may control differences in diatom content. The colour is probably related to greater oxygenation.

Grey mud (facies C)

This facies is a medium grey (N5) silty mud (Fig. 1.5, analysis 4) with thin bedding faintly visible in X-radiographs. There are some beds with abundant granules, and also many scattered granules. Some beds of slightly browner muds are present. Distinct silt laminae occur near the base of the facies.

Alternating moderate brown and grey muds (facies D)

This facies consists of alternations of moderate brown (5YR4/1) clayey silts (Fig. 1.5, analysis 5) and medium grey (N5) silty clays (Fig. 1.5, analysis 6) in beds typically 1-3 cm thick (Fig. 1.6). At the base of, or within, many grey layers are thin silt or sand laminae. The brown layers often include silt laminae, many of which appear less well sorted. The grey layers usually appear to be sharp-based and sometimes are sharp-topped. Both brown and grey layers contain rare scattered granules. In the lower part of this facies, brown beds become more common and siltier, and the transition to facies E is gradational.

Alternating moderate brown mud and thin sands (facies E)

This consists principally of brown muds in beds up to 5 cm thick, but also contains interbedded silty sands 0.2-2 cm thick and some grey mud beds typically 1 cm thick (Fig. 1.7-1.10). There are scattered granules in all facies, and some bioturbation. Sand beds gradually increase in thickness downwards through this facies, which has gradational upper and lower limits. The sands have a high silt matrix (Fig. 1.5, analysis 7), and almost all appear structureless in X-radiographs (Fig. 1.10) with abrupt but indistinct contacts with under and overlying beds (Fig. 1.8). The characteristics suggest deposition directly from suspension fall out, without nearbed current activity.

Sands (facies F)

Sands range from pebbly coarse sands to medium sands (Fig. 1.5, analysis 8) and contain rare grey silty-mud clasts. Occasionally there are interbedded thin sand beds with a silty-mud matrix containing gravel sized clasts (probably analogous to facies H described below). A few thick (≈1m) graded beds are visible. The coarse sand has a very high proportion of granitic clasts. There has probably been some coring disturbance of the sands. No other internal structures are seen.

Well sorted gravel (facies G)

This is an openwork gravel (Fig. 1.5, analysis 9) occurring as a 0.5 m thick unit in core 37. The lower part of this unit is massive, the upper part shows pronounced grading from 2 cm pebbles to coarse sand.

Poorly sorted gravel (facies H)

This facies forms a 0.5 m bed at the base of core 37. The matrix includes 25 per cent silt and 7 per cent clay (Fig. 1.5, analysis 10). Clasts of this lithology occur in the overlying well sorted gravel facies. The sediment appears clast-supported. It is most simply interpreted as an original well sorted ("open work") gravel with the pore space filled by downward percolation of fine sediment, but might be a water-lain till.

Correlation of Cores with Seismic Record

Cores are only located approximately with respect to the Huntec DTS record (Fig. 1.2a,d). Sedimentary facies A and B correspond to the acoustic facies 4 - the uppermost basin filling acoustically transparent unit. Sedimentary facies C and D correspond to acoustic facies 3 (where it overlies facies 2 in basins). The sand at 135 cm in core 39 marks the unconformity between facies 3 and 4. Sedimentary facies E, F, G and H correspond to the upper part of acoustic facies 2 - the highly stratified basin fill. Acoustic facies 1 has not been cored.

Petrology of Muds

There are distinctive variations in mud petrology within the cores. These are exemplified by the contrast between the brown and grey muds in facies D. Brown muds contain a relatively high illite content at the expense of less than 2 micron non-clay minerals (feldspar, amphibole and quartz); in the grey muds, the converse occurs (Fig. 1.11). The brown muds contain little biogenic material (principally diatoms); the grey muds are rich in biogenics and have a much higher proportion of foraminifera to diatoms.

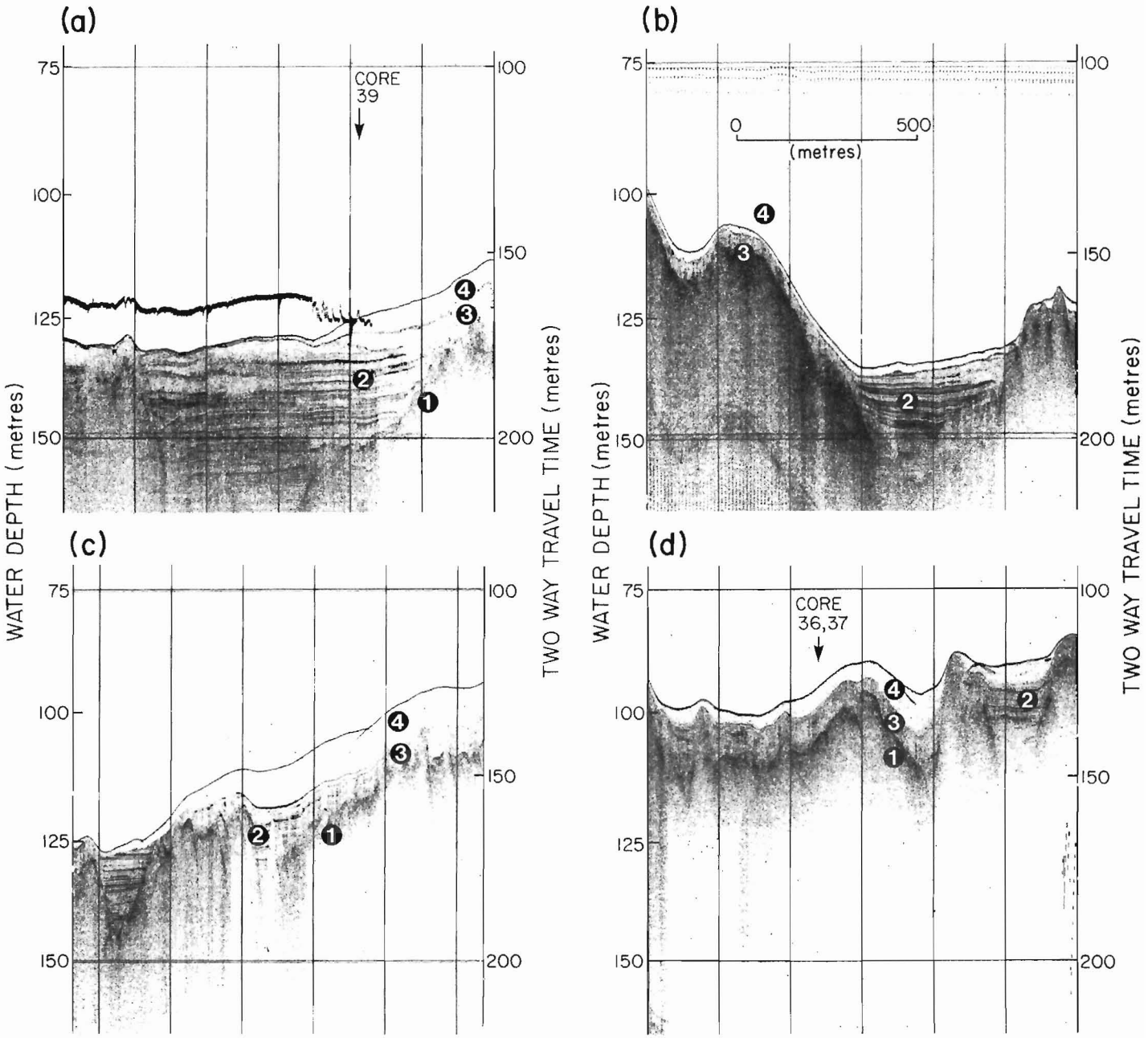

Figure 1.2. Selected Huntec DTS profiles, illustrating acoustic facies 1-4 and approximate location of cores 36, 37 and 39. Profiles located in Figure 1.1.

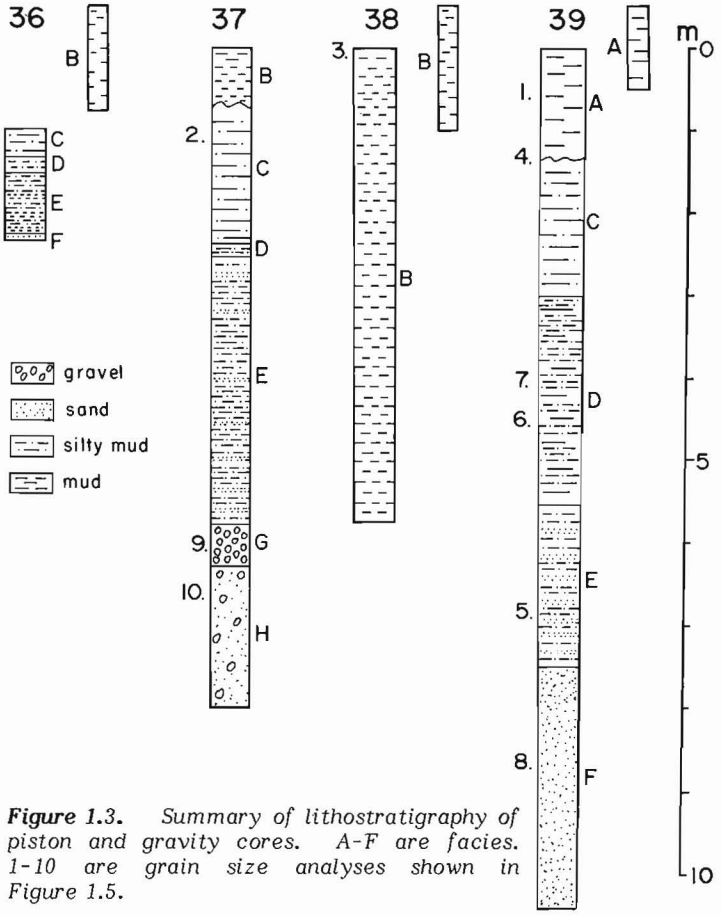

Figure 1.3. *Summary of lithostratigraphy of piston and gravity cores. A-F are facies. 1-10 are grain size analyses shown in Figure 1.5.*

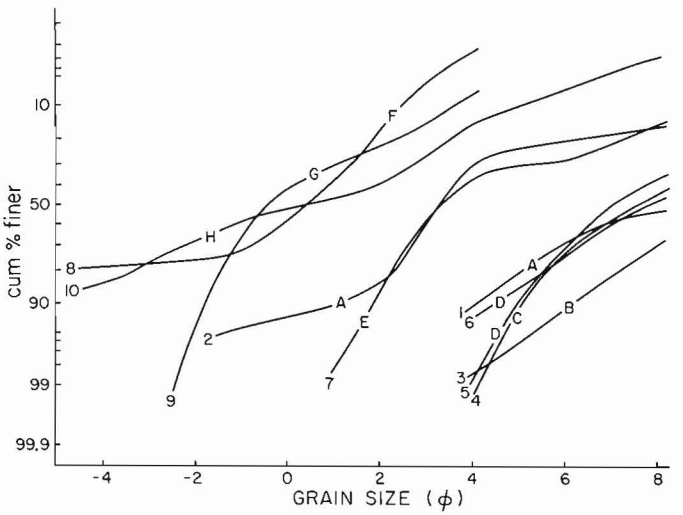

Figure 1.5. *Cumulative frequency plots of representative sediments from facies A-H. Samples 1-10 are located in Figure 1.3.*

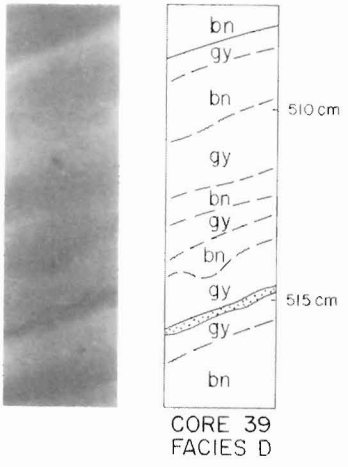

Figure 1.6. *X-radiograph illustrating cyclic sedimentation, of grey (gy) and brown (bn) mud, and silty sands (stippled) in facies D. Darker tones in the X-radiograph indicate sandier or siltier sediment.*

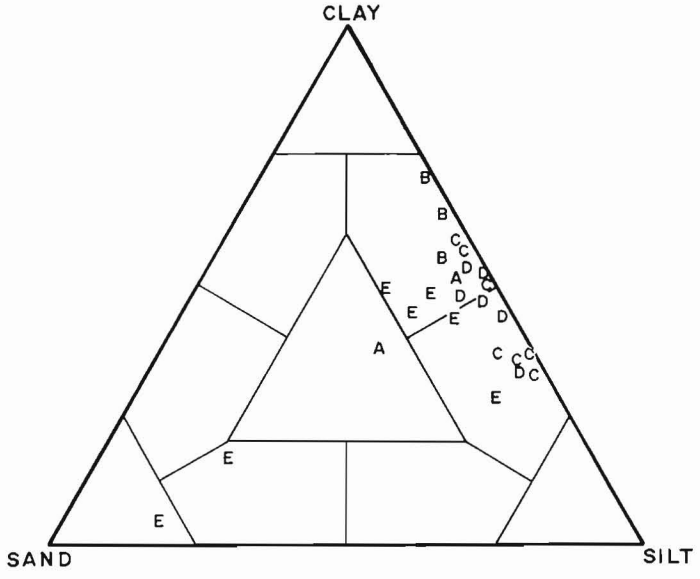

Figure 1.4. *Shepard sand-silt-clay ternary plot showing variation in size distribution of muddy sediments with facies.*

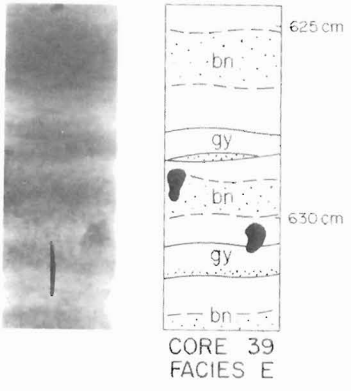

Figure 1.7. *X-radiograph illustrating cyclic sedimentation, facies E. See explanation in Figure 1.6.*

The muds in facies A, B and C have mineralogical compositions between those two extremes. They contain abundant diatoms and foraminifera. Illite abundance may increase seawards in surface samples. Montmorillonite is found throughout the cores in very small amounts, and is most abundant in samples with high feldspar, suggesting a derivation from altered basement rocks.

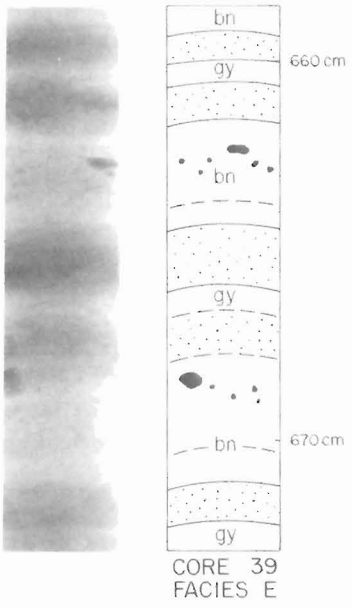

Figure 1.8. *X-radiograph illustrating cyclic sedimentation, facies E. See explanation in Figure 1.6.*

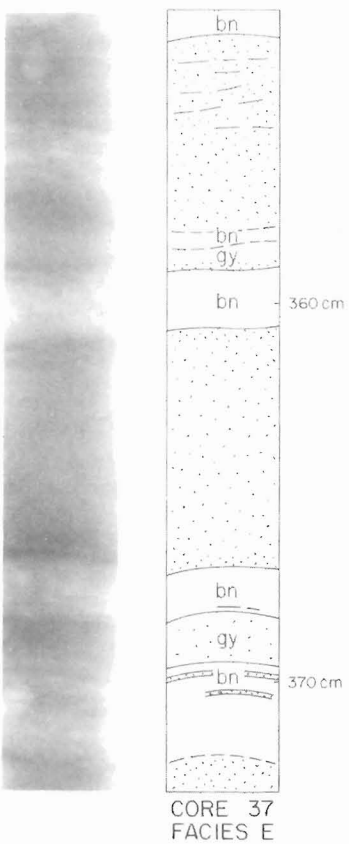

Figure 1.9. *X-radiograph illustrating character of thick sands in facies E. See explanation in Figure 1.6.*

Cyclic Sedimentation in Facies D and E

There is insufficient core available to establish cyclic sedimentation patterns objectively, but visual examination allows a subjective recognition of cyclicity.

The simplest cyclic pattern is an alternation of grey and brown mud (Fig. 1.6), the grey muds sometimes containing thin silt or sand laminae (e.g. 515 cm in Fig. 1.6). A modification of this pattern is illustrated in Figure 1.7 where the grey layer is marked by a basal sand or silt lamina (at 628 and 632 cm in Fig. 1.7), and the brown beds are thicker and coarsest in their middle parts.

Figure 1.8 shows a further development. Thick sands occur at both top and base of the grey muds; the brown muds are fine near the base of beds and they coarsen upwards with scattered granules.

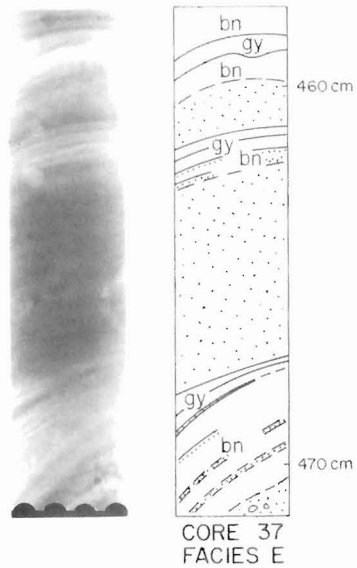

Figure 1.10. *X-radiograph illustrating character of thick sands in facies E. See explanation in Figure 1.6.*

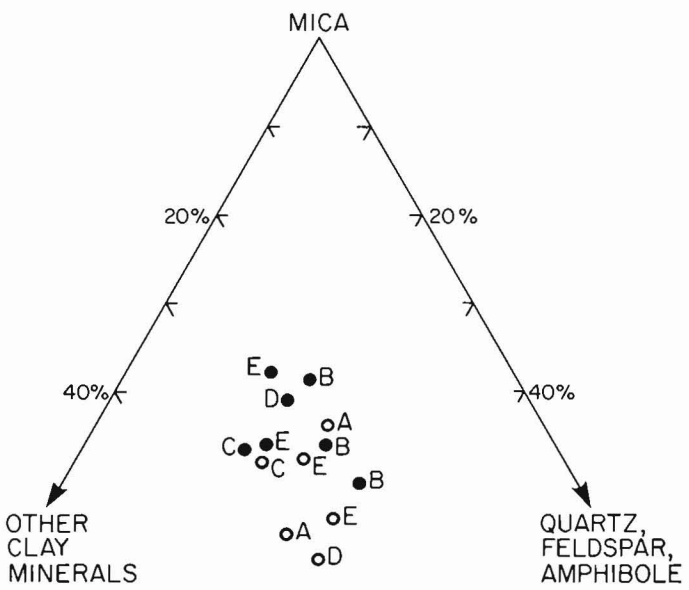

Figure 1.11. *Mineralogy of less than two micron fraction of selected sediments, showing contrast between brown and grey muds in facies D and E, and intermediate compositions of facies A, B and C. Open circles: grey sediments. Solid circles: brown sediments. A-E refer to facies.*

Figures 1.9 and 1.10 show cycles in which sands predominate. The sand beds are often coarsest at the top and base (e.g. 361, 367 cm in Fig. 1.9). Frequently the tops of sand beds pass upwards into alternating laminae of sand and brown mud (352-355 cm in Fig. 1.9; 459-463 and 468-471 cm in Fig. 1.10).

Interpretation of Depositional Environment

The sediments of facies E to H resemble those described by previous workers (e.g. Wightman, 1980) from proglacial deltas. In such environments both graded and ungraded openwork gravels and sands are deposited as foreset beds, and silts falling out of suspension may enter the interstices. Muds with interbedded poorly sorted and stratified sands and silt, depositioned directly from suspension, accumulate as highly proximal bottomsets, within a few kilometres of the river mouth.

However, the Huntec DTS profiles show no clear evidence of foreset beds at basin margins; rather, some reflectors appear to grade into acoustically homogenous strata (e.g. right hand sides of basins in Fig. 1.2a,b). Therefore it is more probable that the sediments accumulated from discharge of subglacial streams beneath floating ice in a marine environment. Sedimentologically, the discharge point of such a stream is in many ways analogous to the mouth of a subaerial outwash stream.

The alternating brown and grey muds of facies D and E probably represent two contrasting depositional environments. The higher biogenic content of the grey muds compared with the brown suggests a slower rate of deposition. The brown muds are rich in illite, which might preferentially flocculate compared to less than 2 micron non-clay minerals on entering saltwater, and the interbedded sands appear to have been deposited directly from suspension. These suggest that the brown muds represent more proximal environments than the grey.

The 5-10 cm thick sand beds that grade up into brown mud in facies E (Fig. 1.9, 1.10) have some characteristics of proximal mass-flow or turbidite deposits, particularly the sharp base overlying grey (biogenic) mud, and the gradational laminated tops of the beds. However, it is difficult to explain all the brown muds as turbidites, particularly those in acoustic facies 3 on basin flanks. The thin coarsening-up mud beds with scattered granules, and thin poorly sorted sand beds (Fig. 1.8) are much more consistent with a model involving direct sedimentation from suspension and ice-rafting, as suggested by Barrie (1980) for Makkovik Bay. If this is so, the cyclicity seen in the sediments might reflect either shifting of discharge points, or an effect of seasonal discharge changes. The interbedded grey mud beds, however, are too thick and rich in biogenics to have been deposited during a single season.

Using the subaerial delta model the sands at the base of the brown mud beds could be explained as the deposits of the spring freshet, with the 3-5 cm brown mud deposited in a single summer season and coarsening up to sand as a delta lobe progrades. This would imply a very proximal environment and annual shifting of distributaries, as a result of winter freezing and the spring freshet. This model, however, does not adequately explain the sands at the base of the grey mud beds where the brown muds do not coarsen up (Fig. 1.7).

Using the floating ice model, brown muds accumulate near discharge points, and grey muds more distally where the effect of ice-margin biota is greater. At times of high discharge, a mud blanket is deposited, but normally sub-ice tidal currents inhibit the deposition of mud, allowing the accumulation of muddy sand layers.

The grey more biogenic muds became commoner upwards through facies D, until they predominate in facies C, but the rare brown mud beds suggest proglacial sedimentation continued during the deposition of facies C. There is some evidence of current-sorted silt laminae. From facies G and H to C, proglacial sediments become increasingly distal. For a subaerial delta model, this would imply a progressive rise in relative sea level. For discharge beneath floating ice, it implies thinning of the ice and retreat of discharge points of subglacial streams. Barrie (1980) has dated sediments of his "conformable cover unit" (our seismic facies 3) at about 10 000 B.P.

We have no independent evidence for the origin of the major unconformity between acoustic facies 3 and 4. Barrie (1980) has discussed a similar unconformity in Makkovik Bay and suggests it is due to wave and storm-induced current erosion during the mid-Holocene 'climatic optimum' when there would have been a shorter period of ice cover protecting the bay from storms. Relative sea level is believed to have been falling at that time, a trend that continues to the present day. Thus facies A and B may only have accumulated once the sill at the entrance to the bay was sufficiently shallow to damp out Labrador Sea waves.

Facies A and B accumulate principally in basins, and have similar textural and mineralogical compositions. The sediment is probably derived from reworking of old pro-delta marine deposits which are subjected to erosion as sea level falls (Piper and Iuliucci, 1978). The colour differences probably reflect oxygen availability related to water depth in the stratified estuary.

Acknowledgments

We thank H. Josenhans and C.Q. Barrie for their constructive criticisms.

References

Barrie, C.Q.
1979: Acoustic reflection stratigraphy of Makkovik Bay, Labrador; in Proceedings of Symposium of Research in the Labrador Coastal and Offshore Region, May 8-10, 1979, Memorial University of Newfoundland, p. 106-132.

Barrie, C.Q.
1980: Marine Geology of Makkovik Bay, Labrador; M.Sc. Thesis, Dalhousie University, Halifax, Nova Scotia.

Barrie, C.Q. and Piper, D.J.W.
1982: Marine geology of Makkovik Bay, Labrador; Geological Survey of Canada, Paper 81-17.

Gandhi, S.S., Grasty, R.L., and Grieve, R.A.F.
1969: The geology and geochronology of the Makkovik Bay area, Labrador; Canadian Journal of Earth Science, v. 6, p. 1019-1035.

Piper, D.J.W. and Iuliucci, R.J.
1978: Reconnaissance of the marine geology of Makkovik Bay, Labrador; in Current Research, Part A, Geological Survey of Canada, Paper 78-1A, p. 333-336.

Piper, D.J.W. and Slatt, R.M.
1977: Late Quaternary clay-mineral distribution on the eastern continental margin of Canada; Geological Society of America Bulletin, v. 88, p. 267-272.

Wightman, D.M.
1980: Late Pleistocene glaciofluvial and glaciomarine sediments on the north side of the Minas Basin, Nova Scotia; Ph.D. thesis, Dalhousie University, Halifax, Nova Scotia.

2.

VOLCANIC ROCKS IN THE LABRADOR SEA AND ENVIRONS AND THEIR RELATION TO THE EVOLUTION OF THE LABRADOR SEA

Project 780042

G.L. Johnson[1], S.P. Srivastava, J. Campsie[2], and M. Rasmussen[2]
Atlantic Geoscience Centre, Dartmouth

Johnson, G.L., Srivastava, S.P., Campsie, J., and Rasmussen, M., Volcanic rocks in the Labrador Sea and environs and their relation to the evolution of the Labrador Sea; in Current Research, Part B, Geological Survey of Canada, Paper 82-1B, p. 7-20, 1982.

Abstract

The chronology of the evolution of the Labrador Sea and environs is examined in relation to dated igneous rocks from land outcrops, continental shelf well samples and dredge hauls from the margins. Results indicate that significant periods of volcanism were associated with initial rifting of the Labrador Sea margins in Late Jurassic and Early Cretaceous. The presence of younger basalts on both the shelf and land fits well with the Paleocene reorientation of the spreading axis in the Labrador Sea. Rock dredges and the shelf magnetic anomalies both suggest the presence of a number of Precambrian and perhaps younger intrusives on the southwest Greenland shelf.

Introduction

The history of development of the Labrador Sea, Davis Strait, and Baffin Bay has long been debated yet serious disagreement still exists between two schools of thought. One group regards these regions as formed by seafloor spreading because of the presence of oceanic crust under them. The other holds that these regions were formed by the subsidence of continental material between Greenland and North America. There are two reasons for this disagreement. Firstly, the large amount of strike slip movement needed along Nares Strait in majority of the seafloor spreading models (Laughton, 1971; Le Pichon et al., 1971; Vogt and Avery, 1974; Kristoffersen and Talwani, 1977; Srivastava, 1978; McWhae, 1981; and Srivastava et al., 1981) is disputed by geologists because of the possible continuation of several geological boundaries and facies across the strait (Christie et al., 1981). Secondly, the well defined magnetic lineations and mid-oceanic ridge are absent in Davis Strait and Baffin Bay regions unlike in the Labrador Sea where they are present (Srivastava et al., 1981). Grant (1980) and Kerr (1981) suggested that the latter can best be explained by the subsidence of the continental crust in these regions.

In spite of the above differences several independent studies support the view that Labrador Sea and Baffin Bay were formed by seafloor spreading: the correspondence between the rate of subsidence of Labrador margin and the cooling of the lithosphere (Keen, 1979; Keen and Hyndman, 1979; Royden and Keen, 1980); the progression of marine conditions from south to north with the opening of the Labrador Sea (Gradstein and Srivastava, 1980); and the presence of a very thin crust under Baffin Bay (Keen and Pierce, in press). Furthermore, studies carried out across passive continental margins have shown that volcanism usually precedes seafloor spreading along the initial plate boundaries (Sleep, 1971; Royden and Keen, 1980; McKenzie, 1978; Keen and Hyndman, 1979). Thus a study of the volcanic rocks present on the shelves bordering the Labrador Sea and Davis Strait should help in deciphering the evolutionary pattern not only of the shelves but also of the adjoining deep basins.

The occurrence of Tertiary basalt on land surrounding the Davis Strait region (Fig. 2.1) has been known for many years (Clarke and Upton, 1971; Clarke and Pedersen, 1976) and occurrences in offshore regions have now been mapped from seismic reflection and magnetic measurements (MacLean et al., 1978, in press; Brett and Zarudzki, 1979). Because of the petrological and geochronological similarities of these basalts on both sides of the strait it has been postulated that they had formed a continuous belt prior to the separation of Greenland from Baffin Island (Hyndman, 1973; Wallace, 1973; Keen and Clarke, 1974; Keen et al., 1974; Hyndman, 1975; Beh, 1975). Basalt has also been encountered in several wells (Fig. 2.1) drilled on the shelves of Labrador, Baffin Island and west Greenland (McWhae and Michel, 1975; Umpleby, 1979; Henderson et al., 1981; Klose et al., 1981). Thus basalt appears to be widespread in the environs of the Labrador Sea. In this paper we examine the ages of these volcanics and their relationship to the evolution of the deep oceanic regions adjacent to them.

Three geographic areas were studied (Fig. 2.1). Area one is the Labrador Shelf which contains reliable well data. Area two includes the Davis Strait region from which reliable well, shallow drill and outcrop data are available whereas area three consists mainly of dredge data, which are less reliable, that were obtained during a geophysical survey of the southwest Greenland margin on board **USNS Lynch** in 1971. One of the primary aims of the cruise was to dredge the outer shelf and slope of Greenland, where it is incised by canyons, in the hope of obtaining in situ samples. Numerous sedimentary and igneous rock samples were collected from a number of dredge hauls whose sedimentologic details were given by Johnson et al. (1974). Included here are the results of petrological and chronological analyses carried out on a few of the volcanic samples collected from the walls of the Julianehaab Canyon and other locations from the southwest Greenland continental margin (Fig. 2.1).

Area One – Labrador Shelf Basalts

A number of wells have been drilled on the Labrador Shelf and some of those, whose information is included here, are shown in Figure 2.1. A summary of the lithostratigraphy obtained from the analyses of well cuttings and examinations of well logs is given in Figure 2.2 (Umpleby, 1979). Precambrian rocks were encountered in Karlsefni, Snorri, Herjolf, Gudrid, and Cartier wells. In the southern part of the Labrador Shelf, four wells penetrated Paleozoic rocks: Ordovician at Freydis, and Carboniferous at Gudrid, Indian Harbour, and Verrazano.

The oldest Mesozoic rocks penetrated by these wells are included in the Alexis Formation (Umpleby, 1979). These comprise variably weathered subaerial basaltic lava flows, aquagene tuffs, and minor sediment giving ages between Beriasian and Hauterivian. Lava flows were encountered in Bjarni, Herjolf, Leif, and Indian Harbour wells. Samples of basalts from these wells show variations in age (Umpleby, 1979; McWhae and Michel, 1975). For example, K-Ar age determinations on the samples collected at 2260 m

[1] Office of Naval Research, Arlington, Va., presently at Dept. of Geology, Univ. of Oslo
[2] Ocean Study Group, Borgergade 34, Copenhagen K, Denmark

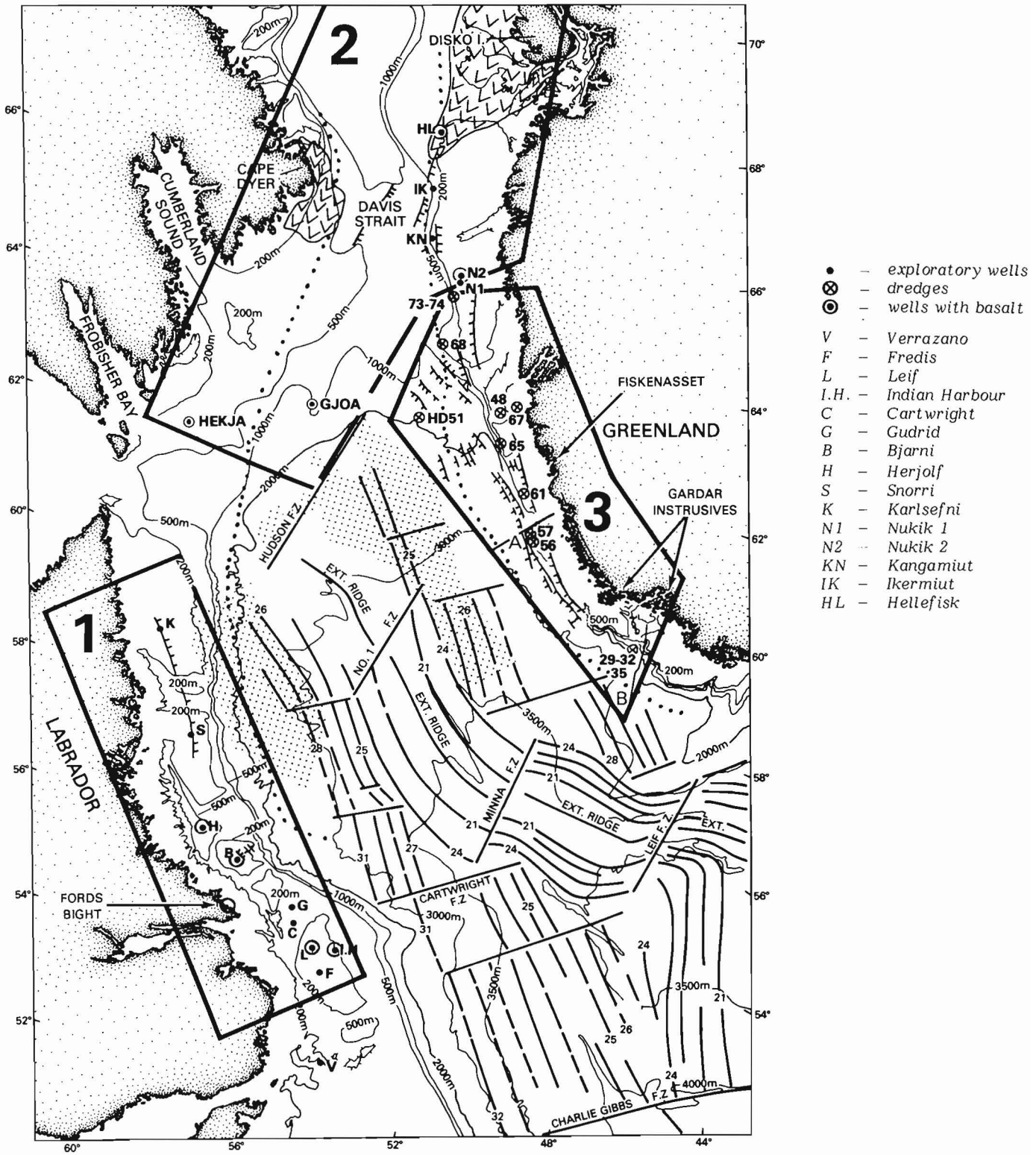

• – *exploratory wells*
⊗ – *dredges*
⊙ – *wells with basalt*

V – *Verrazano*
F – *Fredis*
L – *Leif*
I.H. – *Indian Harbour*
C – *Cartwright*
G – *Gudrid*
B – *Bjarni*
H – *Herjolf*
S – *Snorri*
K – *Karlsefni*
N1 – *Nukik 1*
N2 – *Nukik 2*
KN – *Kangamiut*
IK – *Ikermiut*
HL – *Hellefisk*

Figure 2.1. *Simplified bathymetry and magnetic lineation map of the Labrador Sea and Davis Strait. Stippled pattern with V near Cape Dyer and Disko Island shows the offshore extent of the basalt. Location of seismic lines A and B discussed in the text are shown. Stippled pattern with small crosses in the northern Labrador Sea shows the extent of a flat reflector as seen in the seismic reflection profiles (after Hinz et al., 1979) and interpreted to be Paleocene basalt flows.*

Dotted line marks the ocean-continent boundary as identified by Srivastava et al. (1981).

1, 2, 3 enclosed within thick lines designate regions as discussed in the text.

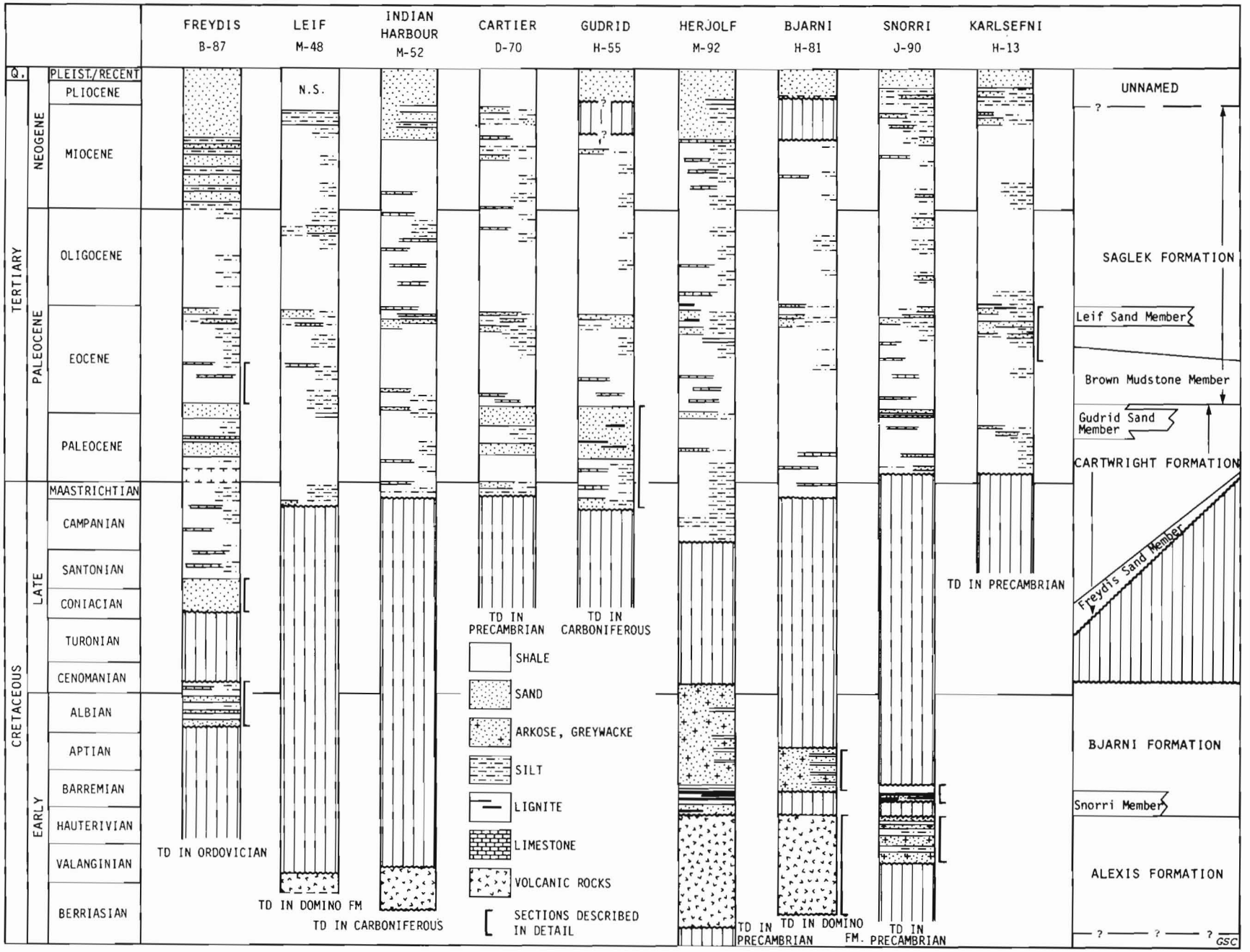

Figure 2.2. *Stratigraphic summary of Labrador Shelf wells after Umpleby (1979).*

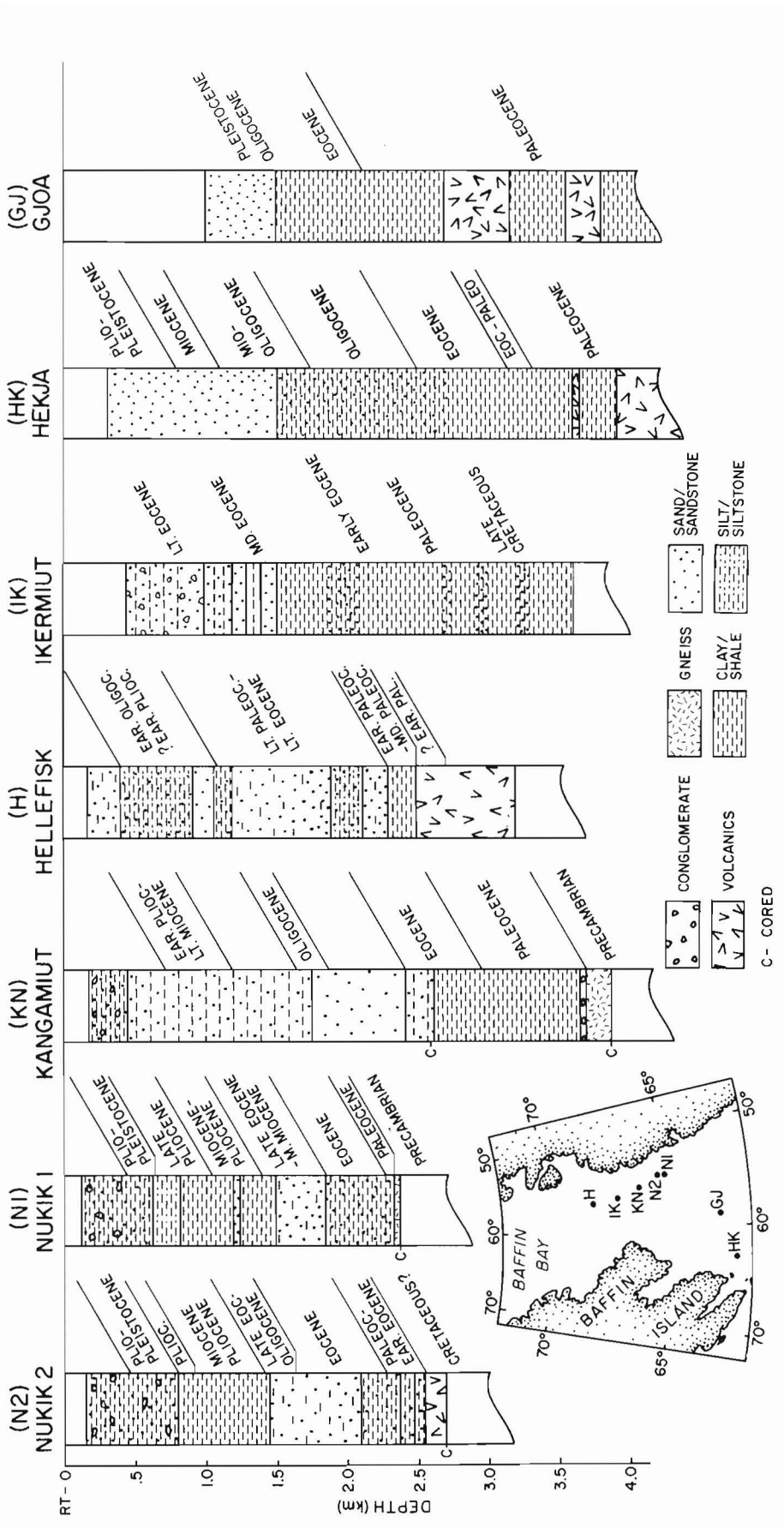

Figure 2.3. *Stratigraphic summary of Greenland and Baffin Island Shelf wells after Greenland Geological Survey (1979) and Klose et al. (1981) respectively.*

and 2510 m depths in Bjarni gave ages of 122 ± 6 and 139 ± 7 Ma respectively. In Herjolf, the radiometric age determination for the sample collected at the top of the lava pile gave an approximate age of 121 ± 5 Ma overlying granitic basement rocks dated at 1427 ± 51 Ma. The youngest basalt flow (90 ± 4 Ma) was encountered in the Indian Harbour well at a depth of 3228 m (Umpleby, 1979).

Isolated outcrops of basalt in the form of lamprophyre dykes occur on the Labrador Coast at Ford's Bight (Fig. 2.1). Radiometric age determinations of these dykes yielded ages from 145 ± 6 to 129 ± 6 Ma (Umpleby, 1979). Igneous intrusives ranging from Late Jurassic to Early Cretaceous in age occur farther south in the Notre Dame Bay area of northeast Newfoundland (Strong and Harris, 1979). The dykes are mainly carbonate lamprophyre; however, basic extrusion and basic to ultrabasic intrusive rocks are also present.

Area Two – Davis Strait Region

Baffin Island Shelf

Volcanic rocks are present onshore in a short, narrow belt near Cape Dyer (Baffin Island) and underlie large areas of the shelf southeast of Cape Dyer (Fig. 2.1) where they have been sampled by shallow drilling and their surface extent outlined by seismic reflection and magnetic profiling (MacLean et al., 1978; MacLean and Falconer, 1979). Strong stratigraphic, petrological, and geochemical similarities exist between these rocks and the Tertiary volcanics of West Greenland (Clarke, 1970; O'Nions and Clarke, 1972). Generally as noted by Clarke (1970) the most notable feature of the basalts from these two areas is the generally high level of MgO with which is correlated high NiO and Cr_2O_3 and low concentrations of the "incompatible elements": Ti, K, P, Zr, Rb, Sr, Ba, and Y. Additionally K_2O/Na_2O and K_2O fall in the 0.06 to 0.16 per cent range. Clarke (1970) also noted that the Baffin Bay basalts belong to a single petrological province characterized by low levels of incompatible elements. The Cape Dyer basalts have been dated as Paleocene by Clarke and Upton (1971) and Parrott and Reynolds (1975).

The volcanic rocks on southeast Baffin Island Shelf near Cumberland Sound form ridge-like structures as seen in the shallow seismic reflection profiles (MacLean et al., in press). Shallow drilled core samples of basalt were recovered from one of these ridges but because they were highly altered no reliable age could be obtained (MacLean et al., in press). The presence of high amplitude and high frequency

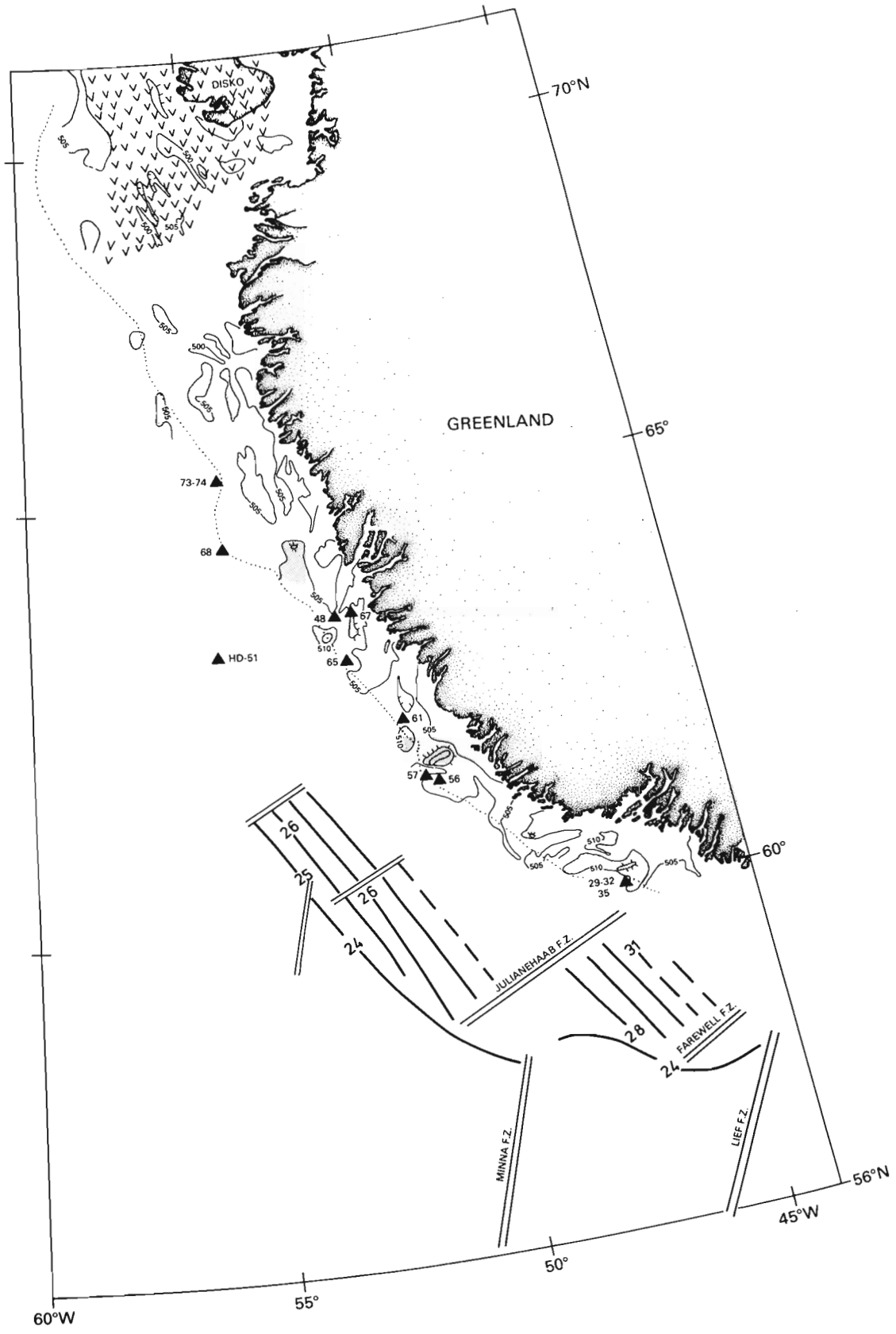

Figure 2.4. *Simplified magnetic anomaly contours of the west coast of Greenland in five hundred of gammas (Greenland Geological Survey Open File, 1979). Ocean anomaly pattern is from Srivastava et al. (1981). Dotted line is shelf break. Positive anomalies on the shelf are shown by a dotted pattern.*

Table 2.1

Dredge haul samples and their descriptions

Dredge	Sample	Position	Depth (fms)	Predicted*	Sample Description		
29	OSG 31	59°57.8N, 46°35.4W	260-320	Gardar	subrounded dolerite	600	g
30	OSG 58	60°03.7N, 46°49.5W	800-950	Tertiary	subangular basalt	125	g
30	OSG 59	- do -	- do -	Tertiary	angular basalt	200	g
31	OSG 83	60°04.6N, 46°50.6W	660-700	Gardar	angular basalt	200	g
32	OSG 69	60°04.8N, 46°44.0W	580-600	Tertiary	subangular dolerite	12	kg
35	OSG 110	60°07.1N, 47°01.7W	405-490	Jurassic	subangular basalt	65	g
56	OSG 549	61°35.5N, 50°37.1W	400-520	Tertiary	angular amygdaloidal basalt	13	kg
57	OSG 558	61°40N, 50°50W	300-400	Gardar	subrounded gabbro	2.3	kg
57	OSG 561	- do -	- do -	Gardar	subrounded dolerite	2.3	kg
61	OSG 567	62°22.3N, 51°13.0W	250-300	Tertiary	grey fine grained basalt	480	g
65	OSG 583	63°07.5N, 52°17.8W	300-440	Tertiary	black medium grained basalt	940	g
67	OSG 594	63°40N, 52°00W	110	Precambrian	fractured subrounded dolerite	3.1	kg
48	OSG 506	63°34.7N, 52°26.5W	60	Tertiary	subrounded dolerite	70	k
68	OSG 598	64°20N, 52°51W	180-240	Precambrian	fractured subrounded dolerite	1.2	kg
73	OSG 599	65°30N, 55°00W	150-180	Precambrian	subrounded dolerite	890	g
74	OSG 600	65°30N, 54°59W	100-150	Tertiary	pillow basalt fragment with one glassy margin	500	g
74	OSG 602	- do -	- do -	Tertiary	subangular basalt	27	g
HD 75	51	63°17N, 55°22W	888	Fault Scarp	basalt		

* Predicted ages based on distinctive petrochemical features of dredged materials compared to known outcrops on land (see also Table 2.3 and Fig. 2.10).

magnetic anomalies over these structures and to the south towards Hudson Strait suggests that basalt may underlie a major portion of the Baffin Island Shelf to the south (Srivastava et al., in press).

Major thicknesses of Paleocene basalts have also been encountered (Klose et al., 1981) in the two offshore wells drilled off Baffin Island (Hekja and Gjoa wells, Fig. 2.3). In Hekja well the bottom 1000 m of drilled section consists of alkalic volcanics interbedded with chalky clays and ranges in age from Danian to Early Cretaceous (Klose et al., 1981). Two thick sheets of volcanics separated by shale were encountered at the Gjoa well. The upper volcanics lie at a depth of 2701 m and are dated as Late Paleocene (Klose et al., 1981).

West Greenland Shelf

Large areas of basalt occur on land and in offshore regions off central West Greenland (Fig. 2.1) and their petrological and chronological similarities and differences have been discussed in detail by Clarke and Pedersen (1976) and Clarke (1977). In general the West Greenland province is characterized by olivine-rich plateau basalts covering hundreds of metres of subaqueous picritic pillow breccias. A greater degree of diversity is present on the Greenland side of Davis Strait, permitting evolution from picritic material at the base to predominantly feldspar-phyric basalts, alkaline basalts including lamprophyres and occasional trachytes in the uppermost layers (Clarke and Pedersen, 1976; Hald, 1976; Larsen, 1977a). Lamprophyre dykes from Ubekendt Ejland just north of Disko Island have been dated as early Oligocene, 30-40 Ma (Parrott and Reynolds, 1975).

Clarke (1975) described 3 dredge hauls from the marine extension of the Disko Island basalt province (Fig. 2.1). The general compositional uniformity of the basalt and its angularity suggest the material was in situ and represented subaerial basalts which had subsided into a marine environment. Both the mineralogy and chemistry were similar to the upper lavas from the West Greenland Tertiary volcanic province.

Five deep exploratory wells (Nukik 1 and 2, Kangamiut, Hellefisk, and Ikermiut) have been drilled to date on the West Greenland Shelf (Fig. 2.1). The preliminary lithostratigraphy of various rock units encountered in these wells is shown in Figure 2.3 (Greenland Geological Survey, 1979). Of the five wells, volcanics were encountered at only two, Nukik 2 and Hellefisk (Fig. 2.1). Their ages, like those from the Labrador Shelf wells, also differ significantly. Late Cretaceous volcanics were present at Nukik 2 (93.4 ± 4.7 Ma, Fergusson, personal communication, 1980; Greenland Geological Survey, 1979) and late Paleocene volcanics at Hellefisk (53 to 54 Ma, Henderson et al., 1981). It should be noted that because of the altered nature of the sample at Nukik 2 its age is questionable and may also be Paleocene (Larsen, personal communication, 1981).

Area Three – Southwest Greenland Margin

A considerable quantity of basalt was collected from extensive dredging carried out along the slope of the west coast of Greenland (Fig. 2.4). Positions of the dredges and sample depths and their description are given in Table 2.1. Results of the geochronological and petrological analyses carried out on some of the samples from these dredges are given in Tables 2.2 and 2.3.

As is well known, dredging in high latitudes such as the Greenland Shelf is complicated by the unknown addition of certain glacial debris from both near and far. Watkins and Self (1972) have demonstrated transport over 30° of latitude in the southern oceans and Rasmussen et al. (1976) have shown an ice-rafted component on the southeastern Greenland margin of over 1000 km. It is difficult to distinguish between ice-rafted and material of possible local origin. In the case of the Greenland continental margin the subareal basalt provinces are relatively well known stratigraphically and petrochemically. Thus by comparison of distinctive petrochemical features one should be able to identify rocks belonging to the various Greenland volcanic provinces and hence isolate volcanic rocks of local origin.

Table 2.2

Major and trace elements of dredged basalts from West Greenland continental margin

dredge	29	30	30	31	32	35	56	57	57	61	65	67	48	68	73	74	74
sample no.	OSG 31	OSG 58	OSG 59	OSG 83	OSG 69	OSG 110	OSG 549	OSG 558	OSG 561	OSG 567	OSG 583	OSG 594	OSG 506	OSG 598	OSG 599	OSG 600	OSG 602
SiO_2	45.60	44.73	47.16	47.77	47.29	49.20	46.44	45.78	52.59	48.47	47.46	49.66	50.73	48.60	52.15	48.10	47.80
Al_2O_3	15.10	13.48	13.62	14.25	13.35	13.59	14.01	15.88	15.62	13.03	12.71	12.77	8.81	14.23	14.81	15.16	15.22
Fe_2O_3	1.77	4.23	3.36	13.13	3.90	4.86	5.95	2.83	0.86	9.81	4.12	3.52	1.86	2.91	2.14	2.50	3.50
FeO	12.45	6.62	10.08	1.51	8.98	8.80	7.53	10.49	10.12	5.09	10.61	13.64	7.73	13.30	10.46	6.74	10.67
MnO	0.16	0.22	0.19	0.17	0.17	0.19	0.20	0.16	0.17	0.21	0.22	0.21	0.20	0.25	0.18	0.17	0.20
MgO	5.51	11.70	7.58	4.46	7.40	4.31	6.88	5.65	4.72	6.53	6.17	4.42	16.28	4.43	4.41	10.85	6.44
CaO	6.95	10.72	11.04	5.91	11.18	8.38	10.93	7.30	7.25	8.49	10.10	8.33	7.21	8.45	8.36	10.89	10.60
Na_2O	4.91	1.92	2.39	3.13	2.21	3.26	1.99	3.49	2.70	2.50	2.71	2.01	1.60	2.36	2.45	1.63	2.20
K_2O	1.79	0.11	0.16	1.89	0.19	1.28	0.15	2.04	1.46	0.42	0.22	1.05	0.34	0.60	1.15	0.08	0.34
TiO_2	2.66	1.01	2.24	2.82	2.07	3.18	2.61	3.01	1.36	2.69	2.93	2.54	0.51	3.05	1.29	0.70	1.35
P_2O_5	1.44	0.10	0.20	0.28	0.22	0.66	0.22	1.46	0.31	0.28	0.30	0.33	0.07	0.30	0.17	0.04	0.09
H_2O	0.12	1.18	0.57	1.87	0.18	0.64	1.31	0.16	0.23	0.78	0.93	0.12	0.10	0.15	0.15	1.04	0.15
loi	1.14	3.55	1.41	2.73	2.16	1.37	1.78	1.76	2.61	1.88	1.52	1.40	4.46	1.37	2.28	2.10	1.44
sum	99.60	99.57	100.00	99.92	99.30	99.72	100.00	100.00	100.00	100.00	99.99	99.99	99.99	99.99	99.99	99.99	99.9
Cu	39	127	221	357	247	82	188	70	55	-	-	418	69	106	168	124	20.9
Rb	35	1.8	1.9	39	1.5	28	0.5	35	32	1.30	1.10	27	-	14	45	0.6	8.5
Ba	2100	not d.	120	560	110	660	39	995	630	125	66.0	396	58	221	320	60	84
Sr	889	102	210	161	17	372	229	868	321	494	200	188	108	189	206	104	143
Ce	55	not d.	not d.	-	-	-	-	-	-	-	-	-	-	-	-	-	-
Nd	35	not d.	not d.	-	-	-	-	-	-	-	-	-	-	-	-	-	-
Y	74	67	74	55	41	73	30	31	32	-	-	46	7	36	28	23	27
Zr	92	75	158	206	157	291	138	163	152	-	-	171	61	142	97	34	82
Ni	18	469	132	119	118	39	84	54	33	103	75	53	660	33	68	277	103
Zn	103	76	105	123	107	145	102	92	104	-	-	156	59	148	112	75	115
Sc	-	-	-	-	-	-	-	24	32	37	40	-	29	-	-	-	33
Co	-	-	-	-	-	-	-	47	40	47	50	-	74	-	-	-	44
Cr	-	-	-	-	-	-	-	29	45	177	105	-	3700	-	-	-	85
Ga	-	-	-	-	-	-	-	18	16	24	27	-	10	-	-	-	12
V	-	-	-	-	-	-	-	168	200	400	430	-	130	-	-	-	300
Feo*/Mgo	2.55	0.89	1.73	2.99	1.69	3.06	1.87	2.31	2.31	2.13	2.32	3.80	0.58	3.59	2.81	0.83	2.15

Comparison Samples

	West Greenland	Baffin I	East Greenland	Gardar Extrusive	Mikis Fjord (E. Greenland)
	48.21	47.5	47.72	46.7	47.61
	14.72	13.8	13.33	15.56	10.92
	3.46	3.3	5.53	10.10	3.80
	8.08	6.7	8.18	2.73	7.25
	0.21	0.17	0.20	0.19	0.19
	7.55	11.8	6.31	4.41	13.49
	11.57	11.7	10.74	8.18	8.07
	2.21	1.53	2.03	2.75	2.74
	0.27	0.10	0.25	1.76	0.10
	1.55	0.97	2.38	0.81	1.58
	0.17	0.10	0.26	0.33	0.17
(H_2O+)	1.28	2.20	2.61	-	H_2O^- 0.58
	0.68	-	-	2.50	3.64
	99.96	100.0	99.50	99.1	-
Pedersen (1977)	-	133	155	-	-
	-	2	2.1	36	-
	-	56	101	394	nil
	-	161	335	785	nil
	-	-	-	81	-
	-	-	9	52	-
	-	21	30	31	-
	-	66	148	205	-
	-	-	48	66	600
	-	57	-	-	Anwar 1950
	-	-	-	-	Wager and Deer 1939
	-	-	48	-	-
	-	-	109	52	-
	-	17	-	-	-
	-	-	343	220	-
		Clarke, (1970)	Brooks et al 1976	Larsen 1977	

Table 2.3

Potassium - Argon Age

Dredge	Sample	Age	K%[1]	Radiogenic Argon%	Remarks
29	31	984 % 36 Ma	1.53	96.7	Calculated age using potassium of 1.53% would be 1007 ± 38 Ma (1.79% K_2O = 1.486% K)
30	58	57.1 % 11.2 Ma	0.09	17.1	
30	59	55.1 % 13.4 Ma	0.18	40.2	Calculated age using 0.16% K_2O = .133% K would be 74.2 ± 18 Ma
57	558	1123 % 27 Ma	1.58	97.4	Calculated age using (2.04% K_2O = 1.69% K) would be 1067 Ma
57	561	1117 % 28 Ma	1.45	97.7	Age calculated using potassium of 1.21% (1.46% K_2O = 1.21% K) would be 1275 Ma
67	594	2311 % 80 Ma	0.71	98.3	Age calculated using potassium of 0.87% (1.05% K_2O = 0.87% K) would be 2054 Ma
HD 75	51	56.9 % 3.2 Ma	0.64	71.9	

[1] K determination based on isotope dilution technique.

About 70-90 per cent of the dredged material consisted of obviously ice-worked boulders and pebbles, generally gneisses and granites, associated with unconsolidated mud. The remainder consisted of a variety of consolidated sediments plus basalts and dolerites. Glacial debris on the shelves of the Labrador Sea appear to be derived mainly from ground moraines of local origin (McMillan, 1973) rather than from melting icebergs. Such debris can be used to broadly infer bedrock geology (Schlee and Pratt, 1970).

Julianehaab Canyon Region

Five dredge hauls (29-32, 35) were collected from the walls of the Julianehaab Canyon (60°15'N, 46°50'W, Fig. 2.4) which extends from middle shelf to the foot of the continental slope – about 60 km long and 8-16 km wide. The canyon in parts is 500-600 m deeper than the adjacent shelf and has fairly smooth walls with 14-15° slopes (Fig. 2.5). The canyon runs roughly north-south and, unlike other West Greenland canyons, is not a submarine continuation of the fiords of the neighboring land area.

The aeromagnetic data in the region of the canyon (Fig. 2.4) show extremely large amplitude high frequency anomalies suggesting that the source of these anomalies lies fairly close to the surface. Comparison of the aeromagnetic data collected over Precambrian rocks with those collected over volcanic rocks (Hood and Bower, 1973) suggests that the anomalies near the dredge site (Fig. 2.4) may arise mainly from volcanic rocks. A **CSS Hudson** geophysical traverse (Fig. 2.6) slightly east of the dredged site (shown as line B in Fig. 2.1) indicated a steep sided basement high about 15 km broad with a maximum residual magnetic value of 1400 nT; it appeared on the seismic reflection record as an arching mass only partly mantled by sediments and may represent a faulted block of intrusive(s) or thick dyke(s).

Statistically the dominant characteristic basaltic rock by weight in the Julianehaab Canyon dredge haul were large angular blocks up to 13 kg with major, minor and trace element characteristics of the East Greenland Tertiary basalt province (Brooks et al., 1976). These large blocks of Tertiary tholeiitic basalt were found in the deeper dredges on the continental slope along with a sedimentary component. Furthermore such large blocks were not found north of 61°35'N. Sample OSG 59 (D 30), which was dated at 55 Ma (Table 2.3), is a typical example of this type; other representative samples of this type are: OSG 69 (D 32) and OSG 549 (D 56). The possibility cannot be ruled out that the samples might be of a local origin, however they chemically resemble tholeiitic plateau basalts from the East Greenland province (Fig. 2.7).

The next most common basalt type in the Julianehaab Canyon region are samples similar to OSG 31 (Table 2.1, 2.2). These have the characteristic chemical features of basic Gardar type extrusives, specifically high TiO_2, FeO (total iron), Na_2O, K_2O and P_2O_5 (Watt, 1966, 1969; Bridgwater and Harry, 1968). Among the trace elements, these rocks appear to be characterized by high contents of Ba and Sr, ranging from 600 to 2500 ppm and 500 to 1200 ppm, respectively. A sample of this type has also been reported by Rasmussen et al. (1976) seaward of Kap Walloe. These samples were found scattered throughout all the dredges from this area, although they made up the largest basalt component of the shallower dredges.

The consolidated sediments found together with basalts were subjected to paleontological and petrographic analyses (Johnson et al., 1974). The preliminary results on two sandy limestones from dredges 32 and 37 suggested a Cretaceous age with some reworked Jurassic material, but a more detailed re-examination indicated that the Cretaceous material is set in a matrix which yielded an Oligocene-Early Miocene age. Further these samples contain Triassic as well

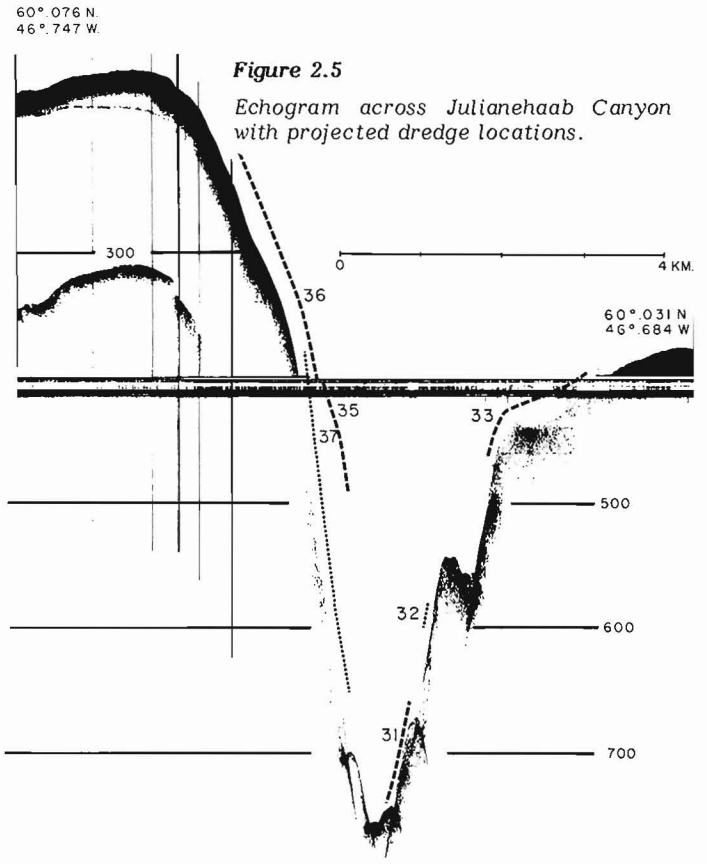

Figure 2.5

Echogram across Julianehaab Canyon with projected dredge locations.

as Jurassic pollen. Such floras do not appear to be known from the subareal West Greenland sediments (K. Raunsgaard Pedersen, personal communication, 1981). Both samples contain fresh volcanic materials, and one even contains a faceted basalt pebble. Mixed ages, similar to those just quoted, were reported from Quaternary morainic debris dredged from the Banan Bank on the outer shelf off Godthaab (Dibner et al., 1963). In addition, the angularity of the volcanic minerals as well as the faceted character of the basalt pebble is suggestive of a high energy regime. We are uncertain if the Julianehaab unconsolidated material is also glacial debris containing Oligocene and Mesozoic fragments, or if it is representative of deeper and more consolidated in situ material from the canyon walls. If the proposed Oligocene age for the sediments is also applied to its contained volcanic grains the volcanic events might relate to episodic mid-Tertiary volcanism confirmed from East Greenland (Brooks, 1980), or West Greenland (Clarke and Pedersen, 1976; Parrott and Reynolds, 1975).

Sample OSG 110 (D 35) has major, minor and trace element concentrations very similar to coast-parallel Jurassic dykes onshore (S. Watt, personal communication, 1981). Particularly distinctive are the relatively high Zr values (291 versus 75-206, Table 2.2). Sample OSG 83 (D 31) had major, minor and trace element contents indistinguishable from those reported from onshore Gardar Basalt Province (Larsen, 1977b). For this latter sample the high degree of oxidation is particularly distinctive, as reflected in its high Fe_2O_3 content. No other samples of these two types were found in the Julianehaab Canyon region.

Dredge 30 (sample 58) was a small fragment of basalt. This sample possesses low TiO_2, K_2O, P_2O_5, Sr (Table 2.2) similar to Prince of Wales Bjaerge lavas in East Greenland (Anwar, 1950), and the basalts from the Hellefisk and Nukik wells (Larsen, personal communication, 1981). It may represent the possibility of long distance transport, or conversely be related to the basalt encountered in the West Greenland drillholes. Note that this sample and samples 506 and 600 lie in a discrete field shown in Figure 2.7.

Central Shelf

Dredges 48 and 56 were recovered from the central region southwest of Greenland (Fig. 2.1). A seismic reflection profile near dredges 56 and 57 (Fig. 2.8, and line A in Fig. 2.1) shows basement to consist of large blocks downfaulted toward the sea. In form it is similar to a multichannel seismic line seaward of Godthaab (Manderscheid, 1980). As noted by Manderscheid (1980) sediment cover in this region seems rather thin with only about 500 m draped over the basement in the shelf region. The rough basement is apparently abutting the most seaward downfaulted block. This block has a 2000 gamma anomaly which may well indicate the presence of an intrusive body. The magnetic anomalies on the shelf tend to strike north-south with occasional circular highs (Fig. 2.4). Dredge 67 lies on the edge of an elongate (N-S) magnetic high and dredges 48-50 and 61 on magnetic highs. Dredge 65 lies in a magnetically quiet area. Assuming dredge 67 is of local origin, its K-Ar age of 2311 ± 80 Ma reported here would seem to support this interpretation.

Farther to the north dredge 56 (OSG 549; Fig. 2.4) recovered almost exclusively large, angular rocks of basalt along with some sedimentary rocks (Johnson et al., 1974). These angular rocks have affinities to the East Greenland Tertiary basalt province (see Fig. 2.1, 2.7, Tables 2.1-2.3). On the other hand dredge 57 (OSG 558, OSG 561) from a shallower depth recovered subrounded rocks of Gardar age (Table 2.3). Both dredges were taken near a large structural and magnetic high (Fig. 2.4, 2.8). It is suggested that these (D 57) samples might be of local origin from the shelf, though now part of the ground moraine. If of local origin they would represent outcrops of Gardar age on the shelf and constitute the northernmost extent of the known Gardar province (Fig. 2.1).

Dredges 61 (OSG 567) and 65 (OSG 583) are from the upper continental slope, whereas dredge 74 (OSG 602) is from the continental shelf. Considering the northerly localities from which these three samples were recovered, their sparse distribution among the dredges and their similarity in major, minor and trace elements, these samples may correlate with the West Greenland Tertiary basalts (Fig. 2.7, Table 2.3).

Dredge 67 (OSG 594) was recovered from the north wall of a transverse canyon at shallow depth and consisted nearly exclusively of dolerite having relatively distintive chemical features with FeO of 14-18%, K_2O of 0.5-1.0% and TiO_2 of 1.5-2.6%. Of the 11 samples analyzed all had similar weathering characteristics with an H_2O value of 0.1% with distinctive variable Cu of 200-450 ppm. This rock was dated as pre-Gardar (2311 Ma, Tables 2.1, 2.3). Dibner et al. (1963) reported a metadiabase having a K_2O value of 0.7% and a K-Ar age of 1840 Ma from Banan Bank seaward of Godthaab. Considering the homogeneity of dredge 67, its location of recovery, and its association with a magnetic high (Fig. 2.4), it would seem likely that this dredge recovered material from local Precambrian intrusives on the shelf. Dredges D 68 (OSG 598) contained basalts which chemically appeared to be related to the Precambrian dolerites like D 67.

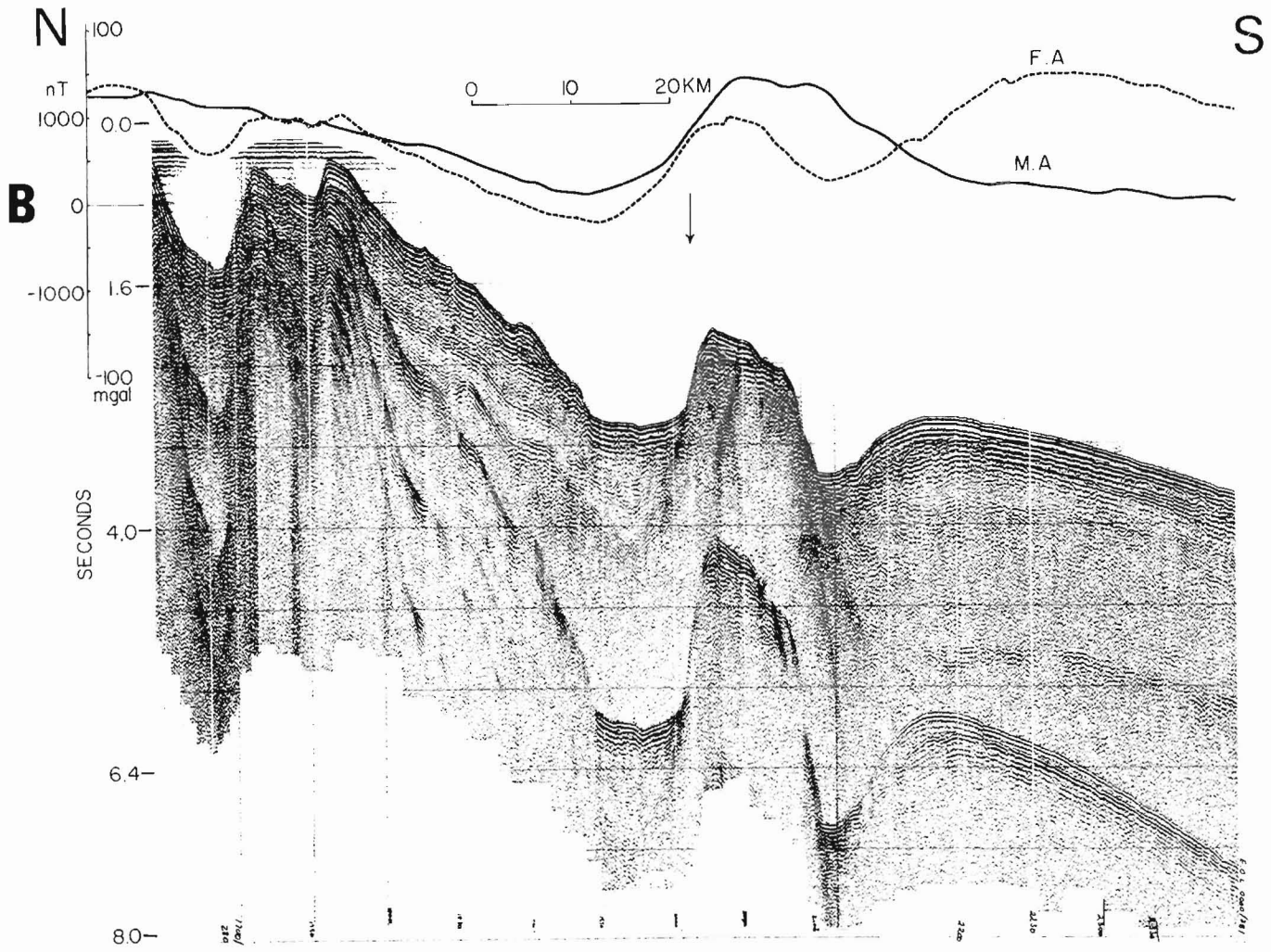

Figure 2.6. *Seismic reflection profile obtained by* ***CSS Hudson*** *just to the south of Julianehaab Canyon. Note the large basement high which is associated with a large gravity (F.A.) and magnetic anomaly (M.A.). Dredges 21-35 were collected along the face of a scarp similar to the one shown by the arrow.*

Dredges 48 (OSG 506) and 74 (OSG 600) recovered basalts with major, minor and trace element concentrations similar to Baffin Island picritic and relatively olivine poor basalts respectively (Clarke, 1970). Sample OSG 600 was an unusually fresh pillow-basalt with a glassy margin. As can be seen in Table 2.2 this sample is similar to Baffin Island basalts. Of course this does not rule out a local basalt with these affinities, as chemically it does resemble basalt from Hellefisk and Nukik 2 holes (Larsen, personal communication, 1981) which were encountered 2500 m below the sediments (Fig. 2.3). Dredge 74 is located very close to Nukik 2 hole. Rocks from this dredge were recovered from a depth of about 200 m and probably represent the upper 350 m of "conglomerate" or Pleistocene-recent debris.

Discussion

The presence of basalt on the shore, shelf and slopes surrounding the Labrador Sea and Davis Strait region indicates it is not confined to the deep basin only. Basalt found on the southwest Greenland shelf and slope is based on dredged samples and unfortunately we cannot with certainty say that we collected any in situ basalts, however, it does not seem unreasonable to assume, based on the foregoing discussion, that some of the basaltic material was of local origin. This is especially true for the Gardar components of the Julianehaab Canyon dredges and dredges 57 and 67 of relatively shallow depth farther north. Furthermore there is

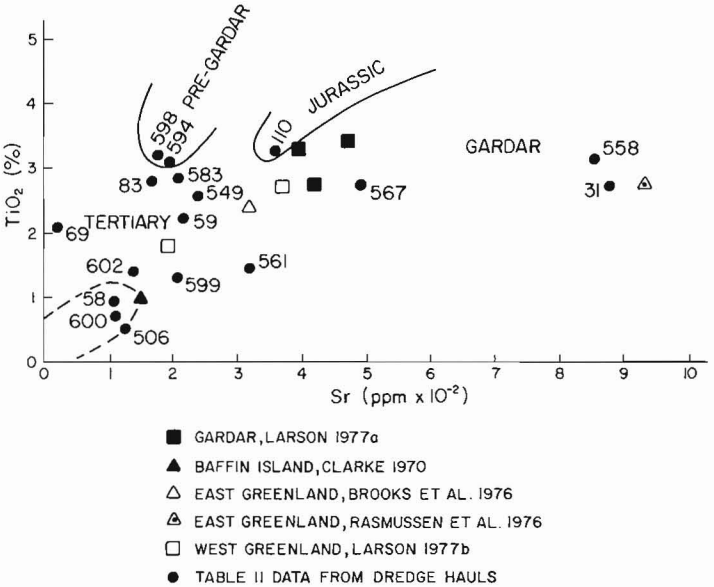

Figure 2.7 *TiO_2 versus Sr diagram for dredged basalts of proposed Tertiary age and representative samples from adjacent igneous provinces (Table 2.2) and cited references in the figure.*

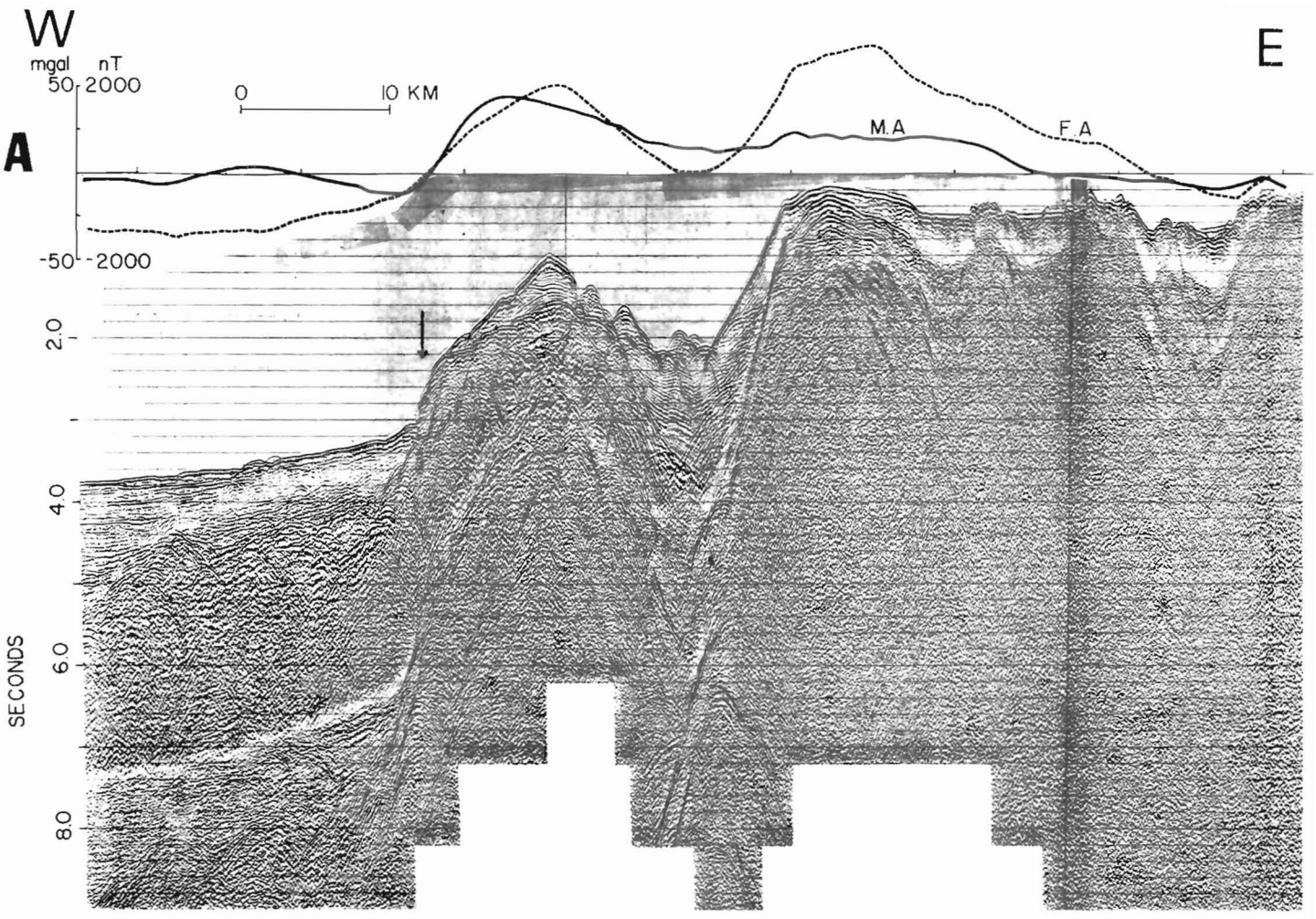

Figure 2.8. *A portion of the multichannel seismic reflection profile in the vicinity of dredges 56 and 57. For location see Figure 2.1.*

no reason to expect that the Jurassic dykes on shore do not extent offshore. Sample OSG 110 (D 35) may well represent these dykes.

As noted earlier, both magnetic and seismic data suggest a presence of basic intrusive bodies on the southwest Greenland shelf. Such intense magnetic anomalies are indicative of a relatively high Fe and Ti concentration in the source material. Both Tertiary and Gardar rocks might generate such anomalies. The two most prominent localities for intrusives would be 60°15'N (D 30-35) and 61°45'N (D 57).

It cannot be ruled out that some of the Tertiary components are of local origin. It is worth noting that no evidence for submarine low-temperature weathering processes have been observed, and none of the recovered basaltic material had ferro-manganese accumulations. Furthermore their Fe_2O_3, H_2O^- and H_2O^+ contents as well as thin section characteristics are indistinguishable from known subareal occurrences in both East and West Greenland. These observations would suggest a limited time of submergence in seawater.

Basalt samples OSG 58 (D 30) and OSG 600 (D 74) appear similar to those reported from Hellefisk and Nukik 2 wells (Larsen, personal communication, 1981). One can of course assume all the Tertiary basalts are ice-rafted from East and West Greenland and this possibility cannot be excluded, however, it seems unlikely in view of the extensive Paleocene volcanism in the Labrador Sea Basin and Davis Strait region (Table 2.4). It is suggested that some of the Tertiary basalts may well represent local events with chemical similarities to other regions.

Results from Table 2.4 show that significant periods of volcanism were associated with initial rifting of the Labrador Sea-Baffin Bay region in Late Jurassic-Early Cretaceous. Occurrence of younger basalts on both the shelf and land fits well with the Paleocene reorientation of the spreading axis in Labrador Sea (Table 2.4). This is in harmony with geometric reconstructions that older basalts should occur on the Labrador Shelf and younger farther to the north and seaward toward the extinct spreading axis. It seems likely the Late Jurassic-Early Cretaceous volcanic event recorded on both the Labrador Coast and West Greenland may also be present on the Greenland Shelf (Dredge D 35). This suggests the early rifting phase of the Labrador Sea may be related to this time, an observation also made by Clarke (1977).

A later period (Paleocene) of volcanism is recognized from the occurrences of volcanics on land and offshore in the Davis Strait region. This includes occurrences of Tertiary basalt at Cape Dyer on Baffin Island, at Disko Island on Greenland and in the deep exploratory wells drilled on the Greenland shelf (Hellefisk) and Baffin Island shelf and slope

Table 2.4

Sequence of events in
Labrador Sea-Baffin Bay region

Eocene – early Oligocene Lamprophyre dykes injected on Ubekendt Ejland (just north of Disko Island) possibly some volcanism in Julianehaab Canyon region.
Late Paleocene – change in direction of spreading axis. Eruption of basalts at Cape Dyer and Disko and Davis Strait (Hellefisk well) regions (Gjoa well, HD-75 sample). Labrador Sea Basin basalts are emplaced. Possible Tertiary dykes scattered along southwest Greenland coast.
Early Paleocene – seafloor spreading commences in the northern Labrador Sea, Baffin Bay (Gjoa well).
Late Cretaceous (Maestrichtian) – seafloor spreading commences in the southern Labrador Sea and Makarov Basin.
Mid-Cretaceous (Cenomanian-Turonian) – volcanism on Greenland Shelf (Nukik 2 well), South Baffin Island Shelf (Hekja well), and outer Labrador Shelf (Indian Harbour well).
Early Cretaceous (Beriasian-Hauterivian) – volcanism on Labrador Shelf (Bjarni, Herjolf and Leif wells).
Late Jurassic-Early Cretaceous (Late Kimmeridgian to Valanginian) – volcanism in western Greenland and possibly shelf: dyke swarm (Fig. 2.1). Lamprophyre dykes along the coast of Labrador (Ford's Bight) northeast Newfoundland, and southwest Greenland.

(Hekja and Gjoa) and a Tertiary (71.9 Ma) basalt sample dredged in the northern Labrador Sea (Table 2.3). The occurrence of basalt in the Davis Strait region has been regarded for a long time as part of the Brito-Arctic Volcanic Province because of the similarity in the ages of the volcanic rocks found in the British Isles and on the east coast of Greenland with those across Davis Strait. However, Clarke (1977) regarded them as two separate units because of geochemical and other differences between them.

A similar later period of volcanism has also been seen in the seismic reflection data collected in the Labrador Sea (Hinz et al., 1979). The flat basement reflector with subbasement reflectors, according to Hinz et al. (1979), represents basalt flows correlated in time with the Late Paleocene volcanism associated with the reorientation of the Labrador Sea spreading centre at anomaly 24. This reflector has a refraction seismic velocity of 5.9 km/s. The extent of the flat basement reflector, as given by Hinz et al. (1979), is shown in Figure 2.1 by a stippled pattern.

The Greenland shelf has been proven by drilling to have at least in the north a significant and shallow Precambrian core. Mayhew's (1970) data suggested this may extend all the way to the Julianehaab region. Both dredge samples and the magnetic anomalies suggest that a number of Gardar and perhaps younger intrusives are present in the southwest Greenland shelf.

Acknowledgments

We wish to thank the following people for their support: The Officers and crew of the **USNS Lynch** for their assistance during the cruise, Dr. Haldis Bollingberg, Dr. John Bailey and B. Moller, Institute of Petrology, University of Copenhagen, for major/minor and trace element analyses. The manuscript was strengthened by the review of J.G. Larsen, C.K. Brooks, D.B. Clarke, and J.M. Woodside. Rock sample dating was done by the Geochronology Laboratory of the Geological Survey of Canada. We are grateful to G.W. Klose, G.G. Zinkan of Esso Resources Canada and E. Malterre and N.J. McMillan of the Cantera Ltd. for allowing us to use simplified lithological logs from Hekja and Gjoa wells in this paper.

References

Anwar, Y.M.
1950: A petrological study of the Prince of Wales Bjaerge lavas, East Greenland; Ph.D. thesis, University of Durham.

Beh, R.L.
1975: Evolution and geology of western Baffin Bay and Davis Strait, Canada; in Canada's Continental Margins and Offshore Petroleum Exploration, ed., C.J. Yorath, E.R. Parker, and D.J. Glass, Canadian Society of Petroleum Geologists, Memoir 4, p. 453-476.

Brett, C.P. and Zarudzki, E.F.K.
1979: Project Westmar – a shallow marine geophysical survey on the west Greenland continental shelf in the region 64° to 69°30'N and a preliminary interpretation of the data; Gröenlands Geologiske Undersoegelse, Rapport 87, 29 p.

Bridgwater, D. and Harry, W.T.
1968: Anorthosite xenoliths and plagioclase megacrysts in Precambrian intrusives of South Greenland; Meddelelser om Gröenland, v. 185, no. 2, p. 243-260.

Brooks, C.K.
1980: Episodic volcanism, epeirogenesis and the formation of the North Atlantic Ocean; Paleogeography, Paleoclimatology, Paleoecology, v. 30, p. 229-242.

Brooks, C.K., Nielsen, T.F.D., and Petersen, T.S.
1976: The Blosseville Coast basalts of East Greenland, their occurrence composition and temperal variations; Contributions to Mineralogy and Petrology, v. 58, p. 279-292.

Christie, R.L., Dawes, P.R., Forsch, T., Higgins, A.K., Hurst, J.M., Kerr, J.W., and Peel, J.S.
1981: Geological evidence against major displacement in Nares Strait; Nature v. 291, p. 478-480.

Clarke, D.B.
1970: Tertiary basalts of Baffin Bay: possible primary magma from the mantle; Contributions to Mineralogy and Petrology, v. 25, p. 203-207.

1975: Tertiary basalts dredged from Baffin Bay; Canadian Journal of Earth Sciences, v. 12, p. 1396-1405.

1977: The Tertiary volcanic province of Baffin Bay in Volcanic Regimes in Canada; ed., W.R.A. Baragar, L.C. Coleman, J.M. Hall, Geological Association of Canada, Special Paper 16.

Clarke, D.B. and Pedersen, A.K.
1976: Tertiary volcanic province of West Greenland; in Geology of Greenland, ed., A. Escher and W.S. Watt, Gröenlands Geologiske Undersoegelse Copenhagen, p. 364-385.

Clarke, D.B. and Upton, B.G.J.
1971: Tertiary basalts of Baffin Island: field relations and tectonic setting; Canadian Journal of Earth Sciences, v. 8, p. 248-258.

Dibner, V.D., Krylov, A.J., Sedova, M.A., and Vakar, V.A.
1963: Age and origin of rocks lifted by trawl from the South-West Greenland shelf; Meddelelser om Gröenland, v. 171, no. 2, 13 p.

Gradstein, F.M. and Srivastava, S.P.
1980: Aspects of Cenozoic stratigraphy and paleo-oceanography of the Labrador Sea and Baffin Bay; Paleogeography, Paleoclimatology, Paleoecology, v. 30, p. 261-295.

Grant, A.
1980: Problems with plate tectonics: Labrador Sea; Bulletin Canadian Petroleum Geology, v. 28, p. 252-278.

Greenland Geological Survey
1979: Well data summary sheets. Wells drilled 1967-1977, Greenland Geological Survey, Copenhagen September 1979, 14 p.

Hald, N.
1976: Early Tertiary flood basalts from Hareoen and Western Nugssuaq; Bulletin, Gröenlands Geologiske Undersoegelse, v. 120, 36 p.

Hansen, K.
1980: Lamprophyres and carbonatitic lamprophyres related to rifting in the Labrador Sea; Lithos, v. 13, p. 145-152.

Hansen, K. and Larsen, O.
1974: K-Ar determinations on Mesozoic lamprophyre dykes near Ravins Storo, Fiskenasset region, southern West Greenland; Rapport Gröenlands Geologiske Undersoegelse, v. 66, p. 9-11.

Henderson, G., Schiener, E.J., Risum, J.B., Croxton, C.A., and Andersen, B.B.
1981: The West Greenland Basin; in Geology of the North Atlantic Borderlands, ed., J.W. Kerr and A.J. Fergusson, Canadian Society of Petroleum Geologists, Memoir 7.

Hinz, K., Schluter, H.U., Grant, A.C., Srivastava, S.P., Umpleby, D., and Woodside, J.
1979: Geophysical transects of the Labrador Sea: Labrador to Southwest Greenland; Tectonophysics, v. 59, p. 151-183.

Hood, P. and Bower, M.E.
1973: Low-level aeromagnetic surveys of the continental shelves bordering Baffin Bay and the Labrador Sea; Geological Survey of Canada, Paper 71-23, p. 571-597.

Hyndman, R.D.
1973: Evolution of the Labrador Sea; Canadian Journal of Earth Sciences, v. 10, p. 637-644.

1975: Marginal basins of the Labrador Sea and the Davis Strait hot spot; Canadian Journal of Earth Sciences, v. 12, p. 1041-1045.

Johnson, G.L., Campsie, J., Rasmussen, M., and Dittmer, F.
1974: Mesozoic rocks from the Labrador Sea – a correction; Nature, v. 247, p. 413-414.

Keen, C.E.
1979: Thermal history and subsidence of rifted continental margins – evidence from wells on the Nova Scotian and Labrador Shelves; Canadian Journal of Earth Sciences, v. 16, p. 505-522.

Keen, C.E. and Hyndman, R.D.
1979: Geographical review of the continental margins of eastern and western Canada; Canadian Journal of Earth Sciences, v. 16, p. 12-747.

Keen, C.E., Keen, M.J., Ross, D.I., and Lack, M.
1974: Baffin Bay: small ocean basin formed by sea-floor spreading; American Association of Petroleum Geology Bulletin, v. 58, p. 1089-1108.

Keen, C.E. and Peirce, J.W.
The geophysical implications of minimal Tertiary motion along Nares Strait; in Nares Strait and the drift of Greenland: a conflict in plate tectonics, ed., P.R. Dawes and J.W. Kerr, Meddelelser om Gröenland, Copenhagen. (in press)

Keen, M.J. and Clarke, D.B.
1974: Tertiary basalts of Baffin Bay: Geochemical evidence for a fossil hot spot; in Geodynamics of Iceland and the North Atlantic Area, ed., L. Kristjansson, D. Reidal (Dordrecht-Holland) Publishers, p. 127-137.

Kerr, J.W.
1981: Stretching of the North American Plate by a now dormant Atlantic spreading centre; in Geology of the North Atlantic Borderlands, ed., J.W. Kerr and A.J. Fergusson, Canadian Society of Petroleum Geologists, Memoir 7, p. 245-278.

Klose, G.W., Zinkan, G.C., Malterre, E., and McMillan, N.J.
1981: Petroleum exploration offshore southern Baffin Island, Northern Labrador Sea, Canada; in Third International Symposium on Arctic Geology, Canadian Society of Petroleum Geologists, abstract only.

Kristoffersen, Y. and Talwani, M.
1977: Extinct triple junction south of Greenland and the Tertiary motion of Greenland relative to North America; Geological Society of America Bulletin, v. 88, p. 1037-1049.

Larsen, J.G.
1977a: Transition from low potassium olivine tholeiites to alkali basalts on Ubekendt Ejland: The Tertiary Volcanic province of West Greenland; Meddelelser om Gröenland, v. 200, no. 1, 39 p.

1977b: Petrology of the late lavas on the Eriks Fjord Formation, Gardar Province, South Greenland; Geological Survey of Greenland Bulletin, v. 125, 31 p.

Laughton, A.S.
1971: South Labrador Sea and the evolution of the North Atlantic; Nature, v. 232, p. 612-617.

Le Pichon, X., Hydman, R., and Pautot, G.
1971: Geophysical study of the opening of the Labrador Sea; Journal of Geophysical Research, v. 76, p. 4724-4743.

MacLean, B., Falconer, R.K.H., and Clarke, D.B.
1978: Tertiary basalts of western Davis Strait: bedrock core samples and geophysical data; Canadian Journal of Earth Sciences, v. 15, p. 773-780.

MacLean, B. and Falconer, R.K.H.
1979: Geological/geophysical studies in Baffin Bay and Scott Inlet-Buchan Gulf and Cape Dyer-Cumberland Sound areas of the Baffin Island Shelf; in Current Research, Part B, Geological Survey of Canada, Paper 79-1B, p. 231-244.

MacLean, B., Srivastava, S.P., and Haworth, R.T.
Bedrock structures off Cumberland Sound, Baffin Island Shelf; in Arctic Geology and Geophysics, ed., A.F. Embry and H.R. Balkwill, Canadian Society of Petroleum Geologists, Memoir 8. (in press)

Manderscheid, G.
1980: The geology of the offshore sedimentary basin of West Greenland; in Facts and Principles of World Petroleum Occurrences, ed., A.D. Miall, Canadian Society Petroleum Geologists, Memoir 6, p. 951-978.

Mayhew, M.A., Drake, C.L., and Nafe, J.E.
1970: Marine geophysical measurements on the continental margins of the Labrador Sea; Canadian Journal of Earth Sciences, v. 7, p. 199-214.

McKenzie, D.P.
1978: Some remarks on the development of sedimentary basins; Earth and Planetary Science Letters, v. 40, p. 25-32.

McMillan, N.J.
1973: Shelves of Labrador Sea and Baffin Bay, Canada; Canadian Society of Petroleum Geologists, Memoir 1, p. 473-517.

McWhae, J.R.H.
1981: Structure and spreading history of the northwestern Atlantic region from the Scotian Shelf to Baffin Bay; in Geology of the North Atlantic Borderlands, ed. J.W. Kerr and A.J. Fergusson, Canadian Society of Petroleum Geologists, Memoir 7, p. 299-332.

McWhae, J.R.H. and Michel, W.F.E.
1975: Stratigraphy of Bjarni H-81 and Lief M-48, Labrador Shelf; Bulletin of Canadian Petroleum Geology, v. 23, p. 361-382.

O'Nions, R.K. and Clarke, D.B.
1972: Comparative trace element geochemistry of Tertiary basalts from Baffin Bay; Earth and Planetary Science Letters, v. 15, p. 436-443.

Parrott, R.J.E. and Reynolds, P.H.
1975: Argon 40/Argon 39 geochronology, age determinations of basalts from Labrador Sea area; Geological Society of America, Abstracts, v. 7.

Rasmussen, M.H., Campsie, J., Dittmer, F.B., and Bailey, J.C.
1976: Basalts from the southeastern Greenland Continental Margin; Bulletin of Geological Society of Denmark, v. 25, p. 73-78.

Royden, L. and Keen, C.E.
1980: Rifting process and thermal evolution of the continental margin of eastern Canada determined from subsidence curves; Earth and Planetary Science Letters, v. 51, p. 343-361.

Schlee, J. and Pratt, R.M.
1970: Atlantic continental shelf and slope of the United States – gravels of the northeastern part; United States Geological Survey, Professional Paper 529-H.

Sleep, N.H.
1971: Thermal effects of the formation of Atlantic continental margins by continental breakup; Geophysical Journal of the Royal Astronomical Society, v. 24, p. 325-350.

Srivastava, S.P.
1978: Evolution of the Labrador Sea and its bearing on the early evolution of the North Atlantic; Geophysical Journal of the Royal Astronomical Society, v. 52, p. 313-357.

Srivastava, S.P., Falconer, R.K.H., and MacLean, B.
1981: Labrador Sea, Davis Strait, Baffin Bay: Geology and Geophysics – A review; in Geology of the North Atlantic Borderlands, ed., J. Wm. Kerr and A.J. Fergusson, Canadian Society of Petroleum Geologists, Memoir 7, p. 333-398.

Srivastava, S.P., MacLean, B., MacNab, R.F., and Jackson, H.R.
Davis Strait: Structure and evolution as obtained from a systematic geophysical survey; in Arctic Geology and Geophysics, ed., A.F. Embry and H.R. Balkwill, Canadian Society of Petroleum Geologists, Memoir 8. (in press)

Strong, D.F. and Harris, A.H.
1974: The petrology of Mesozoic alkaline intrusives of Central Newfoundland; Canadian Journal of Earth Sciences, v. 11, p. 1208-1219.

Umpleby, D.C.
1979: Geology of the Labrador Shelf; Geological Survey of Canada, Paper 79-13, 39 p.

van Bemmelen, R.A.
1949: Geology of Indonesia; 1A General Geology; The Hague Government Printing Office, 732 p.

Vogt, P.R. and Avery, O.E.
1974: Detailed magnetic surveys in the northeast Atlantic and Labrador Sea; Journal of Geophysical Research, v. 79, p. 363-389.

Wallace, F.K.
1973: Geology of the Davis Strait bathymetric sill and associated sediments, offshore Baffin Island, Canada; in Canada: Arctic Geology, ed., J.D. Aitken and D.J. Glass, Geological Association of Canada and Canadian Society of Petroleum Geologists, p. 81-98.

Watkins, N.D. and Self, R.
1972: An examination of the ELTANIN dredged rocks from high latitudes of the South Pacific Ocean; in Antarctic Research Series, v. 19, American Geophysical Union, Washington, D.C., p. 61-70.

Watt, W.S.
1966: Chemical analyses from the Gardar Ingenous Province, South Greenland; Geological Survey of Greenland, Report 6, 92 p.

1969: The coast parallel dike swarm of southeast Greenland in relation to the opening of the Labrador Sea; Canadian Journal of Earth Science, v. 6, p. 1320-1321.

3. GEOLOGY OF STAR LAKE (WEST HALF), SOUTHWEST NEWFOUNDLAND

Project 770026

G.R. Dunning[1], P.J. Carter[2], and M.A. Best[3]
Precambrian Geology Division

Dunning, G.R., Carter, P.J., and Best M.A., Geology of Star Lake (west half), southwest Newfoundland; in Current Research, Part B, Geological Survey of Canada, Paper 82-1B, p. 21-26, 1982.

Abstract

Rocks of the Star Lake area are mainly mid-Paleozoic intrusions with numerous ophiolitic bodies of variable size in the south. Ophiolitic fragments range in composition from harzburgite to gabbro cut by diabase dykes. The largest fragment is fault bounded; the others are intruded and engulfed by tonalite to diorite that may represent partial melts of oceanic crust at an arc-continent collision zone. The tonalite has a strong northeast-trending foliation as do island arc tuffs of Llanvirnian to Llandeilian age preserved in the southeast corner of the area.

Various granites of post-Ordovician age intrude the tonalite, ophiolitic fragments and each other. The largest of these is a subvolcanic alaskitic granite of the Topsails batholith. Rhyolite dykes cut the granite and rhyolite flows are preserved locally.

Diabase dyke intrusion was the last magmatic event in the area.

Introduction

In July and August, 1981, Star Lake (west half; NTS 12A/11 west) was mapped to fill in the gap between Puddle Pond, Rainy Lake, Star Lake (east half) and Victoria Lake map areas (NTS 12A/5, 12A/14, 12A/11 east and 12A/6 respectively), and to further delineate the Annieopsquotch ophiolite belt.

A foliated tonalite to diorite terrane is of major regional importance; it intrudes and engulfs fragments of ophiolitic affinity and is cut by granites of the Topsails batholith.

Previous Work

The Star Lake area (NTS 12A/11) was mapped as part of Red Indian Lake map area (west half) by Riley (1957). Star Lake (east half) was mapped at 1:50 000 scale by Kean (1978), whose map can be broken down into four main subdivisions:

1. volcanics and related intrusions and sediments of the Middle Ordovician Victoria Lake Group in the southern part of the area;
2. granitoid intrusions mostly of unknown ages, including part of the Topsails batholith in the northwest;
3. gabbro, diorite and diabase of presumed Devonian age in the northwest;
4. Carboniferous subhorizontal clastic sediments north of Red Indian Lake.

In 1980, examination of much of the outcrop area of gabbro, diorite and diabase in Star Lake (east half) revealed that it consists of fragments of ophiolite directly comparable to the Annieopsquotch complex to the southwest (Dunning, 1981). It is therefore presumably of lower Ordovician age as is the dated Annieopsquotch complex (T.E. Krogh, personal communication, 1981).

Access

Star Lake (west half) was mapped from flycamps supported by helicopter or floatplane. Lloyds River valley was not mapped in detail as the road which provides access to that area was washed out for much of the summer. Some additional lithologic units may be present in the river valley, by analogy with Star Lake (east half; Kean, 1978).

Physiography

The area can be divided into 3 physiographic regions. The northern region is underlain by part of the Topsails batholith and is composed of barren rock ridges and extensive deposits of boulders and gravel. The majority of the area is part of the Long Range plateau and is chiefly underlain by strongly foliated plutonic rocks which impart a northeast-trending pattern of ridges and valleys; bogs and glacial gravel deposits are extensive. The corner of the area southeast of Lloyds River is part of the Annieopsquotch Mountains and is uplifted along the Lloyds River fault to form 200 metre high northwest-facing cliffs.

Individual map units have distinctive physiographic expressions. Apart from those mentioned above, there is a granite northeast of Lake of the Hills which forms a large flat-topped hill. Syenite forms one hill immediately east of the lake. Hills of resistant ophiolitic gabbro occur east of the fault at Otter Brook, east of Lloyds River fault and northeast of Star Lake just outside the map area.

General Geology

The map area (Fig. 3.1) lies within the Dunnage Zone (Williams, 1979) which represents vestiges of the Iapetus ocean and island arc sequences. The oldest rocks are ultramafic to mafic in composition and occur through the southern part of the area. Harzburgite, clinopyroxenite and gabbro occur as small pods within foliated plutonic rocks and also form large hills and ridges. The suite is interpreted to be ophiolitic by comparison with lithologies of the Bay of Islands and Annieopsquotch complexes (Malpas, 1976; Dunning and Herd, 1980).

Intermediate tuffs of the Ordovician Victoria Lake Group outcrop in the southeast corner of the map area. A much larger area of similar rocks that occurs in the adjacent Victoria Lake map sheet structurally overlies the Annieopsquotch complex (Dunning, 1981).

A foliated tonalitic to dioritic intrusive complex intrudes and engulfs ophiolitic fragments and extends through the central part of the map area. This complex is combined with the mafic-ultramafic suite as a single unit in some areas and separated from it in other areas on the regional map (Riley, 1957).

[1] Department of Geology, Memorial University of Newfoundland, St. John's, Newfoundland, A1B 3X5
[2] Department of Geological Sciences, Queens University, Kingston, Ontario, K7L 3N6
[3] Department of Geology, University of Ottawa, Ottawa, Ontario, K1N 6N5

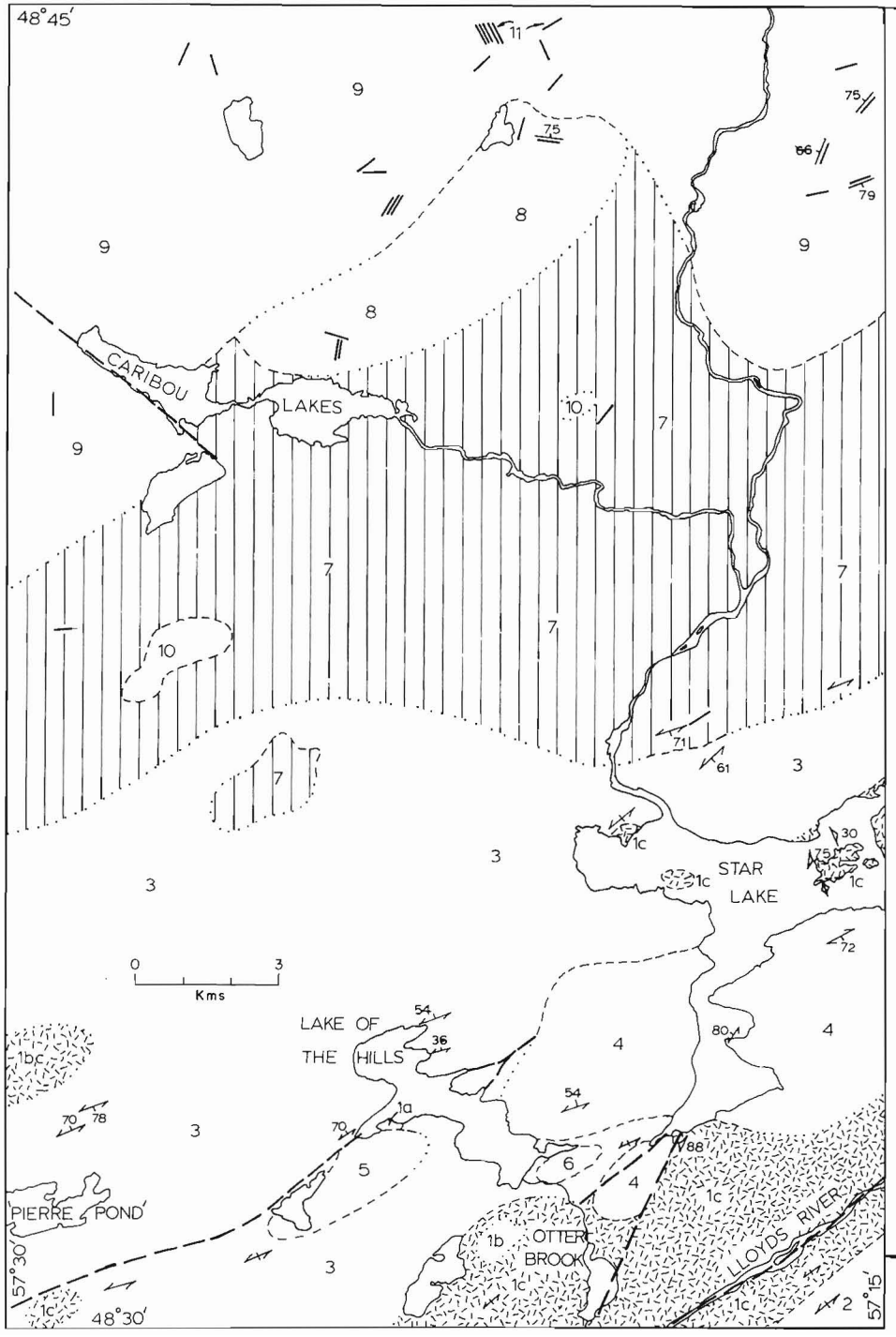

LEGEND

SILURIAN OR YOUNGER

11 Diabase dykes, plagioclase and olivine porphyritic

SILURIAN TO DEVONIAN?

10 Rhyolite flows, orange to red, quartz and feldspar porphyritic, comagmatic with unit 9?

9 Alaskitic granite, brick red, biotite and amphibole bearing, contains miarolitic cavities, coarse grained, massive

8 Monzonite, grey, biotite and hornblende bearing, medium grained, massive

7 Granite, biotite and hornblende bearing, very coarse grained

6 Syenite, red, hornblende bearing, massive

ORDOVICIAN OR YOUNGER

5 Granite, muscovite and locally biotite bearing, rare garnets, buff colour, massive

4 Granite, pink, buff or white, biotite and hornblende bearing, weakly foliated

ORDOVICIAN

3 Tonalite to diorite, biotite and hornblende bearing, strongly foliated, includes small mafic to ultramafic fragments

2 Victoria Lake group, intermediate tuffs

1 Ophiolitic fragments: 1a harzburgite, 1b clinopyroxenite, 1c gabbro, layered and massive, includes trondhjemite pods and diabase dykes of ophiolitic affinity (dashed symbol)

Geological contact approximate, assumed

Fault

70 Strike and dip of dyke

70 Foliation, inclined, vertical, dip unknown

30 Igneous layering, strike and dip

Figure 3.1. *Preliminary geological map of Star Lake, west half, Newfoundland (NTS 12A/11 west).*

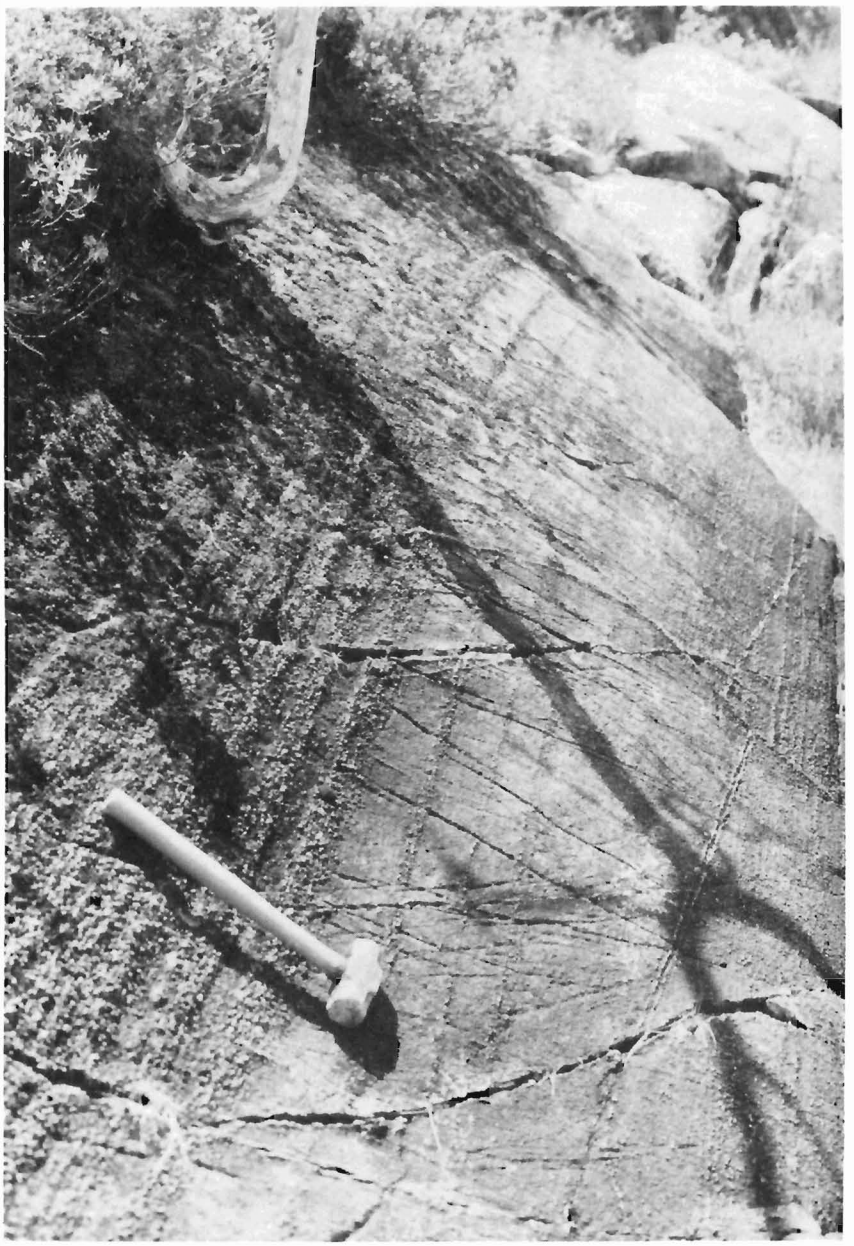

Figure 3.2. *Layered gabbro of Star Lake ophiolitic fragment exposed on easternmost island in lake. Layering due to changes in clinopyroxene: plagioclase ratio. Hammer is 40 cm long. GSC 203546-H*

Granitoid rocks ranging from hornblende granodiorite to alaskitic granite and syenite, all undated, cut the foliated tonalite complex and each other. Alaskitic granite of Topsails batholith underlies much of the northern high barren area and apparently feeds volcanics which occur as erosional remnants at two localities.

Diabase dykes represent the last magmatic activity in the area.

Ophiolite Fragments

The largest of the four areas of ophiolitic rock delineated occurs south of Star Lake. The number of discrete fragments in the Star Lake area is unclear; most of the northern part of the lake may be underlain by mafic rock. Many other coarse grained gabbro and amphibolite pods occur in the foliated tonalite terrane. Too small to show on the map, they form dark green to black patches in the lighter coloured tonalite.

A U-Pb age (zircon) of 483 ± 3 Ma has been determined for trondhjemite of the Annieopsquotch complex (T.E. Krogh, personal communication, 1981), the largest and most complete ophiolite in the Annieopsquotch ophiolite belt (Dunning, 1981). It is thought that the ophiolitic fragments in the Star Lake map area are the same age.

Harzburgite forms one small body exposed on the southwest shore of Lake of the Hills. It is grey green on the weathered surface, dark green on the fresh surface, and distinctive in having very coarse grained poikilitic pyroxenes which weather in relief. It is texturally similar to harzburgite, which is also interpreted to be an ophiolitic fragment, west of Silver Pond (Dunning and Herd, 1980).

Clinopyroxenite, coarse grained and green weathering, occurs interlayered (?) with gabbro in a 1 x 2 km body north of 'Pierre Pond'. Clinopyroxene grains 2 - 5 mm long make up more than 90 per cent of the rock. Associated gabbro contains about 50 per cent pyroxene and is coarser grained. Most gabbro is coarse grained with a subophitic texture composed of near equal amounts of strongly saussuritized plagioclase and clinopyroxene replaced by actinolite and chlorite, with minor amounts of Fe-Ti oxides. It is typical of the 'high-level' gabbro of ophiolite complexes. Trondhjemite pods occur in gabbro in the southwest corner of the area and well layered gabbro is present on the islands in the east arm of Star Lake (Fig. 3.2). Some of the layered gabbro has mineral grading and alignment and cumulate textures, and is fresher and finer grained than the 'high-level' variety.

The Lloyds River gabbro, southeast of the Lloyds River fault (Dunning, 1981), is strongly sheared and bleached along the fault zone. Blocks that have escaped these affects are medium- to coarse-grained, equigranular and cut by diabase dykes. No chemical analyses are available, but this body is interpreted to be ophiolitic as it occurs with other obvious ophiolitic fragments west of the fault and is along strike from the Annieopsquotch complex.

Victoria Lake Group

Tuffs of the Victoria Lake Group occur in the southeast corner of the area. They are andesitic to dacitic in composition, strongly sheared and are composed predominantly of chlorite, epidote, sericite and carbonate. A late Llanvirnian to early Llandeilian age has been determined for Victoria Lake Group tuffs by conodonts in interbeds of limestone along strike near the mouth of the Victoria River at Red Indian Lake (Kean and Jayasinghe, 1980).

Foliated Tonalite Complex

A strongly foliated tonalite to diorite intrusive complex underlies much of the central part of the area. It intrudes and is host to small fragments of ophiolitic harzburgite,

clinopyroxenite, gabbro and amphibolite of probable ophiolitic derivation (Fig. 3.3). Only the largest fragments are distinguished as units on the map.

The diorite contains 10 to 30 per cent hornblende and biotite, 5 to 30 per cent quartz (in most places blue), minor epidote and sulfide, with plagioclase making up the remainder of the rock. The foliation is defined by elongate quartz grains and aligned hornblende and feldspar. A complete range in composition exists from hornblende-rich diorite to tonalite composed almost entirely of quartz and plagioclase, plus secondary albite and epidote.

Medium grained biotite-rich lenses in the diorite are interpreted to be metasedimentary inclusions; most inclusions are mafic, however, and many have a core of coarse grained gabbro rimmed by amphibolite.

It is thought that the complex was originally composed of discrete intrusions varying in composition from hornblende diorite to tonalite and even granodiorite. However, because of the limited outcrop and strong deformation a subdivision of the complex was not attempted. The age of the tonalite complex and its foliation are unknown. They are both thought to be mid-Ordovician based on relationships in the Puddle Pond area (Herd and Dunning, 1979) and because granite of Topsails batholith, of Silurian age, is undeformed.

Granitoid Rocks

Six units of coarse grained granitoid rock are present in the area. No dates are available for these bodies so their relative ages are uncertain. In addition, it is possible that a study of whole-rock chemistry for these bodies would show that some are mineralogically different parts of a single pluton. It is suspected that units 4 and 5 (Fig. 3.1) are related and that the syenite (unit 6) may be related to the Topsails batholith.

Hornblende and biotite-bearing granite (unit 4), that occurs on the south side of Star Lake, is coarse grained, white to pink on fresh surfaces and contains pegmatitic quartz and potassium feldspar pods. It is massive to weakly foliated at the margins and is far less deformed than the adjacent tonalite- diorite terrane. For this reason it is interpreted as younger than the tonalite. The body is bounded by the shores of Star Lake and Lake of the Hills and by bogs. It does intrude ophiolite gabbro on the islands in the east arm of Star Lake where a medium grained marginal phase of the granite is well exposed. An aplite intrudes the foliated diorite on the northeast shore of the Lake of the Hills. The aplite may be related to this hornblende-biotite granite or to the muscovite granite (unit 5) to the southwest.

Coarse grained muscovite granite (unit 5) outcrops southwest of Lake of the Hills. It is buff, massive and locally contains biotite or fine grained garnet. It characteristically contains 1 to 2 cm rusty weathering patches cored by pyrite; some of these appear to be miarolitic cavities with euhedral cubes projecting into the centre of the cavity. Associated with these are zones where the potassium feldspar is bleached white. Contact relationships are obscure but, as with unit 4, unit 5 is interpreted to cut the foliated tonalite complex. This granite is bounded to the southeast by an extensive bog.

A red syenite (unit 6) that appears to occupy a single hill occurs immediately east of Lake of the Hills. It is coarse grained, fresh and undeformed and contains 90 per cent potassium feldspar, 5 to 10 per cent hornblende and about

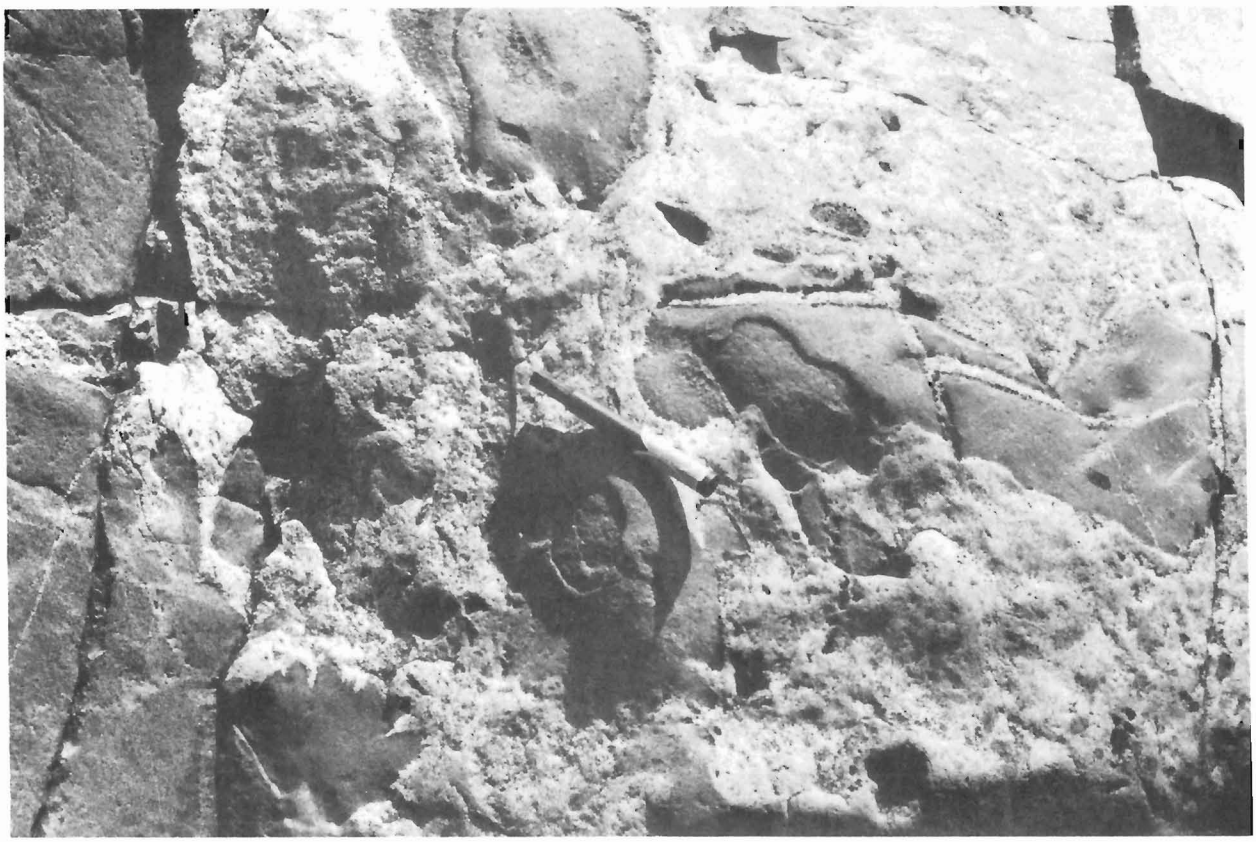

Figure 3.3. *Fragments of gabbro and amphibolite in tonalite, on shore of Star Lake. Marker for scale. GSC 203546-J*

1 per cent quartz. Its contacts were not observed. Another syenite body approximately 1.5 km in diameter cuts the Topsails alaskitic granite just to the east of the map area. It is coarse grained, red on fresh surfaces and forms several steep rounded outcrops in the smoother granite terrane. Possibly these two syenite bodies are related.

The remaining granitoid rocks occur in the north half of the map area and are massive. Several bodies may be essentially the same age. Geochemical and geochronological studies are required to properly subdivide them.

Hornblende and biotite bearing granite to granodiorite (unit 7) underlies the area north of the foliated tonalite complex and one small body of the granite appears to intrude the tonalite. However, there is minimal outcrop in this area so the extent and number of discrete granite bodies is not clear. The body is coarse grained and locally contains quite spectacular well zoned idiomorphic plagioclase. Both the monzonite (unit 8), north of Caribou Lakes, and this granite are cut by granite, rhyolite and diabase dykes (units 9 to 11) but neither was seen to cut the other.

Medium grained biotite and hornblende bearing monzonite (unit 8) that occurs northeast of Caribou Lakes is locally foliated on its northwest side, possibly along a fault. Its boundaries to the southeast are hidden beneath bog and gravel. The monzonite is intruded by granite, rhyolite and diabase dykes (units 9 to 11).

Alaskitic granite (unit 9) is the predominant plutonic rock in the Topsails batholith which underlies the northern part of the area. It is red brown, biotite and amphibole bearing and commonly contains miarolitic cavities with subhedral quartz crystals. This granite, cut by some rhyolite dykes, is believed to be the source of the granite and rhyolite dykes which intrude units 7 and 8, and to be the source of the rhyolite flows that occur in two isolated hills south of the batholith. The granite is also cut by diabase dykes of unit 11.

Rhyolite

Two isolated hills in the north of the area are underlain by rhyolite flows (unit 10). They are orange, red or green, contain quartz or potassium feldspar phenocrysts, typically 2 mm long, and locally show spectacular spherulitic structures up to 1 cm or greater in diameter. Rhyolite breccia contains angular fragments of rhyolite in a fine grained matrix that is locally fluorite bearing. These flows and breccia are believed to be comagmatic with the Topsails batholith and rhyolite dykes which cut it. Some of the dykes show prominent flow banding with alternating dark and light bands. The hills of rhyolite appear to preserve a higher stratigraphical level than the Topsails batholith.

Diabase Dykes

Diabase dykes cut several of the earlier granitic rocks and seem most abundant in the alaskitic granite. They strike predominantly northwest or northeast following joints in the granite. The dykes are 0.3 to 8 m wide, fine grained with chilled margins, very fresh and contain plagioclase or olivine phenocrysts. They are of unknown age; because they cut the youngest granite, they are interpreted to represent the last magmatic event in the map area.

Structure

The map area can be divided into southern deformed and northern undeformed sections. The southern part is underlain by Lower to mid-Ordovician rocks which are affected by a generally northeast-trending foliation and faults. The northern part is undeformed except for local shearing along late faults. Granites in the north are massive and well jointed.

Faults

The largest ophiolitic fragment, south of Star Lake, occurs in part as a block bounded by the Lloyds River and Otter Brook faults. The Lloyds River fault is the most important in the area. Although poorly exposed and of unknown width, it extends southwest past the Annieopsquotch complex to King George IV Lake. Its history is unknown although its most recent movement is certainly post redbed deposition (Devonian?) in the Puddle Pond area. It likely has later movement as poorly exposed conglomerate of possible Carboniferous age is tilted in the Lloyds River valley in the Puddle Pond area.

The fault in Otter Brook is interpreted as a splay off of the Lloyds River fault. The block of ophiolitic gabbro, cut by diabase dykes, which occurs between these two faults, is strongly foliated and feldspars are strongly bleached along subsidiary shear zones within the block.

The fault within the tonalite complex is interpreted southwest of Lake of the Hills, based on a topographic lineament, and northeast of the lake is based on outcrops of sheared tonalite in the bays.

A probable fault, trending northwest from Caribou Lakes, separates a high plateau and valley underlain by the same (?) granite. The dotted geological contact trending southwest from Caribou Lakes may also be a fault (Fig. 3.1).

Foliation

Ophiolitic fragments engulfed in the foliated tonalite complex are weakly foliated parallel to the tonalite or are massive. Most fragments appear to have behaved as rigid blocks in the more strongly deformed tonalite. The actual shape of the large fragments is unknown; they are depicted as oval in Figure 3.1.

Foliation in the tonalite strikes east-northeast in the southwest part of the area to northeast in the central part. It is steep in the 'Pierre Pond' area and moderately northwest dipping in the nearby Lake of the Hills area. The shape of lakes in this area is strongly controlled by the structure in the tonalite.

The only structures noted in the granites underlying the north part of the area are joints, locally well developed, which provided a locus for the intrusion of rhyolite and diabase dykes, as noted above.

Discussion

Relationships in Star Lake (west half) provide an opportunity to decipher events in the Dunnage Zone, especially the destruction of the Iapetus 'ocean' and subsequent intrusion of granites.

The ophiolitic fragments are of unknown affinity and range from mantle to lower crust lithologies. The largest of these fragments is juxtaposed with intermediate tuffs of the Victoria Lake Group that are dated as late Llanvirnian to early Llandeilian in the upper part.

The mafic crust, of whatever affinity, was cut in the mid-Ordovician (?geochronometry in progress) by a suite of diorite to tonalite (and granodiorite?) intrusions. These range from strongly foliated to weakly foliated, in the Puddle Pond area.

The next event recorded is intrusion of weakly foliated to massive biotite and hornblende granite and muscovite granite of unknown ages.

In the north part of the area granites are undeformed and form part of the Topsails batholith. No dates are available and field relationships are, in part, equivocal.

Published Rb-Sr ages of 421 ± 7 Ma for peralkaline granite and 387 ± 16 Ma for alkali feldspar granite from the eastern lobe of the batholith (Bell and Blenkinsop, 1981) may bracket the ages of granites in the batholith in Star Lake area. A new zircon age of 419 to 443 Ma ($^{207}Pb/^{206}Pb$) from an alkali syenite intrusion of the eastern Topsails batholith (R.P. Taylor, personal communication, 1981) tends to confirm a Silurian age for many plutons of the batholith.

Interpretation

The ophiolitic fragments are thought to represent disrupted lower Ordovician oceanic crust. Whether this was a large Iapetus 'ocean' (Williams, 1980) or a marginal or back-arc basin is unknown. Geochemical analysis is underway to try to place some constraints on interpretations of these fragments.

The Victoria Lake Group volcanics are interpreted to be an island arc sequence (Kean et al., 1981) and, in the Victoria Lake map area, are interpreted to structurally overlie the Annieopsquotch complex (Dunning, 1981). One ophiolitic fragment in the Star Lake area is in fault contact with the arc sequence. The ophiolitic fragments may have been basement to the island arc or may represent adjacent marginal basin crust.

Evidence from the tonalite terrane indicates that deformation accompanied intrusion and breakup of the ocean crust as much of the tonalite is strongly foliated. However, intrusion outlasted deformation as some tonalite in the Puddle Pond area is only weakly foliated to massive and well jointed. This tonalite suite may result from partial melting of oceanic crust, disrupted and imbricated on thrusts during subduction. This may be coincident with the approach of an island arc to a continental margin during the mid-Ordovician Taconic Orogeny. Petrological, geochemical and geochronological studies are underway to test and place some constraints on this model.

It is suggested that metasedimentary inclusions in the foliated tonalite terrane may indicate that sedimentary material was involved in the partial melting. These sediments may be Fleur de Lys Supergroup equivalents (cf. Herd, 1978).

Foliated biotite and muscovite granites which cut tonalite terrane presumably were derived from continental or composite crust.

The Topsails granites intrude posttectonically and are presumably derived from continental crust. The diabase dykes, which reflect a local tensional environment, are probably genetically related to the Topsails batholith (Whalen and Currie, 1982).

Acknowledgments

We thank Janet MacManus of the GSC for capable field assistance and Richard Herd for logistical support, advice and encouragement. Helpful discussions with Lesley Chorlton are gratefully acknowledged.

Viking Helicopters Newfoundland Ltd., Newfoundland Air Transport and Fredericton Helicopters provided efficient support in the field.

We thank P. Lassila of Hudsons Bay Oil and Gas Co. for his hospitality, and Environment Canada for the use, once again, of facilities at their Forest Research Centre in Pasadena. H. Williams, and R.K. Herd read the manuscript and suggested improvements.

References

Bell, K. and Blenkinsop, J.
1981: A geochronologic study of the Buchans area, Newfoundland; in The Buchans Orebodies: Fifty Years of Geology and Mining, ed. E.A. Swanson, D.F. Strong and J.G. Thurlow, Geological Association of Canada, Special Paper 22, p. 91-111.

Dunning, G.R.
1981: The Annieopsquotch ophiolite belt, southwest Newfoundland; in Current Research, Part B, Geological Survey of Canada, Paper 81-1B, p. 11-15.

Dunning, G.R. and Herd, R.K.
1980: The Annieopsquotch ophiolite complex, southwest Newfoundland, and its regional relationships; in Current Research, Part A, Geological Survey of Canada, Paper 80-1A, p. 227-234

Herd, R.K.
1978: Geology of Puddle Pond area, Red Indian Lake map sheet, Newfoundland; in Current Research, Part A, Geological Survey of Canada, Paper 78-1A, p. 195-197.

Herd, R.K. and Dunning, G.R.
1979: Geology of Puddle Pond map area southwestern Newfoundland; in Current Research, Part A, Geological Survey of Canada, Paper 79-1A, p. 305-310.

Kean, B.F.
1978: Geology of the Star Lake east half sheet (12A/11E), Newfoundland; in Report of Activities for 1977, Mineral Development Division, Newfoundland Department of Mines and Energy, Report 78-1, p. 129-134.

Kean, B.F. and Jayasinghe, N.R.
1980: Badger map area (12A/16), Newfoundland; in Current Research, Mineral Development Division, Newfoundland Department of Mines and Energy, Report 80-1, p. 37-43.

Kean, B.F., Dean, P.L., and Strong, D.F.
1981: Regional geology of the central volcanic belt of Newfoundland; in The Buchans Orebodies: Fifty Years of Geology and Mining, ed. E.A. Swanson, D.F. Strong and J.G. Thurlow, Geological Association of Canada, Special Paper 22, p. 65-78.

Malpas, J.
1976: The petrology and petrogenesis of the Bay of Islands ophiolite suite, western Newfoundland. Unpublished Ph.D. thesis, Memorial University of Newfoundland, 435 pp.

Riley, G.C.
1957: Red Indian Lake (west half), Newfoundland; Geological Survey of Canada, Map 8-1957.

Whalen, J.B. and Currie, K.L.
1982: Volcanic and plutonic rocks in the Rainy Lake Area (12A/14), Newfoundland; in Current Research, Part A, Geological Survey of Canada, Paper 82-1A, p. 17-22.

Williams, H.
1979: Appalachian orogen in Canada; Canadian Journal of Earth Sciences, v. 16, p. 792-807.

1980: Structural telescoping across the Appalachian orogen and the minimum width of the Iapetus ocean; in The Continental Crust and its Mineral Deposits: A Volume in Honour of J. Tuzo Wilson, Geological Association of Canada, Special Paper 20, p. 421-439.

4.

THE EAST KEMPTVILLE TIN DEPOSIT, NOVA SCOTIA: AN EXAMPLE OF A LARGE TONNAGE, LOW GRADE, GREISEN-HOSTED DEPOSIT IN THE ENDOCONTACT ZONE OF A GRANITE BATHOLITH

E.M.R. Research Agreements 151-4-80 and 87-4-81

J.M.G. Richardson[1], E.T.C. Spooner[1], and D.A. McAuslan[2]
Economic Geology Division

Richardson, J.M.G., Spooner, E.T.C., and McAuslan, D.A., The East Kemptville tin deposit, Nova Scotia: an example of a large tonnage, low grade, greisen-hosted deposit in the endocontact zone of a granite batholith; in Current Research, Part B, Geological Survey of Canada, Paper 82-1B, p. 27-32, 1982.

Abstract

The East Kemptville tin deposit, southwestern Nova Scotia (Yarmouth County) is an example of a large tonnage (38 million tonnes), low grade (0.2% Sn) greisen-hosted deposit. The tin (-tungsten-sulphide) mineralized zone is beneath an irregular inflection in the northwest contact of the southwestern extremity of the South Mountain Batholith (the 'Davis Lake pluton'). The tin mineralization occurs in pods of massive greisen and zoned greisen selvedges flanking thin (0.5-2.5 cm) hydrothermal veins. Tin occurs predominantly as cassiterite and is associated with secondary quartz, muscovite, topaz, pyrite, pyrrhotite, sphalerite, chalcopyrite, arsenopyrite, other sulphides and minor wolframite. Although the style of mineralization is similar to greisen-hosted deposits associated with Hercynian granites in the Krušné hory-Erzgebirge region of Czechoslovakia and East Germany, the batholithic endocontact setting differs, since the latter are related to small (1-3 km) lithium mica-albite cupolas. The complete paragenetic sequence is complex and includes unusual phosphate minerals such as triplite [(Mn, Fe, Mg, Ca)$_2$(PO$_4$) F] and childrenite-eosphorite [(Fe, Mn) Al (PO$_4$) (OH)$_2$ • H$_2$O].

Introduction

The East Kemptville tin deposit is in granitic rocks of the 'Davis Lake pluton' (South Mountain Batholith) immediately below the contact with metasedimentary rocks of the Meguma group, near East Kemptville, Yarmouth County, Nova Scotia (44°16'N, 65°41'W). In 1978, Shell Canada Resources Limited began a geochemical tin exploration program extending throughout southwestern Nova Scotia which led to the discovery of mineralized boulders in the glacial till near East Kemptville. The deposit was evaluated between 1979 and 1982. To date, reserves of 38 million tonnes grading 0.2% Sn at a 0.1% Sn cutoff grade have been defined (Shell Canada Resources Limited, 1980 Annual Report). At present, no other metals are considered economically recoverable. Since the deposit is covered by 3-5 m of glacial overburden, the available information has been obtained from 14 600 m of diamond drill core, two trenches totalling 225 m in length and approximately 1.2 km of underground development.

The purpose of the study overall is to provide a complete geological, petrological, mineralogical and geochemical description of the host rocks, tin mineralization, hydrothermal alteration and later veins. Integration of this information will produce a paragenetic sequence and an understanding of the important factors which controlled tin mineralization. Since the research is still in progress, the material presented here is preliminary.

General Geology

The tin mineralization is in an extension of the extreme southwestern end of the South Mountain Batholith that has been referred to by Shell Canada Resources Limited as the Davis Lake pluton (Fig. 4.1). The South Mountain Batholith is a composite, peraluminous intrusion that is 300 by 60 km. It consists generally of biotite granodiorite into which have been intruded smaller, discrete bodies of two-mica adamellite, porphyritic adamellite, leucoadamellite, aplite and pegmatite (MacKenzie and Clarke, 1975; Charest, 1976; Clarke and Muecke, 1980; Clarke and Halliday, 1980). Five such bodies have been defined and are located near West Dalhousie, Springfield, Lake George, New Ross, and Halifax. Due to poor accessibility and extremely limited exposure, the southwestern extremity of the South Mountain Batholith had not been comprehensively mapped. Detailed boulder mapping by Shell Canada Resources Limited in northern Yarmouth County defined areas of two-mica granite and greisenized granite. Intrusive contacts were observed in large angular boulders west of Second Bear Lake. Based on this evidence, and in keeping with the terminology of Clarke and his co-workers, the name Davis Lake pluton was given to the granitoid rocks near Davis Lake. The location of the northeastern contact of this pluton with the main body of the South Mountain Batholith is uncertain.

In southwestern Nova Scotia, the South Mountain Batholith (Davis Lake pluton) intrudes turbiditic greywacke, quartzite, and argillite of the Cambro-Ordovician Meguma Group (Fig. 4.1) (Taylor, 1967). Whole-rock Rb-Sr isochron ages for the batholith by Clarke and Halliday (1980) are 374 ± 11 Ma (granodiorite) to 361 ± 1.5 Ma (adamellite) (Late Devonian to Early Carboniferous) with moderately high initial $^{87}Sr/^{86}Sr$ ratios of 0.70794 (granodiorite) to 0.71021 (adamellite). Whole rock $\delta^{18}O$ values for the South Mountain Batholith range from +10.1 to +12.0‰ which suggests that it formed by anatexis of ^{18}O-rich clastic metasedimentary rocks (Longstaffe et al., 1980).

Geology of the East Kemptville Tin Deposit

Geological Relationships

The zone of potentially economic tin mineralization shown in Figure 4.1 lies within an irregular protrusion of the Davis Lake pluton into quartzite of the Goldenville Formation (Meguma Group). Figure 4.2 is a more detailed map of the deposit which shows the extent of the mineralized zone, the northeast-trending contact, and the location of two metasedimentary roof pendants within the granitic rocks. The 1500 by 500 m zone of sericitized and greisenized rocks shown here is referred to as the Main Zone. The spatial geological relationships are shown in Figure 4.3, a

[1] Department of Geology, University of Toronto, Toronto, Ontario, M5S 1A1
[2] Shell Canada Resources Limited, Box 400, Terminal A, Toronto, Ontario, M5W 1E1

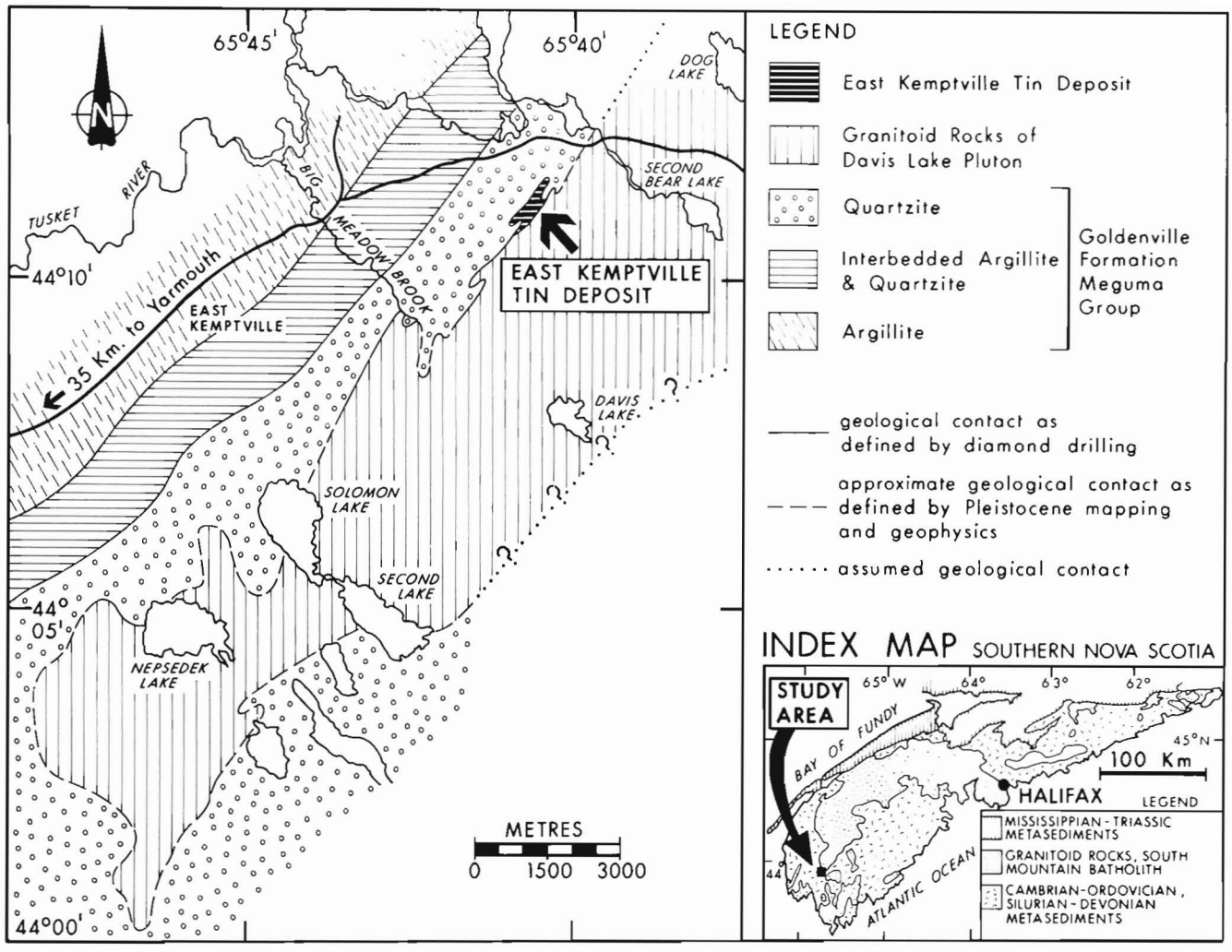

Figure 4.1. *Location and geological setting of the East Kemptville tin deposit, Yarmouth County, Nova Scotia. (Map courtesy of Shell Canada Resources Limited).*

Table 4.1

Paragenetic sequence, East Kemptville tin deposit, Yarmouth County, Nova Scotia

MINERALS	MASSIVE GREISEN	GREISEN-BORDERED VEINS					WHITE QUARTZ ± SULPHIDE + PHOSPHATE			RIBBED VEINS	WHITE QUARTZ ± CARBONATES ± FLUORITE			BARREN QUARTZ	CLAY-FLUORITE	CRUSTS & CRYSTALS
		aspy-wf	cs-py	topaz sulphide	blue quartz	sph-py-cs	sulphide	sulphide + Phos	Phos		Carb	Carb + Fl	Fl			
CASSITERITE	**********	**********	**********	**********	**********	**********	******									
PYRITE	**********	**********	**********	**********	**********	**********	**********	**********				**********	******			**** ****
SPHALERITE	**********	**********		*********		**********	**********	**********								
PYRRHOTITE	**********	**********				**********	**********	*******								
MOLYBDENITE	********															
STANNITE	**********	**********		*********		**********										
ARSENOPYRITE	**********	**********		*********		*******										
WOLFRAMITE		******		*********												
TOPAZ	**********	**********	**********	**********	**********	**********										
GALENA							**********	**********								
BISMUTHINITE	**********	**********		*********		*******										
CHALCOPYRITE	**********	**********		**********	**********	**********	**********	**********								
QUARTZ	**********	**********	**********	**********	**********	**********	**********	**********	**********	**********	**********	**********	**********	*******		
SILVER MICA	**********	**********	**********	**********	**********	**********										
GREEN MICA	**********	**********	**********	**********	**********	**********										
SIDERITE											**********					****** **
DOLOMITE											**********					**
APATITE								**********	**********							
TRIPLITE								**********	**********							
FLUORITE	**********	**********	**********	**********	**********	**********						**********	**********		**********	
VIVIANITE																**
STILBITE																**
CHILDRENITE																**
MARCASITE																**
DICKITE															**********	

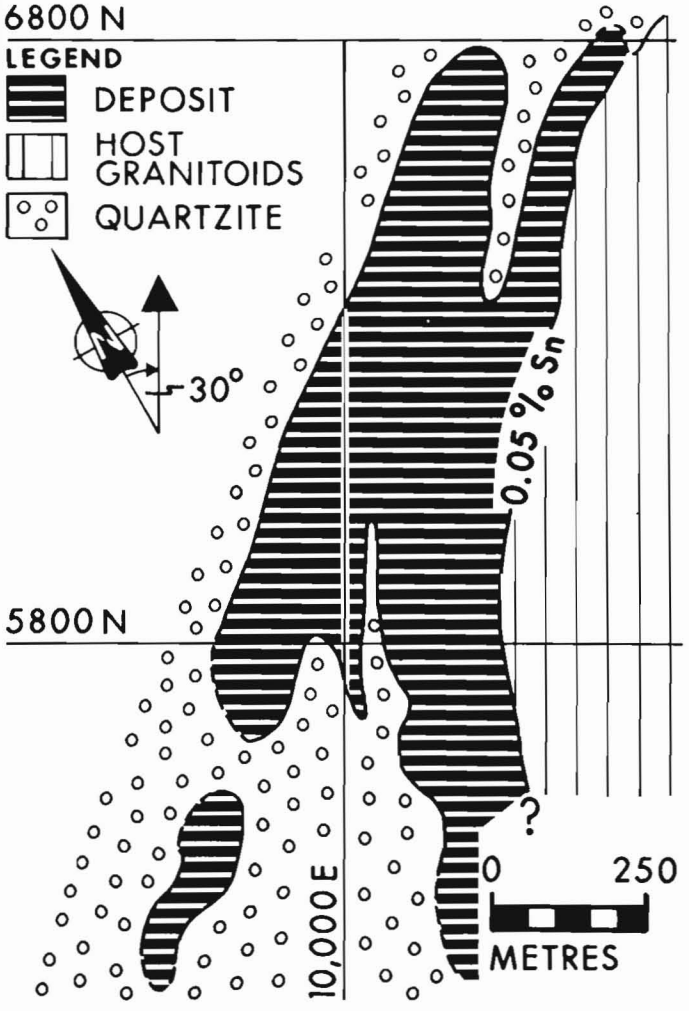

Figure 4.2. *Plan view of the geological relationships of the Main Zone, East Kemptville tin deposit. (Map courtesy of Shell Canada Resources Limited).*

cross-section along L5800N (Fig. 4.2). The zone of mineralized granitic material (>0.05% Sn) lies immediately below what has been interpreted as a slight flattening or corrugation of the normally steeply northwest-dipping contact. To the west, the mineralization does not extend into the metasedimentary rocks. Skarn is not found in the immediate vicinity of the Main Zone. The sericitized and greisenized granitic host rocks grade downward into much less altered and ungreisenized granitoid rock containing less than 500 ppm Sn, not as cassiterite. To the east, this boundary, as defined by a 0.05% Sn cutoff grade, rises gradually to the surface and marks the eastern limit of the deposit as shown in Figure 4.3. The northern and southern boundaries of the deposit, also defined by a 0.05% tin cutoff grade, occur where the broad shallow metasedimentary roof pendants coalesce with the main northwest-dipping contact.

It appears that the main control on the localization of the deposit was the geometry of the contact. The slight flattening and corrugation in the contact between the competent, chemically unreactive quartzite and the granitoid rocks restricted the area of hydrothermal alteration and potentially economic tin mineralization. Although some of this material has been removed by Pleistocene glaciation, a zone 100 m thick, 1500 m long, and 500 m wide still remains.

Paragenesis

The paragenetic sequence illustrated in Table 4.1 was established by trench mapping and verified by core logging and underground mapping. Each major stage was established on the basis of mineralogy, associated alteration, and crosscutting relationships. The characteristics of the major stages overlap slightly.

Greisen-bordered Veins and Massive Greisen Zones. Among the first workers to discuss the term "greisen" were Ferguson and Bateman (1912). They recognized greisen as an "alteration product of granitic rock consisting essentially of quartz and mica, with variable amounts of fluorine- and boron-bearing minerals" (p. 234). Such alteration can occur as envelopes locally bordering veins or microfractures. Alternatively, if the veins are extremely numerous, large masses of rock can be altered. Workers in recent years

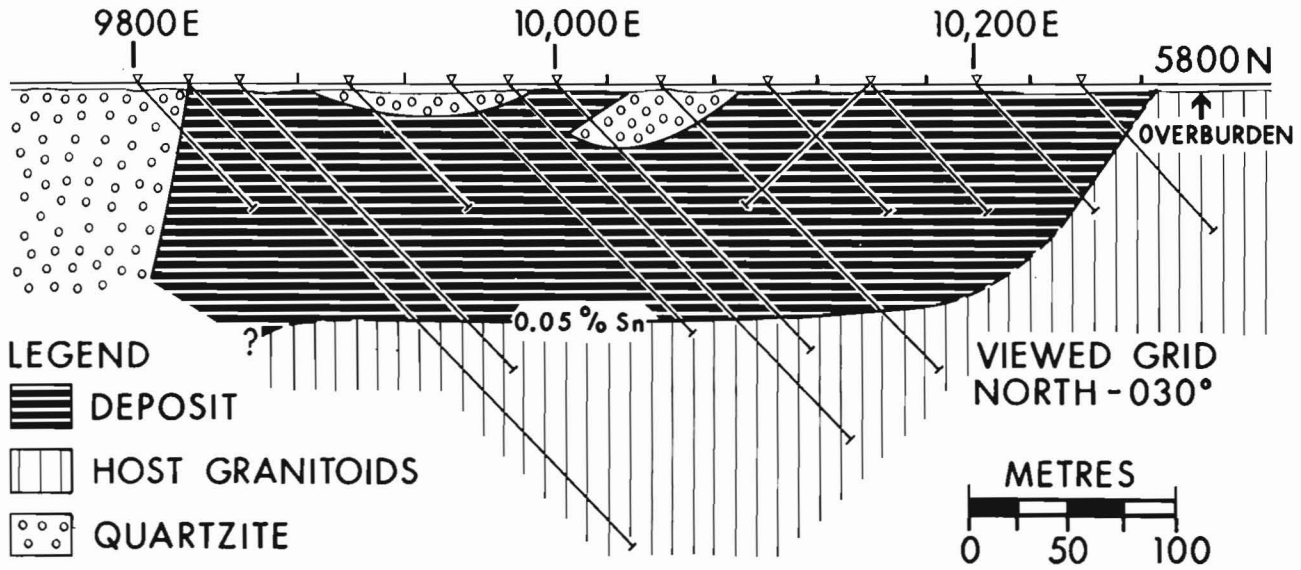

Figure 4.3. *Geologic cross-section of the East Kemptville tin deposit. The location of L5800N is shown in Figure 4.2. The information presented here is derived from drill core, surface mapping and underground development. (Map courtesy of Shell Canada Resources Limited).*

(e.g., Shcherba, 1970; Tischendorf et al., 1971; Groves and Taylor, 1973; Charest, 1976; Farley, 1978) have introduced some variability into the meaning of the term but all definitions are within the scope of Johannsen's (1932) description which listed the essential minerals as quartz and secondary mica and the typical accessory minerals as cassiterite, tourmaline, fluorite, topaz, arsenopyrite and pyrite.

In East Kemptville, the greisen zones consist of bluish grey quartz, topaz, and silver- and green-coloured muscovite with cassiterite, pyrite, sphalerite, chalcopyrite, pyrrhotite, minor wolframite and other sulphide minerals. Recoverable tin occurs exclusively as cassiterite and is restricted to greisen-bordered veins and massive greisen zones. Very minor amounts of stannite occur as exsolution products in sphalerite. The veins and greisen borders range in total width from 0.5-40 cm. They consist of a central vein of variable composition 0.2-2.5 cm wide, symmetrically flanked by a zoned alteration envelope of topaz, quartz and silver and green muscovite. The average width of the alteration envelope on one side of a vein is 4 cm (e.g., Figure 4.4). The central vein may be of blue quartz-cassiterite, fine grained sphalerite ± pyrite ± cassiterite, arsenopyrite-wolframite, topaz-sulphide, or blebs and crystals of cassiterite and pyrite along hairline fractures. Crosscutting relationships among these veins do not indicate a consistent relative chronology.

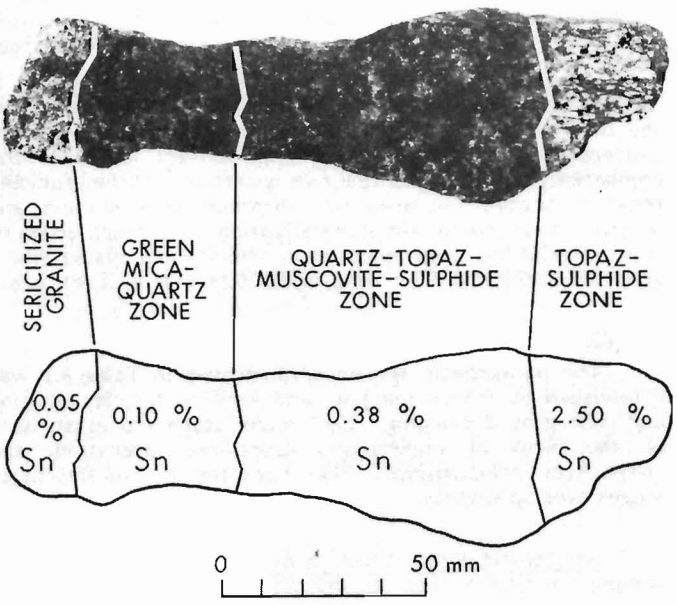

Figure 4.4. Polished slab on one-half of a zoned greisen-bordered vein showing the mineralogical zoning and tin analyses for each zone. (Tin analyses courtesy of Shell Canada Resources Limited).

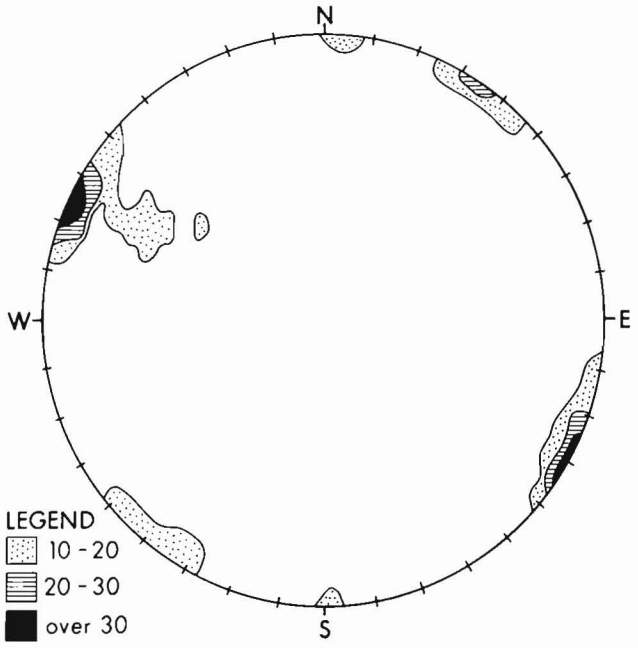

Figure 4.5. Contoured lower hemisphere projection of the poles to 178 greisen-bordered veins located in two surface trenches.

The intensity and extent of greisenization appear to be related to microfracturing and distance from the main sedimentary contact. Other less tangible factors, such as the length of time the fracture was open and the amount and composition of mineralizing fluids which passed through the fractures, were probably important but cannot be evaluated. The greisen alteration envelopes are thought to be the result of fluids passing through a single microfracture and permeating outward to form a well defined mineral zonation. The massive greisen pods are zones up to 20 m wide which show intense greisenization and associated mineralization – disseminated sulphides, topaz and cassiterite or veins of cassiterite, pyrite, topaz and arsenopyrite.

Mapping within the trenches indicates that the greisen-bordered veins are nearly vertical and oriented subparallel (030°) or approximately perpendicular (120°) to the main contact (045°/75°NW) (Fig. 4.5). Some well-defined greisen-bordered veins are more than 20 m in length. Those veins that have been seen to terminate do so gradually, with width and intensity of alteration diminishing. These features are illustrated in Figure 4.6. The orientation and extent of the massive greisen zones are as yet unknown due to the limited exposure.

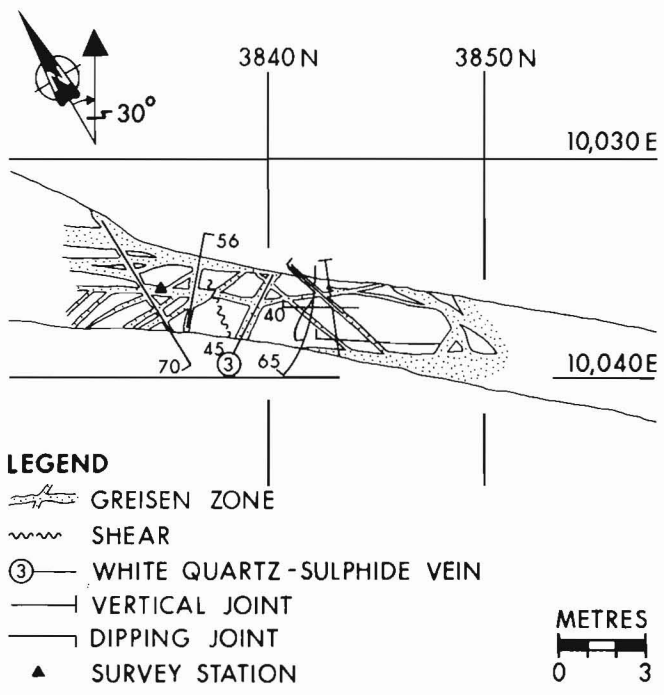

Figure 4.6. A map of a 20 m length of the decline (South Ramp) showing the extent and orientation of the greisen-bordered veins.

Glassy Quartz ± Sulphide ± Phosphate Veins. Veins of this group can be subdivided into three mineralogical subtypes with gradational characteristics. Common properties include the presence of clear glassy quartz and the lack of alteration selvedges. The oldest of the subtypes contains quartz and sulphides (sphalerite, pyrite, pyrrhotite, chalcopyrite and very minor galena). Pink fluorite occurs occasionally where these veins crosscut greisen zones. The second vein type, quartz + sulphide + phosphate, is characterized by the occurrence of coarse grained (0.3-1 cm), anhedral, cream-pink triplite, a rare fluo-phosphate. Subhedral apatite occasionally occurs as small (1-3 mm) green grains. Finally, the quartz-phosphate vein type is distinguished by a lack of sulphides, rare triplite grains (1-3 mm in size), and larger (5 mm) crystals of apatite.

All veins in this group are typically 0.5-1.5 cm in width. Quartz-sulphide and quartz-sulphide-phosphate veins are common throughout the deposit but the extent and orientation of these vein types has not been determined yet. The quartz-phosphate veins are rarer and no structural information is available.

Ribbed Veins. This vein group consists of short (1-50 cm) en-echelon glassy quartz veins that contain apatite and white dolomite. The clear, glassy quartz and dolomite occur in thin (2 mm), alternating bands giving the veins a 'ribbed' or ladder-like appearance. Apatite occurs as small 1-2 mm, subhedral green crystals. These veins are common throughout the deposit and strike perpendicular to the main metasedimentary contact.

Glassy Quartz ± Carbonate ± Fluorite Veins. These veins are characterized by coarse (2-3 cm), anhedral pink or white dolomite, buff siderite and/or blue fluorite. Their attitudes have not been determined due to poor exposure.

Barren Quartz Veins. This category includes several sets of veins that cannot be chronologically separated. Very thin (2 mm), glassy quartz veins are perpendicular (120°/90°) to the main granite-metasedimentary rock contact. Wider (4-5 cm), milky quartz veins with minor accessory muscovite are roughly parallel to this set (126°/68°S). Glassy quartz veins with similar orientations are approximately 1 cm wide, have central cavities and show crystal terminations. None of the minerals mentioned below as crusts or crystals have grown on these quartz crystals.

Clay-Fluorite Veins. These uncommon veins consist of a semiconsolidated yellowish white clay, identified as dickite, mixed with fluorite.

Crusts and Crystals. A complex sequence of carbonate, phosphate and zeolite minerals has been precipitated as open space fillings, on regional joint surfaces, and within shear zones. Blue fluorite forms an anhedral crust on which euhedral stilbite crystals have grown. This stilbite layer is composed of crystals 4-5 mm high which are in some cases overgrown by zoned fluorite crystals dusted with very fine grained pyrite. Commonly, however, the fluorite is absent and the pyrite occurs on the ends of the 'bow-tie' structures of stilbite. Rhombohedral, barrel-shaped, 'worm-like', or botryoidal masses of siderite are intergrown with pyrite or lie directly on stilbite. Other euhedral crystals include tabular vivianite, curved pink blades of dolomite and childrenite-eosphorite.

Hydrothermal Alteration

In addition to the greisenization described above, a pervasive green-yellow-white sericitization of varying intensity occurs throughout the deposit. Rocks showing white sericitization are only slightly altered – orthoclase and plagioclase feldspars show only minor alteration in thin section. A yellow waxy sericitization is produced by the more extensive breakdown of feldspars. A green fine grained sericitic aggregate is the result of complete alteration of feldspars. All rocks showing these stages of hydrothermal alteration contain 100-200 ppm Sn. Since the tin does not occur as cassiterite, it is thought to be contained in the mica lattice.

The relative timing of sericitization has not yet been established. Field evidence suggests that it occurred prior to formation of the quartz-sulphide-phosphate veins, but its relationship to the greisen stage is unclear.

Exotic Mineralogy

Triplite, an unusual iron manganese fluo-phosphate with the composition $(Mn_{1.43}Fe_{0.43}Mg_{0.12}Ca_{0.03})_{2.01}(P_{0.97}O_{3.86})F_{1.14}$ (J.A. Mandarino, Royal Ontario Museum, personal communication, 1981) is commonly found in veins consisting of glassy quartz, sulphides and phosphates. It is light cream-pink in colour, relatively soft (4-5) and occurs in subhedral masses. Triplite typically occurs in minor amounts in phosphate-rich granites, pegmatites and associated mineral deposits, including the Ehrenfreidersdorf tin deposit in Czechoslovakia (Baumann et al., 1974; Stemprok, personal communication, 1981). It is not known to occur in any other Canadian locality.

Childrenite-eosphorite is a solid solution series $[(Fe, Mn)\ Al(PO_4)(OH)_2 \cdot H_2O]$. A mineral belonging to this series is found in the East Kemptville deposit as perfect crystals that have grown on open joint surfaces. It is soft, translucent and yellowish brown in colour. Other known localities include St. Austell, Cornwall, England, the Llallagua tin deposit, Bolivia, and the Ehrenfreidersdorf tin deposit, East Germany.

Comparison with Other Tin Deposits

The East Kemptville deposit is an unusual example of a large tonnage, low grade, greisen-hosted tin deposit in which the dominant ore-controlling factor is the geometry of the granite-metasedimentary rock contact. The style of mineralization is very similar to that of the greisen-hosted tin-tungsten deposits of the Krušné hory Mts.-Erzgebirge area of Czechoslovakia – East Germany. There, the mineralization occurs as massive greisen and greisen-bordered veins in the uppermost zones of small (1-3 km) lithium mica-albite cupolas that coalesce at depth to form a large batholith (Stemprok, 1970; Baumann et al., 1974; Taylor, 1979). This similarity between the deposits has been confirmed by Dr. M. Stemprok, Geological Survey of Czechoslovakia, who examined the East Kemptville deposit in May 1981.

A significant difference, however, between East Kemptville and the Czechoslovakian deposits is that the latter occur in the apical zones of small cupolas whereas mineralization at East Kemptville is located beneath an inflection in the granite-metasedimentary rock contact of a discrete pluton that is part of an extension of an intrusion of batholithic dimensions. Illustrations in Taylor (1979) from Rundquist (1971) suggest that a deposit in Mongolia known as Barun Tsogto is geometrically similar to East Kemptville.

Acknowledgments

This research project is funded by Energy, Mines and Resources under research agreements 151-4-80 and 87-4-81, receipt of which is gratefully acknowledged. Lynn Ann Harlow contributed greatly to field work and sample collection. Subhash Shanbhag and Brian O'Donovan kindly prepared the figures. Shell Canada Resources Limited also provided technical assistance. J.M.G.R. and E.T.C.S. would particularly like to thank the management of Shell Canada Resources Limited for permission to undertake this research project and for supporting J.M.G.R. for eight months in the field. We are very grateful to Dr. J.A. Mandarino of the Royal Ontario Museum for assistance in mineral identification.

References

Baumann, L., Stemprok, M., Tischendorf, G., and Zoubec, V.
1974: Metallogeny of Tin and Tungsten in the Krusné hory-Erzgebirge: Pre-Symposium Excursion Guide I.G.C.P. – Metallization Associated with Acid Magmatism Symposium, Karlovy Vary, 1974, 67 p.

Charest, M.
1976: Petrology, geochemistry and mineralization of the New Ross area, Lunenberg County, N.S.; unpublished M.Sc. thesis, Dalhousie University, 154 p.

Clarke, D.B. and Halliday, A.N.
1980: Strontium isotope geology of the South Mountain Batholith, Nova Scotia; Geochimica et Cosmochimica Acta, v. 44, p. 1045-1058.

Clarke, D.B. and Muecke, G.K.
1980: Igneous and Metamorphic Geology of Southern Nova Scotia – Trip 21: Field Trip Guidebook – Geological Association of Canada – Mineralogical Association of Canada Annual Meeting 1980, 101 p.

Farley, E.J.
1978: Mineralization at the Turner and Walker deposits, South Mountain Batholith; unpublished M.Sc. thesis, Dalhousie University, 252 p.

Ferguson, H.G. and Bateman, A.M.
1912: Geological features of tin deposits; Economic Geology, v. 7, p. 209-262.

Groves, D.I. and Taylor, R.G.
1973: Greisenization and mineralization at the Anchor Tin Mine, N.E. Tasmania; Transactions of the Institution of Mining and Metallurgy, v. 82, p. 135-146.

Johannsen, A.
1932: A Descriptive Petrography of the Igneous Rocks, Vol. 2 – The Quartz-Bearing Rocks; University of Chicago Press, 430 p.

Longstaffe, F.J., Smith, T.E., and Muehlenbachs, K.
1980: Oxygen isotope evidence for the genesis of Upper Paleozoic granitoids from southwestern Nova Scotia; Canadian Journal of Earth Sciences, v. 17, p. 132-141.

MacKenzie, C.B. and Clarke, D.B.
1975: Petrology of the South Mountain Batholith; Canadian Journal of Earth Sciences, v. 12, p. 1209-1218.

Rundquist, D.V., Denisenko, V.R., and Pavlova, I.G.
1971: Greisen Deposits (In Russian); Nedra Publishing House, Moscow, 328 p.

Shcherba, G.N.
1970: Greisens; International Geology Review, v. 12, p. 114-150, 239-255.

Shell Canada Resources Limited
1980: Annual Report.

Stemprok, M.
1970: Petrochemical features of tin-bearing granites in the Krušné hory Mts., Czechoslovakia; Society of Mining Geology, Japan, Special Issue 2, p. 112-118.

Taylor, F.C.
1967: Reconnaissance geology of Shelburne map-area, Queens, Shelburne, and Yarmouth Counties; Geological Survey of Canada, Memoir 349, 83 p.

Taylor, R.G.
1979: Geology of Tin Deposits; Elsevier Scientific Publishing Co., New York, 543 p.

Tischendorf, G., Hosel, G., Lange, H., and Bolduan, H.
1971: Geochemical and structural control of the tin mineralization in the Erzgebirge; IMA-IAGOD Meeting 1970; Society of Mining Geology, Japan, Special Issue 3, p. 15-19.

5.

EVIDENCE FOR GNEISSIC BASEMENT TO THE ARCHEAN YELLOWKNIFE SUPERGROUP IN THE POINT LAKE AREA, SLAVE STRUCTURAL PROVINCE, DISTRICT OF MACKENZIE

R.M. Easton[1], R.L. Boodle,[2] and L. Zalusky[3]
Department of Indian and Northern Affairs

Easton, R.M., Boodle, R.L., Zalusky, L., Evidence for gneissic basement to the Archean Yellowknife Supergroup in the Point Lake area, Slave Structural Province, District of Mackenzie; in Current Research, Part B, Geological Survey of Canada, Paper 82-1B, p. 33-41, 1982.

Abstract

The Point Lake greenstone belt is bounded on the west by an area of gneiss and Kenoran granite. Following 1:30 000 scale mapping in the area, the gneisses have been divided into five units on the basis of crosscutting relationships. Evidence for these gneiss units being basement to Yellowknife Supergroup rocks in the area includes:

i) the presence of several dyke swarms in the gneisses that may be feeders to Yellowknife Supergroup volcanic rocks;

ii) the recognition of several possible unconformities between the gneisses and Yellowknife Supergroup rocks;

iii) the presence of gneiss cobbles in conglomerates of the Yellowknife Supergroup Keskarrah Formation; and

iv) the metamorphic contrast between the gneisses and adjacent supracrustal rocks.

The gneisses underlie an area of about 300 km^2, and extend an unknown distance south into the Winter Lake map area (86A).

Introduction

The nature of the crust underlying Archean greenstone belts has been a subject of continuing interest to geologists. The Slave Structural Province contains several areas of documented and probable granitoid basement to 2.6 to 2.7 Ga greenstone belts (Baragar and McGlynn, 1976; Frith et al., 1974, 1977a,b; Nikic et al., 1980). The best documented case is at Point Lake where altered and deformed granodiorite overlain unconformably by conglomerate is basement to the Point Lake greenstone belt (Stockwell, 1933; Henderson, 1975, 1981; Henderson and Easton, 1977). Henderson and Easton (1977) also suspected that a heterogeneous assemblage of gneiss and schist to the west of the greenstone belt was also older than the Yellowknife Supergroup. Recently completed 1:30 000 scale mapping of the gneisses and other granitoid rocks in National Topographic System map areas 86H/3, H/4, H/5, and H/6 (Easton et al., 1981) revealed both the extent of these gneisses and their age relative to the Yellowknife Supergroup. This paper briefly describes the gneisses, presents evidence suggesting that the gneisses are basement to the Yellowknife Supergroup, and briefly discusses the regional significance of the gneisses.

General Geology

The southern half of the Point Lake map area (86H) can be divided into three geological terranes (Fig. 5.1) – a western granitoid terrane, a north-trending volcanic belt, and a metasedimentary terrane to the east. The metasedimentary and metavolcanic rocks belong to the Yellowknife Supergroup. The contact between the granitoid terrane and the volcanic belt is commonly faulted, and cataclasis has affected rocks on both sides of the contact. Within the area of interest, Bostock (1980) mapped the supracrustal rocks east of the gneiss-greenstone boundary at 1:250 000 scale, Henderson and Easton (1977) mapped the Keskarrah Bay area at 1:50 000 scale, and the metasedimentary terrane was mapped at 1:31 680 scale by King et al. (1980). The granitoid terrane to the west of the volcanic rocks has been mapped at 1:30 000 scale by Easton et al. (1981) and is the subject of this report.

The geology of the granitoid terrane is shown in Figure 5.2. Brief descriptions of the major lithologies are given below. Nomenclature of granitoid rocks follows the recommendations of Streckeisen (1976). Stratigraphic nomenclature of the supracrustal rocks in the area was defined by Bostock (1980).

Pre-Yellowknife Supergroup Rocks and Gneisses

The oldest rocks in the map area are a heterogeneous assemblage of gneisses (Unit 1 to 6) and the previously described basement granodiorite (Unit 7) (Henderson, 1975). Except for Unit 4 and 7, the gneisses are commonly mixed on any one outcrop, with complex contact relationships. To further complicate matters, younger granitoids commonly cut the older gneisses. Age relations are almost impossible to work out on inland, lichen covered outcrop, but they can be determined on the limited clean shoreline exposure at Point Lake.

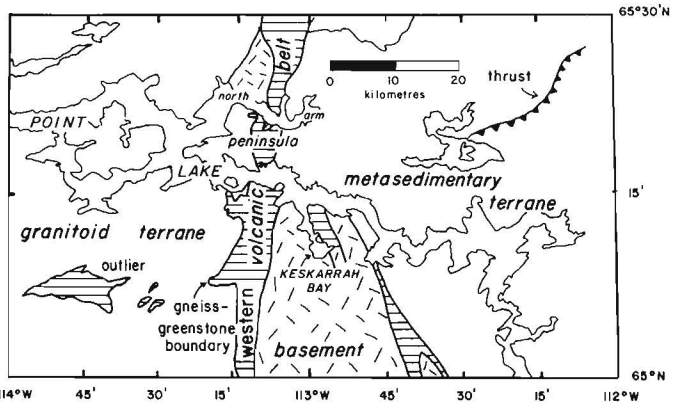

Figure 5.1. *General geology of the southern half of the Point Lake map area (86H), showing the division of the area into a western granitoid terrane, a central volcanic belt, and an eastern metasedimentary terrane. Sources: 112° to 112°45'W – King et al. (1980); 112°45' to 113°15'W – Henderson and Easton (1977), Bostock (1980); 113°10' to 114°W – Easton et al. (1981).*

[1]Department of Earth Sciences, Memorial University, St. John's, Newfoundland, A1B 3X5
[2]Geology Office, Department of Indian and Northern Affairs, Box 1500, Yellowknife, N.W.T., X1A 2R3
[3]Department of Geology, Concordia University, Montreal, Quebec, H3G 1M8

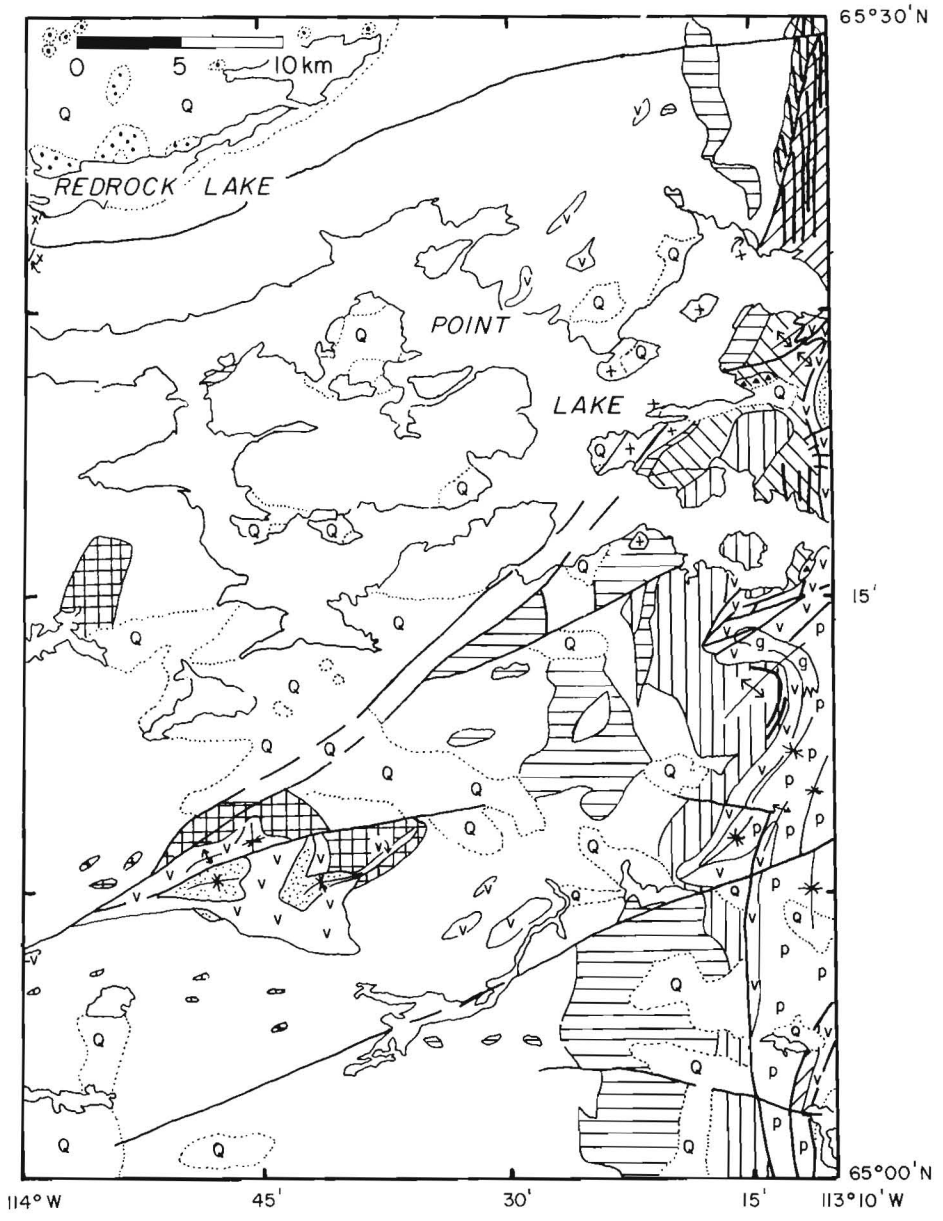

Figure 5.2. *Geological map of the granitoid terrane. Numbers in brackets in legend correspond to units described in the text. Source: Easton et al. (1981).*

Unit 1 consists of 1 to 3 mm thick alternating layers of amphibolite, layers of fine grained biotite tonalite to granodiorite composition, and layers of reddish, fine grained biotite-hornblende granodiorite to monzogranite composition (Fig. 5.3). This prominent layering is folded into north-trending isoclines, but at least two older phases of folding can be observed on clean outcrops. Unit 1 is found only as enclaves in the strongly foliated orthogneisses of units 2 and 3.

Unit 2 is a strongly foliated, layered, grey tonalite orthogneiss with alternating 10 to 200 cm thick layers of fine grained tonalite, medium grained hornblende granodiorite, and dark grey hornblende diorite. The unit is commonly mylonitic (Fig. 5.4).

Unit 3 is a strongly foliated, banded orthogneiss composed mainly of layers of pinkish hornblende granodiorite and amphibolite; layering is 20 to 300 cm thick. In places, amphibolite amounts to over 40 per cent of outcrop area (Easton et al., 1981). A layer within unit 3 that may be a remnant quartz-pebble and granodiorite pebble conglomerate is exposed in a shoreline outcrop 1 km west of the gneiss-greenstone boundary on the south side of the peninsula between the north and south arms of Point Lake. Rafts of unit 2 gneiss are present within unit 3 gneiss. These rafts have been partly assimilated. On several outcrops, layering in unit 3 truncates layering in unit 2 at a very slight angle. Although the contact relations are obscure, it is suspected that unit 2 is older than unit 3. Both units 2 and 3 outcrop near the gneiss-greenstone boundary and have been strongly mylonitized by late movement along this contact. The intensity of late cataclasis decreases westward. The parent to unit 3 could not be determined, but the possible conglomerate and abundant amphibolite is suggestive of a volcano-sedimentary sequence intruded by granitoids.

Unit 4 is the areally most extensive gneiss unit. In the east, it is migmatitic with layers of foliated biotite hornblende granodiorite to tonalite and cordierite-sillimanite-microcline psammitic and pelitic schist. The layers have been folded and refolded (Fig. 5.5). From the contact with the orthogneisses (units 1 to 3), over a distance of a kilometre to the west, the schist layers of the gneiss decrease in abundance to a few schlieren and biotite-rich bands. Locally, minor amphibolite xenoliths are present. Farther west, the gneiss consists predominantly of the foliated granodiorite with minor schileren. The granodiorite phase is interpreted to be a pluton that intruded and metamorphosed a sedimentary sequence. Only a small part of the sedimentary sequence is now exposed. Contact relations betwen units 3 and 4 are poorly exposed, hence, the relative age of units 3 and 4 is unresolved. The greater areal extent of unit 4 may indicate that unit 4 is intrusive into unit 3.

Both units 3 and 4 are cut by weakly foliated plagioclase porphyritic granodiorite and quartz plagioclase pegmatite veins. These veins increase in abundance to the west towards a granodiorite intrusion (unit 13) that is clearly intrusive into the migmatitic gneiss (unit 4). The veins are lithologically and texturally similar to the younger granodiorite (unit 13) and are probably related to it. The samples of the gneiss terrane dated by Krogh and Gibbins (1978) were taken from these younger granodiorite veins (field observations and Gibbins, personal communication, 1981, see Discussion section).

Unit 5 is nebulitic monzogranite orthogneiss with abundant amphibolite xenoliths, and layers and zones of partly assimilated amphibolite. Veins of granitoid material that can be traced to unit 5 cut both unit 3 and unit 4 gneisses. Unit 5 is always in sharp contact with Yellowknife Supergroup rocks, and no granitoid material of unit 5 could be observed cutting the Yellowknife Supergroup rocks. Unit 5 is cut by younger granites of units 12 and 15.

Unit 6 consists of gneisses that cannot be assigned to units 1 to 5 because of their separation from the main body of gneisses by younger granites. Most of these gneisses resemble the orthogneisses of units 2 and 3. The Yellowknife Supergroup outlier topographically overlies unit 6 gneiss. The nature of this contact is discussed later.

Unit 7 is sheared, granodiorite to monzogranite dated by the U-Pb zircon method at 3155 Ma (Krogh and Gibbins, 1978). This is the classic basement unit of Stockwell (1933) and Henderson (1975, 1981). The age relationships between units 1 to 6 and unit 7 have not been determined, as the units were not seen in contact.

Yellowknife Supergroup

The Yellowknife Supergroup succession in the area has been described by Henderson and Easton (1977) and Bostock (1980). The Point Lake Formation (Bostock, 1980) consists of a lower, 100 to 500 m thick member of thinly bedded mafic metatuff (unit 8) commonly overlain by an upper member of pillowed and massive mafic metavolcanic flows. Gabbro sills and irregular intrusions (unit 11) intrude the Point Lake Formation near the tuff-flow member contact. The gabbros were metamorphosed and deformed with the volcanic rocks. Psammitic and pelitic schists of the Contwoyto Formation (unit 10) overlie the Point Lake Formation. The Keskarrah Formation outcrops east of the area shown in Figure 5.2, and consists of a conglomerate member and a sandstone member, both of which interfinger with mafic flows of the Point Lake Formation.

Post-Yellowknife Supergroup Rocks

Unit 12 includes mylonitic and brecciated leucogranite and abundant syenogranite pegmatites, located along the gneiss-greenstone boundary, that cut both the gneisses and Yellowknife Supergroup rocks. These rocks may be related to unit 15, but are distinguished in the field by their strong cataclastic fabric. Unit 13 is a weakly foliated biotite hornblende granodiorite of limited areal extent. Unit 14 is also of local extent, and is a pluton of variable composition ranging from granodiorite to syenogranite. Unit 15 consists dominantly of biotite hornblende syenogranite that contains abundant large angular inclusions of amphibolite, banded amphibolite and metasedimentary rocks. These inclusions are lithologically similar to Yellowknife Supergroup rocks. Locally unit 15 is K-feldspar porphyritic. Unit 15 includes several distinct plutons and is of batholithic extent. Many outcrops between 113°10' to 113°25'W are injection migmatites comprising varied proportions of unit 15 and older gneisses.

Proterozoic clastic rocks of the Odjick Formation are present in the northwest corner of the map area, but the Proterozoic-Archean unconformity is not exposed. Weakly metamorphosed north- and east-trending Proterozoic dykes cut all Archean units. The north-trending dykes intrude the Odjick Formation, and are lithologically distinct from the unaltered north- to northwest-trending Mackenzie diabase dykes common in the area.

Structure

West of 113°18'W, foliation and folds in the gneisses and the supracrustal rocks are east trending. Between 113°18' and 113°10'W, structures become increasingly north trending, and overprinting of easterly structures by north trending structures can be observed in the gneisses. Structures in the volcanic belt are north trending. A 10 to 20 m north-trending mylonite zone is associated with the gneiss-greenstone boundary of most of its length. Cataclasis associated with this mylonite zone has enhanced the

Figure 5.3. *(above)*

Folded layers in unit 1 gneiss. Hammer handle is 30 cm long.

Figure 5.4. *(top right)*

Mylonitized unit 2 orthogneiss, 100 m west of fault contact with mafic tuff member of the Yellowknife Supergroup.

Figure 5.5. *(lower right)*

Deformed migmatitic gneiss (unit 4), 2 m from a sharp contact with amphibolite grade mafic tuff (unit 8). Photograph taken at point A in Figure 5.6.

northerly trends in the gneisses within 500 m of the zone, and has sheared supracrustal and younger granitic rocks within 200 m of the mylonite zone. North-trending mylonite zones 1 to 5 m wide also occur west of the gneiss-greenstone boundary on the peninsula. The east-trending Proterozoic dykes are unaffected by the mylonite zone, hence movement along the mylonite zone was complete by the early Proterozoic. Many of the north-trending faults in the supracrustal rocks adjacent to the mylonite zone (Easton et al., 1981) may be related to it. An older fault set with easterly trends occurs in the northeast corner of the area (Henderson and Easton, 1977). Several large north-easterly trending faults related to deformation in Wopmay Orogen (Hoffman, 1980) cut all units in the area except the Mackenzie diabase dykes.

Metamorphism

Metamorphic grade of supracrustal rocks in the eastern part of the area ranges from upper greenschist to amphibolite facies. Metamorphic grade in the volcanic rocks increases to the south-southwest, coincident with thinning of the volcanic section. Metamorphic grade in the Yellowknife Supergroup outlier is high-amphibolite grade in the volcanic rocks, and with cordierite-andalusite and cordierite-sillimanite assemblages present in the pelitic rocks. Metamorphic grade in the gneiss is difficult to estimate because of the granitic nature of most of the gneisses, but migmatitic gneisses of unit 4 have suffered anatexis and have cordierite-sillimanite-microcline assemblages indicating upper amphibolite grade. Granites that cut metamorphosed Yellowknife Supergroup rocks along the gneiss-greenstone boundary are cataclastic, indicating some movement along the mylonite zone occurred after metamorphism of the Yellowknife Supergroup.

Gneisses as Basement – The Evidence

Cataclasis along the gneiss-greenstone boundary has obscured the original contact relationships between the gneisses and the supracrustal rocks. The relations described below all have a bearing on the nature of the original contact relationship between the gneisses and the Yellowknife Supergroup rocks.

Possible Feeder Dykes

On the south shore of the peninsula between the north and south arms of Point Lake, for a distance of up to 3 km west of the gneiss-greenstone boundary, several amphibolite dykes truncate gneissosity in unit 2 and 3 gneisses at a slight angle (1 to 5 degrees). On vertical faces however, the same dykes cut gneissosity at a high angle (30 to 40 degrees). The amphibolite dykes are metamorphosed to the same degree as adjacent Yellowknife Supergroup volcanic rocks.

In the extreme northeast corner of the map area (Fig. 5.2), a swarm of mafic dykes, now amphibolite, cut unit 2 and 3 gneisses. Several distinct amphibolites are present. Some amphibolite dykes show mutual crosscutting relationships. The dyke swarm is on strike with, and adjacent to a similar swarm of amphibolite dykes cutting basement granodiorite (unit 7), suggesting a genetic relationship. Rocks lithologically similar to some of the amphibolite dykes are present in nearby Yellowknife Supergroup volcanic rocks. The Yellowknife Supergroup volcanic pile is especially thick adjacent to this major dyke swarm (Bostock, 1980).

Near 65°12'N, 113°14'W, medium to coarse grained amphibolite dykes cut unit 5 gneiss and have been folded with the gneiss. The dykes are not cut by the leucosome phase of the gneiss. The dykes are texturally and lithologically similar to gabbros present in nearby Yellowknife Supergroup volcanic

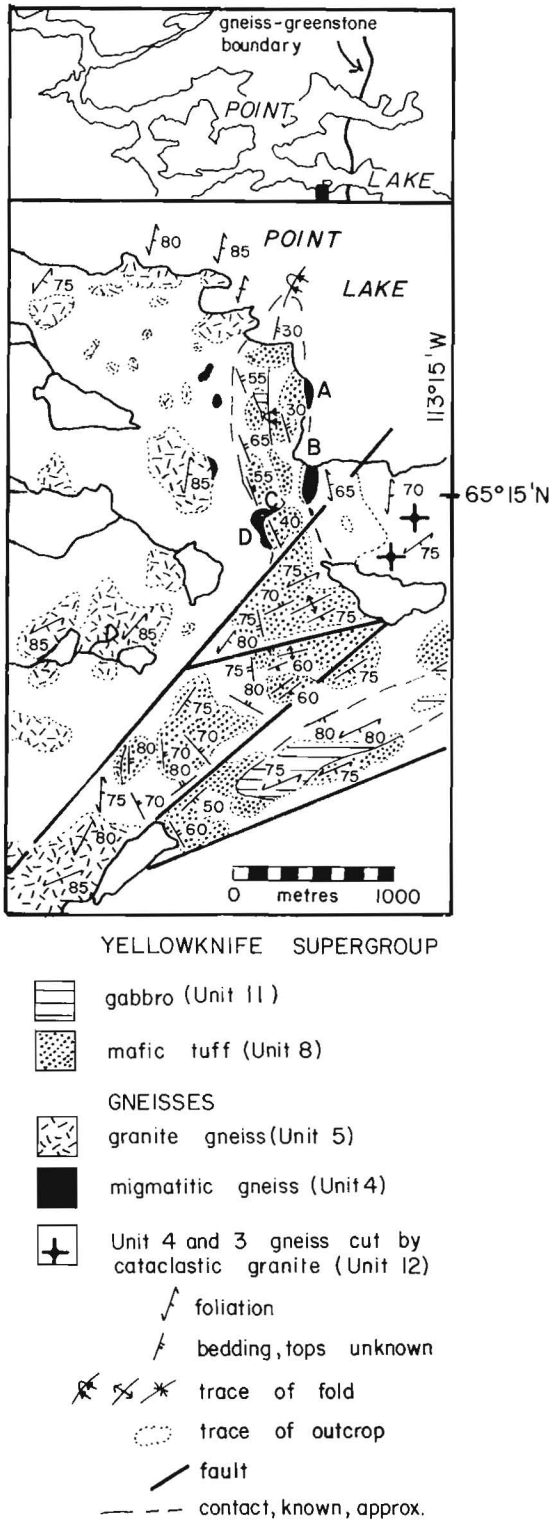

A, B – migmatitic gneiss (unit 4) in sharp contact with amphibolite grade mafic tuffs (unit 8).

C – at this point, conglomerate is present between mafic tuff and weathered gneiss (unit 4).

D – weathered gneiss at this location.

Figure 5.6. *Geological sketch map of area near the gneiss-Yellowknife Supergroup unconformity at 65°15'30"N, 113°16'W. Inset shows location of map relative to Point Lake and the gneiss-greenstone boundary.*

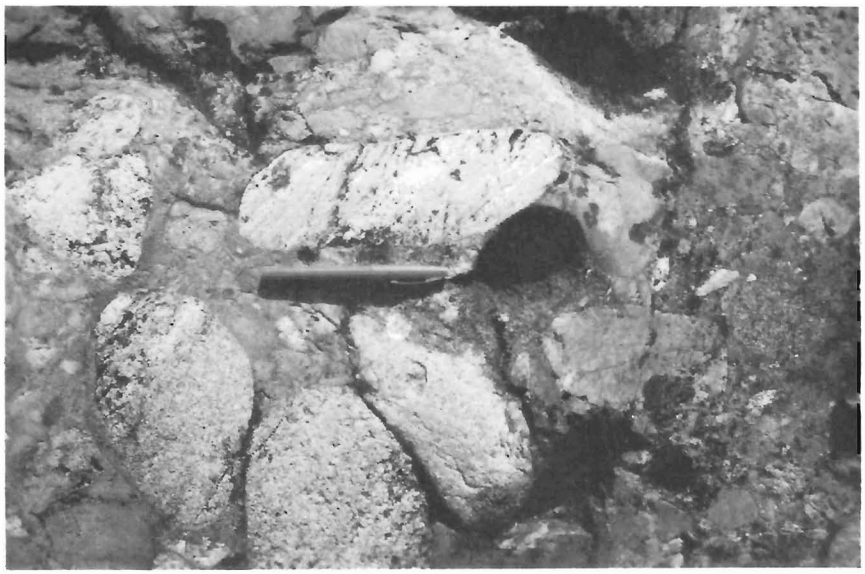

Figure 5.7

Gneiss cobble in the Keskarrah Formation conglomerate member.

rocks, but the dykes cannot be traced to these gabbros. The dykes, gneiss and volcanic rocks are all cut by younger granitoids of unit 12.

The dykes described above are significant because they clearly cut the gneisses – the only units apart from the younger granites (units 12 to 15) and the Proterozoic diabase dykes with such clear relationships. In addition, the dykes are metamorphosed to the same degree, and are lithologically similar to Yellowknife Supergroup volcanic rocks. The dykes are most abundant near the gneiss-greenstone boundary. The dykes had to be intruded prior to metamorphism of the Yellowknife Supergroup, but after formation of the youngest gneiss (unit 5). Thus, although the dykes cannot be shown unequivocally to be contemporaneous with the Yellowknife Supergroup volcanic rocks, it is the most plausible relationship. The amphibolite dykes have geological relationships similar to dykes near a gneiss-greenstone boundary in the Ross Lake area of the southern Slave Province (Baragar, 1966; Davidson, 1972; Baragar and McGlynn, 1976; Lambert, 1982) which have been interpreted to be feeders to Yellowknife supergroup volcanic rocks.

Unconformities

Along the gneiss-greenstone boundary, volcanic rocks of the Point Lake Formation, most commonly the mafic tuff member, are always in fault contact with the gneisses. West of the gneiss-greenstone boundary are three areas where unconformities may be preserved between the gneisses and Yellowknife Supergroup rocks.

A possible unconformity between mafic tuff and gneiss is present at 65°15'30'N, 113°16'W, about 500 m inland (Fig. 5.6). At this locality, the tuff is recumbently folded with the gneiss, the eastern limb being overturned to the west. On this limb, amphibolite grade mafic tuff is in sharp contact with migmatitic gneiss of unit 4 (Fig. 5.6, points A and B). The leucosome of the gneiss does not cut the tuff-gneiss contact. On the western limb, 50 to 100 cm of quartz pebble conglomerate is present between the mafic tuff and strongly weathered, friable migmatitic gneiss (Fig. 5.6, Points C and D). The foliation in the gneiss and tuffs is discordant at a slight angle (2 to 5 degrees). The presence of conglomerate overlying weathered gneiss suggests an unconformity.

Another possible unconformity between gneiss and tuff is located on the north shore of the peninsula between the north and south arms of Point Lake. Here, several small outliers of amphibolite grade mafic tuff are present 1 to 3 km west of the gneiss-greenstone boundary. The tuff in these outliers is infolded with the gneiss. The contact between the tuff and the gneisses, where exposed, is sharp, and the leucosome phase of the gneiss does not cut the tuff. There is slight discordance between the foliation in the gneiss and that in the tuff.

A third possible unconformity may be present in the large Yellowknife Supergroup outlier. The tuffs and metasedimentary rocks lie topographically above the gneiss, dip away and, at one locality, face away from the gneiss, however, 1 to 2 m of cover separates the tuff from the gneiss. At one locality, there is slight discordance between gneissosity and foliation in the tuffs. In several places, 50 to 100 cm of quartz wacke is present between the tuffs and the gneisses. Because of the cover along the contact, the possibility of a fault contact cannot be ruled out.

In the areas described above, there is no evidence for faulting along the contacts, but faulting cannot be ruled out. However, in the first two areas, any fault would have to be paper thin. It is the lack of evidence for faulting that makes these contacts unique within the map area. The geological relationships between the mafic tuffs and the gneisses described above are compatible with interpretation of the contacts as unconformities.

Keskarrah Formation

In addition to the abundant granodiorite cobbles (Stockwell, 1933; Henderson, 1975), cobbles lithologically similar to all the gneiss units are found in the conglomerate member of the Keskarrah Formation east of the map area (Fig. 5.7). The gneiss cobbles are commonly found in beds where over 50 per cent of the granitic cobbles are gneissic. The gneiss-cobble-rich beds are not common, and the bulk of the granitic cobbles in the Keskarrah Formation were derived from the basement granodiorite (unit 7). The foliation in the gneiss cobbles is commonly less intense than in outcrop (but still prominent), probably because the present intensity of the foliation in the gneissic terrane is due, in part, to cataclasis along the gneiss-greenstone boundary that took place after conglomerate deposition.

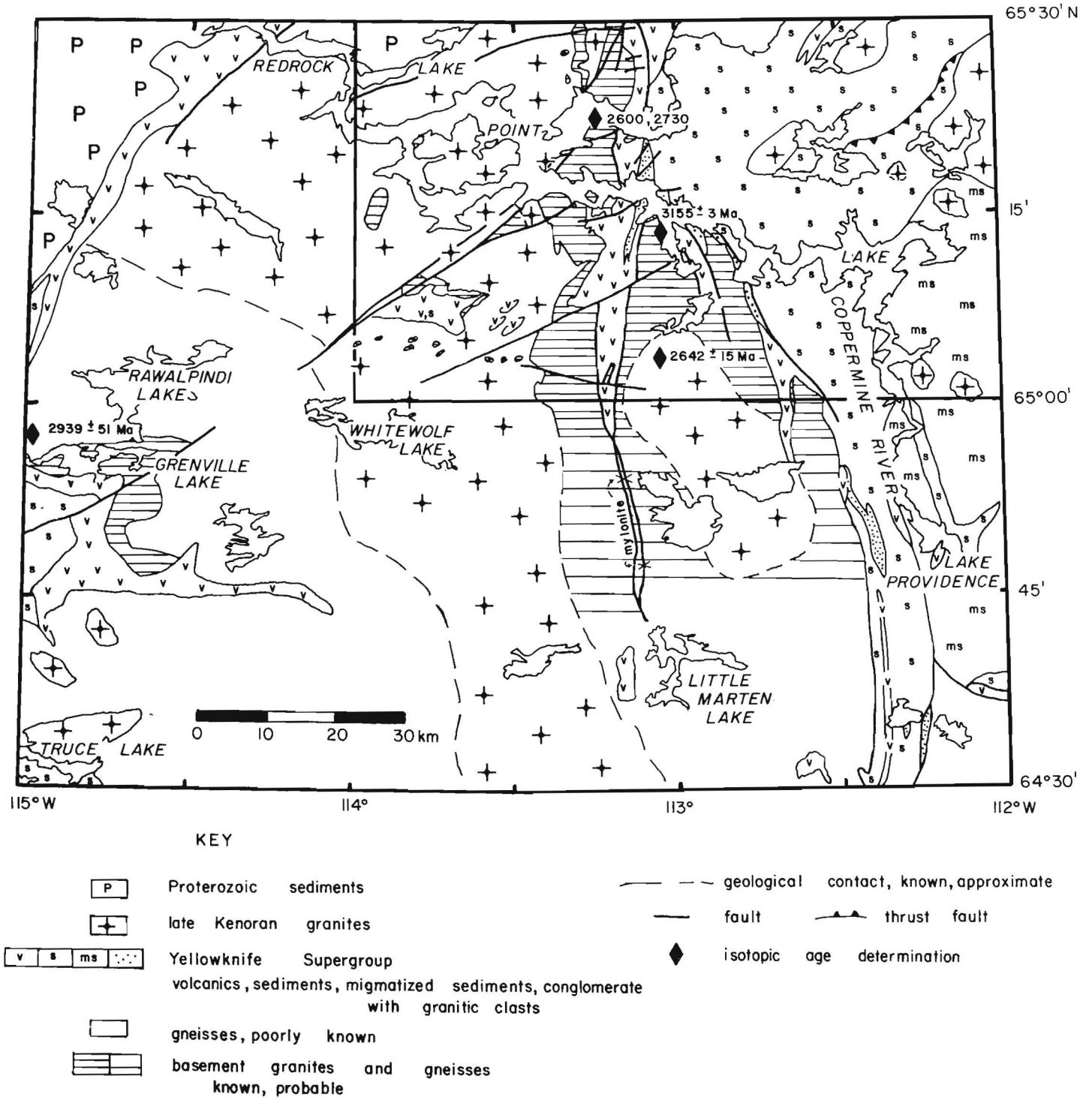

Figure 5.8. *Geological map of the north-central Slave Province showing distribution of greenstone belts, basement and probable basement. Heavy line outlines the Point Lake area shown in Figure 5.1. Zone labelled mylonite is the extrapolated southward extension of the gneiss-greenstone belt through two areas of mylonite shown by Fraser (1969). Data from: Easton et al. (1981), Fraser (1969), Frith et al. (1974, 1977b), Henderson and Easton (1977), and King et al. (1980). Isotopic ages shown are 2939 Ma, Rb-Sr, Frith et al. (1977b); 2642 Ma, zircon, Bostock (1980); 3155, 2600, 2730 Ma, zircon, Krogh and Gibbins (1978). Reported ages use or have been corrected to constants recommended by Steiger and Jäger (1977).*

Metamorphic Contrast

A striking contrast in metamorphic grade is present between lower amphibolite facies metatuffs and greenschist grade metasedimentary rocks of the Yellowknife Supergroup a few hundred metres to the east and the para- and orthogneisses they are in contact with. Cordierite-sillimanite-microcline assemblages indicating upper amphibolite facies metamorphic grade are present in the migmatitic gneisses of unit 4. No rocks gradational in metamorphic grade between the supracrustal rocks and the gneisses have been observed. This contrast is observed throughout the map area.

Discussion

An interpretation of a basement-cover relationship between the Yellowknife Supergroup and the gneisses is consistent with the geological relationships described above. The metamorphosed dykes, which cut the gneisses and are located parallel to, and near the gneiss-greenstone boundary, are best interpreted as being contemporaneous with the volcanic rocks. The gneiss cobbles in Keskarrah Formation conglomerates indicate that a gneissic terrane was exposed and supplying detritus during conglomerate deposition. The metamorphic contrast between the gneisses and the supracrustal rocks, particularly where a faulted contact cannot be demonstrated can be explained if the gneisses were formed before deposition of the supracrustal rocks. The heterogeneous nature of the gneisses suggests a complex history, again, implying that some, if not all of the gneisses formed before supracrustal deposition. Finally, there are localities where unconformable relationships may exist between the gneisses and the supracrustal rocks.

At present, the only unit west of the gneiss-greenstone boundary that has been dated contains weakly foliated granodiorite veins that cut migmatitic gneiss of unit 4. Krogh and Gibbins (1978) separated two sets of zircons from the granodiorite. White, second generation zircons, gave an age of 2600 Ma, probably the age of intrusion. Brown, first generation zircons, have a minimum age of 2730 Ma. The significance of the 2730 Ma age is problematic as the source of the first generation zircons is unknown. These dates establish a minimum age of 2600 Ma for the migmatitic gneiss (unit 4). They do not exclude the possibility that the migmatitic gneiss is older than the circa 2650 to 2680 Ma age of Yellowknife Supergroup rocks in the Slave Province (Henderson, 1981).

The interpreted basement gneisses (units 1 to 6) and the basement granodiorite (unit 7) each underlie an area of about 300 km^2 in the Point Lake area, and may be present in adjacent areas (Fig. 5.8). Although this is only 8 per cent of the Point Lake map area (86H), it is a large area relative to other occurrences of basement rocks in the Slave Province.

The interpreted basement gneisses and the mylonite zone have been traced 3 km south of the Point Lake area (86H, south half) into the Winter Lake map area (86A). The contact between unit 4 and unit 5 of Fraser (1969) in the northwest corner of the Winter Lake map area corresponds to the contact between the gneisses and the late granite batholith (unit 16, this study) near the common boundary of the two map areas (86A, H). If the unit 4/5 contact separates similar rocks to the south, then part of the north-central Winter Lake map area may be underlain by basement gneisses. In addition, Fraser (1969) reported two occurrences of mylonite along a migmatitic zone extending from the common boundary of the two map areas south to Little Marten Lake (Fig. 5.8). These mylonites lie on the extrapolated southward extension of the gneiss-greenstone boundary and may be the southward continuation of this major structure. The large area of probable basement shown in Figure 5.8 also includes rocks on strike with the basement granodiorite (unit 7).

Frith et al. (1977b) dated gneissic basement at Grenville Lake at 2939 ± 51 Ma (recalculated using the $1.42 \times 10^{-11} a^{-1}$ rubidium decay constant) by Rb-Sr whole-rock dating. Grenville Lake is only 30 km south-southwest of interpreted basement gneiss in the Yellowknife Supergroup outlier (Fig. 5.8). A large area of poorly known gneisses that McGlynn (1977) suggested may be older than the Yellowknife Supergroup underlies much of the intervening region (Fig. 5.8). Detailed mapping in this area is needed to determine if basement gneisses do occur between Grenville and Point lakes.

Acknowledgments

Sue Irving, Greg Eiche and Diane McKinnon provided able assistance in the field. Win Bowler did an excellent job of providing logistical support from Yellowknife. This project is part of the mapping program of the Geology Office, Department of Indian and Northern Affairs, Yellowknife in the west-central Slave Province. The co-operation of the Geological Survey of Canada in publishing this report is most appreciated. J.B. Henderson, W.A. Padgham, P. Wonderley and V. Jackson reviewed an earlier version of this report.

References

Barager, W.R.A.
1966: Geochemistry of the Yellowknife volcanic rocks; Canadian Journal of Earth Sciences, v. 3, p. 9-30.

Baragar, W.R.A. and McGlynn, J.C.
1976: Early Archean basement in the Canadian Shield: A review of the evidence; Geological Survey of Canada, Paper 76-14, 20 p.

Bostock, H.H.
1980: Geology of the Itchen Lake area; Geological Survey of Canada, Memoir 391, 102 p.

Davidson, A.
1972: Granite Studies in the Slave Province; in Report of Activities, Part A, Geological Survey of Canada, Paper 72-1A, p. 109-115.

Easton, R.M., Boodle, R.L., Zalusky, L., Eiche, G., and McKinnon, D.
1981: Geology of 86H/3, 86H/4, 86H/5 and 86H/6, District of Mackenzie, Department of Indian Affairs and Northern Development, Preliminary Geological Map EGS-1981-5a,b,c,d, 1:30 000 scale with descriptive notes.

Fraser, J.A.
1969: Geology, Winter Lake, District of Mackenzie; Geological Survey of Canada, Map 1219A, scale 1:253, 440.

Frith, R.A., Frith, R., Helmstaedt, H., Hill, J., and Leatherbarrow, R.
1974: Geology of the Indian Lake area (86B), District of Mackenzie; in Report of Activities, Part A, Geological Survey of Canada, Paper 74-1A, p. 165-171.

Frith, R.A., Fyson, W.K., and Hill, J.D.
1977a: The geology of the Hackett-Back River Greenstone Belt – second preliminary report; in Report of Activities, Part A, Geological Survey of Canada, Paper 77-1A, p. 415-423.

Frith, R., Frith, R.A., and Doig, R.
1977b: The geochronology of the granitic rocks along the Bear-Slave structural province boundary, northwest Canadian Shield; Canadian Journal of Earth Science, v. 14, p. 1356-1373.

Henderson, J.B.
1975: Sedimentological studies of the Yellowknife Supergroup in the Slave Structural Province; in Report of Activities, Part A, Geological Survey of Canada, Paper 75-1A, p. 325-330.

Henderson, J.B.
1981: Archean Basin Evolution in the Slave Province, Canada; in Plate Tectonics in the Precambrian, ed. A. Kroner, Elsevier, Amsterdam, p. 213-236.

Henderson, J.B. and Easton, R.M.
1977: Archean supracrustal-basement rock relationships in the Keskarrah Bay map area, Slave Structural Province, District of Mackenzie; in Report of Activities, Part A, Geological Survey of Canada, Paper 77-1A, p. 217-221.

Hoffman, P.F.
1980: Conjugate transcurrent faults in north-central Wopmay Orogen (early Proterozoic) and the dip-slip reactivation during post-orogenic extension, Hepburn Lake map area, District of Mackenzie; in Current Research, Part A, Geological Survey of Canada, Paper 80-1A, p. 183-185.

King, J.L., Boodle, R.L., and St-Onge, M.R.
1980: Preliminary Geological Map of 86H/1, 86H/8, 86H/2E½ and 86H/7E½, District of Mackenzie; Department of Indian Affairs and Northern Development, Preliminary Map. EGS 1980 – 10a,b, scale 1:31 680.

Krogh, T.E. and Gibbins, W.
1978: U-Pb isotopic ages of basement and supracrustal rocks in the Point Lake area of the Slave Structural Province, Canada; Geological Association of Canada, Abstracts, v. 3, p. 438.

Lambert, M.B.
1982: Synvolcanic Intrusions in the Cameron River Volcanic Belt, District of Mackenzie; in Current Research, Part A, Geological Survey of Canada, Paper 82-1A, p. 165-167.

McGlynn, J.C.
1977: Geology of the Bear-Slave Provinces, Northwest Territories; Geological Survey of Canada, Open File 445, scale 1:1 000 000.

Nikic, Z., Baadsgaard, H., Folinsbee, R.E., Krupicka, J., Leech, A.P., and Sasaki, A.
1980: Boulders from basement, the trace of ancient crust; in Selected Studies of Archean Gneisses and Lower Proterozoic Rocks, Southern Canadian Shield, ed., Morey, G.B. and Hanson, G.N., Geological Society of America, Special Paper 182, p. 169-175.

Steiger, R.H. and Jager, E.
1977: Subcommission on Geochronology: Convention on the Use of Decay Constants in Geo- and Cosmochronology; Earth and Planetary Science Letters, v. 36, p. 359-362.

Stockwell, C.H.
1933: Great Slave Lake-Coppermine River area, N.W.T.; Geological Survey of Canada, Summary Report 1932, Part C, p. 37-63.

Streckeisen, A.
1976: To each plutonic rock its proper name; Earth Science Reviews, v. 12, p. 1-33.

6.

STRATIGRAPHIC PROBLEMS IN THE HAMILTON SOUND AREA OF NORTHEASTERN NEWFOUNDLAND

Project 730044

Karl E. Karlstrom[1]
Precambrian Geology Division

Karlstrom, Karl E., Stratigraphic problems in the Hamilton Sound area of northeastern Newfoundland; in Current Research, Part B, Geological Survey of Canada, Paper 82-1B, p. 43-49, 1982.

Abstract

A new structural interpretation of the Hamilton Sound area involving a subhorizontal enveloping surface for F_2 folds suggests several modifications of existing stratigraphy. (1) The Dunnage Mélange and Davidsville Group are part of a contiguous mélange terrane. (2) Rocks traditionally referred to the Indian Islands Group are repeated by F_2 folding and are correlated with units on the Change Islands, the west side of the Port Albert Peninsula, and the east side of Dog Bay Point; all of these rocks are herein included in the Indian Islands Group. (3) The Botwood Group includes intercalated subaerial volcanic flows, tuffs, and sandstones, and is locally in thrust contact with underlying units.

Introduction

A new structural interpretation of the northeastern Dunnage Zone places important constraints on stratigraphic interpretations. This paper, a progress report of on-going mapping, examines some implications of new structural data to long-standing stratigraphic problems in the Hamilton Sound area. While the final solution to many of these problems is not yet possible, Figure 6.1 presents a simplified stratigraphic interpretation based upon the observation that the enveloping surface of F_2 folds in the area is subhorizontal. This figure indicates that stratigraphic units are repeated by folding, an interpretation that contrasts markedly with prevailing interpretations of fault-bounded, steeply-dipping, northwest-younging homoclinal successions (c.f. Williams, 1964; Kay, 1976; McKerrow and Cocks, 1978; Keen et al., 1981). Figure 6.2 reviews stratigraphic nomenclature used by previous workers. More details on the lithological and sedimentary characteristics of various units are in Williams (1967a,b), Eastler (1969, 1971), Dean (1978), and Currie et al. (1979).

The structure of the eastern Notre Dame area is that of a series of thrust sheets and associated F_1 recumbent folds, folded by upright F_2 asymmetrical folds, and later disrupted by F_3-related high-angle faults. The geometric significance of each of the three generations of folding to the distribution of stratigraphic units has not been fully appreciated by most workers.

The implication of F_1 thrusting is that lithostratigraphic correlations can only be strictly valid within individual thrust sheets (or after palinspastic restoration of the thrust sheets). Thus, an understanding of regional stratigraphy relies in part on the understanding of the geometry of F_1 folds and thrusts. Thrust contacts are difficult to identify, especially when they are strongly deformed by F_2 and F_3. Nevertheless, recognition of the presence of regional-scale thrusting in the Notre Dame Bay area provides a powerful conceptual model to help explain many of the stratigraphic problems of the area.

The geometry of F_2 asymmetrical folds is better understood. F_2 folds (and northeast-striking S_2 axial plane cleavage) are the predominant structures in the area and "unfolding" of F_2 provides the basis for the simplified stratigraphic interpretation presented in Figure 6.1. F_2 folds have subhorizontal enveloping surfaces so stratigraphic units outcrop repeatedly from northwest to southeast across the structural trend of the Dunnage Zone. One example, on the scale of the orogen itself, is the repetition of Caradocian shales (Dean, 1978); another example is the repetition of Ordovician mélanges in the eastern Notre Dame Bay area (the Dunnage and Carmanville mélanges); a third is repetition of turbidites of the Indian Islands Group across the Port Albert Peninsula (Fig. 6.1). All of these examples are discussed below.

F_3 structures include chevron folds, kink bands, and locally developed S_3 crenulation cleavage. Macroscopically, F_3 folding results in gentle warping of F_2 (Fig. 6.1). F_3-related high-angle faults have a major influence on the distribution of stratigraphic units. Even faults of only moderate vertical displacement can juxtapose different thrust sheets creating major discontinuities in surface geology. Major rectilinear faults like the Chanceport, Lukes Arm, Dildo, Reach, and Indian Islands Faults are interpreted to be late high-angle faults which crosscut F_2. Hence, the importance of these faults to stratigraphic interpretations needs to be reassessed.

Ordovician Stratigraphic Problems

Williams et al. (1972, 1974) subdivided the Dunnage Zone into three tectonostratigraphic zones, separated by faults, which they believed to represent terranes with distinct Ordovician or earlier stratigraphic and structural histories. The Reach Fault was interpreted as the boundary between zones E and F (the Exploits and Botwood zones). Subsequent mapping, however, shows that fractured and hornfelsed sandstone of the Botwood Group outcrops on both sides of the trace of the fault at Boyds Cove and that the fault truncates an F_2 synclinorium on the Port Albert Peninsula (Fig. 6.1). The fault is therefore a post-F_2 (post-Middle Silurian) high-angle fault with only moderate displacement. Furthermore, rocks east and west of the fault appear to have undergone the same structural history so there is no reason to postulate that the Reach Fault separates different tectonic zones.

McKerrow and Cocks (1977, 1978) also considered the Reach Fault to be of fundamental importance in the geologic history of the Notre Dame Bay area, as the suture representing the final closure of the Iapetus Ocean in Devonian time. Their evidence was that faunas east of the fault belonged to a European province whereas faunas west of the fault belonged to a North American province. Their argument, however, was based on a single fossil from the Davidsville Group whose identification is uncertain

[1] Department of Geology, University of New Brunswick, Fredericton, N.B., E3B 5A3

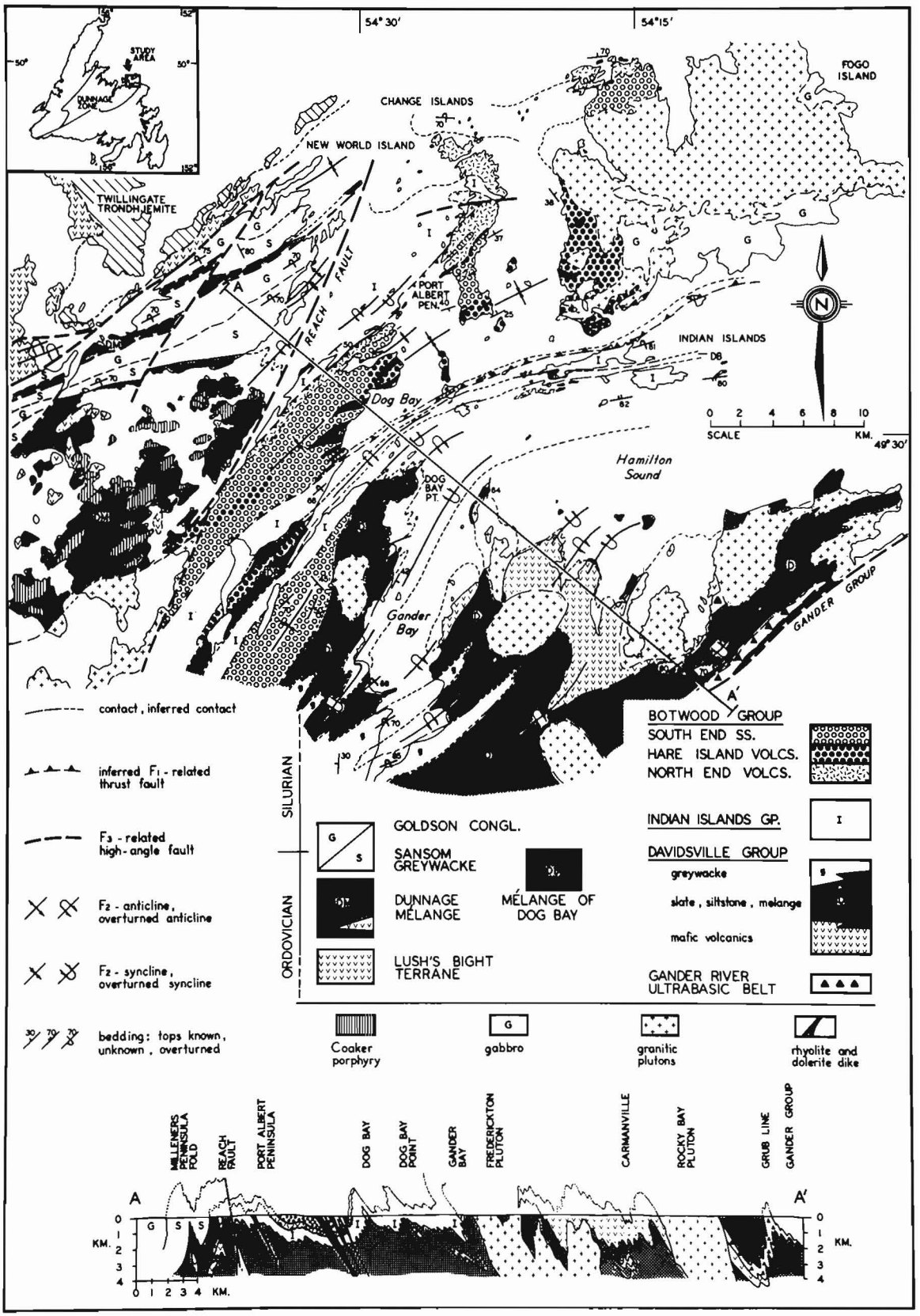

Figure 6.1. *Generalized geologic map and cross-section of the Hamilton Sound area based on new mapping. Includes data from Williams (1964), Baird (1958), Eastler (1971) and Currie et al. (1980a).*

(McKerrow and Cocks, 1977, p. 494). Other workers have suggested that faunas from the Davidsville Group are similar to those found west of the Reach Fault (Stouge, 1980a,b; Nowlan, 1981, p. 10).

In the absence of compelling structural or paleontological evidence for different geologic terranes, it is reasonable to attempt to correlate stratigraphic units across Reach Fault. Indeed, as previously stated, the shallow enveloping surface for F_2 predicts a repetition of stratigraphic units. Pajari et al. (1979, p. 1450) have suggested correlation of the Dunnage Mélange and the Carmanville Mélange of the Davidsville Group on the basis of similar ages and lithologies. I agree with this correlation on the basis of the geometry of macroscopic F_2 folds in the area (Fig. 6.1).

Given such a correlation, the stratigraphy within the Ordovician mélange sequences and correlation of mélanges with more coherent Ordovician stratigraphic units farther west still remain problematical. Dean (1978) has proposed a generalized Ordovician stratigraphy in the eastern Notre Dame Bay area consisting of: 1) pre-Caradocian volcanics, 2) Caradocian shales, and 3) post-Caradocian flysch. The Dunnage Mélange was placed by Dean (1978) into the pre-Caradocian unit because it is interpreted to be a chaotic equivalent of the pre-Caradocian Exploits Group to the southwest and because it appears to conformably underlie Caradocian shales of the Dark Hole Formation (Hibbard and Williams, 1979).

Each lithology in Dean's subdivisions appears to be represented in the Davidsville Group volcanics and volcaniclastic sediments of probable pre-Caradocian age near Carmanville (Pickerill et al., 1981), Caradocian shales near Davidsville (Williams, 1964; Bergstrom et al., 1974) and probable post-Caradocian greywackes near Davidsville (Fig. 6.1). However, stratigraphic succession within the group remains poorly understood. Kennedy and McGonigal (1972) first proposed the name Davidsville Group but did not subdivide it into formations. Subsequently, Currie et al. (1980a,b) Wu (1979), and Blackwood (1981) have all presented lithologic (not stratigraphic) subdivisions of the group (Fig. 6.2). Currie et al. (1980a,b) recognized the presence of coherent sedimentary successions (units 4-8), mélanged equivalents which they interpreted to be olistostromes (units 9, 10), and large allochthons of ultramafics and mafic volcanics (units 1-3) which they interpreted to be both thrust slices (along the Gander River Ultrabasic Belt, i.e. the GRUB line) and olistoliths (west of the GRUB line). Wu (1979) also recognized correlative coherent and chaotic units but he interpreted the volcanic units of the Davidsville Group to be autochthonous volcanic flows and volcaniclastic sediments rather than olistoliths. Blackwood (1981), working farther south, divided the group into three lithological units: conglomerate, shale, and greywacke, overlying the Gander River Ultrabasic Belt. While these lithologic subdivisions are useful, a true stratigraphic understanding of the Davidsville Group has not been possible because of poor understanding of the complex deformation.

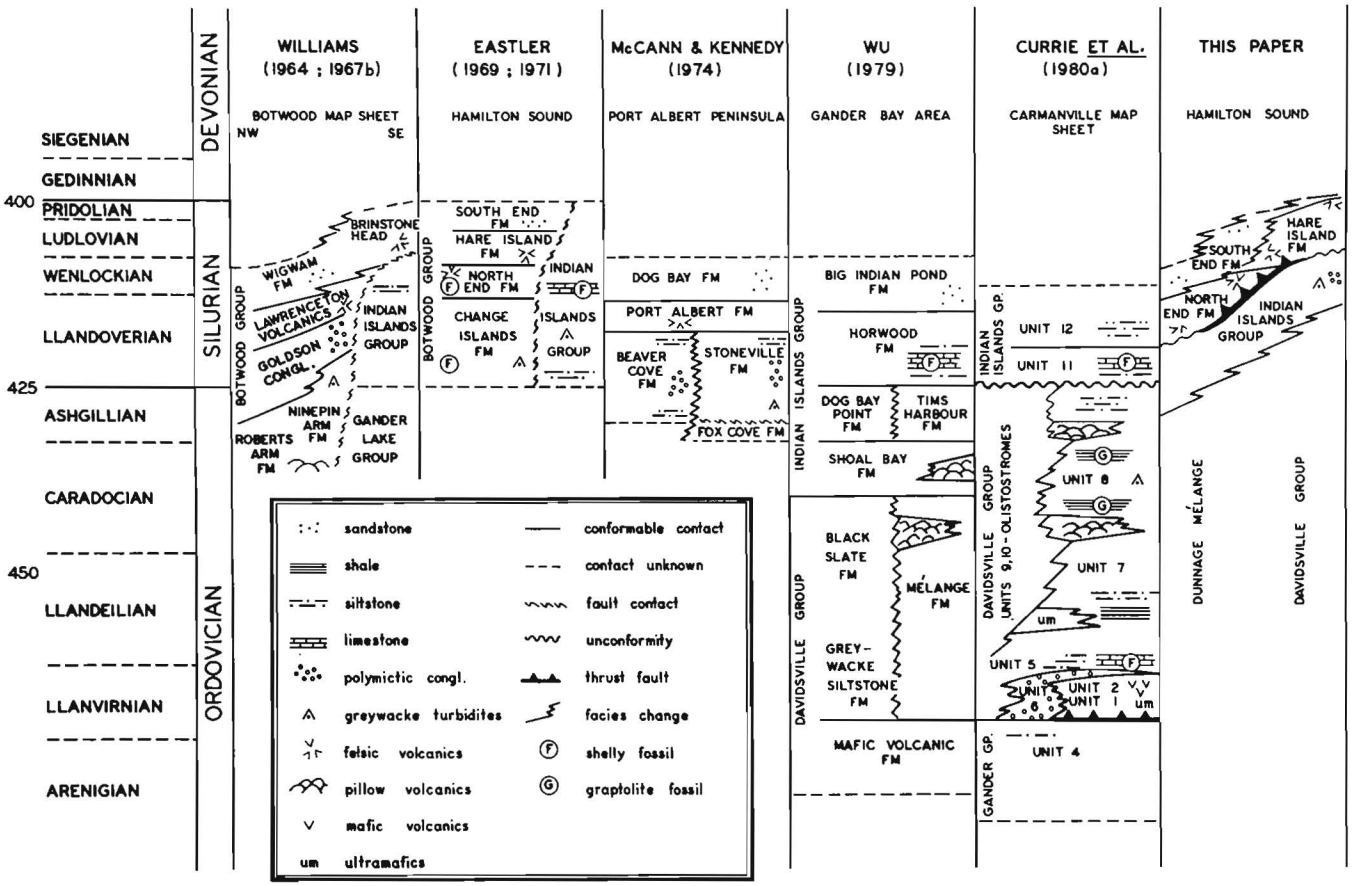

Figure 6.2. *Comparison of stratigraphic nomenclatures used by previous workers in the Hamilton Sound area. Earlier stratigraphic work is reviewed by Williams (1967a) and Dean (1978). The time scale is from Gale et al. (1980).*

All of these workers have assumed a simple northwest-younging homoclinal succession, and have not fully appreciated the effects of F_2 on stratigraphy. Admittedly, where younging evidence is preserved, most beds young towards the northwest. Detailed structural mapping, however, suggests a pattern throughout the Davidsville Group of tight F_2 folds with severely attenuated southeast-younging limbs.

This changes the stratigraphic picture. For example, with the homoclinal interpretation of Currie et al. (1980), the ultramafics west of the Gander River Ultrabasic Belt and the volcanics near Carmanville were believed to be "up-section" from the GRUB line and were interpreted to be large olistoliths derived from an emergent ultramafic thrust slice. In contrast, considering the subhorizontal enveloping surface for F_2, these rocks appear to be part of the GRUB line thrust sheet (or a related thrust sheet), surfacing again due to folding (Fig. 6.1). The syncline just west of the GRUB line is indicated by change of younging directions as well as repetition of ultramafics and volcanics near the Rocky Bay Pluton (see also Currie et al., 1980). The volcanics near Carmanville appear to be related to the GRUB line both chemically and petrologically (Pickerill et al., 1981), and are shown in Figure 6.1 to outcrop in the culmination of a series of doubly plunging F_2 folds. The presence of these folds is well documented in turbidites along the east and west shores of Gander Bay (see also Wu, 1979) and on islands northeast of the volcanics. The folds also affect the volcanics as is shown by the folded trace of the contact between volcanics and adjacent shale and mélange units and by minor folds near this contact.

The present structural interpretation suggests that all the rocks from the Gander Group to Dog Bay Point may be F_2 fold repetitions of the Davidsville Group. The mélange unit extending from Dog Bay to the Indian Islands Tickle (black slate with blocks of siltstone, volcanics, and gabbro) may also be part of the Davidsville Group although no fossils have been found in this unit and its age is therefore not known. In spite of the recognition of F_2 macroscopic folds, no coherent stratigraphy within the Davidsville Group has yet emerged. Apparently the presence of macroscopic F_1 structures, as suggested by the presence of F_1 mesoscopic structures and by downward facing F_2 folds in the Gander Bay area, drastically complicates the stratigraphic picture.

Ordovician – Silurian Transition

Dean's (1978) statement that the Ordovician-Silurian boundary is not well defined in central Newfoundland also applies to the Hamilton Sound area; and attempts by many workers to give this time boundary geologic significance has led to difficulties. The interpretation presented here is that turbidite deposition began in the late Ordovician and continued into Silurian times in the Hamilton Sound area. There is no obvious stratigraphic or structural break which can be ascribed to the Ordovician-Silurian boundary. Williams (1967a) defined the Botwood Group as a Silurian succession consisting of the Goldson Conglomerate, Lawrenceton Volcanics, and Wigwam Formation (Fig. 6.2). He interpreted this succession to represent shallow water deposition which took place in progressively shallowing seas after the closure of the Iapetus Ocean (Williams, 1979), placing great importance upon a pre-Silurian unconformity. However, such an unconformity at the base of the Goldson Conglomerate cannot be demonstrated in the eastern Notre Dame Bay area, as conglomerates are either conformable with or lateral facies equivalents of underlying greywackes (Williams, 1967a, p. 99; Eastler, 1971; Dean, 1978). This led Dean (1978) to remove the Goldson Conglomerate from the Botwood Group and combine it with his post-Caradocian flysch sequence which contains time-transgressive upper Ordovician and lower Silurian sequences. This interpretation is presented in Figure 6.1.

A pre-Silurian unconformity has also been proposed on the basis that Ordovician sequences are more strongly deformed (e.g. contain an extra cleavage) than overlying Silurian successions. This argument was used by Williams (1967a) and Currie et al. (1980b) as evidence that Taconic deformation took place in the eastern Notre Dame Bay area prior to post-orogenic Silurian deposition, the so called "Taconic unconformity". However, this interpretation is questionable in light of structural evidence that Ordovician and Silurian rocks in the Hamilton Sound area record the same three fold generations. Futhermore, my mapping revealed no obvious stratigraphic or structural break between Davidsville Group and Indian Islands Group in the Gander Bay area.

Indian Islands Group

Stratigraphic problems surrounding the Indian Islands Group (Patrick, 1956) have arisen mainly because of a lack of understanding of F_2 deformation. As shown in Figure 6.2, most earlier workers have separated the Indian Islands Group from adjacent units by faults. Williams (1964) distinguished it from the Botwood Group because Indian Islands Group rocks appear more highly sheared. He later suggested that some of the units of the two groups may be correlatives (Williams, 1967a, p. 98). This somewhat ambiguous view was adopted by Eastler (1969, 1971) and Dean (1978). Eastler (1971) believed that the Indian Islands Group was separated from the Botwood Group by the "Indian Islands Thrust" and that the Indian Islands Group represented a separate "structural terrane". However, he suggested that the two "sequences" were stratigraphically identical. Dean (1978) suggested that the Indian Islands Group was probably correlative with parts of the Sansom Greywacke and Goldson Conglomerate.

The confusion can be resolved by recognition of a macroscopic F_2 synclinorium across the Port Albert Peninsula which repeats polymictic conglomerates and turbidites of the Indian Islands Group as well as overlying subaerial volcanics and sandstones of the Botwood Group (Fig. 6.1). Conglomerates on both limbs contain very similar clast assemblages (chert and jasper, rhyolite, dacite and basalt, granitoid, and greywacke, siltstone and limestone) but conglomerates on the east limb are much more highly deformed and the least competent clasts (cherts and sedimentary clasts) are extremely flattened and difficult to distinguish from the matrix. Turbidites on both limbs are thin bedded grey-green siltstones with greywacke, shale, and limestone interbeds. The limestones are locally fossiliferous, frequently containing **Favosites** corals and crinoid fragments. Graded bedding in the turbidites substantiate the synclinal structure across the Port Albert Peninsula. This syncline was also recognized by McCann (1973) and McCann and Kennedy (1974) who proposed new stratigraphic names for all the units on the Port Albert Peninsula. Dean (1978) retained some of McCann's stratigraphic names but applied the names only to the east limb of the syncline. This approach was later followed by Keen et al. (1981).

In Figure 6.1, the following rocks are referred to the Indian Islands Group:

1. turbidites and polymictic conglomerates on the western Port Albert Peninsula previously included in the Farewell Group (Baird, 1958; Patrick, 1956), Goldson Conglomerate (Williams, 1964), Change Islands Formation (Eastler, 1971). Beaver Cove Formation (McCann, 1973) and Sansom Greywacke and Goldson Conglomerate (Keen et al., 1981);

2. strongly deformed turbidites and polymictic conglomerates in eastern Dog Bay, southern Dog Bay Islands, and Indian Islands previously referred to the Indian Islands Group by Patrick (1956), Williams (1964), Eastler (1971) and Keen et al. (1981). Some of these workers also included the overlying volcanics in the Indian Islands Group but I include these in the Botwood Group;
3. siltstones and calcareous siltstones on the east and west sides of Dog Bay Point and on the Dog Islands referred to the Indian Islands Group by Williams (1964) and Currie et al. (1980a, their units 11 and 12) and to both the Davidsville and Indian Islands groups by Wu (1979).

Mappable units in the Indian Islands Group include:

1. grey-green siltstones containing fossiliferous limestones;
2. quartz-rich medium to thick bedded (10-50 cm) turbidites exhibiting well developed Bouma sequences;
3. polymictic conglomerates containing a preponderance of chert pebbles and cobbles; and
4. thin bedded argillites containing an abundance of volcanic detritus. Ultimately, these units can be given formational status but more mapping is required first.

Silurian Subaerial Units

An important stratigraphic break in the Hamilton Sound area is between the marine rocks of the Indian Islands Group (mainly turbidites) and dominantly subaerial rocks of the Botwood Group. In Figure 6.1, the Botwood Group includes subaerial volcanics of the North End Formation (Baird, 1958; Eastler, 1969, 1971), tuffaceous sandstones of the Hare Island Formation (Eastler, 1971), and subaerial sandstones of the South End Formation (Baird, 1958; Eastler, 1969; 1971). For now, I prefer these names to the equivalent names used by other workers, Lawrenceton Volcanics and Wigwam Sandstone (Williams, 1976b; Dean, 1978; Keen et al., 1978), because they provide a better framework to describe local stratigraphic relationships. Most workers agree that these volcanics and sandstones within the Botwood Group are conformably related, and locally intercalated.

The significance of the Botwood Group for regional paleogeographic reconstructions depends upon an interpretation of the lower contact of the group. Dean (1978) suggested disconformity and local faulting on the basis of the contact near Glenwood where Caradocian shales are abruptly overlain by Ludlovian shales in the Wigwam Formation, without the intervening flysch units. Eastler (1971) suggested the contact was partly conformable and partly thrust faulted. The contact near Port Albert can be interpreted to be an F_1-related thrust because of the presence of a zone of F_1 folds along the contact. However, I have also observed areas where the contact appears to be transitional between green siltstones of Indian Islands Group and green volcanogenic rocks of the North End Formation (e.g. western Dog Bay, western Indian Island, and Cann Island).

Perhaps the best interpretation, in view of these various observations, is that subaerial rocks of the Botwood Group were deposited with local conformity and local disconformity upon underlying marine sediments and then were placed in thrust contact with the same units during F_1. (Most contacts were later disrupted by F_3-related high-angle faults.) The similarity in ages between parts of the Indian Islands and Botwood groups, local transitional contacts between the two, and similar faunules found at the base of the North End Formation and in the Indian Islands Group (Eastler, 1971) suggest that depositional conditions underwent a progressive change from deeper to shallower water and terrestrial deposition during the Silurian as suggested by Williams (1979).

Synthesis

The simplest explanation of existing data is that proposed by Dean (1978), that the Ordovician and Silurian stratigraphy of the eastern Notre Dame Bay area is characterized by several broad lithostratigraphic groups. The Davidsville Group appears to represent an attenuated version of the Ordovician sections farther west: pre-Caradocian volcanics and sediments, Caradocian shales, and post-Caradocian greywackes. The stratigraphy within the Davidsville Group appears to have been modified by deformational processes associated with thrusting, olistostromes, or both. The Ordovician-Silurian transition is represented by diachronous deposition of turbidite sequences which generally record shallower depositional conditions with time (Dean, 1978). This shallowing trend continued into Middle Silurian times, as shown by deposition of subaerial volcanics and sandstones of the Botwood Group. The Botwood Group appears to be a para-autochthonous sequence: locally conformable, disconformable, or in thrust fault contact with the turbidites.

This stratigraphic interpretation, combined with an understanding of the subhorizontal enveloping surface of F_2, provides several solutions to stratigraphic problems.

1. It suggests that all of the mélange zones in the northeastern Dunnage Zone (i.e. those in the Cobbs Arm Fault Zone, Dunnage Mélange, Dog Bay, Dog Bay Point, and Carmanville Mélange) could be F_2 fold repetitions of a single extensive Ordovician mélange terrane.
2. It suggests that rocks of the GRUB line (i.e. the thrust slices that make up the GRUB line) outcrop in F_2 fold culminations west of the GRUB line.
3. It suggests repetition of the Indian Islands Group across a syncline in the Port Albert Peninsula and an anticline at Dog Bay Point.
4. It suggests that parts of the Sansom Greywacke and Goldson Conglomerate on New World Island may correlate with the Indian Islands Group.

However, the "unfolding" of F_2 structures does not solve some of the critical stratigraphic problems in the area. One problem is that rocks of the greywacke sequences have varying ages and varying sedimentary characteristics in different areas and it remains unclear how (or if) to correlate them. For example, greywackes on western New World Island are Caradocian and Ashgillian (Dean, 1978; McKerrow and Cocks, 1981); greywackes on eastern New World Island (the Millener's Arm Formation of McKerrow and Cocks, 1978) are late Ordovician and early Silurian and are interpreted to be deep water turbidites; and the Indian Islands Group is Early to Middle Silurian and appears to represent shallower water deposition. These rocks may all represent lateral (and diachronous) facies of a single shelf-slope or fore-arc basin depositional environment. However, if correlation proves untenable on sedimentological or paleontological grounds, these sequences might also represent sediments which were deposited at some distance from each other and juxtaposed during F_1 thrusting.

Another problem is that F_2 deformation provides no explanation for the attenuation and chaotic aspects of the Ordovician sequences. These features have previously been explained in terms of olistostromes (Pajari et al., 1979; Hibbard and Williams, 1979). However, this is just one conceptual model which might be used for the Dunnage Mélange and Davidsville Group. Hsü (1974) noted the difficulty in distinguishing olistostromes from tectonic mélanges where there has been subsequent intense deformation and certainly F_2 folding and cleavage development are intensely developed in the mélange terranes. Furthermore, all of the structural features cited as evidence

for soft rock deformation in these units (e.g. chaotic bedding, disharmonic folds, mélange and boudinage) are also typically found in hard rock terranes which have undergone thrusting.

An alternate working hypothesis is that the observed pre-F_2 stratigraphic and structural complexities are due to thrusting (Brückner, 1978). Thrusting has several advantages as the general explanation for the mélange terranes as well as for the observed distribution of rock units:

1. it explains the widespread temporal and spatial distribution of F_1 structures;
2. it provides a consistent kinematic explanation for the geometry of both F_1 and F_2 structures; and
3. it provides an explanation for the presence and disrupted character of exotic lithologies, like ultramafic rocks of the GRUB line. Obviously, the two interpretations, thrusting and olistostromes, are not mutually exclusive and both would be expected, for example, in subduction complexes (Dickinson and Seely, 1979). However, I share Hamilton's (1979, p. 31) bias that thrusting is by far the more important process in controlling the development and geometry of mélange terranes.

It is important to note that F_1 structures occur throughout the area of Figure 6.1 and in all sedimentary units, from Early Ordovician to Middle Silurian. This suggests that regional thrusting took place in post- Middle Silurian times. If thrusting began earlier, i.e. if it took place over a considerable time interval as might be expected in an orogenic area, F_1 thrusting may have been coincident with the trend towards shallower water depositional conditions. Indeed, it is possible that thrusting, and accompanying thickening and uplift of the sedimentary pile, was the cause of the general shallowing trend.

A plate tectonic model capable of explaining the stratigraphic, sedimentological, and structural features of the area is that of an accretionary terrane associated with subduction. In such a model the mélange sequences represent thrusting within the accretionary wedge; the turbidites represent fore-arc basin deposits; and the subaerial units represent deposition on emergent highlands. As noted by Hamilton (1979, p. 14) sediments commonly are deposited conformably and unconformably on active mélange wedges to subsequently become imbricated into them. This is the situation I envision for the Hamilton Sound area, a subduction-related accretionary terrane active and being deformed in Late Ordovician and Silurian times. The paleogeographic context of this accretionary terrane, i.e. the position of island arcs, continental slopes, subduction zones, etc., will only be understood after we have a better understanding of the extent and geometry of F_1 thrust sheets in the eastern Notre Dame Bay area.

Acknowledgments

Research was sponsored by a Postdoctoral Fellowship from the University of New Brunswick and by E.M.R. Grant No. 179-4-81 to G.E. Pajari. Structural interpretations are the result of collaboration with P.F. Williams and B.A. van der Pluijm. Thanks are due to G.E. Pajari who arranged the postdoctoral fellowship, organized the field project, and spent considerable time acquainting me with the field area. K.E. Currie provided air photographs and useful field discussions. R.K. Pickerill reviewed the manuscript and provided useful and animated discussions during the writing stage. Sherri Townsend typed several versions of the manuscript; Gary Landry drafted the illustrations.

References

Anderson, F.D. and Williams, H.
1964: Gander Lake, (west half), Newfoundland; Geological Survey of Canada, Map 1195A.

Baird, D.M.
1958: Fogo Island map-area, Newfoundland (2E/9, mainly); Geological Survey of Canada, Memoir 301.

Bergstrom, S.M., Riva, J., and Kay, M.
1974: Significance of conodonts, graptolites, and shelly faunas from the Ordovician of western and north central Newfoundland; Canadian Journal of Earth Sciences, v. 11, p. 1625-1660.

Blackwood, R.F.
1981: Geology of the west Gander River area, Newfoundland; in Current Research of the Newfoundland Department of Mines and Energy, Mineral Development Division, Report 81-1, p. 50-56.

Brückner, W.D.
1978: Carmanville map area, Newfoundland; the northeastern end of the Appalachians – Discussion; in Current Research, Part C, Geological Survey of Canada, Paper 78-1C, p. 127-129.

Currie, K.L., Pajari, G.E., and Pickerill, R.K.
1979: Tectonostratigraphic problems in the Carmanville area, northeastern Newfoundland; in Current Research, Part A, Geological Survey of Canada, Paper 79-1A, p. 71-76.

Currie, K.L., Pajari, G.E., and Pickerill, R.K.
1980a: Geological map of the Carmanville Map Area (2E/8), Newfoundland; Geological Survey of Canada, Open File 721.

Currie, K.L., Pajari, G.E., and Pickerill, R.K.
1980b: Comments on the boundaries of the Davidsville Group, northeastern Newfoundland; in Current Research, Part A, Geological Survey of Canada, Paper 80-1A, p. 115-118.

Dean, P.L.
1978: The volcanic stratigraphy and metallogeny of Notre Dame Bay, Newfoundland; Memorial University of Newfoundland, St. John's, Newfoundland, Geology Report 7.

Dickinson, W.R. and Seely, D.R.
1979: Structure and stratigraphy of forearc regions; American Association of Petroleum Geologists Bulletin, v. 63, p. 2-31.

Eastler, T.E.
1969: Silurian geology of Change Islands and eastern Notre Dame Bay, Newfounland; in North Atlantic Geology and Continental Drift, M. Kay, ed., American Association of Petroleum Geologists, Memoir 12, p. 425-432.

Eastler, T.E.
1971: Geology of Silurian rocks, Change Islands and eastern-most Notre Dame Bay, Newfoundland; Unpublished Ph.D. thesis, Columbia University, New York, 143 p.

Gale, N.H., Beckinsale, R.D., and Wadge, A.J.
1980: Discussion of a paper by McKerrow, Lambert, and Chamberlain on the Ordovician, Silurian and Devonian time scales; Earth and Planetary Science Letters, v. 51, p. 9-17.

Hamilton, W.
1979: Tectonics of the Indonesian region; United States Geological Survey, Professional Paper 1078, 345 p.

Hibbard, J.B. and Williams, H.
1979: Regional setting of the Dunnage Mélange in the Newfoundland Appalachians; American Journal of Science, v. 279, p. 993-1021.

Hsü, K.
1974: Mélanges and their distinction from olistostromes; in Modern and Ancient Geosynclinal Sedimentation, R.H. Dott, Jr., ed., Society of Economic Paleontologists and Mineralogists, Special Publication 19, p. 321-333.

Kay, M.
1976: Dunnage Mélange and subduction of the protacadic ocean, northeast Newfoundland; Geological Society of America, Special Paper 175, 49 p.

Keen, B., Dean, P.L., and Strong, D.F.
1981: Regional geology of the central volcanic belt of Newfoundland; in The Buchans Orebodies: Fifty years of Geology and Mining, E.A. Swanson, D.F. Strong, and J.G. Thurlow, ed., Geological Association of Canada, Special Paper 22.

Kennedy, M.J. and McGonigal, M.H.
1972: The Gander Lake and Davidsville Groups of northeastern Newfoundland: new data and geotectonic implications; Canadian Journal of Earth Sciences, v. 9, p. 453-459.

McCann, A.M.
1973: Structural and stratigraphic relationships in Silurian rocks of the Port Albert – Horwood area, Fogo – Twillingate districts, Newfoundland; Unpublished M.Sc. thesis, Memorial University of Newfoundland, 102 p.

McCann, A.M. and Kennedy, M.J.
1974: A probable glacio-marine deposit of Late Ordovician-Early Silurian age from the north central Newfoundland Appalachain belt; Geological Magazine, v. 111, p. 549-564.

McKerrow, W.S. and Cocks, L.R.M.
1977: The location of the Iapetus Ocean suture in Newfoundland; Canadian Journal of Earth Sciences, v. 14, p. 488-495.

1978: A Lower Paleozoic trench-fill sequence, New World Island, Newfoundland; Geological Society of America Bulletin, v. 89, p. 1121-1132.

1981: Stratigraphy of eastern Bay of Exploits, Newfoundland; Canadian Journal of Earth Sciences, v. 18, p. 751-764.

Nowlan, G.S.
1981: Some Ordovician conodont faunules from the Miramichi Anticlinorium, New Brunswick; Geological Survey of Canada, Bulletin 345, 35 p.

Pajari, G.E., Pickerill, R.K., and Currie, K.L.
1979: The nature, origin and significance of the Carmanville ophiolitic mélange, northeastern Newfoundland; Canadian Journal of Earth Sciences, v. 16, p. 1439-1451.

Patrick, T.O.H.
1956: Comfort Cove, Newfoundland; Geological Survey of Canada, Paper 55-31 (map).

Pickerill, R.K., Pajari, G.E., and Currie, K.L.
1981: Resedimented volcaniclastics in the Carmanville area, northeastern Newfoundland – depositional remnants of Early Paleozoic oceanic islands; Canadian Journal of Earth Sciences, v. 18, p. 55-70.

Stouge, S.
1980a: Conodonts from the Davidsville Group, northeastern Newfoundland; Canadian Journal of Earth Sciences, v. 17, p. 268-272.

1980b: Conodonts from the Davidsville Group, northeastern Newfoundland: Reply; Canadian Journal of Earth Sciences, v. 17, p. 1600-1601.

Twenofel, W.H. and Shrock, R.R.
1937: Silurian strata of Notre Dame Bay and Exploits Valley, Newfoundland; Geological Society of America Bulletin, v. 48, p. 1743-1772.

Williams, H.
1964: Botwood map-area, Newfoundland; Geological Survey of Canada, Paper 64-17, pt. II, p. 22-29.

1967a: Silurian rocks of Newfoundland; in Geology of the Atlantic Region; Geological Association of Canada, Special Paper 4, p. 93-137.

1967b: Stratigraphy of Botwood map-area, northeastern Newfoundland; Geological Survey of Canada, Open File 113, 103 p.

1979: Appalachian Orogen in Canada; Canadian Journal of Earth Sciences, v. 16, p. 792-807.

Williams, H., Kennedy, M.J., and Neale, E.R.W.
1972: The Appalachian structural province; in Variations in Tectonic Styles in Canada, R.A. Price, R.Y.W. Douglas, ed., Geological Association of Canada, Special Paper 11, p. 181-262.

1974: The northeastward termination of the Appalachian orogen; in The Ocean Basins and Margins, Volume 2, A.E.M. Nearn and F.G. Stehli, ed., Plenum Press, New York, p. 79-123.

Wu, T.W.
1979: Structural, stratigraphic and geochemical studies of the Horwood Peninsula – Gander Bay area, northeast Newfoundland; Unpublished M.Sc. thesis, Brock University, Ontario, 185 p.

7. **DÉPÔTS MEUBLES DU SECTEUR AVAL DE LA RIVIÈRE COPPERMINE, TERRITOIRES DU NORD-OUEST**

Convention de recherche 2-4-80

Denis A. St-Onge[1] et Hélène C. Bruneau[1]
Division de la science des terrains

St-Onge, Denis A. et Bruneau, Hélène C., Dépôts meubles du secteur aval de la rivière Coppermine, Territoires du Nord-Ouest; dans Recherches en cours, partie B, Commission géologique du Canada, Étude 82-1B, p. 51-55, 1982.

Résumé

L'étude des dépôts meubles du secteur aval de la rivière Coppermine a permis de reconnaître une série de deltas emboîtés et de plages soulevées qui marquent la régression marine postglaciaire depuis un maximum de 170 m a.n.m. En s'encaissant dans ces dépôts, la rivière Coppermine a abandonné des terrasses. Des coquilles marines, des horizons de tourbe et des débris de bois permettront de dater la séquence d'événements depuis la disparition des glaces des basses-terres du golfe du Couronnement.

Introduction

La région étudiée (fig. 7.1, juillet '81) est limitée au sud par les monts Coppermine et September et au nord par le golfe du Couronnement. Les limites est et ouest sont de 5 à 10 km de part et d'autre de la rivière Coppermine. Le but du travail est d'élucider la séquence d'événements qui, depuis la déglaciation, a façonné cette partie des basses-terres du golfe du Couronnement dans la partie nord-centrale du district du Mackenzie, Territoires du Nord-Ouest.

Des travaux antérieurs ont établi l'existence d'un lac glaciaire dans la vallée de la rivière Coppermine au sud des monts September. Le "Lac glaciaire Coppermine" était retenu par la masse de glace qui occupait les basses-terres entre le golfe du Couronnement et les monts September (St-Onge, 1980; St-Onge et al. 1981). Les travaux de Craig (1960) ont en outre établi que le retrait de la glace vers l'est a dû se faire avant 8 300 ans B.P. puisqu'une date obtenue sur des coquilles marines à une altitude d'environ 131 m près de l'embouchure de la rivière Asiak (fig. 7.2) a donné un âge de 8 275 ± 220 ans (I (GSC) -22).

Les levés sur le terrain, effectués au cours du mois de juillet 1981 et une analyse détaillée des photographies aériennes ont permis de dresser une carte des dépôts meubles. Sur celle-ci on distingue très clairement une succession de deltas inscrits dans des sédiments glaciaires et fluvio-glaciaires dans la partie sud de la région et dans des dépôts marins dans le secteur nord. L'apex du plus haut de ces deltas se trouve à 170 m a.n.m. La figure 7.2 schématise les résultats consignés.

Les unités lithologiques

En aval des monts September et Coppermine, la vallée de la rivière Coppermine est entaillée dans des gabbros, des basaltes et des grès du Précambrien (Baragar et Donaldson, 1973). Le pendage vers le nord et la différenciation lithologique ont permis aux agents d'érosion de dégager de spectaculaires cuestas. Dans la partie sud de la région étudiée le relief atteint 300 m.

La roche en place est recouverte d'un till à matrice silteuse qui tapisse complètement les dépressions. Sur les sommets cette unité est discontinue et souvent représentée uniquement par des blocs erratiques épars. Aux rares endroits où elles peuvent être mesurées, les stries indiquent un écoulement vers le nord-ouest. Dans le segment de la vallée occupé par les rapides Muskox (fig. 7.3) un esker composé de crêtes au tracé anastomosé occupe la partie est du fond de la vallée. Après avoir été tronqué par la rivière Coppermine en aval du ruisseau Willow, ce complexe fluvio-glaciaire se poursuit vers le nord-nord-ouest.

Suite au retrait du front glaciaire, l'invasion marine atteint la cote actuelle de 170 m a.n.m. Ce niveau maximum est marqué par un delta dont l'apex (point A, fig. 7.2) se distingue bien sur la photo aérienne (fig. 7.3). La partie amont se trouve en contact avec l'esker et il est vraisemblable que la rivière Coppermine ancestrale a remanié une partie des sédiments fluvio-glaciaires lors de la mise en place de ce haut delta. La surface plane du delta est constituée de blocs, graviers et sables et est parcourue par de nombreux chenaux abandonnés, en partie occupés par des lacs ou des étangs. Deux autres deltas soulevés marquent des phases du retrait de la mer postglaciaire, suite au relèvement isostatique.

À 2 km en amont de Bloody Fall 40 m de silts, d'argiles et de sables fins interstratifiés témoignent de l'importance de la sédimentation de fines dans les parties profondes (30-60 m) du bras de mer postglaciaire. Dans quelques horizons, de 5 à 8 m d'épaisseur, la stratification de ces rythmites marines a été profondément déformée par des courants de turbidité.

Dans les parties peu profondes de la mer, de grandes quantités de sables ont été mis en place. Ces sédiments tapissent de grandes étendues de faible relief entre les collines de roche en place, depuis le niveau actuel de la mer jusqu'à 160 m a.n.m. On trouve également des plages soulevées constituées de sables grossiers et de petits graviers. Ces dépôts, mis en place par l'action des vagues et de courants marins à partir de sédiments fluviatiles, ont été soulevés jusqu'à 70 m a.n.m. lors du relèvement isostatique postglaciaire. En général, ces sables reposent sur des silts marins, et au contact de ces deux unités il est fréquent de trouver d'abondants coquillages marins.

Le lit de la rivière actuelle est souvent encaissé dans la roche en place, mais des sédiments grossiers forment des îles et des lambeaux de plaine alluviale. Les principaux rapides tels ceux de Muskox, Sandstone, Escape et Bloody Fall correspondent à des seuils de roches plus résistantes.

Sur les revers de cuesta, les mouvements de masses ont remanié les sédiments. Le processus le plus important est certes la solifluxion qui forme des lobes qui garnissent la partie inférieure des crêtes et collines.

La tourbe atteint des épaisseurs de 3 m dans les fonds d'anciens lacs. Des débris de buissons sont une partie importante de ces dépôts organiques.

[1] Département de géographie, Université d'Ottawa, Ottawa, Ontario, K1N 6N5

Figure 7.1. *Carte de localisation et synthèse des travaux antérieurs*

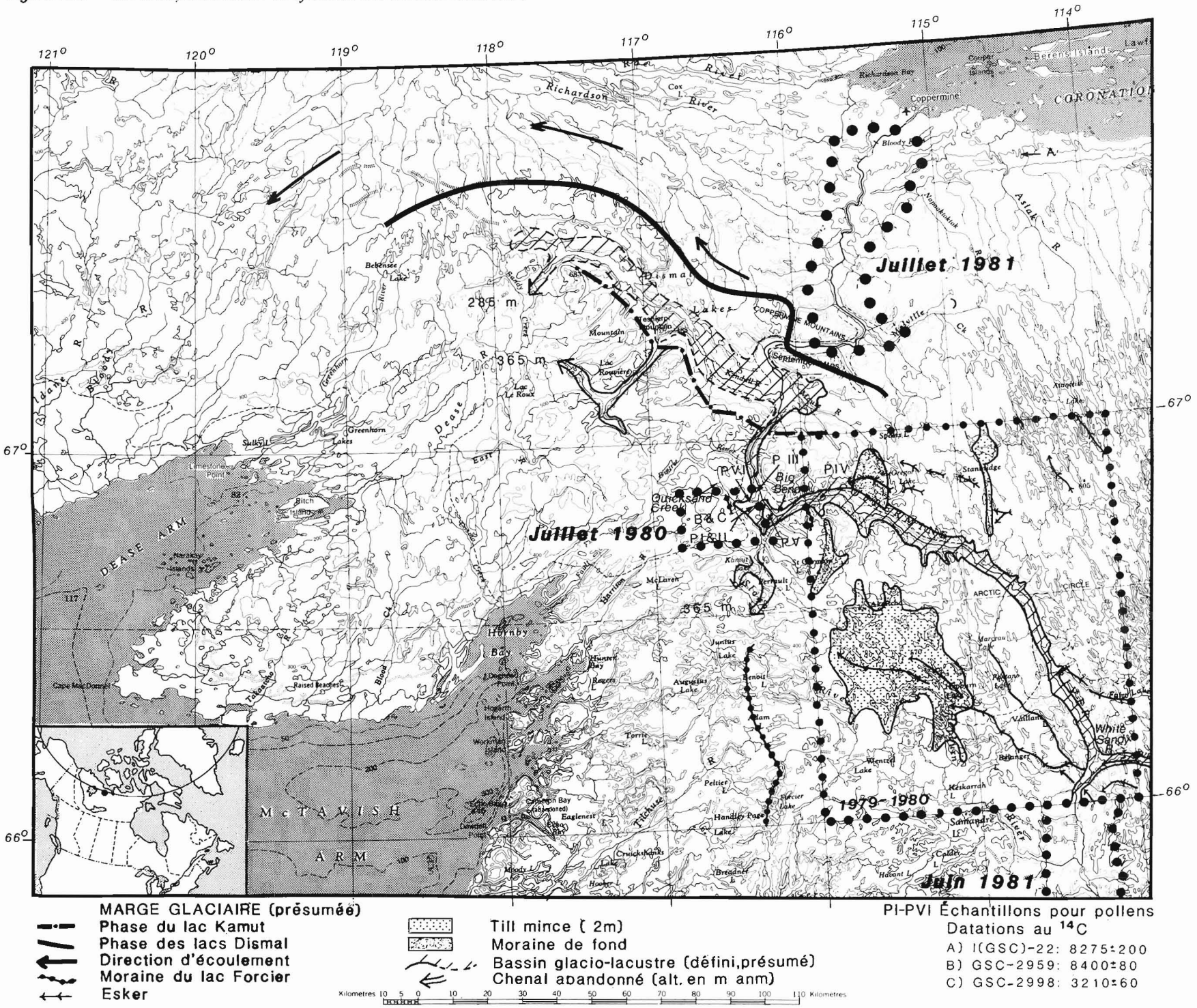

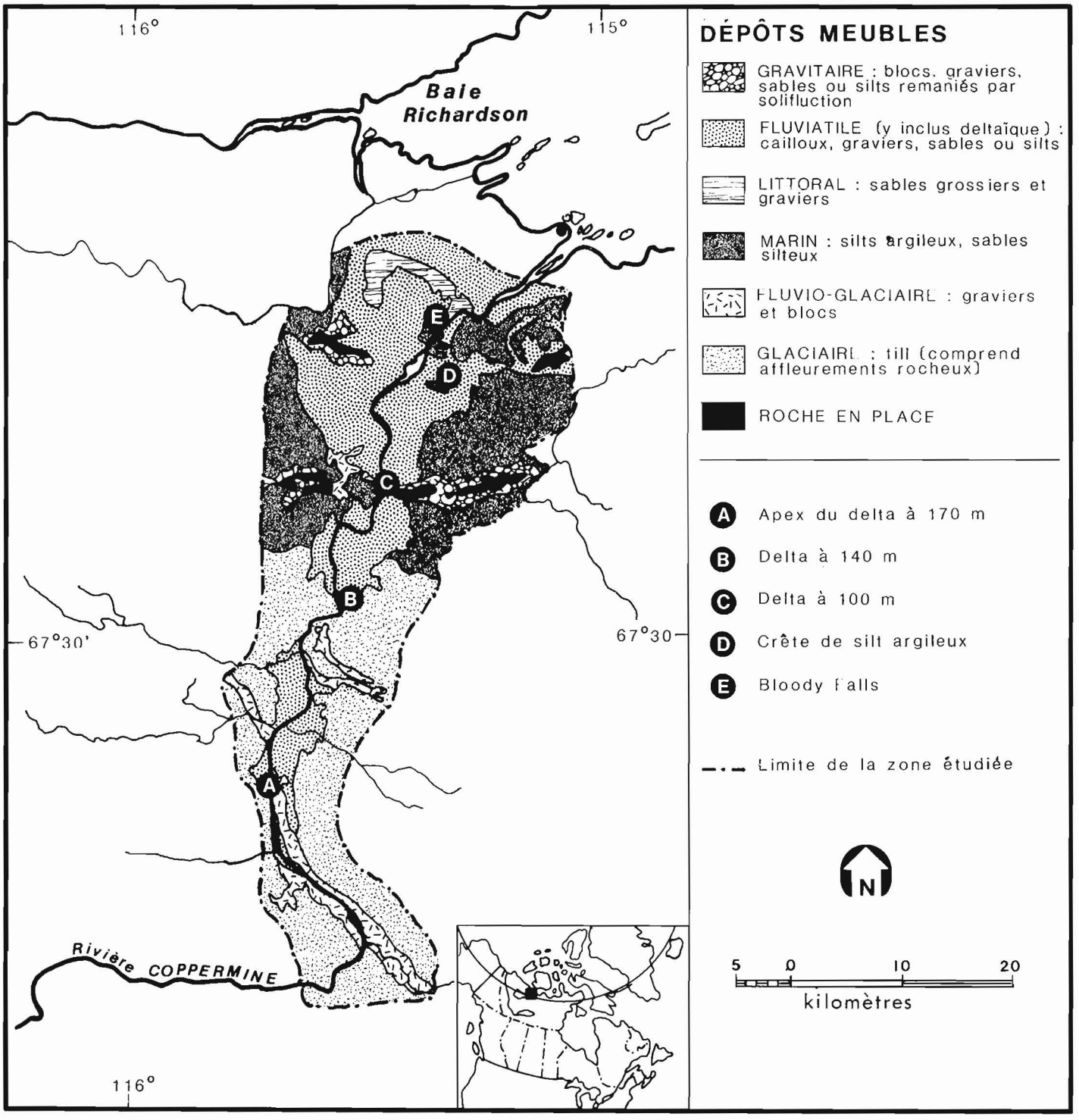

Figure 7.2. *Lithologie des dépôts meubles*

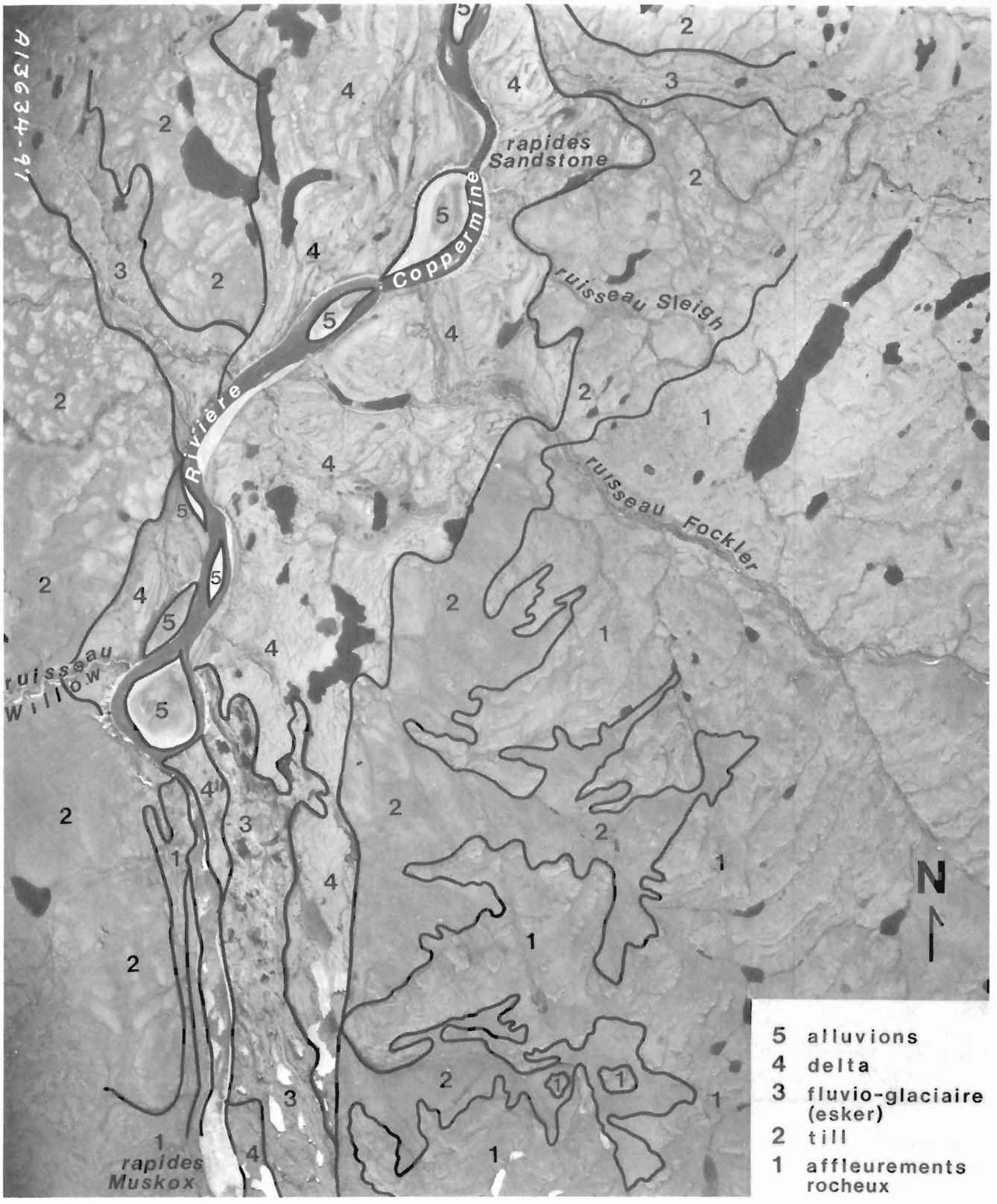

Figure 7.3 *Complexe deltaïque de 170 m a.n.m. (région du point A de la figure 7.2)*

Interprétation

Le résultat (W. Blake, comm. pers.) d'une datation au ^{14}C de coquillages marins à 110 m a.n.m. (9820 ± 90 ans, GSC-3327) indiquent que les basses-terres du golfe du Couronnement étaient libres de glace il y a plus de 10 000 ans. Ce retrait du front glaciaire a permis à la rivière Coppermine de reprendre son tracé vers le nord et au lac glaciaire, qui occupait une partie de sa vallée en amont des monts September et Coppermine, de se vidanger.

Un diamicton qui remplit un réseau de vallées entaillées dans la roche en place entre les monts September-Coppermine et les chutes de Bloody Fall représente, vraisemblablement, une sédimentation résultant d'une ou plusieurs coulées de laves torrentielles. Cette unité lithologique fera l'objet d'une étude ultérieure.

Les sédiments grossiers transportés par la rivière Coppermine sont mis en place sous forme de très grands deltas qui progressent vers le nord au fur et à mesure du relèvement isostatique. Les sables sont redistribués par les courants et les vagues le long des rivages successifs étagés entre 160 m a.n.m. et la côte actuelle. Les argiles et les silts, déposés en eau plus profonde, sont maintenant exposés dans des coupes de plus de 40 m de hauteur.

Le soulèvement isostatique, qui fait migrer le rivage vers le nord, provoque l'encaissement de la rivière dans ses propres sédiments puis dans les assises rocheuses sous-jacentes. C'est à ce mécanisme que l'on doit les nombreuses terrasses étagées en escalier et les gorges étroites à parois verticales taillées dans les grès rouges des groupes de Rae et de Coppermine River (Baragar et Donaldson, 1973).

Faute de datations au radiocarbone, il n'est présentement pas possible d'établir une courbe d'émersion. Les travaux de cartographie ont cependant permis de fixer l'altitude maximale de la transgression marine postglaciaire et d'établir les principaux jalons de l'évolution géomorphologique de la partie aval de la vallée de la rivière Coppermine. Les travaux des étés à venir permettront de détailler cette première ébauche.

Remerciements

Des subventions offertes par le Groupe de recherches nordiques de l'Université d'Ottawa, le Conseil national des recherches, le ministère de l'Énergie, des Mines et des Ressources et le ministère des Affaires indiennes et du Nord ont permis le travail sur le terrain. Nous sommes particulièrement reconnaissants à M.W. Padgham, géologue résident, M.A.I.N., Yellowknife et à M.P. Hoffman de la Commission géologique du Canada pour l'aide logistique.

Bibliographie

Baragar, W.R.A. and Donaldson, J.A.
1973: Coppermine and Dismal Lakes map-areas; Commission géologique du Canada, Étude 71-39, 20 p.

Craig, B.G.
1960: Surficial geology of north-central District of Mackenzie, Northwest Territories; Commission géologique du Canada, Étude 60-18, 8 p., carte 24-1960.

St-Onge, D.A.
1980: Glacial Lake Coppermine, north-central District of Mackenzie, Northwest Territories; Journal canadien des sciences de la Terre, vol. 17, n° 9, p. 1310-1315.

St-Onge, D.A., Geurts, M.A., Guay, F., Dewez, V., Landriault, F., et Léveillé, P.
1981: Aspects of the deglaciation of the Coppermine River region, District of Mackenzie; dans Recherches en cours, partie A, Commission géologique du Canada, Étude 81-A, p. 327-331.

8.

GOLD AND TUNGSTEN ABUNDANCE VS. GRAIN SIZE IN TILL AT WAVERLEY, NOVA SCOTIA

Project 780016

R.N.W. DiLabio
Terrain Sciences Division

DiLabio, R.N.W., Gold and tungsten abundance vs. grain size in till at Waverley, Nova Scotia; in Current Research, Part B, Geological Survey of Canada, Paper 82-1B, p. 57-62, 1982.

Abstract

The abundances of gold and tungsten were determined in up to 11 grain size fractions separated from the matrix (<4.0 mm) of till collected near a former gold mine. Gold levels in the samples drop markedly from >10 000 ppb to <500 ppb in the first 300 m down-ice from the source, and the most auriferous size range shifts from all fractions <0.5 mm to the 0.063-0.002 mm fractions over the same distance. The <0.063 mm fraction is recommended as the optimum size fraction for gold analysis of till derived from the Meguma Group. Tungsten is most abundant in the 2.0 to 0.25 mm and <0.002 mm fractions, and the 0.5 to 0.25 mm fraction is recommended for analysis. Grains of gold and scheelite were identified in the samples by SEM techniques.

Introduction

One of the common problems faced in the geochemical analysis of till in mineral exploration is the choice of a representative grain size range for analysis. This report presents data on the abundance of gold and tungsten with respect to grain size in till collected down-ice from a saddle reef gold deposit in Nova Scotia. Additional work of this type on a larger set of trace elements in till is in progress (W.W. Shilts, personal communication, 1981).

Dreimanis and Vagners (1971) have shown that minerals are glacially comminuted (crushed and abraded) so that each mineral species in till has peaks of abundance in specific size ranges, although the position of the size ranges on the grain size scale may be dependent on the texture of source rocks for the till (Haldorsen, 1977). For each specific set of source rocks, therefore, the choice of the optimum size ranges for geochemical analysis of till should take into account the size ranges to which ore minerals are glacially comminuted, a consideration that is often omitted in routine orientation surveys.

Although detailed work has been performed on the abundance of common rock-forming minerals in different grain size fractions of till (Dreimanis and Vagners, 1971; Lindén, 1975; Haldorsen, 1977), most studies concerned with ore minerals and elements have been limited to selected size fractions (Kauranne, 1967; Shilts, 1973; Ayras, 1977). Only a few studies have dealt with ore minerals and elements in the full range of grain sizes in till matrix (<2 mm) (Eriksson, 1973; Smith and Gallagher, 1975; Klassen and Shilts, 1977; DiLabio, 1979, 1981).

Procedures

Samples known to contain significant amounts of gold and tungsten were selected from an archived collection to represent increasing distances down-ice from the exhausted gold deposit at Waverley, about 20 km north of Halifax. Coarse grained gold occurred there with scheelite and arsenopyrite in a narrow quartz-carbonate vein in greywackes of the Meguma Group. This deposit is considered to be representative of several others in Nova Scotia (Malcolm, 1929).

A portion of each sample was dry sieved to recover composite samples of fines (<0.037 or <0.063 mm), then the oversize was wet sieved to wash out adhering fines, dried, and dry sieved at 1ϕ intervals. Fractions coarser than 0.063 mm were ground to powder. A fraction <0.002 mm was recovered by centrifugation and decantation of a separate portion of each sample.

Gold analysis was performed by the fire assay-atomic absorption technique after digestion in HCl-HNO_3. Ten grams of sample was analyzed, except for the <0.002 mm fraction, of which only 1.0 to 2.5 g was available for analysis. Tungsten analysis was performed by colorimetry after sintering. Analyses were performed by Bondar-Clegg and Co. Ltd., Ottawa.

Heavy minerals were recovered from the 0.25 to 0.063 mm fraction of selected samples using methylene iodide (s.g. = 3.3) as the heavy liquid. These separates were examined with a scanning electron microscope (SEM) using CRT displays of both secondary and backscatter electron images. Qualitative analyses of grains seen in the displays were obtained using energy dispersive X-ray techniques.

Gold in Till

As expected, the gold content of the till samples decreased with increasing distance down-ice from the source (Table 8.1, Fig. 8.1). The decrease is most pronounced in the first 250 m; beyond that distance, gold contents of most of the fractions are relatively low. This rapid decrease in gold abundance with distance down-ice is consistent with the logarithmic-like abundance curve postulated by Shilts (1976) for glacially dispersed rocks and minerals. An attempt was made to map the gold content of the till, but this failed because till was absent in much of the area, most of the available samples are gold-poor (<10 ppb), and because the village of Waverley is built on most of the land that should have been sampled. In addition, high within-site variation at sites near the source would have made mapping difficult. The variability is illustrated by the data for eight samples collected from a soil profile 250 m down-ice from the source (Table 8.1). Although almost all the data for the eight samples are considered highly anomalous, orders of magnitude shifts in gold content of the same size fraction are evident in samples collected only 25 cm apart. This within-site variation could have been caused by the so-called 'nugget effect', by the original mineralogical variability in the till, or by hydromorphic redistribution of gold during postglacial weathering. The nugget effect occurs when a small but variable number of gold-rich grains controls the gold content of a large volume of sample. It is believed to have caused the high gold contents in the 4-2 mm fraction of samples 78 NS 165 and 78 NS 162 because high gold contents were not detected in adjacent size ranges in these samples. The nugget effect is also suspected in the 1-0.5 mm fraction of sample 79 NS 48 and in the 0.5-0.25 mm fraction of sample 78 NS 170.

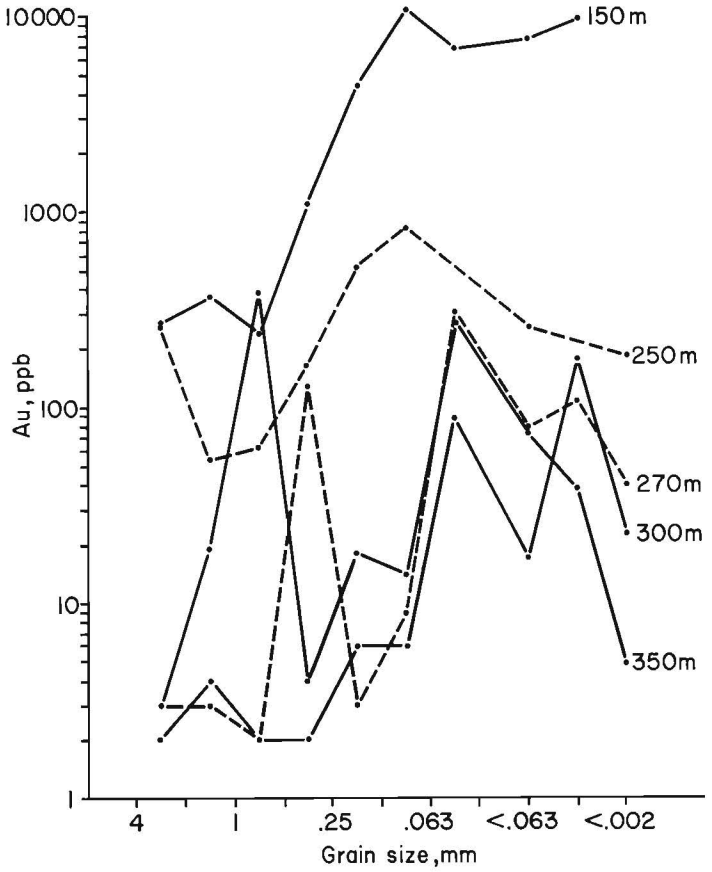

Figure 8.1. *Abundance of gold vs. grain size of analyzed fraction of till at varying distances down-ice from the gold deposit at Waverley, Nova Scotia. Curve for 250 m is the average of data for eight samples (Table 8.1); other curves represent one sample each. Curves for samples at 250 and 270 m down-ice are dashed for clarity.*

Circumstantial evidence exists for hydromorphic redistribution of gold in a comparison of gold data (Table 8.1) with tungsten data (Table 8.2) for samples 78NS159 to 78NS166. If it is assumed that the tungsten in the till is purely a clastic component (the resistate scheelite, identified in these samples by SEM), and that scheelite and gold had exactly the same bedrock source, the data for the two metals should follow similar shifts from high to low values up the section. Because the data are dissimilar, it could be said that gold has been redistributed hydromorphically in the upper metre of the soil profile. This interpretation is, however, tentative.

In the choice of the optimum grain size range for geochemical analysis for gold, one must consider which size range is most auriferous, whether different size ranges are useful at different distances from the source, and whether an adequate quantity of the chosen size range is recoverable by simple techniques. Ignoring the high data that are believed to have been caused by the nugget effect in the coarse size ranges, gold is most abundant in the fine sand, silt, and clay sizes of most of the samples (Table 8.1, Fig. 8.1). Near the source, gold is abundant in all size ranges, but it is most abundant in size ranges finer than 0.5 mm (sample 79 NS 53). Farther down-ice, represented by samples 250 m from the source, a mode appears in the abundance curve in the size range 0.25-0.063 mm; significantly less gold is found in finer and coarser size ranges. At distances more applicable to the size of 'typical' geochemical sampling programs, ie., greater than 250 m from the source, the mode in the abundance curve seems to have shifted into the size range 0.063 to 0.002 mm. The overall decrease in gold content and the shifts in the mode in the abundance curve with increasing distance down-ice may have been the combined result of a number of factors: glacial smearing of gold on other grains, a process that would reduce the grain size of the gold; the deposition of auriferous till; and the erosion of gold-poor rock down-ice from the source, which would lower the gold content of the debris in transport. The glacial comminution of gold cannot be compared directly to the comminution of the more common minerals studied by Dreimanis and Vagners (1971) because of the high malleability and ductility of gold. In addition, the samples from Waverley are all from the oxidized part of the soil profile, and hence some hydromorphic redistribution of gold may have taken place, as suggested above for samples 78 NS 159 to 78 NS 166.

Based on the data from Waverley, differing optimum grain size ranges for geochemical analysis might be proposed for use at different distances from a presumed gold source, but it is more efficient to choose one size range that is useful at all distances. Because of the mode in the abundance curves of samples collected more than 250 m from the source, the chosen size range should include the 0.063 to 0.002 mm range. The use of only one sieve would simplify recovery of the fraction to be analyzed, and thus a choice of the <0.063 or <0.037 mm fraction seems warranted. Because of the more sturdy construction and lower cost of 0.063 mm sieve cloth in comparison to 0.037 mm sieve cloth, and because of the relative ease with which an adequate weight of sample (>10g) can be recovered from even very sandy till with a 0.063 mm sieve, the <0.063 mm (<230 mesh) fraction is recommended for gold analysis. It must be noted that this recommendation is made only for till derived from the Meguma Group and use of the <0.063 mm fraction is not recommended in other terranes unless similar grain size experiments show that the <0.063 mm fraction is more widely applicable.

When the <0.063 mm fraction is compared to the traditional <0.177 mm (<80 mesh) fraction that is commonly used in soil geochemistry, it can be seen that the <0.177 mm fraction will be diluted by gold-poor fine and very fine sand (Table 8.1). The three samples collected more than 250 m from the source have very low gold levels in their 0.25 to 0.063 mm fractions, a feature which suggests that analysis of the <0.177 mm fraction would produce gold levels that are partially dependent on the fine sand content of the samples. Therefore, the <0.177 mm fraction is not recommended for gold analysis of the Meguma-derived till.

Tungsten in Till

Only the eight samples collected from a soil profile 250 m down-ice from the ore zone contained significant quantities of tungsten (Table 8.2), so down-ice variations in tungsten content could not be determined.

As noted above in the discussion of the gold data, there is high within-site variation in the tungsten data. Again, if it is assumed that the tungsten in the till is a chemically stable clastic component (scheelite), then the original mineralogical variability of the till and the nugget effect could have caused the high variation in tungsten content down the soil profile. In spite of this variation, tungsten is clearly most abundant in the same grain size ranges of all eight samples. The peaks of abundance are in the size ranges 2 to 0.25 mm and <0.002 mm. This distinct bimodal distribution of tungsten may have resulted from glacial abrasion of coarse grains of relatively soft, cleavable scheelite which produced the second mode in the <0.002 mm fraction.

Although the <0.002 mm fraction is highly enriched in tungsten, this fraction is not recommended for analysis unless the sample preparation laboratory is equipped to recover fine fractions by centrifugation and decantation. As an

alternative, a coarse fraction provides essentially the same information and requires only simple sieving techniques. Because of the smaller number of grains present in equal volumes of coarser fractions than finer fractions, coarser fractions are more prone to the nugget effect. Therefore, the 0.5 to 0.25 mm fraction is recommended for tungsten analysis. The same caveat stated in reference to gold analysis concerning the restriction of this recommendation to Meguma-derived till must be applied to the selection of the optimum size fraction for tungsten analysis.

Comparison of the 0.5 to 0.25 mm fraction to the traditional <0.177 mm fraction (<80 mesh) shows that the <0.177 mm fraction would be diluted by tungsten-poor fine sand and silt; therefore, the <0.177 mm fraction is not recommended for tungsten analysis of Meguma-derived till, at least for samples within 250 m of a presumed source. A larger set of samples should be tested to show the applicability of the 0.5 to 0.25 mm fraction or a finer one at greater distances.

Mineralogy of the Till

In an attempt to identify particulate gold in the till, the nonmagnetic heavy minerals (s.g. >3.3) in the most auriferous samples were examined with a binocular microscope and the SEM. Identification of the minerals was based on grain morphology, colour, and qualitative analysis by energy-dispersive X-ray techniques during examination with the SEM. In the backscatter electron image produced by the SEM, the brightness of a grain is proportional to its average atomic number, so gold grains can be found easily by this technique.

The heavy mineral suites are dominated by ilmenite, garnet, and unidentified silicate minerals. Zircon, scheelite, and monazite are present in small amounts (Fig. 8.2). The scheelite grains are clean, slightly pitted, unevenly fractured, and most show one set of cleavage planes (Fig. 8.2c).

Gold was not seen in heavy mineral separates from fractions containing 1000 to 3000 ppb gold. Light mineral fractions were also searched unsuccesfully for gold which may have been present as composite grains with vein quartz or smeared on light minerals. The apparent lack of gold grains in samples containing 1000 to 3000 ppb gold in their fine sand fractions could occur because 1 to 3 grains per million gold could easily be absent from the small samples used in the SEM. Moreover, gold may be present in coatings on other grains as very small detrital or reprecipitated grains that are below the resolving power of the SEM.

Sand-sized gold was found in sample 79 NS 53, which contained 4500 to 11 000 ppb in its fine sand fractions (Table 8.1). In the backscatter mode of the SEM, the gold grains appear as bright, globular flakes surrounded by grey grains of other minerals (Fig. 8.3). The gold has a rough surface, and pits in its surface are packed with aluminosilicate-rich mud (dark patches on backscatter images, Fig. 8.3c) that probably consists of clay minerals and iron oxides. The gold itself contains trace amounts of silver. The shape of the gold grains suggests that they have not been transported far or that they are secondary grains, unlike the thin striated flakes described by McDonald (1966) which probably were deformed during glacial transport.

Table 8.1

Gold content (ppb) of various grain size ranges of till at increasing distances down-ice from the vein

Distance from vein (m)	Sample number	Depth (cm)	Grain size (mm) 4-2	2-1	1-0.5	0.5-0.25	0.25-0.125	0.125-0.063	0.063-0.037	<0.063	<0.037	<0.002
150	79 NS 53	50	270	370	240	1110	4500	10900	7000	7800*	10100	-
250	78 NS 166	50	35	65	110	120	1955	3445	-	285*	-	200
250	78 NS 165	110	925	30	30	45	50	145	-	210	-	200
250	78 NS 164	135	20	35	55	50	35	45	-	190*	-	170
250	78 NS 163	160	25	70	35	520	1210	1155	-	145*	-	150
250	78 NS 162	185	945	70	95	295	250	1330	-	600*	-	250
250	78 NS 161	210	65	70	40	40	65	260	-	240*	-	280
250	78 NS 160	245	30	55	60	30	15	25	-	220*	-	150
250	78 NS 159	280	15	35	75	230	635	290	-	150*	-	100
270	78 NS 170	150	3	3	2	130	3	9	310	80	110	41
300	78 NS 169	150	< 2	4	2	2	6	6	90	25	180	23
350	79 NS 48	50	3	19	390	4	18	14	280	75*	39	5

*Average of two determinations

Table 8.2

Tungsten content (ppm) of various grain size ranges of till

Sample number	Depth (cm)	Grain size (mm) 4-2	2-1	1-0.5	0.5-0.25	0.25-0.125	0.125-0.063	<0.063	<0.002
78 NS 166	50	3	90	< 2	4	< 2	2	7*	12
78 NS 165	110	2	3	4	12	3	2	8	20
78 NS 164	135	16	18	14	14	3	2	9*	10
78 NS 163	160	40	550	950	390	300	240	155*	390
78 NS 162	185	36	100	110	70	70	65	85*	200
78 NS 161	210	34	500	220	180	110	110	85*	560
78 NS 160	245	16	20	110	80	40	36	25*	200
78 NS 159	280	19	16	36	32	20	20	25*	52

*Average of 2 determinations

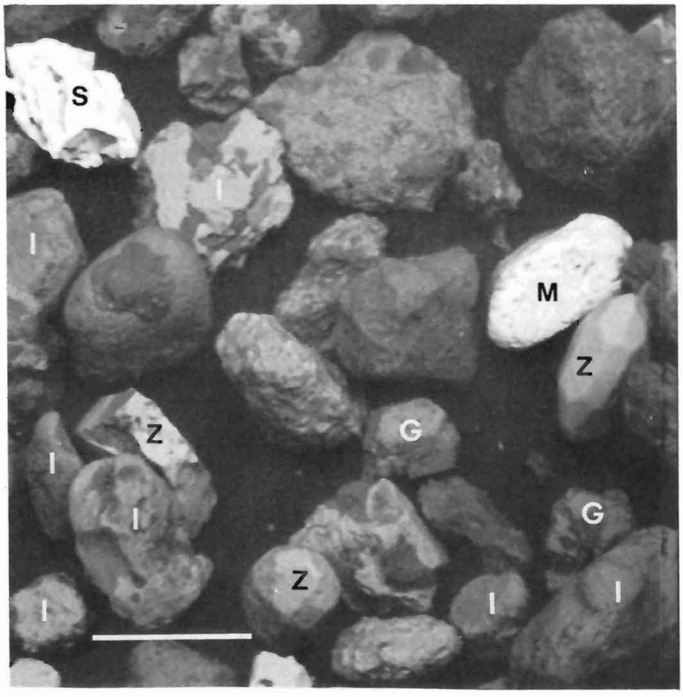

(a)

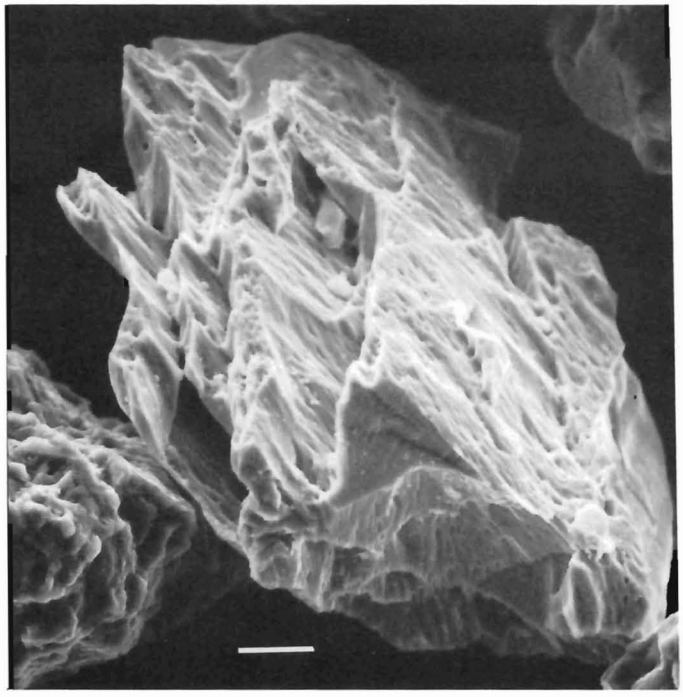

(c)

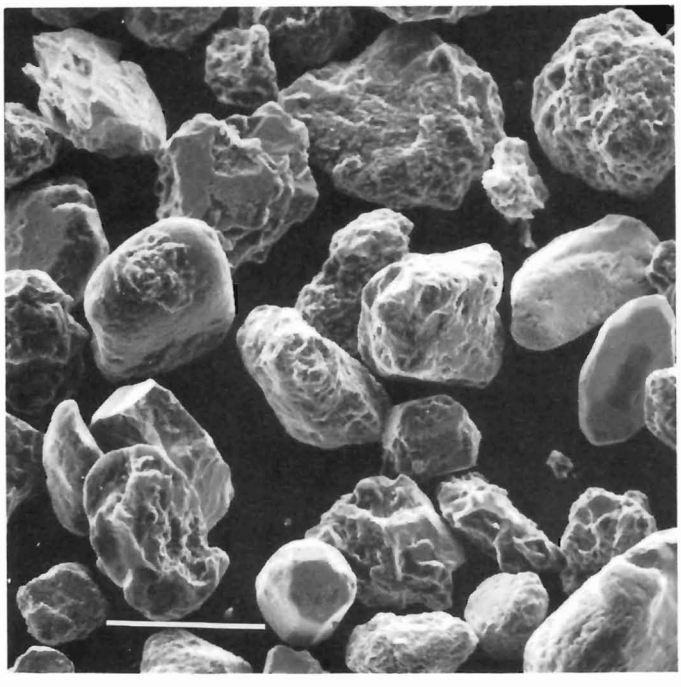

(b)

Figure 8.2. *SEM photos of sand-sized heavy minerals in sample 78 NS 163.*

(a) Backscatter image.
I = ilmenite, S = scheelite,
G = garnet, M = monazite;
Z = zircon,

unlabelled grains are unidentified silicate minerals. Scale bar is 0.1 mm long.

(b) Secondary image of the same field shown in Figure 8.2a. Scale bar is 0.1 mm long.

(c) Secondary image of scheelite grain shown in Figure 8.2a, b. Scale bar is 0.01 mm long.

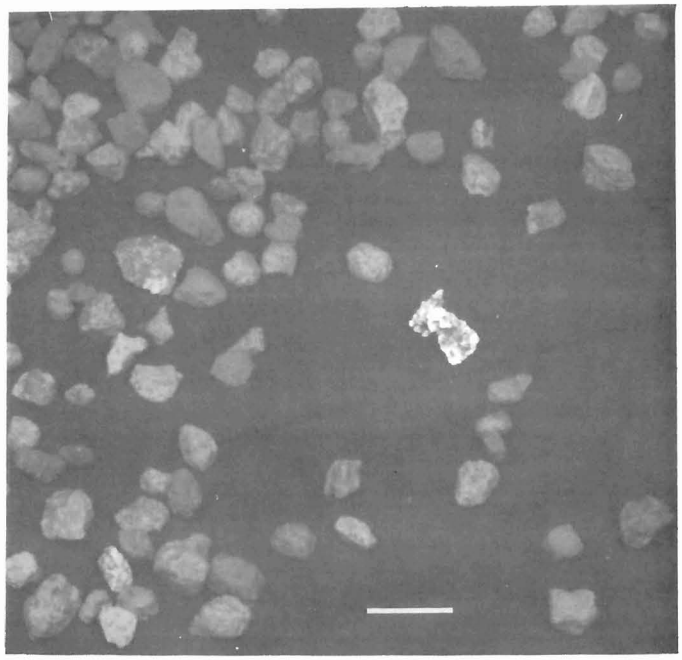

(a)

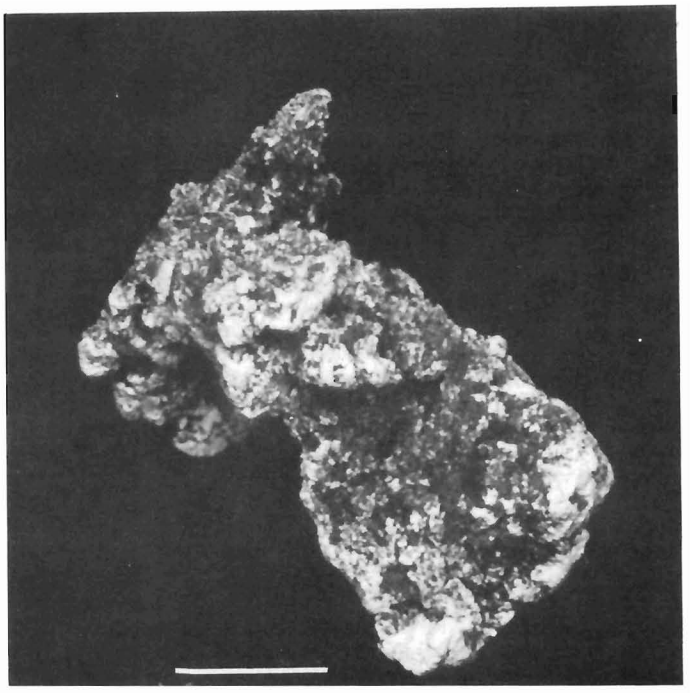

(c)

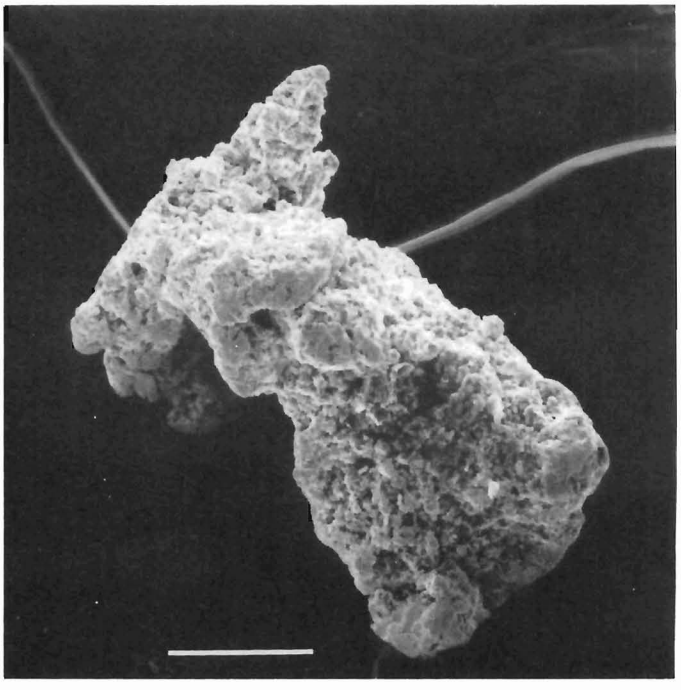

(b)

Figure 8.3. *SEM photos of sand-sized heavy minerals in sample 79 NS 53.*

(a) Backscatter image showing bright gold grain. Scale bar is 0.5 mm long.

(b) Secondary image of gold grain shown in Figure 8.3a. Scale bar is 0.1 mm long.

(c) Backscatter image of gold grain shown in Figure 8.3a. Scale bar is 0.1 mm long.

Conclusions

In the till at Waverley, the most auriferous grain size range shifts rapidly from < 0.5 mm to 0.063 - 0.002 mm and the gold content of the samples decreases with increasing distance down-ice from the gold source. The <0.063 mm fraction is recommended as the optimum size fraction for gold analysis of till derived from the Meguma Group. Particulate gold was found only in the most auriferous sample. The form in which the gold is present in the other samples is unknown, but the small size of the samples searched with the SEM does not eliminate particulate gold as one of the forms.

Tungsten is most abundant in the size ranges 2 to 0.25 mm and < 0.002 mm in the small number of samples that were examined. The 0.5 to 0.25 mm fraction is recommended as the optimum size fraction for tungsten analysis of till derived from the Meguma Group. Scheelite grains are common in the heavy minerals of the tungsten-rich samples.

Acknowledgments

The author thanks M. Rupners and P. Wyatt for their cheerful work in the field. D.A. Walker, M. Bonardi, and D. Paré helped with the SEM work. Valuable criticism of the manuscript was made by R.W. Boyle and W.W. Shilts.

References

Äyräs, M.
1977: Statistical observations on the element distribution in the fine material of till, Sodankylä, northern Finland; Geological Survey of Finland, Report of Investigation No. 14, 41 p.

DiLabio, R.N.W.
1979: Drift prospecting in uranium and base-metal mineralization sites, District of Keewatin, Northwest Territories, Canada; in Prospecting in Areas of Glaciated Terrain 1979, Institution of Mining and Metallurgy, London, p. 91-100.

1981: Glacial dispersal of rocks and minerals at the south end of Lac Mistassini, Quebec, with special reference to the Icon dispersal train; Geological Survey of Canada, Bulletin 323, 46 p.

Dreimanis, A. and Vagners, U.J.
1971: Bimodal distribution of rock and mineral fragments in basal tills; in Till/A Symposium, ed. R.P. Goldthwait; Ohio State University Press, Columbus, p. 237-250.

Eriksson, K.
1973: The distribution of some metals in different till fractions; Bulletin of the Geological Institutions of the University of Uppsala, v. 5, p. 157-164.

Haldorsen, S.
1977: The petrography of tills - a study from Ringsaker, South-eastern Norway; Norges Geologiske Undersøkelse, Nr. 336, 36 p.

Kauranne, L.K.
1967: Facts to be noticed in pedogeochemical prospecting by sampling and analysing glacial till; in Geochemical prospecting in Fennoscandia, ed. A. Kvalheim; Interscience, New York, p. 273-277.

Klassen, R.A. and Shilts, W.W.
1977: Glacial dispersal of uranium in the District of Keewatin, Canada; in Prospecting in Areas of Glaciated Terrain 1977, Institution of Mining and Metallurgy, London, p. 80-88.

Lindén, A.
1975: Till petrographical studies in an Archaean bedrock area in southern central Sweden; Striae, v. 1, p. 1-57.

Malcolm, W.
1929: Gold fields of Nova Scotia; Geological Survey of Canada, Memoir 156, 253 p.

McDonald, B.C.
1966: Auriferous till in the eastern townships, southeastern Quebec; in Report of Activities, Geological Survey of Canada, Paper 66-2, p. 51-54.

Shilts, W.W.
1973: Drift prospecting; geochemistry of eskers and till in permanently frozen terrain: District of Keewatin, Northwest Territories; Geological Survey of Canada, Paper 72-45, 34 p.

1976: Glacial till and mineral exploration; in Glacial Till, ed. R.F. Legget; Royal Society of Canada, Special Publication No. 12, p. 205-224.

Smith, R.T. and Gallagher, M.J.
1975: Geochemical dispersion through till and peat from metalliferous mineralization in Sutherland, Scotland; in Prospecting in Areas of Glaciated Terrain 1975, ed. M.J. Jones; Institution of Mining and Metallurgy, London, p. 134-148.

9. SAPROLITE IN THE BIG BALD MOUNTAIN AREA, NEW BRUNSWICK

Project 730019

J.J. Veillette and F.M. Nixon
Terrain Sciences Division

Veillette, J.J. and Nixon, F.M., Saprolite in the Big Bald Mountain area, New Brunswick; in Current Research, Part B, Geological Survey of Canada, Paper 82-1B, p. 63-70, 1982.

Abstract

Three holes were drilled in the Big Bald Mountain area of New Brunswick during October 1980 to sample at depth and to provide geological control for seismic refraction surveys aimed at determining the thickness of saprolite. Cores showed that granite and metasediments occur in this part of the granitic batholith and are chemically altered to depths of several metres and at one location to at least 26 m. No evidence of glacial transport was found at the drilling sites. A model, which consists of an upper layer of loose surficial sediments, an intermediate saprolite layer containing lenses of relatively fresh rock, and a lowermost layer of unaltered rock, is derived from the drilling information. It is presented to assist in the interpretation of the seismic refraction data for the area and possibly for other locations where saprolite is found in Eastern Canada. Ultrasonic wave velocity and bulk density measured on 20 core samples showed that a positive correlation exists between the two properties. Strongly altered granite samples have velocities 30 to 50% those of fresh rock.

An organic, water soluble drilling fluid additive (Revert) allowed drilling and sampling of saprolite using a light-weight rotary drill without the need for casing. Highly viscous Revert mixed with Borax powder diluted in water was effective in sealing fractured rock where excess loss of circulation fluid was experienced.

Introduction

Gauthier (1980) described grus several metres thick and chemically altered granite in the Big Bald Mountain area of north-central New Brunswick. The unusual thickness of the grus led to further investigation; seismic refraction surveys were run during the summers of 1979 and 1980 (Gagne, 1982) to determine depth to competent bedrock and as such provide an estimate for the thickness of the grus. The 1980 seismic survey was done along closely spaced grid lines to map bedrock topography and to identify subsurface materials on the basis of seismic velocities.

Four holes were drilled for this study during the period October 16-31, 1980 in the same area covered by the 1980 seismic survey (Fig. 9.1) in order to provide geological control for the interpretation of the seismic refraction data and to obtain samples of grus and saprolite (rock rotted in situ, i.e. chemically altered but coherent and not texturally disintegrated; Becher, 1895) at depth. Ultrasonic wave velocity and bulk density were measured on selected core sections in the laboratory.

The combination of stratigraphic, structural, lithological, and geophysical information derived from this drilling project results in a subsurface model that not only complements the seismic refraction surveys done in the Big Bald Mountain area but may be of assistance in other areas with similar covers of thick saprolite.

Drilling equipment and field procedure are described in Appendix 1.

Acknowledgments

C. Gauthier selected the drilling sites and provided information on the terrain conditions while planning the project. C. Wang, Agriculture Canada, estimated the degree of chemical alteration of four core samples, and C. Kamineni, Atomic Energy of Canada Ltd., described thin sections of the metamorphic rock. Bulk density of selected core samples was measured by J.A. Baker in the Soil Classification Laboratory, Land Resource Institute, Agriculture Canada, Ottawa. Core sections were prepared for ultrasonic wave velocity measurements in the Lapidary Laboratory of the Geological Survey of Canada. R. Good measured the ultrasonic wave velocities. A.S. Dyke critically read the paper.

Geology

Big Bald Mountain is underlain by the northeastern extension of a Devonian granitic batholith (Fig. 9.1). The batholith is surrounded by greywackes, metabasalts, schists, and phyllites of the Ordovician Tetagouche Group.

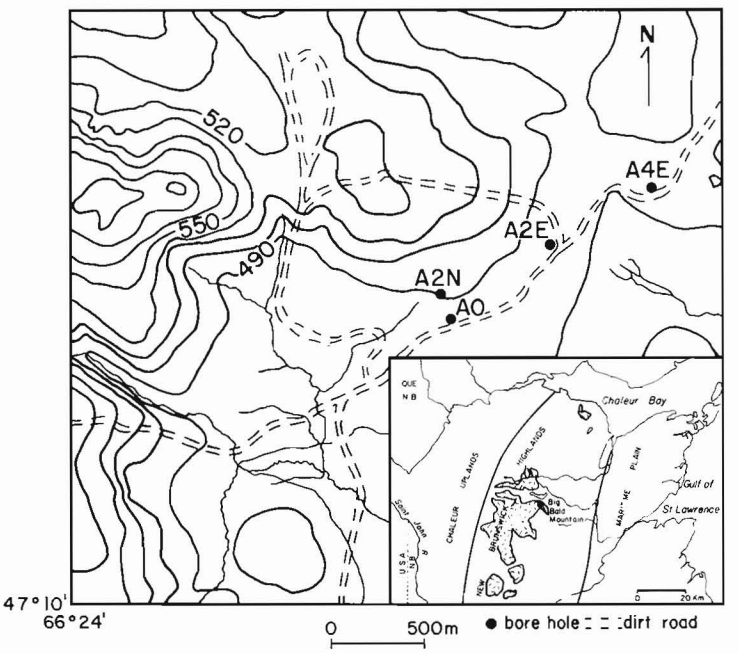

Figure 9.1. Location of boreholes and extent of the Devonian granitic batholith (after Gauthier, 1980) in the Big Bald Mountain area of north-central New Brunswick. Elevation in metres.

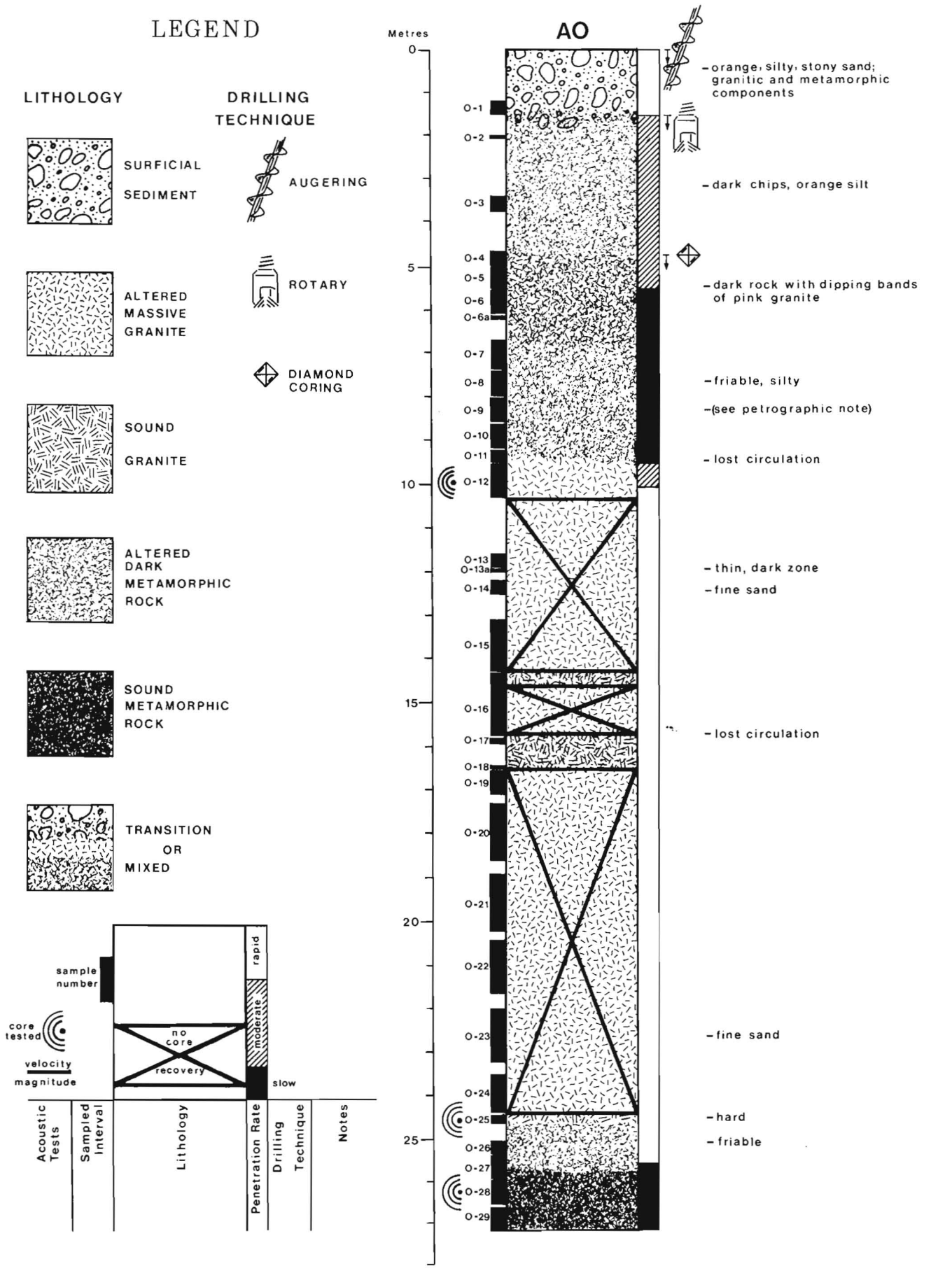
LEGEND
LITHOLOGY
DRILLING TECHNIQUE
SURFICIAL SEDIMENT
AUGERING
ROTARY
ALTERED MASSIVE GRANITE
DIAMOND CORING
SOUND GRANITE
ALTERED DARK METAMORPHIC ROCK
SOUND METAMORPHIC ROCK
TRANSITION OR MIXED
sample number
core tested
velocity magnitude
no core recovery
rapid
moderate
slow
Acoustic Tests
Sampled Interval
Lithology
Penetration Rate
Drilling Technique
Notes
Metres
AO
0-1
0-2
0-3
0-4
0-5
0-6
0-6a
0-7
0-8
0-9
0-10
0-11
0-12
0-13
0-13a
0-14
0-15
0-16
0-17
0-18
0-19
0-20
0-21
0-22
0-23
0-24
0-25
0-26
0-27
0-28
0-29
- orange, silty, stony sand; granitic and metamorphic components
- dark chips, orange silt
- dark rock with dipping bands of pink granite
- friable, silty
- (see petrographic note)
- lost circulation
- thin, dark zone
- fine sand
- lost circulation
- fine sand
- hard
- friable

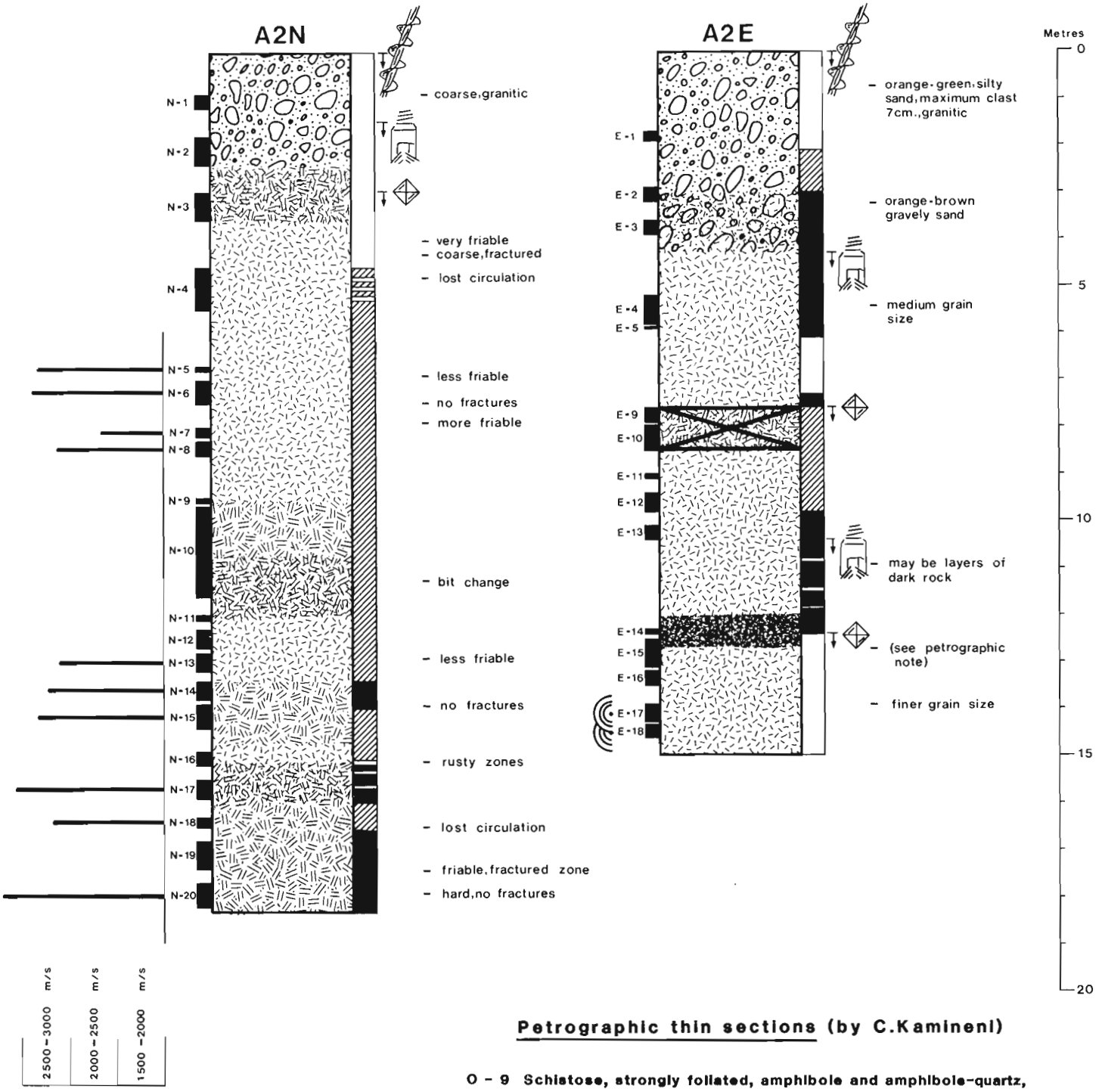

Petrographic thin sections (by C.Kamineni)

O - 9 Schistose, strongly foliated, amphibole and amphibole-quartz, plagioclase layers. Amphibole layers leached of iron oxides. Fracture fill goethite. Amphibolite facies

E - 15 Folded fine amphibole , clinopyroxene, quartz, plagioclase, epidote, biotite, and opaque minerals layer and coarse grained olive pyroxene, garnet, sphene, and plagioclase layer. Amphibole facies.

Figure 9.2. Drill logs showing subsurface conditions and drilling data at A0, A2N, and A2E. Seismic velocities from selected A2N samples are shown.

Drillhole logs are shown in Figure 9.2 for three holes, designated AO, A2E, and A2N, where bedrock has been mapped as intrusive Devonian granite (Gauthier, 1980). Another hole (A4E, Fig. 9.1), not described here, was the first hole drilled in the area and, from the point of view of field procedure, was largely experimental. It reached a depth of 2.60 m and had chips of a black metamorphic rock at the base interpreted as Ordovician rocks of the Tetagouche Group correctly mapped as such at this location.

Holes AO, A2N, and A2E confirm the presence of deep in situ chemical alteration in both massive intrusive granite and metamorphic rock. The unconsolidated surface materials at all three sites appear to have been derived solely from the underlying bedrock. Hand lens and microscopic examination of the sand fraction of samples in this upper zone failed to reveal mineral constituents other than those present in the underlying bedrock. Near AO, especially south of it, large black boulders and blocks of metamorphic rock occur, but these are similar to the metamorphic rock drilled through at AO. This suggests that these boulders and blocks are 'weathered out' inclusions rather than glacial erratics. At A2E from 12 to 12.5 m depth metamorphic rock of possible intrusive origin occurs in the granite, whereas at A2N, granite is the only rock present in the subsurface. At A2E and A2N no boulders or blocks of black metamorphic rock were observed at the surface in the immediate vicinity of the holes.

Some disagreement exists as to the location of the contact between granite and metasediments in the southern Big Bald Mountain area. Anderson (1969) placed the contact between the granite and the metasediments farther north than did Fyffe (1972a,b) and Irrinki (1972). Gauthier (1980) accepted Anderson's contact on the inference that the contact location of Fyffe and Irrinki may have been influenced by the presence of metasedimentary 'erratics' within the batholith margins. Numerous blocks and boulders ('weathered out' inclusions) south and southwest of AO and the thickness of metasediments drilled at AO show that metasediments do outcrop in the area. Although these observations are valid only for the immediate vicinity of AO, the possibility of mistaking "weathered out" inclusions for glacial erratics in other parts of the Big Bald Mountain area must be considered.

Gauthier (1980) recognized till overlying grus on parts of the batholith. The till was identified primarily on the basis of a high percentage of erratic granules and pebbles of parasedimentary rock, volcanic rock, and schist. The possibility that the 'erratic' materials are also 'weathered out' inclusions should be retained. The "weathering out" hypothesis finds support in past and possibly present intense chemical weathering and related erosional features, the latter being numerous in the Big Bald Mountain area.

Drilling, in addition to pointing out the problems associated with the use of lithological indicators to explain ice movement, showed that saprolite, present at all drill sites, extends to a depth of 26 m at AO. This is still a minimum depth, for chemical alteration may be present below this level at other locations. Samples E-1 and E-15 (1.8 m and 13 m) at A2E and N-8 and N-19 (8.5 m and 17 m) at A2N (Fig. 9.2) have been chemically altered (C. Wang, personal communication, 1981), with the intensity of alteration decreasing with depth. Gibbsite and kaolinite are found in the upper part of the bedrock whereas only kaolinite occurs at greater depth.

Subsurface Model

A subsurface model (Fig. 9.3) based on drilling information is presented to assist in the interpretation of seismic data. The model applies specifically to areas where granitic loose surficial sediments or granite outcrops and is based primarily on holes A2E and A2N. The assumption is made that the lithology and subsurface conditions shown in the model are representative for most of the areas underlain by granite and that the number of occurrences of nongranitic rocks at shallow depth decreases inward from the batholith margins. Big Bald Mountain is in the eastern extension of the batholith, where the granitic rock forms a narrow band bounded by nongranitic rocks (Fig. 9.1). This proximity to the margin may explain the presence of metasediments in two of the three drillholes. For this reason, metamorphic rock is included in the model. It could be omitted for areas well behind the batholith margins where only granite is likely to occur.

The model shows a loose sandy, silty, gravelly sediment in the uppermost layer, an intermediate saprolite layer (granite cores were commonly found to be sufficiently coherent to be preserved in the core barrel but could be easily crushed between the fingers), and a lowermost layer of hard, massive granite.

Structural discontinuities were encountered in all three boreholes. These were revealed by 'rotten' or lost sections of core, by major losses of drilling fluid, and by drill behaviour such as sudden short rapid advances of the bit and local high rates of penetration. Rock fractures enlarged by weathering are probably responsible for the major losses of circulation fluid experienced at AO and especially in the granite at A2N at 5 and 17 m (Fig. 9.2). Infiltration of meteoric water along these fracture planes may have created major zones of discontinuity in the bedrock extending well below the weathering front (Fig. 9.3).

As both the metamorphic and granitic rocks of Big Bald Mountain are chemically altered it is important to try to evaluate the effects that variations in chemical alteration of

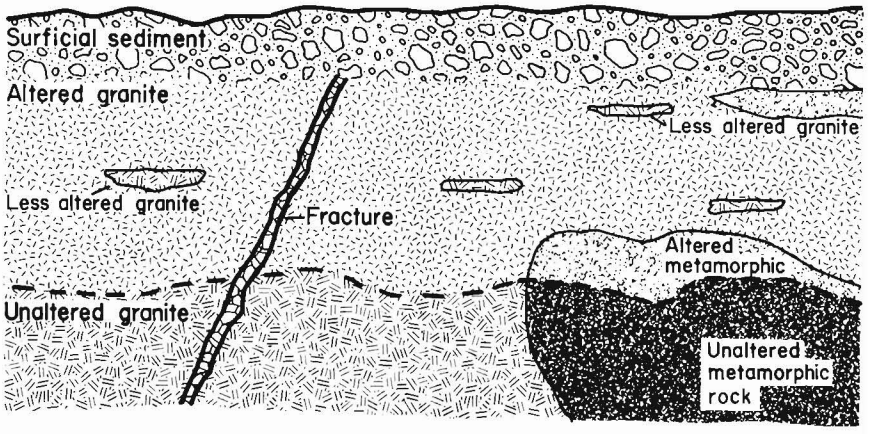

Figure 9.3

Subsurface model for saprolite on the batholith in the Big Bald Mountain area, north-central New Brunswick. The interface between chemically unaltered and less altered granite is referred to as the weathering front.

the same lithology have on seismic velocities. Although chemical weathering generally decreases with increasing depth, abrupt variations exist in degree of chemical alteration especially in the intermediate saprolite layer where relatively 'fresh' rock is found within 'rotten' rock (Fig. 9.2). The less altered rock, from the point of view of seismic refraction, is a high velocity refractor, so an appreciation for these subsurface conditions is of special concern for the interpretation of seismic refraction data.

Implications of Subsurface Conditions on the Interpretation of Seismic Results

R.M. Gagne (personal communication, 1981) converted the geological model into a basic three-layer velocity model for the interpretation of seismic data. From preliminary interpretation of seismic data, Gagne, prior to drilling had suspected the presence of high velocity refractors within the subsurface (which drilling revealed to be dense metamorphic rocks). Because high velocity refractors may also result from sound, fresh, or less weathered granite lenses occurring within a 'rotten' granitic mass, core samples representative of different chemical alteration conditions for the granite were selected for laboratory measurements of bulk density and ultrasonic wave velocity (Table 9.1) to be correlated with velocities obtained in the field. The apparatus and procedure used to measure the acoustic wave velocities of core samples are described by Kurfurst (1977).

Because of suspected porosity in certain cores due to chemical alteration and because of their irregular shapes, bulk density had to be determined by immersion in water. The method selected (McKeegue, 1970, p. 32) and commonly used by pedologists for determining bulk density for soil samples involves coating the cores with Dow Saran Resin to prevent water penetration. The cores were then prepared for ultrasonic wave velocity measurements by removing the resin coating with the circular steel brush of a bench-grinder before being soaked in hot epoxy liquid. This last step was necessary to prevent disintegration of the saprolite when trimmed with a diamond saw. More friable cores or those with marked planes of weakness, despite this precaution, could not withstand the pressures applied during the ultrasonic tests and some failed. Cores for ultrasonic wave velocity measurements must be cylinders with both extremities at right angles to the core axis. Although the epoxy liquid in the cores theoretically could have affected the ultrasonic velocities, this was probably negligible because the epoxy acted as a jacket on the surface of the cylinders and did not penetrate deeply into the core.

The velocities obtained on granite cores at A2N show that high velocity refractors (harder, less chemically altered granite lenses) are erratically distributed within the saprolite. A general increase in velocity with increasing depth is necessary for a successful application of the seismic refraction method. If these lenses are large, they could probably prevent an accurate determination of depth to competent bedrock using the seismic refraction method; if, on the other hand, the hard granite lenses are of limited extent, the intermediate layer (saprolite) of the model (Fig. 9.3) can be treated as one more or less homogeneous layer from a seismic refraction point of view. Although drilling at A2N was not deep enough to establish a distinct passage from saprolite to unaltered granite at each of the three sites, penetration rate (Fig. 9.2), bulk density, and seismic velocity of cores (Table 9.1) towards the base of the hole suggest that a zone of transition, more abrupt than gradual, was reached.

The presence of important structural 'discontinuities' within the subsurface, interpreted as fractures enlarged by weathering, will, especially if they extend well below the weathering front, result in an overestimate of 'overburden' thickness.

Table 9.1

Density, ultrasonic wave velocities, and visual characteristics of 20 selected core samples from the Big Bald Mountain area. Core diameter is 41.3 mm.

Sample	Depth (m)	Bulk Density	Core Length (mm)	Compressional Velocity (m/s)	Test Pressure (kPa)	Remarks
A0-4	4.8	3.03	Sample unsuitable for velocity test			- dark rock, dense, heavy
A0-12	10.3	2.46	83.4	2490	1378	- strongly altered granite
A0-25	24.6	2.55	84.1	4924	1378	- hard granite, more K-spar
A0-27	25.7	2.90	82.7	4285	1102	- dark rock, dense
A0-28	26.6	2.67	83.8	5601	1102	- dark rock, dense
A2N-5	6.8	2.49	83.9	2837	1378	- strongly altered granite
A2N-6	7.5	2.49	85.1	2924	1378	- moderately altered granite
A2N-7	8.2	2.40	84.7	2148	827	- strongly altered granite
A2N-8	8.6	2.40	84.1	2620	1378	- strongly altered granite
A2N-11	12.4	2.53	Sample unsuitable for velocity test			- fresh granite
A2N-13	13.2	2.50	82.1	2605	1654	- moderately altered granite
A2N-14	13.8	2.52	88.5	2717	1378	- moderately altered granite
A2N-15	14.4	2.50	83.7	2818	1378	- moderately altered granite
A2N-16	15.2	2.43	Sample failed during test			- strongly altered granite
A2N-17	15.9	2.49	84.1	3057	1654	- hard, more K-spar granite
A2N-18	16.5	2.54	84.3	2677	1378	- fresh, hard granite
A2N-20	18.2	2.57	83.1	3209	1378	- fresh, hard granite
A2E-15	13.0	3.05	84.8	7380	1102	- dark rock, dense, heavy
A2E-17	14.3	2.48	83.3	2398	1378	- moderately altered granite
A2E-18	14.6	2.48	81.7	2577	1378	- moderately altered granite

Conclusions

Drilling in this part of the Big Bald Mountain area revealed primarily that (1) granite and metasediments occur in the subsurface (<30 m), (2) no evidence exists of glacial transport at the drill sites, (3) chemical alteration of bedrock occurred at depth in both granite and metasediments, and (4) evidence of chemical alteration exists to a depth of 26 m.

A subsurface model derived from drillhole information serves as an aid in the interpretation of refraction seismic surveys aimed at mapping the thickness of the saprolite. Although the model is specifically for use in the Big Bald Mountain area, it may be of assistance to those interested in subsurface investigation of saprolite at other locations in Eastern Canada.

The measurement of ultrasonic wave velocity and bulk density in the laboratory on selected core samples showed that a positive correlation exists between the two properties. The more chemically altered the sample, the lower the bulk density and velocity measurements. Velocities of strongly altered granite samples are 30 to 50 per cent those of fresh granite or metamorphic rock.

References

Anderson, F.D.
1969: Geology of Big Bald Mountain, New Brunswick; Geological Survey of Canada, Map 1220A, scale 1:50 000.

Becher, G.F.
1895: Reconnaissance of the gold fields of the southern Appalachians; in Annual Report of The United States Geological Survey, no. 16, pt. 3, p. 251-331.

Fyffe, L.
1972a: Geology of lower North Branch Little S.W. Miramichi River; Mineral Resources Branch, New Brunswick Department of Natural Resources, Plate 72-80, Map M-10, scale 1:15 625.

1972b: Upper parts South Branch Sevogle River; Mineral Resources Branch, New Brunswick Department of Natural Resources, Plate 72-89, Map M-9, scale 1:15 625.

Gagne, R.M.
1982: Shallow refraction seismic survey Big Bald Mountain, New Brunswick area; Geological Survey of Canada, internal Report, 7 p., maps and diagrams.

Gauthier, C.
1980: Decomposed granite, Big Bald Mountain area, New Brunswick; in Current Research, Part B; Geological Survey of Canada, Paper 80-1B, p. 277-282.

Irrinki, R.R.
1972: Upper parts of South Branch Sevogle River; Mineral Resources Branch, New Brunswick Department of Natural Resources, Plate 72-92, Map N-10, scale 1:15 625.

Kurfurst, P.J.
1977: Acoustic wave velocity apparatus; in Report of Activities, Part A; Geological Survey of Canada, Paper 77-1A, p. 16.

McKeegue, J.A.
1978: Manual on Soil Sampling and Methods of Analysis; Canadian Society of Soil Scientists, Ottawa, 212 p.

Veillette, J.J. and Nixon, F.M.
1979: Portable drilling equipment for shallow permafrost sampling; Geological Survey of Canada, Paper 79-21, 35 p.

APPENDIX 1

Drilling Equipment and Field Procedure

Drilling in the Big Bald Mountain area presented some difficulty. The main constraints were (1) the unusual material to sample, i.e. grus and saprolite, (2) the need to recirculate a drilling mud in the holes due to the inability of water alone to adequately remove the cuttings, (3) a scarcity of water near the drill sites, and (4) difficult access conditions for wheeled vehicles. These fields conditions called for a light-weight mobile drill and provided an opportunity to assess Terrain Sciences' ATV-drill (Veillette and Nixon, 1979). Drilling through zones of highly fractured rock resulted in excessive loss of circulation fluid; this was solved, with little lost drilling time, by using small amounts of a water-soluble drilling fluid additive which produces a gel that seals the fracture. This is the most important result of the technical part of the project.

The bulk of the drilling equipment taken to the field consisted of:

- the drill (Fig. 9.4)
- open flight augers and bits (7.6 cm hole) for augering in dry, unconsolidated deposits
- light-weight magnezium-zirconium drill rods (BW size)
- tri-cone roller bit (7.6 cm hole)
- BWM (60.3 mm hole diameter, 41.3 mm core diameter) double tube swivel-type core barrel
- a few tens of metres of casing (7.6 cm I.D.)
- a 64 kg drop hammer
- a hydraulic capstan adapted to the ATV-drill to drive casing if necessary
- Iwan and spiral type samplers (5 and 7.6 cm diameter) for sampling loose material.

Considering that none of the four sites is within a practical pumping distance of a water source, special attention was given to the drilling fluid recirculation system. A four-wheel drive vehicle with a 1135 L bladder (normally used for gasoline) installed in the back was used to haul water as far as 2.5 km. A light-weight piston pump designed for water and viscous fluids was used so that drilling mud could be recirculated. Sedimentation tanks consisted of pre-cut plywood containers which were assembled in the field and soaked in water to seal the joints.

In planning the project, emphasis was on those problems normally encountered in sampling unconsolidated loose sediments because preliminary interpretation of seismic and surficial geology data indicated the presence of thicker grus than was actually encountered in the field. To avoid time-consuming positioning of casing in such deposits it is necessary to circulate a drilling fluid of a sufficient viscosity to 'cake' the interior of the hole; this also prevents losses of circulating fluid and keeps the hole open. Conventional native clay mud such as bentonite was rejected because (1) transportation of the mud was not logistically feasible and (2) contamination by clay minerals in the mud could invalidate results of some of the analyses planned for the samples (C. Gauthier, personal communication, 1980). After consultation with Johnson Division, Universal Oil Products Company, Minnesota, the drilling fluid additive, Revert, was selected.

Revert is made from guar gum, is entirely organic, and as such does not contaminate samples of mineralogic origin; methyl blue is the only additive (G. Carpenter, personal communication, 1980). Revert also has viscosity-building properties about 10 times those of bentonite in the viscosity range used in normal water-well drilling. The name Revert is derived from its property of reverting back to a liquid as thin as water after a period varying from a few hour to a few days.

Figure 9.4. *Coring with ATV-drill using an organic drilling fluid (Revert) recirculated by a light-weight mud pump. 203506-H.*

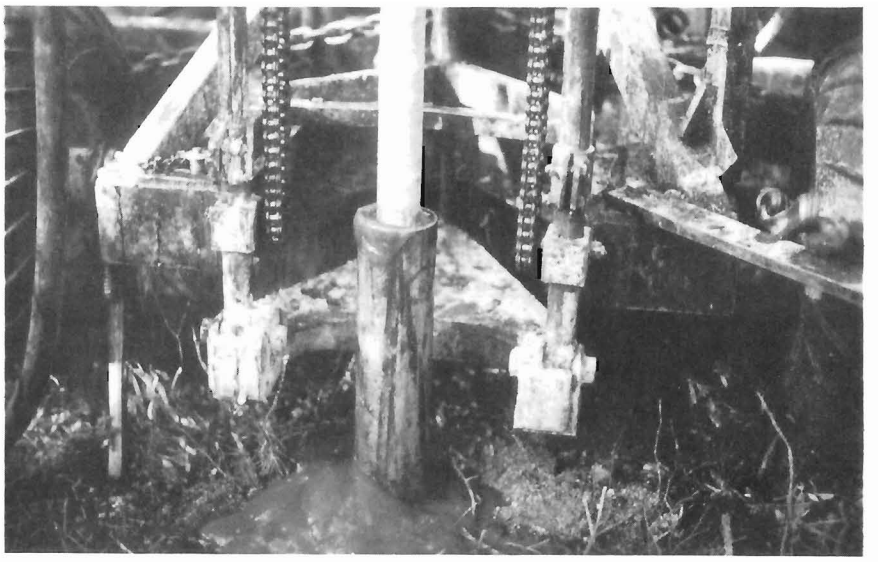

Figure 9.5. *Gel used to seal cavities in bedrock. The semi-solid, stringy mass pouring out of the casing results from adding Borax solution to high viscosity Revert drilling fluid. 203506-G.*

Early field trials indicated that Revert of relatively low viscosity, 30 to 40 seconds Marsh Furnel Viscosity (MFV, water has a MFV of 26 seconds), could hold the upper uncased portion of a hole in near-surface loose unconsolidated deposits, and allowed the hole to be flushed free of cuttings in the saprolite below. Coarse sand and even fine granules could be lifted at viscosity of about 40 seconds MFV. Trials using water without any Revert added proved disastrous because cuttings adhered to the interior of the hole and settled at the bottom, plugging the bit ports and stopping the circulation of the drilling fluid.

Very viscous Revert (80-150 sec MFV), when mixed with Mule Team Borax powder diluted in water, produces a thick, stringy mass (Fig. 9.5). This mixture was used to seal zones where excess lost circulation of drilling fluid was encountered. This was the greatest advantage of using Revert. It made drilling possible at hole A2N, where several hundred litres of fluid were lost in openings in granite at 5 m and 17 m depth. Revert alone, even at 80 seconds MFV, could not seal the upper zone, but the gel produced by the addition of Borax did. By making drilling possible below zones of lost circulation, this product allowed logging of structural discontinuities (joints, fractures, faults?) which otherwise would have been missed had water alone or even a bentonite drilling mud been used as drilling fluid.

Most of the drilling was expected to be in unconsolidated sediments (grus and till) and, as such, the equipment available was better suited for techniques other than continuous diamond drilling. Subsurface conditions were, however, different from those expected, and 71 per cent of the drilling had to be done with a diamond core barrel, which slowed drilling considerably. Also the only core barrels available took 60 and 68 cm cores instead of the standard 152 or 309 cm lengths. Where hard rock was encountered, the tri-cone roller bit had to be replaced by the diamond core barrel, due to the slower penetration of the roller bit.

A total of 63 m was drilled: 15% in loose near-surface sediments; 22% in largely unconsolidated granite or grus; 44% in granite in various stages of chemical alteration; and 19% in a black metamorphic rock in various stages of chemical alteration. Seventy-three (3 were lost) samples, both chips and core samples, were collected for description in the laboratory.

10. CAMBRIAN MEDUSOIDS FROM THE ST. JOHN GROUP, SOUTHERN NEW BRUNSWICK

Project 730044

R.K. Pickerill[1]
Precambrian Geology Division

Pickerill, R.K., Cambrian medusoids from the St. John Group, southern New Brunswick; in Current Research, Part B, Geological Survey of Canada, Paper 82-1B, p. 71-76, 1982.

Abstract

Over one hundred well preserved specimens of cnidarian medusoids have been discovered on the upper surface of a bedding plane of quartz arenite exposed in a road cut in the city of Saint John. The rocks probably belong to the Agnostus Cove Formation of the St. John Group, which is of early Late Cambrian age.

Introduction

Since the pioneering work of G.F. Matthew in the late nineteenth century (e.g. Matthew 1890, 1891, 1892), many geologists have been attracted to the Cambro-Ordovician succession (the St. John Group) of Saint John and adjacent areas, southern New Brunswick. Matthew (1890, 1891, 1892) described the macrofaunas in detail and more recently Landing et al. (1978) and Landing (1980) described a selection of the microfaunas. A newly constructed highway through the city of Saint John, the McKay Highway (Fig. 10.1), has exposed several new and important sections of Cambro-Ordovician strata. One of these sections has exposed the upper surface of a bedding plane of quartz arenite of probable early Late Cambrian age. This surface has preserved over 100 specimens of previously undescribed cnidarian medusoids, which are, of course, extremely rare fossils in rocks of any age. Because medusoids of Cambrian age in Canada have only been previously described from the Burgess Shale of British Columbia (Walcott, 1911; Conway Morris, 1978) the locality represents a unique and fortunate discovery. The following report is, therefore, intended to document the discovery and comprises initial results of but a single aspect of a current multidisciplinary project in the Saint John area (Currie et al., 1981; Nance, 1982). The detailed taxonomy of the medusoids is currently in progress in association with Mary Wade, Queensland Museum, Australia. In view of the long term nature of this taxonomic work (where each medusoid will be individually analyzed) it is perhaps timely to report on the occurrence of these previously undescribed medusoids and make preliminary comment on their taxonomic affinity.

Locality and Stratigraphical Setting

Within the city of Saint John, the Cambro-Ordovician St. John Group of Matthew (1863) is generally poorly and discontinuously exposed in strongly faulted and folded terrain. Hayes and Howell (1937) and Alcock (1938) subdivided the group into ten formations (Fig. 10.2), but unfortunately these were improperly defined on a biostratigraphical rather than lithological basis (North, 1971). In the absence of faunal control it is, therefore, extremely difficult to accurately locate specific exposures because apart from the Ratcliffe Brook and Glen Falls Formations, which are lithologically distinctive and easily recognizable, the remainder of the succession is generally lithologically indistinguishable, consisting essentially of interbedded shales and micaceous quartz arenites.

The medusoid fossils are located on the upper surface of a steeply dipping micaceous quartz arenite on the northwestern side of the McKay Highway, 0.75 km northwest of Courtenay Bay, immediately below Wright Street, which runs parallel to the new highway (Fig 10.1). The only associated fossils, found as disarticulated and broken fragments in strata above and below the medusoid horizon, are poorly preserved lingulid (**Lingulella** sp.) shells. Associated shales are extremely bioturbated and **Skolithos, Planolites, Fraena** and **Laevicyclus**-like structures are recognizable trace fossils observed particularly at sand/shale interfaces.

Although, as outlined above, it is impossible to state with absolute certainty the precise stratigraphical location of the medusoids, the following observations can be made:

i) The locality is in stratigraphical continuity and overlies **Paradoxides**-bearing strata of Middle Cambrian age. The strata correspond to the "coarse beds of Division 2" (Johannian) of Matthew (1890, p. 126), thus implying a Late Cambrian age and therefore, either the Agnostus Cove or Black Shale Brook Formations of Hayes and Howell (1937) and Alcock (1938). This is also in agreement with Yoon (1970) who regarded the immediately underlying Wright Street section as Late Cambrian in age.

ii) The exposed strata consist of interbedded shales and quartz arenites. The latter are most conspicuous and make-up at least 75 per cent of the total succession. Of the two aforementioned Upper Cambrian formations, the sequence can, therefore, best be lithologically correlated with the Agnostus Cove Formation, as the Black Shale Brook Formation, as its name suggests, is dominantly shale (see Hayes and Howell, 1937; Alcock, 1938).

Thus, it is suggested that the medusoid fossils are probably located in the Agnostus Cove Formation and consequently are, therefore, of early Late Cambrian age.

The Medusoids

Preservation

Over 100 specimens of the medusoids have so far been observed on the upper surface of the exposed bedding plane of the 10 cm thick, parallel laminated, micaceous quartz arenite which possesses a ripple marked and weakly scoured upper surface (Fig. 10.3). The bedding plane itself is approximately 20 m high and 5-6 m long, but the medusoids are (fortunately) restricted to the lower 2-2.5 m of the exposure: above this they are absent. This specific and linear distribution (on outcrop scale) suggests that the medusoids were gregarious and as a result of some unknown event and concomitant mass mortality, upon settlement they were quicky buried. Many species of Recent medusae are known to be gregarious and, for example, similar 'clumped' occurrences of **Ediacara flindersi** and **Medusinites asteroides** in the Precambrian sandstones of south Australia were suggested by Glaessner and Wade (1966) to have resulted from a gregarious mode of life. Alternatively, however, the medusoids could

[1]Department of Geology, University of New Brunswick, Fredericton, N.B. E3B 5A3

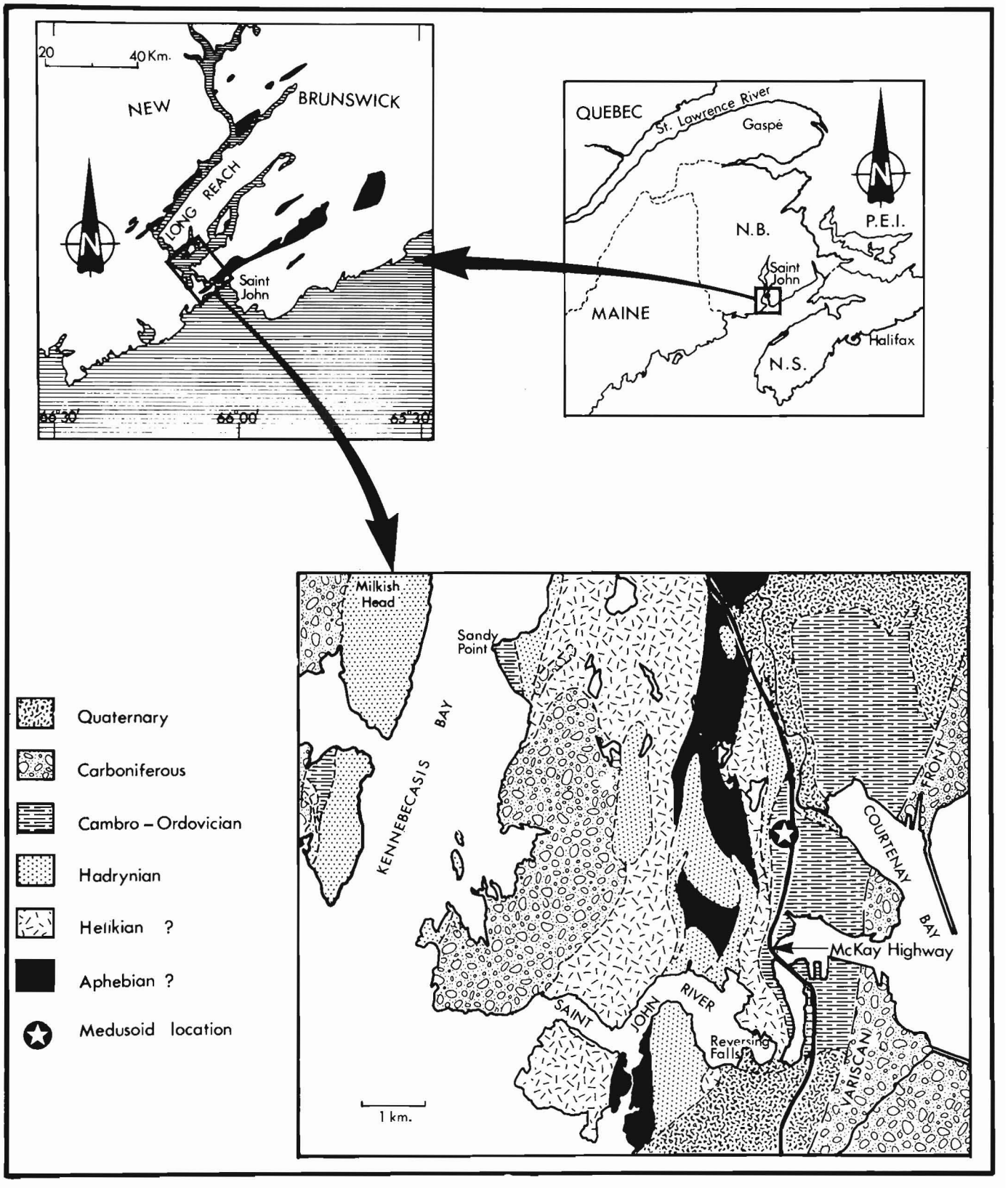

Figure 10.1. *Location and geological map of Saint John and vicinity. Modified after Currie et al. (1981).*

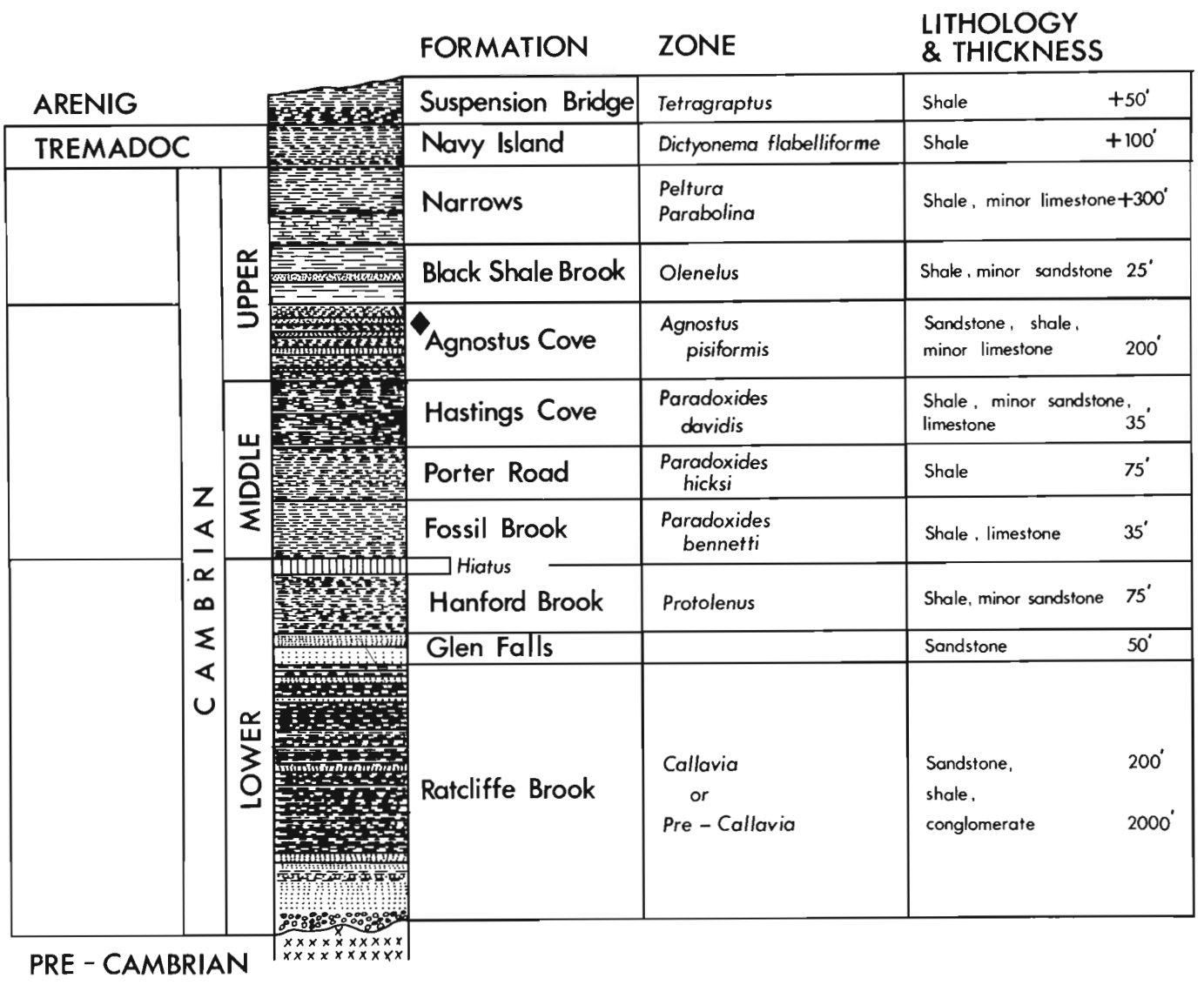

Figure 10.2. *Stratigraphical succession of the St. John Group. Modified after Hayes and Howell (1937). Medusoid fossils occur at the level marked by the diamond.*

possibly have been washed onto a shoreline or offshore bar and stranded as swash accumulations at or above immediate high tide level during a period of storm or unusual tidal activity. Recent medusae are commonly stranded during such periods (Hyman, 1940). The research by Lincke (1956) has also indicated that mass strandings consisting almost exclusively of one species can occur during periods of fair weather. During fair weather conditions medusoids rise to the surface and are easily driven onshore by weak winds.

Unfortunately, there is no specific evidence preserved to indicate which of these alternatives (or perhaps combination of alternatives) was responsible for the medusoid distribution. Associated strata do contain evidence of shallow water deposition (e.g. linsen bedding, double crested ripples) but no valid evidence of periodic emergence. Underlying and overlying formations are strictly marine, as indicated by their contained faunas, but water depth is of course indeterminate. One possible solution, as yet not fully resolved, will be detailed examination of preservation of the medusoids. Medusae are characteristically stranded exumbrella side up in shoreface or extremely shallow water conditions (Walcott, 1898; Schafer, 1941; Wade, 1968), but in water of more than critical depth (>2/3 of their total diameter) characteristically settle exumbrella side down (Wade, 1968). Although the medusoids are variably preserved and even the distinction of exumbrellar, subumbrellar and composite moulds is sometimes very difficult, future analysis may potentially prove meaningful.

Irrespective of their distribution, the medusoids must have been covered by sediment relatively quickly. Hertweck (1966), for example, observed that a recently dead medusa "collapsed to a film" in only 10 days and Schafer (1972) pointed out that typically, medusoid moulds form within the first few hours after settlement. Thus, the overlying shales with thin and lenticular rippled and cross-laminated siltstones were probably rapidly deposited, and it was this that in part contributed to the chance preservation of the medusoids. The preservation of medusoids on upper surfaces of coarse grained sediment is not usually the 'norm' (see Wade, 1968, Schafer, 1972). The example here, however, can possibly be attributed to localized erosion of the quartz arenite between individual medusoids following their settlement. The subsequent deposition of mud within the hollowed 'scours' and on the medusoid 'mounds', followed by postdepositional differential compaction would result in their preservation as positive features on the upper surface of the quartz arenite. This suggestion is perhaps substantiated by the observation of scour-like structures between the

Figure 10.3 *Artistic sketch of the medusoid location illustrating the lower 2.5-3 m of the bedding plane exposure and the distribution of medusoids on the plane.*

medusoids and the rarely observed examples of medusoids which are moderately convex with their margins apparently draping down the sides of the mound on which they were preserved. Whether or not the gastro-vascular system and radial canals branching from it were filled with sediment prior to mud deposition is unknown, though this is apparently a frequently observed process with Recent stranded medusoids (see Schafer, 1972, p. 189 for details).

Description

As the purpose of this report is essentially to record the occurrence of the medusoids and detailed analysis is still being continued, the following description has been kept as short and concise as possible and only general morphological details are included.

The medusoids are circular, subcircular or elliptical discs preserved as positive structures on the upper surface of the quartz arenite. Cross-sections may be moderately convex, gently convex or alternatively may be crater-like, with marginal ridges and furrows (see below) separating a broadly concave depression. The cross-sectional shape is somewhat dependent on the position of preservation (ripple troughs, crests) but also probably reflects variation in parameters such as scouring, decay, compaction, etc. (see Schafer, 1972). Size is variable, ranging from 20-120 mm in diameter, the majority falling within the range of 60-80 mm. Preservation is variable, some showing fine detail, others showing no internal detail but merely being recognized by the raised external circular or elliptical outline.

The majority of specimens, where recognizable, are apparently composite moulds, shaped by the flattened exumbrellars. Well preserved specimens exhibit a central circular stomach and radial canals in multiples of 12 or more, commonly 16. Occasionally a poorly preserved more centralized structure resembling an unspecialized mouth can be observed (Fig. 10.4). Radial canals are unbranched and are preserved as delicate ridges which extend from the stomach to the margins of the discs. The centralized stomach region usually preserves no fine detail and typically constitutes about 30-35 per cent of the total diameter of individual specimens. The margins are composed of concentric ridges (typically two) and furrows, most probably produced as a result of thinning of the gelatinous discs towards their edges (M. Wade, personal communication, 1981). These external ridges and furrows are typically slightly more elevated than features within the discs apart from when the medusoids have a distinctly convex cross-sectional profile.

Affinities

Historically, medusoids have been distinguished as hydrozoan or scyphozoan with little caution, but as Glaessner (in Robison and Teichert, 1979) has pointed out, because of nonpreservation of diagnostic characters, conclusions must be made with extreme caution. The differentiation of hydrozoa and scyphozoa is largely dependent on characters which are typically not preserved in many fossilized medusoids, such as the position and presence or absence of coelenteron gonads, gastric filaments and pouches, the presence or absence of subumbrellar furrows etc. None of these, or other, diagnostic differentiating criteria have been observed with the medusoids described herein. Nevertheless, although for the time being they should be regarded as still of uncertain affinity, it is tentatively concluded that they were most probably scyphozoans.

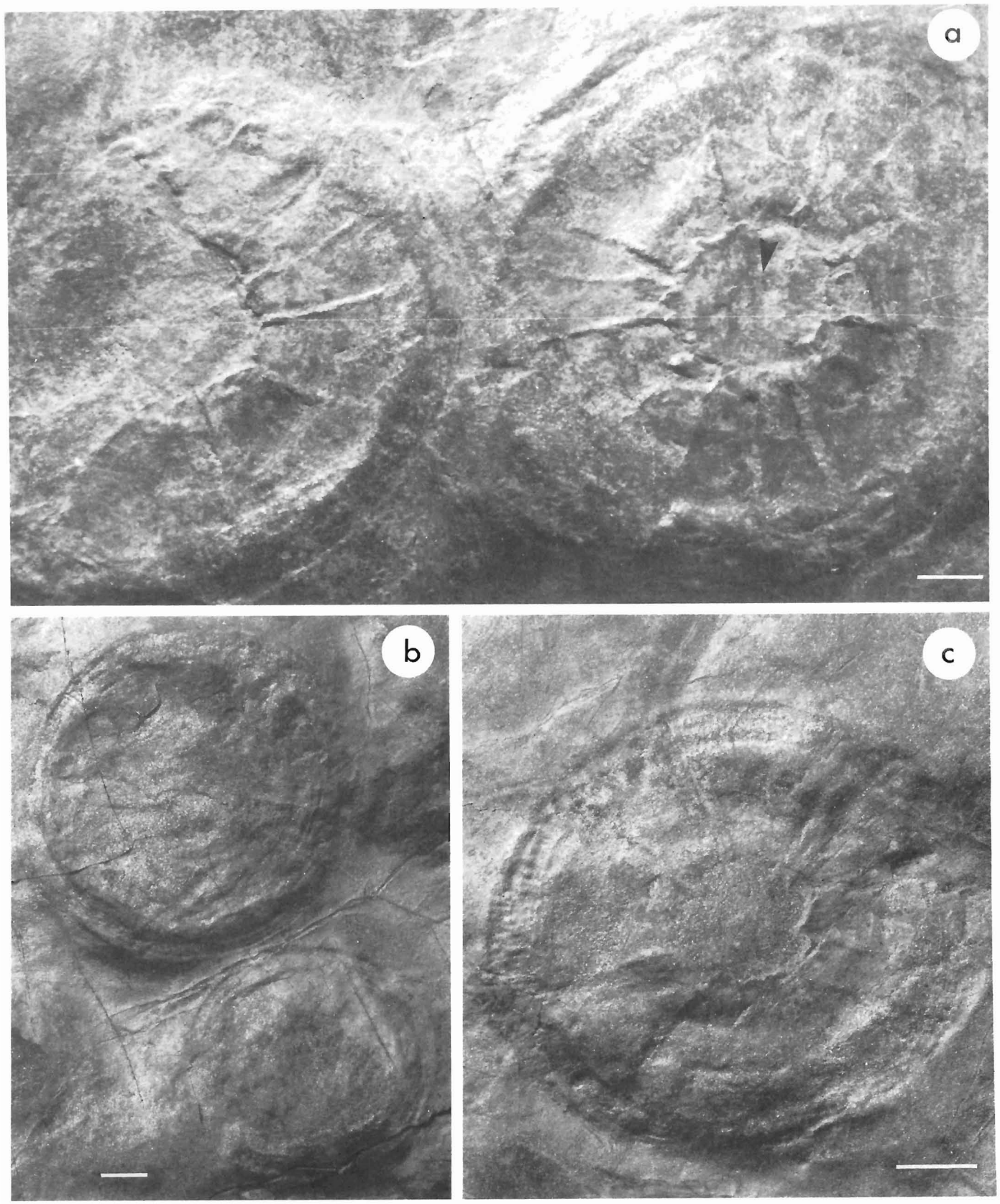

Figure 10.4. *A selection of medusoids from the St. John Group. Note the well preserved radial canals, the stomach outline and the possible central and unspecialized mouth in a (arrowed), b and c illustrate the more typical preservation. Note the well defined external margins defined by concentric ridges and furrows in b. Specimen c also preserves a possible centralized mouth. Bar scale is 10 mm.*

Hydromedusae are not as solidly built as scyphomedusae and are less likely to leave impressions in clastic rocks (M. Glaessner, personal communication, 1981). The majority of Recent hydromedusae are craspedote (i.e. possess a velum) but this has not been observed in any of the Saint John medusoids. Furthermore, hydromedusae commonly possess four, six or eight radial canals whereas scyphomedusae, when present, possess four or multiples or four (Hyman, 1940). Finally, although not an absolutely convincing distinguishing criterion, the large size of the specimens is more suggestive of a scyphomedusoid affinity (M. Foster, personal communication, 1981).

It is likely that the medusoids represent a new and distinctive species. They vaguely resemble **Velumbrella czarnockii** Stasinska, 1960 from the Cambrian of Poland but they differ from this in that there are no tentacles, they do not possess a velum nor do they possess 28 radial canals (see Stasinska, 1960). They are also reminiscent of **Peytoia nathorsti** Walcott, 1911 from the Burgess Shale but again, possess fewer radial canals and do not possess the four major lobes and marginal lappets characteristic of this species. Otherwise, the medusoids bear no resemblance to any previously described hydromedusoid or scyphomedusoid.

Acknowledgments

It is a pleasure to acknowledge fellow members of the Saint John interdisciplinary working group, K.L. Currie, G.E. Pajari, and R.D. Nance. Thanks are also extended to M.F. Glaessner, M. Foster, M. Wade, and R.A. Robison for their useful comments regarding affinities of the medusoids.

References

Alcock, F.J.
1938: Geology of Saint John region, New Brunswick; Geological Survey of Canada, Bulletin 216, 65 p.

Conway Morris, S.
1978: **Laggania cambria** Walcott: a composite fossil; Journal of Paleontology, v. 53, p. 494-500.

Currie, K.L., Nance, R.D., Pajari, G.E., and Pickerill, R.K.
1981: Some aspects of the pre-Carboniferous geology of Saint John, New Brunswick; in Current Research, Part A, Geological Survey of Canada, Paper 81-1A, p. 23-30.

Glaessner, M.F. and Wade, M.
1966: The late Precambrian fossils from Ediacara, South Australia; Palaeontology, v. 9, p. 599-628.

Hayes, A.O. and Howell, B.F.
1937: Geology of Saint John, New Brunswick; Geological Society of America, Special Paper 5, 146 p.

Hertweck, G.
1966: Moglichkeiten des Fossilwerdens von Quallen – im Experiment; Natur und Museum, v. 96, p. 456-462.

Hyman, L.H.
1940: The Invertebrates: Protozoa through Ctenophora; McGraw-Hill New York and London, 726 p.

Landing, E.
1980: Late Cambrian early Ordovician macrofaunas and phosphatic microfaunas, St. John Group, New Brunswick; Journal of Paleontology, v. 54, p. 752-761.

Landing, E., Taylor, M.E., and Erdtmann, B.D.
1978: Correlation of the Cambrian-Ordovician boundary between the Acado-Baltic and North American Faunal provinces; Geology, v. 6, p. 75-78.

Linke, O.
1956: Quallen-Spulsaume Okologische Voraussetzung und aktuogeologische Aausdeutung; Natur und Volk; v. 86, p. 119-127.

Matthew, G.F.
1863: Observations on the geology of St. John County, New Brunswick; Canadian Naturalist, v. 8, p. 241-259.

1890: Illustrations of the fauna of the St. John Group, No. V; Transactions of the Royal Society of Canada, v. 8, p. 123-166.

1891: Illustrations of the fauna of the St. John Group, No. VI; Transactions of the Royal Society of Canada, v. 9, p. 33-65.

1892: Illustrations of the fauna of the St. John Group, No. VII; Transactions of the Royal Society of Canada, v. 10, p. 95-109.

Nance, D.
1982: Structural reconnaissance of the Green Head Group, Saint John, New Brunswick; in Current Research, Part A, Geological Survey of Canada, Paper 82-1A, p. 37-43.

North, F.K.
1971: The Cambrian of Canada and Alaska; in Cambrian of the New World, ed. C.H. Holland, Wiley-Interscience, London-Toronto, p. 219-324.

Robison, R.A. and Teichert, C.
1979: Treatise on Invertebrate Paleontology, Part A, Introduction; Geological Society of America and University of Kansas, Boulder, Colorado, and Lawrence, Kansas, 569 p.

Schafer, W.
1941: Fossilations-Bedingungen von Quallen und Laichen; Senckenbergiana, v. 23, p. 189-216.

1972: Ecology and Palaeoecology of Marine Environments; Oliver and Boyd, Edinburgh, 568 p.

Stasinska, A.
1960: Velumbrella czarnockii n. gen., n. sp. – méduse du Cambrien Inférieur des Monts de Sainte-Croix; Acta Palaeontologica Polonica, v. 5, p. 337-344.

Wade, M.
1968: Preservation of soft-bodied animals in Precambrian sandstones at Ediacara, south Australia; Lethaia, v. 1, p. 238-267.

Walcott, C.D.
1898: Fossil Medusae; United States Geological Survey, Monograph 30, 201 p.

1911: Cambrian geology and paleontology II, Number 3 – Middle Cambrian holothurians and medusae; Smithsonian Miscellaneous Collections 57, p. 41-68.

Yoon, T.
1970: The Cambrian and Lower Ordovician stratigraphy of the Saint John area, New Brunswick; Unpublished M.Sc. thesis, University of New Brunswick, 92 p.

11.

RECONNAISSANCE PALEOMAGNETISM OF THE EOCENE METCHOSIN VOLCANICS, VANCOUVER ISLAND, BRITISH COLUMBIA

Project 730036

E.J. Schwarz[1] and J.E. Muller[2]

Schwarz, E.J. and Muller, J.E., Reconnaissance paleomagnetism of the Eocene Metchosin Volcanics, Vancouver Island, British Columbia; in Current Research, Part B, Geological Survey of Canada, Paper 82-1B, p. 77-82, 1982.

Abstract

Alternating field and thermal demagnetization of 51 cores (9 sites, 5 or 6 cores each) from Eocene Metchosin Volcanics from southern Vancouver Island yielded stable directions of remanent magnetizations with very high dispersion. The grouping of easterly-up direction distinguished in some of the cores is significantly improved after rotating the flow planes to horizontal around strike. Thermal cleaning indicates the presence of a westerly-down direction which may be the reverse of the easterly-up direction. The easterly-up direction ($D = 74$, $I = -66$, $k = 78$, $\alpha_{95} = 14°$) yields a North pole at 11°E, 25°S, $dm = 23°$, $dp = 19°$, which suggest substantial post-Eocene movement (rotation) of this area with respect to cratonic North America. The pole is also greatly different from other early Tertiary paleomagnetic pole positions from the Western Cordillera suggesting limited coherency in movements of different blocks.

Introduction

A number of paleomagnetic studies of the Upper Triassic Karmutsen basalts of Vancouver Island have yielded results that are incompatible with the Triassic paleomagnetic pole positions of the North American craton (Symons, 1971; Irving and Yole, 1972; Schwarz et al., 1980; Yole and Irving, 1980). Muller (1977a) suggested that Vancouver Island, as well as other parts of the Insular Belt, were rifted off the continental margin far to the south and that outflow of Late Triassic Karmutsen basalts was a direct result of this rifting process. The allochthonous Insular Belt, characterized by a heterogeneous assemblage of Paleozoic to Cretaceous volcanic, crystalline and sedimentary rocks, was sutured onto the interior cordillera in the Middle Jurassic to Late Cretaceous time interval.

Vancouver Island also contains on its southernmost tip a small region, not belonging to the Insular Belt but to the pacific Belt (Muller, 1977a), extending into Olympic Peninsula and Washington and Oregon Coast Ranges. It is separated from the Insular Belt by the fundamental San Juan

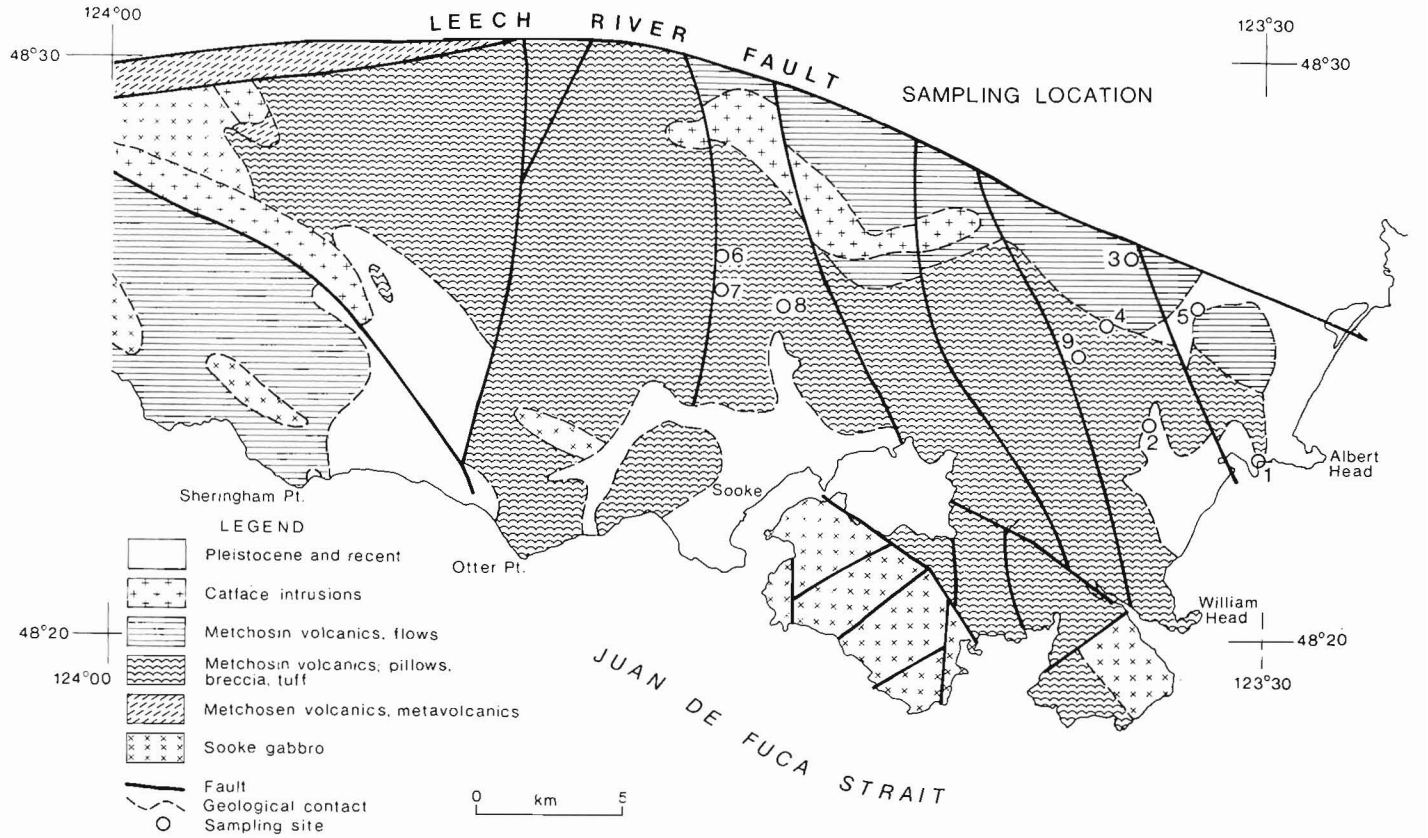

Figure 11.1. *Geological map of southern Vancouver Island indicating sample locations.*

[1] Departement de génie minéral, Ecole Polytechnique C.P. 6079, succursale A, Montréal, Qué. H3C 3A7
[2] Cordilleran Geology Division

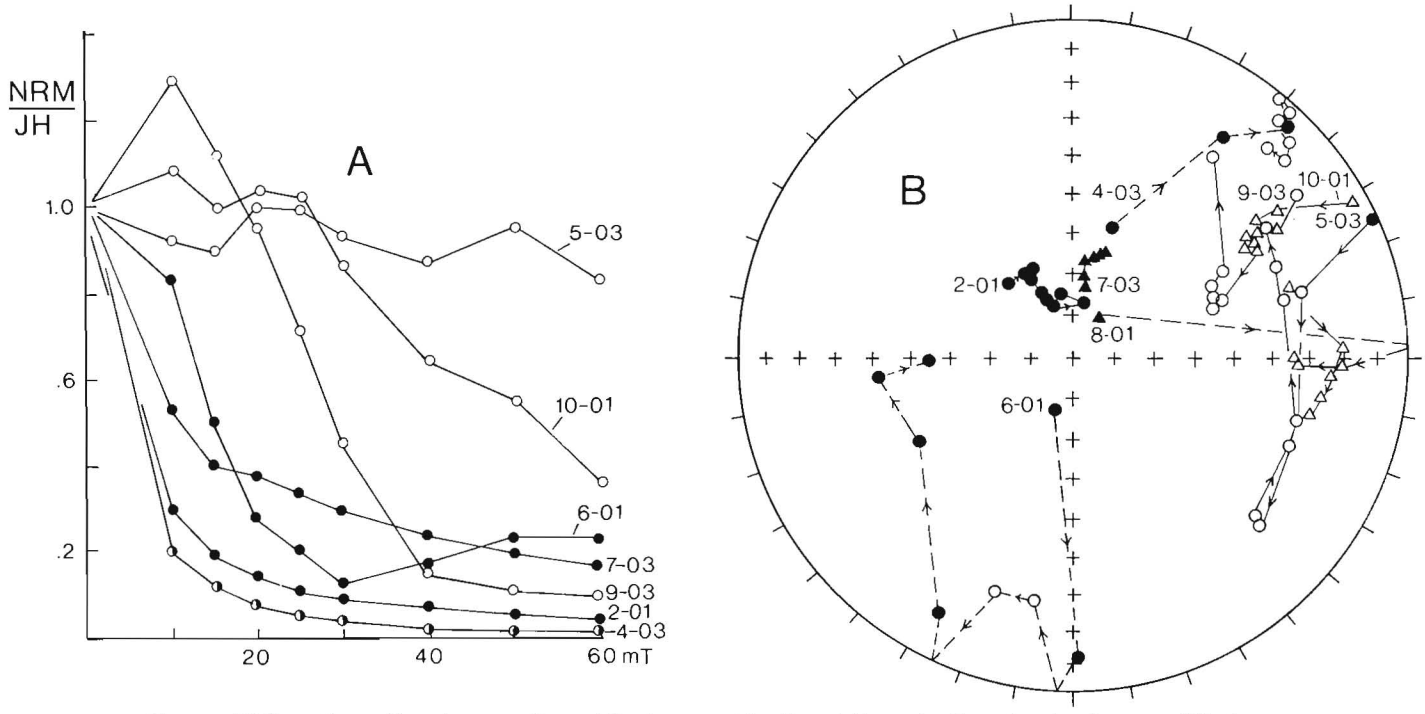

Figure 11.2. *Intensity decay after AF demagnetization (A) and directional changes (B) for specimens from different sites.*

and Leech River faults. The suture between the two belts is marked by a zone of melange and highly deformed and schistose volcanic and sedimentary rocks of late Mesozoic age. The Pacific Belt is composed of Tertiary clastic sediments overlying Eocene tholeiitic basalt and locally associated basic dykes and gabbro. The basalt formations are the Metchosin Volcanics of Vancouver Island and the correlative Crescent Formation and Black Hills lavas of Washington and the Siletz River, and several other Eocene basaltic volcanics of Oregon. This crustal block, apparently composed of early Tertiary tholeiitic ocean floor, volcanic islands and overlying sediments, was sutured to the Cordilleran margin in Tertiary time, long after the emplacement of the Insular Belt.

The present study is a first attempt to obtain data on post-Eocene movement of this northern geological extension of the Oregon and Washington Coast Ranges, the Pacific belt, in respect to other parts of that domain, as well as in respect to adjacent parts of the Insular Belt on Vancouver Island.

Geology and Sampling

Metchosin Volcanics are a series of tholeiitic basalts, composed of a lower portion of submarine pillow lavas and breccias and an upper part of flows, believed to be subaerial. Volcaniclastic beds, about at the level of transition between pillows and flows, contain a layer with well preserved **Turritella** indicating early Eocene age (Muller, 1977b). Chemistry of the basalts suggests a ridge-island type of tectonic setting, similar to that of Iceland (Muller, 1980).

Sooke Gabbro and Catface Intrusions are respectively gabbroic and quartz dioritic plutonic masses, formerly considered together as Sooke Intrusives (Clapp and Cooke, 1917). The gabbro occurs as coarse grained plutonic masses and as finer grained dyke complexes. The largest mass of gabbro of East Sooke is in fault contact with Metchosin Volcanics. It may be coeval and comagmatic with the volcanics, or could be somewhat older.

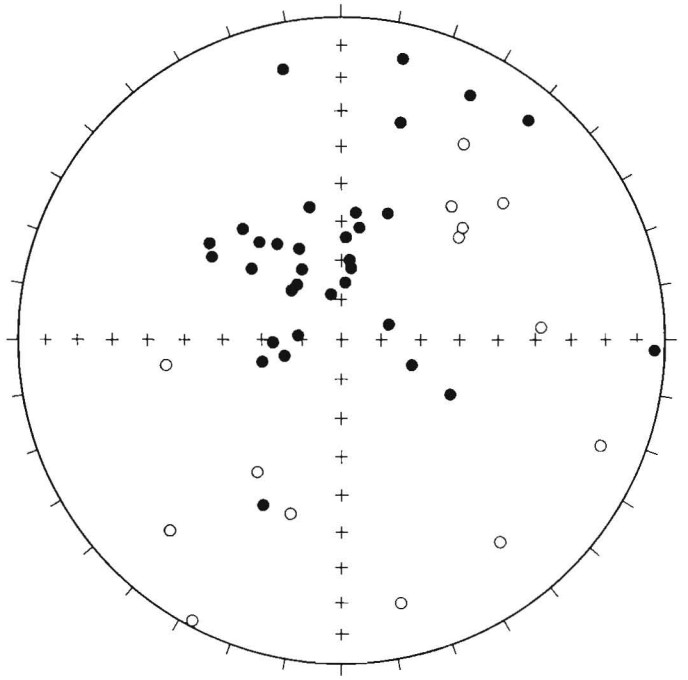

Figure 11.3. *All accepted directions after 40 mT treatment.*

Catface Intrusions are small plutons, dykes and sills of generally quartz dioritic composition. They intrude Metchosin Volcanics and also Sooke Gabbro as partly agmatitic dykes. The granitoid intrusions, postdating Sooke Gabbro, have locally metasomatized the gabbroic rocks resulting in the formation of amphibolite and coarse grained hornblendite and the concentration of copper ore. Available K-Ar ages date the emplacement of Catface Intrusions into Metchosin Volcanics and Sooke Gabbro as follows:

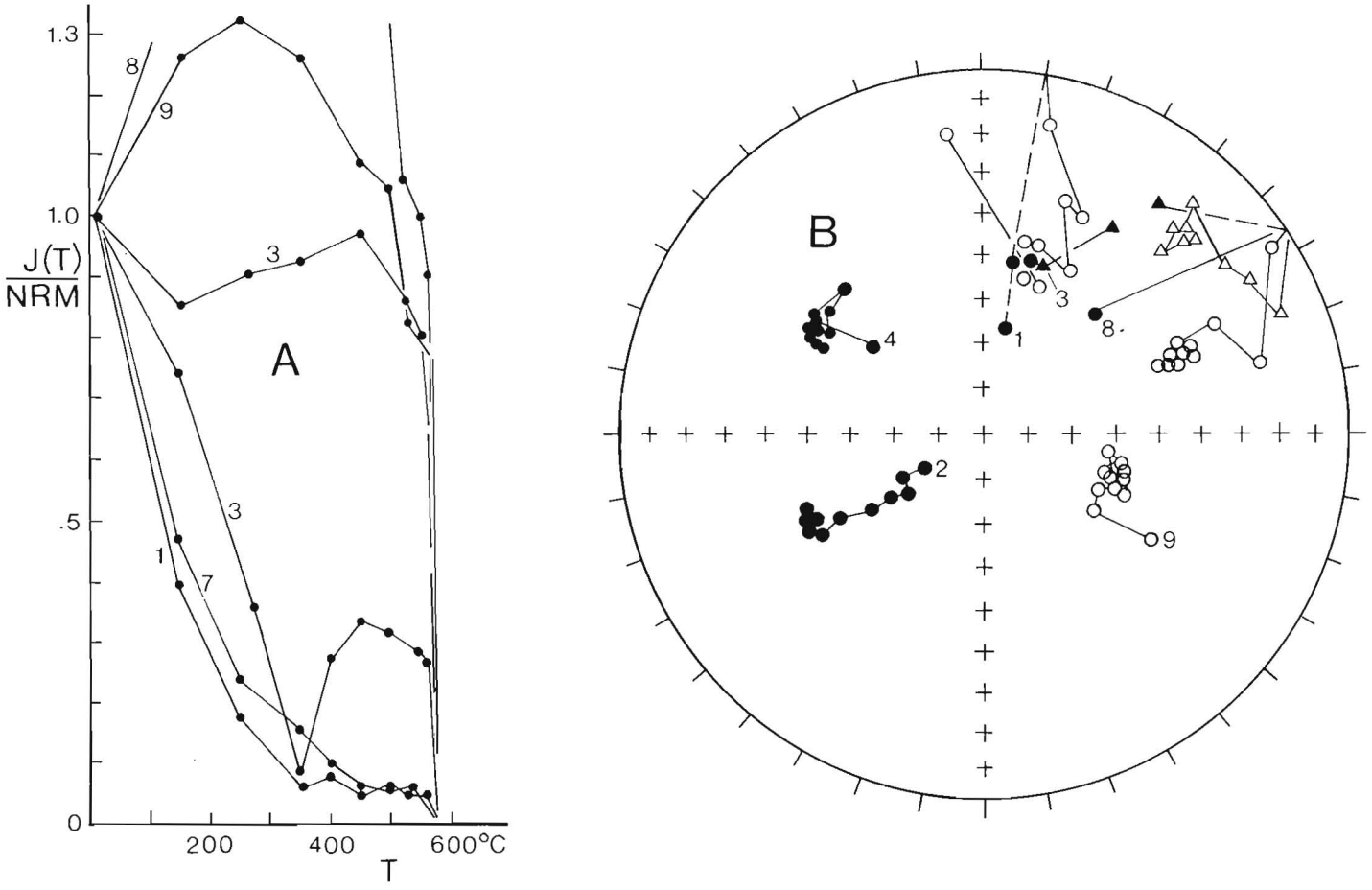

Figure 11.4. *Intensity decay (A) after thermal demagnetization (150, 250, 300, 350, 400, 450, 500, 525, 540, 550, 560, 570°C) and directional changes (B).*

Biotite from trondhjemite, Jordan River (GSC 65-13, Wanless et al., 1967): 39 ± 10 Ma.

Hornblende from Jordan River Mine ore (GSC 70-36, Wanless et al., 1972): 44 ± 6 Ma.

Hornblende from mineralized hornblendite (GSC 72-25, Wanless et al., 1973): 31 ± 15 Ma.

The age relationships of Metchosin Volcanics with Sooke Gabbro and Catface Intrusions have a significant bearing on the interpretation of paleomagnetic data for the Sooke Gabbro (Symons, 1973). Clapp and Cooke (1917) recognized that the "granite" of what is now named Catface Intrusions intrudes Sooke Gabbro. Also, paleontological data now indicate early Eocene age for Metchosin Volcanics and Miocene to Pliocene age for the Sooke Formation. It is suggested here that in the oceanic island setting of Metchosin basalts and related plutonic rocks it is more likely that the gabbro represents either a magma chamber directly related to the volcanics or an "oceanic" gabbroic basement, while the quartz dioritic intrusions represent late subvolcanic phases or a younger, unrelated volcanic event. The gabbro and the volcanics are considered to be 50 Ma old, while Catface Intrusions are, according to the quoted K-Ar dates, about 40 Ma old.

Five or six oriented drill cores (diameter is 2.5 cm) were collected at each of nine sites (Fig. 11.1) from amygdaloidal flows (sites 4 and 6) and from pillow lavas (all other sites). The sites were collected on the basis of minimal alteration. Orientation of the cores in the field was

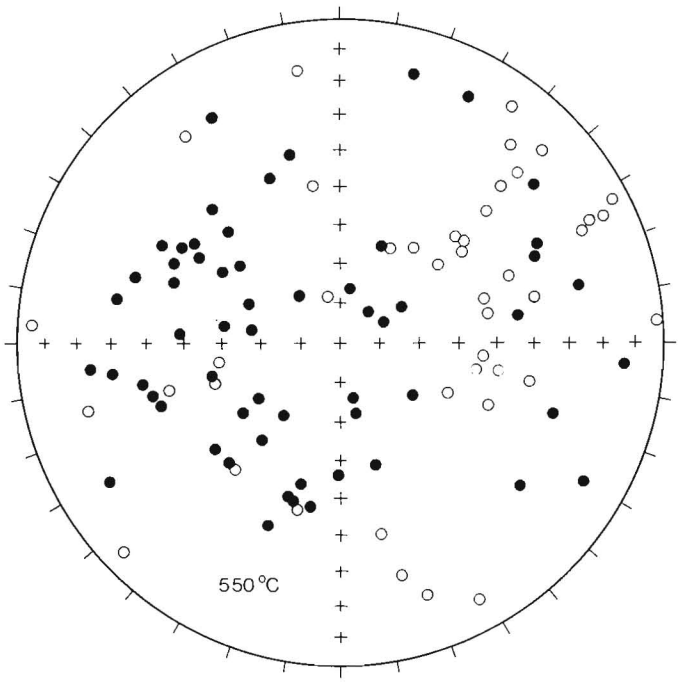

Figure 11.5. *All accepted directions after 550°C treatment.*

Table 11.1

Remanent magnetization data for Metchosin Volcanics

SITE	N	NRM D	NRM I	NRM k	NRM α_{95}	AF (30 or 40 mT) D	AF I	AF k	AF α_{95}	AF N	AF n	AF* D	AF* I	AF* k	AF* α_{95}	T (530-570°C) D	T I	T k	T α_{95}	T N	T n	T* D	T* I	T* k	T* α_{95}
1	5	345	+77	22	10	7	+75	13	19	4	6	7	+75			251	+36	7	50	3	3	251	+36		
2	6	298	+84	20	10	252	+81	2	26	4	6	68	+84			72	+84	2	120	3	3	71	+69		
3	6	345	+74	13	13	20	+18	6	34	4	5	20	-20			49	-28	16	24	3	4	62	-67		
4	6	329	+65	78	5	311	+56	105	8	4	5	290	+54			297	+48	62	10	5	5	283	+42		
5	5	285	+72	6	21	264	+69	5	36	4	6	264	+69			262	+33	6	31	6	6	262	+33		
6	6	12	+82	22	10	11	+62	9	23	4	6	38	+19			106	+67	7	30	5	5	78	+22		
7	6	91	+72	2	49	-	-	-	-		-	-	-			120	-25	11	40	3	3	(127	-8)		
8	6	47	-14	3	31	56	-47	35	13	4	5	46	-66			83	-51	9	26	5	5	95	-70		
9	5	149	-63	2	45	68	-41	29	23	3	3	64	-50			73	-49	8	36	4	4	68	-58		
Average	all sites	7	+76	2.5		11																			
	sites 1, 2, 4, 5, 6					354	+70	14	31	20	29	351	+73	5	38										
	sites 3, 8, 9					46	-26	4	75	11	13	40	-51	12	38	82	-41	9	33	12	13	74	-66	78	14
	sites 1, 4, 5															268	+40	18	30	14	14	265	+38	37	21
	sites 2, 6															62	+65	8	47	8	8				

N – is number of cores
n – is number of specimen endpoints
AF and T – represent data after Alternating Field and Thermal demagnetization in the field strength and temperature ranges as indicated
* – indicates the data after rotation of the flow planes to horizontal around strike
k and α_{95} – statistical parameters are based on site means and are worse than those based on individual core directions

by sun compass or by magnetic compass sighting of prominent topographic features used as a check. The cores were cut up in 2.3 cm long cylinders. The remanent magnetization of these specimens was determined after AF and thermal testing.

Experimental Results

The NRM directions grouped by site are listed in Table 11.1. In general, the within-site directions are poorly grouped with all but sites 8 and 9 showing positive inclinations. Coherency between the sites is also low and decreases by tilting the flow planes to horizontal around strike. The NRM intensity is fairly constant and of the order of 10^{-4} emu/cc (10^{-1} SI).

Two specimens per site were demagnetized in alternating fields (AF) up to 600 oe (60 mT) in 8 steps. The results were highly variable (Fig. 11.2A), the directions of some specimens hardly being affected while others showed considerable change. A number of specimens in the latter group do not reach endpoints (e.g. 6-01 in Fig 11.2A) and these are excluded from futher consideration. Figure 11.2B shows that the decay of the NRM intensity with increasing AF is also highly variable. Rapid decay to about 2 per cent of the original intensity is observed for some northerly-down directions (e.g. 2-01 on Fig. 11.2A). Northeast-up directions (e.g. 9-01) generally show much slower decay. On the basis of these results, one specimen of each core was subjected to fields of 30, 40, and 45 mT yielding the data shown on Figure 11.3. The directions are strongly scattered with a tendency to group towards north-down. This agrees with Symons' (1973) suggestion also based on AF data, that the original Metchosin direction is in this general direction. However, the strong scatter (Table 11.1) is increased by tilting the beds to horizontal around strike showing that the north-down magnetization is secondary.

Another group of samples, from sites 3, 8, and 9 displays consistently negative inclinations with northeasterly declinations. Vectors removed during the AF testing are consistent for this group of sites suggesting an essentially single component magnetization. Rotation of the flow planes to horizontal results in a considerable improvement in grouping (Table 11.1).

Thermal demagnetization was carried out on two specimens per site. Decay of NRM is shown on Figure 11.4A for representative examples and shows great variation. Specimens from sites 8 and 9 show the removal of a downward directed low blocking temperature (Tb) component and the presence of a relatively large component with Tb = 550°C suggesting magnetite as the carrier (Fig. 11.4B). These sites show stable north easterly-up magnetizations with relatively high coercivity as discussed earlier. Specimens from sites 1 and 2 with northerly-down, low median coercivity magnetization show a large, low-Tb component. Westerly-down specimens from sites 4 and 5 (and some from site 1) show an intermediate mode of decay (e.g. specimen from site 1).

The end points of the individual specimens after thermal demagnetization form a pattern which differs in several respects from that obtained after AF demagnetization. The easterly-up direction is much better represented (Fig. 11.3, 11.5) with several specimens from other sites (6, 3, 4) showing this direction in addition to those from site 8. The north (west)-down direction which is well represented in Figure 11.3 by specimens from, in particular, sites 4, 6, 2 is not apparent after the thermal treatment. There is, however, a group of westerly-down directions in particular represented by site 5 specimens after thermal treatment which is not present in the AF plot. About 40 per cent of the thermal end points do not belong to either easterly-up or westerly-down direction. Table 11.1 also shows that for both the AF and thermal data the core directions are based on only one specimen endpoint. The data set as a whole is clearly of low quality.

The thermal treatment was more effective than the AF treatment in particular for site 8 and 9 specimens and revealed a westerly-down direction of which the grouping is

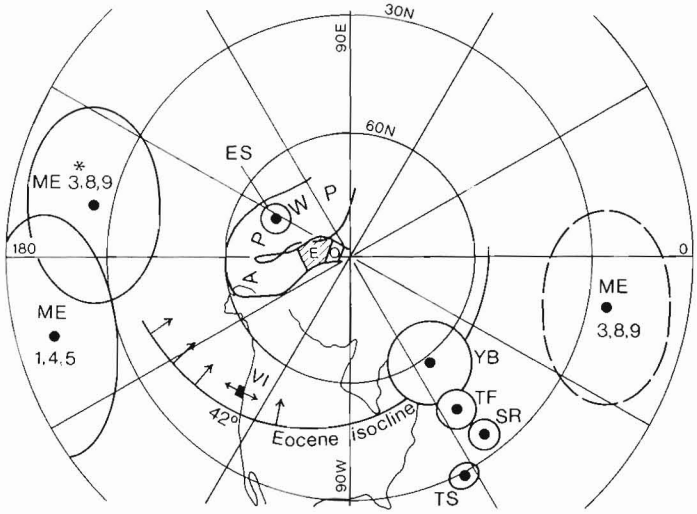

Figure 11.6. *Apparent polar wander path for cratonic North America (APWP, E indicates Eocene portion, Irving, 1979) and Eocene poles from the western Cordillera (ES, East Sooke Gabbro, Vancouver Island; YB, Yachats basalt, Oregon; TS, Twin Sisters dunite, Washington; TF, Tyee – Flournoy Formation, Oregon; SR, Silets River series, Oregon; and Metchosin, ME sites 3, 8, 9 and 1, 45). ME* is the reversed position of ME 3, 8, 9. The 42° paleoisocline is indicated, in which vicinity the Metchosin volcanics may have been formed. Arrows on the isocline indicate the direction of the horizontal component after magnetization in the magnetic field represented by ME*. Arrows on the square representing south Vancouver Island (VI) show direction of horizontal component of easterly-up remanent magnetization and its reverse.*

Table 11.2

Pole positions derived from data presented in Table 11.1 given in longitude (LO), latitude (LA), and semi-axes (dm, dp) of the area of 95% confidence around the position listed

	AF				AF*				T				T*			
SITES	LO	LA	dm	dp	LO	LA	dm	dp	LO	LA	dm	dp	LO	LA	dm	dp
1, 2, 4, 5, 6	159W	84N	54	46	147W	78N	67	60								
3, 8, 9	10E	16N	80	43	22E	3N	51	34	12W	12S	40	25	11E	25S	23	19
1, 4, 5									163E	16N	36	22	165E	12N	24	14

somewhat better after correction for bedding tilt (Table 11.1). Better grouping is also observed after tilt correction for the easterly-up specimen directions (Table 11.1) which is significant at the 95 per cent confidence level according to McElhinney's (1964) table of k ratios for both the AF and thermal results. This is, however, not the case for the westerly-down direction. Furthermore, Table 11.1 shows that the westerly-down direction is almost the exact opposite of the northeast-up direction before rotating the beds to horizontal but that these directions differ by only 156° afterwards. This inconsistency may be ascribed to inaccuracy of the westerly-down average direction due to contamination by other remanence components.

The following conclusions may be drawn from the experimental evidence:

1. There is an easterly-up group of directions in a strongly dispersed assemblage of generally downward directions. The grouping of the easterly – up directions is significantly improved after rotating the flow planes to horizontal indicating that the magnetization predates deformation.
2. The downward directions are predominantly to the west and may contain a group of normal magnetization directions reversed relative to the northeast-up magnetization. This suggests that the easterly-up direction is either primary or the result of oxydation soon after extrusion of the basalt.
3. The north-down direction shows a significant decrease in grouping after rotation of the flow planes to horizontal indicating that this component postdates deformation.

Pole Position

The pole positions for the different groups of sites (Table 11.2) were calculated from the mean site directions both before and after rotating the flow planes to horizontal. The two positions in the last column, obtained after thermal demagnetization and rotation to horizontal, are plotted on Figure 11.6 which also shows the apparent polar wander path (APWP) for the North American paleocontinent as compiled by Irving (1979) and other Eocene pole positions for western North America (also listed by Irving, 1979). The possible megatectonic significance of these pole positions with respect to APWP will be examined in a further study.

References

Clapp, C.H. and Cooke, H.C.
1917: Sooke and Duncan map-areas, Vancouver Island; Geological Survey of Canada, Memoir 96.

Irving, E.
1979: Paleopoles and paleolatitudes of North America and speculations about displaced terraines; Canadian Journal of Earth Sciences, v. 16, p. 669-694.

Irving, E. and Yole, R.W.
1972: Paleomagnetism and the kinematic history of mafic and ultramafic rocks in fold mountain belts; Publications of the Earth Physics Branch, Department of Energy, Mines and Resources, Ottawa, v. 42, p. 87-95.

McElhinny, M.W.
1964: Statistical significance of the fold test in paleomagnetism; Geophysical Journal of the Royal Astronomical Society, v. 8, p. 338-340.

Muller, J.E.
1977a: Evolution of the Pacific margin, Vancouver Island and adjacent regions; Canadian Journal of Earth Sciences, v. 14, p. 2062-2085.

1977b: Metchosin Volcanics and Sooke Intrusions of southern Vancouver Island; in Report of Activities, Part A, Geological Survey of Canada, Paper 77-1A, p. 287-294.

1980: Chemistry and origin of the Eocene Metchosin Volcanics, Vancouver Island, British Columbia; Canadian Journal of Earth Sciences, v. 17, p. 199-209.

Schwarz, E.J., Muller, J.E., and Clark, K.R.
1980: Paleomagnetism of the Karmutsen basalts from southeast Vancouver Island; Canadian Journal of Earth Sciences, v. 17, p. 389-399.

Symons, D.T.A.
1971: Paleomagnetic notes on the Karmutsen basalts, Vancouver Island, British Columbia; Geological Survey of Canada, Paper 71-24, p. 9-24.

1973: Paleomagnetic zones in the Oligocene East Sooke Gabbro, Vancouver Island, British Columbia; Journal of Geophysical Research, v. 78, no. 23, p. 5100-5109.

Wanless, R.K., Stevens, R.D., Lachance, G.R., and Delabio, R.N.
1972: Age determinations and geological studies, K-Ar Isotopic Ages, Report 10; Geological Survey of Canada, Paper 71-2.

1973: Age determinations and geological studies, K-Ar Isotopic Ages, Report 11; Geological Survey of Canada, Paper 73-2.

Wanless, R.K., Stevens, R.D., Lachance, G.R., and Edmonds, C.M.
1967: Age determinations and geological studies, K-Ar Isotopic Ages, Report 7; Geological Survey of Canada, Paper 66-17.

Yole, R.W. and Irving, E.
1980: Displacement of Vancouver Island: paleomagnetic evidence from the Karmutsen Formation; Canadian Journal of Earth Sciences, v. 17, p. 1210-1228.

12. **VAMPIRE FORMATION, A NEW UPPER PRECAMBRIAN(?)/LOWER CAMBRIAN FORMATION, MACKENZIE MOUNTAINS, YUKON AND NORTHWEST TERRITORIES**

Project 650024

W.H. Fritz
Institute of Sedimentary and Petroleum Geology, Ottawa

Fritz, W.H., Vampire Formation, a new Upper Precambrian(?)/Lower Cambrian formation, Mackenzie Mountains, Yukon and Northwest Territories; in Current Research, Part B, Geological Survey of Canada, Paper 82-1B, p. 83-92, 1982.

Abstract

The Vampire Formation of dark coloured siltstone and interbedded fine grained quartzite is exposed along the southwestern margin of the Mackenzie Mountains. These strata belong to the latest Precambrian(?) and early Lower Cambrian. They represent slope deposits that are intermediate between shallow water quartzites of the upper member of the Backbone Ranges Formation, and basinal strata that at least in part belong to the upper member (maroon siltstone) of the "grit unit". Map unit 13 of Blusson is a tongue of the Vampire Formation that overlies a tongue of the upper member of the Backbone Ranges Formation.

Introduction

A new formation is proposed for strata that are the lateral equivalent of the upper member of the Backbone Ranges Formation. These strata, herein named the Vampire Formation, comprise siltstone and interbedded, very fine- to fine-grained quartzite, both of which weather a dark rust. Vampire strata differ significantly from those of the upper member of the Backbone Ranges Formation, which consist mainly of fine- to coarse-grained quartzite. The latter quartzites weather to various shades of orange, grey, maroon or purple, and are interbedded with far less siltstone than are the quartzites of the Vampire Formation.

Previous Work and Geographic Distribution

Strata of the Vampire Formation were first mapped in the Nahanni map area as map unit 3 (Green and Roddick, 1961; Green et al., 1967). Immediately north of the Nahanni area, in the Sekwi Mountain map area, Blusson (1971) mapped a tongue of Vampire strata as map unit 13. To the north and west of the Sekwi Mountain area, Blusson (1974) included map unit 13 as part of the Backbone Ranges Formation on a series of Geological Survey of Canada open file maps. The writer (Fritz, 1976, 1978, 1979b) has described 26 stratigraphic sections that extend down into map unit 13 in the areas mapped by Blusson, although these studies were directed primarily toward understanding of the overlying Sekwi Formation.

Gabrielse and others (1973) assigned Vampire strata in the South Nahanni Anticline (east of the Nahanni map area) to the Backbone Ranges Formation. This assignment of beds was also made by Gordey (1979, Fig. 2.1, section C) in the

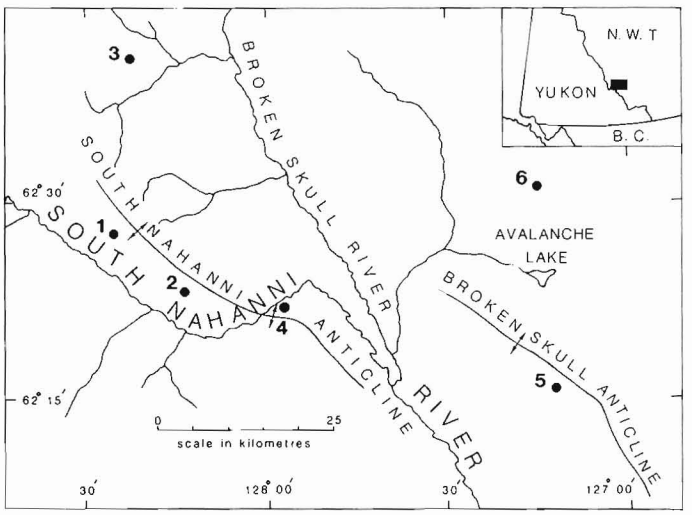

Figure 12.1. *Index map locating the type section (4) of the Vampire Formation and sections (5, 6) containing laterally equivalent strata in the upper member of the Backbone Ranges Formation. These three sections are shown in Figure 12.3. Sections at 1 (Fritz, 1979a) and at 2 and 3 (Fritz, 1981) have been published in studies mainly focused upon younger Cambrian strata; nevertheless, each contains a description of strata belonging to the upper part of the Vampire Formation.*

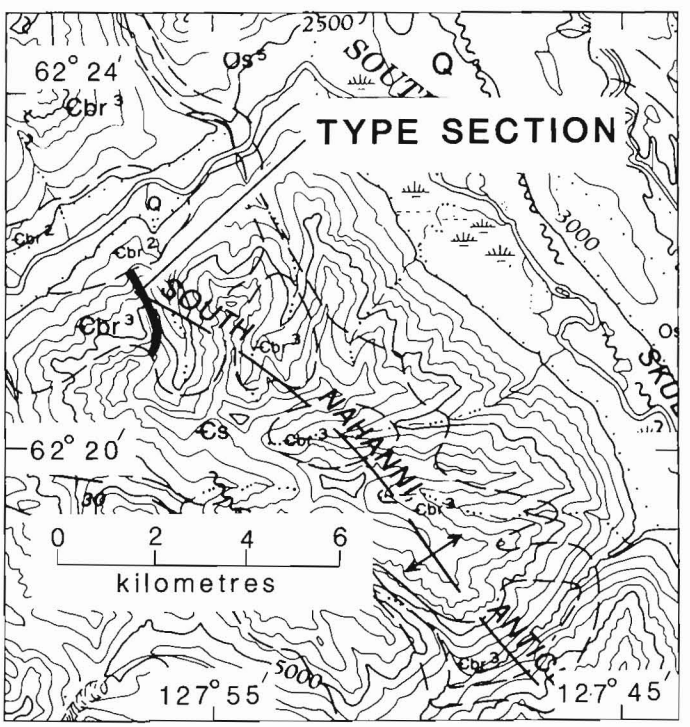

Figure 12.2. *Geological map reproduced from Gabrielse et al. (1973) to show location of type section of Vampire Formation. Symbols include: €Cbr², middle member of Backbone Ranges Formation; €Cbr³, Vampire Formation; and €Cs, Sekwi Formation.*

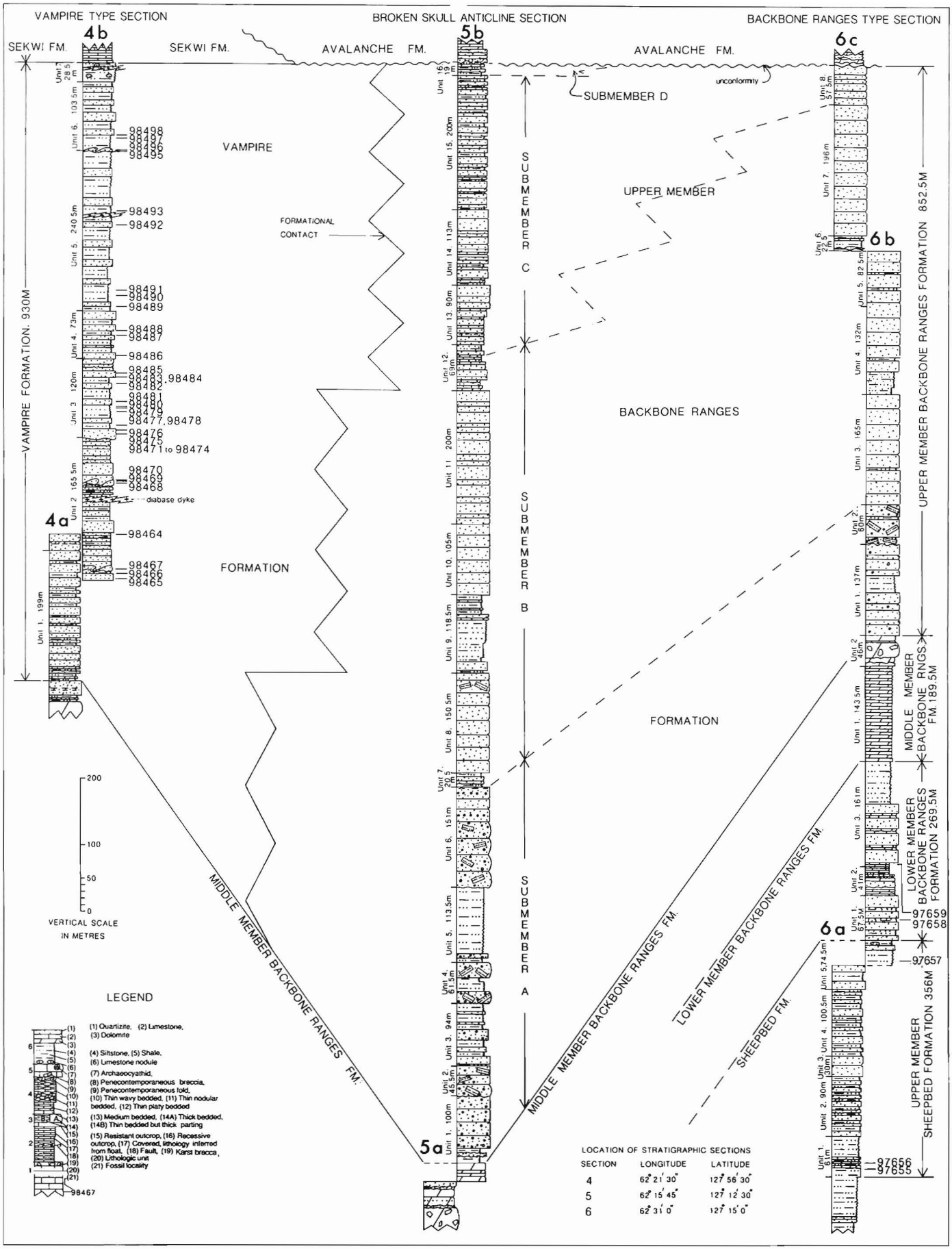
VAMPIRE TYPE SECTION
BROKEN SKULL ANTICLINE SECTION
BACKBONE RANGES TYPE SECTION
4b
5b
6c
SEKWI FM.
SEKWI FM.
AVALANCHE FM.
AVALANCHE FM.
unconformity
SUBMEMBER D
VAMPIRE
FORMATIONAL CONTACT
UPPER MEMBER
SUBMEMBER C
BACKBONE RANGES
SUBMEMBER B
FORMATION
SUBMEMBER A
VAMPIRE FORMATION. 930M
UPPER MEMBER BACKBONE RANGES FORMATION 852.5M
MIDDLE MEMBER BACKBONE RNGS FM. 189.5M
LOWER MEMBER BACKBONE RANGES FORMATION 269.5M
UPPER MEMBER SHEEPBED FORMATION 356M
MIDDLE MEMBER BACKBONE RANGES FM.
LOWER MEMBER BACKBONE RANGES FM.
SHEEPBED FM.
diabase dyke
98498
98497
98496
98495
98493
98492
98491
98490
98489
98488
98487
98486
98485
98483,98484
98482
98481
98480
98479
98477,98478
98476
98475
98471 to 98474
98470
98469
98468
98464
98467
98466
98465
97659
97658
97657
97656
97655
4b
4a
5a
6b
6a
VERTICAL SCALE IN METRES
200
100
50
0
LEGEND
(1) Quartzite, (2) Limestone, (3) Dolomite
(4) Siltstone, (5) Shale, (6) Limestone nodule
(7) Archaeocyathid, (8) Penecontemporaneous breccia, (9) Penecontemporaneous fold, (10) Thin wavy bedded, (11) Thin nodular bedded, (12) Thin platy bedded
(13) Medium bedded, (14A) Thick bedded, (14B) Thin bedded but thick parting
(15) Resistant outcrop, (16) Recessive outcrop, (17) Covered, lithology inferred from float, (18) Fault, (19) Karst breccia, (20) Lithologic unit, (21) Fossil locality
98467
LOCATION OF STRATIGRAPHIC SECTIONS
SECTION LONGITUDE LATITUDE
4 62° 21' 30" 127° 56' 30"
5 62° 15' 45" 127° 12' 30"
6 62° 31' 0" 127° 15' 0"

Nahanni map area. Gordey's terminology was questioned by the writer (Fritz, 1979a, p. 123), who suggested that the Nahanni strata more closely resemble those of map unit 13 to the north, and therefore recommended a delay in reassigning map unit 3 of Green and Roddick (1961) until new data could be obtained.

H. Gabrielse and S.P. Gordey suggested that the writer carry out a detailed study of outcrops at the south end of Nahanni Anticline. In 1980 the writer spent one week measuring a section in this area and one week studying the type section of the Backbone Ranges Formation (Gabrielse et al., 1973, section 12) 36 km to the east. From the study the writer concluded (Fritz, 1981, p. 152) that the beds of the South Nahanni Anticline are lithologically distinct from the upper member of the Backbone Ranges Formation, that a new name was needed for the lateral equivalent of the upper member, and that the type section of the new formation should be located at the south end of the South Nahanni Anticline. In 1981 the writer measured a second stratigraphic section (type section of this report) in the South Nahanni Anticline and studied equivalent Backbone Ranges strata exposed in the Broken Skull Anticline located 39 km to the southeast (Fig. 12.1-12.3; sections 4 and 5, respectively).

Location of Type Section and Name of Formation

The type section for the Vampire Formation is in the southwestern part of Mackenzie Mountains where the South Nahanni Anticline is crossed by the South Nahanni River (Fig. 12.1). The section is on a high slope overlooking the river from the southeast and 7 km southwest of the point where the course of the South Nahanni River turns abruptly from east-northeast to southeast (Fig. 12.2). Photographs showing the base, top and various stratigraphic horizons of the section are shown in Plates 12.1 and 12.2. The centre of the section lies at latitude 62°21'30"N and longitude 127°56'30"W.

The formation name is taken from Vampire Peaks, which are numerous rock spires that stand along the South Nahanni Anticline. The spires start at the South Nahanni River and extend 15 km to the southeast. The name Vampire Peaks has been approved by the Canadian Board on Geographical Names (now Canadian Permanent Committee on Geographical Names) and is reserved for future maps, but, to the writer's knowledge, the name has not yet appeared on a map.

General Lithology

Typical outcrops of the Vampire Formation weather dark brownish grey and form recessive slopes that contrast with those of the overlying carbonate of the Sekwi Formation and the underlying dolomite of the middle member of the Backbone Ranges Formation. Slopes underlain by the Vampire Formation are commonly covered with plates of siltstone and very fine- to fine-grained quartzite, which are the formation's two main lithologies. The siltstone is generally interbedded with the quartzite, but at several levels within the formation the quartzite forms successive medium and thick beds that outcrop as ribs in an otherwise uniform slope (Plate 12.1, number 4).

Figure 12.3 *(opposite). Stratigraphic sections illustrating the type section of the Vampire Formation (4) and laterally equivalent strata in the upper member of the Backbone Ranges Formation (5, 6). Section 6 is the type section for the Backbone Ranges Formation. The section locations are shown in Figure 12.1. Fossil locality numbers refer to collections of trace fossils or pseudo-trace fossils.*

Viewed at close range, the quartzites are a dark rust with minor areas of orange, medium brownish grey, and light brown. The bedding is thin to thick, blocky, and planar laminae are visible on some beds, especially the thinner ones. Crossbedding is rare. Load casts, ball and pillow structures, and penecontemporaneous folds are present at some levels. Fresh quartzite surfaces are medium grey, greenish grey or light brownish grey, and the quartzite is very fine- to fine-grained.

The siltstone weathers medium brownish grey, greenish grey or rust. Fresh surfaces are medium grey or greenish grey. Very fine grained sandstone is commonly intermixed with the siltstone.

Base and Top of Formation

The base of the Vampire Formation is at the top of the highest, orange weathering dolomitic sandstone bed in the predominantly dolomitic middle member of the Backbone Ranges Formation. Dolomite in orange weathering, thick to massive beds is present 30.5 m below the Vampire-Backbone Ranges formational contact (Plate 12.2, number 3). In the interval 21.5 to 30.5 m below the contact are interbeds of dark grey siltstone and orange weathering, thin and medium bedded quartzite. The interval 0 to 21.5 m contains orange weathering dolomitic quartzite in thick beds and some dolomite free of quartz clasts. The quartz grains are fine to coarse. Immediately above the base of the Vampire Formation are interbedded, rusty weathering siltstone and fine grained quartzite (further described under "stratigraphic unit 1", below). No interbedded dolomite was seen in the lower part of the Vampire Formation, although some interbeds of dolomitic sandstone are present near the 200 m level.

Consideration was given to locating the base of the Vampire Formation at the horizon 30.5 m below the present level, as this is a level where a major lithological change takes place. However, from a distance the predominantly quartzite beds in the 0 to 20.5 m interval appear similar to the thick dolomite beds below, and therefore are easier to map as part of the same formation.

At the top of the Vampire Formation is 28.5 m of light greenish-grey siltstone (stratigraphic unit 7) that is abruptly overlain by 3 m of maroon and orange weathering limy siltstone that forms the basal beds of the Sekwi Formation. The limy siltstone contains orange weathering limestone nodules that are susceptible to weathering so that cavities give the siltstone a "Swiss cheese" appearance. Above the siltstone is medium light grey weathering, platy limestone typical of the lower Sekwi of this region.

Diabase Dykes

The type section is cut by three diabase dykes that cross the measured traverse in the intervals 272 to 278 m, 698.5 to 703 m, and 921 to 922 m above the base of the Vampire Formation. There is only minor displacement at the horizon where the dykes pass from the Vampire into the Sekwi Formation and little displacement was seen within the Vampire Formation. The dykes are included in the measured section as an aid in locating position in any later study of this monotonous succession of rocks.

Stratigraphic Units

Unit 1, 199 m

The basal unit in the Vampire Formation comprises rust weathering, thin to thick bedded quartzite (three-fourths) that is fine- to coarse-grained in the lower 54 m and fine grained above. Unweathered quartzite surfaces are medium light grey. Interbedded with the quartzite is rust weathering

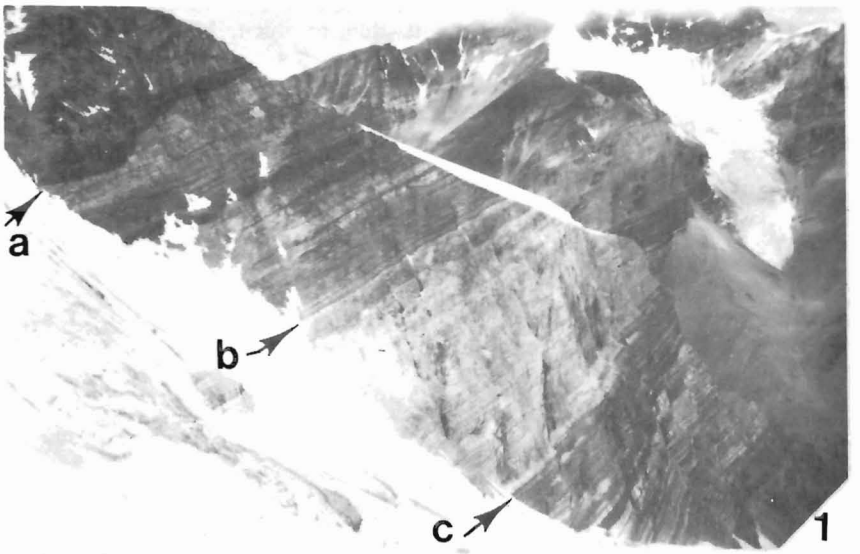
a
b
c
1


2

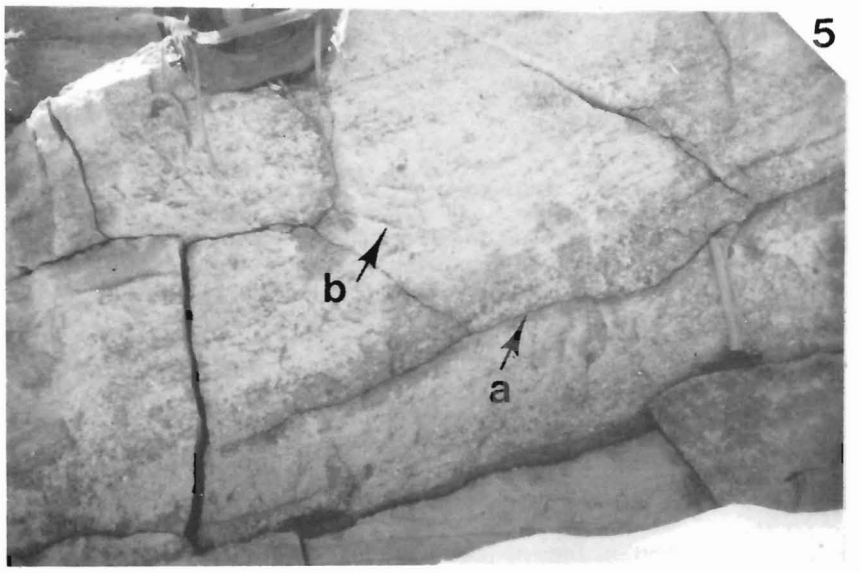
b
a
5

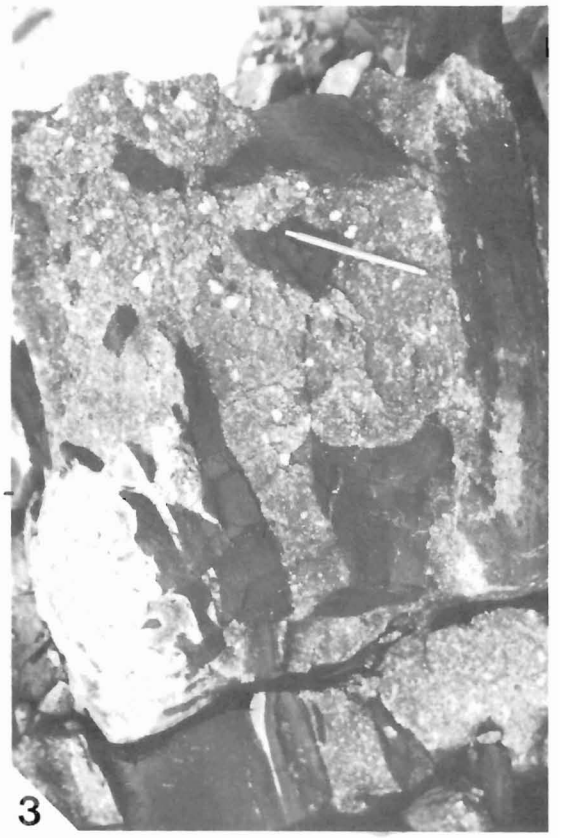
3

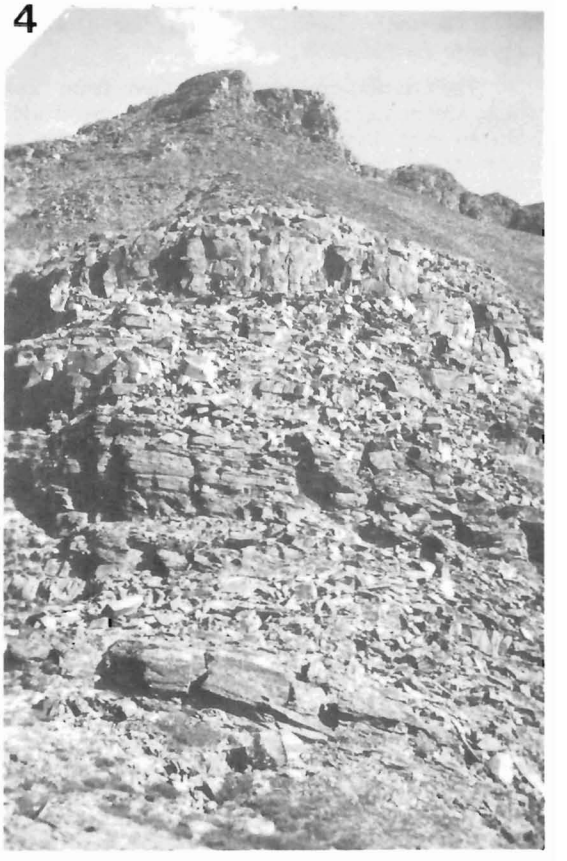
4

siltstone (one-fourth) that is dark grey on unweathered surfaces. Interval 154 to 158 m above the base contains orange weathering quartzite (two-thirds) that is light maroon on fresh surface and is interbedded with maroon siltstone (one-third). Interval 158 to 170 m contains quartzite (three-fourths) that is medium greenish brown on weathered and fresh surfaces and is interbedded with siltstone (one-fourth) of a similar colour. Penecontemporaneous slump folds are present at 154, 167.5, 170 and 184 m above the base. Near the latter horizon are symmetrical transverse ripple marks on a single bedding surface indicating a current from either the northeast or southwest. The description of unit 1 from the base to the 154 m level is from section 4a located west of the small gully shown in Plate 12.2, numbers 1 to 3. The remainder of the section (4b) was measured along a continuous route east of the gully.

Unit 2, 165.5 m

At the base of this unit is 6 m of orange weathering, dolomitic sandstone in thick beds. The sand grains are fine and the dolomitic sandstone is light brown on unweathered surfaces. The interval from 6 m to the base of a diorite dyke occupying the interval 73 to 79 m is mainly covered, but float indicates that the lithology is similar to the main lithologies mentioned in unit 1. The interval 79 to 123.5 m contains rust to medium greenish brown weathering quartzite (three-fourths) in thin to thick beds that are medium grey on fresh surfaces, and bright rust weathering siltstone (one-fourth) that is medium light greenish grey on fresh surfaces. At the top of the unit is 36 m of bright rust weathering quartzite in thin to thick beds. Fresh surfaces are light greenish grey and are fine grained. Orange to pink weathering dolomite in thick beds is present 88 to 91 m above the base and penecontemporaneous slump folds are present in the interval 102 to 103 m and 108 to 108.75 m above the base. The latter folds are shown in Plate 12.2, number 6.

Unit 3, 120 m

Unit 3 is mainly rust to yellowish orange weathering siltstone and very fine grained sandstone that weathers to plates with flat to broadly cuspate parting surfaces. Unweathered surfaces are medium light grey to greenish grey. Interbedded with the siltstone and sandy siltstone is a subordinate amount of thick bedded, fine grained quartzite that weathers rust to medium dark brownish grey with a slight purple cast. Unweathered quartzite surfaces are medium greenish grey. At the base of the unit is 8 m of cliff-forming (Plate 12.2, number 4), medium brownish grey weathering quartzite in very thick beds. The quartzite is fine grained and was deposited on a surface that has been scoured at least 0.5 m into the underlying unit. In the uppermost 27.5 m of the unit the quartzite is in thin to thick interbeds, some of which are purple weathering or have a purple cast.

Unit 4, 73 m

Half of this unit consists of thick bedded, very fine grained quartzite. It is white on weathered and unweathered surfaces near the base and darkens upsection until, near the top, it is rust weathering and medium grey on fresh surfaces. Near the base, the quartzite is marked by small (0.2 mm) limonite spots. Interbedded with quartzite is fine grained sandstone and siltstone that weather rust and are medium to dark grey on fresh surfaces.

Unit 5, 240.5 m

Unit 5 is rust weathering siltstone (three-fourths) that is dark grey on unweathered surfaces, and thin to thick bedded, very fine grained quartzite (one-fourth) that is medium brownish to greenish grey on fresh surfaces. The lower third of this unit forms a bench on the ridge followed while measuring the type section (Plate 12.2, numbers 1, 2). A diabase dyke cuts the unit in the interval 74.5 to 79 m above the base.

Unit 6, 103.5 m

Medium greenish grey, rust and yellow-orange weathering siltstone (three-fourths) predominates in this unit. Unweathered surfaces are medium light greenish grey. Rust weathering, very fine grained quartzite (one-fourth) in thick beds is interbedded with the siltstone and is the same colour on fresh surfaces. Penecontemporaneous slump folds with northeast-trending axes are present in the intervals 0 to 0.5 m and 11 to 11.3 m above the base and prominent load casts (Plate 12.2, number 5) are developed 94 m above the base.

Unit 7, 28.5 m

A thick bedded to massive unit of siltstone that is light greenish grey on weathered and fresh surfaces forms the uppermost unit in the Vampire Formation. Orange weathering pods (averaging 3 cm in diameter) of fine grained quartzite are also present.

Age of Formation

Thirty-four horizons containing trace fossils or pseudo-trace fossils were collected at the type section of the Vampire Formation. The fossil material is under study by G.M. Narbonne at the University of Montreal, and only preliminary identifications are available. Narbonne reports (personal communication, 1981) that the only trace fossils of definite Cambrian age are at GSC locality 98470 located 301 m above the base of the formation. Forms present are described as cf. **Rusophycus** sp. and arthropod scratch marks. At GSC locality 98498 the writer noted the presence of a small, cone-shaped, shelly fossil, **Circotheca**? sp. This locality is 107 m below the top of the formation. Similar fossils identified as **Circotheca**? sp. have been found (Fritz, 1981, p. 15) in section 2 (see Fig. 12.1) at 90.5 to 85.5 m below the top of the formation.

Plate 12.1

1. View west to outcrop of Backbone Ranges Formation, section 6. Channel at base of unit 2 in upper member is at "a", and top and base of middle member are at "b" and "c". GSC 200875-W
2. Large clast of light green siltstone (near hammer handle) in fine breccia; 26 m above base of unit 2, upper member of Backbone Ranges Formation, section 5. GSC 203775E
3. Large clast of maroon siltstone in channel breccia; 4.5 m above base of unit 2, upper member of Backbone Ranges Formation, section 6. GSC 200875-U
4. View south and upsection of a typical exposure of Vampire Formation. Location is 2 km west of type section. Camera is 451 m above base of formation. GSC 203775
5. Layer of grit-sized quartzite in small channels with base at "a". Faintly outlined high angle crossbeds in coarse grained quartzite are at "b". Location is 119 m above base of unit 6, upper member of Backbone Ranges Formation, section 5. GSC 203775-B

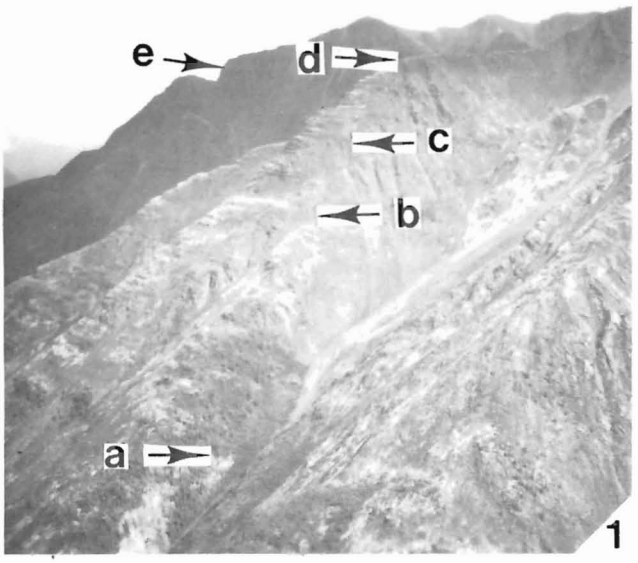
e
d
c
b
a
1

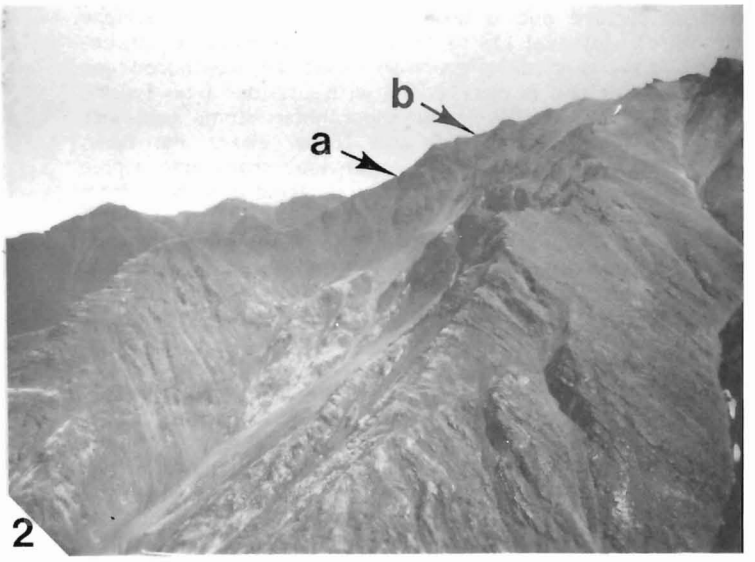
b
a
2

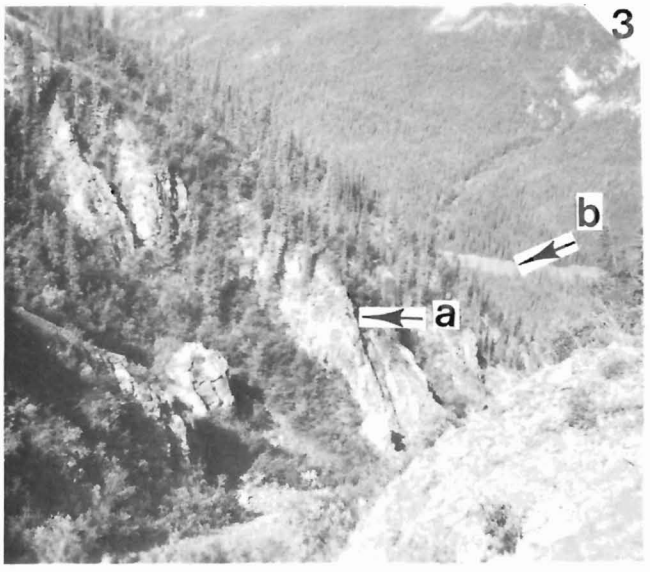
3
b
a


4


5


6

Parafallotaspis grata Fritz has been reported (Fritz, 1981, p. 152) in local float 1 m above the top of the Vampire Formation in section 3, so it is clear that the formation can be no younger than early Lower Cambrian. This observation and the noted trace fossils at GSC locality 98470, indicate that at least the upper two-thirds of the formation belongs to the early Lower Cambrian. Lithological correlations (see below and Fig. 12.4) with map units 11 and 12 of Blusson (1971) in the Sekwi Mountain map area suggest that part of the lower third of the formation belongs to the Precambrian.

Correlations

The Vampire Formation at the type section is clearly the lateral equivalent of the upper member of the Backbone Ranges Formation at its type section and in the Broken Skull Anticline: at all three localities the map units are underlain by the middle member of the Backbone Ranges Formation and overlain by younger Cambrian strata (Fig. 12.3). At its type section the Vampire Formation is overlain with a normal depositional contact by the Lower Cambrian Sekwi Formation, whereas at section 5 and 6 the upper member of the Backbone Ranges Formation is separated by an unconformity from the Middle Cambrian Avalanche Formation. It appears at the latter two localities that erosion has not cut deeply into the Backbone Ranges Formation.

No fossils were found in the upper member of the Backbone Ranges Formation at sections 5 and 6. The lack of fossils at the latter two sections is believed to be the result of an inhospitable environment and not to the age of the strata. Questionable trace fossils are present in the lower member of the type section of the Backbone Ranges Formation at GSC locality 97658 and **Planolites** sp. is present in the same member at GSC locality 97659.

Plate 12.2

1. View from helicopter looking east at type section of Vampire Formation. Base of formation, at outcrop short distance east of measured segment 4a, is at "a", diabase dyke cutting section 272 m above base of formation is at "b", base of unit 3 is at "c", and base of unit 5 is at "d". Measured but undescribed Vampire section 2 km east of type section is on ridge "e". GSC 203775-G
2. View from helicopter looking east at Vampire Formation. Diabase dyke cutting type section 698.5 m above base of formation is at "a", and top of formation is at "b". GSC 203775-L
3. View northwest and down gully shown at "a" in Figure 12.1. Top of thick bedded to massive dolomite 30.5 m below base of Vampire Formation in segment 4a of measured section is at "a". South Nahanni River is at "b". GSC 203775-N
4. Base of unit 3 in type section of Vampire Formation is at top of 1.5 m measuring staff. Note that basal, thick bedded to massive quartzite in unit 3 rests on irregular surface with relief of at least 0.5 m eroded into underlying strata. GSC 203775-D
5. Strongly developed load casts in fine grained quartzite (dark beds) and interbedded siltstone. Type section for Vampire Formation, unit 6, 93.5 m above base of unit. GSC 203775-C
6. Quartzite (at base of hammer handle) in penecontemporaneous detached fold. Type Vampire section, unit 2, 103 m above base of unit. GSC 203775-O

The lithological change between the upper member of the Backbone Ranges Formation in sections 5 and 6 and the Vampire Formation at section 4 (type section) is appreciable, and no major tongues or marker beds extend from sections 5 and 6 into section 4. There are, however, three thick lithological submembers within the upper member of the Backbone Ranges Formation at sections 5 and 6, and a thin fourth submember at section 5 that reflect a general fining upward within the upper member. The four submembers have been designated as submembers A, B, C, and D on Figure 12.3. The submembers are discussed below and are compared with strata of the Vampire Formation in section 4, which also fines upward, although more subtly because of a narrower range of grain sizes.

Submember A forms the lower quarter of the upper member of the Backbone Ranges Formation at sections 5 and 6. This consists of thick-bedded to massive, poorly sorted quartzite beds with few visible internal structures, but locally with channels 4 to 150 cm deep (Plate 12.1, numbers 1, 5). Grit- and pebble-sized quartz and feldspar clasts are common but rarely exceed 25 mm in diameter. Clasts of maroon, purple, and greenish grey siltstone are common at various levels, and some exceed 1.5 m in length (Plate 12.1, numbers 2, 3). These clasts of siltstone are "floating" in the finer matrix of quartz and feldspar grains and are tilted at various angles to the bedding. The siltstone of the clasts closely matches siltstone in local interbeds. The coarse size, poor sorting, and presence of channels combine to suggest a high energy, shallow environment at the two Backbone Ranges sections. Abundant large feldspar clasts and the high angularity of the clasts indicate rapid transport and burial. The presence of scattered sulphide fragments up to 7 mm in diameter in unit 4 of section 5 supports the rapid transport and burial concept.

Submember B of the upper member of the Backbone Ranges Formation at sections 5 and 6 is composed of fine- and medium-grained quartzite in thick beds that exhibit crossbedding and small channels. Although some layers of grit are present, pebbles and siltstone fragments are rare, and it seems likely that these strata were laid down in a shallow water, offshore environment. Twenty-six crossbeds in submember B at the Broken Skull Anticline section (section 5) indicate flow to the northwest.

The lithological differences that permit submembers A and B to be recognized as separate entities at sections 5 and 6 are not evident in equivalent strata at the type Vampire section, where the colour, grain size, and geometry of the beds are uniformly monotonous. There is, however, a greater concentration of quartzite in the lower four units of the Vampire Formation.

Submember C of the Backbone Ranges Formation in sections 5 and 6 consists of white weathering quartzite in thin to thick beds and interbedded dark grey siltstone. The uniform composition and fine grain size of the quartzite indicate a greater maturity than is typical of subunits A and B in the upper member. A similar white quartzite was noted in the lower part of unit 4 in the Vampire Peaks type section. Above unit 4 in the Vampire section there is a general change in grain size with quartzite giving way to a dominance of siltstone. This change in grain size may be a basinward reflection of the abrupt change in grain size between submembers B and C in the upper member of the Backbone Ranges Formation.

The highest submember, D, of the Backbone Ranges Formation in section 5 comprises only 19 m of rust weathering, fine grained quartzite and interbedded siltstone. The strata of this submember are almost identical to those of the Vampire Formation, and the submember might in fact

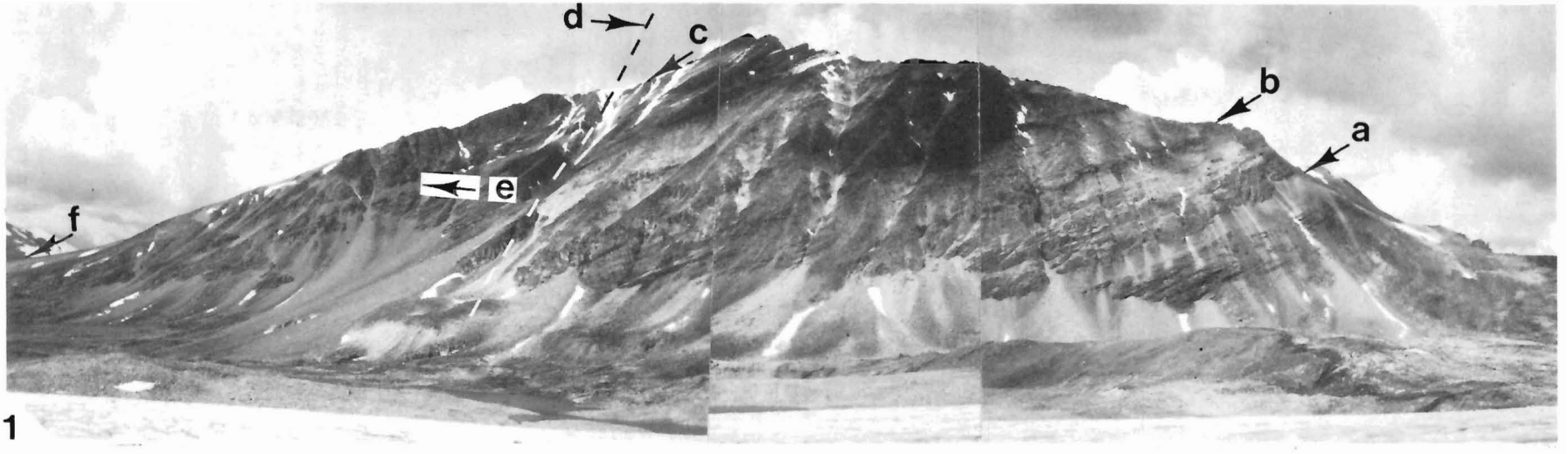

1

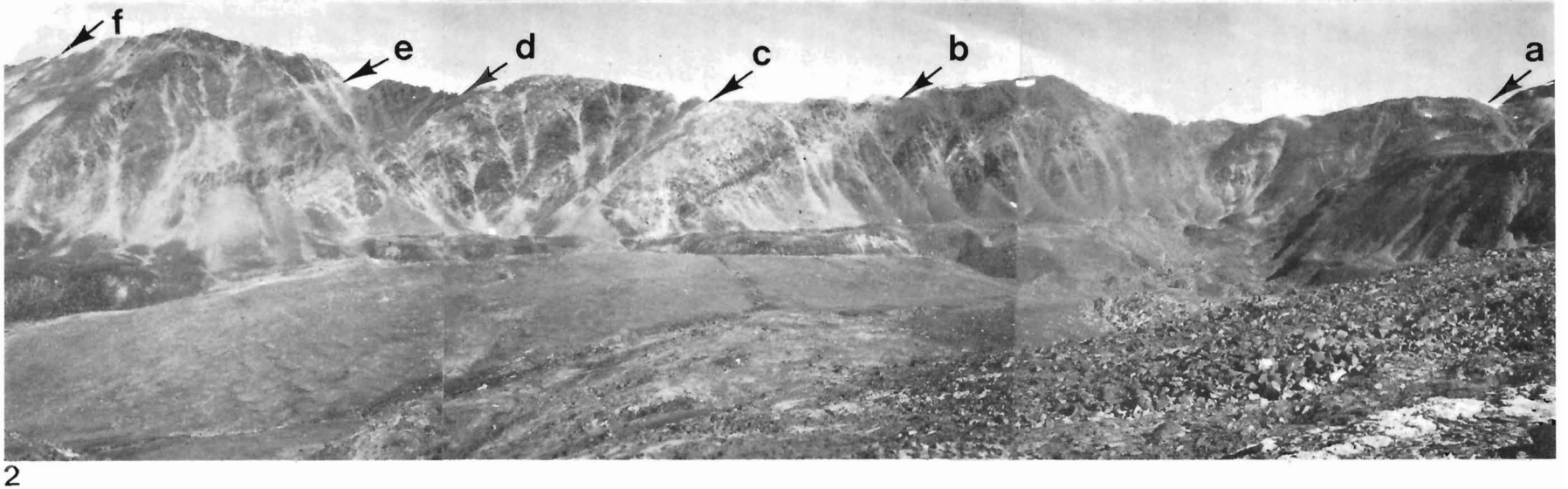

2

Plate 12.3

1. View northwest to upper member of Backbone Ranges Formation. Type section, described in Gabrielse and others (1973, section 12), was measured in valley in foreground; section 6, shown in Figure 12.3 in this paper, was measured along crest of ridge on skyline. Base of upper member of Backbone Ranges Formation is at "a", base of unit 2 is at "b", base of unit 6 is at "c" and "e", fault cuts section at "d", and top of Backbone Ranges Formation is at "f". Figure is composite of GSC 200875-X, 200875-Y, and 200875-Z.

2. View northwest to upper member of Backbone Ranges Formation in Broken Skull Anticline (Fig. 12.3, section 5). Location of section is shown on GSC map 1314A (Gabrielse et al., 1973), but no description was given by these authors. Shale at base of unit 1 is at "a", base and top of unit 6 is at "b" and "c", base and top of unit 9 is at "d" and "e", and base of unit 12 is at "f". Figure is composite of GSC 203775-A, 203775-I, and 203775-J.

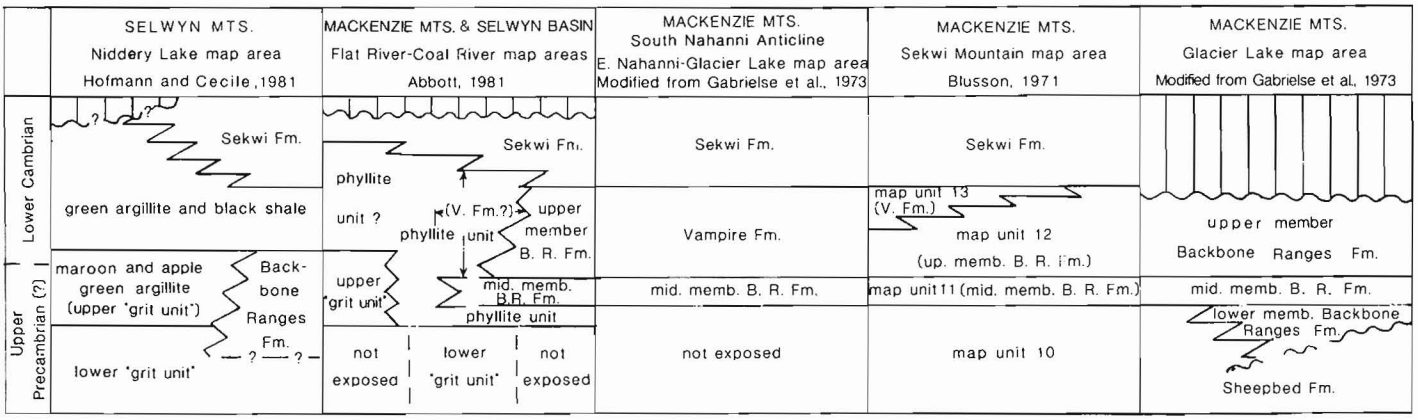

Figure 12.4. *Correlation chart for the Vampire Formation and certain other map units. Vampire Formation in brackets (V. Fm.) has been added to those map units that are here proposed for recognition as being part of the Vampire Formation. Backbone Ranges Formation is abbreviated to "B. R. Fm." in some parts of the chart.*

represent a thin edge of an eastward extending tongue of the formation. The minor thickness of submember D precludes its being mapped in this area as part of another formation.

Middle and Northern Mackenzie Mountains

Strata equivalent to those in the Vampire Formation type section and to the upper member of the Backbone Ranges Formation in its type section have been assigned to map units 12 and 13 (Blusson, 1971) in the Sekwi Mountain map area. These two map units are overlain by the Sekwi Formation and are underlain by map unit 11. Map unit 11 is the basinward extension of the middle member of the Backbone Ranges Formation. Map unit 12 is mainly fine and medium grained, light coloured quartzite and should be assigned to the upper member of the Backbone Ranges Formation, whereas overlying map unit 13 is composed of dark siltstone and interbedded very fine grained quartzite that can be assigned to the Vampire Formation. Eight published sections (Fritz, 1978, 1979b) from the Sekwi Mountain area include descriptions of map unit 13. Additional data on map unit 13 are available in an unpublished thesis by F.F. Krause (1979).

The Precambrian-Cambrian Boundary Working Group (I.U.G.S., I.G.C.P.) has tentatively placed the Precambrian-Cambrian boundary within the interval 350 to 370 m above the top of map unit 11 (Fritz, 1980, p. 44). Assuming that the top of the middle member of the Backbone Ranges Formation (top of map unit 11) is approximately synchronous in the Sekwi Mountain map area and in the South Nahanni Anticline, then the Precambrian-Cambrian boundary should lie within the lower part of the Vampire Formation at the type section.

In the Mount Eduni and the eastern part of the Bonnet Plume Lake map areas, the Vampire Formation is absent and the Sekwi Formation rests directly on the upper member of the Backbone Ranges Formation (Fritz, 1978, sections 16, 17; 1979b, section 31/4). The eastern edge of the Vampire Formation lies just east of the centre of the Bonnet Plume Lake area (Fritz, 1978, section 18, unit 3) where it directly underlies the Sekwi Formation. A tongue of the Vampire Formation lies below the Sekwi Formation and above the upper member of the Backbone Ranges Formation in the western part of the Bonnet Plume Lake area (Fritz, 1978, section 13; 1979b, section 27) and in part of the adjoining Nadaleen River map area to the west (Fritz, 1978, section 11). In the latter area the middle member of the Backbone Ranges Formation is thin, but it abruptly thickens immediately north of the Snake River near the mouth of Duo Creek and the mouth of Goz Creek where it hosts the Goz Creek lead-zinc deposits. A short distance north (lat. 64°28'30"N, long. 132°36'30"W) and to the east (lat. 64°25'45"N, long. 132°22'30"W) of the deposit, the Vampire Formation occupies the entire interval between the middle member of the Backbone Ranges Formation and the Sekwi Formation, and is therefore fully developed.

Selwyn Basin

Hofmann and Cecile (1981) have correlated a sub-Sekwi shale northeast of the Selwyn Valley (Niddery Lake map area) with the lower part of an unnamed Lower Cambrian green argillite and black shale map unit southwest of the valley (see Fig. 12.4). Underlying the shale to the northeast is the undivided Backbone Ranges Formation that is shown to correlate, at least in its upper part, with the upper part of the "grit unit" (unit 1 of Green and Roddick, 1961) to the southwest. In the latter area, the Lower Cambrian trace fossil **Oldhamia** is reported to be present high in the upper member of the "grit unit". The sub-Sekwi position of the shale and upper Backbone Ranges Formation to the northeast and the correlation of these two map units to the shale and **Oldhamia**-bearing "upper grit" member to the southwest suggests that in the latter area at least the lower part of the greenish grey phyllite and the upper part of the upper member of the "grit unit" correlate with the Vampire Formation.

In the Nahanni map area west of the South Nahanni Anticline, Gordey (1980) has recognized a maroon shale as being the upper member of the "grit unit". Directly above the maroon shale is a buff weathering shale with archaeocyathids in breccia at the base (Gordey, 1980). The presence of the archaeocyathids suggests that the buff shale is the lateral equivalent of the Sekwi Formation, and their position indicates that at least part of the underlying maroon shale is the lateral equivalent of the Vampire Formation.

Southeast of the Nahanni map area, in the Flat River and Coal River map areas, Abbott (1981, Fig. 2, 3) has studied the transition between the Backbone Ranges Formation to the east and the "grit unit" to the west. The usual three-fold subdivision of the Backbone Ranges Formation is shown and the formation is reported to be overlain by the Sekwi Formation and underlain by a "phyllite unit". The middle member of the Backbone Ranges Formation extends for a considerable distance to the west

but the upper and lower members to the west are replaced by the phyllite unit. In this transition zone, the strata between the Sekwi Formation and the middle member of the Backbone Ranges Formation occupy the same interval as the Vampire Formation at the type section, and therefore the lithology of this zone should be reviewed to see whether or not the reported phyllite unit is similar in lithology to the siltstone and interbedded quartzite of the type Vampire Formation. If similar, the Vampire Formation can be extended for a distance of at least 75 km south-southeast of the type section.

Farther basinward in Abbott's (1981) cross-section the lower member of the "grit unit" is shown to be overlain by the phyllite unit and then in turn by the Sekwi Formation. Still farther basinward, the upper part of the upper member of the "grit unit" is shown to be the lateral equivalent of the Backbone Ranges Formation. There the "grit unit" is overlain by the questionably identified phyllite unit that is there mainly equivalent to the lower part of the Sekwi Formation. Dolomite that is probably the basinward extension of the upper part of the Sekwi Formation overlies the questionable phyllite unit. As outcrops representing the latter two parts of the cross-section are poor, the relationships shown are tentative until further field work is done (G. Abbott, personal communication, 1981). However, Abbott's present interpretation closely matches that provided by Hofmann and Cecile (1981) in the Niddery Lake map area to the northwest.

References

Abbott, G.
1981: A new geological map of the upper Coal River area; Yukon Geology and Exploration 1970-80, Department of Indian and Northern Affairs, p. 51-54.

Blusson, S.L.
1971: Sekwi Mountain map-area, Yukon Territory and District of Mackenzie; Geological Survey of Canada, Paper 71-22, 17 p.

1974: Geological Survey of Canada, Open File Report 295; Maps 106 A, B, C and 105 O.

Fritz, W.H.
1976: Ten stratigraphic sections from the Lower Cambrian Sekwi Formation, Mackenzie Mountains, northwestern Canada; Geological Survey of Canada, Paper 76-22, 42 p.

1978: Fifteen stratigraphic sections from the Lower Cambrian of the Mackenzie Mountains, northwestern Canada; Geological Survey of Canada, Paper 77-33, 18 p.

1979a: Cambrian stratigraphic section between South Nahanni and Broken Skull rivers, southern Mackenzie Mountains; in Current Research, Part B, Geological Survey of Canada, Paper 79-1B, p. 121-125.

Fritz, W.H. (cont.)
1979b: Eleven stratigraphic sections from the Lower Cambrian of the Mackenzie Mountains, northwestern Canada; Geological Survey of Canada, Paper 78-23, 18 p.

1980: International Precambrian-Cambrian Boundary Working Group's 1979 field study to Mackenzie Mountains, Northwest Territories, Canada; in Current Research, Part A, Geological Survey of Canada, Paper 80-1A, p. 41-45.

1981: Two Cambrian stratigraphic sections, eastern Nahanni map area, Mackenzie Mountains, District of Mackenzie; in Current Research, Part A, Geological Survey of Canada, Paper 81-1A, p. 145-156.

Gabrielse, H., Blusson, S.L., and Roddick, J.A.
1973: Geology of Flat River, Glacier Lake, and Wrigley Lake map-areas, District of Mackenzie and Yukon Territory; Geological Survey of Canada, Memoir 366, 153 p.

Gordey, S.P.
1979: Stratigraphy of southeastern Selwyn Basin in the Summit Lake area, Yukon Territory and Northwest Territories; in Current Research, Part A, Geological Survey of Canada, Paper 79-1A, p. 13-16.

1980: Stratigraphic cross-section, Selwyn Basin to Mackenzie Platform, Nahanni map area, Yukon Territory and District of Mackenzie; in Current Research, Part A, Geological Survey of Canada, Paper 80-1A, p. 353-355.

Green, L.H. and Roddick, J.A.
1961: Nahanni, Yukon Territory and District of Mackenzie; Geological Survey of Canada, Map 14-1961.

Green, L.H., Roddick, J.A., and Blusson, S.L.
1967: Nahanni, District of Mackenzie and Yukon Territory; Geological Survey of Canada, Map 8-1967.

Hofmann, H.J. and Cecile, M.P.
1981: Occurrence of Oldhamia and other trace fossils in Lower Cambrian(?) argillites, Niddery Lake map area, Selwyn Mountains, Yukon Territory; in Current Research, Part A, Geological Survey of Canada, Paper 81-1A, p. 281-290.

Krause, F.F.
1979: Sedimentology and stratigraphy of a continental terrace wedge: the Lower Cambrian Sekwi and June Lake formations (Godlin River Group), Mackenzie Mountains, Northwest Territories, Canada; unpublished Ph.D. thesis, University of Calgary, 252 p.

13.

DEVONO-MISSISSIPPIAN (EARN GROUP) AND YOUNGER STRATA IN EAST-CENTRAL YUKON

Project 790007

S.P. Gordey, J.G. Abbott[1], and M.J. Orchard
Cordilleran Geology Division, Vancouver

Gordey, S.P., Abbott, J.G., and Orchard, M.J., Devono-Mississippian (Earn Group) and younger strata in east-central Yukon; in Current Research, Part B, Geological Survey of Canada, Paper 82-1B, p. 93-100, 1982.

Abstract

Devono-Mississippian to Triassic strata in Nahanni, southeast Niddery Lake, and western Sekwi Mountain map areas comprise shale, chert, chert pebble conglomerate, chert quartz sandstone, and siltstone (Earn Group) overlain by sandstone, shale, limestone, chert and siltstone. Regional correlation of these strata on the basis of age control provided by 24 new conodont localities suggests: (1) the base of the Earn Group is diachronous, in places of least as old as Early Devonian, (2) the Earn Group can be regionally subdivided into two units separated by an unconformity, (3) correlation of coarse conglomeratic members of the Earn Group is only locally feasible because they are found at different stratigraphic levels throughout the group, (4) the Earn Group is overlain unconformably by an extensive shallow marine quartz sandstone of mid-Mississippian (Visean) age, and (5) Upper Mississippian and Lower Pennsylvanian shale and thick limestone is found above the quartz sandstone in some areas, but elsewhere overlying possibly equivalent strata consist of post-Mississippian to pre-Permian shale and sandstone.

Introduction

In early to mid-Paleozoic time, shallow water carbonate of Mackenzie Platform and offshelf, deeper water shale, limestone and chert of outer Selwyn Basin fringed the northwest margin of North America. Sedimentation changed dramatically in Late Devonian time when transgressive shale and/or chert blanketed the platform far to the east and thick sequences of basin-derived chert conglomerate and related clastic sediments accumulated in a number of submarine fan complexes to the west. In mid-Mississippian time, shallow marine, clean quartz sandstone blanketed most of the area, and indicates a return to normal marine shelf clastic sedimentation. Units as young as Triassic show that the extensive shallow water carbonate platform was never re-established.

Coarse clastics of Devono-Mississippian age in the northern Cordillera are often included in the 'black clastic group', a field term which has never been formally defined. We prefer the term Earn Group, a synonomous, but formally introduced name used by Campbell (1967) that includes Devono-Mississippian shale, chert, limestone, and chert-pebble conglomerate in Glenlyon map area (105 L).

In the Macmillan Pass-Nahanni area of eastern Yukon (Fig. 13.1) the Earn Group hosts economically significant stratabound barite and lead-zinc-silver-barite deposits and has been the subject of considerable debate. Work by many government and industry geologists in separate areas, without benefit of accurate paleontological control, has resulted in confusing informal terminology and incorrect regional stratigraphic correlations.

This report is a first attempt to clarify the complicated stratigraphy of the Earn Group and of the Carboniferous through Triassic units succeeding it. It is based on recent regional mapping in Nahanni map area (105 I) (Gordey, 1981), southeast Niddery Lake (105 O), and southwest Sekwi Mountain (105 P) map areas, as well as a brief examination of stratigraphic sections in west-central Sekwi Mountain map area by Abbott and Gordey, and paleontological control provided mainly by conodonts identified by M.J. Orchard.
The authors are grateful for the co-operation and assistance provided by Hudson Bay Mining and Smelting Co. Ltd., Pan Ocean Oil Ltd., Cominco Ltd., and AMAX Minerals Exploration Ltd.

Earn Group

Two regionally mappable, sharply delineated units (Fig. 13.2) containing shale, chert, quartz sandstone, grit and chert pebble conglomerate have been identified within the Earn Group. The lower unit, or lower Earn Group, locally spans most of the Devonian and is distinguished regionally by its predominantly gun-blue weathering siliceous shale and chert. The upper Earn Group is post- mid-Famennian to mid-Mississippian and is characterized by mainly brown weathering shale (not highly siliceous); bedded chert is

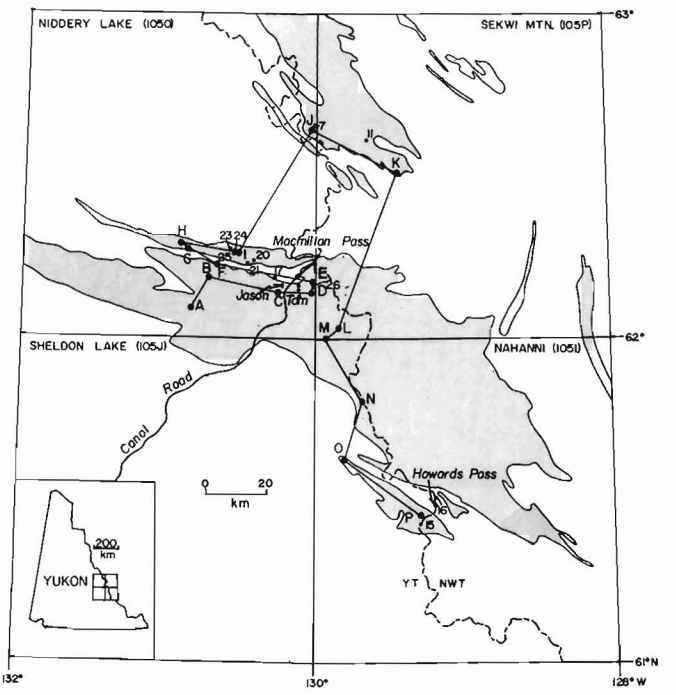

Figure 13.1. *Exposure of Devono-Mississippian and younger strata (shaded) in Nahanni, Sheldon Lake, Niddery Lake, and Sekwi Mountain map areas. Letters refer to sections shown in Figure 13.2. Numbers refer to fossil localities (Fig. 13.2) projected onto line of section.*

[1] Department of Indian Affairs and Northern Development, Whitehorse, Yukon.

Figure 13.2. *Stratigraphic correlation of Earn Group and younger strata. Section locations shown in Figure 13.2. Lower Earn Group shaded for clarity. Mineral deposit names are indicated. Ba = barite; all other abbreviations are standard.*

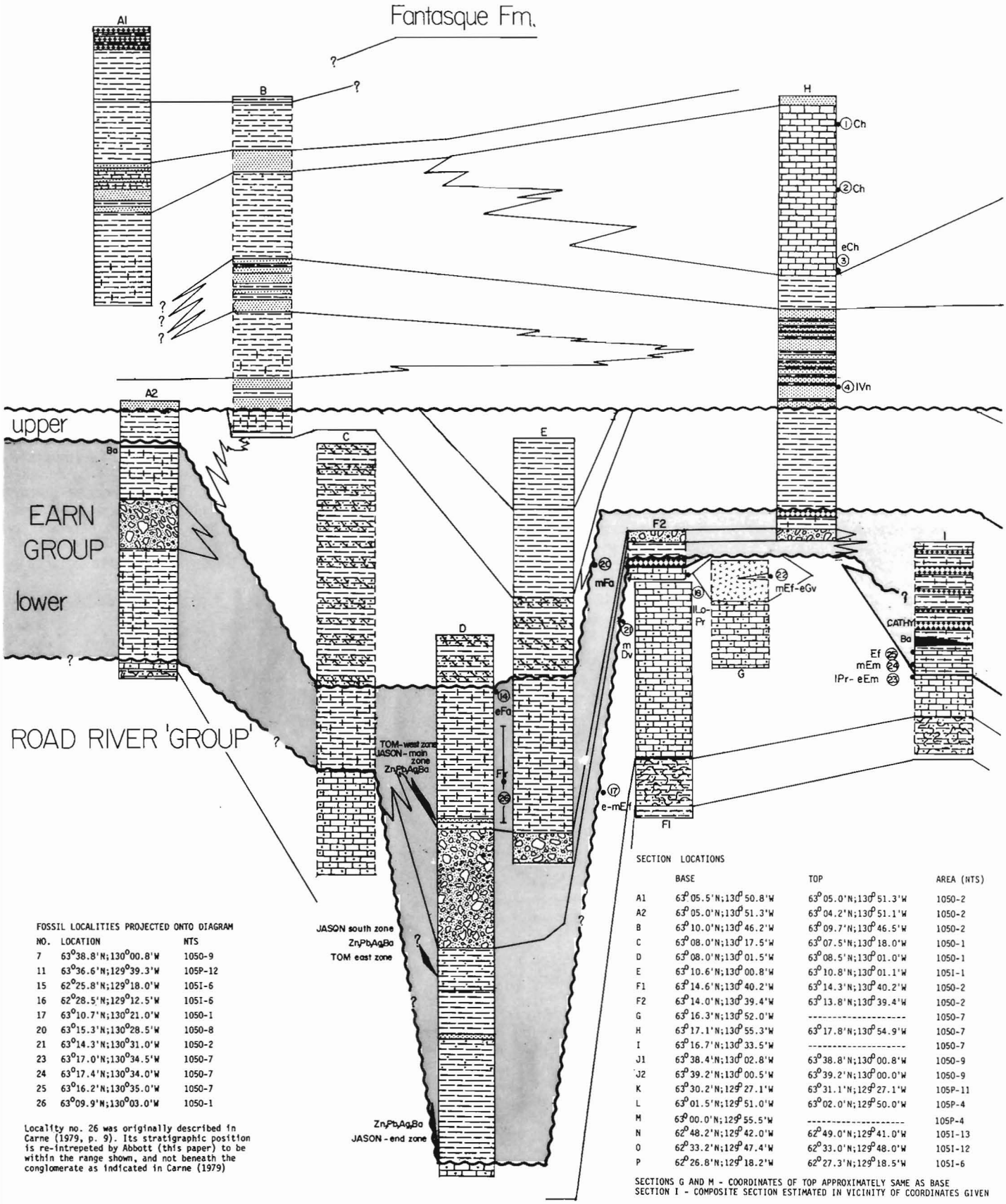

FOSSIL LOCALITIES PROJECTED ONTO DIAGRAM

NO.	LOCATION	NTS
7	63°38.8'N;130°00.8'W	1050-9
11	63°36.6'N;129°39.3'W	105P-12
15	62°25.8'N;129°18.0'W	105I-6
16	62°28.5'N;129°12.5'W	105I-6
17	63°10.7'N;130°21.0'W	1050-1
20	63°15.3'N;130°28.5'W	1050-8
21	63°14.3'N;130°31.0'W	1050-2
23	63°17.0'N;130°34.5'W	1050-7
24	63°17.4'N;130°34.0'W	1050-7
25	63°16.2'N;130°35.0'W	1050-7
26	63°09.9'N;130°03.0'W	1050-1

Locality no. 26 was originally described in Carne (1979, p. 9). Its stratigraphic position is re-intrepeted by Abbott (this paper) to be within the range shown, and not beneath the conglomerate as indicated in Carne (1979)

SECTION LOCATIONS

	BASE	TOP	AREA (NTS)
A1	63°05.5'N;133°50.8'W	63°05.0'N;133°51.3'W	1050-2
A2	63°05.0'N;133°51.3'W	63°04.2'N;133°51.1'W	1050-2
B	63°10.0'N;133°46.2'W	63°09.7'N;133°46.5'W	1050-2
C	63°08.0'N;133°17.5'W	63°07.5'N;133°18.0'W	1050-1
D	63°08.0'N;133°01.5'W	63°08.5'N;133°01.0'W	1050-1
E	63°10.6'N;133°00.8'W	63°10.8'N;133°01.1'W	105I-1
F1	63°14.6'N;133°40.2'W	63°14.3'N;133°40.2'W	1050-2
F2	63°14.0'N;133°39.4'W	63°13.8'N;133°39.4'W	1050-2
G	63°16.3'N;133°52.0'W	----------	1050-7
H	63°17.1'N;133°55.3'W	63°17.8'N;133°54.9'W	1050-7
I	63°16.7'N;133°33.5'W	----------	1050-7
J1	63°38.4'N;133°02.8'W	63°38.8'N;133°00.8'W	1050-9
J2	63°39.2'N;133°00.5'W	63°39.2'N;133°00.0'W	1050-9
K	63°30.2'N;129°27.1'W	63°31.1'N;129°27.1'W	105P-11
L	63°01.5'N;129°51.0'W	63°02.0'N;129°50.0'W	105P-4
M	63°00.0'N;129°55.5'W	----------	105P-4
N	62°48.2'N;129°42.0'W	62°49.0'N;129°41.0'W	105I-13
O	62°33.2'N;129°47.4'W	62°33.0'N;129°48.0'W	105I-12
P	62°26.8'N;129°18.2'W	62°27.3'N;129°18.5'W	105I-6

SECTIONS G AND M - COORDINATES OF TOP APPROXIMATELY SAME AS BASE
SECTION I - COMPOSITE SECTION ESTIMATED IN VICINITY OF COORDINATES GIVEN

Figure 13.2 (cont.)

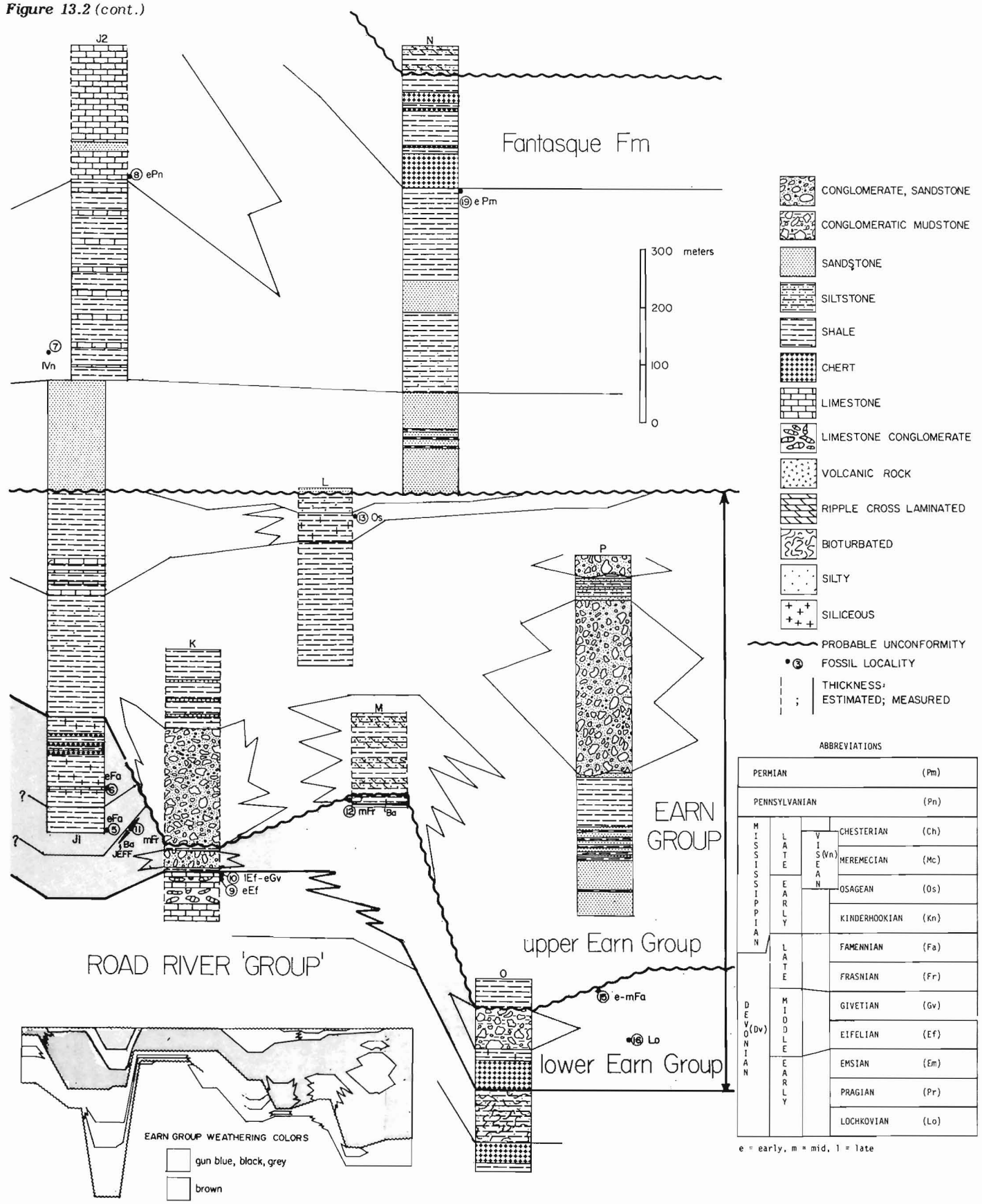

Table 13.1

Fossil determinations and age assignments by M.J. Orchard except macrofossil collections nos. 18 and 26 by A.W. Norris and W.W. Nassichuk respectively

No.	GSC Loc. No.	Age	Faunal List
1.	C-087569	Chester, Late Mississippian	*Gnathodus bilineatus* (Roundy), ?*G. girtyi* Hass, ?*G. defectus* Dunn, *Rhachistognathus muricatus* (Dunn), *R.* cf. *R.* sp. B Tynan.
2.	C-087568	Chester, Late Mississippian	*Gnathodus bilineatus* (Roundy), *G. girtyi simplex* Dunn, *G. g.* cf. *collinsoni* Rhodes, Austin & Druce, *Paragnathodus* cf. *P. commutatus* (Branson & Mehl), *Rhachistognathus muricatus* (Dunn), *R.* sp. B Tynan, *Polygnathus*? sp. indet.
3.	C-087567	Late Visean, L. Carboniferous	*Gnathodus girtyi collinsoni* Rhodes, Austin & Druce, *G. texanus* Roundy, *G. bilineatus* (Roundy), *Cavusgnathus* sp., *'Spathognathodus'* sp., *Palmatolepis*? sp.
4.	C-087566	Late Visean, L. Carboniferous	*Gnathodus girtyi collinsoni* Rhodes, Austin & Druce, *G. g.* cf. *girtyi* Hass, *Paragnathodus* aff. *P. commutatus* (Branson & Mehl), *'Spathognathodus'* cf. *'S.' campbelli* Rexroad, 'S.' sp.
5.	C-087561	Early Famennian (U. Palmatolepis triangularis-crepida Zone), Late Devonian	*Palmatolepis tenuipunctata* Sannemann, *Polygnathus* sp., *Pelekysgnathus*? sp.
6.	C-087562	Early Famennian (U. crepida Zone), Late Devonian	*Palmatolepis glabra pectinata* Ziegler morphotype 1 Sandberg & Ziegler, *P. g. lepta* Ziegler & Huddle, *P. quadrantinodosalobata* Sannemann morphotype 1 Sandberg & Ziegler, *P. subperlobata* Branson & Mehl, *P.* cf. *P. regularis* Cooper, *P.* cf. *P. tenuipunctata* Sannemann, *P. minuta* Branson & Mehl, *Polygnathus nodocostatus* Branson & Mehl group.
7.	C-087565	Late Visean, L. Carboniferous	*Gnathodus* cf. *G. bilineatus* (Roundy), *G.* cf. *G. texanus* Roundy, *G. girtyi collinsoni* Rhodes, Austin & Druce, *Paragnathodus* cf. *P. commutatus* (Branson & Mehl), *Metalonchodina sp.*
8.	C-087570	Early Pennsylvanian	*Idiognathoides sinuatus* Harris & Hollingsworth, *I. attenuatus* Harris & Hollingsworth, ?*Declinognathodus noduliferus* (Ellison & Graves), *Gnathodus* cf. *G. bilineatus* (Roundy), *G.*? n. sp., *Paragnathodus* cf. *P. commutatus* (Branson & Mehl), *Rhachistognathodus muricatus* (Dunn), ?*R. primus* Dunn.
9.	C-087555	Early Eifelian (patulus-costatus Zone), M. Devonian	*Polygnathus angusticostatus* Wittekindt s. l., *P. serotinus* Telford, *Ozarkodina* sp. of Klapper, Perry & Lenz, ?*Icriodus* n. sp. A Chatterton, *Belodella* sp., *Panderodus* sp.
10.	C-087556	Late Eifelian-Early Givetian (ensensis Zone), M. Devonian	*Polygnathus pseudofoliatus* Wittekindt, *P. xylus ensensis* Ziegler & Klapper, *P.* n. sp. M Johnson, Klapper & Trojan, *P. schwartzi* Chatterton, *P. parawebbi* Chatterton, *P. linguiformis linguiformis* Hinde, *P. l.* ?epsilon morphotype Ziegler, Klapper & Johnson, *Ozarkodina brevis* (Bischoff & Ziegler), *Pandorinellina*? n. sp. B Chatterton, ?*'Coelocerodontus' Klapperi* Chatterton, *Belodella* sp.
11.	C-087558	Mid Frasnian (L. gigas Zone), Late Devonian	*Palmatolepis gigas* Miller & Youngquist, *P. subrecta* Miller & Youngquist, *P. hassi* Müller & Müller, *Ancyrodella nodosa* Ulrich & Bassler, *Polygnathus*? *ancyrognathoidea* Ziegler.
12.	C-087557	Mid Frasnian (Ancyrognathus triangularis-U. gigas Zone), Late Devonian	*Palmatolepis subrecta* Miller & Youngquist, *Ancyrodella nodosa* Ulrich & Bassler, *Polygnathus* sp.
13.	C-087563	Osagean (U. typicus-anchoralis/latus Zone), mid Mississippian	*Pseudopolygnathus oxypageus* morphotype 2 Lane, Sandberg & Ziegler, *Polygnathus communis* Branson & Mehl, *'Spathognathodus'* sp., *Metalonchodina* sp.

14.	C-087560	Early Famennian (U. P. triangularis-M. crepida Zone), Late Devonian	*Palmatolepis triangularis* Sannemann, *P. perlobata perlobata* Ulrich & Bassler, *P.* cf. *P. delicatula clarki* Ziegler, *Polygnathus* sp.
15.	C-86285	Early-Mid Famennian (U. crepida-velifera Zone) Late Devonian	*Palmatolepis glabra* cf. *lepta* Ziegler & Huddle, *Polygnathus* sp.
16.	C-086424	Lochkovian (pesavis Zone), Early Devonian	*Icriodus steinachensis* Al-Rawi, *Ozarkodina* aff. *O. selfi* Lane & Ormiston, *Pandorinellina steinhornensis* (Ziegler), *Belodella* sp., *Panderodus* sp.
17.	C-087554	Eifelian, M. Devonian	*Polygnathus angusticostatus* Wittekindt s. l., *P.* cf. *P. parawebbi* Chatterton, *Pandorinellina* sp., *Pelekysgnathus* sp., *Tortuodus*? sp., *Pseudooneotodus* sp., *Belodella* sp., *Panderodus* sp.
18.	C-88004	late Lochkovian-Pragian, Early Devonian	*Nowakia acuaria* (Richter), *Styliolina* sp., monograptid? impression.
19.	C-087590	Early Permian, ?late Sakmarian	*'Neogondolella' bisselli* (Clark & Behnken) group, *Sweetognathus merrilli* Kozur s. l.
20.	C-087685	Mid Famennian (marginifera Zone), Late Devonian	*Palmatolepis glabra distorta* Branson & Mehl, *P. g. lepta* Ziegler & Huddle, *P. g. pectinata* Ziegler, *P. g. prima* Ziegler & Huddle, *P. marginifera marginifera* Helms, *P. gracilis gracilis* Branson & Mehl, *Polygnathus* sp.
21.	C-087686	M. Devonian	*Polygnathus* cf. *P. linguiformis* Hinde, *Panderodus* sp.
22.	C-087687	Mid Eifelian-early Givetian (australis-ensensis Zone), M. Devonian	*Polygnathus trigonicus* Bischoff & Ziegler, *P. linguiformis linguiformis* Hinde, *P.* cf. *P. pseudofoliatus* Wittekindt, *P.* cf. *P. angustipennatus* Bischoff & Ziegler, *Tortuodus kockelianus* Bischoff & Ziegler, *Icriodus expansus* Branson & Mehl s. l., *Pandorinellina*? sp. indet., *Belodella* sp.
23.	C-087688	Late Pragian-early Emsian (Kindlei-dehiscens Zone), Early Devonian	*Polygnathus pireneae* Boersma, *Icriodus* cf. *I. steinachensis* Al-Rawi.
24.	C-087689	Mid Emsian (inversus Zone), Early Devonian	*Polygnathus inversus* Klapper & Johnson, *P. laticostatus* Klapper & Johnson, *P.* cf. *P. pireneae* Boersma, ?*Pandorinellina optima* (Moskalenko), *Panderodus* sp.
25.	C-087690	Probably Eifelian, M. Devonian	*Polygnathus* cf. *P. costatus* Klapper, *Pelekysgnathus* sp.
26.	C-49975	Frasnian, Late Devonian	*Ponticeras* cf. *P. tschernyschewi* (Holzapfel)

NOTES

Nos. 1,2,8 include species of *Rhachistognathus* previously recorded only from the North American midcontinent, in which series nomenclature the faunas are dated. Slightly older faunas (Nos. 4,7) are more readily determined in European terms. Nos. 2 and 3 each contain a single fragment of late Devonian (*Palmatolepis* sp. and ?*Polygnathus*) or early Mississippian (*Polygnathus*) aspect. These may indicate late Mississippian erosion of older strata. No. 10 was collected from talus regarded as originating within a narrow but unexposed interval. No. 23 The icriodid in this fauna is not well preserved and may correspond to *I. nevadensis* Johnson & Klapper, in which case the younger zone would apply. No. 24 includes species that suggest an older fauna is also represented in this carbonate: *P. pireneae* and *P. optima* are indicative of the late Pragian *kindlei* Zone.

uncommon. The base of the Earn Group is regionally mappable, and delineated by the lower limit of siliceous shale, chert, and generally fine clastic rocks above bioturbated siltstone, silty limestone, and locally volcanic rocks of the 'Road River group'[1]. Facies changes result in the base of the Earn Group being diachronous. The upper contact of the Earn Group is at the base of a widespread shallow marine quartz sandstone. Correlation within the Earn Group without fossil control is difficult because lithologies and weathering colour typical of one unit are found in the other, thickness and facies changes are dramatic, and unconformities locally cut out significant thickness of strata.

Compositionally and sedimentologically the coarse clastics that occur within both units are similar. Grey weathering chert-pebble conglomerate is characterized by rounded pebbles to cobbles of grey, black, white, or green chert, minor quartz sandstone, and outsize shale clasts in a fairly clean matrix of chert and quartz sand. Conglomerate and medium- to coarse-grained, quartz-chert sandstone form massive channel deposits up to several hundred metres thick. Local conglomeratic mudstone containing large shale, chert- and quartz-sandstone cobbles forms thin to thick (up to 70 m) isolated lenses and occurs within the channel deposits. Where interbedded with shale, the chert-quartz sandstone is even bedded, locally graded and has flute and groove casts on the base of some beds.

Lower Earn Group

In western Nahanni map area the lower Earn Group is composed almost entirely of gun-blue weathering, thin bedded, black chert and siliceous shale up to 300 m thick. Muddy chert-quartz sandstone and conglomeratic mudstone occur locally in this area (Section O), in contrast to the normally clean sandstone and conglomerate typical of the Earn Group.

Partly equivalent strata in the Macmillan Pass area can be subdivided into several members. At sections D and E the lower Earn Group consists of about 370 m of brown weathering shale, silty shale and minor chert grit, which is overlain abruptly by 200 m of massive chert-pebble conglomerate. A thin feldspar-porphyry dyke intrudes the contact. The conglomerate is succeeded by 230 m of blue-black weathering, platy graphitic mudstone.

West of Macmillan Pass the lower Earn Group is undated. At section C, 150 m of blue-black weathering, siliceous shale and silty shale could be equivalent to part or all of the lower Earn Group seen in section D immediately to the east. At section A2 the lower Earn Group is 370 m thick and includes 90 m of chert conglomerate enclosed by black siliceous shale. The conglomerate wedges out to the east and is not continuous with that in sections D and E.

In west-central Sekwi Mountain map area at section J1, the lower Earn Group consists of 150 m of gun-blue weathering black siliceous shale and chert overlying recessive brown weathering shale of unknown thickness. Siliceous shale also occurs beneath the brown member east of section J1. To the southeast at section K the lower Earn Group comprises 30 m of chert-pebble conglomerate over and underlain by a few metres of black siliceous shale and minor chert.

The base of the lower Earn Group and its contact with the older Road River group strata is diachronous. In western Nahanni map area the lower Earn Group is at least as old as Early Devonian (Table 13.1, no. 16) and rests conformably? (previously considered unconformable, Gordey, 1981) on bioturbated silty shale of Silurian age. In Sekwi Mountain map area at section K, the lower Earn Group rests conformably? on silty limestone of early Givetian age (no. 9, 10). In the Macmillan Pass area and to the west, underlying Road River group limestone is also Middle Devonian (no. 17, 21). At section I minor bioclastic limestone in the lower 50 to 70 m of the lower Earn Group yielded conodonts of mid-Emsian (no. 24) to probably Eifelian age (no. 25), and those from the underlying Road River silty limestone are late Pragian or early Emsian (no. 23). The youngest known ages of the lower Earn Group range from mid-Frasnian to mid-Famennian (no. 12, 14, 20, and 6).

Unconformable relations beneath the lower Earn Group are suggested in the Macmillan Pass area and to the west by the sharp upper contact and rapid thinning of the underlying Road River group silty limestone, although the latter may be accounted for by a rapid facies change.

The age of the oldest coarse clastics within the Earn Group is not well bracketed. Conglomerate at sections D and E is of post-early Middle Devonian (no. 17, 21) and pre-early Famennian (no. 14), possibly Frasnian in age (no. 26). Conglomerate at section K is post-early Givetian (no. 9, 10). The conglomeratic mudstone in Nahanni map area at section O is undated but its relatively high stratigraphic position indicates it may be Late Devonian.

Early workers (e.g., Blusson, in Dawson, 1977) correlated lower Earn Group strata with the Canol Formation of Mackenzie Mountains. The present work shows that in both lithology and age it is quite different from the Canol Formation as described at its type section (see Bassett, 1960). The lower Earn Group correlates with the siliceous shale unit of Gordey (1981) in Nahanni map area, with units D2 and D3 of Cecile (1981) in northeast Niddery Lake map area, and with units 1, 2, and 3 of Carne (1979) in the Macmillan Pass area. In Sekwi Mountain map area lower Earn Group equivalents are included in unit 26 of Blusson (1971). The brown weathering shale member at section J1 correlates with his unit 26B.

Upper Earn Group

In Nahanni map area upper Earn Group strata comprise at least 600 m of brown weathering shale, sandstone, grit and chert conglomerate (section P). The conglomerate is compositionally and sedimentologically similar to lower Earn Group conglomerate at Macmillan Pass (section D, E).

In Sekwi Mountain map area at section K, the basal upper Earn Group consists of massive chert-quartz sandstone and chert-pebble conglomerate at least 200 m thick, overlain by brown weathering shale with minor interbeds of turbiditic chert grit and sandstone. The conglomerate unit and sandstone beds above it contain abundant distinctive turquoise chert clasts.

In the Macmillan Pass area at sections C, D, and E, and to the southeast at section M the basal unit of the upper Earn Group is thin bedded, ripple crosslaminated siltstone and evenly interbedded brown shale. Its thickness varies from at least 400 m at section C to less than 150 m at section E, partly because of facies change to brown weathering shale and silty shale by loss of the crosslaminated siltstone component.

At sections B, E, and L there are members of gun-blue weathering, locally siliceous shale near the top of the upper Earn Group that are tentatively correlated. Black weathering shale with thin beds of limestone at section J1 may also be correlative. At section L a thin interval of brown weathering siltstone and silty shale occurs above the gun-blue weathering shale member whereas beneath it strata are mostly brown weathering shale.

The upper Earn Group rests unconformably on lower Earn Group strata over most of the area; the brown weathering clastics above contrast sharply with the typical gun-blue weathering rocks below (Fig. 13.2).

[1]Road River Formation is here informally given group status.

Fossil collections from immediately beneath the unconformity range from mid-Frasnian (no. 12) to mid-Famennian (no. 14, 15, 20). Carne (1979) suggested the existence of this unconformity at Macmillan Pass on sedimentological grounds (at the base of his unit 4). At section J1 a thick section of lower Earn Group rocks lies above an early Famennian conodont locality (no. 6), which does not confirm the existence of the unconformity in that area, consequently the relationship there is tentatively shown as conformable. Only one fossil collection was made from within the upper Earn Group, and it is Osagean (no. 13). Collections from above (no. 4) and below the upper Earn Group (no. 14, 6 and 20) bracket it between post-mid Famennian and pre-Late Mississippian.

Early work led to correlation of upper Earn Group strata by Blusson (in Dawson, 1977) with the Imperial Formation of Mackenzie Mountains. This study shows that they are regionally different in lithology and age (see the descriptions of the Imperial Formation at its type section by Bassett, 1960; Chi and Hills, 1974). The upper Earn Group is included in unit 26 of Blusson (1971) in Sekwi Mountain map area. Blusson tentatively included conglomerate at section K with clean quartz sandstone (quartz arenite unit of this paper) in his unit 27. The two however, are sedimentologically distinct and widely separated stratigraphically. The upper Earn Group is equivalent to the combination of units DMsh, DMss, DMu, and CPshl of Cecile (1981) in northeast Niddery Lake map area, unit 4 of Carne (1979) in the Macmillan Pass area, and to the 'black clastic' unit of Gordey (1981) in Nahanni map area.

Carboniferous to Triassic

Quartz Arenite Unit

Succeeding the Earn Group is a clean quartz sandstone, typically fine- to medium-grained and up to 200 m thick (section J1). At some localities (section J1, N) it contains little shale but at others a major amount (section H, B). In shale-free intervals the sandstone is typically resistant and massive, and bedding is defined by thick parting. Where interbedded with shale most of the sandstone is clean, except for rare mud chips, and forms thick, massive beds with sharp planar contacts. At most localities where the base of the unit is in sharp contact with underlying shale, the basal sandstone is not different from that stratigraphically higher. At section H, however, the basal sandstone is calcareous and laminated, and is interbedded with considerable bioturbated shale. At section B a thick, mostly brown weathering shale member, siliceous and blue-black weathering at its base, occurs within the quartz arenite unit. Sandstone beneath this member is clean, massive and similar to that found elsewhere; sandstone above the member has a muddy matrix and forms beds several centimetres to 2 m thick, interbedded with shale.

The quartz arenite is probably unconformable with the underlying Earn Group. A conodont fauna of late Visean age was collected 33 m above the base of the quartz arenite from calcareous ripple crosslaminated siltstone at section A (no. 4), whereas only 40 m below the quartz sandstone, at section L, Osage conodonts (no. 13) were collected from the Earn Group. Elsewhere (e.g. section A2 to E) the thickness of upper Earn Group strata changes dramatically and locally its upper gun-blue weathering member is absent. The age of the quartz arenite is bracketed within the Visean (no. 13, 4, 7).

The massiveness, compositional maturity, and marine fauna (no. 4) of the quartz arenite suggest a shallow marine depositional environment. It is correlated with the coal-bearing Mattson Formation of the southwestern District of Mackenzie, which contains much quartz sand and whose base is approximately early late Visean (Bamber and Mamet, 1978).

Post-Quartz Arenite Stratigraphy

In Nahanni map area (section N), stratigraphy above the quartz arenite has been described previously by Gordey et al. (1981). It consists of dark quartz siltstone and pale green weathering shale, overlain by Lower Permian chert which is correlated with the Fantasque Formation of southwestern District of Mackenzie. A thick section of Triassic ripple crosslaminated siltstone and sandstone, with thin interbeds of shale overlies the chert.

In the Niddery Lake map area (section H, J) thick, grey, to light orange weathering bioclastic limestone and minor clean quartz sandstone of Late Mississippian and Early Pennsylvanian age (no. 1, 2, 3, and 8) forms the uppermost unit. The carbonate forms medium to thick massive beds containing abundant crinoid, coralline, and shelly debris. The apparent lateral discontinuity of the carbonate, its thickness and limited age range, suggest it formed rapidly as local? reef buildups. The carbonate contrasts markedly with noncalcareous strata at sections A1, B, and N between the quartz arenite unit and Lower Permian chert.

West of Macmillan Pass (sections A1, B) the quartz arenite is overlain by brown weathering shale and silty shale, within which is a thick member of sandstone. At section A1 the sandstone is a thick bedded, grey, clean quartz arenite, interbedded with calcareous siltstone and shale. At sections B and H correlative? sandstone is massive clean quartz arenite.

Orange weathering, resistant green shale and chert form the uppermost unit at sections A1 and B, and are in sharp contact with the underlying shale. Part or all of this upper unit correlates with the Fantasque Formation at section N.

Barite-Lead-Zinc-Silver Occurrences

Bedded barite occurs within the siliceous shale facies of the lower and possibly upper Earn Group at Macmillan Pass and sedimentary exhalative zinc-lead-silver-barite deposits occur within clastic facies of the lower Earn Group. The origin of both types of deposits is poorly understood. The bedded barite occurs discontinuously over large areas and at more than one stratigraphic horizon, forming thick deposits only locally. Regional phenomena such as seawater chemistry and more local factors such as block faulting may have been important depositional controls. The sulphide-bearing deposits are hydrothermal in origin (Carne, 1979).

Thick, bedded barite deposits near Macmillan Pass are both younger and older than the sulphide deposits. The oldest are Givetian and possibly Eifelian. They are 1 to 30 m thick and occur intermittently within a structurally complex west-northwest-trending belt at least 50 km long and 10 km wide. At the Cathy deposit (section I), Givetian conodonts have been collected from within the barite. Barite also occurs near the top of the lower Earn Group in discontinuous beds less than 1 m thick. At section M, a thin bed of mid-Frasnian limestone at the top of the lower Earn Group (no. 12) is less than 5 m above thin, bedded barite (see also section A2).

In Sekwi Mountain map area a mid-Frasnian conodont fauna (no. 11) was obtained from a barite and shaly barite member (Jeff deposit) more than 50 m thick. To the northwest in northeast Niddery Lake map area Cecile (1981) noted many occurrences of barite (in his unit D3), which may be of similar age. In Nahanni map area bedded barite of uncertain age(s) is widespread but discontinuous in the lower Earn Group. Thicknesses range from a few centimetres to many tens of metres (e.g. Oro and GHMS deposits).

The zinc-lead-lead-silver-barite deposits at Macmillan Pass (Tom, Jason) (near sections D, E) are post-early Middle Devonian (no. 17, 21) and pre-early Famennian (no. 14), possibly Frasnian (no. 26). The sulphide deposits occur at two, possibly three stratigraphic levels within a single submarine fan complex. The middle level (i.e. Jason south and Tom east zones, Fig. 13.2) may represent a separate mineralizing event or it could be structurally repeated upper level mineralization (i.e. Tom west and Jason main zones, Fig. 13.2). Although the deposits may be related to contemporaneous faulting, the nature of the faults, including their location, extent and relationship with coeval beds is obscure.

References

Bamber, E.W. and Mamet, B.L.
1978: Carboniferous biostratigraphy and correlation, northeastern British Columbia and southwestern District of Mackenzie; Geological Survey of Canada, Bulletin 266, 65 p.

Basset, H.G.
1960: Devonian stratigraphy, central Mackenzie River region, Northwest Territories, Canada; in Geology of the Arctic, v. 1, ed. G.O. Raasch, Alberta Society of Petroleum Geologists and University of Toronto Press, p. 481-495.

Blusson, S.L.
1971: Sekwi Mountain map-area, Yukon Territory and District of Mackenzie; Geological Survey of Canada, Paper 71-22, 17 p.

Campbell, R.B.
1967: Reconnaissance geology of Glenlyon map area, Yukon Territory; Geological Survey of Canada, Memoir 352.

Carne, R.C.
1979: Geological setting and stratiform mineralization Tom Claims, Yukon Territory; Department of Indian and Northern Affairs, Canada, Report EGS 1979-4, 30 p.

Cecile, M.P.
1981: Geology of northeast Niddery Lake, NTS 1050-9, 10, 15, 16; Geological Survey of Canada, Open File 765.

Chi, B.I. and Hills, L.V.
1974: Stratigraphic and paleoenvironmental significance of Upper Devonian megaspores, type section of the Imperial Formation, Northwest Territories, Canada; in Canadian Arctic Geology, ed. J.D. Aitken and D.J. Glass, Geological Association of Canada – Canadian Society of Petroleum Geologists Symposium, Saskatoon, Saskatchewan, p. 241-257.

Dawson, K.M.
1977: Regional metallogeny of the northern Cordillera; Geological Survey of Canada, Report of Activities, Part A, Paper 77-1A, p. 1-4.

Gordey, S.P.
1981: Geology of Nahanni map-area (105 I), Yukon Territory and District of Mackenzie; Geological Survey of Canada, Open File 780.

Gordey, S.P., Wood, D.H., and Anderson, R.G.
1981: Stratigraphic framework of southeastern Selwyn Basin, Nahanni map area, Yukon Territory and District of Mackenzie; in Current Research, Part A, Geological Survey of Canada, Paper 81-1A, p. 395-398.

14. STRATIGRAPHY AND STRUCTURE OF SYLVESTER ALLOCHTHON, SOUTHWEST McDAME MAP AREA, NORTHERN BRITISH COLUMBIA

Project 770016

S.P. Gordey, H. Gabrielse, and M.J. Orchard
Cordilleran Geology Division, Vancouver

Gordey, S.P., Gabrielse, H., and Orchard, M.J., Stratigraphy and structure of Sylvester Allochthon, southwest McDame map area, northern British Columbia; in Current Research, Part B, Geological Survey of Canada, Paper 82-1B, p. 101-106, 1982.

Abstract

The Sylvester Allochthon in southwestern McDame map area is composed of at least three discrete mildly deformed fault bounded assemblages overlying autochthonous strata of the North American miogeocline. A basal thrust sheet of greenstone, chert, shale and serpentinite of Mississippian? and Permian age is overlain by another thrust sheet of Pennsylvanian to Permian augite porphyry basalt, shale, chert, and limestone, and undated shale and sandstone. The two assemblages have little in common stratigraphically, implying considerable distance between their original depositional sites. A third assemblage of lapilli tuff, quartz diorite, and quartz sandstone and shale of unknown age is in steep fault contact with the other assemblages. It may comprise a separate thrust sheet, or be autochthonous with respect to either of the dated sequences and entirely older or younger. Age control is not strict enough to rule out other major thrust faults within any of the three assemblages.

Introduction

The Sylvester Allochthon in north-central British Columbia comprises upper Paleozoic chert, greenstone, clastic and ultramafic rocks thrust over autochthonous or parautochthonous strata of the North American continental margin in mid-Jurassic to Early Cretaceous time (Fig. 14.1), and intruded later by mid- to Late Cretaceous quartz monzonite. The relationship between the Sylvester Allochthon and allochthonous Paleozoic and Mesozoic strata to the southwest (Gabrielse and Dodds, 1982) and to the Cache Creek Group farther southwest (Monger, 1975) is uncertain. Those assemblages are roughly equivalent in age and gross lithology but stratigraphic and faunal differences (Monger and Ross, 1971) appear numerous. In general Sylvester Group rocks seem much less disrupted by tectonism than those of the Cache Creek Group.

The Sylvester Allochthon comprises most of what was originally mapped as autochthonous Sylvester Group by Gabrielse (1963). Pyritic black shale, and minor chert-quartz sandstone and chert-pebble conglomerate included in the basal part of the group were excluded when strata above this level were later considered allochthonous (Gabrielse and Mansy, 1980). Gabrielse (1963) recognized and described all the major lithologies within the group, but the scale of his work did not allow subdivision. Diakow and Panteleyev (1981) subdivided and briefly described part of the Sylvester Group in the northwest part of the present area.

To document the stratigraphy and structure of the allochthon a strip across it was mapped at 1:50 000 scale in an area known to be structurally simple, and thought to expose relatively high stratigraphic levels (Fig. 14.2). In this region the allochthon is composed of three discrete assemblages preserved in a gentle syncline above autochthonous Upper Devonian pyritic black siliceous shale which, in turn, is underlain by Devonian dolostone and limestone (units A, B, and C: Gabrielse, 1963; Gabrielse and Mansy, 1980). The basal assemblage (lower thrust sheet), of Mississippian? and Permian age, consists of shale, chert, greenstone, and serpentinite. Strata which are partly time equivalent and include sandstone, shale, augite basalt, chert and limestone form an upper thrust sheet. Lapilli tuff, purple lapilli tuff, gritty quartz sandstone and quartz diorite of unknown age are in steep fault contact with the other two assemblages.

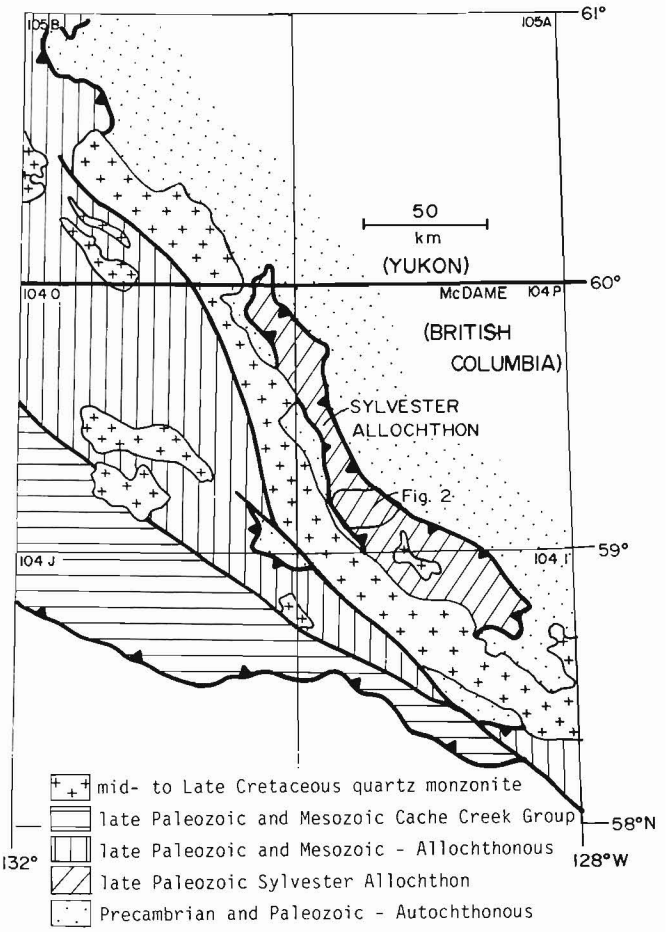

Figure 14.1. *Location and geological setting of Sylvester Allochthon. Modified from Tipper, Woodsworth and Gabrielse (1981).*

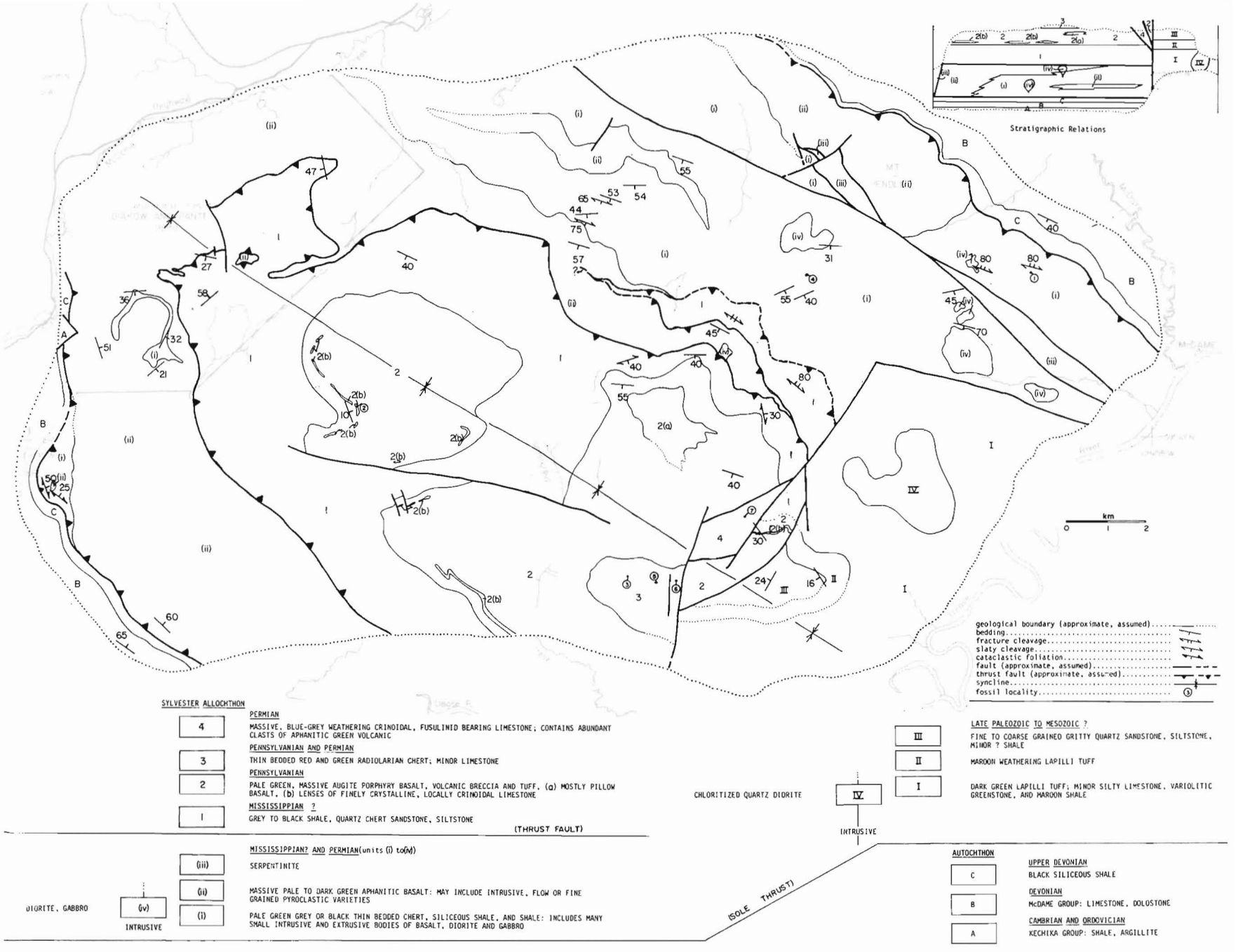

Figure 14.2. *Geological map across central Sylvester Allochthon, southwestern McDame map area. Location shown in Figure 14.1.*

Allochthon Stratigraphy

Lower Thrust Sheet (units (i) to (iv))

Dark weathering, well laminated, uniformly thin bedded shale, siliceous shale and grey to pale green chert form unit (i), which locally includes thick members of massive shale. The only limestone seen, a bed 2 m thick, yielded conodonts of Carboniferous, probably Mississippian age (Table 14.1, no. 1). Thin bedded black chert southeast of Blackfox Mountain contains Lower Permian conodonts (Table 14.1, no. 4). As the unit has no recognized base, its thickness is unknown, but apparently about 600 m+. The structure, however, may be complex; marker horizons are absent.

Dark grey-green weathering, aphanitic, pale green, massive volcanic rocks form unit (ii). The origin of most of the unit, whether intrusive, extrusive or pyroclastic, is not discernible in outcrop, although tuffaceous textures are evident locally. Thin section study shows that at least some of the volcanics are of 'flow type' composed of highly saussuritized plagioclase surrounding a few per cent of unaltered augite. Tremolite, chlorite, carbonate and epidote group minerals form an extensive alteration assemblage. Small to large intrusive and (?) extrusive bodies of unit (ii) greenstone are numerous within unit (i) and suggest that the two units may be partly temporal equivalents. The thickness of unit (ii) is unknown but is probably at least as thick as unit (i), i.e. 600 m+. Serpentinite of unit (iii) is spatially associated and in contact with unit (ii) greenstone, and is not found with volcanic rocks in the upper thrust plate.

Unit (iv) consists of medium grained equigranular gabbro, typically containing 10 to 15 per cent augite in a matrix of highly saussuritized plagioclase with rare hornblende, biotite and minor quartz. The euhedral to subophitic augite shows minor alteration to tremolite. Patchy carbonate and scattered chlorite are common alteration minerals. Numerous intrusive bodies of unit (iv) cut strata of unit (i) and may be related to eruption of unit (ii) greenstone.

Upper Thrust Sheet (units 1 to 4)

Unit 1 is composed of dark to black recessive weathering shale, siltstone and lesser sandstone. The sandstone is a fine- to coarse-grained, moderately sorted wacke, and consists of subrounded to subangular quartz and chert in equal abundance, with rare squashed mud clasts and detrital muscovite. Most of the chert grains contain some argillaceous material as expressed by crowded platelets of white mica. Quartz grains have silica overgrowths. Petrographically the sandstones are remarkably similar to Upper Devonian and Mississippian clastic rocks of the autochthonous succession. The unit is so recessive that bedding style and other features are not easily studied. Thickness is probably about 300 m+.

Green-grey weathering volcanic rocks of unit 2 overlie unit 1 along a sharp contact. They consist of augite porphyry basalt, breccia and tuff (Fig. 14.2), with lenses of crinoidal limestone. In most places the rocks are massive and breccia or tuffaceous texture is seen only on suitably weathered surfaces. A sequence of basalt flows 60 m ± thick with well developed pillows was noted south of Juniper Mountain (Fig. 14.3), and near the peak and on the west slope of the mountain. All rock types within the unit are very well indurated. In thin sections of the porphyry the augite is relatively fresh, but the matrix of tiny interlocking feldspar crystals is completely altered, with epidote and chlorite being common alteration products. Unit 2 volcanics can be distinguished easily from those of unit (ii) by their structural and stratigraphic position and their plentiful augite phenocrysts. About 70 m above the base of unit 2 lenses up to 20 m thick of grey weathering crinoidal limestone (unit 2b) locally yielded Lower Pennsylvanian conodonts (Table 14.1, no. 2). The thickness of unit 2 is estimated at about 600 m ±.

South of Juniper Mountain unit 2 is overlain by thin bedded red and green chert and minor limestone of unit 3. Both red and green chert range from relatively pure to argillaceous with thin bands and laminae of tuffaceous? material. Thicker interbeds consist of graded fine sand and silt. The limestones within unit 3 are at least several metres thick, are white weathering, massive, and finely crystalline; one yielded Middle Pennsylvanian conodonts (Table 14.1, no. 3). The underlying volcanics of unit 3 are thus bracketed between Early and mid-Pennsylvanian. Another limestone and chert from the unit yielded Lower? Permian conodonts (Table 14.1, no. 5, 6). The thickness of the red and green chert that may either lie above the younger limestone or separate the two limestones is now known. The thickness of the unit including the limestone members is difficult to estimate because of tight folding but the exposed thickness appears to be about 100 m ±.

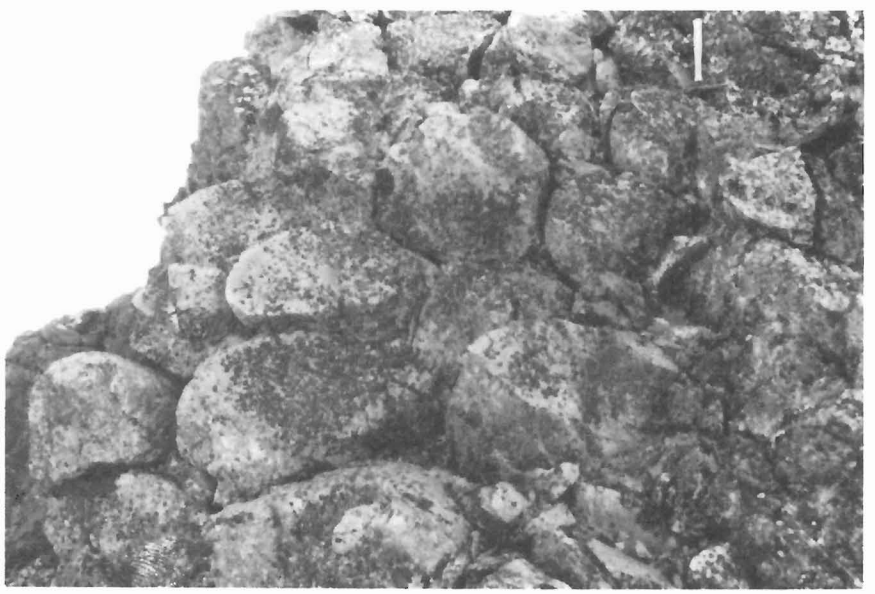

Figure 14.3

Well developed pillows in unit 2(a) augite porphyry basalt.

Table 14.1

Fossil determinations and age assignments for conodont collections from southwest McDame map area, Sylvester Allochton

No.	GSC No.	Lat./Long.	Unit	Lithology	Fauna and Age
1.	C-087675	59°12.3'N; 129°18.2'W	(i)	limestone	*'Spathognathodus'* cf. *'S.' stabilis* (Branson & Mehl), *Metalonchodina* sp. Age: ?Mississippian
2.	C-087676	59°10.5'N; 129°36.2'W	2	limestone	*Idiognathoides* cf. *I. sinuatus* Harris & Hollingsworth, *Neognathodus bassleri* Harris & Hollingsworth, *N. symmetricus* (Lane), *Gnathodus*? n. sp. Age: Early Pennsylvanian
3.	C-087677	59°08.2'N; 129°29.0'W	3	limestone	*Idiognathodus delicatus* Gunnel, *Neognathodus medadultimus* Merrill, *Streptognathodus*? sp., *'Neogondolella' laevis* (Kosenko & Kozitskaya), *'N.'* sp., *Gnathodus*? spp. Age: Middle Pennsylvanian
4.	C-087682	59°12.2'N; 129°24.2'W	(i)	chert	*'Neogondolella' bisselli* (Clark & Behnken) - *'N.' idahoensis* (Youngquist, Hawley & Miller) group Age: Early Permian
5.	C-087679	59°08.1'N; 129°28.2'W	3	chert	age and fauna same as C-087682
6.	C-087680	59°08.1'N; 129°27.7'W	3	limestone	age and fauna same as C-087682
7.	C-087678	59°09.0'N; 129°25.8'W	4	limestone	age and fauna same as C-087682
8.	C-087683	59°02'N; 128°47'W	-	chert	age and fauna same as C-087682

Numbers 4 to 8 are all low diversity fragmented neogondolellid faunas which are not well enough preserved to be confident of species determination. Fragments display characteristics of the group which includes the two named species as 'evolutionary end members' of a series that is in need of substantial taxonomic clarification, with particular emphasis on ontogenetic changes.

1 to 7 correspond to locations on Figure 14.2
8 is from northern Cry Lake map area (104I)
Identifications and age assignments by M.J. Orchard

Blue-grey weathering limestone of unit 4 is commonly a coarsely crystalline crinoidal or fusulinid hash. It contains abundant angular clasts, up to 1.5 m across, of orange weathering, fine grained, green volcanic rock both scattered within the limestone and as concentrations along certain horizons outlining bedding. Below a sharp contact at the base of the limestone are pebbly sandstone and minor pebble volcanic-clast conglomerate a few metres thick. Small 'flames' of the sandstone project upward into the limestone. Unit 4 is fault bounded and its relationships with other units remain uncertain. It yielded conodonts dated broadly as Permian (Table 14.1, no. 7), perhaps equivalent in age to the limestone within the chert of unit 3. The unit is at least 200 m thick.

Assemblage of Unknown Age (units I to IV)

Units I to IV form an assemblage in steep fault contact with those previously described. Unit I consists of massive, dark brown, recessive weathering, weakly cleaved and somewhat poorly indurated fragmental volcanic rock, mostly lapilli tuff. Within the volcanics thin interbeds of thin bedded to massive limestone up to 20 m thick, make up about 5 per cent of the unit. The limestone ranges from argillaceous to fairly pure, and from finely crystalline to sugary textured. Minor members include clean quartz sandstone (locally associated with the limestone), maroon siltstone, shale, and chert, and fine grained variolitic volcanic rock. The unit is probably at least several hundred metres thick although structural repetitions are possible but cannot be documented because of a lack of structural and stratigraphic data.

Unit I is apparently overlain by distinctive maroon to purple-red weathering tuff (Unit II) about 100 m ± thick which contains lapilli-size fine grained green volcanic fragments in a maroon to purple fine grained matrix. The upper and lower contacts are not exposed.

Overlying? unit II is fine- to coarse-grained, fairly pure, medium bedded quartz sandstone, calcareous sandstone, and shale (Unit III). The sandstone is moderately sorted and consists of monocrystalline and polycrystalline undulose quartz, and 5 to 10 per cent microcline and plagioclase. The matrix is extensively recrystallized to a mat of fine grained felsic minerals, mostly quartz, and abundant white mica. Fine grained green volcanic tuff and coarse grained diorite are found within the unit but their extent and distribution are unknown. The top of the unit is not exposed, but its thickness is probably at least 70 m.

Unit IV is a small intrusive body of medium grained quartz diorite. It consists of about 5 per cent completely chloritized mafic mineral(s) (originally hornblende?), 15 per cent quartz, minor interstitial microcline, and highly saussuritized plagioclase. Augite occurs as scattered small unaltered crystals within the chlorite masses. The rocks of unit I are not significantly metamorphosed at the contacts with the quartz diorite.

Figure 14.4

Chert augen within argillaceous matrix; cataclastic texture seen in rocks of unit (i)? near base of Sylvester Allochthon at Needlepoint Mountain.

Structure

The Sylvester Allochthon is preserved as a mildly deformed, flat, imbricated sheet within a broad synclinorium. Deformation possibly related to the sole fault was seen only near Needlepoint Mountain. There, a lens of (unit (i)?) shale, chert, and minor tuff or tuffaceous sandstone above the sole thrust has a weak transposition fabric. Augen of chert and tuffaceous sandstone developed from disruption of competent beds are set in a sheared and rodded shale matrix (Fig. 14.4). The rock commonly splits along irregular surfaces showing a well developed microrodding and wrinkle lineation. The lineation and the long axes of chert and sandstone augen generally trend northwest – southeast and plunge gently in either direction. Where the rock is more strongly transposed a gently dipping planar cataclastic foliation is developed containing the linear elements. The foliation generally has a shallow northeast dip and seems concordant with the underlying sole thrust. The sole thrust is not exposed. Rocks of the autochthon immediately beneath are recessive weathering, pyritic, black siliceous shale.

Deformation within the allochthon is mild and heterogeneous, although the effects of possible structural repetition on stratigraphic thickness cannot be assessed. Unit (i) locally shows slaty cleavage and fracture cleavage, but minor folds were not seen. Local thick members of massive shale contrast with the well bedded nature of most of the unit. The massive character may have been structurally produced but the rocks do not possess consistent planar or linear structural elements. In unit 1 some small outcrops of shale are not cleaved and display fine sedimentary lamination, yet in others tight folds and slaty cleavage are developed. Thin bedded chert and minor limestone of unit 3 are highly contorted southwest of Juniper Mountain. The competent volcanic rocks of unit 2 beneath are apparently undeformed, as are the greenstones of unit (ii).

A thrust fault is thought to separate units (i) to (iv) from units 1 to 4 because of older over younger relationships indicated by conodont ages. Unit (i) includes strata at least as young as Permian whereas unit 2 of the upper thrust sheet is in part demonstrably Lower Pennsylvanian. The contact of upper and lower thrust plates is sharp although not well exposed where seen by the authors. Diakow and Panteleyev (1981, p. 61) state that where examined by them "the contact in many areas appears to be a plane of dêcollement (possibly a major thrust fault). Argillite beds along the contact are crumpled, and locally contain large boudins of dyke material". Conodont ages seem to indicate a normal younging upward succession for the upper thrust sheet. Age control, however, is not strict enough to rule out other thrust faults within either the upper (e.g., at base of unit 2) or lower thrust plates. East of Juniper Mountain units of both lower and upper thrust sheets are repeated. Although tentatively shown as resulting entirely from imbrication, it is unclear exactly how the observed distribution was produced.

The lower and upper thrust sheets, broadly equivalent in age, seem to have little in common stratigraphically, which implies a significant distance between their original sites of deposition.

The relationship of the two dated assemblages with the third is not known. The latter may form a separate allochthonous slice of equivalent age or it may be autochthonous with respect to either of the dated assemblages and be entirely older or younger. The contacts of units I to III within the third assemblage are presumably stratigraphic. The possibilities that the units themselves are discrete thrust slices or alternatively that they young systematically upwards in depositional sequence cannot be demonstrated without paleontological control.

Regional Relationships within Sylvester Allochthon

The stratigraphic and structural complexities of the Sylvester Allochthon described above imply that two important volcanic and or subvolcanic units seem to be present. The most widespread and structurally lowest is commonly spatially related with ultramafic rocks. It underlies most of the rugged peaks southeast of Mount Pendleton, extending through southern McDame map area and into Cry Lake map area. The other, of Pennsylvanian age, appears to be less extensive.

Limestone units (including these described here) of Late Mississippian (Late Visean to Early Namurian; Mamet and Gabrielse, 1969), Pennsylvanian, Permian and Triassic (Gabrielse, 1963) ages have been identified within the allochthon. Their distribution suggests the allochthon consists of discontinuous lithological units complicated by low and high angle faults perhaps related to its emplacement.

The steep fault marked by discontinuous sheared serpentinite bodies southwest of Mount Pendleton can be traced southeastward into Cry Lake map area where its continuation is marked by a conspicuous lineament and the occurrence of more ultramafic pods and lenses. Near the boundary of McDame and Cry Lake map areas it separates rocks as old as Late Mississippian (Nizi Formation) to the west from rocks as young as Permian to the east (see Table 14.1, no. 8). Thus it may represent the sole fault of another major imbrication within the allochthon.

References

Diakow, L.J. and Panteleyev, A.
1981: Cassiar gold deposits, McDame map area; in Geological Field Work, 1980, B.C. Ministry of Energy, Mines and Petroleum Resources, Paper 1981-1, p. 55-62.

Gabrielse, H.
1963: McDame map area, British Columbia; Geological Survey of Canada, Memoir 319, 138 p.

Gabrielse, H. and Dodds, C.J.
1982: Faulting and plutonism in northwestern Cry Lake and adjacent map areas, British Columbia; in Current Research, Part A, Geological Survey of Canada, Paper 82-1A, p. 321-323.

Gabrielse, H. and Mansy, J.L.
1980: Structural style in northeastern Cry Lake map area, north-central British Columbia; in Current Research, Part A, Geological Survey of Canada, Paper 80-1A, p. 33-35.

Mamet, B.L. and Gabrielse, H.
1969: Foraminiferal zonation and stratigraphy of the type section of the Nizi Formation (Carboniferous System, Chesterian Stage), British Columbia; Geological Survey of Canada, Paper 69-16.

Monger, J.W.H.
1975: Upper Paleozoic rocks of the Atlin Terrane, northwestern British Columbia and south-central Yukon; Geological Survey of Canada, Paper 74-47, 63 p.

Monger, J.W.H. and Ross, C.A.
1971: Distribution of fusulinaceans in the western Canadian Cordillera; Canadian Journal of Earth Sciences, v. 8, no. 2, p. 259-278.

Tipper, H.W., Woodsworth, G.J., and Gabrielse, H.
1981: Tectonic assemblage map of the Canadian Cordillera and adjacent parts of the United States of America; Geological Survey of Canada, Map 1505A.

15. ECOSTRATIGRAPHIC AND PALEOMAGNETIC STUDIES OF LATE QUATERNARY SEDIMENTS ON THE NORTHEAST NEWFOUNDLAND SHELF

P.J. Mudie and J.-P. Guilbault
Atlantic Geoscience Centre, Dartmouth

Mudie, P.J. and Guilbault, J.-P., Ecostratigraphic and paleomagnetic studies of Late Quaternary sediments on the northeast Newfoundland Shelf; in Current Research, Part B, Geological Survey of Canada, Paper 82-1B, p. 107-116, 1982.

Abstract

Two piston cores from the inner northeast Newfoundland Shelf contain a correlatable sequence of sediment units, including: unsorted red till and stratified red till of Late Wisconsinan age; banded brown glaciomarine mud; gravelly periglacial mud (brownish below, grey above); and olive-grey Holocene mud. Studies of foraminifera in one core show that the red till is unfossiliferous or has a mostly reworked fauna; banded and gravelly brown muds have a calcareous ***Islandiella-Cassidulina*** *fauna, with common* ***Elphidium excavatum****; gravelly grey mud has a similar fauna but with agglutinated species also present; the Holocene mud has a diverse fauna, partly dominated by* ***Nonion labradoricum*** *but overlain by a surface layer with an agglutinated fauna. Magnetostratigraphy of the cores shows some evidence of a major inclination excursion at the base of the Holocene mud and a shallower excursion at the top of the brownish periglacial mud. The usefulness of paleomagnetic data for lithofacies correlations is limited, however, by variable core recovery of very soft sediments and, possibly, by other sources of disturbances, such as bioturbation and irregular deposition of ice-rafted debris.*

Introduction

The continental shelf off northeastern Newfoundland is dissected by numerous broad channels and deep troughs (Fig. 15.1), which were probably formed by glacial erosion (Grant, 1972). High resolution seismic reflection studies (Dale and Haworth, 1979) show that, in Notre Dame and White bays, 5 to 9 m of mud overlies an acoustic reflector which denotes the surface of unstratified glacial till. The till probably marks the last advance of the Wisconsinan ice sheet over the northeastern Newfoundland Shelf; however, the age of this ice advance has formerly been uncertain.

We describe here preliminary results of a study of two piston cores and their trigger weight gravity cores which were obtained from the Notre Dame Channel about 50 km offshore (Fig. 15.1). The core sites are about 200 m apart and both piston cores appear to contain a continuous sequence of postglacial sediments overlying unstratified till at the base. The purposes of this report are:

i) to describe the core lithostratigraphies and preliminary foraminiferal ecostratigraphies;

ii) to date the major paleoecological events recorded in the cores; and

iii) to evaluate the usefulness of paleomagnetic data for correlation of late Quaternary marine sediment cores.

Methods

During **CSS Hudson** Cruise 78-023, two piston cores (Core 20P and 21P) were obtained from an area of flat bottom topography about 50 km offshore in the Notre Dame Channel, at a water depth of 286 m. A trigger weight gravity core was recovered in conjuction with each piston core. These gravity cores (Cores 20G and 21G) represent samples of the surface mud about 1 m away from the piston cores. Methods of navigation, coring and seismic reflection profiling are described by Dale and Haworth (1979). X-radiographs were taken before the cores were split in 1978. The split cores were visually described and sediment texture was semi-quantitatively studied using smear slides and counts of the clasts in the X-radiographs, following the method of Piper (1976). The cores were wrapped in plastic and stored in a refrigerator at 4°C. Cores 20P and G were sampled for foraminifera in 1978 and again in 1980, at which time there was no visible evidence of gypsum precipitation or fungus growth. In 1981, all the cores were sampled for palynomorphs and paleomagnetism measurements. The methods used to prepare the microfossil samples and to measure the natural remanent magnetism are described with the results of these studies.

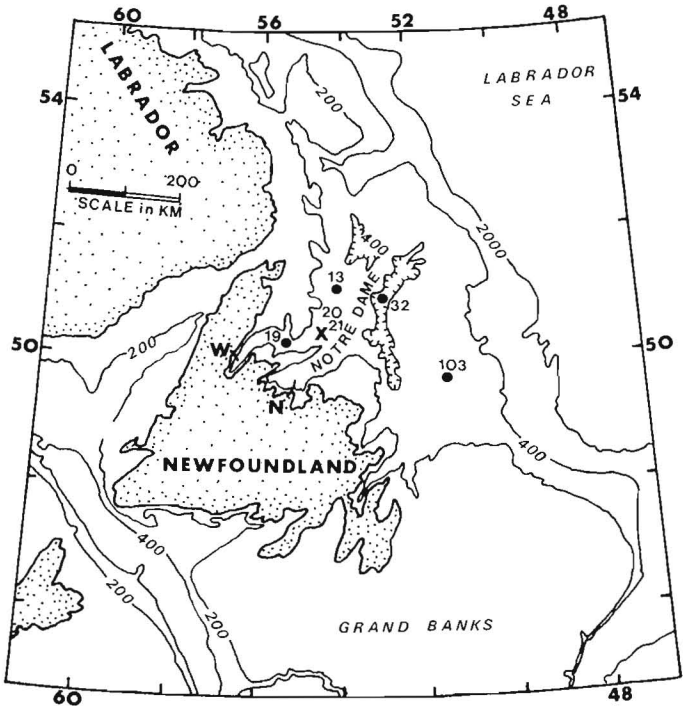

X = cores in this study
o = other cores referred to in the text
W = White Bay
N = Notre Dame Bay; NOTRE DAME indicates the Notre Dame Channel

Figure 15.1. *Geographic location of core sites and bathymetry (in metres).*

Sediment

Five lithological units are recognized which are stratigraphically correlatable between Cores 20 and 21 and can be related to lithofacies in other cores from the northeast Newfoundland Shelf described by Dale (1979) and Piper et al. (1978). The correlation between Cores 20 and 21 is shown in Figure 15.2; for clarity, however, only the lithostratigraphy of Core 20 is described in detail as follows.

Unit 5 (1005-1095 cm). The base of the piston cores consists of about 1 m of unstratified, very stiff, greyish red to brown (2.5 YR – 5 YR 4/3) gravelly mud. The mud is either unfossiliferous or contains very few, poorly preserved foraminifera, diatoms and Paleozoic spores. This unit has a poorly sorted silty clay matrix, with about 5 per cent sand, abundant angular granules and scattered gravel to cobble-sized clasts. The sand contains many iron-oxide stained grains and coal fragments; Barss (in Dale, 1979) reported that the coal is of Westphalian A (Late Carboniferous) age. This semi-consolidated diamicton has the characteristics of lodgement till (Dreimanis, 1976) and it must have been transported by ice which eroded Upper Carboniferous bedrock. The closest source for the coal is an area of Mississippian-Permian sandstone (Haworth et al., 1976) which lies about 1 km west of the core sites. On seismic records (Dale, 1979), the unstratified till unit appears to cover an extensive area, being thicker inshore at sites 19 and 13 (Fig. 15.1) and thinner offshore at site 32.

Unit 4 (910-1005 cm). About 1 m of laminated greyish red (10 R 4/2) mud overlies the unstratified till. This mud is also essentially unfossiliferous, although a small number of foraminifera are present. The lower half of the unit contains iron-stained sand, coal and Carboniferous spores. The sediment is stiff and consists of layers (0.5 – 20 cm thick) of poorly sorted silty mud with 5 per cent sand and fine to medium gravel, alternating with thinner (0.25 – 5 cm) layers of clayey mud. Most of the laminae are sharp-based, grading upwards to coarser or finer lithologies. This laminated mud shows evidence of sorting (silt to silty clay couplets) within the clayey laminae.

Unit 3 (685-910 cm). About 2 m of banded mud overlies the laminated sediment. This mud contains abundant marine diatoms. Small numbers of planktonic and benthonic foraminifera are found in the lower part of the unit, becoming fairly abundant towards the top. The banding consists of relatively thick (2-10 cm) layers of brown (10 YR 3/2) silty or gravelly mud, alternating with thin (0.5 cm) layers of olive grey (5 Y 4/1) or brown (5 YR 3/4) mud containing abundant well preserved cylindric diatoms (**Chaetoceros atlanticus**) and small centric diatoms (cf. **Melosira**). Unit 3 has the textural characteristics of glaciomarine sediments which are presently found under and proximal to Antarctic ice shelves (Anderson et al., 1980). The diatom-rich laminae suggest the periodic upwelling of nutrient-rich water at the edge of a floating ice shelf (Foldvik and Kvinge, 1977).

Unit 2 (95-685 cm). A thick (4-6 m) sequence of fossiliferous greyish mud, with scattered granules and occasional sandy or gravelly layers, overlies the banded mud. This lithofacies is divided into 3 subunits on the basis of differences in colour and gravel content which coincide with major changes in diatom and carbonate content.

Subunit 2C (400-685 cm) consists of about 2.5 m of greyish brown (2.5 YR 4/1) to olive (5 Y 5/2 or 4/1) silty mud. The mud is poorly sorted, with scattered gravel and occasional thin (<2 cm) silty layers. Well preserved, small centric diatoms are common but larger diatoms (**C. atlanticus** and **Coscinodiscus** spp.) are mostly broken. Bioturbation is indicated by burrows and mottles and by discontinuous or gradational laminae. The mud is relatively firm and coarse textured below and grades upwards to soft mud. The upper mud shows diffuse to sharp-based laminae in the X-radiographs: the laminae consist of thin (ca. 1 cm) layers of coarse silt, about 10 per cent sand and abundant granules, alternating with wispy layers of poorly sorted silty mud containing abundant small centric diatoms.

Subunit 2B (358-400 cm) consists of about 50 cm of greyish-brown (10 YR 5/2) silty carbonate-rich mud which grades upwards to a greyish-green mud sequence, Subunit 2A. The carbonate-rich mud corresponds to Dale's (1979) Unit 2 and contains carbonate lithologies in all grain size classes. However, much of this carbonate seems to reside in the abundant calcareous foraminifera which mark this subunit. The heavy mineral and clay fractions (see Dale, 1979) are not significantly enriched in calcite or dolomite relative to other sections of the cores. Well preserved large **Coscinodiscus** frustules are common to abundant within faintly discernable diatom-rich laminae. Dale's correlation of this lithofacies with Aksu and Piper's (1979) ice-rafted carbonate layer is therefore questionable and it seems more likely that subunit 2B marks a late glacial ice margin environment which is commonly characterized by an **Elphidium excavatum** acme zone in eastern Canadian shelf sediments (Vilks, 1981).

Subunit 2A (95-358 cm) consists of dark grey (2.5 Y 4/1) to greenish (5 Y 5/2) gravelly mud which is significantly thicker (3 m) in Core 20 than in Core 21 (ca. 1 m). Subunit 2A is similar to subunit 2C but it contains more fine sand and (towards the base) a larger amount of coarse gravel and it lacks the brownish hues which characterize subunit 2C. Subunit 2A contains abundant large **Coscinodiscus** frustules, both whole and broken. The texture of the mud in subunit 2A is similar to that of the iceberg zone mud lithofacies proximal to a modern Alaskan tidewater glacier (Powell, 1980).

The relatively high organic and microfossil content of unit 2 suggests that it was deposited in the absence of a permanent ice cover. However, subunit 2C corresponds to a strongly stratified acoustic-morphologic unit (Dale and Haworth, 1979) which may indicate a proglacial environment (cf. Parrott et al., 1979). Subunit 2A is acoustically transparent and the sand and gravel probably indicate frequent deposition of ice rafted detritus. The sand in this subunit lacks iron-oxide coatings and appears fresher (less worn) than that in subunit 2C and unit 3.

Unit 1 is found in the gravity cores and the tops of the piston cores. It consists of dark olive grey (5 Y 3/2) to olive brown (7.5 YR) mud which is structureless or bioturbated. The mud is soft to soupy in consistency and is highly fossiliferous, with abundant small centric diatoms and large **Coscinodiscus** frustules. The lithofacies is tentatively divided into subunits on the basis of gravel content. Subunit 1B (3-95 cm in Core 20P) contains scattered fine gravel which is most frequent near the base. Subunit 1A (Core 20G and Core 20P, 0-3 cm) is mostly fine grained, with rare silty or sandy-gravelly mud layers, notably at the tops of the cores.

Foraminifera

Core 20 was sampled for foraminifera at about 20 cm intervals. The samples (20 cm^3 volume) were prepared by washing through a 63 µm sieve mesh, then drying and floating the specimens, using standard foraminiferal separation techniques. The total numbers of **Cibicides lobatulus, Islandiella helenae, I. norcrossi,** and **Nonion labradoricum** were counted in both the piston and

gravity cores. These results are shown in Figure 15.3, columns 1-3 and in Figure 15.4. It should be noted that the two **Islandiella** species have been grouped as a single entry. Aksu (in Dale, 1979) counted the number of planktonic foraminifera, benthonics, and **Elphidium excavatum** in Core 20P; these data and the percentage frequency of **E. excavatum** are also shown in Figure 15.3 (column 4). In addition to counts of the calcareous species listed above, which will be used for future oxygen isotope studies at Dalhousie University, notes were made of the major arenaceous foraminifera species and other important calcareous species in Cores 20G and P. The main results are summarized as follows (also see Fig. 15.9).

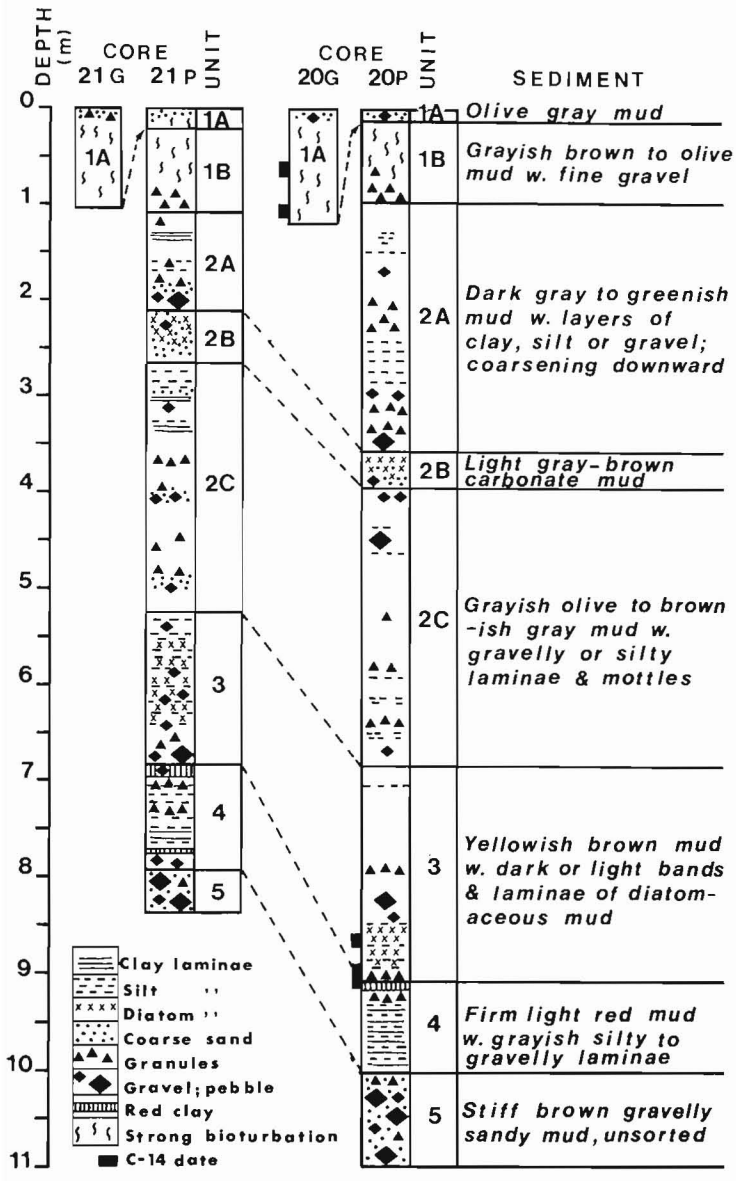

Figure 15.2. *Lithostratigraphic correlation of Cores 20 and 21; G and P denote gravity and piston cores, respectively.*

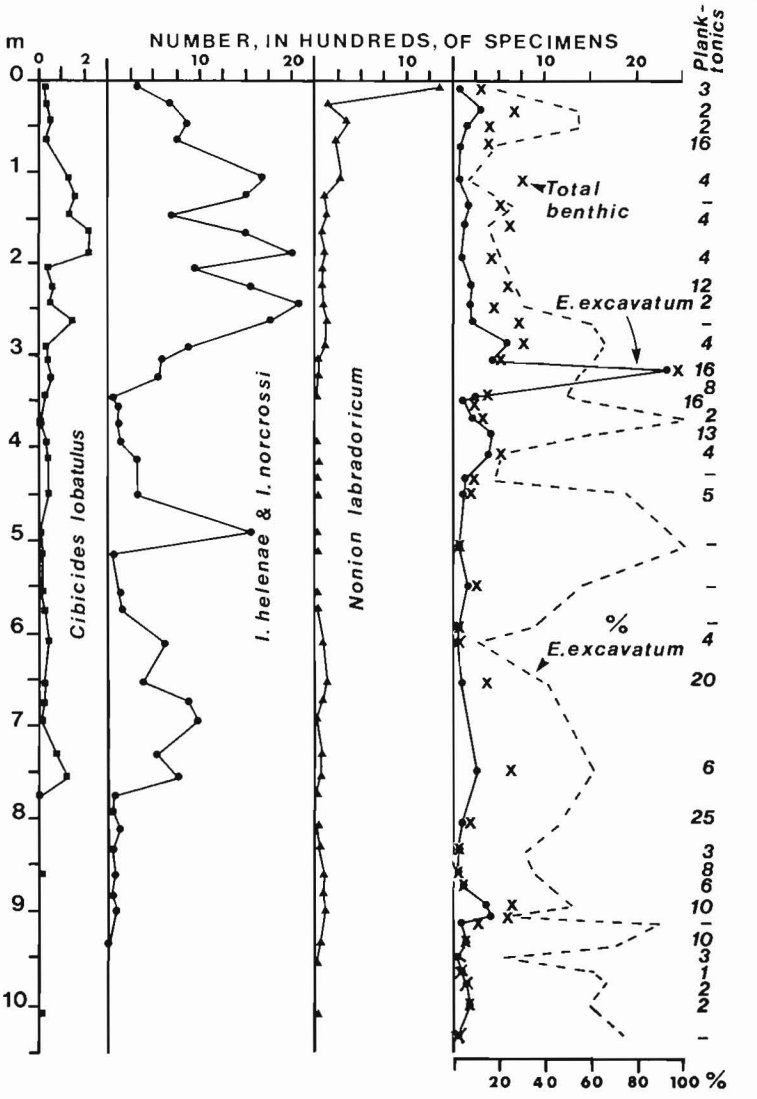

Figure 15.3. *Abundance of major foraminifera species vs. depth in Core 20P. Horizontal scales show: at top, number of specimens per sample; at bottom right,* ***Elphidium excavatum*** *as a percentage of total benthic foraminifera per gram. All data in the right-hand column are from Dale (1979).*

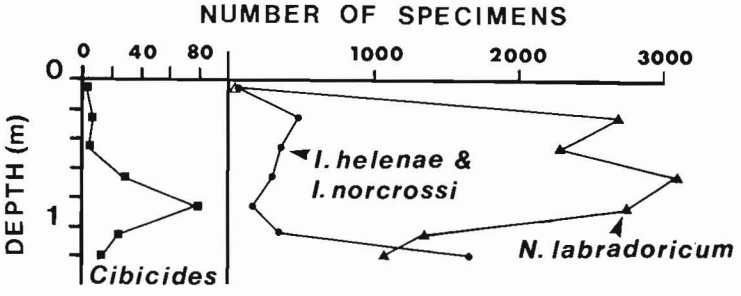

Figure 15.4. *Abundance of major foraminifera species vs. depth in Core 20G. Horizontal scale shows numbers of specimens per sample.*

Table 15.1

Foraminifera in samples of (A) stratified till and (B) diamicton from Core 20. Sample A is a one-fifth split and B is a one-half split

	A		B	
Core interval (cm)	998-1000		1008-1010	
Elphidium excavatum	80		116	
Cassidulina reniforme	77		77	
Bucella hannai	7		22	
B. frigida	23		12	
Cibicides lobatulus	2		6	
Haynesina orbiculare	8		6	
Elphidium albiumbilicatum	-		6	
E. cf. subarcticum	8		-	
Islandiella helenae	3		6	
I. norcrossi	5		-	
I. indeterminate	4		-	
Astrononion gallowayi	8		6	
Virgulina schreibersiana	6		-	
Nonion labradoricum	5		5	
Other species	9	(7 spp.)	19	(12 spp.)
Indeterminates	22		43	
	267		324	

Units 5 and 4. Below 920 cm, the faunas are sparse and the tests, although not etched, show traces of abrasion and breakage. The dominant forms are **E. excavatum** and **Cassidulina reniforme; Virgulina schreibersiana** is rare and **E. groenlandicum** is present sparingly. Samples from the base of unit 4 (998-1000 cm) and the top of unit 5 (1008-1010 cm) were analyzed in detail as shown in Table 15.1. Large numbers of indeterminates in these samples reflect the poor preservation of the fauna and suggest transport and redeposition. Asku (in Dale, 1979) reported that a few foraminifera (total = 117) are present in a sample from 1030 cm depth. The amount of foraminiferal redeposition seems maximum at the base of the stratified mud, and it decreases upwards gradually until a seemingly in situ fauna is found at 920 cm. The till below 1030 cm has not been sampled in detail but it appears to contain no recognizable foraminifera.

Unit 3 and lower Subunit 2C. From 920 to 500 cm, the fauna is also mostly sparse and is low in diversity. Only calcareous species are present. The predominant species are **E. excavatum, Islandiella** spp. (mainly **I. norcrossi**) and **Cassidulina reniforme; V. schreibersiana** is very variable but is occasionally dominant. **N. labradoricum** is a minor constituent except in the 860-920 cm interval.

Subunit 2C to lower 2A. From 500-200 cm, the dominant species is **E. excavatum,** with variable amounts of **Islandiella** spp. and **C. reniforme.** The calcareous fauna is also accompanied by agglutinated species, mainly **Spiroplectammina biformis** and **Reophax arctica.**

Subunit 2A to 1B. From 200-3 cm in Core 20P, the number and diversity of benthonic foraminifera increase, **E. excavatum** tends to be replaced by **Islandiella** spp., and the abundance of **C. lobatulus** and **N. labradoricum** increases. The agglutinated fauna also changes, becoming dominated by **Adercotryma glomerata** and **Cribrostomoides crassimargo,** with common **Reophax subfusiformis.**

Unit 1A. At the top of the piston core (0-3 cm) and in most of the gravity core (see Fig. 15.4), the fauna is dominated by vast numbers of **Nonion labradoricum** which are frequently fragmented, with the last chamber(s) broken off. **I. helenae** is also fairly common and a few **Globobulimina auriculata** are present. The arenaceous fauna accompanying this calcareous fauna is similar to that in subunit 1B. The distribution of this foraminiferal assemblage establishes that there is a slight overlap (ca. 20 cm) between the stratigraphy of the gravity and piston cores. At the top of Core 20G (0-5 cm), however, the gravelly layer contains a very different fauna which is not present in Core 20P. This surface fauna contains only a few poorly preserved calcareous forms and it is dominated by the agglutinated species, **A. glomerata, S. biformis** and **C. crassimargo.**

Discussion

Five foraminiferal assemblages are recognized in Core 20: I. a reworked assemblage; II. an **Elphidium-Islandiella-Cassidulina** assemblage; III. an **Elphidium-Islandiella-Cassidulina**-arenaceous assemblage; IV. a **Nonion labradoricum** assemblage; and V. an **Adercotryma glomerata** assemblage. The environmental characteristics of these faunal assemblages are discussed as follows.

I. Reworked assemblage (1030-920 cm). The samples from below 920 cm contain only a few well preserved specimens, mainly **E. excavatum** and **C. reniforme.** The assemblage appears to contain mostly redeposited tests and it probably represents, at least in part, reworked material flushed from a melting ice front or ground moraine. The similarity in faunal composition suggests that the assemblages in unit 4 may have been derived from the fauna in unit 5.

II. **Elphidium-Islandiella-Cassidulina** assemblage (920-500 cm). This assemblage comprises calcareous foraminifera. It occurs extensively in all clayey deposits formed during the retreating phase of the last glaciation. It occurs on the Labrador Shelf (Vilks, 1980), in Hudson Bay (Leslie, 1965), Frobisher Bay (Osterman, personal communication), in raised marine deposits around the St. Lawrence Estuary (Guilbault, unpublished data) and in Champlain Sea sediments (Guilbault, 1980). Where seismic reflection data are available, this assemblage is associated with an acoustically stratified unit, possibly deposited by a floating ice shelf.

III. **Elphidium-Islandiella-Cassidulina**-arenaceous assemblage (500-3 cm). The main difference between this and the previous assemblage (II) is the presence of arenaceous forms in III. Assemblage III presently occurs in Hudson Bay, on the Labrador Shelf, near the coasts of Greenland, on the Grand Banks and in the Gulf of St. Lawrence. In the last area, this fauna is associated with a cold water layer, with salinities of 30-32‰, between the seasonal less saline surface layer and the more saline oceanic bottom water. On the Labrador Shelf, the assemblage is not found in the surface mud of box cores but occurs immediately beneath and may represent the taphrocoenosis derived from early diagenetic destruction of the numerous arenaceous species present on the seafloor (Vilks et al., 1982). The advent of the arenaceous species in postglacial sediments has been observed in Hudson bay, Lake Melville, and on the Labrador Shelf and it seems to be related to the end of the glacial influence in these regions. However, insufficient data are available to interpret the paleoecological significance of the different arenaceous assemblages with certainty.

Table 15.2

Radiocarbon dates, based on total organic matter (t.o.m.) for Core 78-023-20, and palynomorph data for subsamples of the dated sediment

Core No. and Sample Depth (cm)	Radiocarbon Lab. No.	Measured ^{14}C Age (years B.P.)	Palynomorphs per gram dry weight Quaternary	pre-Quat.	'Graphite'
78-023-20G (53-65 cm)	GX7765	9 185 ± 359	12 425	0.05%	2%
78-023-20G (105-115 cm)	GX7764	9 525 ± 315	8 462	1.5%	1%
78-023-20P (861-869 cm)	GX7763	21 980 ± 1135	1 050	10%	33%
78-023-20P (890-912 cm)	GX6404	25 490 $^{+1570}_{-1310}$	0	850	75%

IV. **Nonion labradoricum** assemblage (Core 20P, 0-3 cm, Core 20G, 10-100 cm). Modern analogues of the **N. labradoricum** assemblage are few and their distribution is poorly known. The assemblage is found on the Scotian Shelf (Williamson, personal communication) as a variant of the **Bulimina marginata** assemblage which inhabits the warm, saline Atlantic water at the base of deep basins. On the other hand, high abundances of **N. labradoricum** and **G. auriculata** may indicate transport, because they are easily carried by currents. Living specimens are mostly found on the edges of basins from where they can easily be transported downslope. In the Laurentian Channel, Cole (unpublished data) found both species (living and dead) in greatest abundance below 300 m depth, in saline water with a temperature of about 5°C. On the Tail of the Grand Banks, Sen Gupta (1971) found large numbers of living **N. labradoricum** and **G. auriculata** in an area where warmer Atlantic water laps onto the shelf edge. The dead fauna in Sen Gupta's samples has a completely different composition and is probably relict Pleistocene. Thus, on the Grand Banks, tests of **N. labradoricum** and **G. auriculata** are being generated but are probably carried away soon after their death.

In summary, the **N. labradoricum** assemblage seems to be related to waters warmer than those dominated by the **Elphidium-Islandiella-Cassidulina**-arenaceous assemblage and may therefore indicate an incursion of Atlantic water into Notre Dame Channel. On the other hand, it may represent a change in the mode of sediment transport, causing different substrate conditions or a preferential concentration of dead **N. labradoricum** tests.

V. **Adercotryma glomerata** assemblage (Core 20G, 0-5 cm). This assemblage presently occurs in coastal water on the Scotian Shelf at depths of 0-250 m, and on the upper Labrador Slope, in normal marine conditions at depths of 300-500 m. The ecological implications of the fauna at the top of Core 20G must await further study of this widely distributed arenaceous assemblage.

Radiocarbon Dates

Four radiocarbon dates were obtained from total organic matter (t.o.m.) in mud from the core intervals shown in Table 15.2. It is well known, however, that radiocarbon dates from highly inorganic muds are usually erroneously old (Olsson, 1968; Stuckenrath, 1977; Nambudiri et al., 1980) and that the apparent radiocarbon ages should be corrected by estimates of the amount of old carbon contamination. A modification of the method using pre-Quaternary palynomorph counts to estimate the relative amount of contamination (Nambudiri et al., 1980) has been applied here. This modified method considers both the quantity of pre-Quaternary spores and other organic material (kerogen) showing a high degree of thermal alteration. Hence, counts were made of the 'graphite' (=highly reflective coal particles) in the <150 µm fraction (Table 15.2) and in the coarser sediment fraction. The palynomorphs and 'graphite' are considered to constitute the major sources of old carbon contamination because treatment with hot hydrochloric acid prior to ^{14}C measurement removes most of the nonrefractory amorphous hydrocarbons and calcium carbonate sources other than dolomite, which was not found in the radiocarbon sample lithologies. A very small volume (<0.5%) of orange-brown wood fragments were observed in the gravity core samples but not in the piston samples. It is not possible to assign a definite age to these slightly altered wood particles but they can be ignored here because their quantity is very small relative to the number of well preserved Quaternary pollen, spores and dinoflagellate cysts in the gravity core.

Using the data in Table 15.2 and the carbon correction graphs of Olsson (1968) and Stuckenrath (1977), it is estimated that the apparent radiocarbon dates for Core 20 should be corrected as follows.

1. The gravity core samples contain about 3% v/v of nonradiogenic carbon; hence, the apparent ages of 9185 and 9525 years B.P. may be up to 500 years too old. The similarity of the spruce-tree birch pollen assemblages in the two samples, however, is in accord with the small difference between the apparent radiocarbon ages.
2. The sample from about 860 cm in Core 20P contains about 40 per cent old carbon; therefore, the apparent age is about 5000 years too old. When corrected, the apparent ^{14}C age of ca. 21 980 years B.P. yields a 'true age' of ca. 16 980 years B.P. This 'true age' for unit 4 is consistent with a date of 17 000 ± 270 years B.P. obtained from barnacles in relict littoral sand on the southwestern Grand Banks (Slatt, 1974).
3. The sample from about 900 cm contains at least 75 per cent inert carbon in the fine fraction and it is not clear if any of the total organic matter represents an autochthonous biota. The radiocarbon date is of finite age, however; hence, the total organic matter must contain some penecontemporaneous reworked organics.

Foraminifera are the only obvious source of this organic material. The simplest assumption is that the foraminifera are derived from the top of the youngest Wisconsinan interstadial (Plum Point) which is dated at ca. 24 000 years B.P. (Bowen, 1978). If a ratio of ca. 1:1 Plum Point carbon (foram linings) to inert carbon is assumed, then correction of the apparent age of 25 400 years yields a 'true age' of ca. 18 000-19 000 years B.P. This age is consistent with the average age of the Late Wisconsinan glacial maximum based on ^{14}C dates from deep-sea foraminifera and periglacial peats.

Paleomagnetism

Use of magnetostratigraphy to date sediments by correlation of small-scale magnetic excursions has met with some success in the Great Lakes region and eastern Canada (see reviews by Verosub and Banerjee, 1977; Barendregt, 1981). Because of the problems of dating unfossiliferous tills and highly inorganic pre-Holocene marine sediments, paleomagnetic studies were made of Cores 20 and 21 in an attempt to answer the following questions:

i) are short-lived regional polarity changes, such as the Erieau and Lake Michigan excursions, also recorded in sediments of the northeast Newfoundland area and,

ii) how similar is the magnetostratigraphy of piston-gravity core pairs spaced 200 m apart in an area of flat bottom topography and flat-lying subbottom acoustic reflectors?

Natural remanent magnetization (NMR) was measured from samples (8 cm^3) taken at approximately 10 cm intervals from Cores 20G, 20P, 21G and 21P. A Schonstedt Digital Spinner Magnetometer was used to measure inclination, declination and intensity after systematic demagnetization at 50 Oe steps (where 1 Oe = 79.6 A/m in SI units) in an alternating magnetic field. During the spinning, some samples of very soft mud from Core 21 began to slide within the sampler sleeves. Therefore, tests were done to determine the effect of freezing the samples in their sleeves before demagnetization. This treatment was found to have little effect (<5°) on NRM polarity or on magnetic intensity up to a demagnetization field of 250 Oe, after which the samples started to melt and slide. All measurements for Core 21 were therefore made using frozen samples. The polarity data reported here are arithmetic means of

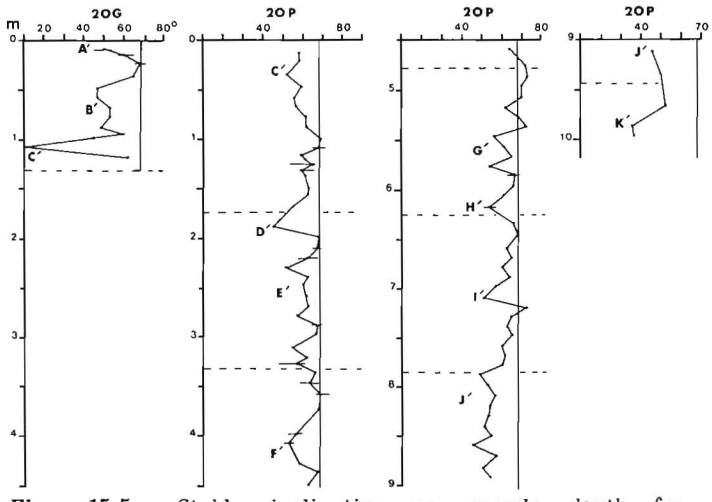

Figure 15.5. *Stable inclination vs. sample depth for Core 20G and 20P. Letters denote excursions of ≥10° from the centred axial dipole. Dashed lines indicate core sections; horizontal bars show the range of values/sample where this exceeds 4°.*

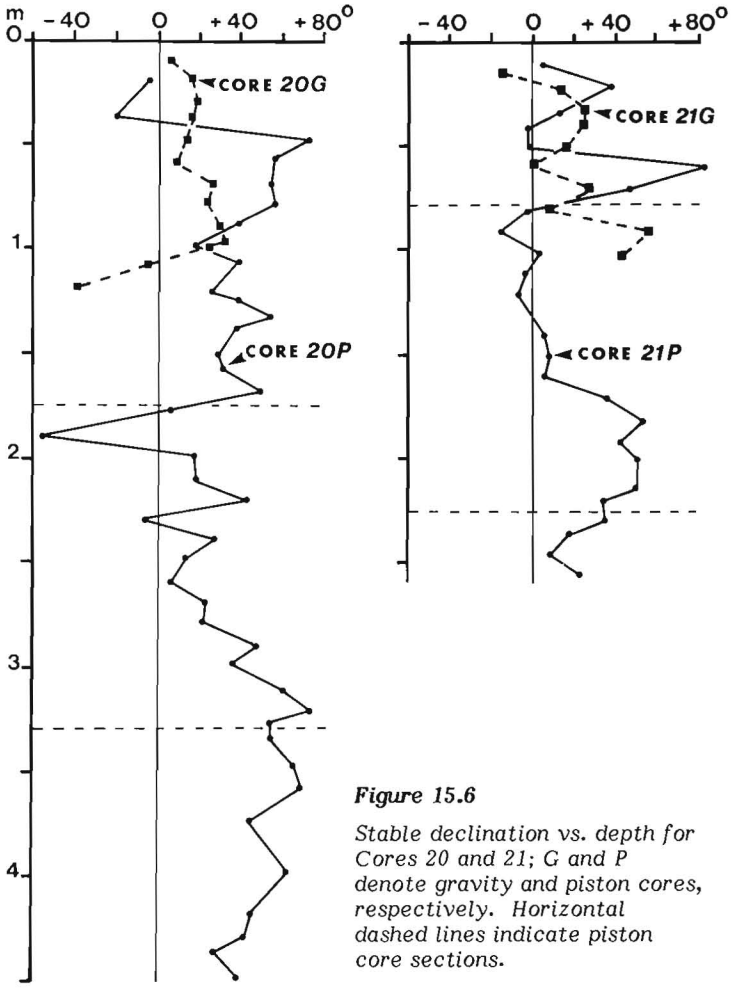

Figure 15.6

Stable declination vs. depth for Cores 20 and 21; G and P denote gravity and piston cores, respectively. Horizontal dashed lines indicate piston core sections.

4-5 measurments obtained before demagnetization step 300 Oe. The magnetic intensity values are those obtained at step 200 Oe.

Stable inclination for Core 20 (Fig. 15.5) shows that most of the secular variations are within ± 10° of the centred axial dipole inclination (68°) for the core site latitude. No reversals were found but significant departures from the dipole inclination are recorded in the lower part of Core 20G and in Core 20P at 170-190 cm and 925-1000 cm. The largest inclination excursion, designated Event C', corresponds to a 60° rotation of the stable declination (Fig. 15.6) in the gravity core; the excursion at 170-190 cm (Event D') in Core 20P corresponds to a 90° rotation. In contrast, smaller changes in stable inclination (e.g. Event E' in Fig. 15.5) are marked by irregular fluctuations in declination (Fig. 15.6) and/or magnetic intensity (Fig. 15.7). The minor inclination excursions appear to be related to lithological irregularities, e.g. presence of ice-rafted detritus; hence these small magnetic excursions are not fully documented or described in detail here.

The radiocarbon dates show that Event C' in Core 20G falls within the age range (8000-13 000 years B.P.) of similar excursions reported for the Great Lakes and European lakes (Verosub and Banerjee, 1977) and for Core 103 (see Fig. 15.1) from the outer northeast Newfoundland Shelf (Piper et al., 1978). Hence, the excursion in Core 20G appears to mark a geographically widespread magnetic event and the question arises as to why this large change in dipole inclination is not clearly evident in Core 20P (Fig. 15.5) or in Core 21 (Fig. 15.8). Detailed comparison of the stratigraphy of the cores may provide some answers to this question, as explained below.

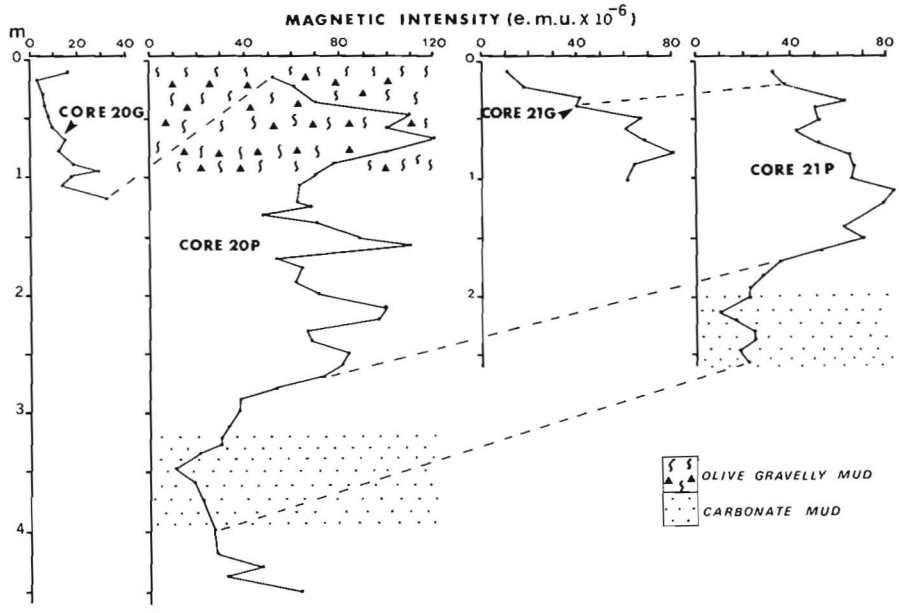

Figure 15.7. *Magnetic intensity vs. sample depth for Cores 20 and 21; G and P denote gravity and piston cores, respectively. Dashed lines indicate tentative magnetostratigraphic correlations.*

The foraminiferal data for Core 20 (Fig. 15.3, 15.4) suggest that the gravity and piston core lithologies overlap in the top 20 cm. The microfossil evidence is further supported by the correlations between magnetic intensity values as shown in Figure 15.7. Therefore, Event C' should be recorded in Core 20P and it is postulated that it may be represented in a modified form because of the different depositional histories of sediments in the gravity and piston cores (see Fig. 15.2). Firstly, if sedimentation rates in the piston core during Event C' were much slower than the gravity core, the magnetic signal would be recorded in a shorter core length; hence, it would be more difficult to sample the excursion adequately because the size of the core area required for the paleomagnetic samples is relatively large (diameter ca. 5 cm) and the excursion appears to be of short duration in Core 20G. Bioturbation is also more likely to smear out the magnetic signal if the sedimentation rate is relatively low.

Radiocarbon dates for Core 20G indicate a sedimentation rate of ca. 150 cm/1000 years for the lower half of the core and Event C' seems to have occurred within about 100 years. Sedimentation rates in Cores 20P and 21 appear to be lower. If the corrected age of 16 980 years is taken for Core 20P and it is assumed that the piston core top has an age of ca. 10 000 years, it appears that the average sedimentation rate for Core 20P is about 120 cm/1000 years. If it is further assumed that subunit 2B in Cores 20 and 21 are time correlative, an average sedimentation rate of ca. 50 cm/1000 years is obtained for Core 21P. Thus the relatively slow sedimentation rate for Core 21P may account for the absence of a clearly marked polarity excursion, but this factor alone is unlikely to explain the magneto-stratigraphy of Core 20P.

Secondly, modification of a regional paleomagnetic signal may also result from the local influx of ice-rafted detritus. As described earlier, a significantly greater amount of coarse grained sediment is present throughout the piston cores as compared to the gravity cores. It is postulated that this influx could have disrupted the paleomagnetic signal so that it is now only evident as a discontinous series of relatively shallow inclination excursions, such as those labelled C' and D' in Core 20P (Fig. 15.5) and 21P (Fig. 15.8).

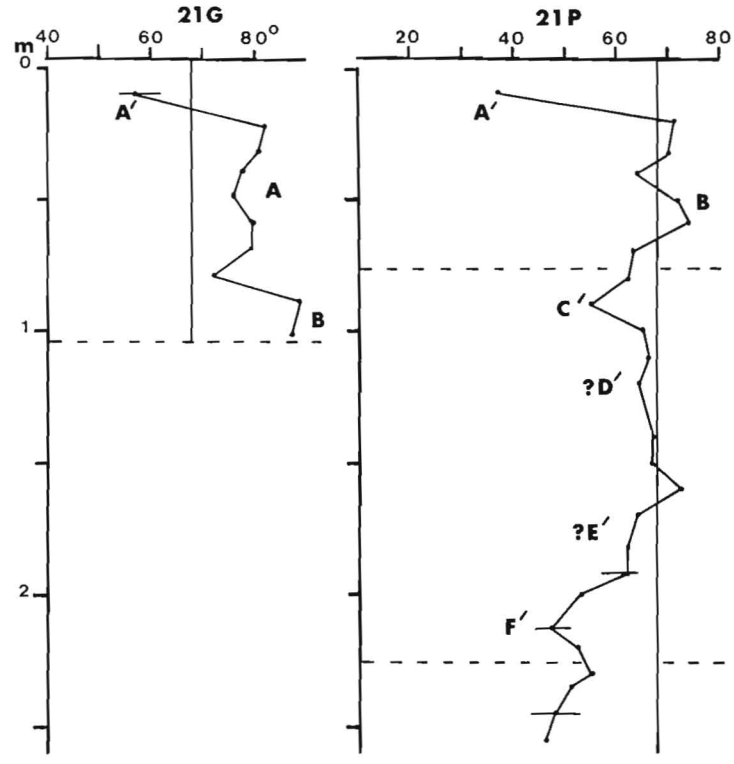

Figure 15.8. *Stable inclination vs. sample depth for Core 21G and upper sections of Core 21P. Letters denote excursions of >10° from the centred axial dipole. Dashed lines indicate core sections; horizontal bars show the range of values per sample where this exceeds 4°.*

Figure 15.9

Summary of the ecostratigraphy for Core 78-023-20. GC and PC denote gravity and piston cores, respectively. Approximate radiocarbon ages (in 1000 years B.P.) are shown on the left. IRD = ice rafted detritus.

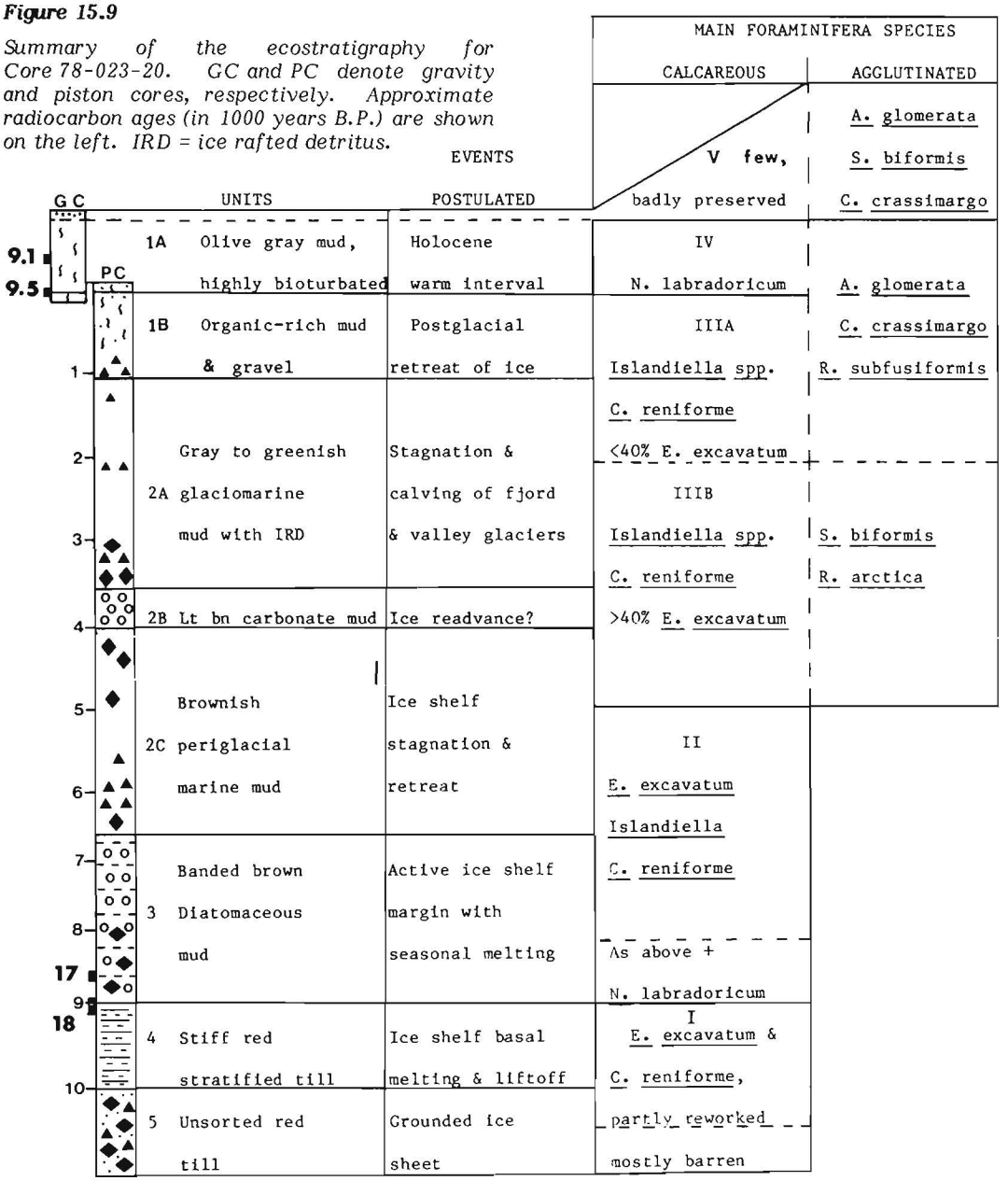

If the above arguments are valid, then it seems that a postglacial magnetic excursion comparable to the Erieau or Lake Michigan excursions can be traced in three of the four cores from Notre Dame Channel but is absent in Core 21G due to the short length of this gravity core. In general, however, correlation between the magnetostratigraphy in the sediments below unit 1A is very unclear. It is suggested that the magnetic variability of lithofacies 1B and 2A is largely due to the sporadic influx of ice-rafted detritus. This detritus may randomly introduce magnetite-rich clasts (e.g. basalt) and rapid deposition of a large volume of ice-rafted detritus might rearrange the soft surface mud. It may be significant, however, that Cores 20P and 21P both show a shallow inclination trough, designated Event F', which corresponds to the carbonate mud facies (subunit 2B). Event F' is marked in both cores by a ca. 40° rotation of stable declination occurring within an interval of very low magnetic intensity. If this late-glacial polarity excursion can be traced in other cores from the Newfoundland region, it may serve as a useful marker for correlation of lithologies in which the carbonate-rich facies in not clearly denoted by sediment colour and microfossil compostition.

Paleoenvironmental Interpretation

Figure 15.9 summarizes the major lithological features and microfossil changes recorded in Core 20 and it lists the ecostratigraphic events which are considered most likely to account for these data.

The lithostratigraphy of Cores 20 and 21 appears to record a continuous sequence of sedimentological events which accompanied the retreat of Late Wisconsinan ice from the northeast Newfoundland Shelf. The oldest event is represented by a reddish brown, unsorted till (unit 5) which is essentially barren of Quaternary microfossils. This semiconsolidated diamicton appears to be a lodgement till that was deposited by ice which over-rode the Carboniferous bedrock a few kilometres west of the core sites. The unstratified till is overlain by laminated red mud (unit 4) which contains very few microfossils, including a large proportion of reworked Quaternary foraminifera (assemblage I). This stiff red mud is interpreted as a stratified till. Evidence of current sorting suggests that this till was deposited in water shortly after lift-off of the grounded ice. The top of the stratified red till is older than 17 000 years.

The red glacial sediments are overlain by several metres of brownish organic-rich marine mud (unit 3 and subunit 2C), with a periglacial shelf foraminiferal fauna (assemblage II). The banded diatom-rich mud of unit 3 may reflect upwelling at the edge of a floating ice shelf. The calcareous **Elphidium-Islandiella-Cassidulina** assemblage probably represents a periglacial environment in which the ice front stood near the core site or was slowly melting back. Except for a possible low salinity interval suggested by absence of planktonics and a high percentage of **E. excavatum** from 600-500 cm in Core 20P, there is no indication of highly brackish water that might suggest quick and intense melting. The sea was probably not permanently ice covered, as indicated by

i) abundant diatoms and

ii) the occurrence of a fauna similar to assemblage II in Champlain Sea sediments where there is good evidence for wave-washing of landforms.

The presence of fossiliferous periglacial mud suggests that rapid thinning of the Wisconsinan ice sheet started at about 17 000 years. The appearance of agglutinated foraminifera in the upper part of unit 2C may mark the further retreat of the ice front and the start of conditions more similar to those of the present Labrador Shelf, but the paleoenvironmental significance of the arenaceous fauna is presently uncertain.

Light brown carbonate mud (subunit 2B) marks the end of the prominance of red Carboniferous lithologies and the start of lithofacies dominated by non-oxidized sediments. The carbonate mud contains abundant **Elphidium excavatum** and it is associated with a biofacies (IIIA) in which **E. excavatum** usually comprises more than 40 per cent of the benthic foraminifera. It is not clear, however, whether subunit 2B represents an Arctic-type temperate ice shelf environment (cf. Reading and Walker, 1966) or reflects increased runoff at the start of the final deglaciation stage. The carbonate mud is overlain by greyish fossiliferous mud with abundant gravelly ice rafted detritus at the base (subunit 2A). This grey sediment has textural features similar to those characterizing the iceberg zone peripheral to a temperate tidewater glacier (Powell, 1980); hence, this lithofacies is referred to here as a glaciomarine sediment. The exact age of unit 2a is unknown, but by extrapolation from the corrected radiocarbon dates, it has a maximum age of ca. 14 000 years.

The upper part of subunit 2A and subunit 1B are marked by a gradual decrease in the amount of coarse gravel and by a decline in the proportional representation of the ice margin indicator, **E. excavatum.** The change in the calcareous fauna (assemblage IIIB) is accompanied by a change in the arenaceous fauna (from linear to spiral morphotypes). This change in the arenaceous fauna may be related to the increased organic content of the sediment but more data on the relationship between the morphology of the tests and ecology are required before this observation can be verified.

Unit 1 represents postglacial and Holocene mud, with the **Nonion labradoricum** assemblage (IV) in subunit 1A possibly indicating an interval during which warm Atlantic water moved into the Notre Dame Channel. This condition appears to have prevailed until recent times when the calcareous assemblage was replaced by the **A. glomerata** assemblage (V). This arenaceous fauna may mark the change to an environment of sediment erosion or very slow accumulation, but the paleoecological meaning of this assemblage is presently uncertain.

Correlation

Since the present water depth at the core sites is 286 m and relative sea level was probably no more than 100 m lower during the Wisconsinan glacial maximum, it seems unlikely that much sediment has been eroded from the top of the stiff red till. Unit 5 therefore probably marks the presence of grounded ice during the maximum extent of the Late Wisconsinan glaciation. The corrected radiocarbon ages of ca. 18 000 years for the top of the unstratified red till and 17 000 years for the base of the banded glaciomarine sediment are consistent with the average age reported for the last glacial maximum. An age of about 14 000 years for the grey glaciomarine sediment (subunit 2A) is comparable to that of the St. George's River Drift of southwest Newfoundland, which is overlain by marine deposits dated 13 200-13 600 years (Brookes, 1974).

The occurrence of two glacial sediment units off northwest Newfoundland is consistent with the Pleistocene geology of the Sheffield Lake area (ca. 50 km southwest of Notre Dame Bay) which was studied by Alley and Slatt (1976). Here, a heavily oxidized, indurated, gravelly Lower Red Till with a high Fe content (10%) is unconformably overlain by a lightly oxidized, friable, sandy Upper Grey Till with about 2% Fe. The Lower Red Till is undated but the Upper Grey Till appears to have been deposited by a glacial readvance during the final stage of the Wisconsinan glaciation and is probably correlative with till studied by Tucker (1974) at the head of the Notre Dame Bay. This till is overlain by marine and deltaic deposits dated at about 12 000 years.

Work is in progress to study the foraminifera in Core 21 and to obtain oxygen isotope data for foraminifera from cores 20 and 21 to assist in the interpretation of the ecostratigraphic data. Effort will continue to find better means of dating the cores. Magnetostratigraphic correlation might be improved by use of corers which uniformly recover the soupy surface sediment and have a greater barrel width to allow for closer sampling of short-lived magnetic excursions. However, major differences in sedimentation rates and ice-rafted detritus composition of periglacial lithofacies will probably remain substantial 'noise' factors which limit the usefulness of this technique for correlation of glacial marine sediments. Thus radiocarbon dating will continue to be the most widely applicable method of correlation, although apparent radiometric ages should always be critically evaluated in conjunction with detailed study of the nature of the organic material to be dated.

Acknowledgments

This work was carried out through an NSERC strategic grant to study Quaternary paleo-oceanography of Eastern Canada (QPEC) and was also supported by an NSERC postdoctoral scholarship to J.-P. Guilbault. We gratefully acknowledge the assistance of Dalhousie University technicians Chloe Younger and Jacqueline Clark for preparation of the foraminifera and paleomagnetic samples, and to Charles Walls for assisting with paleomagnetic measurements. We thank Drs D.B. Scott, J.M. Hall and D.V. Subba Rao for help with the foraminifera, paleomagnetism and diatom studies, respectively. This report was critically reviewed by D.J.W. Piper and G. Vilks of the Atlantic Geoscience Centre.

References

Aksu, A.E. and Piper, D.J.W.
1979: Baffin Bay in the past 100,000 yr; Geology, v. 7, p. 245-248.

Alley, D.W. and Slatt, R.M.
1976: Drift prospecting and glacial geology in the Sheffield Lake-Indian Pond area, northcentral Newfoundland; in Glacial Till, R.L. Legget, ed., Royal Society of Canada Special Publications, No. 12, p. 249-266.

Anderson, J.B., Kurtz, D.D., Dormack, E.W., and Balshaw, K.M.
1980: Glacial and glacial marine sediments of the Antarctic continental shelf; Journal of Geology, v. 88, p. 399-414.

Barendregt, R.W.
1981: Dating methods of Pleistocene deposits and their problems: VI. Paleomagnetism; Geoscience Canada, v. 8, p. 56-64.

Bowen, D.Q.
1978: Quaternary Geology; Pergamon Press, Oxford and New York, 221 p.

Brookes, I.A.
1974: Late Wisconsinan glaciation of southwestern Newfoundland, with special reference to the Stephenville map area; Geological Survey of Canada, Paper 73-40 and Map 15-1973.

Dale, C.T.
1979: A study of high resolution seismology and sedimentology on the offshore late Quaternary sediments northeast of Newfoundland; M.S. Thesis, Dalhousie University, Halifax, 180 p.

Dale, C.T. and Haworth, R.T.
1979: High resolution reflection seismology studies on late Quaternary sediments of the northeast Newfoundland continental shelf; in Current Research, Part B, Geological Survey of Canada, Paper 79-1B, p. 357-364.

Dreimanis, A.
1976: Tills: their origin and properties; in Glacial Till, R.L. Legget, ed., Royal Society of Canada Special Publications, No. 12, p. 11-49.

Foldvik, A. and Kvinge, T.
1977: Thermohaline convection in the vicinity of an ice shelf; in Polar Oceans, M. J. Dunbar, ed., Arctic Institute of North America, Calgary, p. 247-255.

Grant, A.C.
1972: The continental margin off Labrador and eastern Newfoundland – morphology and geology; Canadian Journal of Earth Sciences, v. 9, p. 1394-1429.

Guilbault, J.-P.
1980: A stratigraphic approach to the study of the Late-Glacial Champlain Sea deposits with the use of foraminifera; Unpublished Licentiat Thesis, Aarhus University, Aarhus, Denmark, 194 p.

Haworth, R.T., Poole, W.H., Grant, A.C., and Sanford, B.V.
1976: Marine geoscience survey northeast of Newfoundland; in Report of Activities, Part C, Geological Survey of Canada, Paper 76-1C, p. 61-70.

Leslie, R.J.
1965: Ecology and paleoecology of Hudson Bay foraminifera; Bedford Institute of Oceanography Report 65-6; unpublished manuscript, 192 p.

Nambudiri, E.M.V., Teller, J.T., and Last, W.M.
1980: Pre-Quaternary microfossils – a guide to errors in radiocarbon dating; Geology, v. 8, p. 123-126.

Olsson, I.U.
1968: C-14/C-12 ratios during the last several thousand years and the reliability of C-14 dates; in Means of Correlation of Quaternary Successions, R.B. Morrison and H.E. Wright, ed., Proceedings of the VIIth Congress, International Association for Quaternary Research, p. 241-252.

Parrott, D.R., Dodds, D.J., King, L.H., and Simpkin, P.G.
1979: Measurement and evaluation of the acoustic reflectivity of the sea floor; Canadian Journal of Earth Sciences, v. 17, p. 722-737.

Piper, D.J.W.
1976: Manual of Sedimentological Techniques; Dalhousie University, Department of Geology, Halifax, 106 p.

Piper, D.J.W., Mudie, P.J., Aksu, A.E., and Hill, P.R.
1978: Late Quaternary sedimentation 50°N, Northeast Newfoundland Shelf; Geographie physique et Quaternaire, v. 32, p. 321-332.

Powell, R.D.
1980: Holocene glaciomarine deposition by tidewater glaciers in Glacier Bay, Alaska; Ph.D. Thesis, Ohio State University, Columbus, Ohio.

Reading, H.G. and Walker, R.G.
1966: Sedimentation of Eocambrian tillites and associated sediments in Finmark, Northern Norway; Paleogeography, Paleoclimatology and Paleoecology, v. 2, p. 177-212.

Sen Gupta, B.K.
1971: The benthonic foraminifera of the Tail of the Grand Banks; Micropaleontology, v. 17, p. 69-98.

Slatt, R.M.
1974: Continental shelf sediments off eastern Newfoundland: a preliminary investigation; Canadian Journal of Earth Sciences, v. 11, p. 362-365.

Stuckenrath, R.
1977: Radiocarbon: some notes from Merlin's Diary; New York Academy of Science Annals, v. 288, p. 181-188.

Tucker, C.M.
1974: A series of raised Pleistocene deltas, Halls Bay, Newfoundland; Maritime Sediments, v. 10, p. 1-7.

Verosub, K.L. and Banerjee, S.K.
1977: Geomagnetic excursions and their paleomagnetic record; Reviews of Geophysics and Space Physics, v. 15, p. 145-155.

Vilks, G.
1980: Postglacial basin sedimentation on the Labrador Shelf; Geological Survey of Canada Paper 78-28, 28 p.

1981: Late glacial – postglacial foraminiferal boundary in sediments of eastern Canada; v. 8, p. 48-55.

Vilks, G., Deonarine, B., Wagner, F.J., and Winters, G.V.
1982: Foraminifera and mollusca in surface sediment of southeastern Labrador Shelf and Lake Melville, Canada; Geological Society of America Bulletin, v. 93, p. 225-238.

16. SNOWSHOE FORMATION (1982), CENTRAL BRITISH COLUMBIA

Project 680066

L.C. Struik
Cordilleran Geology Division, Vancouver

Struik, L.C., Snowshoe Formation (1982), central British Columbia; in Current Research, Part B, Geological Survey of Canada, Paper 82-1B, p. 117-124, 1982.

Abstract

The term Cariboo Group has mistakenly been applied to two contrasting rock suites. The two suites are separated by a northwest-trending, east-dipping fault, the Pleasant Valley thrust. The Snowshoe Formation is restricted to the Cariboo Group southwest of the fault.

Introduction

Several geographic names used throughout the text do not appear in the figures but can be found on published topographic maps (see NTS 93H/3, 4, 93A/13, 14). The Snowshoe Formation was defined (Holland, 1954) as the highest unit of the Cariboo Group at Yanks Peak in the Cariboo District of British Columbia (Fig. 16.1). The Cariboo Group terminology has subsequently been extended eastward to include Hadrynian and Cambrian age rocks of the Cariboo Mountains.

These notes contain: 1) a description of the Cariboo Group where it includes the Snowshoe Formation, 2) a proposal for a late Paleozoic age for part of the Snowshoe Formation, 3) a description of the important structures displayed in the rocks, and 4) a discussion arguing that the Cariboo Group at Yanks Peak is not the same as the Cariboo Group of the Cariboo Mountains and that they are separated by an east-dipping fault.

Stratigraphy

Struik (1981) divided the rocks between Wingdam and Wells into 5 sedimentary units. They outcrop discontinuously southeastward into the Yanks Peak area where Holland (1954) defined part of the Cariboo Group including the Snowshoe Formation. A brief description of the 5 units and their correlation, if any, with the Cariboo Group follows.

Unit 1

Unit 1 consists of olive to grey micaceous quartzite, pelite and conglomerate. The quartzite and conglomerate contain clasts of glassy light grey and minor blue quartz and some feldspar. The conglomerate also has white quartzite clasts that outnumber other clast types. It occurs near the contact with unit 2. The description of Struik (1981) includes rocks of the Sugar Creek area, but they may be younger.

Unit 2

Unit 2 is thin, discontinuous and characterized by light grey weathering, white to grey marble and calcareous clastics. It does not extend south of the head of Peter Creek, or east of the Dragon-Burns Mountain ridge, except for one possible locality in the Swift River area.

Unit 3

Unit 3 consists of 3 subunits. The lower subunit consists of olive and grey phyllite and medium to fine grained micaceous quartzite and thin beds of chlorite phyllite that resembles metatuff. It is correlative with the type Yankee Belle Formation of Yanks Peak. The middle subunit is composed of white, pink and grey orthoquartzite. It exists locally and is less than 5 m thick. It correlates with the type Yanks Peak Formation of Yanks Peak. The upper subunit comprises thinly bedded grey medium and fine grained micaceous quartzite and phyllite and occurs only at Pinegrove Mountain. It may be in fault contact with the other subunits.

Unit 3 is recognized only in the western part of the map area. In the northwest it is underlain by the thin and discontinuous calcareous rocks of unit 2 or the quartzite of unit 1. In the southeast however, stratigraphic relationships of the lower contact remain unresolved (see the discussion of the Ramos Creek succession of unit 5). Unit 3 is overlain, by black pelite and/or grey and olive micaceous quartzite of unit 4.

Unit 4

Unit 4 is characterized by dark grey to black, thin bedded siltite, argillite, slate and phyllite that are interbedded with micaceous quartzite, black orthoquartzite, muddy conglomerate and grey limestone and marble. The limestone occurs mainly near the top, whereas the other subsidiary rock types are found throughout the succession. The muddy conglomerate has clasts of dark grey, grey and minor blue glassy quartz supported in a black pelite matrix. Similar clasts are found in the micaceous quartzite and dense orthoquartzite. In the areas transected by cross-sections A through C (Fig. 16.2) unit 4 is dominated in the northeast by black siltite and phyllite and changes southwestward to include more grey micaceous quartzite. The micaceous quartzite with its dark grey quartz clasts is a lithology characteristic of the Snowshoe Formation in its type locality. A lateral facies change from grey and dark grey micaceous quartzite to black siltite and phyllite was observed on the ridge southwest of Harveys Creek. A similar vertical change exists on the ridge east of Aster Creek. The grey quartzite at this locality is purplish weathering; the matrix contains abundant secondary white mica and minor green mica. This type of quartzite also occurs on Mount Agnes in contact with black siltite and phyllite. The black rocks that dominate this unit have been mapped throughout the area and include the type Midas Formation of Yanks Peak.

Unit 4a

Unit 4a consists of conglomerate and quartzite. The conglomerate clasts (Fig. 16.3) vary in size from granule to cobble and are mainly pebbles. They are composed of white poorly sorted orthoquartzite and lesser amounts of grey micaceous and dark grey quartzite, black siltite, light olive and light grey phyllite, glassy quartz, limestone and minor grey chert. The micaceous quartzite clasts resemble quartzite common through the Dragon-Amador ridge system, the ridges south of the Little Swift River and the Snowshoe Plateau. The black siltite and limestone clasts resemble rocks of unit 4. The orthoquartzite clasts have no obvious source in the area underlain by the conglomerate.

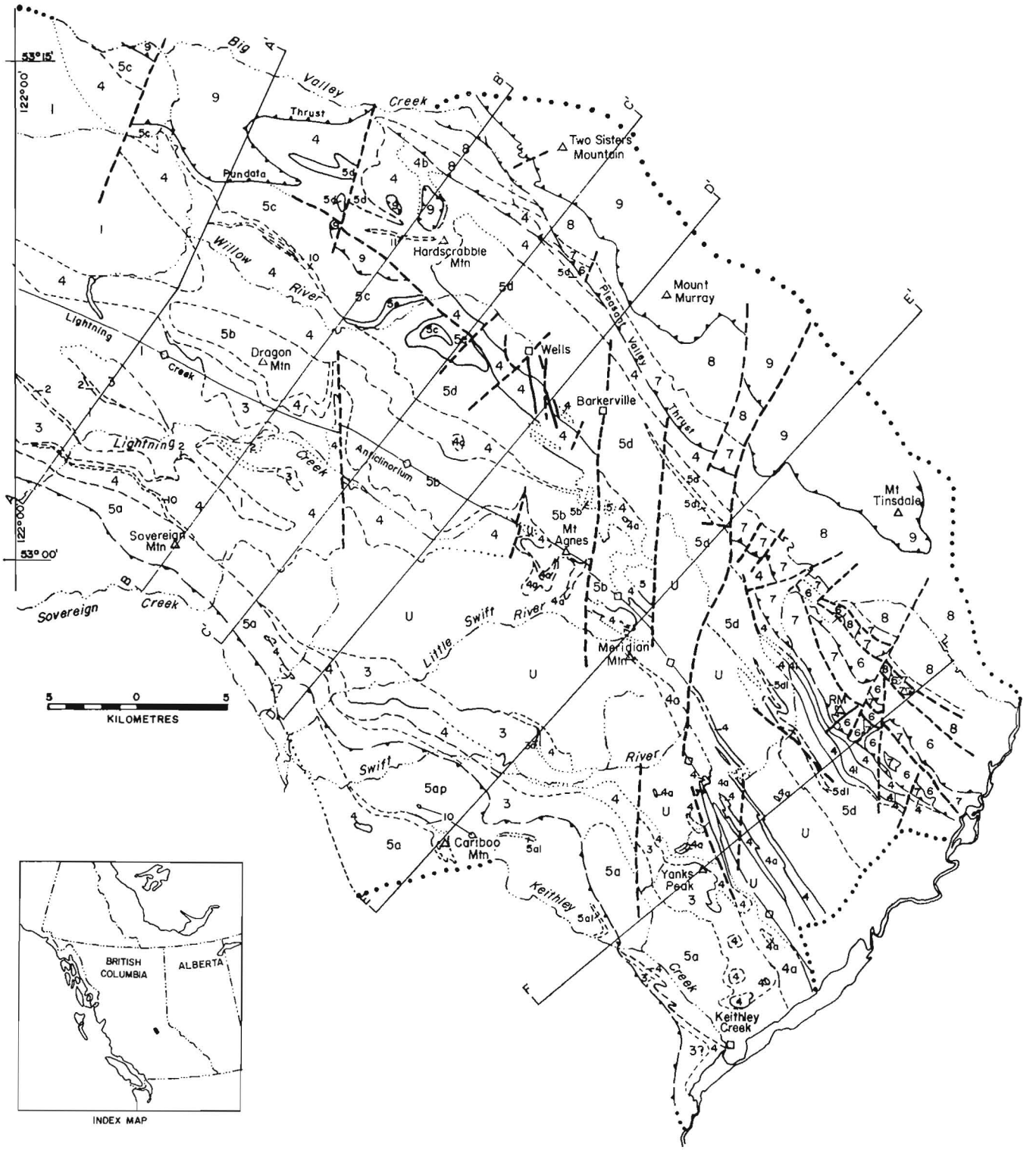

Figure 16.1. *Geological map of study area.*

The matrix of the conglomerate is most commonly light grey sericitic quartzite but can also be a black phyllite or sandy limestone.

The quartzite is poorly sorted and has an average grain size that varies from coarse grained to granule. It is composed of glassy clear, grey and minor blue quartz and local concentrations of feldspar. The matrix is fine quartz and minor sericite. The quartzite appears to be a lateral facies change of the conglomerate. They are discontinuous and most abundant in the area of the Snowshoe Plateau. Small amounts of coarse conglomerate occur at Mount Agnes, Amador Mountain, Cornish Mountain and Cooper Creek. Holland (1954) mapped the conglomerate and quartzite of unit 4a as part of the basal and lower members of the Snowshoe Formation.

Unit 5

This unit is divided into 4 rock successions that may or may not be correlative. They are from northeast to southwest the 1) Downey Creek, 2) Tom Creek, 3) Dragon Mountain and 4) Ramos Creek successions. They are distinguished by lithologic differences or by possible differences in stratigraphic position. Except for the Tom Creek and part of the Downey Creek successions, the remainder form 3 continuous northwest-southeast-trending belts.

The Downey Creek succession is best exposed at Downey, Grouse, Antler and Cunningham creeks and in exploration trenches on Barkerville Mountain. The package consists of green, grey and purple slate and phyllite, light grey, olive grey and tan micaceous quartzite, green metatuff?, grey limestone and marble and calcareous clastic rocks. The limestone is interbedded with the green and purple slates which are locally chlorite rich and may in part be metapyroclastic. Diorite layers parallel to bedding increase volumetrically southeastward and are found with the limestones of this succession in the area of Cunningham Creek and Pearce and Peter gulches. The amount of quartzite appears to vary considerably along strike although this may be partly because of structural complexities. The quartzite of this succession is generally ankeritic and as a result, brown weathering. It is poorly sorted with clasts of glassy translucent and blue quartz supported in a micaceous matrix. Feldspar, although not abundant, occurs locally.

The micaceous quartzite, grey phyllite and lesser limestone underlying the southwestern parts of Island, Cow and Richfield mountains are correlated with the Downey Creek succession because of the calcareous green metatuffs? found on Cow Mountain. Holland (1954) included the limestone and chlorite phyllite of the Downey Creek succession in the upper member of the Snowshoe Formation.

The Downey Creek succession may be in part Mississippian. The age assignment is made by correlating known Mississippian marble, slate and crinoidal limestone of Stewart Creek in the northwestern part of the map area with similar marble and slate within the Downey Creek succession. The Mississippian rocks of Stewart Creek were dated from conodonts extracted from the crinoidal limestone (M.J. Orchard, personal communication, 1982). The dating of the Downey Creek succession is suspect because the lithologic correlation involved is uncertain.

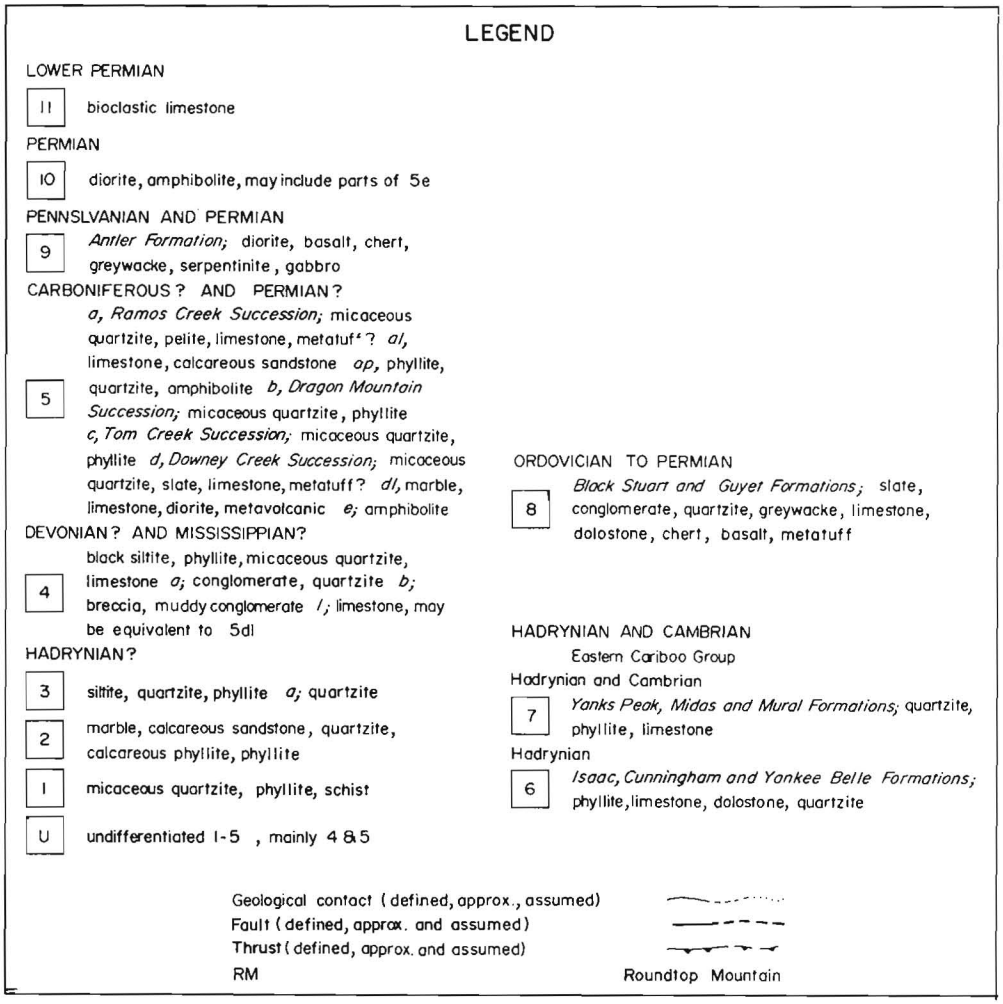

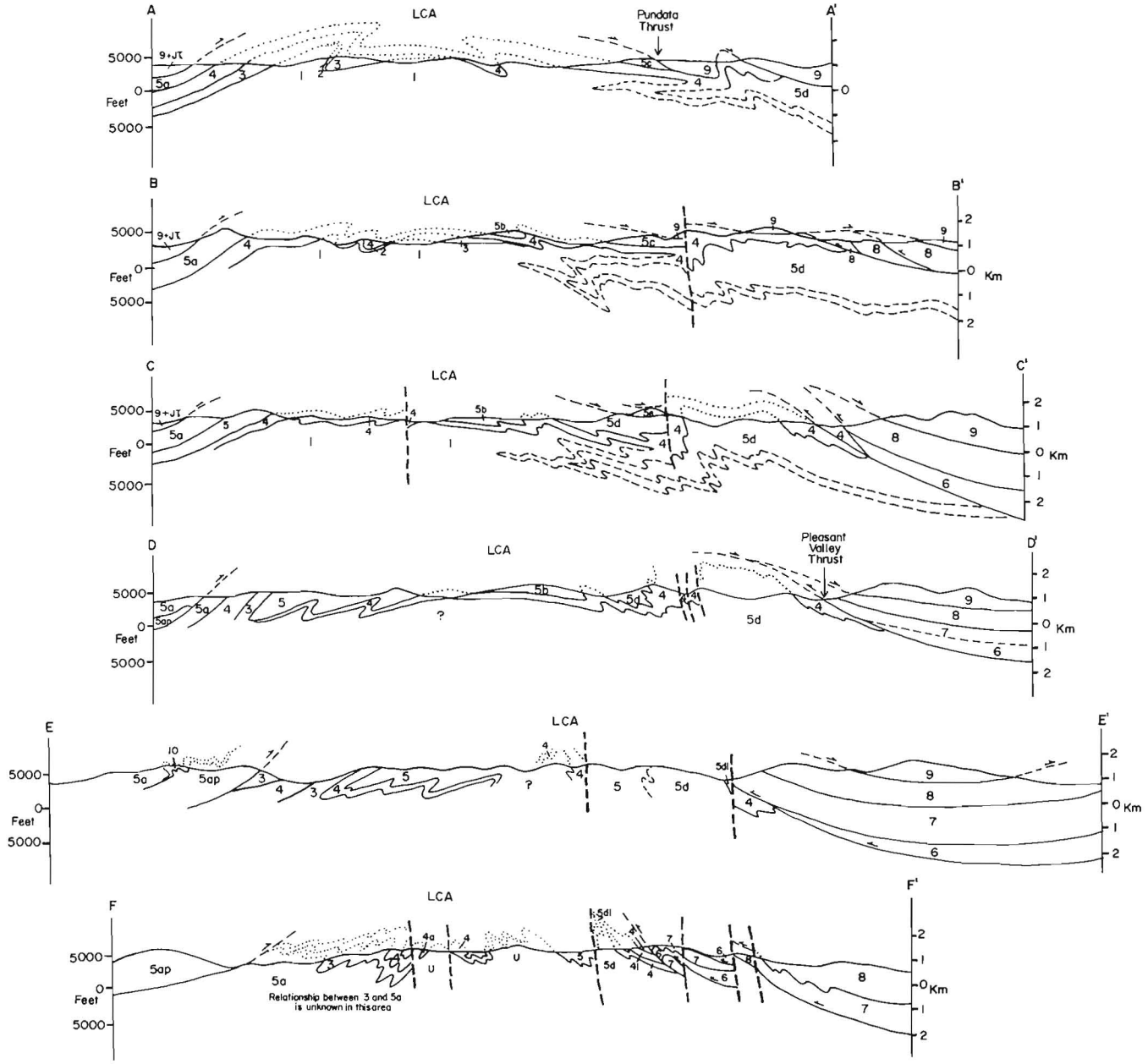

Figure 16.2. *Cross-sections A-A' to F-F'. Stratigraphic units and the locations of the sections are described in Figure 16.1. Vertical equals horizontal scale. LCA is the Lightning Creek Anticlinorium. The nappe shown in sections A-A' to C-C' is hypothetical and accounts for the assumption that unit 4a underlies unit 5d in the Hardscrabble Mountain Area. The nappe would exist also in sections D-D' to F-F' but has not been drawn in.*

The Tom Creek succession structurally overlies the Downey Creek succession on the ridge between Mount Tom and the Willow River. It is made up of poorly sorted quartzite, in part micaceous, phyllite, schist and cataclastic rocks. The quartzite is similar to that of the Downey succession but is volumeterically more important. The photograph of graded quartzite in Struik (1981, Fig. 28.6) is of an outcrop on Pundata Creek that is considered part of the Tom Creek succession. The phyllite and schist are generally grey with less olive varieties and there are no equivalents to the chloritic green slates and metatuffs? of the Downey succession. Quartzofeldspathic cataclasites and muscovite schist occur near the contact of the Tom Creek succession with the underlying Tom Creek-Island Mountain amphibolite and with the overlying Antler Formation diorite and serpentinite. The contact with the underlying Tom Creek-Island Mountain amphibolite may be a shallow fault. The contact with the Antler Formation is a thrust fault because the Antler is older than rocks it overlies in the area of Sliding Mountain and Spectacle Lakes.

The Dragon Mountain succession overlies unit 4 along the ridge from Dragon Mountain southeast to Mount Agnes. It is dominated by poorly sorted quartzite and phyllite. Micaceous quartzite is olive and grey, non-micaceous quartzite is light grey. Phyllite is primarily grey and dark grey with some olive types. Quartzite is more abundant than phyllite, is thin and thick bedded, and commonly the olive and grey varieties alternate throughout the sequences. The clasts are mainly light and dark glassy quartz with lesser amounts of feldspar and blue quartz. There are minor green micas in

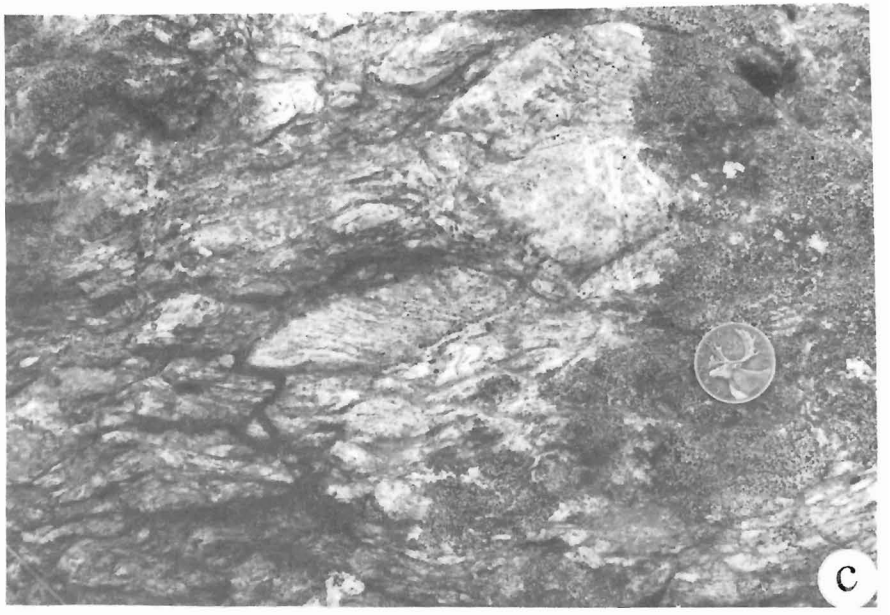

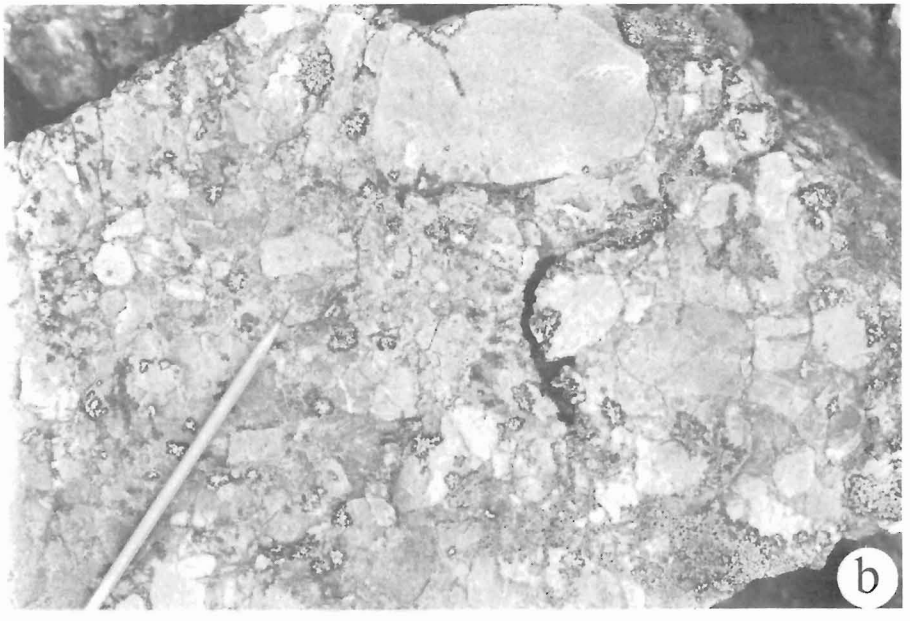

a) *coarse variety from near Mount Agnes,*

b) *also from near Mount Agnes, note the variety from angular to subrounded forms,*

c) *from north of Luce Creek,*

d) *muddy conglomerate from upper part of French Snowshoe Creek (quarter as scale).*

Figure 16.3. *Quartzite clast conglomerate of unit 4a.*

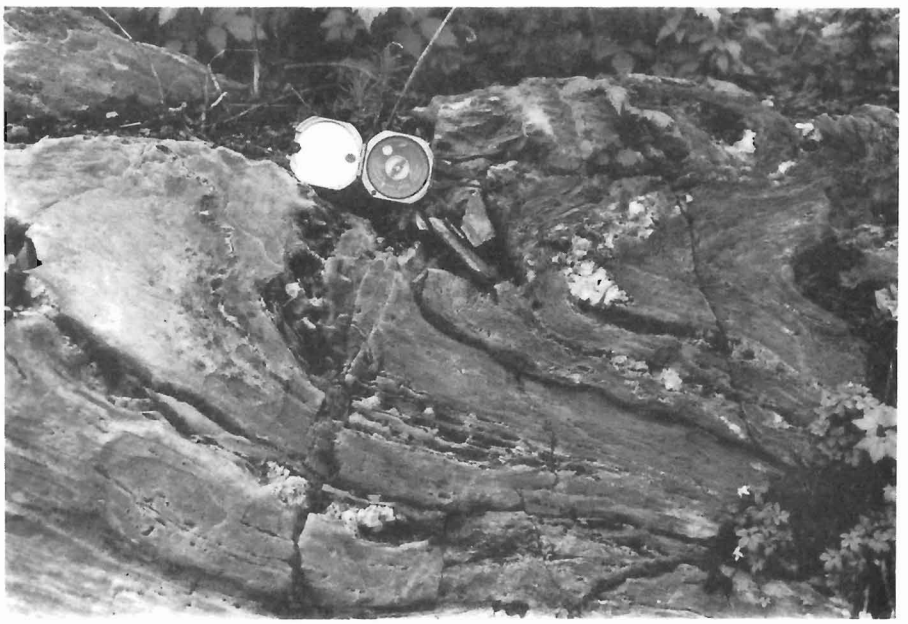

Figure 16.4

Poly folded calcareous amphibolite found in a logged parcel of land south of the Little Swift River, near where it crosses the Swift River forest road. This amphibolite is similar to the one on Tom Creek and Island Mountain.

some places and this quartz resembles that described as gradational with unit 4 black phyllite. The Dragon Mountain differs from the Downey Creek succession by its lack of tuffaceous rock and limestone and by the common presence of dark glassy quartz clasts and more abundant grading and colour variation in the quartzite.

The Ramos Creek succession can be traced discontinuously from Ramos Creek southeast to Keithley Creek. It consists of micaceous and non-micaceous quartzite and granule conglomerate, grey and olive phyllite, metatuffs?, black siltite, calcareous quartzite, limestone and various types of amphibolite.

A distinctive coarse grained olive micaceous quartzite recurs throughout the length of the belt underlain by the Ramos Creek succession and does not have a counterpart in any of the other successions of unit 5. Southeastward from Ramos Creek calcareous quartzite and limestone appear for the first time at Fontaine Creek where they are underlain and overlain by poorly sorted quartzite. Dense light grey coarse quartzite occurs with micaceous quartzite at Sovereign Mountain. Within the micaceous quartzite are several areas of black siltite of unknown relationship. In the area of Wingdam Lake and southeast in the Keithley Creek area are poorly sorted quartzites with detrital muscovite. At Wingdam Lake it does not appear as deformed as the remainder of the quartzites. Calcareous and non-calcareous amphibolites occur in the sequence from Sovereign Mountain southeastward. They are prominent in the Cariboo Mountain area and on the northeast side of Keithley Creek. Several amphibolite horizons (Fig. 16.4) closely resemble those of Tom Creek and Island Mountain. Common through the Ramos Creek succession and the associated rocks of unit 4 are diorite sills that in places are seen to be isoclinally folded.

The stratigraphic position of the succession is uncertain. At Ramos Creek graded beds in medium grained quartzite imply the section is facing westward and overlies black siltites which in turn structurally overlie unit 3 of Pinegrove Mountain. However, southwest of Keithley Creek graded quartzite beds suggest the quartzites underlie a black siltite unit. Northeast of Keithley Creek, the apparent same black siltite unit can be traced discontinuously to Yanks Peak; here Holland (1954) suggested the black siltite overlies the Yanks Peak and Yankee Belle formations, inferring the Ramos Creek succession is laterally equivalent to part of unit 3.

Undifferentiated Rocks

Quartzite and phyllite that extend from Mount Campbell to Meridian Mountain and in a belt through the upper part of the Cunningham Creek area are left undifferentiated. The rocks have characteristics of the Dragon Mountain succession of unit 5.

Structure

Folds occur in all rocks, and vary from early macroscopic folds to later crinkles and kinks. Cleavage is axial planar to folds and parallel to bedding and some faults. Faults formed after the deposition of the youngest rocks (Permian).

Folds are mainly asymmetric and verge toward an axis that traverses the area from northwest to southeast (the Lightning Creek Anticlinorium, Fig. 16.5). They have a parallel form and range from open to isoclinal, except for the youngest generation represented by crinkles and kinks. Fold trends are generally northwest-southeast with the greatest deviation occurring southwest of the Lightning Creek Anticlinorium (Fig. 16.5). There is no obvious correlation between the generation of a fold and its orientation (Fig. 16.5). Refolded folds were previously recognized near Wells (Benedict, 1945) and Yanks Peak (Holland, 1954). They are now recognized also in the Swift River and northern Snowshoe Plateau areas. A nappe with a limb length in excess of 6 km must exist in the area of Wells, if the conglomerate of unit 4a overlies unit 4 (Fig. 2b). If the conglomerate underlies unit 4 then a nappe of similar scale must exist along the length of the Dragon Mountain - Mount Agnes ridge. The existence of such a nappe depends on two assumptions: that all the black siltite belongs to unit 4, and that there is only one conglomerate horizon (4a). The lower limbs required for either of these hypothetical structures cannot be found within the map area (Fig. 16.1).

Faults are post-Permian and formed prior to and after the peak of metamorphism. Their style and sequence are described in Struik (1981) and only 3 thrusts of possible large displacement will be mentioned. The first is a postmetamorphic thrust, interpreted in the region of Swift River and Keithley Creek to account for the fact that biotite and garnet bearing rocks overlie chlorite bearing ones. The hanging wall contains the Quesnel Lake gneiss and overlies the low greenschist facies sedimentary rocks of the Keithley

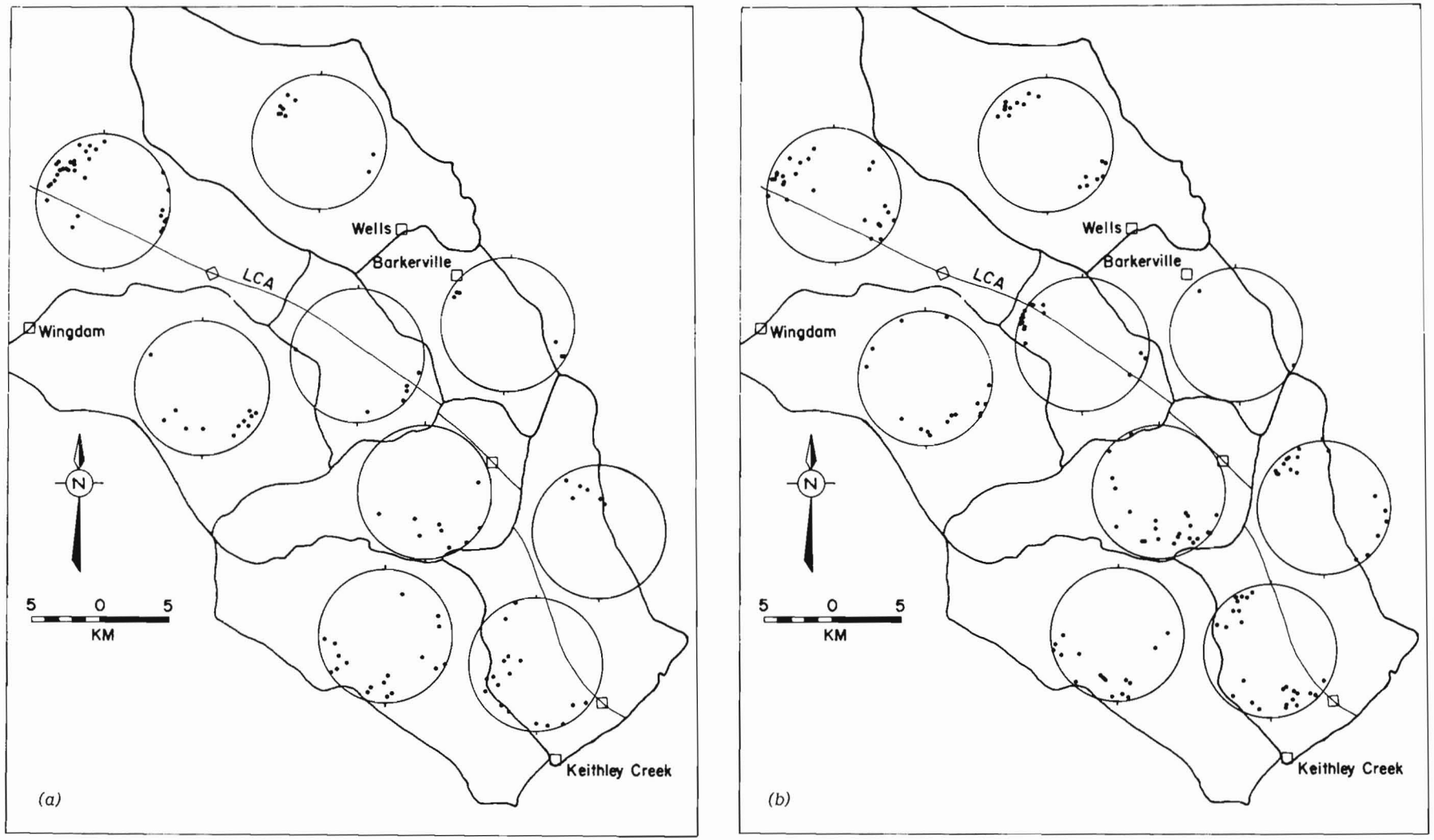

Figure 16.5. *Distribution of the trends of first (a) and second (b) phase fold axes throughout arbitrarily chosen domains plotted on Lambert nets. Note the more scattered attitudes southwest of the Lightning Creek Anticlinorium.*

Creek valley. The second thrust is postulated to separate the Tom Creek from the underlying Downey Creek succession and accounts for the cataclastic rocks seen overlying and included within the Island Mountain amphibolite. This thrust would be broadly folded with the amphibolite. The third thrust is the east-dipping Pleasant Valley fault which has contrasting rock suites and structural complexities between its hanging and footwall successions. It crosses the map area (Fig. 16.1) from northwest and southeast and may continue southeastward as the Little River Fault (Klepacki, 1980).

Discussion

Two different groups of rock underlie the map area (Fig. 16.1) and both have been called the Cariboo Group. The two are separated by the east-dipping Pleasant Valley fault (Fig. 16.1, 16.2). The western Cariboo Group (WCG) consists of the 5 units as outlined which include the Yankee Belle, Yanks Peak, Midas and Snowshoe formations defined by Holland (1954) in the Yanks Peak area. The eastern Cariboo Group (ECG) comprises the Isaac, Cunningham, Yankee Belle, Yanks Peak, Midas, Mural and Dome Creek formations as defined by Struik (1980) in the Roundtop Mountain area. The differences between the eastern and western Cariboo Groups are discussed below.

The Isaac Formation is characterized by grey marls everywhere it is found in the ECG. The marls have no western equivalents. If the Isaac existed in the WCG it would be below unit 2; this stratigraphic level contains conglomerate and micaceous quartzite. The Cunningham Formation of the ECG is massive limestone 200 to 500 m thick at its westernmost exposures; it may be represented in the west by the thin discontinuous limestone and calcareous clastic rocks of unit 2. The Yankee Belle Formation of the ECG is mostly medium grained quartzite and limestone that is generally thicker than the phyllite and fine grained quartzite of the Yankee Belle of the WCG. The Yanks Peak Formation of the ECG consists of interbedded pure orthoquartzite, micaceous quartzite and phyllite and varies from 0 to 60 m thick; by contrast, the Yanks Peak Formation of the WCG is very discontinuous consisting of pure orthoquartzite that rarely exceeds 10 m in thickness. The Midas Formation of the ECG consists of olive to grey phyllite, slate and quartzite, some of which is crossbedded; whereas the Midas of the WCG consists of black phyllite and siltite and dark grey poorly sorted micaceous quartzite and minor limestone. Correlation between the Midas of the eastern and western Cariboo Groups is unlikely. The Midas Formation of the WCG is overlain by conglomerate, micaceous quartzite, phyllite, limestone, metatuff? and diorite of units 4a and 5 whereas the Midas of the ECG is gradational with the Lower Cambrian limestone of the Mural Formation. As suggested by Campbell (1968), the Mural has no obvious lateral relationship with the succession that overlies the Midas of the WCG.

Rocks of units 1 to 3 of the WCG may be lateral facies changes of the lower parts of the ECG. However, units 4, 4a and 5 are distinct from any sequence in the ECG. They may be distal equivalents of the Black Stuart and Guyet formations as suggested by Campbell (1978). Correlations of this type between the eastern and western Cariboo Groups require large displacement on the Pleasant Valley thrust, a western source terrane for a Paleozoic sequence of coarse greywackes, and an unconformity separating units 3 and 4.

Acknowledgments

Marcel and Paul Guiget and Vic Hollister kindly shared their geological understanding of the Island Mountain, Mosquito Creek and Cariboo Gold Quartz Mines.

References

Benedit, P.C.
1945: Structure at Island Mountain Mine, Wells, B.C.; Canadian Institute of Mining and Metallurgy, Transactions, v. 48, p. 755-770.

Campbell, R.B.
1968: McBride (93H) map area, British Columbia; in Report of Activities, May to October, 1967, Geological Survey of Canada, Paper 68-1, Part A, p. 14-19.

1978: Quesnel Lake, British Columbia; Open File 574.

Holland, S.S.
1954: Yanks Peak-Roundtop Mountain area, British Columbia; British Columbia Department of Mines, Bulletin 34.

Klepacki, D.W.
1980: The Little River Fault - a low angle boundary fault of the northern Shuswap Complex, Quesnel Lake, British Columbia; in Geological and Mineralogical Associations of Canada, Program with Abstracts, v. 6, p. A-32.

Struik, L.C.
1980: Geology of the Barkerville - Cariboo River area, central British Columbia; unpublished Ph.D. thesis, University of Calgary.

1981: Snowshoe Formation, central British Columbia; in Current Research, Part A, Geological Survey of Canada, Paper 81-1A, p. 213-216.

17.

OPTIMUM FIELD TECHNIQUES FOR BEDROCK REFLECTION MAPPING WITH THE MULTICHANNEL ENGINEERING SEISMOGRAPH

J.A. Hunter, R.A. Burns, R.L. Good, H.A. MacAulay and R.M. Gagné
Resource Geophysics and Geochemistry Division

Hunter, J.A., Burns, R.A., Good, R.L., MacAulay, H.A., and Gagné, R.M., Optimum field techniques for bedrock reflection mapping with the multichannel engineering seismograph; in Current Research, Part B, Geological Survey of Canada, Paper 82-1B, p. 125-129, 1982.

Abstract

Where large velocity contrasts exist between unconsolidated overburden and bedrock, reflections from this interface can be some of the most prominent later events on engineering seismograms. With modern multichannel engineering seismographs having filtering capability, seismograms can be tailored to enhance these events. Interfering ground-roll events can be minimized through the use of high frequency geophones and decoupling at the seismic source. Optimum geophone-source separations are dependent on ground-roll velocities and reflector depth and can be selected to obtain good reflector move-out for velocity determinations yet minimize reflector phase changes found at wide angles of incidence. Reflection profiling of the bedrock interface can effectively replace refraction profiling techniques at bedrock depths in excess of 30 m.

Introduction

During the past year, we have begun investigating the application of multichannel reflection techniques to mapping the overburden-bedrock interface using a 12-channel digital enhancement engineering seismograph.

Increasing importance is being placed these days on the mapping of buried river valleys in southern Canada as potential aquifer sources.

Over much of southern Canada glacial drift is relatively thick, commonly greater than 30 m; hence, mapping of buried valleys may involve drift thicknesses in excess of 60 m.

With such thick overburden, shallow refraction methods often come to grief in that:

1. refraction arrays necessarily have to be long, with offset shots which may have associated problems of overburden velocity variations along a spread.
2. bedrock refraction signal levels are often low; hence, one may have to replace the hammer source with an environmentally less acceptable explosive device.
3. the time to set up and shoot a long refraction array coupled with explosives costs makes this type of profiling quite expensive.

Based on earlier work by Hunter and Hobson (1977) and by Mooney (1973) and others, we believed that reflections from the top of bedrock at these depths might be identifiable as separate events in the rather clusttered wave packets one generally ignores following the first arrival on engineering refraction records.

Recording Equipment

We began with the premise that to develop a viable technique we would use equipment that would be readily available to a small engineering geophysics company and keep specialized arrays and hardware to a minimum.

Hence, we selected a Nimbus 1210F 12-channel enhancement seismograph with filtering capability. Other similar multichannel enhancement seismographs can be used equally as well.

We selected a 91.5 m 12-channel seismic cable with equispaced geophone take-outs at 7.6 m spacing with one geophone per take-out. The one non-standard component is the geophone; we use 100 hertz phones to minimize low frequency content on the seismic record; however, usable records can be obtained with standard low frequency phones used in refraction work.

Model Studies

Let us examine a simple earth model (Fig. 17.1) consisting of a 90 m thick overburden layer with a P-wave velocity of 1600 m/sec lying on a plane bedrock surface with a P-wave velocity of 5000 m/sec.

The travel-time-distance plot on the lower portion of the figure shows the relative arrival-time positions of the overburden P-wave, the bedrock refracted P-wave and the

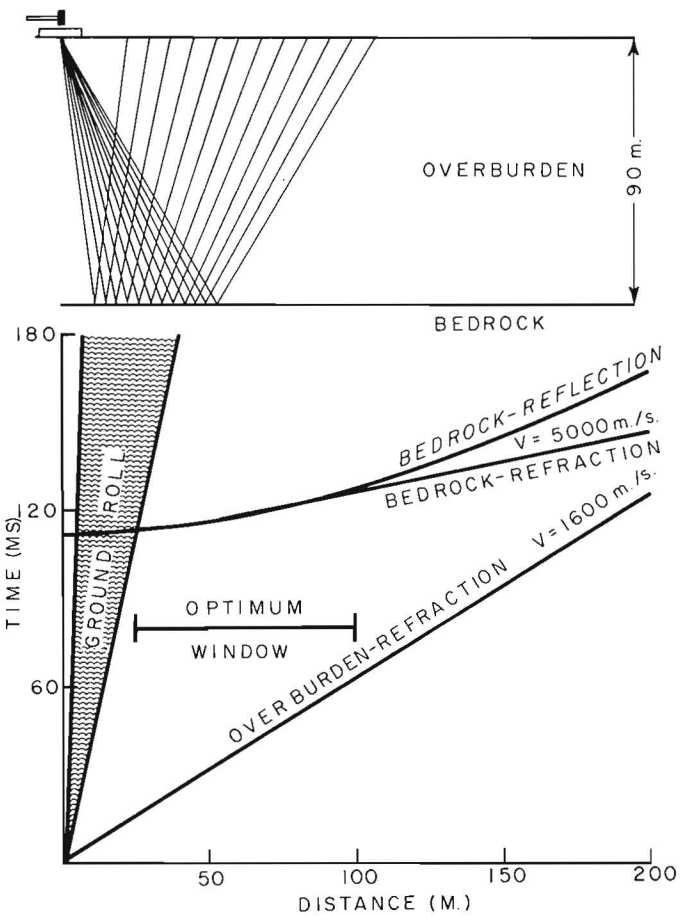

Figure 17.1. *Two layer reflection model and travel-time curve with an overburden thickness of 90 m, overburden velocity of 1600 m/sec, and bedrock velocity of 5000 m/sec.*

bedrock reflection. Also shown is the position of a wedge of large amplitude, many-cycled packets of Rayleigh-type waves known as ground-roll.

To identify the bedrock reflection, an optimum window (Fig. 17.1) on the time-distance curve must be selected; that is, an optimum shot offset and geophone spacing must be chosen.

As in the large scale deep seismic reflection practice it would be better to identify the reflector at near-normal incidence close to the source for best structural interpretation; however, the ground-roll in this zone is often quite severe and no amount of selective band-pass filtering can reduce the ground-roll sufficiently to separate out the reflector. Also, the reflector move-out in this zone is quite small and with no other source of velocity information, normal-move-out velocity determination on this event can be quite inaccurate.

The reflector at very wide angles can be subject to interference effects from the refractor ahead of it in time and possibly even the overburden arrival. Average velocity determination can be quite accurate but errors on intercept time estimations can be large.

As a compromise, for optimum velocity and intercept time determination one should attempt to obtain a window in an area as close as possible to the leading edge of the ground-roll, spanning a zone where the reflector shows maximum curvature yet not extending the window into the wide-angle zone where possible interference effects may occur.

But is the reflector identifiable as a separate event in this optimum window? Hunter and Hobson (1977) suggested, based on modelling done by Cervany and Ravindra (1971), that the reflection amplitude should be much larger than the bedrock refraction over much of the range. The relative amplitude of the overburden P-wave is difficult to estimate as is the pulse shape; that is, will the later cycles of the overburden event interfere with the reflector?

For reflections in the optimum viewing window, normal incidence reflection coefficients do not apply and the amplitude observed at non-normal angles of incidence is,

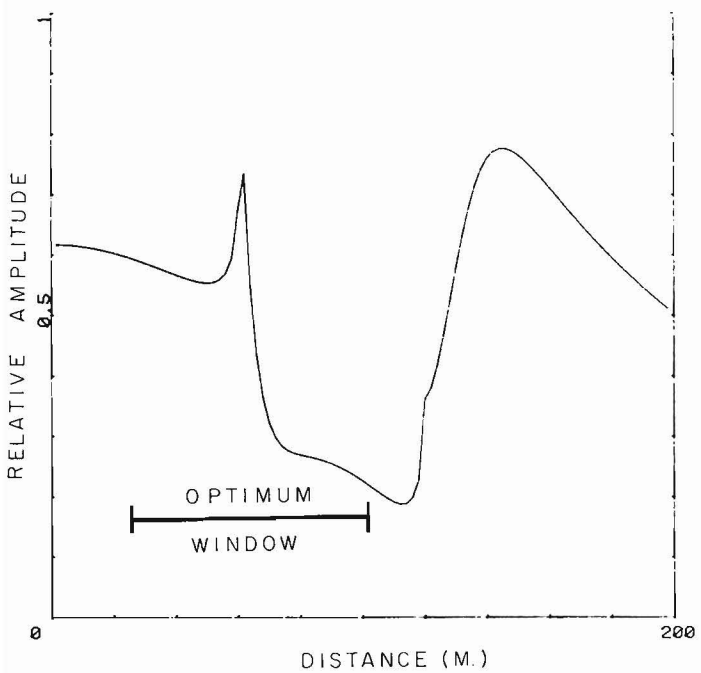

Figure 17.2. *Reflection relative amplitude curve for model shown in Figure 17.1.*

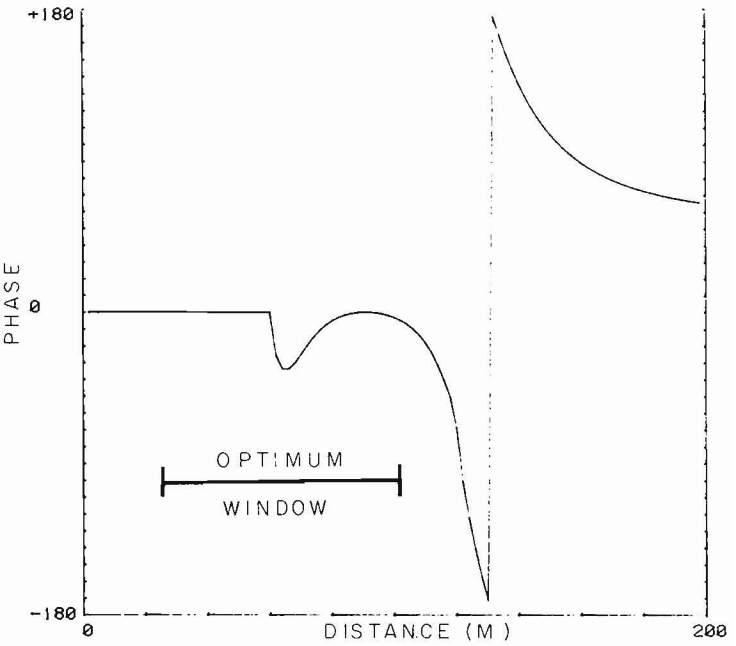

Figure 17.3. *Reflection phase curve for model shown in Figure 17.1.*

even for this simple model, the result of complex amplitude partitioning at the reflecting boundary and is a function of angle of incidence, densities and P and shear wave velocities for the two media, assuming perfect elasticity.

Shown in Figure 17.2 is the reflection amplitude variation with shot-geophone distance computed for the two layer model given in Figure 17.1. The curve was computed from solutions of the Zoeppritz (1919) amplitude equations for a plane P-wave incident at a plane overburden-bedrock boundary. Although corrections were made for wave spreading, no effects of wave-front curvature, near surface velocity variation or free surface amplitude partitioning have been considered. However, the curve is a useful guide to first-order amplitude variations which may be expected.

The inflections shown in the curve of Figure 17.2 result from changes in amplitude partitioning related to "critical" angles of P and S waves at the boundary. The positions of the inflections will vary with velocities and reflector depths chosen for the model.

For near vertical angles of incidence (at small source-geophone distances) the reflection amplitude is uniform. For very large angles of incidence (at large source-geophone distances), large reflection amplitudes should be observed.

With the optimum viewing window, considerable amplitude variation can be expected with a trend towards amplitude attenuation with source-geophone distance.

Will the reflection wavelet retain its signature over the optimum viewing window? Figure 17.3 shows the phase response associated with the amplitude curve computed for the model. Note that at near-vertical angles of incidence close to the source, there is no phase variation. At extremely wide angles of incidence (at large source-geophone spacing), large phase variations exist which translate to a change in wavelet characteristics. The interpreter might mispick the onset of reflector by a half-cycle or more.

In the optimum viewing window, some relatively minor phase variation does exist. Hence, the relative amplitudes of the first peak to first trough of a wavelet may vary, a point to consider when attempting trace to trace correlation.

Field Testing

Having established by modelling the possibility of identifying the bedrock reflection event in thick overburden cases, we selected a field test site near Ottawa where bedrock, at a depth of about 91 metres (determined by drilling) is overlain by glacial till and a surface layer of silt. We chose a hammer source offset from the first geophone of 22.9 m and a geophone spacing of 7.6 m.

Figure 17.4 shows a seismic record recorded at this site with the Nimbus 1210F. Two hammer blows were necessary to build up the record and no field filtering was applied.

The overburden P-wave, and a clearly defined event in the 120-130 millisecond range (interpreted as the bedrock reflection) can be seen across all traces.

Trace one (22.9 m spacing) also shows a large degree of low frequency which is the leading edge of the ground-roll: for optimum viewing the source offset should have been slightly larger (30 m).

Figure 17.5 shows a similar record shot close to that shown in Figure 17.4, but with a low-cut field filter of 100 hertz. The low frequency ground-roll on trace one is virtually eliminated. This is an exception rather than the usual case; however, the application of low-cut filters may help to extend the optimum viewing window into the ground-roll area.

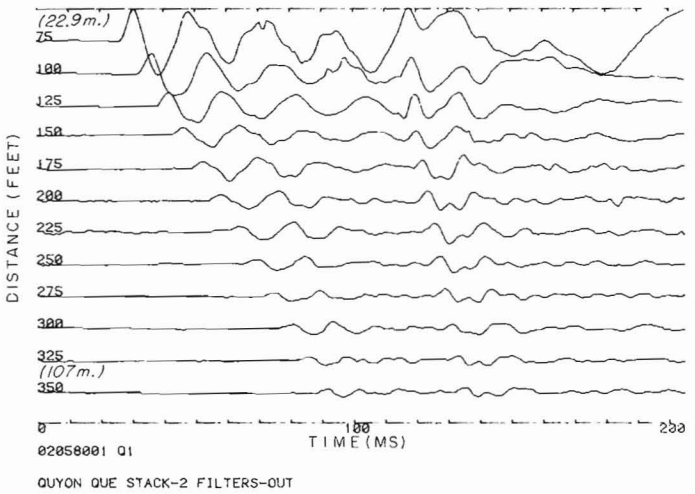

Figure 17.4. *Reflection record showing a bedrock reflection at a depth of 91 m near Quyon, Quebec. No filtering has been applied.*

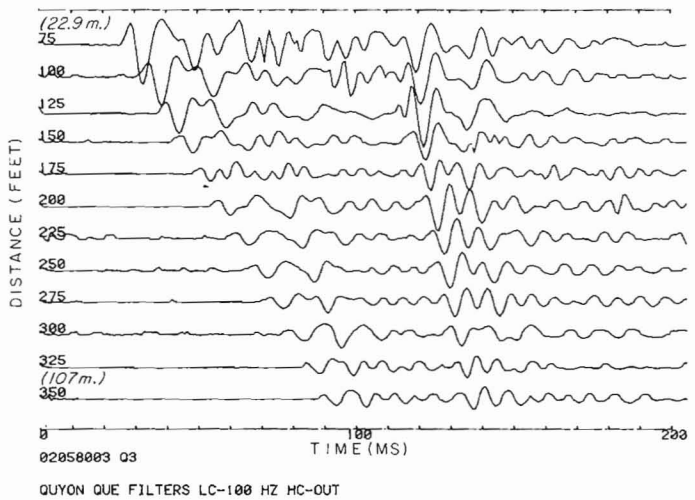

Figure 17.5. *Reflection record at the same site as Figure 17.4. Low cut (100 hz) filtering applied.*

The interpreted reflection appears to have a higher amplitude and slightly higher frequency content than the first arrival overburden P-wave. The amplitude of the reflection decreases with distance but not as severely as the overburden P-wave. There is no indication of the bedrock refraction as a separate event.

The first half cycle of the bedrock reflection appears to be observable over the entire record. This facilitates picking of travel-time for computing the normal move-out velocity. The least-squares fit was 1600 m/sec.

Additional tests at other sites in eastern and southern Ontario, where thick overburden was known from drilling records, showed that, with few exceptions, a bedrock reflection was rather straightforward to map once the optimum viewing window had been selected. To illustrate some of the possible pitfalls with the technique, Figure 17.6 shows a poor quality record taken in eastern Ontario with the same field parameters as the record in Figure 17.5. The record was shot on a windy day, with amplifier gains reduced, requiring 4 hammer blows to build the signal. The geophones were placed on surface (with a spike base). We have found that to reduce the noise level and to ensure uniform ground coupling it is worth the extra effort to bury the geophones.

The overburden P-wave cannot be correlated across the record, however, the reflection from bedrock can be seen on most traces in the 80 to 120 millisecond range. The

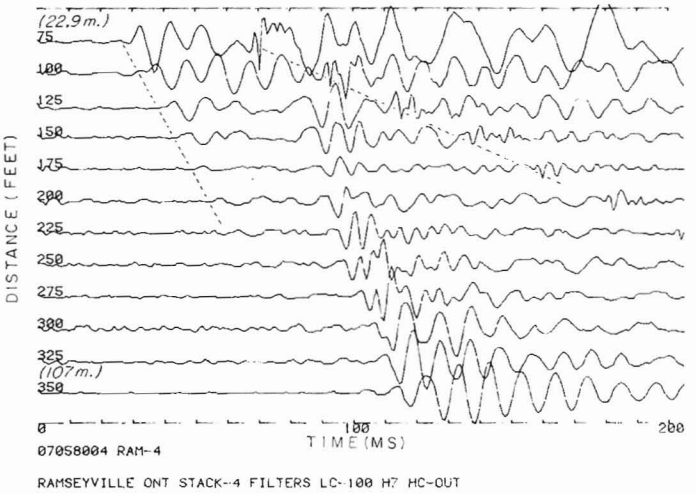

Figure 17.6. *Poor quality reflection record showing ground-roll, ground-coupled air wave and wide-angle reflection effects.*

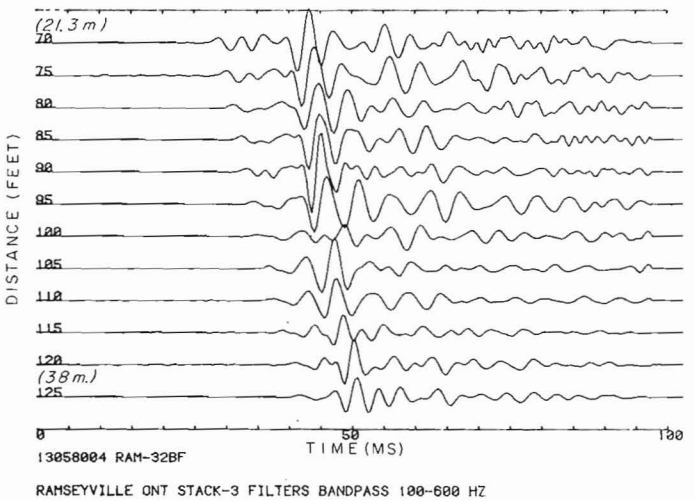

Figure 17.7. *Reflection record from shallow bedrock surface (30 m depth). The shallow limit of the reflection method.*

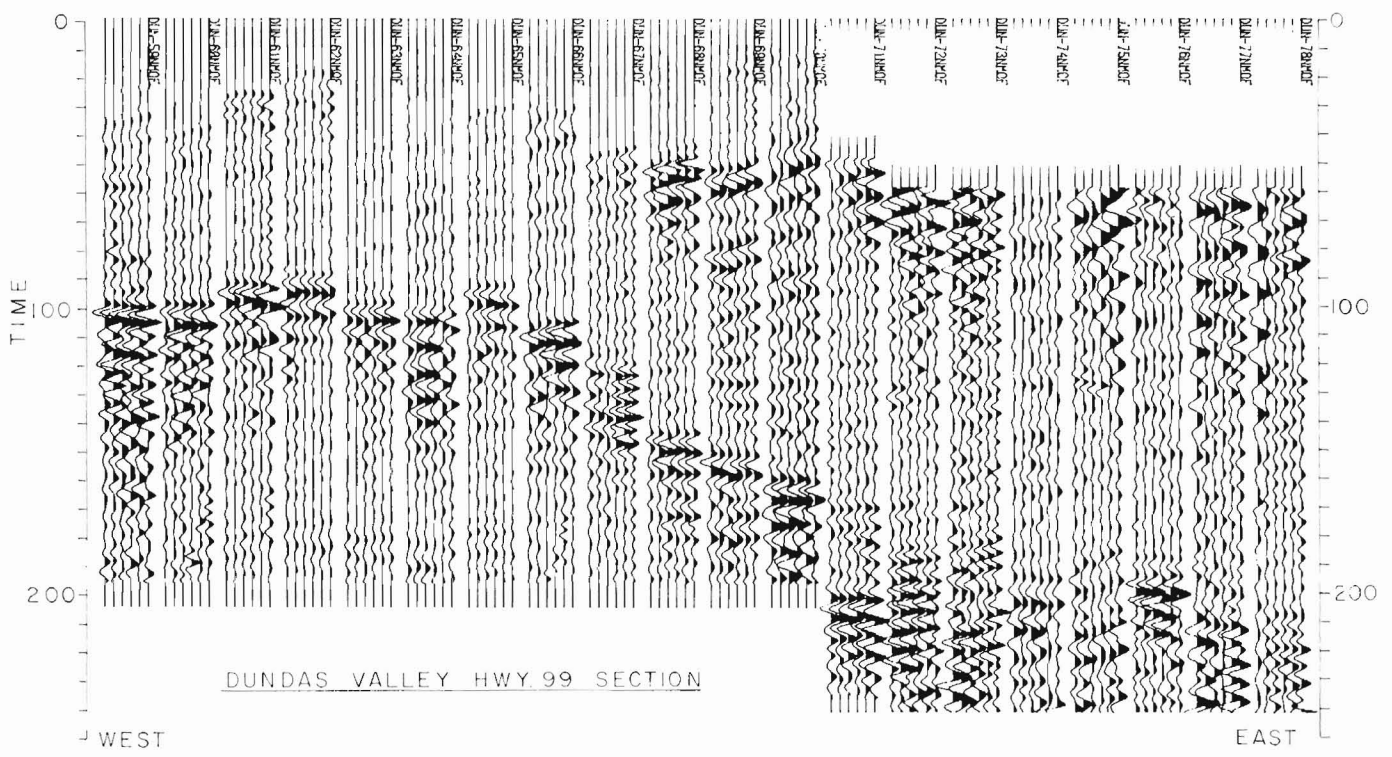

Figure 17.8. *Reflection record section across one edge of the Dundas "buried" valley near Hamilton, Ontario. NMO velocities are in the range of 1550 - 1600 m/sec.*

reflection is at a much shallower depth than that shown in Figure 17.5 hence, with the large spread length the farthest 4 traces are showing large amplitude wide-angle characteristics. The optimum viewing window should have been between 30-75 m for this site.

The close traces at 22.1 m and 30.4 m show considerable interference from ground-roll despite field low-cut filtering at 100 hertz. A very spiky large amplitude low velocity event, the ground-coupled air wave, is visible on the near 6 traces. Since it is a broadband signal no amount of selective filtering can remove it. However, we have found that placing a 1.25 x 1.25 m sheet of styrofoam at the hammer source, blocking the direct path of the wave through air to the geophones is an effective way of reducing the amplitude of the event substantially.

This record was made using the 0 to 200 millisecond recording span of the Nimbus 1210F. The record should have been recorded on the 0-100 millisecond scale using a 30 millisecond recording delay. This would have resulted in a higher digital rate on our computer system and would have allowed a higher low-cut filter setting and probably sharper definition of the onset of the bedrock reflection.

We found that the minimum depth of bedrock from which we could observe a separate reflected event was in the order of 30 m as shown in Figure 17.7. The reflector is in the range of 40 to 50 milliseconds. The first geophone to source offset is 21.3 m and the geophone spacing is 1.52 m. The offset is sufficiently far away to avoid ground-roll interference, however, the reflector is becoming relatively wide angle and the last few traces cannot be utilized. The minimum depth limitation of the technique is site specific, depending on the ground-roll conditions and the width of the overburden arrival wavelet.

Having gained experience with the reflection technique we initiated a reflection survey over the Dundas "buried" valley near the city of Hamilton in southwestern Ontario. The valley is probably of Pleistocene age and was the site of a major river cutting through the same escarpment of Paleozoic rock which forms Niagara Falls and the associated Niagara River canyon. The surface expression of the valley is nonexistent in its upper reaches and drill control is sparse. Groundwater geologists have predicted an abrupt end to this canyon with an associated falls. The canyon is thought to be completely filled with several sequences of tills capped with a thin layer of lacustrine deposits.

A seismic line composed of reflection spreads was shot down the shoulder of a highway, which was thought to run down the axis of the valley, in an attempt to map the upstream end of the canyon. Figure 17.8 is a section from this line comprising 6 trace records which have been normal move-out corrected, band pass filtered from 100-300 hertz and gain adjusted. The details of mating the engineering seismograph with the computer and the techniques involved are given in a paper by Hunter et al. (1982).

The geophone spacing used on this line is approximately 3 m with a spacing of 75 m between adjacent records.

These records were shot in a seismically noisy area with both highway traffic and Canadian National Railways mainline traffic to contend with. Hence, amplifier gains were set low and often 5 or 6 hammer blows were stacked per record. The last two records on the east side were shot using a seismocap and a primer charge.

The section shows a prominent reflector which can be followed from 100 ms at the west end down to 200 ms at the east end. At the east end the reflector is not as prominent and several reflectors are evident leading to some difficulty in deciding which is the bedrock reflector.

Normal move-out velocities were in the range of 1550-1660 m/sec. The bedrock surface has been interpreted to drop from 75 m below surface at the west side down to 160 m depth at the east side with an approximate drop of 90 m in a horizontal distance of 500 m at the canyon edge. From other sections shot in the area we now believe that this section cuts the canyon edge at an angle of 45°.

Summary

Good quality bedrock reflections can be obtained in a rapid, cost-effective manner using a 12-channel enhancement seismograph and a standard 12-geophone array, with an optimum viewing window. The optimum viewing window depends upon:

1. the position, on the time-distance plot, of the leading edge of ground-roll interference,
2. the depth (time position) of the bedrock reflector and hence,
3. the position in distance of the onset of wide-angle amplitude and phase changes on the reflection and,
4. the interference effects of the bedrock refractor and the overburden P-wave.

In most areas where large velocity contrasts exist between overburden and bedrock, a reflection from the top of bedrock should be easily observable for overburden thicknesses in excess of 30 m.

References

Cervany, V. and Ravindra, R.
1971: Theory of Seismic Head Waves; University of Toronto press.

Hunter, J.A. and Hobson, G.D.
1977: Reflections on shallow seismic refraction records; Geoexploration, v. 15, p. 183-193.

Hunter, J.A., Burns, R.A., Gagné, R.M., Good, R.L., and MacAulay, H.A.
1982: Mating the digital engineering seismograph with the small computer: some useful techniques; in Current Research, Part B, Geological Survey of Canada, Paper 82-1B, Report 18.

Mooney, H.M.
1973: Handbook of Engineering Geophysics; Bison Instruments Inc., Minneapolis, Minn.

Zoeppritz, K.
1919: Uber Erdbebenwellen, VII 6; Gottingen Nachrichten, p. 66-84.

18.

MATING THE DIGITAL ENGINEERING SEISMOGRAPH WITH THE SMALL COMPUTER – SOME USEFUL TECHNIQUES

Project 800018

J.A. Hunter, R.A. Burns, R.M. Gagné, R.L. Good and H.A. MacAulay
Resource Geophysics and Geochemistry Division

Hunter, J.A., Burns, R.A., Gagné, R.M., Good, R.L., and MacAulay, H.A., Mating the digital engineering seismograph with the small computer – some useful techniques; in Current Research, Part B, Geological Survey of Canada, Paper 82-1B, p. 131-138, 1982.

Abstract

The development of multichannel, digital, engineering seismographs capable of talking with inexpensive small computers has the potential to increase substantially interpretation and display capabilities for the engineering seismologist. In the past, the application of shallow refraction and reflection techniques to groundwater and unconsolidated overburden problems has been limited by the inability to digitally process field records. With digital recording now available, field records can be filtered, gain enhanced, and stacked. Interactive use of a computerized CRT record display results in rapid interpretation using standard refraction and reflection methods. Inexpensive hard copy displays of interpretations and seismic sections can greatly improve report preparation.

Examples of refraction and reflection surveying, using the Nimbus 1210F seismograph, G-724S digital recorder, and Apple II computer with periferal devices, are given.

Introduction

The past few years have seen the rapid development of multichannel, digital, enhancement engineering seismographs. Although most engineering seismographs offer digital stacking and recording capability, most often the end product is in the form of a paper record showing an analog trace display. The engineering seismologist is then forced to hand-pick events and transfer them to a graph plot for interpretation. Unlike deep reflection seismic work in the oil exploration business, the engineering seismologist does not generally have access to a large computer centre with a wealth of software interpretive capability at his disposal. Obviously, the scale of the investment is not justified.

The past few years have also seen the rapid proliferation of low cost computers and it is now possible to mate an engineering seismograph with an inexpensive desk-top computer to enhance both the interpretation aspects and display capabilities associated with engineering seismic work.

At the Geological Survey of Canada, we have begun designing a seismograph-computer system for engineering work which would be relatively cost-effective and within the range of capital outlay capability of a small engineering geophysics company.

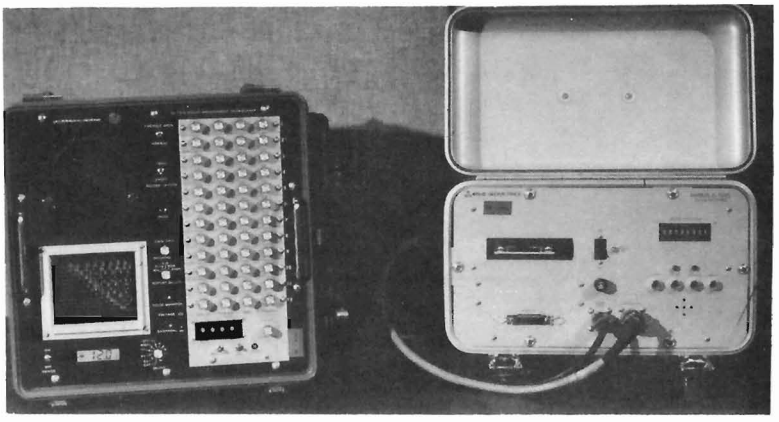

Figure 18.1. *Nimbus 1210F digital engineering seismograph and G-724S digital tape recorder.*

Figure 18.2. *Apple II computer system with printer, plotter and digitizer.*

System Design

We began by selecting a 12-channel digital enhancement seismograph as the basic recording system. Although 6 and 24 channel seismographs are available we decided that the 12-channel unit would be the most versatile for general engineering work.

The seismograph system required a digital recording facility and the ability to transfer the data to a small computer via an RS-232 serial output.

We selected the Nimbus 1210F seismograph complete with the G-724S digital tape recorder (Fig. 18.1). It must be pointed out, however, that other seismographs are available which can be mated to a small computer equally as well.

The computer for our system had to be relatively inexpensive yet powerful enough to store and manipulate a complete 12-channel digital seismic record, to easily accept digital data from the seismic tape recorder, to have interactive screen display capability, and to have sufficient input/output ports to drive periferal hard copy units.

We selected the Apple II computer, designed for the home computer market, with 48 K bytes memory and the following attachments and periferals (Fig. 18.2):

1. a CRT monitor (a conventional TV set can also be used),
2. a disk drive using a 5 inch floppy disk,
3. a printer,
4. a small 8" x 11" plotter (a Houston Instruments model),
5. a small digitizer pad (a Houston Instruments model).

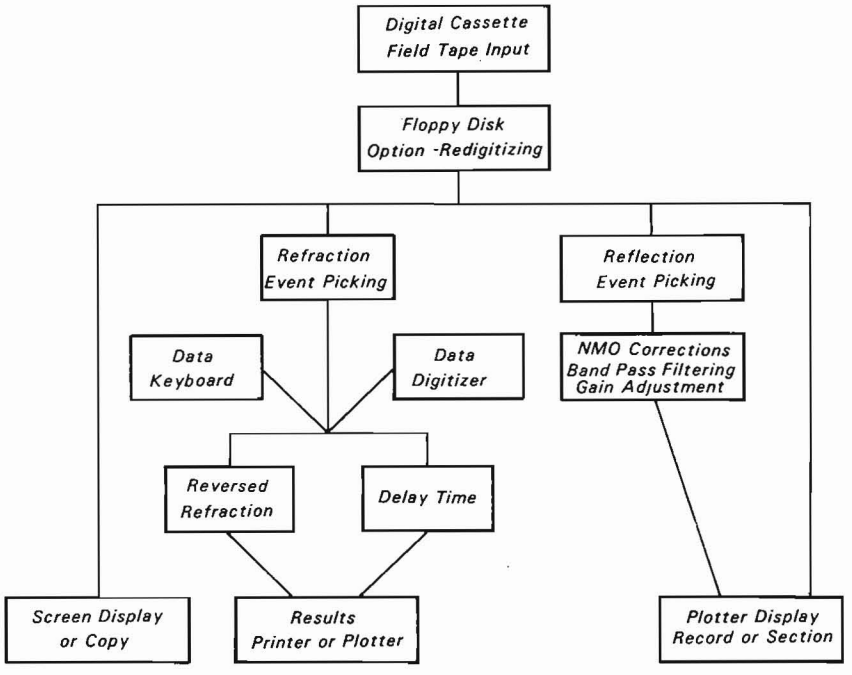

Figure 18.3. *Flow diagram of software applications to engineering seismic data.*

Figure 18.4. *Transferring seismograms from digital tape recorder to floppy disk via the computer.*

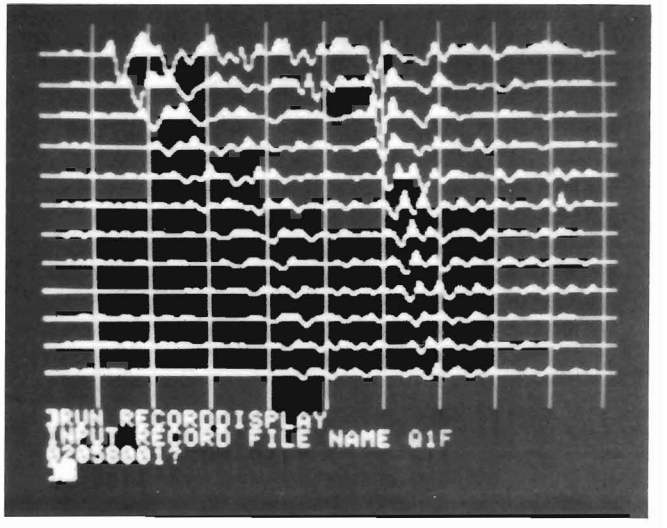

Figure 18.5. *Variable area screen display of a seismogram.*

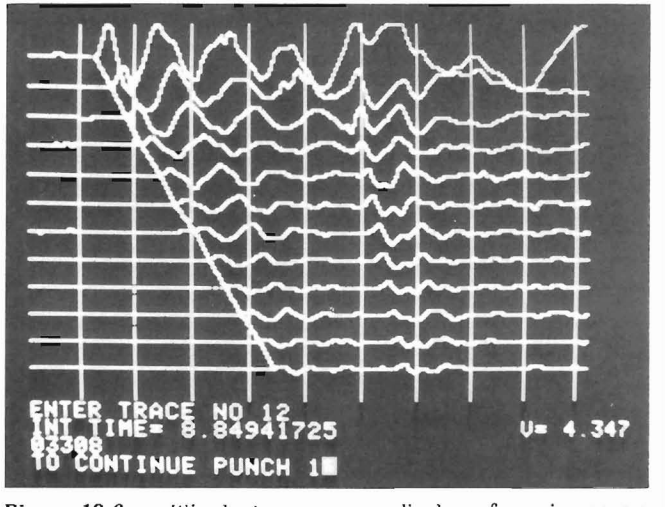

Figure 18.6. *Wiggle trace screen display of a seismogram showing a refractor picked using a screen cursor interactively with the computer.*

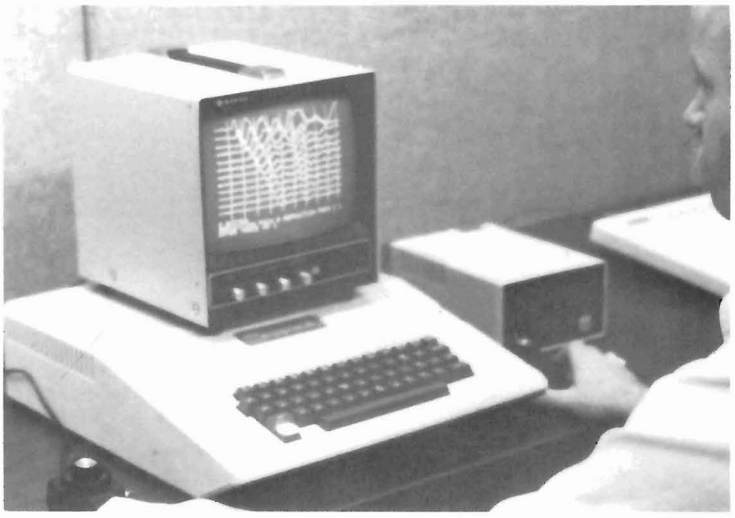

Figure 18.7. Operator using screen cursor via game paddles to interactively pick seismic events.

Figure 18.8. Operator interactively interpreting refraction layering from screen display of first arrival time-distance plot.

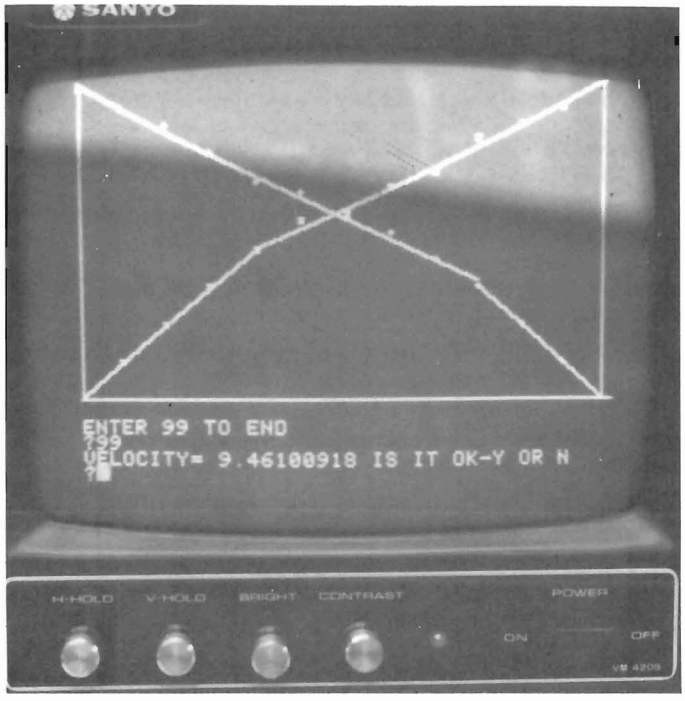

Figure 18.9. Screen display of interactive refraction interpretation showing a time-distance plot.

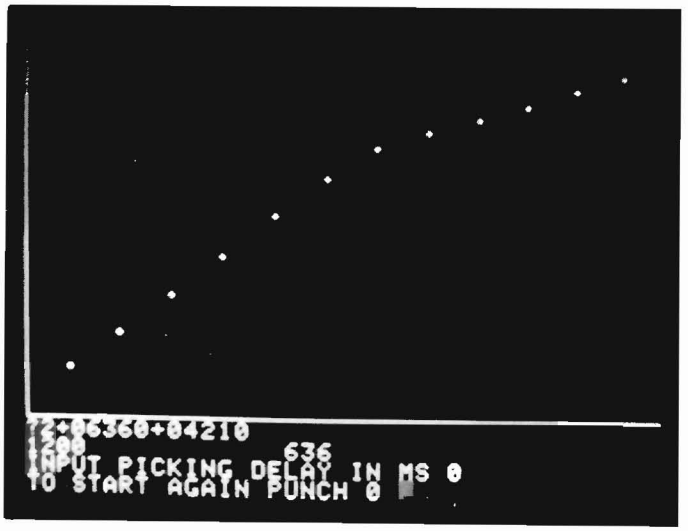

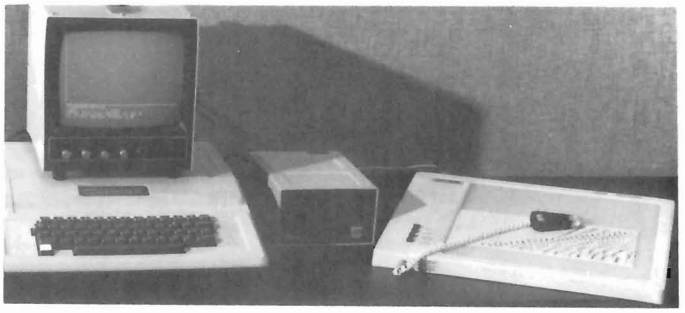

Figure 18.10. Digitizing time-distance data from a seismogram. Data are written on floppy disk and output of digitized data are shown at top of figure.

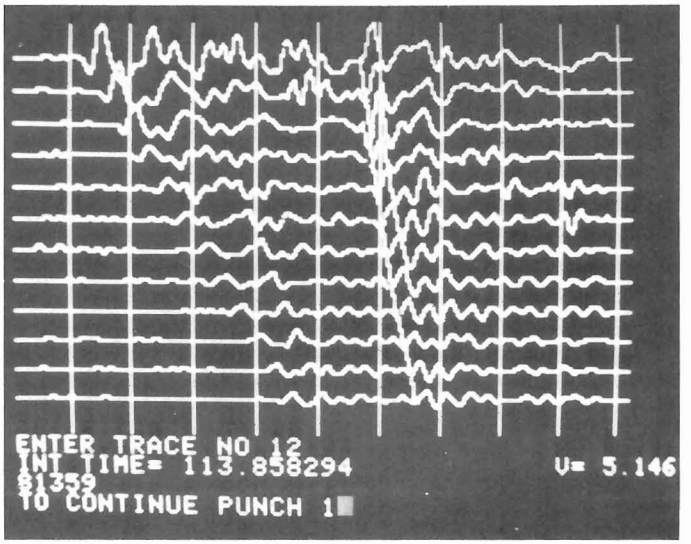

Figure 18.11. Screen display of a seismogram showing an interactive pick of a reflection.

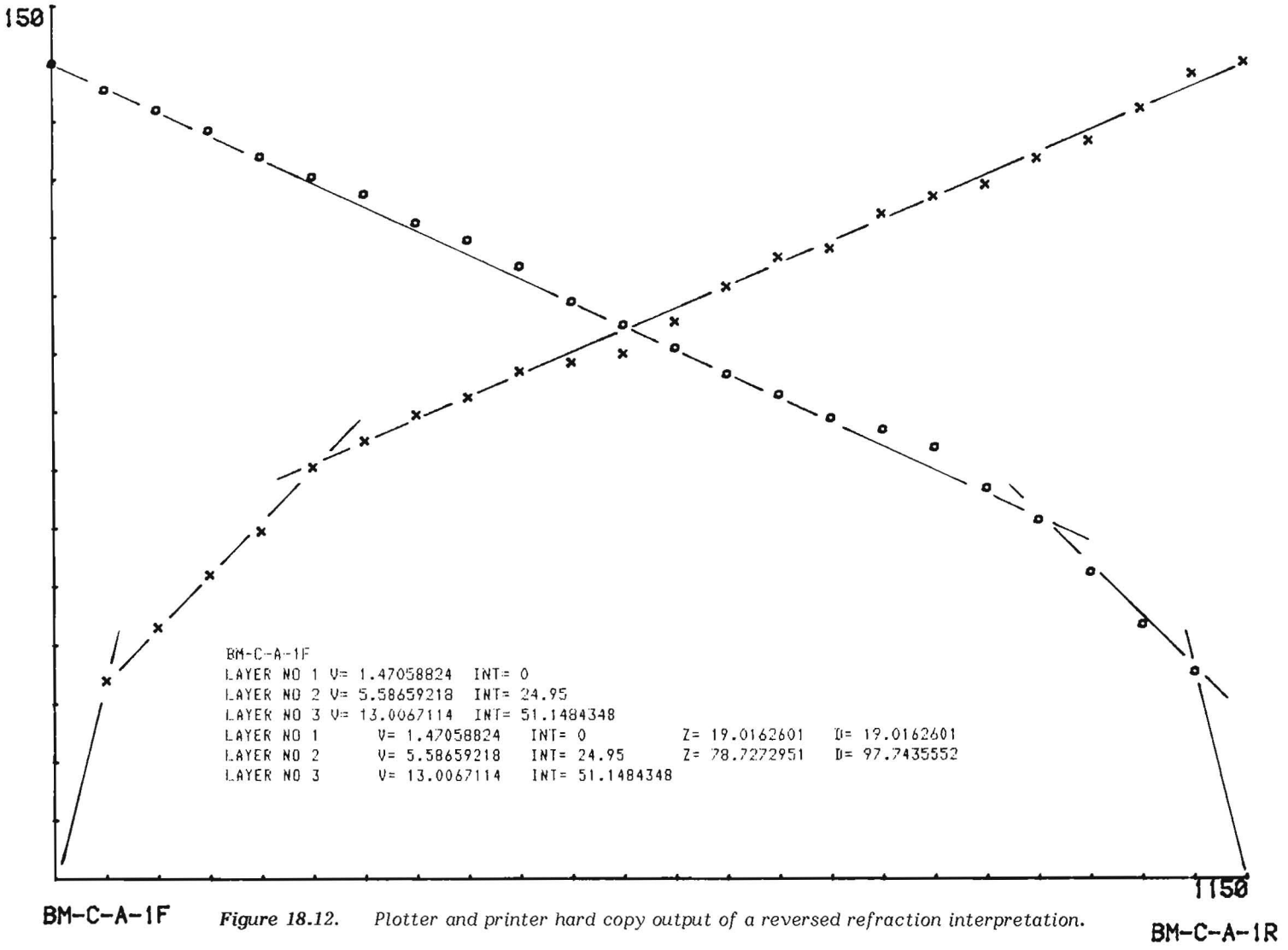

Figure 18.12. Plotter and printer hard copy output of a reversed refraction interpretation.

The Apple II computer like most others of its kind, uses the program language BASIC; a language which is in widespread use and one which is easily comprehended by the novice programmer.

Of interest may be some relative costs. The Apple II system as shown (Fig. 18.2) with the associated periferal devices is approximately 30 per cent of the cost of the Nimbus seismic system and is most certainly worth the extra investment.

Software Development

The first step in software programming development (Fig. 18.3) involved acquiring the seismic data from the digital tape recorder and storing it in the computer system in a form whereby the data could be rapidly accessed. The easiest way was to store the data on floppy disk.

The seismic data are played back from the tape recorder into the computer's memory (Fig. 18.4), decoded, resampled and written to disk in a matter of a few minutes. The details of the formatting and decoding procedure will not be given here since they are peculiar to the Nimbus and Apple II systems.

We routinely store seismic data on disk and clean and re-use the digital tapes since records can be stored on disk at one fifth the cost of tape storage.

The next step in software development was to display the data on a CRT screen so that time and distance measurements could be made interactively for both refraction and reflection interpretation.

The Apple II has relatively good high resolution screen plot capability and seismic records can be displayed at any gain level in either variable area (Fig. 18.5) or wiggle trace (Fig. 18.6) modes.

Using paddles (Fig. 18.7) normally used for playing computer games, a cursor display is used to move from trace to trace to enter time and distance picks into the computer's memory. The time required to produce a display is in the order of a couple of minutes.

Once time and distance information has been entered into computer memory, several options are available. One can:

1. store time-distance data on disk file and/or obtain screen copies of data or seismograms via the printer, or
2. in refraction work, obtain least squares fits of arrival time line segments for velocities and intercept times or,
3. in reflection work, compute least squares average velocities and intercept times for future normal move-out corrections to seismic records.

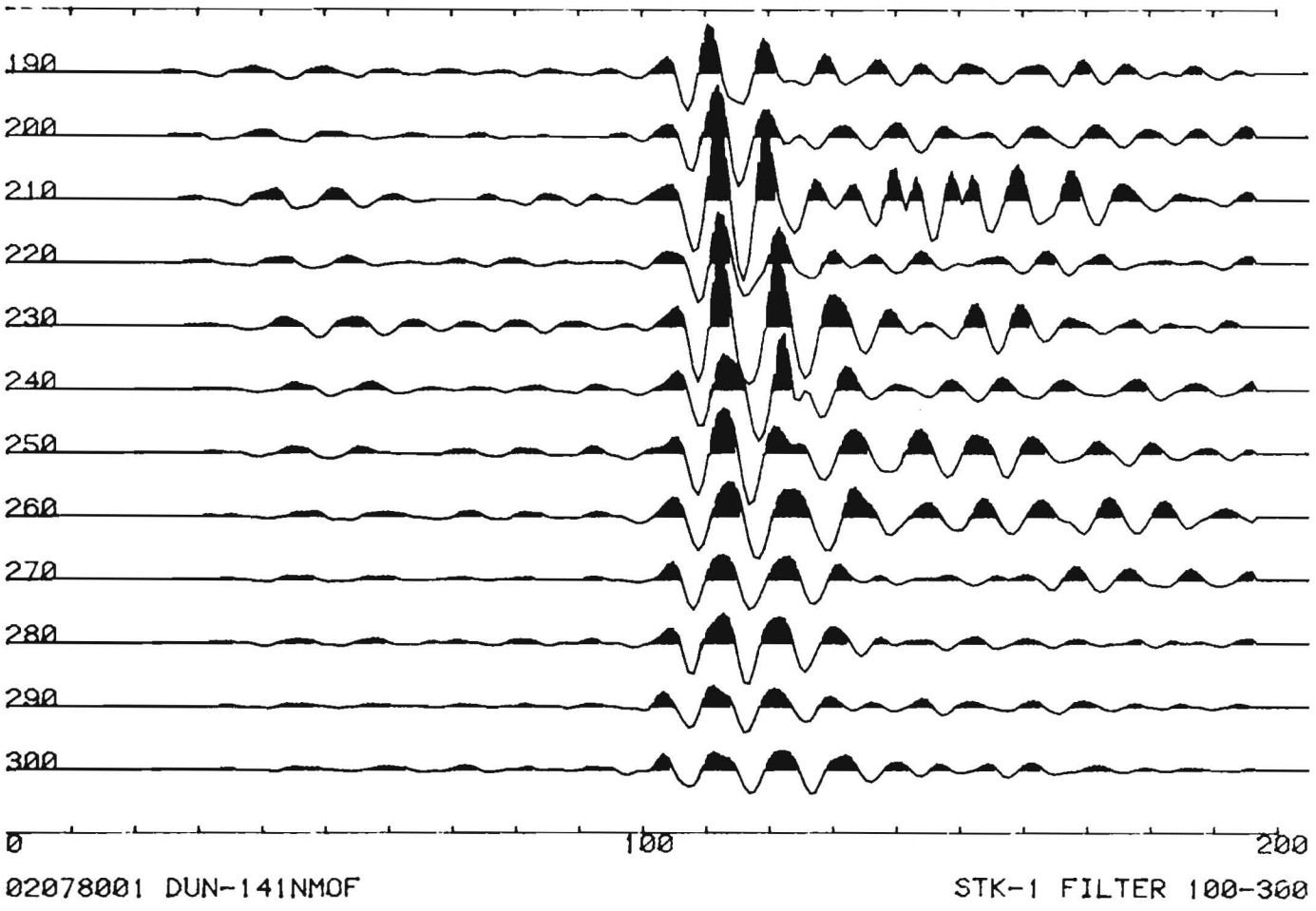

Figure 18.13. *Variable area hard copy plot of a seismogram.*

Let us examine a simple refraction reversed profiling technique. With the raw time-distance data in disk storage the interpreter can call this information back to the screen in the form of a time-distance plot (Fig. 18.8, 18.9). At this point several decisions must be made:

1. Are the data OK or are there points which need to be omitted? An easy task for the computer.
2. Where are the break-over points; that is, which points should be grouped to fit a straight line velocity? If the interpreter is not satisfied with the fit he has the option of starting over or altering individual segments.
3. Finally, which velocity segments on forward and reverse profiles indicate sloping interfaces?

These functions are those which the interpreter in the past has generally artfully performed on graph paper, and now can quickly perform on the CRT screen.

For more detailed refraction analyses using delay-time techniques, the computer can be utilized interactively to select data and perform velocity and depth computations.

Hard copy results can be obtained on the printer or through the use of the plotter (Fig. 18.10).

In shallow reflection work, the first interpretation step, as mentioned previously, is to obtain average velocity estimates to each reflector by interactively picking the reflection record on the screen (Fig. 18.11). The ultimate goal is to produce a record which is Normal Move-Out corrected to form a record section. Normal Move-Out corrections are done by manipulating the record in time in the computer memory and writing the corrected record into a disk file. On our system this takes approximately 7 minutes per record. In conjunction with Normal Move-Out corrections one often performs band-pass filtering and gain adjustments.

Admittedly, the computation rate of our system is orders of magnitude slower than that of a large-scale seismic-oriented computer centre, but in engineering seismic operations, the quantity of data processed is on a much smaller scale.

Before turning to display capabilities of the small computer system (Fig. 18.3), we should discuss the mountain of seismic data that the small engineering firm may already have in the form of times and distances or in analog paper record format.

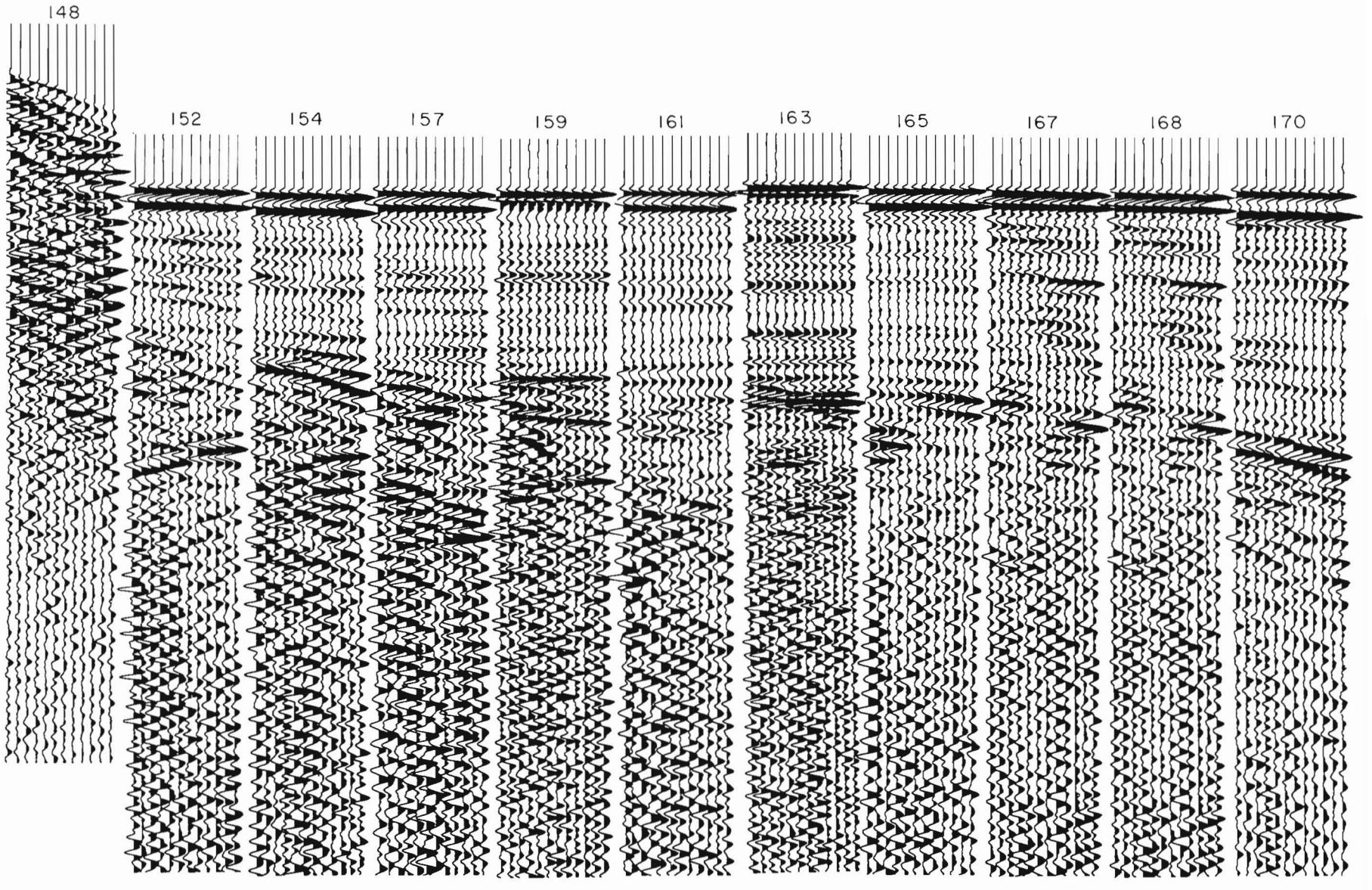

Figure 18.14. *Variable area reflection section hard copy plot. The data were recorded via the Nimbus seismograph and processed via the Apple computer.*

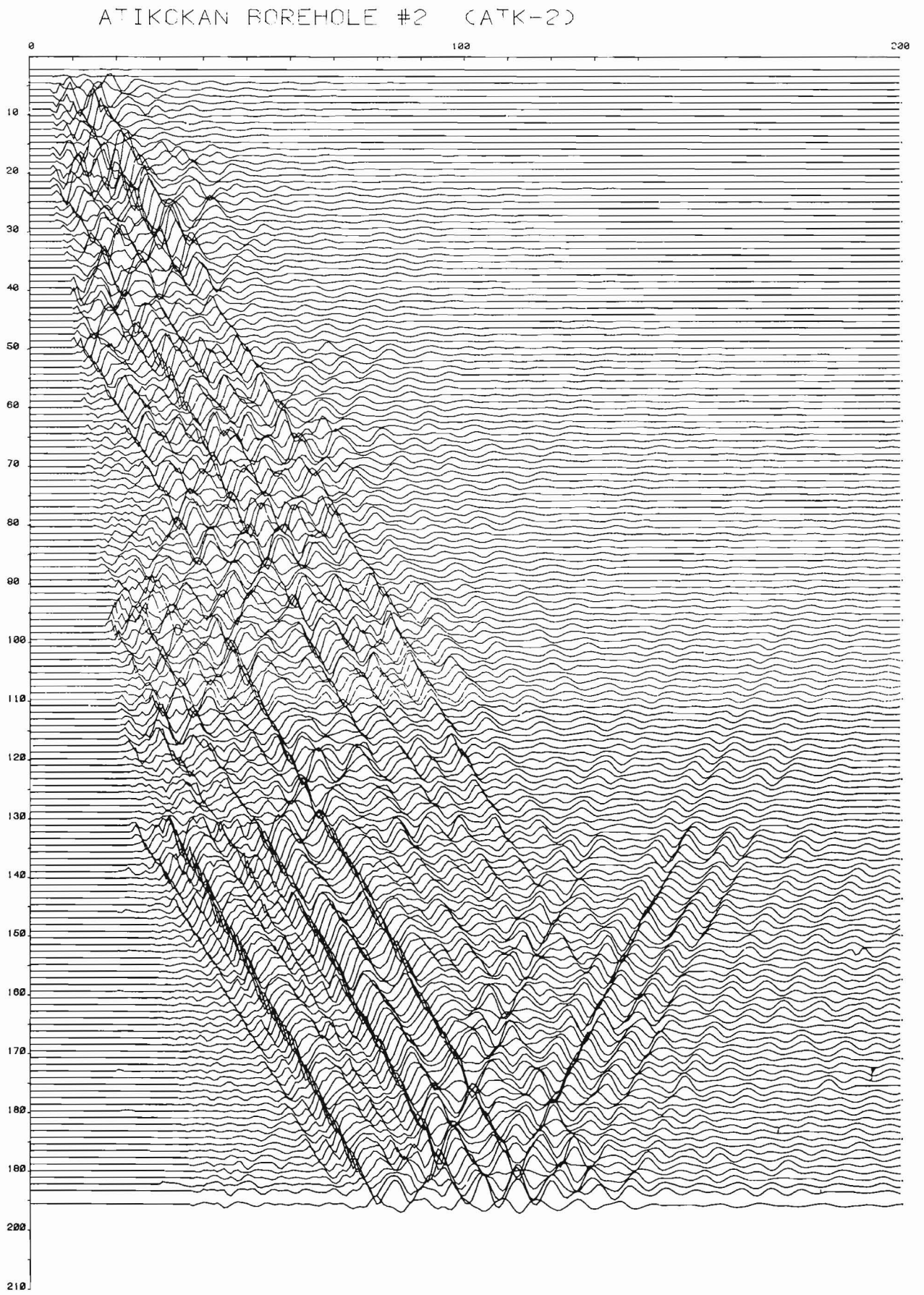

Figure 18.15. *Borehole seismic section hard copy plot recorded on the Nimbus seismograph and plotted via the Apple computer. Gains have been adjusted to enhance later "tube"-wave events.*

Programs previously mentioned which were designed to obtain data by interactively viewing seismograms on the CRT can also accept data from the keyboard. Thus, data in the form of numbers, either from single channel seismographs or hand-picks of paper records can be interpreted.

Records in the form of analog traces can be picked using a small digitizer pad as shown in the bottom of Figure 18.12. Time-distance values entered via the digitizer cursor are entered into disk file, displayed on the screen and analyzed.

Hardcopy Display Capabilities

Perhaps the most valuable aspect of mating the engineering seismograph with the small computer is the hardcopy display capability.

With the client in mind, it is far superior to produce a report-quality plot of a field record than to submit a photocopy of the raw field monitor. Variable area displays (Fig. 18.13) are much more definitive, especially when it is possible to improve the display via computer through filtering and gain adjustment.

It is possible to produce seismic record sections through the plotter periferal of the small computer. Figure 18.14 shows an example of a variable area display of marine reflection records. This section was shot on the sea-ice near the north pole and displays 2 seconds of record below seabottom. Although the section is not on an engineering scale it does demonstrate the engineering seismograph-computer capabilities since the data were replayed from a conventional seismic recording system (Sercel 338) into the Nimbus seismograph. The records were recorded on the G724S digital tape recorder, dumped via the Apple computer to floppy disk, were Normal Move-Out corrected, deghosted, band-pass filtered, gain-adjusted and plotted in variable area format on the small plotter. The section was glued together from individual plots.

A further example is shown in Figure 18.15. We have used the engineering seismograph in conjunction with a 12-hydrophone borehole cable (known as the crystal-cable) to measure compressional wave and later events in boreholes in crystalline rock where the shot is detonated near the hole on surface. The hydrophone spacing is 1 m and the crystal cable is lowered in the hole at 12 m intervals per shot. This record suite was produced from Nimbus tape recordings which were transferred to computer disk, edited, gain adjusted, and plotted. The gains have been substantially reduced so that the first arrival compressional wave is barely discernible yet the large amplitude tube wave events (Huang and Hunter, 1981) associated with micro-fractures in the borehole wall are on-scale and correlatable across the suite. Post data-acquisition time to completion of report-ready record suite was six hours.

Summary

The small inexpensive computer, when linked to the engineering seismograph, is portable and can be operated in a variety of field situations, provides an inexpensive means of storing seismic information on disk, can automate and speed up interpretation in the field and in the office, and can provide the client with the optimum hard copy display of work and interpretation performed.

The software programs discussed in this paper have been published as Geological Survey of Canada Open File 552.

Reference

Huang, C.F. and Hunter, J.A.M.

1981: The correlation of "tube wave" events with open fractures in fluid-filled boreholes; in Current Research, Part A, Geological Survey of Canada, Paper 81-1A, p. 361-376.

SEISMIC RECONNAISSANCE PROFILES ACROSS THE SVERDRUP BASIN, CANADIAN ARCTIC ISLANDS

Project 770018

A. Overton
Resource Geophysics and Geochemistry Division

Overton, A., Seismic reconnaissance profiles across the Sverdrup Basin, Canadian Arctic Islands; in Current Research, Part B, Geological Survey of Canada, Paper 82-1B, p. 139-145, 1982.

Abstract

Seismic data may be described as multifold reversed profile data, with multiplicities ranging from 300 to 700% in each direction of the reversed profile. The viewpoint that reversed refraction profiles are more determinate than unreversed profiles is stringently tested for these deep sedimentary basins, and results show that great quantities of data complicate rather than simplify interpretations. Attempts to use traditional reversed profile refraction analyses based on a layered model with dipping interfaces failed to reveal unique velocities, dips and structures for the layers which could be matched bidirectionally.

A different analytical approach, using a model with velocities gradually increasing with depth, so that seismic events may be treated as wide angle reflections near critical incidence, appears to be justified. This approach yielded delay time-velocity profiles which match perfectly for the two directions of the reversed profile and uses all the available seismic data without internal conflict. The delay time-velocity structures are also consistent with observed gravity anomalies.

Introduction

In 1972, industry and the Federal Government jointly sponsored detailed shallow and deep seismic refraction and gravity studies along a profile located 60 km south of, and parallel to, the axis of the Sverdrup Basin (Fig. 19.1) in the Canadian Arctic Islands. G.D. Hobson of the Geological Survey of Canada (GSC) initiated and organized the project and led the operations. The Earth Physics Branch (EPB) of Energy Mines and Resources, Canada, conducted the gravity profiling and the deep crustal seismic sounding. Six oil companies participated: Canada Southern Petroleum Limited, Canadian Reserve Oil and Gas Limited, Deminex (Canada) Limited, Dome Petroleum Limited, Mobil Oil Canada Limited, and Panarctic Oils Limited. Details of the joint responsibilities are described by Hobson (1972). In 1973, the GSC and EPB extended the profile eastward across Amund Ringnes Island, and in 1974 added the north-south profile off the east coast of Ellef Ringnes Island (Fig. 19.1). Analytical problems relating to the seismic data for the sedimentary section were reported by Overton and Hobson (1977). Interpretation of the deep seismic refraction data is reported by Forsyth et al. (1979). This report documents the logistic details and the interpretation problems encountered with the unique multifold seismic refraction coverage obtained for the sedimentary section.

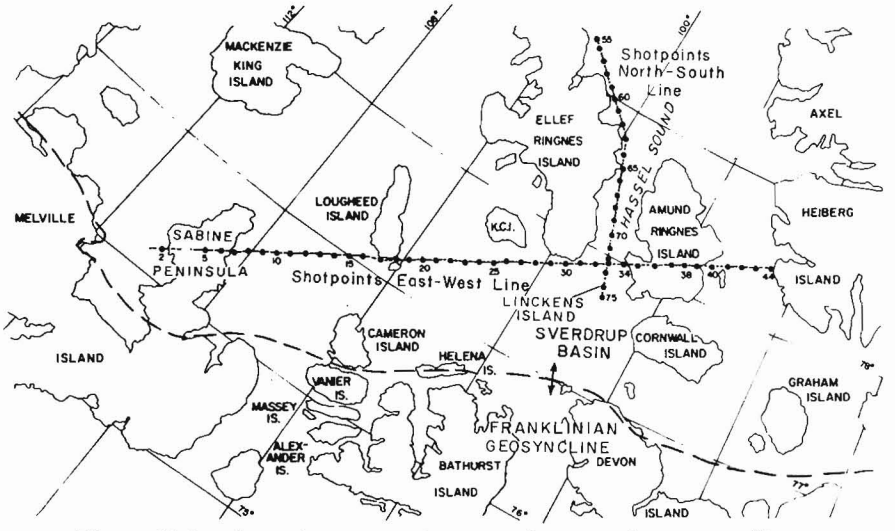

Figure 19.1. *Location map and extent of reconnaissance profiles.*

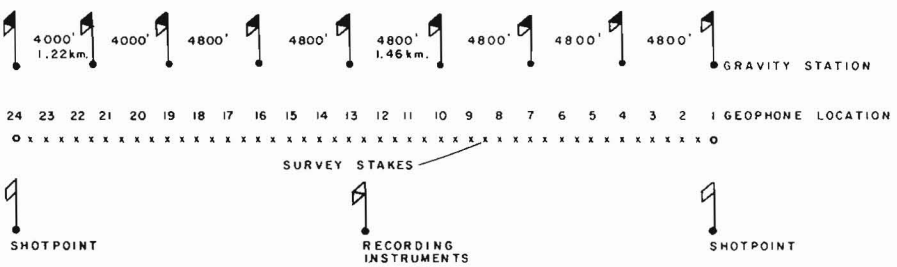

Figure 19.2. *Details of seismometer array, shotpoints and gravity stations.*

Logistics, Operations, and Instrumentation

Three campsites were established in 1972 as the work progressed east from Melville Island: at Drake Point on Sabine Peninsula, on Stupart Island at the southern tip of Lougheed Island, and at Sun Oil's King Christian Island airstrip. This last campsite was used in 1973 and 1974.

The operations involved up to 9 staff members of GSC and EPB, and Inuit Labour from Cambridge Bay and Resolute were employed each year.

The principal means of mobilizing and demobilizing the bulk of equipment, personnel, fuel and supplies during the winter season was by fixed-wing aircraft; field operations used helicopters. In the 1972 operation a cat train transported and housed the surveying crew as the line was surveyed and flagged from Sabine Peninsula to Axel Heiberg Island. Extensive use was made of snowmobiles for laying out and picking up the seismometers and cables; during 1973 and 1974 they were used to survey and flag the profiles.

For surveying, in 1972, elevations on land were determined by levelling and tying into base stations on Sabine Peninsula, Lougheed Island, King Christian Island, Linckens Island, Amund Ringnes Island, Ellef Ringnes Island and Axel Heiberg Island. Water depths were measured using an echo sounder coupled to the ice surface at every gravity station at intervals ranging from 980 to 1460 m. The accuracy of gravity station locations is within 30 m. Elevations are accurate within 0.3 m, and water depths are estimated to be accurate within 1 m. In 1973 and 1974, the surveying was done by triangulation from control points on King Christian Island and Ellef Ringnes Island using two snowmobiles. The lines were flagged by chaining and staking, using visual backsiting, every 243.8 m along bearings established from the triangulation control. These procedures proved to be very successful.

The seismic refraction profiling of the sedimentary section was conducted using 48-seismometer linear arrays, one seismometer per station, with 243.8 m station spacing for the east-west profile. Seismometers were Mark Products LIU, 4.5 Hz. An 11 460 m cable (Fig. 19.3) connected seismometers to the recording instruments at the centre of the array. The cable and seismometers were laid out using two snowmobiles except where extremely rough ice made helicopter airlifting necessary. The arrays were laid end to end along the profile with end seismometers common on adjacent arrays. Shotpoints were placed at increasing distances from both ends of the array, at equal intervals (array lengths, Fig. 19.3), until a first arrival velocity of 6 to 6.8 km/s was obtained. These velocities were taken to represent granitic or Ordovician limestone basement, respectively (Overton, 1970). For the north-south profile a 24 seismometer array was used with 487.6 m station spacing (Fig. 19.2) in order to minimize logistic problems. Apparently, no disadvantage resulted from this compromise.

Shots consisted of 60% geogel in 23 kg centre-tunneled cylinders. Charges made up in weights ranging from 23 kg to 68 kg were detonated on the ground surface on the islands and in the water on the seafloor, or at a depth of 60 m where water depth exceeded 60 m. Shots located on land or in shallow water on the shore were ineffective seismic sources and were not recorded beyond one cable length. Shotholes were drilled in the ice, generally about 2 m thick, using a gasoline powered auger. Charges were electrically detonated, producing a time reference pulse which was transmitted by radio to the recording seismograph. The 48 channel amplifier bank was made up of four 12-channel Texas Instruments VLF-2 systems modified to equalize signals to two SIE-PMR-20, 24 channel FM tape systems which were coupled mechanically and electrically. Adjustments to the PMR-20 proved to be extremely critical and sensitive to vibrations and temperature changes in the instrument shack. The drive mechanism was prone to freezing, and moisture condensation caused ice accumulations on the magnetic tapesand heads. Also the tape systems

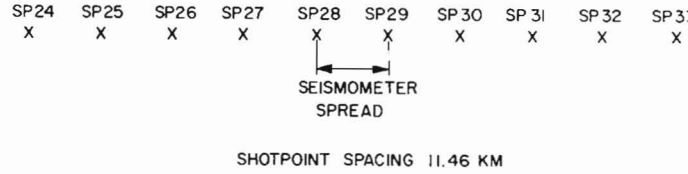

Figure 19.3. *Seismometer array and shotpoint details used in generating the reversed profile multifold seismic data.*

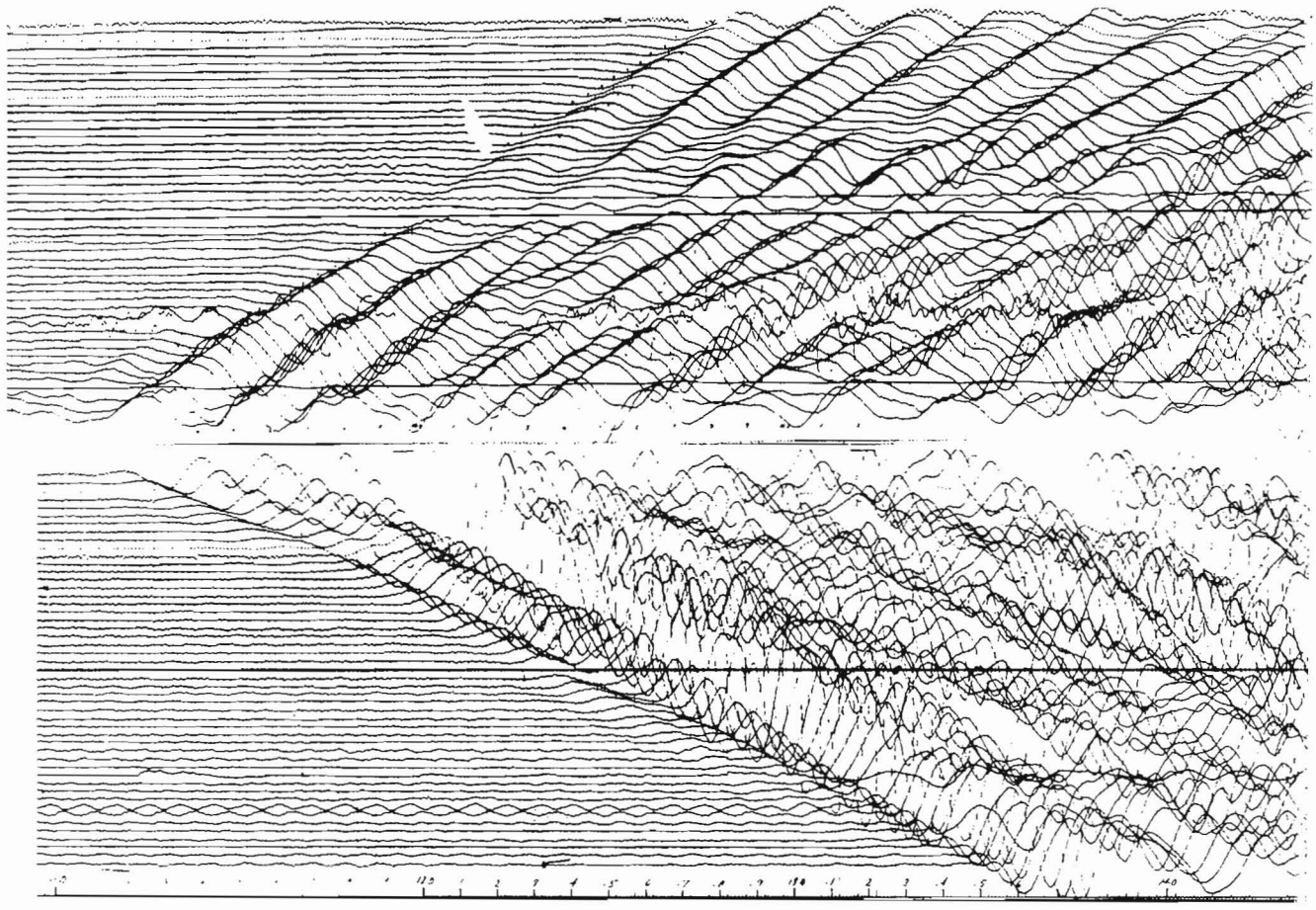

Figure 19.4. *Two examples of the reversed profile seismograms.*

caused a great deal of electrical interference on the seismograph amplifiers. These problems forced an early abandonment of attempts to record the data on magnetic tapes. A Texas Instruments RS-8U oscillograph using liquid developer and fixer was used with difficulty in the cold climate, only because an electrostatic oscillograph was not available. Oscillograph paper speed was 16.6 cm per sec. System bandpass response was 6 db down at 5 Hz and 48 Hz.

Results

Two sample records from the east-west line are shown in Figure 19.4. The first arrivals are characterized by weak onsets followed by stronger phases. The interpreter is compelled to pick progressively later events within the first arrival wavetrain, as the distance of the traces increases from the shotpoint. This results in an en-echelon pattern of segments on the time-distance plots, often causing timing conflicts in the interpretation. Early attempts to interpret these data were by conventional reversed profile methods which sought to establish layered velocity models on the basis of the reversed profile time-distance plots. All first arrivals and conspicuous secondary arrivals were plotted. Figure 19.5 is an example of the time-distance graphs. The method of recording shots from various distances into a stationary array is a sensitive indicator of velocity changes associated with depth of seismic penetration; variations of 0.25% can be significant depending upon the dispersion of the residual times about their regression line. Most velocity differences are larger than this and are highly significant. Figure 19.5 shows the difficulty in selecting a discretely layered model, and the difficulty of matching reversed profile segments for any given velocity. Velocity changes are subtle, with some obvious distortions due to local structures. Note the change to 5.33 km/s between shotpoints 29 and 30 decreasing to 5.12 km/s between shotpoints 28 and 29. This makes reversed profile matching of velocity segments virtually impossible. The subtlety of velocity variation is further illustrated in Figure 19.6 which shows frequency distributions of velocities for each direction of each of the reversed profiles. No discrete pattern of velocity layering is noticeable. No velocity shifts between the distributions for the reversed profiles are apparent. Regional dips (which would contribute to such shifts) of up to on half degree would produce bilateral velocity differences no greater than one class interval.

On the east-west line the prominent peak at 2.74 km/s represents ice arrivals at small distances. The north-south line shows several observations at 1.52 km/s which represent ice coupled water arrivals. Velocities greater than 6.75 km/s represent events modified by local structures and probably some diffractions.

Interpretation

The velocity distributions suggest complex multilayered models; however, the number of layers remains obscure. The velocity histograms do not indicate a lower limit. Even allowing one layer for each class interval, the problem of matching reversed profile segments to avoid conflicting structures persists. The interpreter is forced to accept each velocity segment of the time-distance plot at face value and to consider the concept of gradually increasing velocities with depth, a concept which has been used routinely to interpret reflection data in sedimentary basins for decades (Slotnick, 1936).

Another problem remains with head wave interpretations; that is, which part of the subsurface span between the shotpoint and the seismometers does an event represent? The simplest approach is to think of the seismic events as wide-angle, or near-critical, reflections. In this way the events may be viewed as representing the halfway point on the subsurface. This can be done for each direction of the reversed profile. A comparison of the bidirectional results may provide insight into interpretational refinement. Further to the concept of gradually increasing velocities with depth, near-critical reflection trajectories are commonly curved (circular for strictly linear velocity increases), with the apparent velocities representing the velocity at the maximum depth penetrated (Dobrin, 1952). This provides the most convenient approach for interpretation because it solves all the mechanical problems; that is, since the recorded events are considered to be wide angle reflections, they would represent the halfway subsurface span. Also in the sense that the events are critical reflections, their apparent velocities are representative of those at the maximum depths of penetration, and may also be interpreted as head waves. In this way, the time-distance-velocity values for each event may be reduced to a delay time. This fully describes the method: for each direction of the reversed profiles, velocities and associated delay times were computed for all segments of the time-distance graphs. The delay times were plotted on sections, and annotated with their velocities, halfway between the shotpoints and seismometers. Velocity contours were then drawn on these sections. The two directions for the reversed profiles were then compared and, with minor modifications to the contours, were found to match. The results from the two directions, now being compatible, were combined (Fig. 19.7, 19.8). This was considered a major accomplishment, especially since prior interpretations using reversed profile headwave analyses and layered models produced gross conflicts in structures. Thus, a fundamental prerequisite is satisfied: the interpretation utilizes all of the data systematically without internal conflicts. The practical meaning, as with any interpretation, requires substantiation.

Discussion

Certainly for the deep Sverdrup and Franklinian sedimentary basins (Thorsteinsson and Tozer, 1960) composed of an alternating sequence of marine and nonmarine sediments, faulted and folded, containing igneous, carbonate, gypsum and halite intrusions, the complexity of the seismic refraction results is not surprising. Previous seismic studies in this area (Hobson and Overton, 1967; Overton, 1970; Sander and Overton, 1965) used layered velocity models and headwave interpretations simply because the data were sparse and no conflicts were encountered. The highly detailed work of this experiment has demanded attention to these conflicts.

The most serious criticisms of the interpretation are:

1. the resulting velocity contours do not correspond with, or even resemble the results of seismic reflection work over the same area (reported in Forsyth et al, 1979), and
2. the velocity contours do not correspond with the stratigraphy as it is known from borehole control.

These criticisms are easily dismissed as the refraction method, with wide ranging soundings, traverses a highly diverse geological environment and in the process it does a lot of averaging of structures. The borehole and seismic reflection correlations show detailed, localized structures.

As for geological implications the 3 km/s contour approximates the water delay time and it shows the highly variable seafloor topography. Other geological correlations are obscure and are undoubtedly complicated by stratigraphic variations. However, some general regional effects may be seen. Judging from depth estimates the 5.25 km/s contour in Figures 19.7 and 19.8 appears to approximate the base of the Sverdrup Basin. It shows a general thickening from the west toward the east (Fig. 19.7) and from the north toward the south (Fig. 19.8) approaching the axial region of the basin.

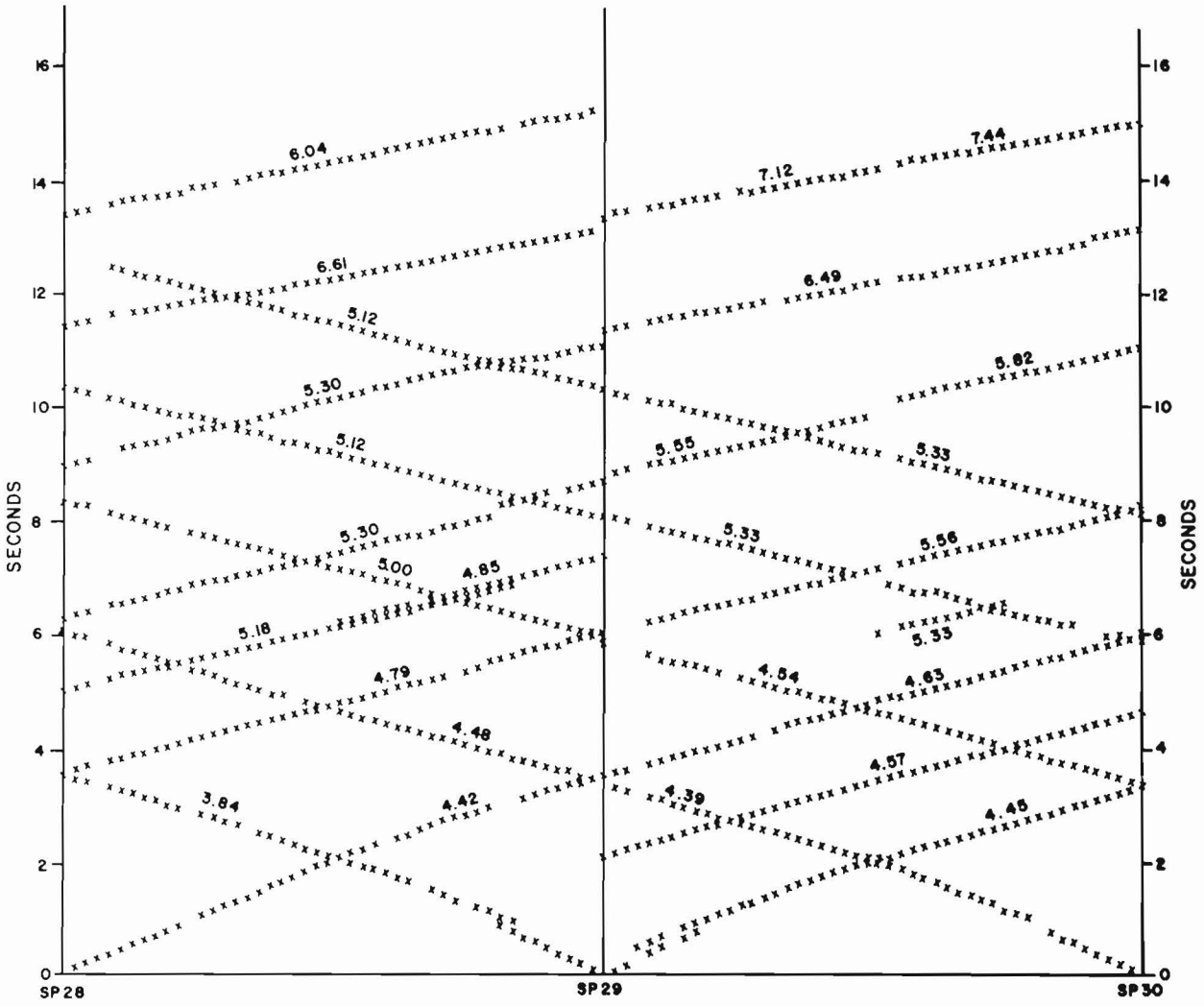

Figure 19.5. *Example of reversed profile time-distance plots. Velocities are in kilometes per second.*

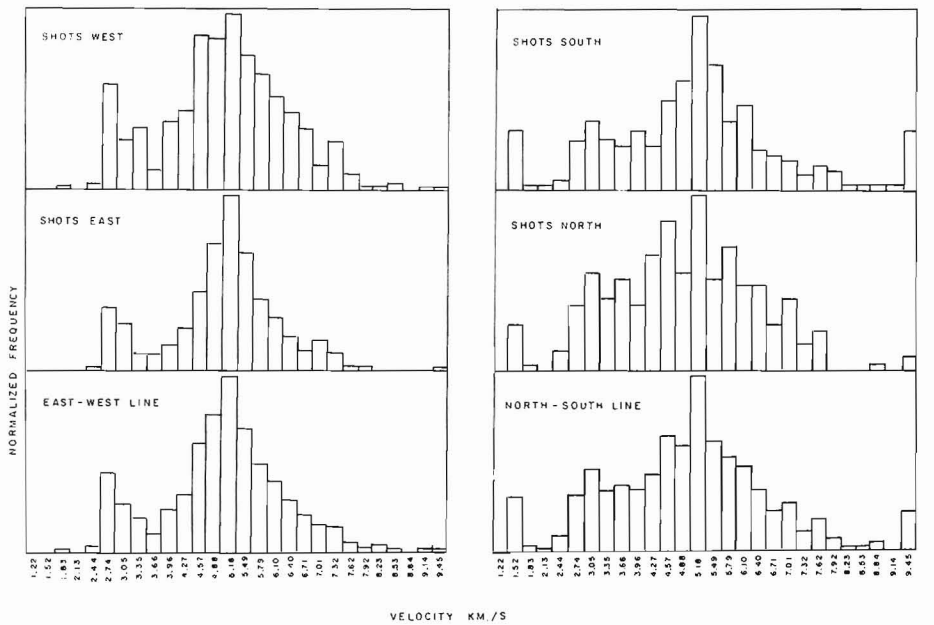

Figure 19.6. *Histograms of first arrival velocities for reversed profile multifold seismic refraction data.*

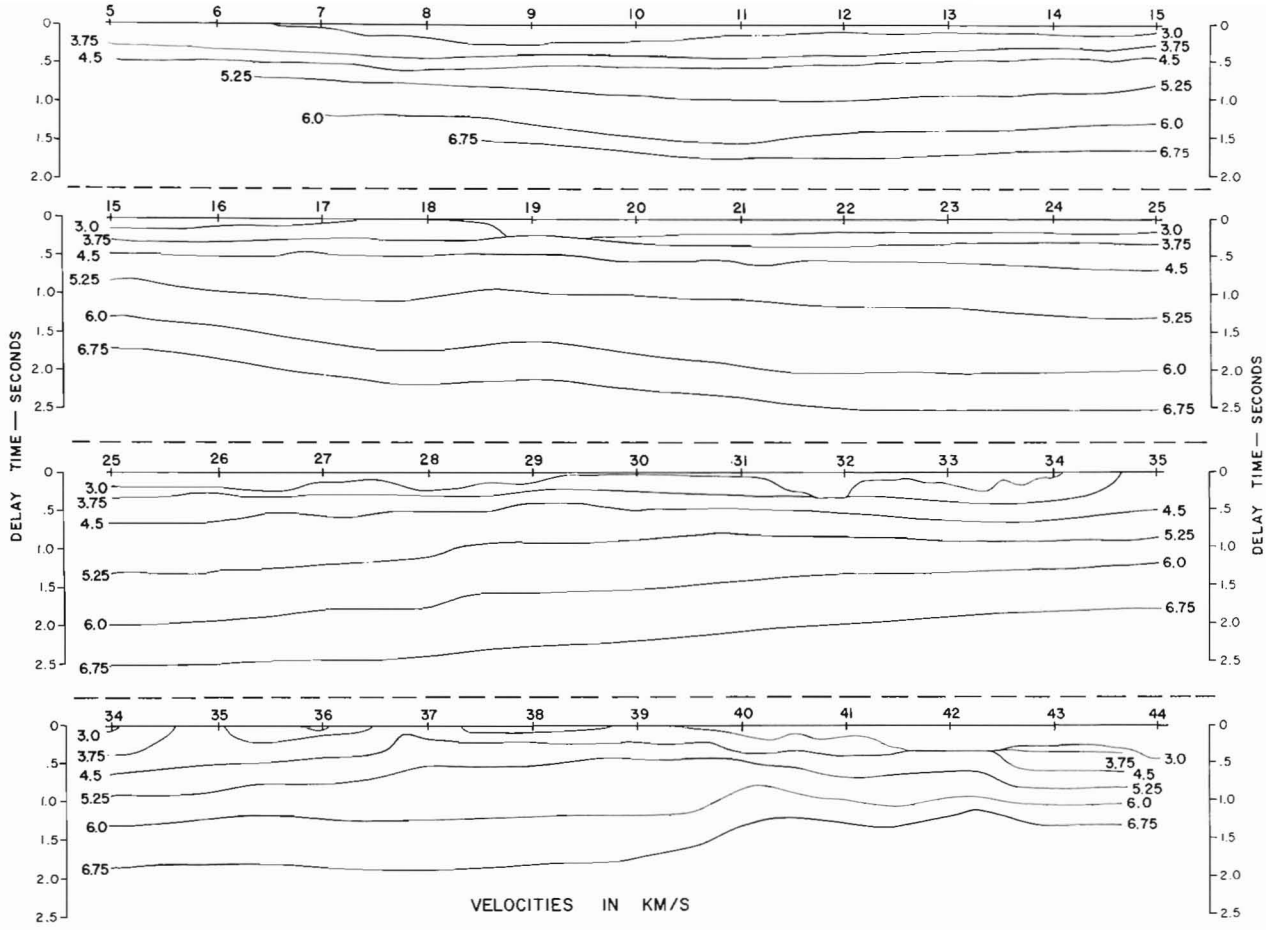

Figure 19.7. Contoured velocity-delay time profile for the east-west line.

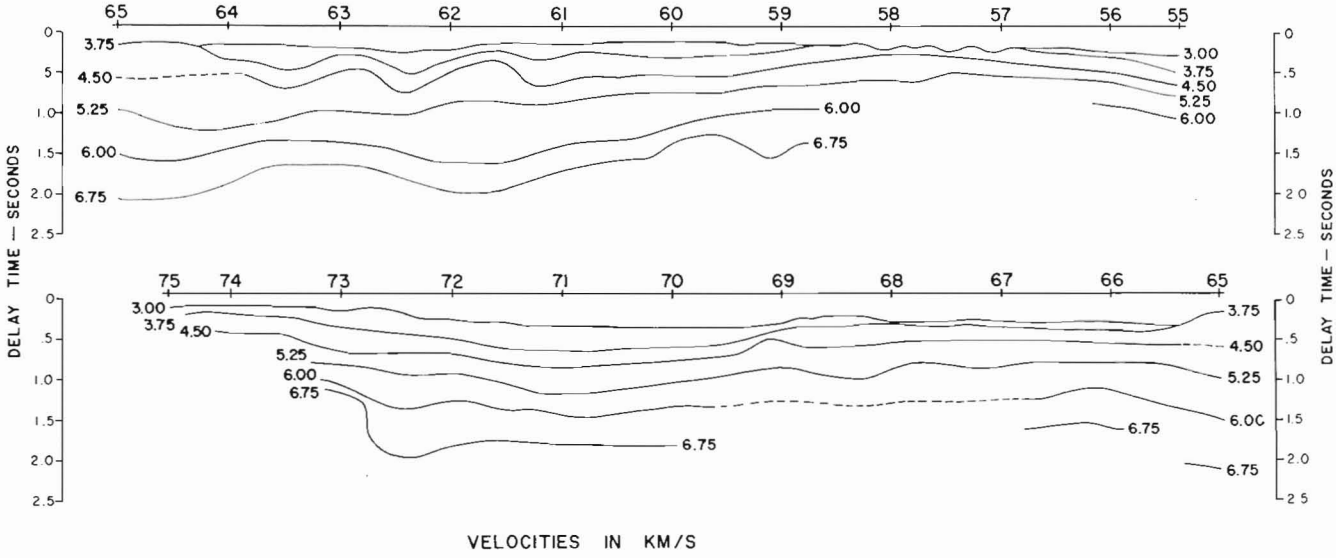

Figure 19.8. Contoured velocity-delay time profile for the north-south line.

The 6.75 km/s contour is ubiquitous on the east-west section (Fig. 19.7) and is considered to be seismic basement, and coincides with early Paleozoic carbonate belts which fringe the Sverdrup Basin. The seismic refraction method is very effective in mapping these carbonate belts.

Another basin-like thickening is suggested for these deeper Paleozoic strata, and may represent the Franklinian geosyncline underlying the Sverdrup Basin. Increased complexity of folding east of Ellef Ringnes Island, across Amund Ringnes toward Axel Heiberg is in accordance with known geological models, as well as structural complexities on Amund Ringnes Island.

Figure 19.8, the contoured velocity-delay time section for the north-south profile shows a sharp rise in the 6.75 km/s contour at shotpoint 73 which appears to be significant. This coincides with a pronounced local gravity feature which may be related to the northern extension of the Boothia Arch and the Cornwallis Fold Belt (Thorsteinsson and Kerr, 1968; Kerr, 1977). Poorly controlled contours are dashed. The absence of the 6.75 km/s contour between shotpoints 67 and 70 may signify a change from carbonate to shale or clastic facies. This effect has been observed in previous work (Overton, 1970) near Emerald Isle, between Prince Patrick Island, Mackenzie King Island and Sabine Peninsula where a high velocity basement was absent. Truncation of sedimentary beds on the seafloor is suggested on an arch centred under shotpoints 57 and 58 (Fig. 19.8) This feature coincides with a 60 mgal positive gravity anomaly (Sobczak et al., 1963). The pronounced folding at shotpoints 62 and 63 on the shallow contours is the most conspicuous seismic feature. This coincides with a 30 mgal negative gravity anomaly representing a gypsum piercement structure.

Further support for this seismic interpretation is discussed in a manuscript by Sobczak and Overton (submitted to Earth Physics Branch).

Depth Conversions

Alterating sequences of marine and nonmarine sediments in sedimentary basins invariably cause velocity inversions which complicate depth conversions, particularly for the seismic refraction method which only shows monotonically inceasing velocities. Delay times obtained from refraction profiling, however, are directly related to these inversions. Thus it is necessary to examine the effect of these inversions on depth estimates. In the absence of velocity information from deep boreholes or from deep seismic reflection data, it is necessary to examine reasonable

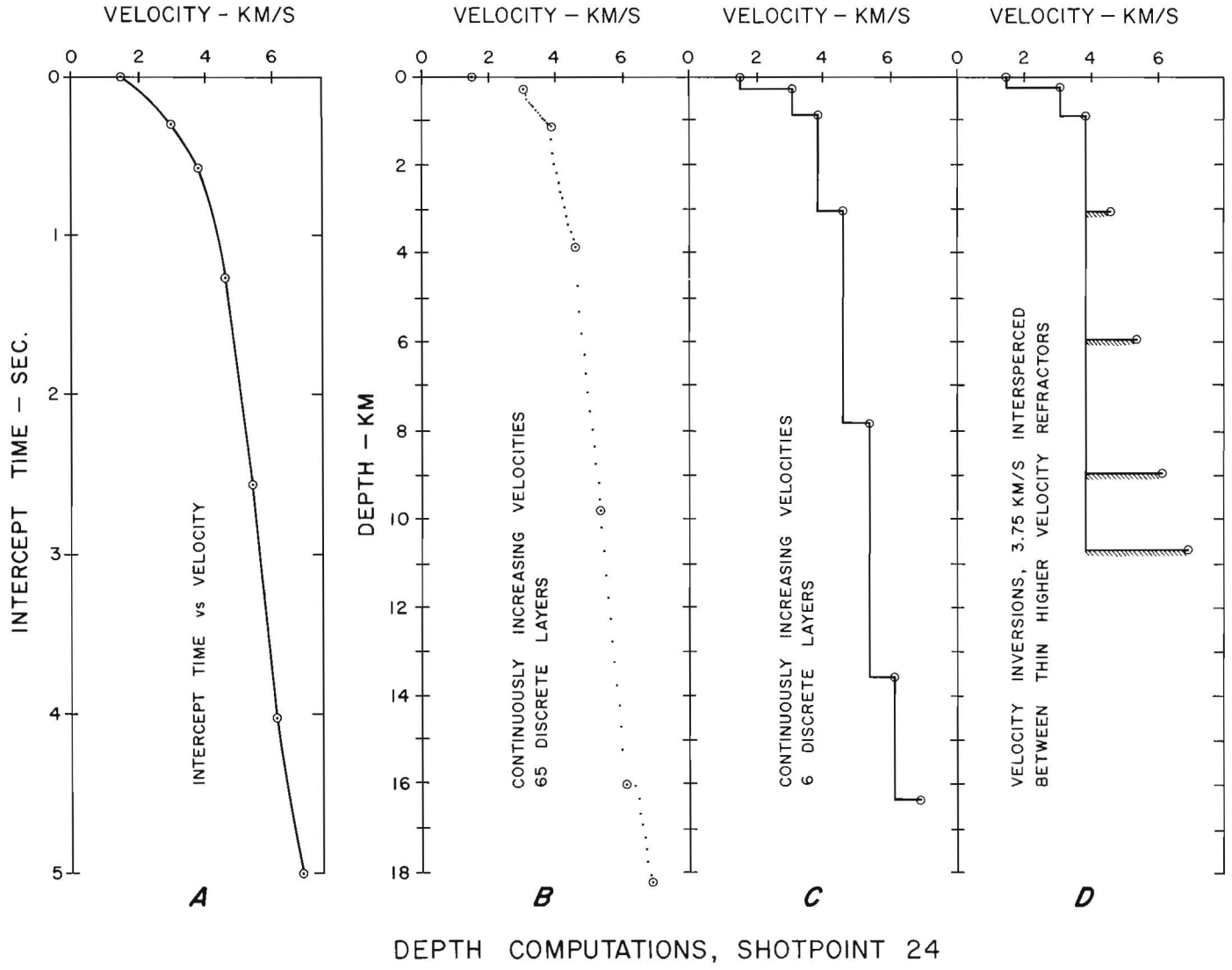

Figure 19.9. *Comparison of depth conversions for selected velocity models.*

possibilities for velocity models. Three methods were tested for the purpose of comparison. First, Figures 19.7 and 19.8 indicate the monotonically increasing velocities characteristic of refraction profiling. Accepting these as representing one possible model with a large number of increasing velocity layers gives one set of depth estimates. Second, Figures 19.7 and 19.8 may be taken to represent six discrete velocity layers overlying the 6.75 km/s basement, giving another set of depth estimates. Third, the velocity contours of Figures 19.7 and 19.8 may be considered as representing thin refractors interspersed within a low velocity matrix. Figure 19.9 shows the depths resulting from these three models for shotpoint location 24. The greatest difference in computed depths is given by Figure 19.9D for which an extreme degree of inversion has been assumed. The model in Figure 19.9C represents depth uncertainties of 10%, compared with the model in Figure 19.9B and models assuming a moderate degree of velocity inversion.

Conclusions

Reversed seismic refraction profiling in the Sverdrup and Franklinian basins has produced data which generate conflicting and confused structures by traditional headwave analyses and discretely layered velocity models. An interpretation which assumes that first arrivals represent wide angle critical reflections appears to eliminate these conflicts and allows the data to be mapped as contoured velocities on delay time sections. The resulting sections are consistent for reversed profiles and utilize all the available data.

Details of structures are not seen in these wide ranging seismic refraction measurements, while the broad, well known features of depth variations, folding and faulting complexities and diapiric structures are evident in the interpretations. The seismic refraction method is effective in mapping the high velocity Paleozoic carbonates of the Franklinian geosyncline. Depth estimates appear to be within expected limits, allowing for reasonable variation in the velocity model.

Acknowledgments

The considerable efforts of G.D. Hobson, initially the leader of the seismic team, the later the Director of the Polar Continental Shelf Project, in planning, contracting and organizing the project, and in manuscript revision, are gratefully acknowledged.

This work was supported in 1972 by Canada Southern Petroleum Limited, Canadian Reserve Oil and Gas Limited, Deminex (Canada) Limited, Dome Petroleum Limited, Mobil Oil Canada Limited and Panarctic Oils Limited.

The Earth Physics Branch conducted the gravity measurements during all three field seasons, and the long range seismic refraction surveys of 1972 and 1973. Several people were involved in various aspects of the field work, which was often conducted under harsh conditions. The bulk of this work was done by, or under the supervision of, H.A. MacAulay, R.A. Burns and R.M. Gagne.

The author thanks C.E. Waboso for critically reading the manuscript, and also K.A. Richardson for much revision and assistance.

References

Dobrin, M.B.
1952: Introduction to Geophysical Prospecting; McGraw-Hill Book Company, Inc., New York, 1952, p. 224-229.

Hobson, G.D. and Overton, A.
1967: A seismic section of the Sverdrup Basin, Canadian Arctic Islands; in Seismic Refraction Prospecting, ed. A.W. Musgrave, Society of Exploration Geophysicists, Tulsa, Oklahoma, p. 550-562.

Hobson, G.D.
1972: Sverdrup Basin Project Geological Survey of Canada. Internal report to participants.

Forsyth, D.A., Mair, J.A., and Frazer, I.
1979: Crustal structure of the central Sverdrup Basin; Canadian Journal of Earth Sciences, v. 16, p. 1581-1598.

Kerr, J.W.
1977: Cornwallis Fold Belt and the mechanisms of basement uplift; Canadian Journal of Earth Sciences, v. 6, p. 1374-1401.

Overton, A.
1970: Seismic refraction surveys, western Queen Elizabeth Islands and Polar Continental Margin; Canadian Journal of Earth Sciences, v. 7, p. 346-365.

Overton, A. and Hobson, G.D.
1977: Seismic reconnaissance profiles across the Sverdrup Basin, Canadian Arctic Islands. Paper presented at the Society of Exploration Geophysicists Conference, Calgary, Alberta, September, 1977.

Sander, B.W. and Overton, A.
1965: Deep seismic refraction investigation in the Canadian Arctic Archipelago; Geophysics, v. 30, p. 87-96.

Slotnick, M.M.
1936: On seismic computations, with applications, I; Geophysics, v. 1, p. 9-22.

Sobczak, L.W., Weber, J.R., Goodacre, A.K., and Bisson, J.L.
1963: Preliminary results of gravity surveys in the Queen Elizabeth Islands with maps; Dominion Observatory, Gravity Map Series No. 12-15.

Thorsteinsson, R. and Kerr, J.W.
1968: Cornwallis Island and adjacent smaller islands, Canadian Arctic Archipelago; Geological Survey of Canada, Paper 67-64.

Thorsteinsson, R. and Tozer, E.T.
1960: Summary account of the structural history of the Canadian Arctic Archipelago since Precambrian time; Geological Survey of Canada, Paper 60-7.

EFFECTS OF THE 1929 GRAND BANKS EARTHQUAKE ON THE CONTINENTAL SLOPE OFF EASTERN CANADA

Project 810047

David J.W. Piper and William R. Normark[1]
Atlantic Geoscience Centre, Dartmouth

Piper, David J.W. and Normark, William R., Effects of the 1929 Grand Banks earthquake on the continental slope off eastern Canada; in Current Research, Part B, Geological Survey of Canada, Paper 82-1B, p. 147-151, 1982.

Abstract

In 1929, the largest historical earthquake on the Atlantic margin of Canada was followed by a series of breaks in trans-Atlantic telegraphic cables on the deep seafloor south of the Laurentian Channel. Both slumping and turbidity currents generated by the slumps are thought to have caused the cable breaks. It is necessary to know the approximate recurrence interval of similar earthquakes to allow an assessment of the seismic risk for this part of the Canadian margin. Sparker and airgun seismic-reflection profiles of the upper Laurentian Fan and superjacent slope, together with recently obtained core samples and 3.5 kHz high-resolution acoustic profiles, confirm that slumping of surficial sediment on the slope and upper Laurentian Fan is common within 100 km of the earthquake epicentre. Most slumps involve the uppermost several tens of metres of sediment and expose late Pleistocene sediment at the seafloor. One large debris flow that originated near the earthquake epicentre is locally more than 200 m thick and extends more than 100 km down the eastern valley on the Laurentian Fan. Deep seismic reflection profiles from the upper Laurentian Fan suggest that earthquakes with effects similar to that of 1929 have recurrence intervals of hundreds of thousands of years.

Introduction

The Grand Banks earthquake of November 18, 1929, which had an estimated magnitude of 7.2 and an epicentre just south of the southeast edge of the Laurentian Channel (Doxsee, 1948; Stewart, 1979), was the largest historical earthquake to have occurred in Atlantic Canada. Epicentres of subsequent earthquakes in the southern Laurentian Channel suggest that the 1929 event occurred on a major fault system that runs from the Cobequid-Chedabucto fault of Nova Scotia, through the Orpheus graben, to the transform continental margin of the southwestern Grand Banks (Glooscap fault system of King and MacLean, 1976).

Numerous deep sea cables (Fig. 20.1) were broken, either during or shortly after the earthquake (de Smitt, 1932; Doxsee, 1948), and these breaks, together with the discovery of a turbidite bed on the surface of the Sohm Abyssal Plain led to the suggestion by Heezen and Ewing (1952) that the earthquake triggered a slump and major turbidity current. Although the relative importance of slumping (Terzaghi, 1956; Piper and Normark, in press) and the precise path and velocity of the subsequent turbidity current (Heezen and Drake, 1964; Uchupi and Austin, 1979) have been disputed, this general interpretation is widely accepted.

With the recent expansion of hydrocarbon exploration on the Atlantic continental margin of Canada, there is a need to assess the risk posed by a seismically active zone in Laurentian Channel. In this report we use geological data, including some quite recently obtained, to estimate a recurrence interval for earthquakes with effects similar to those of the 1929 event.

The principal data, from cruise 81-044 on **CSS Dawson**, December 4-15, 1981 (Fig. 20.2), include 3.5 kHz profiles, piston and gravity cores, and unprocessed analogue records from a high-resolution multichannel seismic-reflection survey; navigation was by Loran-C. In addition, we use data (Fig. 20.3) from an earlier single-channel sparker survey from cruise 78-022 (Normark, in press; Piper and Normark, in press) and the piston cores studied by Stow (1977). This earlier work was partly supported by the Natural Science and Engineering Research Council (NSERC) and the U.S. Geological Survey.

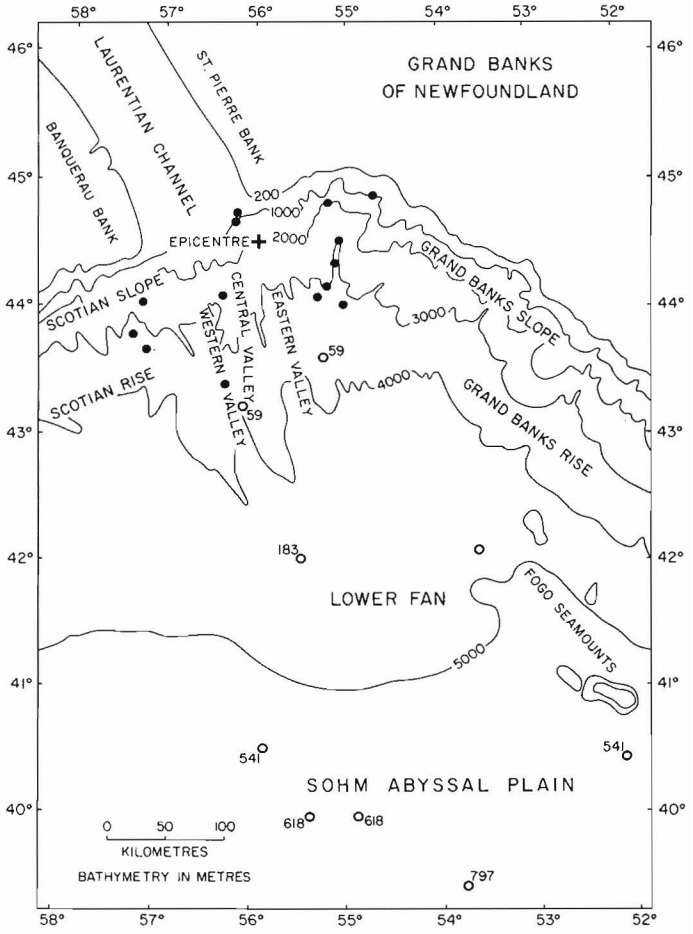

Figure 20.1. *Laurentian Fan and adjacent area, showing epicentre of 1929 earthquake and locations and times of cable breaks (after Heezen and Ewing, 1952). Dots, instantaneous breaks; circles, later breaks. Numbers are times (in minutes) after earthquake.*

[1]U.S. Geological Survey, 345 Middlefield Road, Menlo Park, CA 94025, U.S.A.

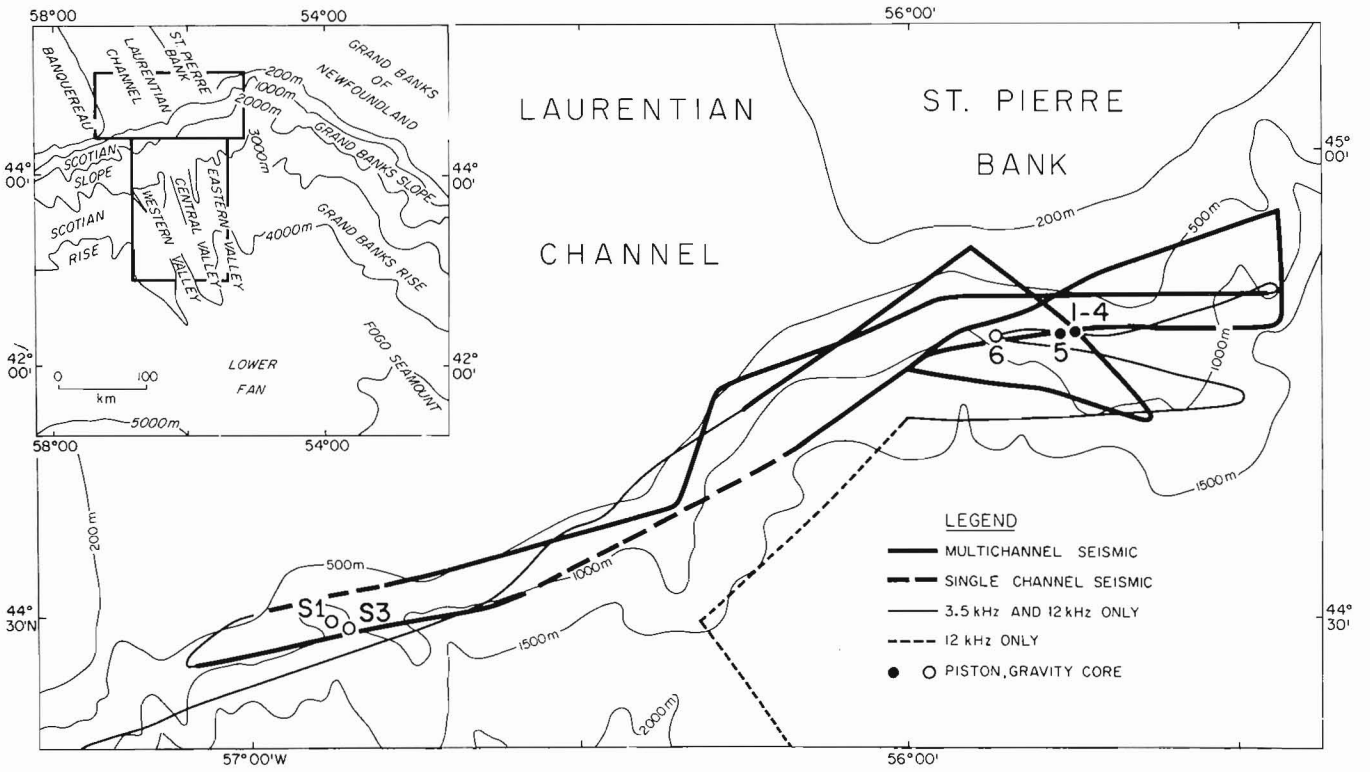

Figure 20.2. *Track chart for cruise 81-044 off the Laurentian Channel and St. Pierre Bank. (Inset shows location of this figure and Figure 20.3) S1 and S3 are cores of Stow (1977); other cores are from cruise 81-044.*

In this report, the thicknesses on acoustic records are given in two-way traveltime (in milliseconds): for surficial sediment, 1 ms two-way traveltime is approximately equivalent to 1 m of sediment thickness.

The Debris Flow and Turbidity Current

Both field and laboratory studies (Hampton, 1972) suggest that turbidity currents develop from slumps through an intermediate stage of debris flow; the debris flows themselves commonly occur downslope from large slump scars. Such debris flows may be kilometres wide and as much as hundreds of metres thick, although thicknesses of only a few metres or tens of metres are normal in distal environments. Damuth (1980) reviewed the criteria that are useful in identifying debris flows from high-resolution acoustic data, and good examples of modern debris flows were described by Embley (1980) and Damuth and Embley (1981).

The large eastern valley of the Laurentian Fan (Fig. 20.3), below the 1929 epicentre, has long been known to contain a low central ridge, here identified as a debris-flow deposit (Stow, 1977; Edgar and Piper, 1979; Uchupi and Austin, 1979). This feature is seen to have a rough surface topography on 3.5 kHz reflection profiles, suggestive of a debris flow (Damuth, 1980). A 160 kj sparker profile that crosses the feature shows a complex of hyperbolic reflectors (again suggesting irregular unstratified sediment) overlying a prominent valley floor or slope reflector that continues to either side (Damuth, 1980). Long-range sonar (GLORIA) records by D.G. Roberts (personal communication, 1980) also confirm the presence of a large debris flow here. In most areas this debris flow is less than 40 m thick, but near its upslope limit it is more than 100 m thick. A second, smaller possible debris flow is recognized in sparker seismic profiles in the central valley of the upper fan (Fig. 20.3) as far south as latitude 43°30'N, although its surface morphology is

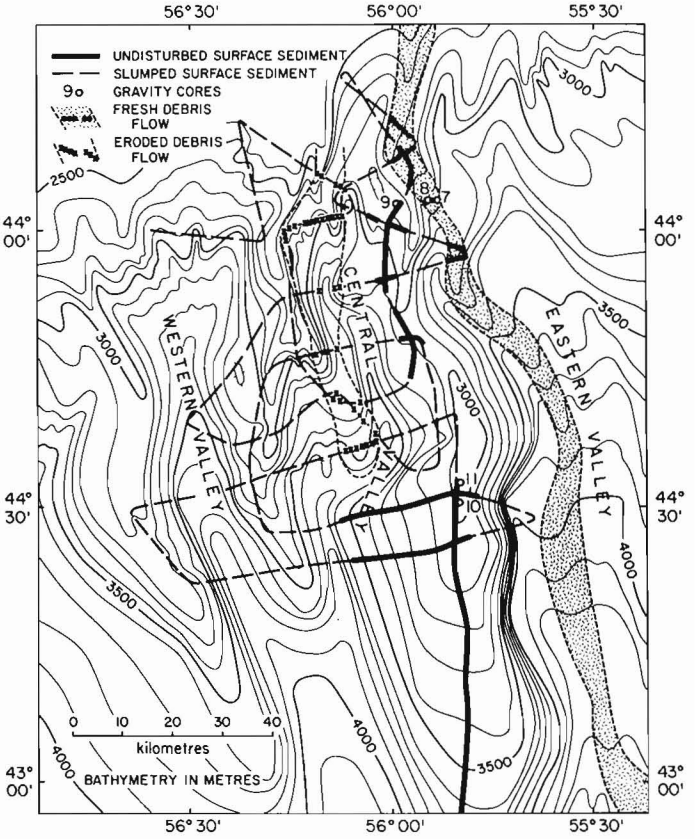

Figure 20.3. *Track chart of single-channel sparker survey on upper Laurentian Fan (Piper and Normark, in press), showing locations of debris flows, cores, and undisrupted surficial sediment. See Figure 20.2, for location.*

a - abruptly missing sedimentary sequence, contrasting with complete sequence to east.
b, c - missing sedimentary sequences on valley wall.
d - disturbed surficial sediment.
e - missing sedimentary sequences on both valley walls, contrasting with complete sequence to west.
f - missing sedimentary sequences on valley wall.
g, h - missing sedimentary sequences on valley floors.
i - possible slump deposit or debris flow.

Figure 20.4. *Example of 2.5 kHz record from slope south of St. Pierre Bank, between 5 and 6 in Figure 20.2. Depths in two-way traveltime.*

smoother on higher frequency analogue records and in places it is deeply dissected by the central valley. This second debris flow appears to be onlapped by stratified sediment at one locality; thus, it appears to be a substantially older feature than the debris-flow deposit in the eastern valley.

Pleistocene turbidites on the Laurentian Fan and Sohm Abyssal Plain comprise a distinctive red mud, whereas the overlying Holocene sediment is hemipelagic and olive grey (Piper, 1975; Stow, 1977, 1981). The red colour of the 1929 turbidite on the Sohm Abyssal Plain (Fruth, 1965) also indicates that much of its source material may be Pleistocene sediment. These observations suggest that the finer grained sediment of the 1929 turbidite on the Laurentian Fan may be recognized as a distinctive red mud at the top of the cores, overlying Holocene olive-grey hemipelagic sediment.

Piston cores from the Laurentian Fan in the vicinity of latitude 42°10'N (Stow, 1977, 1981) show surface sand and gravel in channels that may be derived from the 1929 turbidite. Red mud occurs on some low valley walls, but overbank red mud is absent on the levees more than 170 m above the valley floor.

We sampled the debris flow and adjacent valley floor at about latitude 44°N. Both gravity cores (cores 7 and 8, Fig. 20.3) washed out, probably after bottoming in sand, but penetrated 30-50 cm of red mud (preserved on the outside of the barrel). Any overlying olive-grey sediment, if present at all, must have been very thin. These cores presumably penetrated the 1929 turbidite. On the adjacent levee, 250 m above the crest of the debris flow, no red mud is present at the surface (core 9, Fig. 20.3).

Ground Shaking on the Upper Fan

Our 1978 sparker survey of the upper fan showed that the sediment surface is commonly very rough, and gives hyperbolic returns, not only on the steep valley walls but also on the relatively flat levee crests. A transition occurs on the levee crests downfan to smooth seafloor at about latitude 43°30'N. New 3.5 kHz data indicate that this transition is marked by the loss of 5-20 ms (approximately 5-20 m) thicknesses of surface sediment from the rough upslope side, presumably by slumping (Fig. 20.4). This conclusion was confirmed by coring (cores 10 and 11, Fig. 20.3). The smooth seafloor has an upper layer of Holocene olive-grey hemipelagic mud; this layer is absent, however, on the rough seafloor, where red mud and sand (both characteristically Pleistocene sediment types) were noted at the surface. Core 10 had a slight red tinge in the uppermost surficial hemipelagic sediment: whether this material was derived from levee spillage of the 1929 turbidity current or from resuspension of sediment during slumping away of the surficial sediment sequences is unclear.

We have insufficient 3.5 kHz data to confirm whether all the areas that show surface roughness on the 160 kj sparker profiles have undergone surficial slumping: probably in some areas the roughness results from valley-wall erosion by turbidity currents (Piper and Normark, in press). Nevertheless, our data indicate that few of the levee crest areas south of latitude 43°30'N are disturbed, whereas between latitudes 43°30'N and 44°10'N, only small areas of undisturbed levee crest occur.

The area of widespread ground shaking and slumping during the 1929 earthquake can be estimated from the distribution of instantaneous cable breaks (Fig. 20.1). These breaks, which occurred as far south as latitude 43°25'N, correlate well with our observations on surface slumping. The distribution of cablebreaks occurring after the initial earthquake suggests that a turbidity current was not restricted to the eastern valley below the epicentre; instead several breaks appear to have taken place near the lower part of the western valley.

Ground Shaking on the Continental Slope

The steep continental slope is presumably the source area for most of the slump material that formed the debris flows and turbidity current. We can distinguish two strikingly different areas: the slope off Laurentian Channel, and the slope off St. Pierre Bank.

The continental slope off the Laurentian Channel lies in 400 to 2000 m water depth. The upper slope (to 1300 m) is very steep, scalloped in plan, and somewhat resembles a glaciated mountain slope with cirques separated by arêtes (Fig. 20.2). High-resolution 3.5 kHz profiles show a hard bottom, and the few attempts at coring in this environment (Stow, 1977) yielded almost no sediment. High-resolution common depth point seismic-reflection profiles, using a 40 in^3 airgun sound source, also show no continuous reflectors. We suggest that the slope here is underlain by thick glacial till and that the cirquelike features represent major slump scars.

The slope off St. Pierre Bank is much more gentle, and is dissected by shallow channels that show multiple cut-and-fill sequences on the multichannel seismic records. The well stratified sedimentary sequence (to 1 s subbottom) shows no evidence of major slumps. High-resolution 3.5 kHz profiles show well stratified surficial sediment in water depths of more than 500 m. Absence of acoustic penetration in shallower waters is probably due to the presence of surficial sand. Over large areas (estimated at 60 per cent of the total survey area), the uppermost 5-30 ms of stratified sediment is missing, and abrupt transitions occur between the truncated and the complete stratified sequences (Fig. 20.4). Piston cores (2, 5, and 6, Fig. 20.2) confirm that Holocene sediment is missing where the 3.5 kHz profiles show that the upper part of the stratified sequence has been stripped away. This observation suggests that the missing sedimentary sequences have been removed by late Holocene slumping.

Recurrence Interval of Major Seismic Events

The 1929 Grand Banks earthquake was a major seismic event. The evidence of instantaneously broken cables indicates that it caused slumping to as far as 100 km from the epicentre. Subsequently, a powerful turbidity current is thought to have broken cables as far south as latitude 39°30'N on the Sohm Abyssal Plain.

The timing of the breaks suggests current velocities approximately 10 m/s (e.g., Heezen and Ewing, 1952). On the continental slope, Laurentian Fan, and Sohm Abyssal Plain, we saw abundant evidence of a major late Holocene slump and turbidity current event. Slumping was widespread to as far as 100 km from the epicentre, some as far as 130 km away. The morphologically fresh debris flow and small slump scars have no recognizable Holocene sediment resting on them. The widespread turbidite on the Sohm Abyssal Plain, with a volume of more than 50×10^9 m^3, is not overlain by pelagic sediment (Fruth, 1965); furthermore the surficial sediment in mid-fan channels is composed of thick sorted and graded gravel to coarse sand rather than pelagic mud (Stow, 1977).

The similarities in scale and extent between the inferred late Holocene slump/turbidity current event on the continental slope – Laurentian Fan-Sohm Abyssal Plain, as well as the observed effects of the 1929 earthquake in the same area, argue that these two are causally related. It is highly improbable that the inferred slump/turbidity current event represents an earlier larger unrecorded late Holocene earthquake. The absence of earlier slump events revealed in the sedimentary sequences on 3.5 kHz profiles of both the slope off St. Pierre Bank and the upper Laurentian Fan suggests that no other major shaking event of the same style occurred during the accumulation of the upper 40 ms of sediment. The sedimentation rate data of Stow (1977) and Alam (1979) suggest that this interval corresponds to at least the past 100 000 years. Therefore, we conclude that the 1929 event was the only earthquake of that magnitude to occur at the edge of the Laurentian Channel within at least the past hundred thousand years. Large earthquakes, however, may have occurred farther northwest on the Glooscap fault system, and smaller earthquakes may well have occurred, with effects less visible on 3.5 kHz profiles.

On deeper seismic-reflection profiles from the Laurentian Fan (Normark, in press; Piper and Normark, in press), there is evidence of occasional earlier major slump and debris-flow events within the Pleistocene section. The age of the dissected debris flow in the central valley is uncertain. On the west levee of the eastern valley, at latitude 43°20'N, there are two subsurface horizons with evidence of surficial slumping above marker horizon A of middle Pleistocene age (Piper and Normark, in press). At latitude 41°20'N, near the terminus of the western valley, is a thick debris flow some 0.3 s subbottom, also of inferred middle Pleistocene age.

Turbidites of Wisconsinan (latest Pleistocene) age, which are common on the lower Laurentian Fan and Sohm Abyssal Plain (Stow, 1977; Wang et al., in press), appear to be more common than seismic events of the magnitude of the 1929 earthquake. The turbidites may well have been formed by slumping of glaciomarine sediment transported down the Laurentian Channel; this slumping may have been initiated either by sediment overloading on steep slopes or by small earthquakes that triggered slumps only very close to the epicentres. Some of the currents must have been large as they reached the distal Sohm Abyssal Plain 1200 km to the south (Wang et al., in press). Such turbidity currents probably eroded the older debris-flow deposits from the valley floors.

Conclusions

Extensive ground failure occurred as far as 100 km from the epicentre of the 1929 Grand Banks earthquake. Earthquakes with such effects probably have a recurrence interval of hundreds of thousands of years. Earthquakes with lesser, but significant, effects could be considerably more common.

Acknowledgments

This study was supported by the Canada Office of Energy Research and Development, program of long term studies in marine geology. We thank Geomarine Associates and the officers and crew of **CSS Dawson** for efficient field operations. The manuscript was reviewed by J. Adams, C.F.M. Lewis and B. Edwards.

References

Alam, M.
1979: The effects of Pleistocene climatic change on sediments around the Grand Banks; unpublished Ph.D. thesis, Dalhousie University, Halifax, N.S., 295 p.

Damuth, J.E.
1980: Use of high frequency (3.5 - 12 kHz) echograms in the study of near-bottom sedimentation processes in the deep sea. A review; Marine Geology, v. 38, p. 51-75.

Damuth, J.E. and Embley, R.W.
1981: Mass transport processes on Amazon Cone, Western Equatorial Atlantic; American Association of Petroleum Geologists Bulletin, v. 65, p. 629-643.

de Smitt, V.P.
1932: Earthquakes in the North Atlantic as related to submarine slides; American Geophysical Union Transactions, v. 13, p. 103-109.

Doxsee, W.W.
1948: The Grand Banks Earthquake of November 18, 1929; Publications of the Dominion Observatory, v. 7, no. 7, p. 323-336.

Edgar, D.C. and Piper, D.J.W.
1979: A new bathymetric map of the middle Laurentian Fan; Maritime Sediments, v. 15, p. 1-3.

Embley, R.W.
1980: The role of mass transport in the distribution and character of deep ocean sediments with special reference to the North Atlantic; Marine Geology, v. 38, p. 23-50.

Fruth, L.S.
1965: The 1929 Grand Banks turbidite and the sediments of the Sohm Abyssal Plain; unpublished M.Sc. thesis, Columbia University, New York, 257 p.

Hampton, M.
1972: The role of subaqueous debris flows in generating turbidity currents; Journal of Sedimentary Petrology, v. 42, p. 775-793.

Heezen, B.C. and Drake, C.L.
1964: Grand Banks slump; Geological Society of America Bulletin, v. 48, p. 221-225.

Heezen, B.C. and Ewing, M.
1952: Turbidity currents and submarine slumps and the 1929 Grand Banks earthquake; American Journal of Science, v. 250, p. 849-873.

King, L.H. and MacLean, B.
1976: Geology of the Scotian Shelf; Geological Survey of Canada, Paper 74-31, 31 p.

Normark, W.R.
Progradation de la levée et les autres caractères du lobe de la deposition dans le cone de Laurentian, le marge Atlantique du Canada; Institut de Géologie du Basin d'Aquataine, Bulletin no. 31. (in press)

Piper, D.J.W.
1975: Late Quaternary deep water sedimentation off Nova Scotia and the western Grand Banks; Canadian Society of Petroleum Geologists, Memoir 4, p. 195-204.

Piper, D.J.W. and Normark, W.R.
Quaternary sedimentation and erosion on the channelled upper Laurentian Fan; Canadian Journal of Earth Sciences. (in press)

Stewart, G.S.
1979: The Grand Banks earthquake of November 18, 1929 and the Bermuda earthquake of March 24, 1978. A comparative study in relation to their intraplate location; EOS, v. 60, p. 312.

Stow, D.A.V.
1977: Late Quaternary stratigraphy and sedimentation on the Nova Scotian outer continental margin; unpublished Ph.D. thesis, Dalhousie University, 360 p.

1981: Laurentian Fan: morphology, sediments, processes and growth pattern; American Association of Petroleum Geologists Bulletin, v. 65, p. 375-393.

Terzaghi, K.
1956: Varieties of submarine slope failures; Proceedings 8th Texas Conference on Soil Mechanics and Foundation Engineering, Special Publication 29, 41 p.

Uchupi, E. and Austin, J.
1979: The stratigraphy and structure of the Laurentian cone region; Canadian Journal of Earth Sciences, v. 16, p. 1726-1752.

Wang, Y., Piper, D.J.W., and Vilks, G.
Surface texture of turbidite sand grains, Laurentian Fan and Sohm Abyssal Plain; Sedimentology. (in press)

21. STRUCTURAL AND LITHOLOGICAL CHRONOLOGY OF THE ARCHEAN HOPEDALE BLOCK AND THE ADJACENT PROTEROZOIC MAKKOVIK SUBPROVINCE, LABRADOR: REPORT 4

Project 780025

Ingo F. Ermanovics, John A. Korstgård[1], and David Bridgwater[2]
Precambrian Geology Division

Ermanovics, I.F., Korstgård, J.A., and Bridgwater, D., Structural and lithological chronology of the Archean Hopedale block and the adjacent Proterozoic Makkovik Subprovince, Labrador: Report 4; in Current Research, Part B, Geological Survey of Canada, Paper 82-1B, p. 153-165, 1982.

Abstract

Archean tectonics in Hopedale block of southern Nain (Nutak) Province are dominated by large scale shears. Two stages of deformation are recognized. Stage one – the Hopedalian – resulted in NW-trending planar structures and SE-plunging linear structures in volcanic rocks (Hunt River belt and Weekes amphibolite) and in already polydeformed tonalites and granodiorites (Maggo gneiss) older than 3200 Ma. Stage two – the Fiordian – resulted in NNE-SSW planar structures and mainly NE-plunging linear structures. This deformation has a sinistral shear sense as evidenced by the deflection of Hopedalian structures; it followed the deposition of Florence Lake volcanics and the emplacement of Kanairiktok intrusions about 2830 Ma ago.

In the southern part of Hopedale block these Archean rocks and structures were deformed during the early Proterozoic and formed the Makkovik Subprovince. Deformation is associated with syn- and post-kinematic phases of the Island Harbour granite emplaced about 1970 Ma ago. Initially deformation was dominated by strain of pure shear type with formation of poorly defined NE-trending zones of ductile simple shear. The boundary between Archean Nain Province and Proterozoic Makkovik Subprovince is defined in rocks of Nain Province along Kanairiktok Bay where one such zone of ductile shear coincides with an amphibole isograd of Proterozoic age.

Introduction

This report summarizes the results of mapping, structural studies and detailed collecting for geochemical and isotopic work during the fourth and final year of this project. The mapping was designed to complete field work for three map sheets at 1:100 000 (Fig. 21.1) covering the areas in NTS 13N, K and O, and complementing work by geologists of the Newfoundland Department of Mines and Energy (e.g. Ryan and Kay, 1982; Hill, 1981). Structural and lithological chronology for the Archean block presented in previous reports (Ermanovics and Raudsepp, 1979; Ermanovics, 1980; Ermanovics and Korstgård, 1981) can be extended into Makkovik Subprovince where it is modified by Proterozoic deformation, metamorphism and intrusive events. The structural and lithological framework was used as a basis for collections from selected outcrops designed to study possible geochemical and isotopic modifications of original early Archean gneisses during later Archean and Proterozoic deformation and high grade metamorphism. Subsidiary collections were made from Proterozoic intrusions in the Makkovik Subprovince for comparison with the lithologically similar and contemporaneous plutonic rocks from the Ketilidian fold belt of South Greenland.

The use of the term Nain Province in this report follows the common usage by geologists of the Newfoundland Department of Mines and Energy and is synonymous with Nutak Province (Douglas, 1972) and Eastern Nain Subprovince of Nain Province (Stockwell, 1982).

The Archean Block

The Hopedale trend

Structures. The earliest recognizable regional trend in Hopedale block (Fig. 21.2) is a NW-striking, steeply mainly SW-dipping planar trend (Fig. 21.3a) combined with a SE-plunging linear trend (Fig. 21.3b). This trend is characteristic of the rocks between Hopedale and the outer coast, but is also found as relicts in the structurally younger Fiord trend areas (Fig. 21.2).

Lithologies. The main rock units having Hopedale trend had a complex history prior to the development of the dominant regional structure mapped as Hopedalian. We recognize the following major rock types:

1. Early amphibolites (Weekes amphibolite, Ermanovics and Raudsepp, 1979). These occur as rafts and inclusions, a few square metres to hundreds of square metres in area, enclosed within grey gneisses. They are veined and partly broken up by the surrounding tonalites and by several generations of younger quartzo-feldspathic gneisses and pegmatite. As the oldest rocks in the coastal area they are provisionally correlated with rocks of the Hunt River belt (Fig. 21.1), a group of amphibolitic and ultramafic rocks forming a 80 km continuous belt trending NNE (Fiordian) in the northwestern part of the area (Ermanovics and Korstgård, 1981; Collerson et al., 1976; Jesseau, 1976). Alternatively the Weekes amphibolites and the grey gneisses surrounding them could represent a basement to rocks of the Hunt River belt.

The Weekes amphibolites are mainly dark rocks with prominent metamorphic layering at a scale of 10-20 cm. Some of the outcrop scale layering is due to concordant sheets of gneiss intruded into the amphibolites and reaction between gneiss and amphibolite. Other layering appears to be due to primary variation in the chemistry of the suite so that between 10 and 45 per cent of some outcrops consists of garnet amphibolite or a pale leucoamphibolite of intermediate composition. The Weekes amphibolites locally contain ultramafic layers (talc-actinolite schist), garnet-rich quartzofeldspathic gneiss (Fig. 12.2b in Ermanovics and Korstgård, 1981), and orthopyroxene-bearing units. No primary sedimentary units have been identified and the amphibolites could represent either basic lavas from a supracrustal succession or layered basic intrusive rocks. The garnet-rich, quartzofeldspathic gneisses of Weekes amphibolite may have some textural and compositional similarities to the Upernavik supracrustal rocks of the Saglek area (Bridgwater and Collerson, 1976).

[1]Department of Geology, Aarhus University, DK-8000 Aarhus C, Denmark
[2]Geological Museum, Copenhagen University, DK-1350 Copenhagen K, Denmark

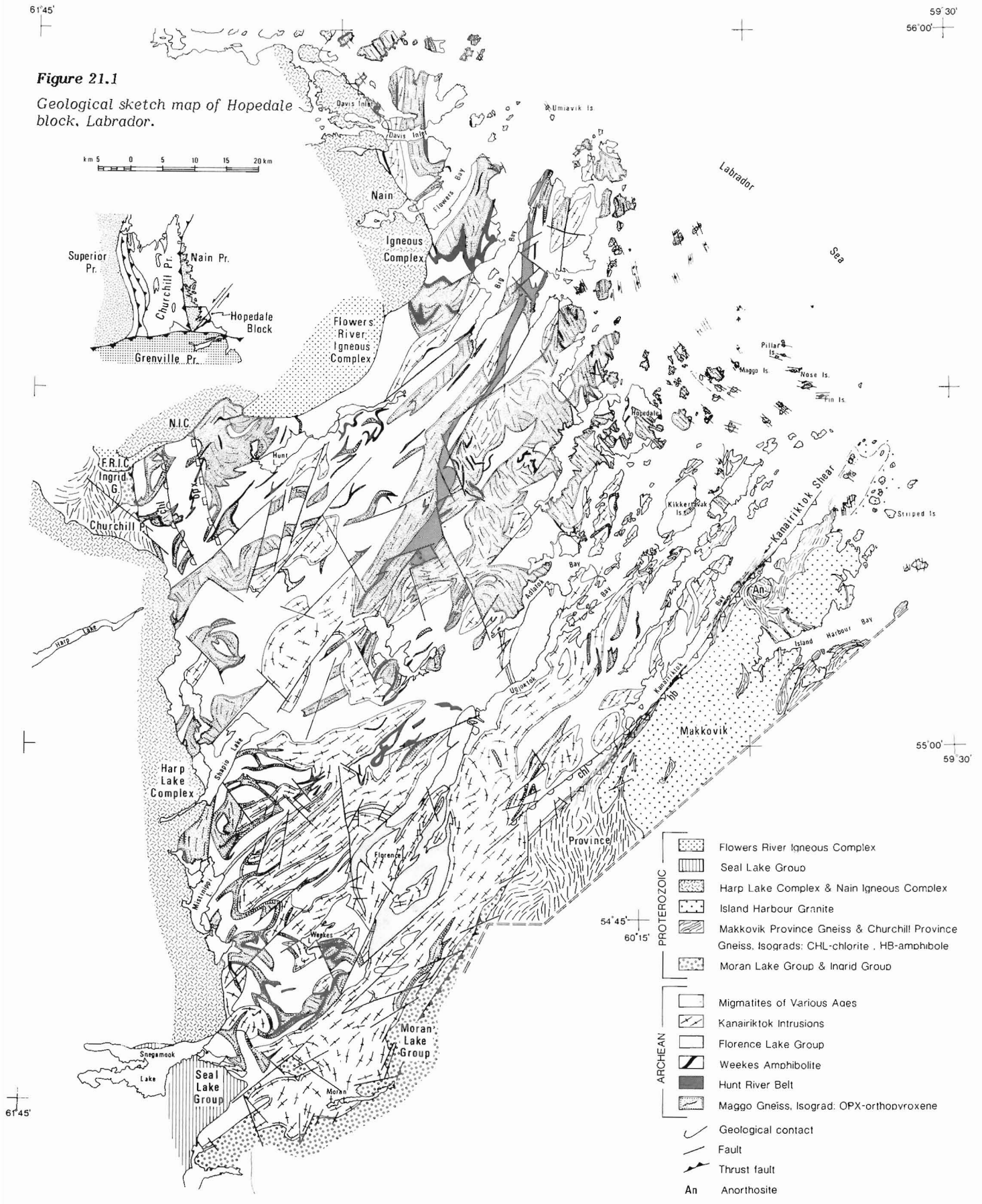

Figure 21.1

Geological sketch map of Hopedale block, Labrador.

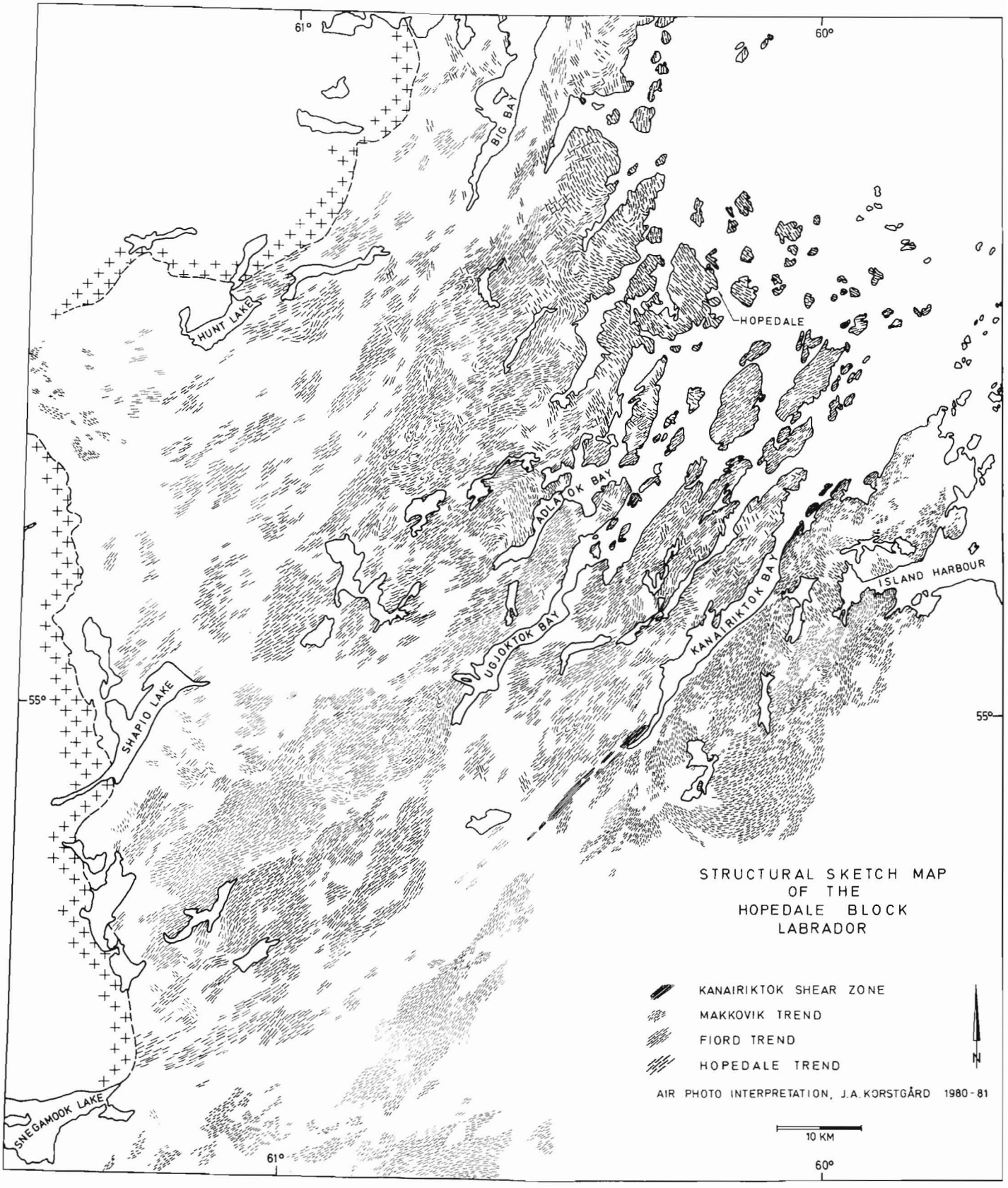

Figure 21.2. *Trends of foliation in the Hopedale block. The Kanairiktok shear zone runs along the southeast coast of Kanairiktok Bay and the Makkovik trend is southeast of the bay. Crosses indicate Elsonian intrusions.*

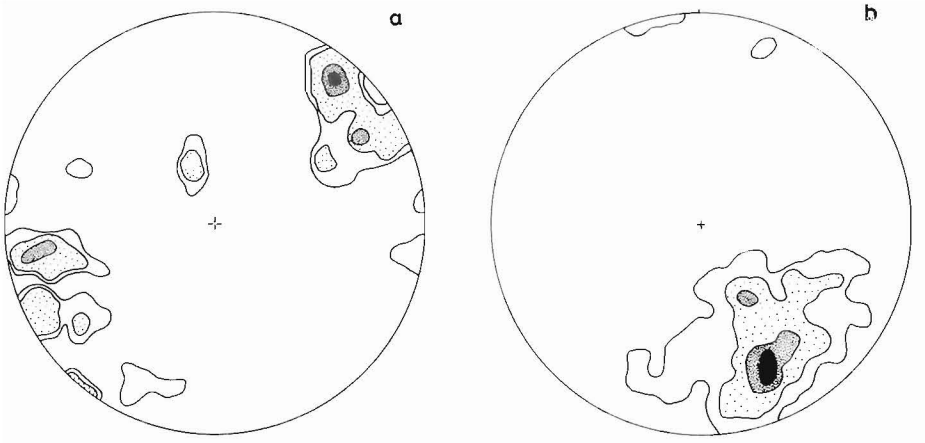

Figure 21.3. *Orientation of structures with the Hopedale trend.*

a – 56 poles to planar structures. Contours at 3%, 5%, 10% per 1% area, maximum 16%.

b – 94 linear structures. Contours at 1%, 5%, 10% per 1% area, maxium 16%. Equal area, lower hemisphere projection.

2. Early grey gneisses (Maggo gneiss, Ermanovics and Raudsepp, 1979). These form the dominant lithology throughout the Archean block but have been modified to such an extent by later processes that we consider the former term Maggo gneiss best restricted to quartzofeldspathic gneiss with Hopedale trend which has not been affected by strong later migmatization (Fig. 21.1). There is a considerable range in composition, from medium grained hornblende-plagioclase-quartz leucotonalite to coarser grained porphyroblastic granodiorites. Relations between individual phases are obscured by later deformation. However we interpret variations in composition seen on outcrop scale to represent primary plutonic layering. The contacts between granodiorite and fine grained leucotonalite suggest that the sequence of lithologies of Maggo gneiss was from early dark phases to progressively more leucocratic rocks.

3. Early amphibolite dykes (Hopedale dykes; Fig. 37.1 in Ermanovics and Raudsepp, 1979). The early grey gneisses are characterized by the presence of concordant to slightly discordant elongate pods and sheets of medium grained amphibolite interpreted as derived from diabase dykes recrystallized and tectonically thinned during one or more phases of post-dyke metamorphism (Fig. 21.4). Dykes may be strongly attenuated and complexly folded to give intricate outcrop patterns in which individual bodies remain remarkably coherent. Both in appearance and in local chronological importance the Hopedale dykes resemble the Saglek dykes of northern Labrador (Bridgwater et al., 1975) and the Ameralik dykes of West Greenland (McGregor, 1973). Detailed studies of the Archean block between Hopedale and Saglek are not complete and are hampered by the presence of large Proterozoic igneous intrusions. However, scattered examples of similar dykes have been observed in Archean gneisses at Ford Harbour east of Nain suggesting it may be possible to use metadiabase dykes to control the chronology throughout the Labrador Archean block.

4. Migmatization in areas with Hopedale trend. The deformation that impressed the planar and linear fabric used to define the Hopedale trend was accompanied by strong recrystallization of the earlier rocks. Local partial melting and migmatization ranged from formation of a few scattered pegmatitic schlieren to wholescale break-up of the early structures in agmatite zones. Transitions between units of comparatively low deformation and migmatization are commonly abrupt so that a new lithological layering develops on a 10-100 m scale between zones with old structures well preserved and zones with a high proportion of neosome. Comparable (and possibly contemporaneous) structures have been described from the Saglek area where the dominant NNW-SSE late Archean shear deformation is concentrated in tightened synforms and is accompanied by migmatization and intrusion of granite sheets (Bridgwater et al., 1975).

The degree of partial melting and possibly the response to the Hopedalian deformation is apparently partly controlled by the composition of the grey gneisses. Where these are leucotonalitic or basic tonalites, the Hopedale dykes are thin and relatively continuous with some evidence of local discordances preserved. Where the country rocks are granodioritic, the dykes are commonly over 50 cm wide, there is less evidence of a pre-dyke foliation in the country rocks and the dyke fragments now appear to 'float' in a more homogeneous matrix (Fig. 21.4c,f).

Migmatization develops as a series of irregular veins, the margins of which are apparently formed by the recrystallization of the earlier grey gneiss probably with the introduction of alkalies so that biotite forms at the expense of hornblende. The centre of the veins are coarse grained and contain markedly more alkali feldspar than seen in the country rocks. Most of the veins, including the diffuse marginal zones, cut through the Hopedale dykes suggesting that there has been considerable post-dyke mobility (Fig. 21.4f). The final products of migmatization are seen at Hopedale village where the amount of mobile material is equal to or exceeds the earlier gneisses. A veined complex is developed in which the earlier rock types can only be recognized as recrystallized schlieren separated and intruded by several generations of leucocratic material.

The only guide to the degree of late migmatization and mobility in the gneisses are the Hopedale dykes and their detailed relations with individual phases in the surrounding gneiss distinguished by slight changes in colour or grain size. As a regional character, the degree of post-dyke migmatization, recrystallization and mobility is greater in the Hopedale gneisses than in the main outcrops of Amitsoq gneiss (West Greenland) or in the best preserved outcrops of Uivak gneiss and Saglek dykes from farther north in Labrador. Recrystallization appears to have taken place in the dykes and country rocks after the former had been folded and separated into boudins so that the fabrics in the dykes or immediate country rocks show no relation to their contorted forms. Pegmatite material emplaced or formed by partial melting during the Hopedale migmatization commonly follows dyke margins. Some thin dykes or apophyses become engulfed in pegmatite and recrystallize as coarser grained biotite-bearing amphibolite that develops irregular cuspate margins against the surrounding quartzofeldspathic rocks. Finally, this process produces narrow, relatively coarse grained basic schlieren in migmatite, the origin of which can only be judged by progressive stages from recognizable dyke to partly digested enclave.

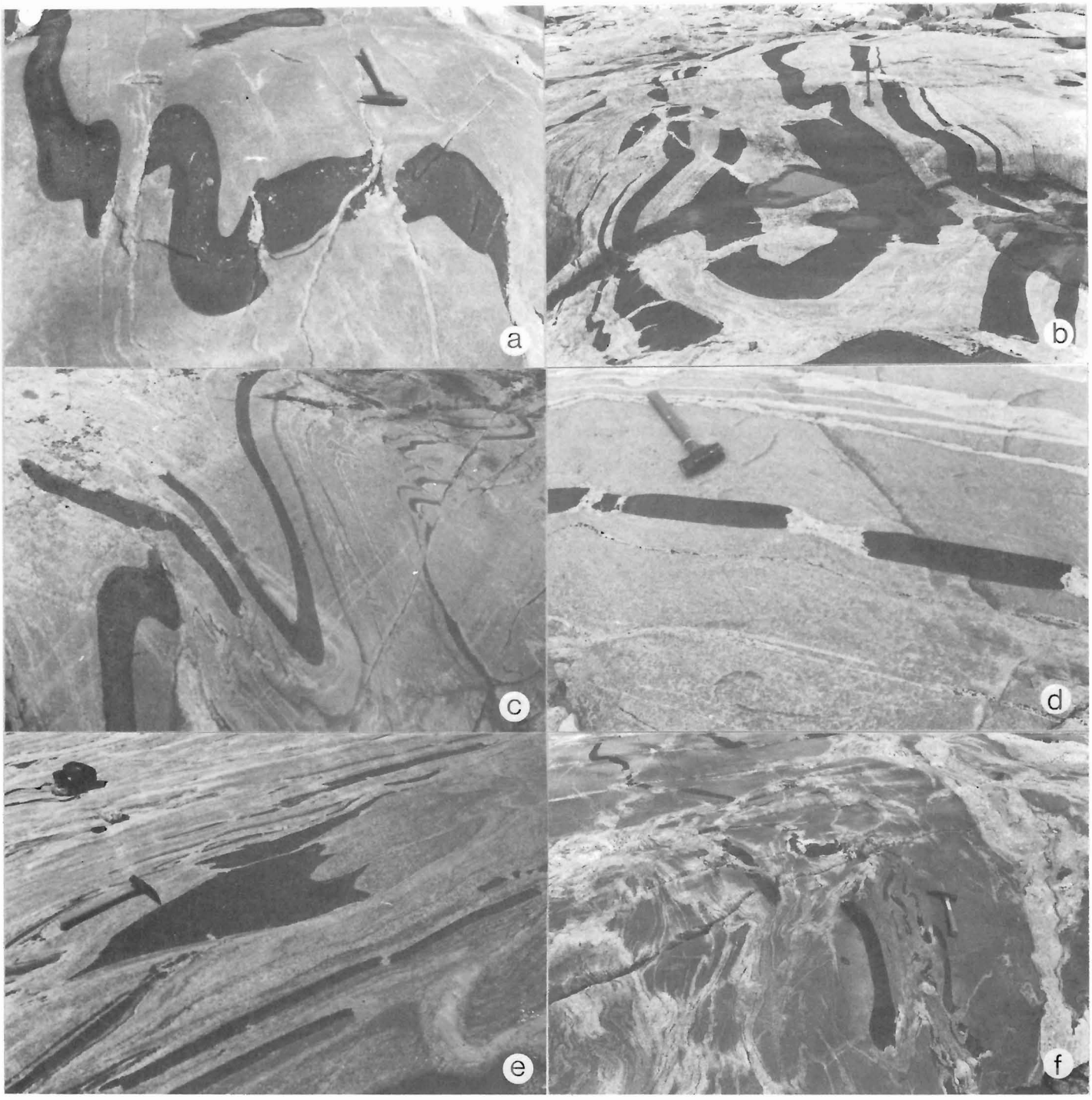

Figure 21.4. *Hopedale dykes in Maggo gneiss deformed with Hopedale trend, (F2 folds):*

a – porphyritic dyke, GSC 189188
b – GSC 189151
c – GSC 177296
d,e,f – dykes affected by Hopedale migmatite, GSC 189149, GSC 177341 and DB 3-81 respectively.

The Fiord trend

Structures. The Fiord trend (Fig. 21.2) is the dominant structural trend of the Hopedale block and parallels the NE-SW main fiord directions. It is particularly well developed in the south of the area between Ugjoktok Bay and Kanairiktok Bay and in a belt extending from the coast southward on either side of the Hunt River belt. The borders of the area affected by this younger deformation are diffuse but the belts map out as 15-30 km wide structures cutting through and partly modifying the older gneisses.

The Fiord trend is characterized by a NNE- to NE-trending subvertical planar fabric (Fig. 21.5a) and a persistent moderately steep NE-plunging linear structure (Fig. 21.5b). In several places within the zones affected by Fiord trend deformation the earlier Hopedale planar structures are preserved but the regional NE-plunging linear Fiord trend structures are well developed.

Lithologies. The lithological units described from the area affected by Hopedale trend deformation form the main rock types in the Fiord trend areas where they show various degrees of structural and metamorphic reworking. In the area between Ugjoktok Bay and Kanairiktok Bay and in the western part of the study area new intrusives ranging from tonalites to granodiorites were emplaced. These are grouped collectively as the Kanairiktok intrusions (Fig. 21.1) and were emplaced after the formation of the Hopedale migmatites but before or at the same time as the Fiord trend deformation.

The Kanairiktok intrusions. In the northeastern part of the map area the Kanairiktok suite (Ermanovics and Raudsepp, 1979; Ermanovics 1980) occurs as group of small elongate plutonic bodies, and extends, as a group, southwestward to underlie large areas of map sheet 13K (Fig. 21.1). The intrusions are composed of homogeneous tonalite to granodiorite with trains of cognate diorite inclusions and occasional net-veined diorite bodies, suggesting the contemporaneous intrusion of acid and basic magma. There are local reactions between acid and basic components to form orbicular diorites which have been stretched by the prevailing Fiord trend deformation.

The contacts of the Kanairiktok plutons are difficult to define since the country rock is largely agmatite gneiss and it is virtually impossible to distinguish between younger intrusive material with inclusions and country rock with an earlier mobilizate, particularly when both types of rock are involved in strong shear movements during and after formation.

Early rocks.

1. Gabbro anorthosites. In addition to the Weekes amphibolites and the Maggo gneisses, the early Archean rocks in areas with Fiord trend include scattered occurrences of coarse grained anorthositic gabbro and leucograbbro set in leucocratic gneisses (Fig. 21.6). The inclusions are identical to the anorthositic inclusions and layers found 200 km north of the present study area (Wiener, 1981) and in other parts of the North Atlantic craton (e.g. Myers, 1975; Bridgwater et al., 1976). The gabbro anorthosites do not occur as continuous units in the coastal outcrops and their relationship to the Weekes amphibolite and early grey Maggo gneisses is not certain. A major body of leucogabbro with identical lithologies and textures to that found in some of the inclusions occurs at margins of the Hunt River belt (Collerson et al., 1976; Jesseau, 1976) and elsewhere with preserved Hopedalian structures. If the correlation of Weekes amphibolites with the Hunt River belt is correct, then the anorthosites can be regarded as a separate lithology within the Weekes amphibolite assemblage.

The gabbro anorthosites exposed in the coastal area (e.g. Umiavik Islands, Fig. 21.1) show a bewildering range in lithologies from coarse grained mafic rocks (largely hornblendic but locally with pyroxene) through to gabbro anorthosite with nearly spherical plagioclase crystals 10-20 cm across set in hornblende (Fig. 21.6c,e). The anorthositic rocks were subjected to varying degrees of deformation before their inclusion in their present quartzofeldspathic host. Adjacent fragments separated by 2-3 m of host rocks may show the complete range in both lithology and deformation state. There has either been considerable transport of material or the original body was layered on a scale of 1-2 m and was affected by very inhomogeneous deformation. Contacts between the matrix and inclusions are generally sharp (Fig. 21.6b,c). Individual fragments are not elongated parallel with the regional strike, and layering in the fragments is randomly orientated (Fig. 21.6b). The quartzofeldspathic matrix is generally more leucocratic and coarse grained than the regional gneiss, suggesting that at one stage original layered leucogabbros were broken up by pegmatitic granitic sheets (possibly during the Hopedale migmatization event). The matrix contains irregular fragments of white feldspar apparently derived from mechanical breakdown either of the included material or an originally coarser grained host. Layering in the host rock is highly irregular and is controlled by the large ductility contrast between the massive very coarse grained competent inclusions and the more easily deformed and mobilized host.

2. Weekes amphibolites, early grey gneisses and Hopedale migmatites. The obvious effect of the Fiord trend deformation is the rotation of the earlier fabrics described above. Over large parts of the area this was accompanied by marked changes in the lithology of the earlier units on both a microscopic and mesoscopic scale suggesting that the rocks were recrystallized under conditions approaching partial melting. The grey granodioritic gneisses, which are probably the most extensive of the earlier rocks, become coarser grained with the growth of

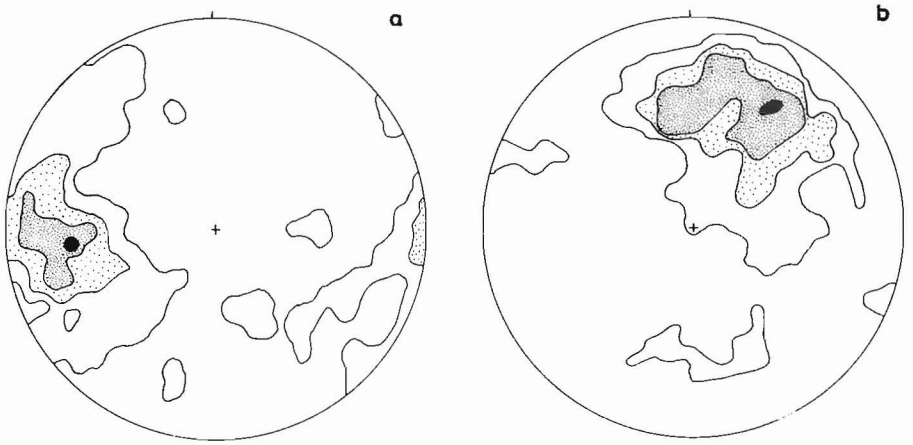

Figure 21.5. *Orientation of structures with the Fiord trend:*

a – 154 poles to planar structures. Contours at 1%, 3%, 5% per 1% area, maximum 9%

b – 191 linear structures. Contours at 1%, 3%, 5% per 1% area, maximum 9%. Equal-area, lower hemisphere projection.

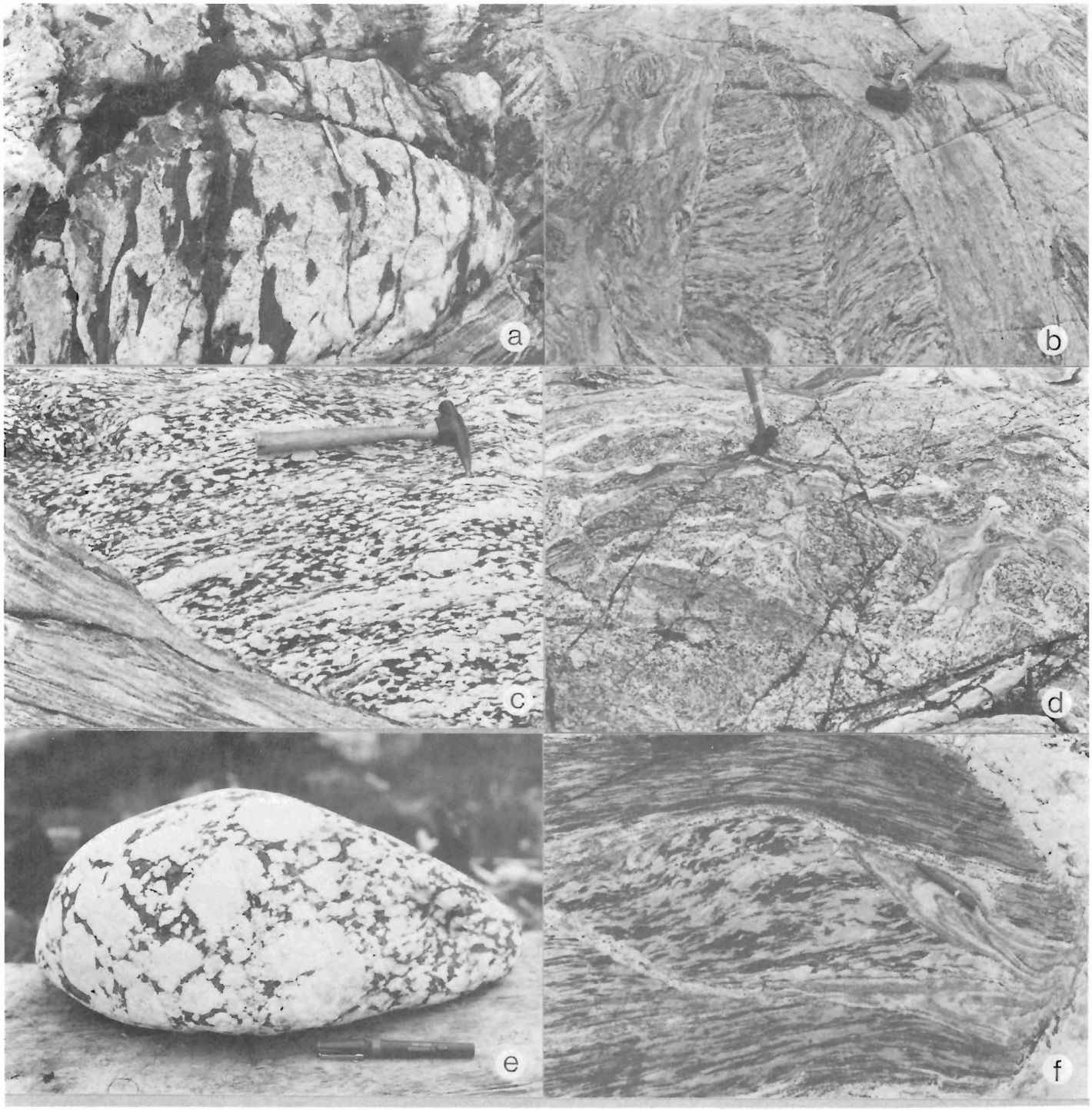

Figure 21.6. *Gabbroic anorthosites:*

a – in Hopedale trend area, GSC 189126
b,c,d – in Fiord trend area, GSC 189115, 189121 and 189122 respectively
e – tectonic-shaped inclusion from area of Figure b, GSC 189239
f – in Proterozoic Makkovik trend area, GSC 189091.

a
b
c
d

new hornblende crystals and an obliteration of earlier structures. There is a widespread development of "agmatites" in which coarser grained quartzo-feldspathic gneisses enclose fragments of Weekes amphibolite, layered grey gneiss and Hopedale migmatite ranging from a few metres to centimetres in diameter. The formation of agmatites is interpreted as a more general case of the breakup of earlier layered rocks from the layered anorthosite described above. The agmatites are particularly abundant in 3 to 5 km wide zones along the northeastern margins of the Kanairiktok intrusions, and agmatite formation is at least partly connected to the emplacement of those bodies. In places, dyke-like sheets of homogeneous quartzofeldspathic gneiss crowded with disoriented older gneiss fragments cut through the regional gneisses and have the appearance of having crystallized from younger magmas intruded into the complex during deformation. However, only a very small proportion of the outcrops show convincing evidence that the matrix was a melt at the time of the formation of the agmatites. Characteristically the textures of the gneisses forming the matrix to the agmatites appear as though they were formed by mechanical breakdown of older rocks. We suggest that many of the agmatites were formed mechanically when one component in the gneisses became markedly more ductile than other layers and became mobile, possibly on a regional scale (cf. Talbot, 1979). We suggest that this occurred during the intense deformation associated with the formation of the Fiord trend and was probably aided by a rise in local thermal gradients related to the intrusions of the Kanairiktok granitoid suite.

Archean metamorphism

The Archean gneiss block is polymetamorphic. We have no convincing field evidence about the pre-Hopedale dyke metamorphic history of the area except to note that it must have reached amphibolite facies. There is no evidence for an early granulite facies event (cf. West Greenland, Griffin et al., 1980, or the Saglek area, Bridgwater et al., 1978). On the coast, metamorphism during both the formation of the Hopedale migmatites and the Fiord trend was at amphibolite facies grade and during both events reached temperatures and pressures at which partial melting of quartzofeldspathic material took place. Inland along the margin of the Proterozoic Churchill Province (Fig. 21.1) a deeper level is exposed and granulite facies conditions were attained earlier than the formation of the Fiord trend. These rocks were subsequently partly downgraded following the deposition of the Proterozoic cover (e.g. Ingrid group).

Posttectonic diabase dykes (Kikkertavak dykes)

The Archean block is cut by several generations of basic dykes which postdate the Archean metamorphism and tectonism but the majority of which predate strong Proterozoic deformation and plutonism seen in the Makkovik Subprovince to the southeast. Although there are intersections between different generations no regional chronology has been worked out since most of the dykes are concentrated in areas affected by the Fiord trend and strike subparallel to the regional foliation (Fig. 21.7). Two types of early Proterozoic intrusion are recognized: normal dykes up to 50-100 m wide that can be followed for tens of kilometres, and less regular gabbroic pods that commonly form more isolated intrusions elongated with the regional NE-SW structure. There is a regional tendency for a greater concentration of dykes and for a greater irregularity in intrusive form as the margin of the Proterozoic subprovince is approached.

The dykes vary from olivine gabbros to fine grained tholeiitic basalts. Some are full of inclusions of country rock concentrated centrally. Others contain large plagioclase phenocrysts in places concentrated along one margin or in apophyses. Most of the dykes within 5-10 km of the border of the Proterozoic subprovinces show some postmagmatic recrystallization. This is also seen in the country rocks and is usually concentrated along distinct brittle fracture zones with reddening and the formation of some epidote.

The Proterozoic Block

The transition from the Archean to the Proterozoic block (the Makkovik Subprovince) is sudden and takes place within perhaps less than one kilometre. In the coastal region the boundary is situated somewhere in Kanairiktok Bay and the actual transition is not exposed. Three main features mark the boundary: reworking of Archean rocks and Kikkertavak dykes, emplacement of major masses of granitic rocks, and formation of a major transcurrent shear zone at the northwestern margin of the Proterozoic, along the southeast coast of Kanairiktok Bay.

The Makkovik trend

Structures. No drastic change in structure is apparent from the structural sketch map of Figure 21.2 across the Archean/Proterozoic boundary. Planar structures are more variable in Makkovik Subprovince (Fig. 21.8a), mainly N-S but do not define a good trend. Lineations however, show a radical change from shallow NE-plunging in rocks of the Archean Fiord trend to subvertical in the Makkovik Subprovince (Fig. 21.8b), indicating a major change in deformation pattern.

Archean lithologies. Recognition of Archean lithologies within the Makkovik Subprovince is facilitated by the occurrence of deformed and metamorphosed equivalents of the Kikkertavak dykes (Ermanovics, 1980). These rocks now occur as foliated amphibolites subparallel to planar structures in quartzofeldspathic gneisses (Fig. 21.7c,d). They have acquired strong planar and linear structures (Fig. 21.7d) and have been rotated into parallelism with country rock structures. In spite of the strong deformation the dykes still occur as coherent bodies and have preserved their character as originally intrusive rocks (Fig. 21.7c).

The country rocks of the Kikkertavak metadykes can be separated into two groups. The first encompasses reworked equivalents of what was probably Weekes amphibolite, early grey gneisses, Hopedale migmatites and similar rocks in the Fiord and Hopedale trend areas. Although recognition of the various subdivisions of Archean gneiss becomes increasingly

---

Figure 21.7. *Kikkertavak dyke and metadyke, and reworked xenolith in Island Harbour granite:*

- *a – Kikkertavak dyke subconcordant to planar structure in Fiord trend gneiss, JK-919*
- *b – xenolith of Archean age deformed during the Proterozoic and intruded by an early phase of Island Harbour granite (top one third of photo). The xenolith comprises the following lithologies from left to right: Kanairiktok granitoid, Maggo gneiss, gabbroic anorthosite and Fiord-trend migmatite; the xenolith is cut by a vein of granitic aplite. JK-1123*
- *c – Kikkertavak metadyke in reworked Archean gneiss with Makkovik trend (Makkovik gneiss)*
- *d – steeply plunging lineation in Kikkertavak metadyke of, Figure c, JK-830.*

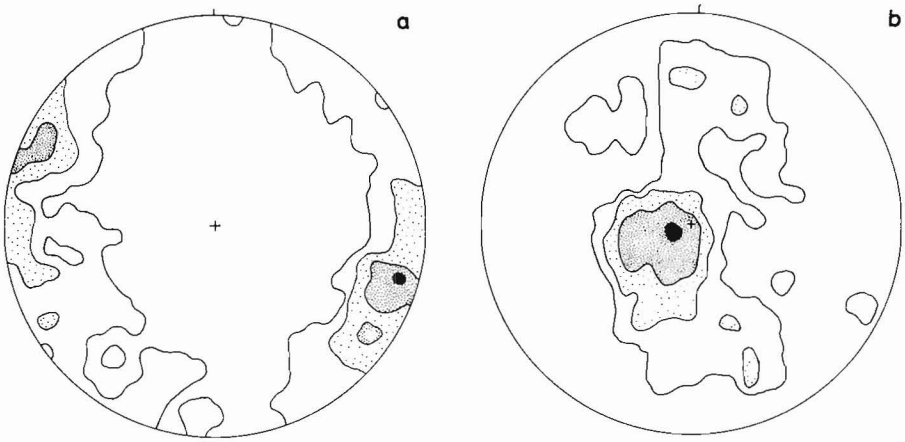

Figure 21.8. *Orientation of structures with the Makkovik trend:*

a – 193 poles to planar structures. Contours at 1%, 3%, 5% per 1% area, maximum 8%

b – 162 linear structures. Contours at 1%, 3%, 5% per 1% area, maximum 10%. Equal area, lower hemisphere projection.

difficult southwards into the Proterozoic block, some units such as the gabbroic anorthosites can survive as major inclusions (area "An" in Fig. 21.1) or as rafts virtually unchanged in field appearance (Fig. 21.7b). Recognition of distinctive rock types such as the gabbroic anorthosites may allow estimates of the total extent of early Archean rock involved in the Proterozoic mobile belt. The Proterozoic reworking impresses a very well marked schistosity on both older gneisses and metamorphosed Kikkertavak dykes indicating, at least locally, very high strains that consequently hamper recognition of the older rocks.

The second group or rocks which are cut by metamorphosed Kikkertavak dykes, and therefore are of Archean age, are the Kanairiktok granitoids. Where these rocks are relatively little affected by Proterozoic reworking they are clearly recognizable on account of their uniform nature, relatively coarse grain size, cognate diorite inclusions, and xenoliths of older gneisses.

Proterozoic lithologies. Over fifty per cent of the study area south of the Proterozoic margin is occupied by major intrusive masses. These range from coarse grained hornblende gabbroic rocks that include appinites (Ryan and Kay, 1982) with spectacular layering through to true granites. Individual outcrops may contain up to 5 generations of basic, intermediate and granitic dykes many of which are net-veined or contain pillowed structures of a mafic component in a lighter phase. Many of the dykes were emplaced along active shear zones and developed foliations. Some of the basic dykes show evidence of crystallization under stress with leucocratic material squeezed out to leave hornblendite dykes. Both the lithologies and mechanisms of emplacement are closely comparable to the Proterozoic intrusions of the South Greenland Ketilidian mobile belt (Allaart, 1976; Watterson, 1965). The youngest plutonic rocks mapped are coarse grained, porphyritic posttectonic granites and granodiorites (Island Harbour granites, Fig. 21.1). Locally these show mineral layering and we interpret them as thick sheet-like bodies. They are cut by swarms of red weathering amphibole diorite sills (Fig. 2.4, in Ermanovics, 1980).

The main phases of the Island Harbour granite have textural, chemical and possibly temporal similarities with coarse grained granodiorites of the Benedict Mountains Intrusive Suite (Gower, 1981) located 100 km southeast of Island Harbour Bay. Both intrusions have similar K + Na + Ca values (Fig. 21.9). However, normative plots of Qz + Or + Pg and Qz + Ab + Or of both populations show that the Island Harbour granite is more siliceous. The normative femic content of the Island Harbour granite is 6.5 per cent and that of the Benedict Mountains suite is 7.7 per cent.

The Kanairiktok shear zone

A linear zone of strong deformation separates the Archean block to the north and the Proterozoic Makkovik Subprovince to the southeast. (Ermanovics, 1980). The zone strikes NE, is less than 2 km wide, and can be followed for more than 50 km. It is situated along the southeast coast of Kanairiktok Bay where its southeastern boundary is exposed at several localities along the bay. The northern boundary lies somewhere in the bay and is not well exposed in the inland areas to the southwest. The zone represents the last major structural event in the Hopedale block.

Structures. Linear and planar structures in the Kanairiktok shear zone are characterized by a high degree of parallelism. Linear structures in the zone are subhorizontal within subvertical planar structures trending NNE (Fig. 21.10a,b). Earlier structures are clearly reoriented into the shear zone direction and the geometry of reorientation is consistent with a sinistral simple shear deformation.

Lithologies. Deformation in the Kanairiktok shear zone probably affected most of the rocks known from the Archean block. However, within the zone deformation was so intense that most rocks are not recognizable. Southeast of the shear zone less deformed rocks can be traced into the zone but rocks were already deformed at least once during Proterozoic plutonic activity before being sheared. A porphyritic variety of the Island Harbour granite is very common within and east of the shear zone. Outside the zone it is only slightly deformed whereas it becomes progressively more deformed as the shear zone is approached and finally develops into mylonite. Numerous pegmatites of various generations cut the gneisses and the porphyritic granite in the vicinity of the shear zone. They all have a tectonite fabric and appear to have intruded during the final stages of deformation.

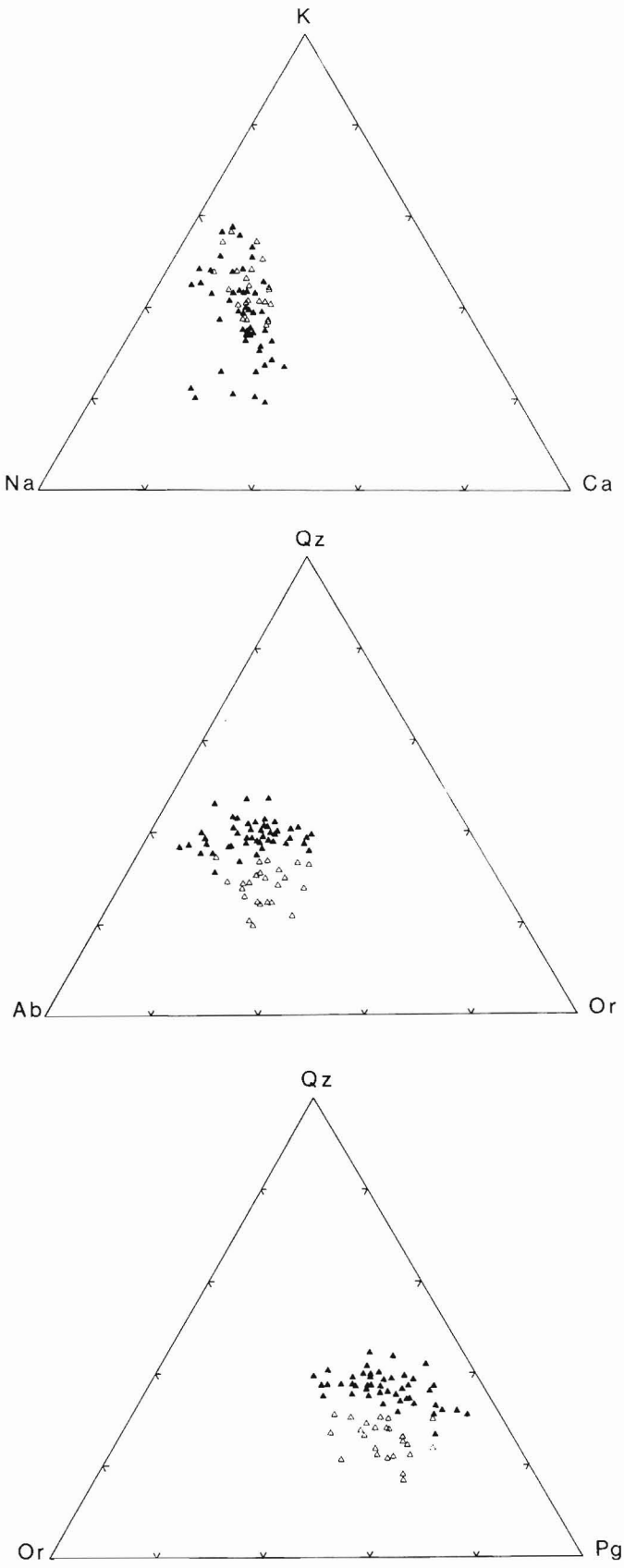

Summary

Previous reports (Ermanovics and Raudsepp, 1979; Ermanovics, 1980; Ermanovics and Korstgård, 1981) and maps placed on open file (Ermanovics, 1979, 1981a, 1981b) give the results and show the progress made in gaining an understanding of the geology of the study area since 1978. A simplified chronology of events in Archean Hopedale block and adjacent Proterozoic terranes, not all of which are discussed in this report, is as follows:

1. (?) Deposition of supracrustal rocks (Hunt River belt); mainly tholeiitic flows, ultramafic rocks and mafic dykes; minor greywackes and rare Al-rich sediments.
2. Intrusion of anorthositic, gabbroic and dioritic rocks; minor ultramafic rocks.
3. (?) Intrusion of tonalite and porphyritic granodiorite (Maggo gneiss) associated with Weekes amphibolite (Hunt River remnants).
4. Deformation and metamorphism.
5. Intrusion of diabase dykes (Hopedale dykes).
6. Deformation and metamorphism. Upper amphibolite facies metamorphism accompanied by migmatization. Deeper levels are metamorphosed to granulite facies either in this event or in event 4. Development of northwest-striking planar trend and southeast-plunging linear trend defined as Hopedalian. A Rb-Sr whole-rock age of either this or an earlier metamorphism is about 3230 Ma. (N. Grant, Miami University, Oxford, Ohio, personal communication, 1981).
7. Deposition of Florence Lake supracrustals (Fig. 21.1), 30 % mafic to intermediate lavas and 60 % intermediate to felsic volcanoclastic sediments; minor serpentinites and limestones.
8. Intrusion of Kanairiktok granitoids about 2830 Ma ago (U-Pb zircon concordia age, D. Loveridge, GSC. personal communication, 1981). Contact metamorphism and migmatization over large areas. Intrusions may be in part coeval with deformation of event 9.
9. Deformation and metamorphism. Hopedalian structures are deflected into a northeast-striking planar and northeast-plunging linear trend defined as Fiordian. Metamorphism is at lower amphibolite facies. Regional retrograde metamorphism (lower greenschist facies) confined mainly to shear zones may be related to tectonic activity in adjacent Churchill and Makkovik provinces in early Proterozoic time. Rb-Sr whole-rock and K-Ar hornblende analyses of sheared Kanairiktok granitoids yield errorchron ages (e.g. 2316 ± 530 Ma) and updated ages, e.g. 2390 Ma and 1860 Ma) respectively, indicative of Proterozoic time. (N. Grant personal communication, 1981; R.D. Stevens, G.S.C., personal communication, 1981).
10. Intrusion of Kikkertavak diabasic and gabbroic dykes in early Aphebian time. These are metamorphosed on approaching the Churchill and Makkovik provinces and contain schistose margins throughout the study area.

Figure 21.9. *Ternary plots of porphyritic main phases of the Island Harbour granite (closed triangles) and the Benedict Mountains Intrusive Suite (open triangles; data from C. Gower, Newfoundland Department of Mines and Energy, personal communication, 1982). K, potassium; Na, sodium; Ca, calcium; Normative values (CIPW, Mesonorm with biotite and hornblende option); Qz, quartz; Ab, albite; Or, orthoclase; Pg, plagioclase, (Ab + An) Normative femic content of Island Harbour granite is 6.5 per cent; that of the Benedict Mountains Suite is 7.7 per cent.*

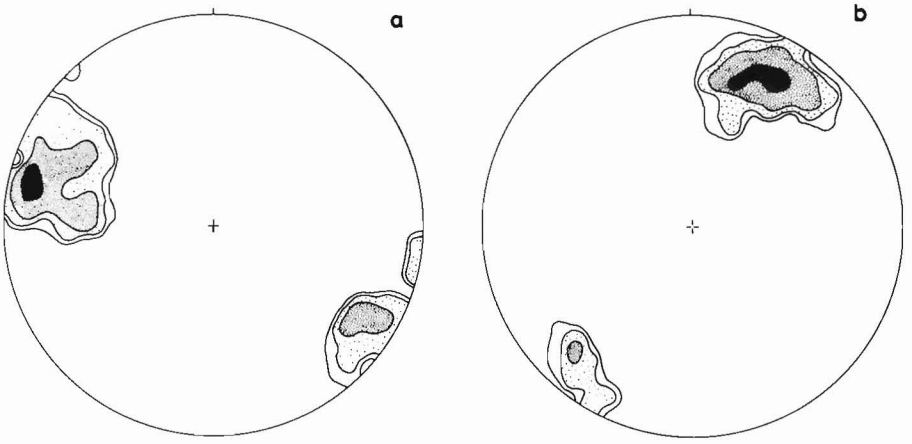

Figure 21.10. *Orientation of structures in the Kanairiktok shear zone:*

a – 58 poles to planar structures. Contours at 3%, 5%, 10% per 1% area, maximum 20%

b – 59 linear structures. Contours at 3%, 5%, 10% per 1% area, maximum 17%. Equal-area, lower hemisphere projection.

11. Deposition of Moran Lake Group and Ingrid group: the former is a succession of marginal basin deposits overlain by basalts; the latter is a succession of subaerial mafic lavas and polymictic conglomerates.

12. Deformation and metamorphism. Fiordian structures are transformed initially to poorly defined NE-SW planar and well defined subvertical linear trends, and subsequently to narrow NNE-trending transcurrent shear zones. Metamorphism is at amphibolite facies outside the shears (e.g. the Kanairiktok shear zone). This structural trend defines Proterozoic Makkovik Subprovince southeast of Kanairiktok Bay. A N-S planar and as yet unspecified linear trend defines Churchill Province west of Ingrid group.

13. Intrusion of Island Harbour granitoids east and south of Kanairiktok Bay in Makkovik Subprovince. Early phases are syntectonic to event 12. The main and later phases are posttectonic and yield a Rb-Sr whole-rock age of 1810 Ma (Striped Island, N. Grant, personal communication, 1981) and a U-Pb zircon concordia age of 1970 Ma (possibly an early syntectonic phase of the Island Harbour granite, Brooks 1982).

14. Intrusion of subhorizontal dioritic sills and dykes in Makkovik Subprovince and in Archean terrane immediately west of Kanairiktok Bay. "A Rb-Sr whole-rock age for these dykes from Striped Island is 1640 ± 59 Ma (B. Fryer, Memorial University, personal communication, 1982)."

15. Intrusion of Harp Lake Complex (Emslie, 1980) and Nain Igneous Complex (Hill, 1981), members of a group of Elsonian plutonic complexes (Fig. 21.1). A U-Pb zircon age of associated olivine-bearing granites is 1450 Ma for the Harp Lake Complex.

16. Deposition of anorogenic subaerial plateau basalts and sediments of the Seal Lake Group (Fig. 21.1) about 1320 Ma ago (Baragar, 1981).

17. Intrusion of Harp (?) diabase dykes. A preliminary Rb-Sr whole-rock age is about 1200 Ma from fresh diabase on the west shore of Kanairiktok Bay (F. Voner, Miami University, Oxford, Ohio, personal communication, 1982).

18. Intrusion of peralkaline granites and associated felsic volcanic rocks of the Flowers River Igneous Complex (Hill, 1981; Fig. 21.1). A U-Pb zircon concordia age of peralkaline granite is 1270 Ma. (Brooks, 1982).

Acknowledgments

We thank B. Ryan and R. Wardle of the Newfoundland Department of Mines and Energy for their help in providing us with a better understanding of the regional geology of Labrador. I.F. Ermanovics is grateful to student assistants N. Fraser (University of Toronto), S. Perreault, (University of Montreal) and J. Scodnick (Concordia University) for their assistance during the 1981 field season. A. Davidson kindly read and improved the manuscript of this report.

References

Allaart, J.H.
1976: Ketilidian mobile belt in South Greenland; in Geology of Greenland, ed. A. Escher and W. Watt; Geological Survey of Greenland, p. 121-151.

Baragar, W.R.A.
1981: Tectonic and regional relationships of the Seal Lake and Bruce River magmatic provinces; Geological Survey of Canada, Bulletin 314, 72 p.

Bridgwater, D., Collerson, K.D., Murst, R.W., and Jesseau, C.W.
1975: Field characters of the early Precambrian rocks from Saglek, coast of Labrador; in Report of Activities, Part A, Geological Survey of Canada, Paper 75-1A, p. 287-296.

Bridgwater, D. and Collerson, D.
1976: The major petrological and geochemical characters of the 3,600 m.y. Uivak gneisses from Labrador; Contributions to Mineralogy and Petrology, v. 54, p. 43-59.

Bridgwater, D., Collerson, K.D., and Myers, J.S.
1978: The development of the Archean gneiss complex of the North Atlantic region; in Evolution of the Earth's Crust, ed. D.H. Tarling, Academic Press, London, p. 18-36.

Bridgwater, D., Keto, L., McGregor, V.R., and Myers, S.
1976: Archean gneiss complex of Greenland; in Geology of Greenland, ed. A. Escher and W. Watt; Geological Survey of Greenland, p. 19-75.

Brooks, C.
1982: Third report on the geochronology of Labrador; Department of Mines and Energy, Newfoundland, Internal Report.

Collerson, K.D., Jesseau, W.C., and Bridgwater, D.
1976: Contrasting types of bladed olivine in ultramafic rocks from the Archean of Labrador; Canadian Journal of Earth Sciences, v. 13, p. 442-450.

Douglas, R.J.W.
1972: A revision of Precambrian structural provinces in northeastern Quebec and northern Labrador: Discussion; Canadian Journal of Earth Sciences, v. 9, p. 925-930.

Emslie, R.F.
1980: Geology and petrology of the Harp Lake Complex, central Labrador: An example of Elsonian magmatism; Geological Survey of Canada, Bulletin 293, 136 p.

Ermanovics, I.F.
1979: Geology Adlatok Bay-Florence Lake area, Labrador; Geological Survey of Canada, Open File 580.

1980: Geology of the Hopedale block of Nain Province Labrador: Report 2, Nain-Makkovik boundary zone; in Current Research, Part B, Geological Survey of Canada, Paper 80-1B, p. 11-15.

1981a: Geology, Ingrid Group map-area, Newfoundland (13N/5); Geological Survey of Canada, Open File 755.

1981b: Geology, Hunt River map-area Labrador, Newfoundland (parts of 13N/7, 9, 10, 15, 16); Geological Survey of Canada, Open File 778.

Ermanovics, I. and Raudsepp, M.
1979: Geology of the Hopedale block of eastern Nain Province Labrador: Report 1; in Current Research, Part B, Geological Survey of Canada, Paper 79-1B, p. 341-348.

Ermanovics, I. and Korstgard, J.A.
1981: Geology of Hopedale block and adjacent areas, Labrador: Report 3; in Current Research, Part A, Geological Survey of Canada, Paper 81-1A, p. 69-76.

Gower, F.
1981: The geological and geochemical characteristics of the Benedict Mountains Intrusive Suite, Labrador; in Abstracts, Geological Association of Canada, Annual Meeting, p. A 22.

Griffin, W.L., McGregor, V.R., Nutman, A., Taylor, P.N., and Bridgwater, D.
1980: Early Archean granulite-facies metamorphism south of Ameralik, West Greenland; Earth and Planetary Science Letters, v. 50, p. 59-74.

Hill, J.D.
1981: Geology of the Flowers River area, Labrador; Newfoundland Department of Mines and Energy, Report 81-6, 40 p.

Jesseau, C.W.
1976: A structural, metamorphic and geochemical study of the Hunt River supracrustal belt, Nain Province, Labrador; unpublished M.Sc. thesis, Memorial University of Newfoundland.

Myers, J.S.
1975: Igneous stratigraphy of Archaean anorthosite, at Majorqap gâva, near Fiskenaesset, Southwest Greenland; Geological Survey of Greenland, Report 74, 22 p.

McGregor, V.R.
1973: The early Precambrian gneisses of the Godthåb district, West Greenland; Philosophical Transactions of the Royal Society of London, Part A, v. 273, p. 343-358.

Ryan, B. and Kay, A.
1982: Basement-cover relationships and plutonic rocks in the Makkovik Subprovince, north of Postville coastal Labrador (13J/13, 13 0/4); in Current Research, Newfoundland Department of Mines and Energy, Report 82-1, p. 109-121.

Stockwell, C.H.
1982: Proposals for time classification and correlation of Precambrian rocks and events in Canada and adjacent areas of the Canadian Shield, Part 1: A time classification of Precambrian rocks and events; Geological Survey of Canada, Paper 80-19, 135 p.

Talbot, C.J.
1979: Infrastructural migmatitic upwelling in East Greenland interpreted as thermal convective structures; Precambrian Research, v. 8, p. 77-93.

Watterson, J.
1965: Plutonic development of the Ilordleq area, South Greenland. I: Chronology, and occurrence and recognition of metamorphosed basic dykes; Geological Survey of Greenland, Bulletin 51, 147 p.

Wiener, W.
1981: Tectonic setting, rock chemistry, and metamorphism of an Archean gabbro-anorthosite complex, Tessiuyakh Bay, Labrador; Canadian Journal of Earth Sciences, v. 18, p. 1409-1421.

22. THE NEW INTERNATIONAL GEOMAGNETIC REFERENCE FIELDS: HOW GOOD ARE THEY?

Project 730081

K.G. Shih and Ron Macnab
Atlantic Geoscience Centre, Dartmouth

Shih, K.G. and Macnab, Ron, The new International Geomagnetic Reference Fields: how good are they?; in Current Research, Part B, Geological Survey of Canada, Paper 82-1B, p. 167-168, 1982.

Abstract

Theoretical values of the earth's main magnetic field have been calculated by evaluation of the new International Geomagnetic Reference Fields and compared with selected multiyear sets of marine magnetic data. The new reference fields are better than the old at modelling the main magnetic field and its secular variation. When applied to large amounts of data, the new model may increase computer execution time; workers who only have access to limited computer resources would benefit from a simpler but equivalent formulation of the model to speed up the process.

The New Reference Fields

Five new International Geomagnetic Reference Fields have been recently proposed as a computational model for the earth's main magnetic field and its secular variation (IAGA, 1981). This model is intended to replace older geomagnetic reference fields – IGRF 1965 and IGRF 1975 – that exhibit serious deficiencies in their secular variation components (Dawson and Newitt, 1978).

The new model consists of: three definitive reference fields for the years 1965.0, 1970.0, and 1975.0 (DGRF 1965, DGRF 1970, and DGRF 1975); a provisional reference field for the interval 1975.0-1980.0 (PGRF 1975); and a predictive reference field for the interval 1980.0-1985.0 (IGRF 1980). The provisional reference field PGRF 1975 will be superseded if and when a definitive reference field for 1980 is adopted (which may be different from IGRF 1980).

Each definitive reference field is a 120-term spherical harmonic expansion that expresses the main geomagnetic field at a particular date: 1965.0, 1970.0, or 1975.0. The predictive reference field incorporates a similar 120-term main-field expression for 1980.0, plus an 80-term secular variation expression for 1980.0-1985.0.

In this proposed scheme, the main field at a particular date within the interval 1965.0-1975.0 is derived in a two-step process: (1) linear interpolation of the coefficients of the appropriate definitive reference fields; (2) evaluation of the 120-term expansion using the new coefficients. For instance, to calculate the magnetic field at a given location for the date 1973.5, one would first interpolate the DGRF 1970.0 and DGRF 1975.0 coefficients, then use the new coefficients to compute the 120-term expansion.

Field and variation values for the 1975.0-1980.0 interval are derived by a process similar to that described above, involving the DGRF 1975 coefficients and the IGRF 1980 main-field coefficients. Values for the 1980.0-1985.0 interval are derived directly from IGRF 1980, which evaluates both the main field and the secular variation.

We recently reported on comparisons between various candidate models for the new geomagnetic reference fields using sample AGC data sets (Shih and Macnab, 1982). Following IAGA's publication of the proposed model coefficients, we set out to check the performance of the recommended reference fields by applying them to some of the data sets that were used in our previous investigation.

Test Data and Their Locality

Data were extracted from six cruise files spanning the interval 1968-1979 inclusive, and restricted to the one-degree square 40°-41°N, 59°-60°W. The cruise tracks represented by these data are a composite of survey and reconnaissance patterns that cut through various parts of the one-degree square.

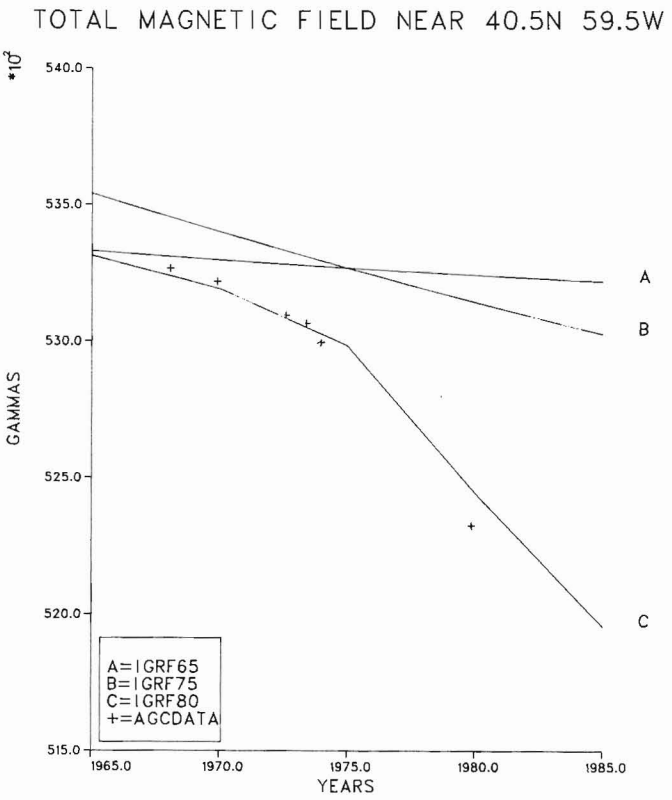

Figure 22.1. *Comparison of six AGC marine magnetic data sets to theoretical values of the earth's main magnetic field at 40.5°N, 59.5°W. Data sets were extracted from a one-degree square in the northwest Atlantic centred at 40.5°N, 59.5°W, and averaged for comparison purposes. Theoretical values of the main field were derived from the now superseded IGRF 1965 and IGRF 1975 models (lines A and B, respectively), and the new standard reference fields: DGRF 1965, DGRF 1970, DGRF 1975, and IGRF 1980 (line C).*

This particular one-degree square was selected because: (a) several cruises had worked in the area over the years; (b) it lies in the Quiet Magnetic Zone (QMZ), a band of low magnetic relief located over the Northwest Atlantic abyssal plain, and oriented roughly parallel to the continental shelf. The magnetic anomaly field in the one-degree square ranges between a few scattered highs and lows of ± 50 nanotesla; the mean value over the area is close to zero. This is a favourable region for the comparison of multiyear sets of overlapping and contiguous marine magnetometer data, because variations caused by local features in the anomaly field are relatively small.

Our approach here is somewhat analogous to that of a land-based surveyor, who reoccupies a fixed station several times over a period of years in order to obtain some indication of long-term magnetic variations in that locality. In the marine situation, it is difficult to establish an equivalent oceanic reference point with any sort of accuracy, let alone to reoccupy it regularly and precisely. It is a compromise to compare marine data sets from a common area of low magnetic relief, but use of the method does confer at least two benefits: (1) it serves to validate the new geomagnetic model for marine use, as it was derived from observations that were largely nonmarine; (2) it approximates the actual end use of the geomagnetic model, which is applied to data sets that feature much more relief over much broader areas.

Comparisons Between "Real" and "Theoretical" Data

Point values of total magnetic field were averaged for each cruise segment contained within the one-degree square, and the mean values were plotted against the midtime of the segment (Fig. 22.1). Also shown in this figure are three representations of the total theoretical magnetic field at the midpoint of the one-degree square. These were derived from three different models: IGRF 1965, IGRF 1975, and the new 1981 version. It is clear that the new model composite produces a closer approximation to the time-varying total field than does either IGRF 1965 or IGRF 1975. Theoretical values in the 1968-1974 interval all fall within 10-15 nanotesla of the mean values. That for 1979 is about 70 nanotesla too high, but agreement is still quite good when compared to the old models.

The reason for the 1979 discrepancy is not clear. It could be due to: a problem with the provisional geomagnetic field; a bias introduced in the mean value on account of the nonuniform distribution of data points throughout the one-degree square; or a field disturbance caused by a temporal variation other than secular variation (e.g. diurnal variation, geomagnetic storm). When future cruises collect additional magnetometer data in this region, it will be interesting to carry out similar comparisons with IGRF 1980, and so to determine whether similar discrepancies exist with the predictive model. An opportunity to do this may arise late in 1982 following a proposed survey of the southwestern part of the Scotian Margin.

Computing Considerations

The new geomagnetic reference fields are demonstrably superior to the old versions, but at the cost of some increase in computing overhead and complexity: the new field expressions contain 120 terms where the old expressions had 80, and programs must now handle four sets of main field coefficients instead of two.

Modifying existing software to cope with the new model has in our case proved to be relatively straightforward. We have no figures yet to back up or to quantify our expectation that use of the new model will increase computer processing time compared to use of the old models. The old models, however, were not noted for computational brevity. What is required now is a method of reducing the execution time of this compute-bound process with little or no sacrifice in accuracy. This would improve the situation considerably for those who have to run their jobs on saturated mainframes or on slower minicomputers.

One solution would be to use the new reference fields as bases for deriving models with fewer terms that are valid only within regions of limited extent and/or over fairly short time spans. The generation of such models could be carried out "on line" and automatically as an integral procedure in the processing of magnetic data. Alternatively, several sets of models could be generated for different years and different regions, to be kept in computer storage and invoked whenever needed. We plan to investigate various means of generating such models.

Conclusions

The new geomagnetic reference fields are better than the old fields at modelling the main magnetic field and its secular variation, but some technique is needed to make them more tractable from a computational view-point.

References

Dawson, E. and Newitt, L.R.
1978: IGRF comparisons; Physics of the Earth and Planetary Interiors, v. 16, p. 1-6.

International Association of Geomagnetism and Aeronomy (IAGA) Division 1, Working Group 1
1981: International Geomagnetic Reference Fields: DGRF 1965, DGRF 1970, DGRF 1975, and IGRF 1980; American Geophysical Union, Transactions, v. 62, p. 1169.

Shih, K.G. and Macnab, R.
1982: Geomagnetic field models: some brief preliminary comparisons; in Current Research, Part A, Geological Survey of Canada, Paper 82-1A, p. 221-223.

23.

CONTRIBUTION TO THE DIATOM FLORA OF ARCTIC CANADA: REPORT 3. ON THE OCCURRENCE OF CHAETOCEROS SPP. FO. CLAVIPES IN THE SOUTHERN BEAUFORT SEA

Project 720078

Sigrid Lichti-Federovich
Terrain Sciences Division

Lichti-Federovich, Sigrid, Contribution to the diatom flora of Arctic Canada: Report 3. On the occurrence of ***Chaetoceros*** *spp. fo.* ***clavipes*** *in the southern Beaufort Sea; in Current Research, Part B, Geological Survey of Canada, Paper 82-1B, p. 169-171, 1982.*

Abstract

The morphological aberrants ***Chaetoceros atlanticus*** *fo.* ***clavipes****,* ***Chaetoceros convolutus*** *fo.* ***clavipes****, and* ***Chaetoceros decipiens*** *fo.* ***clavipes*** *occur in phytoplankton offshore samples from the southern Beaufort Sea. Distribution of these teratological forms shows positive correlation to the allochthonous freshwater diatom component of phytoplankton samples collected from stations within the Mackenzie River discharge area. Lowered and fluctuating salinities are a likely causal factor of foreshortening and distal thickening of setae of these morphological anomalies.*

Introduction

Although this report deviates somewhat from previous contributions to this series (Lichti-Federovich, 1979, 1981) with regard to format and to the treatment of subject matter, its relevance to the taxonomic and ecological aspects of the diatom flora of Arctic Canada renders it suitable for inclusion into the series.

Phytoplankton samples collected during the 1970 **CSS Hudson** cruise were floristically analyzed. Whereas species enumeration and frequency data form the basis of a separate report, one of the more intriguing aspects emerging from this diatom analytical investigation is reported here. It relates to the occurrence and distribution of morphological aberrants of the genus **Chaetoceros** whose structural abnormality is expressed by a foreshortening and distal thickening of setae (Fig. 23.1, 23.2). The descriptive account and taxonomic determination of an aberrant **Chaetoceros convolutus** as fo. **clavipes** manifested by the lack of one seta as well as the distinct thickening of another shortened seta, cited from the coastal waters off northern Iceland, represents the first recorded occurrence of this anomalous form (Paasche, 1961).

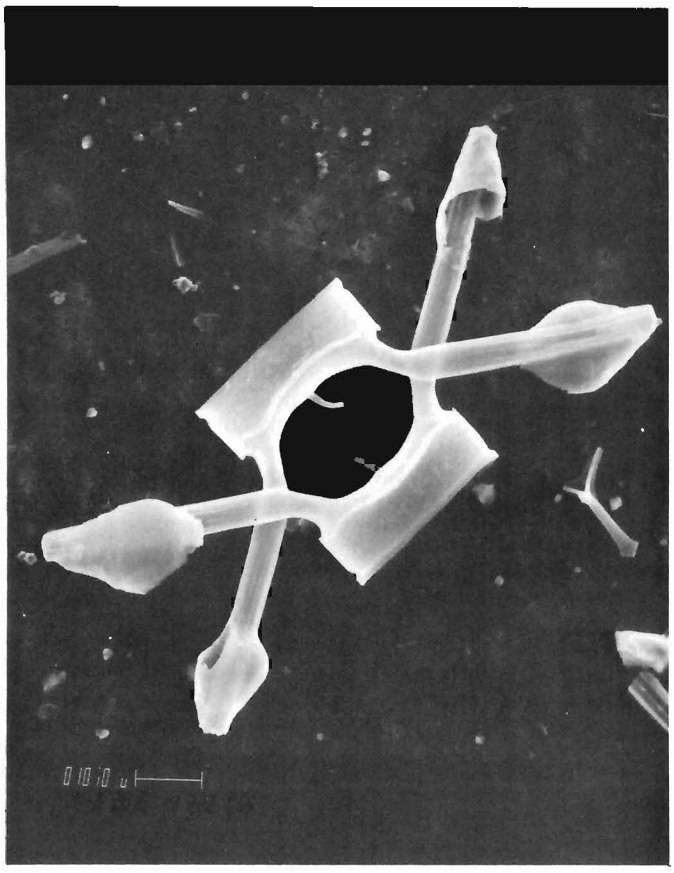

Figure 23.1. ***Chaetoceros atlanticus*** *Cleve (SEM x 1500).*

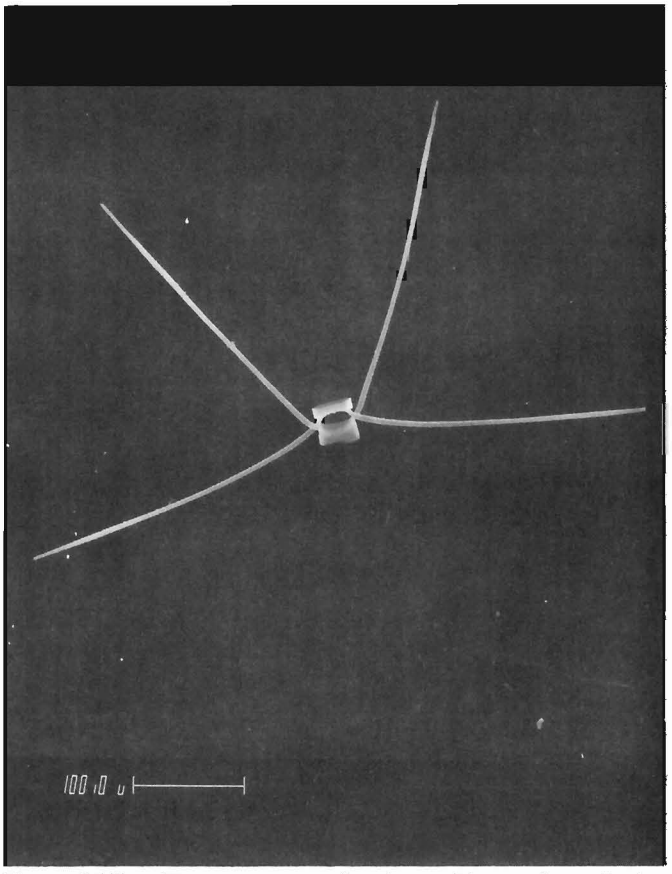

Figure 23.2. ***Chaetoceros atlanticus*** *Cleve fo.* ***clavipes*** *Paasche (SEM x 9000). Anomalous form.*

Brunel (1970), documenting **Chaetoceros convolutus** fo. **trisetosa** from the St. Lawrence estuary and from several stations in Chaleur Bay in the Gulf of St. Lawrence, provides a more recent account of an aberrant **Chaetoceros convolutus** characterized by the total absence of one seta. Additional records of this particular teratological form from northern Canada include Trinity Bay, Newfoundland, and Robertson Bay, Belcher Island (J. Brunel, personal communication with A. Bursa). In his detailed account, by literature reference, Brunel (1970) also relates the presence of anomalous forms of **Chaetoceros subtilis** in the Gulf of Panama, Black Sea, and South Atlantic, likewise characterized by the absence of one seta.

The occurrence in Chaleur Bay of identical **Chaetoceros convolutus** aberrants to the one depicted by Paasche induced Brunel (1970) to suggest that fo. **clavipes** as described by Paasche represents a transitional form and that his fo. **trisetosa** portrays the end result in reduction.

From purely morphological considerations, I fully support his proposition relating to transitional phases expressed by distal thickening between a normal **Chaetoceros convolutus** valve and the ultimate reduction stage, manifested by a total lack of setae. It should be emphasized, however, that these structural modifications are limited neither to one or two species of the genus **Chaetoceros** nor to number and position of setae as is clearly evidenced by the aberrants from the Beaufort Sea.

Materials and Methods

The sample material was collected during a cruise of **CSS Hudson** between August 26 and September 22, 1970. Qualitative analysis and distributional data are based on 200 µm mesh net vertical and horizontal hauls recovered from several offshore stations located within the southern Beaufort Sea (Fig. 23.3, 23.4).

Routine preparation of these phytoplankton samples for floristic analysis followed the procedure outlined by Lichti-Federovich (1981). The technique used for scanning electron (SE) analytical and photographic work have been detailed by Lichti-Federovich (1979).

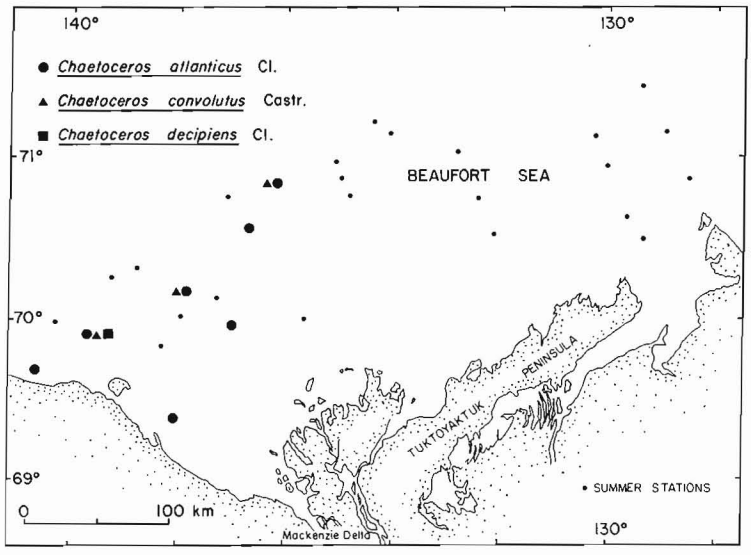

Figure 23.3. *Distribution of anomalous forms of* ***C. atlanticus*** *Cl.,* ***C. convolutus*** *Castr., and* ***C. decipiens*** *Cl. in the southern Beaufort Sea.*

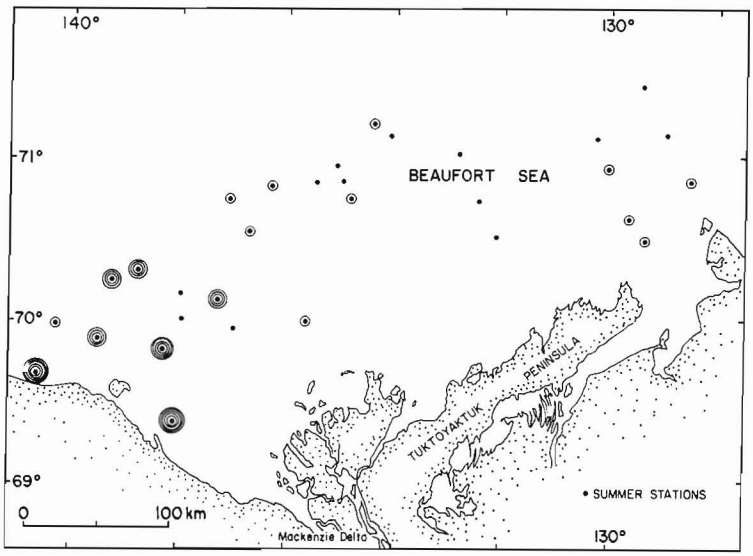

Figure 23.4. *Distribution of allochthonous freshwater diatoms in the southern Beaufort Sea. Number of circles represents number of freshwater taxa.*

Results and Discussion

Chaetoceros atlanticus fo. **clavipes, Ch. convolutus** fo. **clavipes** and **Ch. decipiens,** fo. **clavipes** appear to manifest in response to environmental stress conditions. This inference does not rest on purely speculative grounds but is clearly substantiated by the recorded occurrence of this aberrant form in the literature. Without exception, all finds to date derive from marginal marine areas, i.e. environments subject to considerable hydrographic changes (Paasche, 1961; Brunel, 1970). It is difficult, however, to designate with certainty any particular environmental factor or type of stress as the cause of this morphological anomaly. Nevertheless, it appears most likely that this structural modification is attributable principally to pronounced osmotic changes caused by the lowered and fluctuating salinities of marine coastal waters. In this context mention should be made of the skillful demonstration by Schmid (1979) of salinity sensitivity and resultant structural aberrations of some benthic brackish and freshwater diatoms.

Interpretation of the occurrence of **Chaetoceros** spp. fo. **clavipes** in terms of environmental stress due to salinity fluctuations is strengthened by the incidence of these aberrants within the Mackenzie River discharge area (Fig. 23.3). A close positive correlation between the pattern of distribution of the anomalous **Chaetoceros** species (Fig. 23.3) and that of the allochthonous freshwater diatom component (Fig. 23.4) also attests to this inference. Furthermore, the autecological characterization of **Chaetoceros atlanticus** and **Chaetoceros convolutus** as oceanic, high salinity forms, sensitive to osmotic pressure oscillations, lends additional support to the likely manifestation of structural changes in response to the injurious effect of salinity fluctuations. If one accepts the validity of the proposed cause and effect relationship, then the occurrence of **Chaetoceros decipiens** fo. **clavipes** suggests a significant freshening influence, since **Chaetoceros decipiens** represents a neritic taxon favouring a lowered optimal salinity of 23.2‰ (Cleve-Euler, 1951).

Although the various postulates enumerated seem to support a causal salinity-stress/distribution hypothesis, further studies are needed to systematically evaluate the range of phenotypic characters in a succession of progressively modified forms and to fully assess the structural response of **Chaetoceros** to various environmental stress conditions.

Acknowledgments

The plankton samples examined were provided by G. Vilks, Atlantic Geoscience Centre, Dartmouth. I am indebted for his kindness. I also acknowledge with gratitude and appreciation the technical skill of D. Walker, Geological Survey of Canada who took the scanning electron micrographs. Sincere thanks are also extended to H.C. Duthie who critically reviewed the paper.

References

Brunel, J.
1970: Le Phytoplancton de la Baie Chaleurs; 2nd ed., Les Presses de L'Université de Montréal, Montréal, Canada, 365 p.

Cleve-Euler, A.
1951: Die Diatomeen von Schweden und Finnland; I.-K. Svenska Vet.-Akad. Handiingar, Fjärde Serien, v. 2, p. 1-163.

Lichti-Federovich, S.
1979: Contributions to the Diatom Flora of Arctic Canada: Report 1. Scanning electron micrographs of some freshwater species from Ellesmere Island; in Current Research, Part B, Geological Survey of Canada, Paper 79-1B, p. 71-82.

1981: Contribution to the diatom flora of Arctic Canada: Report 2. Arctic representatives of the genus **Navicula**; in Current Research, Part A, Geological Survey of Canada, Paper 81-1A, p. 57-62.

Paasche, E.
1961: Notes on Phytoplankton from the Norwegian Sea; Institute for Marine Biology, Section B, University of Oslo, p. 197-211.

Schmid, A.-M.M.
1979: Influence of environmental factors on the development of the valve in diatoms; Protoplasma, v. 99, p. 99-115.

24.

DENSITY GRADIENTS AND INJECTION STRUCTURES IN MUDBOILS IN CENTRAL DISTRICT OF KEEWATIN

Project 770035

P.A. Egginton and L.D. Dyke[1]
Terrain Sciences Division

Egginton, P.A. and Dyke, L.D., Density gradients and injection structures in mudboils in central District of Keewatin; in Current Research, Part B, Geological Survey of Canada, Paper 82-1B, p. 173-176, 1982.

Abstract

Mud injection structures in mudboils are explained by the collapse of a relatively dense mud carapace into an underlying less dense zone of supersaturated muds. According to the model, mud injection is a late summer phenomenon.

The moisture content of the carapace, the ice content and distribution at the bottom of the active layer, and rate and depth of annual thaw determine whether the carapace will fail in a given year. In addition, a change in mudboil diameter over time, such as by the encroachment of border vegetation, will affect the frequency of carapace failures.

Introduction

Mudboils, a patterned ground form, are common on the marine muds and till (here collectively termed muds) of central District of Keewatin. Similar forms are common throughout Arctic Canada (Zoltai and Tarnocai, 1981) and other permafrost areas (i.e. Washburn, 1969). Shilts (1978) and Egginton (1979) have reported injection structures, referred to as diapirs by Shilts (1978), in the red till belt near Victory Lake, District of Keewatin. Field evidence indicates that the structures are formed when mud, from the base of the thaw zone, is injected into overlying drier mud, typically beneath the centre of a mudboil. At Victory Lake the injection structures are visible because of textural and colour contrasts between the upper washed, and hence coarser, grey mud and the underlying finer red mud (Fig. 24.1). In areas above the postglacial marine limit (≈170 m a.s.l.), where strong textural and colour contrasts do not exist between the upper and lower parts of the active layer, injection structures are not easily identified; however, even at these sites occasional extrusions of mud to the surface have been observed suggesting that injection occurs. Several mechanisms have been suggested by Shilts (1978) for the formation of these mud structures in District of Keewatin including: 1) differential hydrostatic head (artesian pressure), 2) differential cryostatic pressure, and 3) differential loading. The possibility that the intrusion of supersaturated muds from the base of the active layer upward into the overlying muds results from density variations in mudboils in later summer is discussed here.

Acknowledgments

The paper was critically reviewed by A.S. Dyke and D.A. Hodgson; their comments greatly improved the original manuscript.

Mudboil Structure and Properties

The typical mudboil is either a high- or low-centre feature, essentially circular, 1 to 3 m in diameter, and has a vegetated border. The active layer is 1.5 to 2 m thick beneath mudboil centres, and typically only 1 m thick beneath vegetated borders.

During freeze-back, ice in a mudboil can be concentrated at both the top and bottom of the active layer (Egginton, 1979; Dyke and Zoltai, 1980; Veillette, 1980). This phenomenon is common in permafrost areas and has been reported for similar patterned ground forms and other surficial material elsewhere (i.e. Mackay, 1970, 1980). Ice contents within frozen soils are not constant. In summer, water in the upper active layer may migrate to the lower active layer and underlying permafrost (Parmuzina, 1978, cited in Mackay, 1980). Thus a considerable volume of ice may accumulate at the base of the thaw zone by late summer.

The thaw of the top ice-rich zone in early summer can result in rapid surface displacements of muds (Egginton, 1979); however, by midsummer this upper zone or carapace typically dries out. Shilts (1978), working below marine limit, found textural as well as moisture contrasts between the upper and lower active layer. He termed the upper portion 'carapace' and the lower, 'thawed mud subtrate'. Above marine limit these textural variations are not found; however, moisture contrasts typically do exist. In this report the term carapace is used to describe that portion of the active layer that overlies the ice-rich zone – in late summer the zone of supersaturated mud at the bottom of the active layer. The term does not have any textural connotation.

The ice-rich zone at the bottom of the active layer thaws in late summer. Hydraulic conductivities of the carapace vary but are typically of the order 1.0×10^{-6} cm/s. Late in the season, if thaw is rapid, water released by the melting of the ice-rich zone may not be able to drain because of the low permeability of the overlying mud and because of the bowl shape of the active layer (Fig. 24.2). This leads to an unstable condition – a reverse density gradient – dense muds overlie less dense muds that contain a considerable volume of excess water.

The Carapace as a Beam

As thaw proceeds to the bottom of the active layer it progresses more rapidly under the bare centre of the mudboil than under the vegetated border. In a two-dimensional model of conditions in a mudboil in late summer, the carapace can be treated as a relatively dry mud beam overlying a supersaturated mud (Fig. 24.2). Since little thaw per unit time occurs in the borders relative to the mudboil centre, the beam is supported at the borders. As the beam is denser than the supersaturated mud, the beam may collapse into the underlying muds. Assuming the carapace and underlying mud are uniform throughout, the beam may fail in tension. Whether the beam fails or not depends upon its thickness, its length, and its tensile strength.

[1]Geology Department, Queen's University, Kingston, Ontario

Figure 24.1

An excavated mudboil showing an area of diapiric injection (dark toned mud) Victory Lake, District of Keewatin, (courtesy W.W. Shilts, GSC 201696-P).

Tensile Strength

Tensile strengths, S, were calculated from laboratory test data using the formula derived from beam bending theory for a simply supported beam of rectangular cross-section:

$$S = \frac{3FL}{2BD^2} \qquad (1)$$

where F = the applied force at failure, L = beam length, B = unit width, and D = beam thickness (Fig. 24.3).

Critical Thickness

For a beam of given length, width, and tensile strength, failure will take place unless the beam has a critical thickness. This thickness is obtained by rewriting equation (1):

$$D = \sqrt{\frac{3FL}{2BS}} \qquad (2)$$

and using for F one half the beam weight (W). This follows from the consideration that for the supported beam (Fig. 24.2), a force equal to one half the beam weight applied midway between the supports will be the force (see arrows, Fig. 24.2) necessary to prevent bending. Thus,

$$F = \frac{\rho LBD}{2} \qquad (3)$$

where ρ = density of the material composing the beam. Equation (3) would apply to a mudboil with a carapace overlying but not supported by the supersaturated mud. If the carapace is supported by the underlying mud (i.e., there is a buoyancy effect),

$$F = \frac{\Delta\rho LBD}{2} \qquad (4)$$

where $\Delta\rho$ is the difference in density between the carapace and the supersaturated mud. These two situations (equations (3) and (4)) represent the field extremes. Equation (2) can now be rewritten in terms of beam weight:

$$D = \frac{3\rho L^2}{4S} \quad \text{or} \quad D = \frac{3\Delta\rho L^2}{4S} \qquad (5)$$

Equation (5) can be used to predict the critical thickness, based on mud densities, and tensile strengths given by different moisture contents (Fig. 24.3) for beams of various lengths.

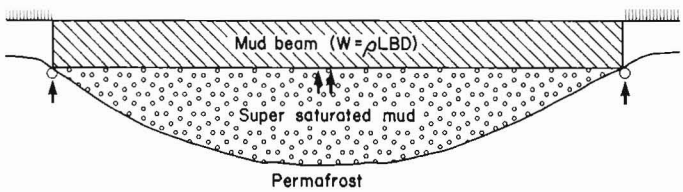

Figure 24.2. *A schematic cross-section of a mudboil having a vegetated border. A mud beam overlies a supersaturated mud (see text).*

Mudboil Diameter

The diameter of the mudboil, or in the two-dimensional model the beam length (L), is important in determining whether the beam will or will not fail. Equation (5) was solved for various beam lengths with $\Delta\rho$ = 1.0 g/cm^3 and ρ = 2.0 g/cm^3, respectively (Fig. 24.4, 24.5). The density of the carapace increases as its moisture content increases; however, in late summer it is at or below saturation. On the other hand, the mud at the bottom of the active layer is supersaturated. The greater the ice content at the bottom of the active layer, the greater the density difference between the carapace and the underlying mud when it thaws. A maximum upper limit for $\Delta\rho$ is 1.0 g/cm^3. Carapace field densities varied but values of about 2.0 g/cm^3 were fairly typical.

When the other variables are held constant, as beam length increases, so must beam thickness in order to prevent failure. In central District of Keewatin, carapace moisture contents reach values of 10% (or more) in late summer (Shilts, 1978). If ρ = 2.0 g/cm^3, then a mudboil 1.5 m in diameter requires a carapace 2.25 m thick to prevent failure, whereas a mudboil 2.0 m in diameter requires a carapace 4.0 m thick to prevent failure (Fig. 24.5). If $\Delta\rho$ = 1.0 g/cm^3, then the same mudboils (L = 1.5 and L = 2.0) require carapace thicknesses of 1.1 and 2.0 m, respectively to prevent failure. Typically, in the field the active layer rarely exceeds 2.0 m, and the carapace must necessarily be thinner than the active layer; therefore, a mudboil requiring a carapace (beam) thicker than that available (say 1.8 m) will fail under its own weight. From the foregoing, it would appear that carapace (beam) collapse can be expected when the mudboil diameter (beam length) is in excess of 1.5 m, as is common in central District of Keewatin.

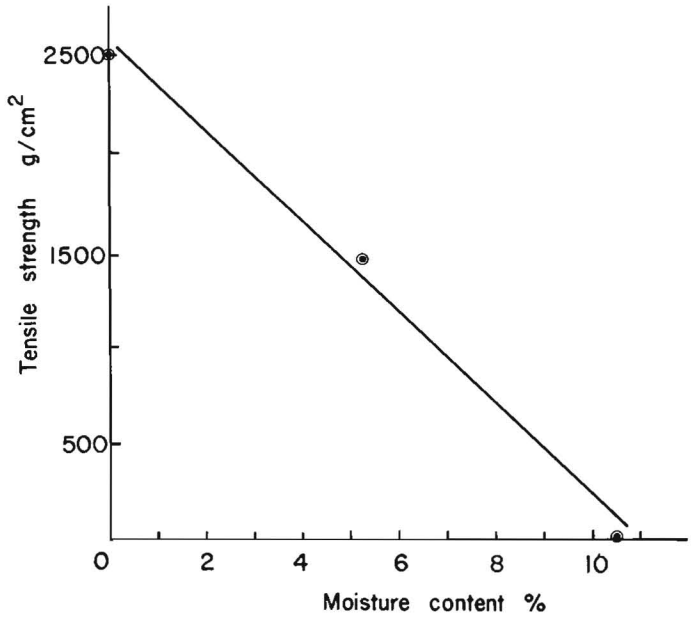

Figure 24.3. Tensile strength of a typical carapace mud as a function of moisture content.

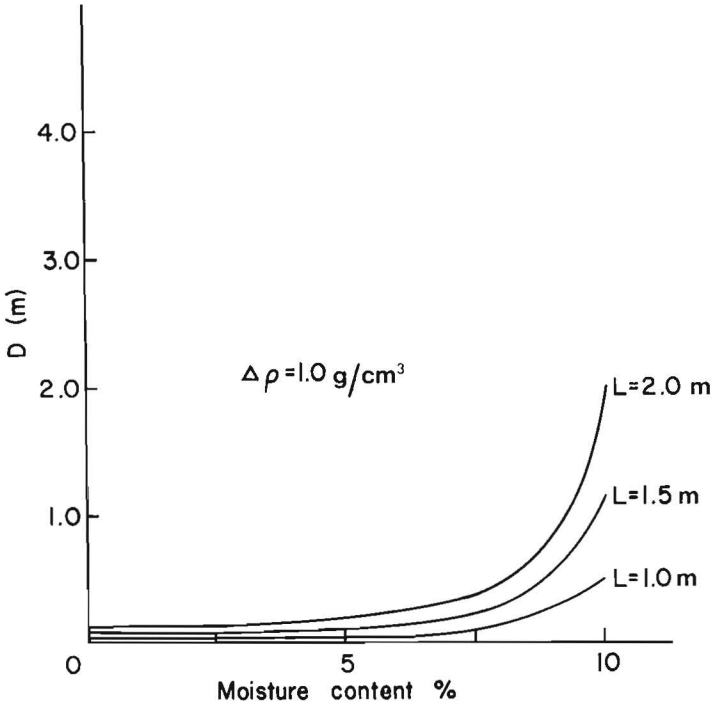

Figure 24.4. The critical beam thickness (D) required to prevent carapace failure for various moisture contents and beam lengths. A buoyancy effect is assumed (i.e. $\Delta\rho$ = 1.0 g/cm^3).

Mud Injection

The actual downward displacement of the carapace (beam) on failure may be slight, contrary to the impression given in Figure 24.2. The carapace is thick relative to the zone of supersaturated mud, as pointed out above; therefore, failure does not imply a complete overturning of the two muds, merely a displacement of the lower mud. The quantity

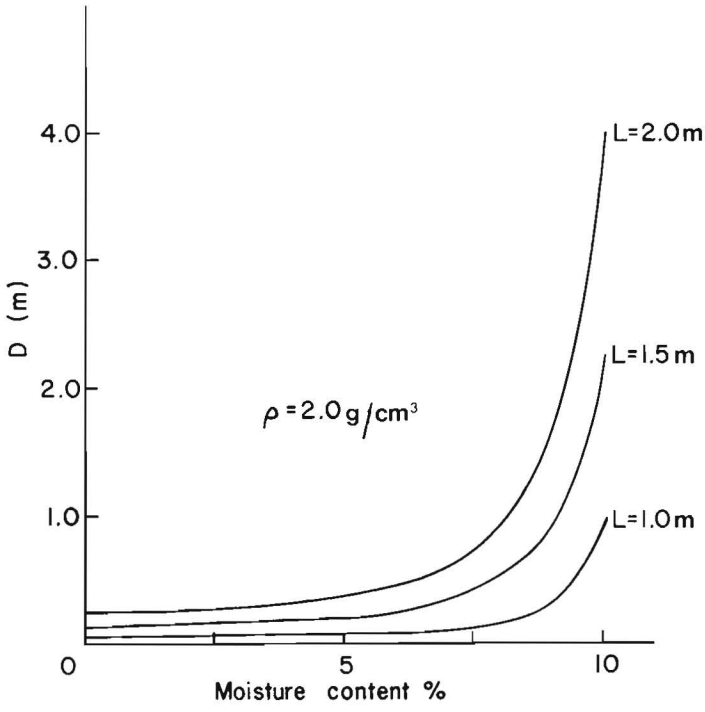

Figure 24.5. The critical beam thickness (D) required to support the carapace for various moisture contents and beam lengths. The beam is not supported by the underlying supersaturated mud (i.e. $\Delta\rho$ = 2.0 g/cm^3).

and manner in which the underlying mud is injected depends upon whether the beam is supported or unsupported by the underlying mud. If it is supported, the melt and subsequent decrease in volume of the underlying mud may cause a gradual failure of the carapace; injection may be limited. On the other hand, if the beam is unsupported, the failure and collapse may be rather sudden and injected mud may reach the carapace surface.

The moisture content of the carapace, the ice content and distribution at the bottom of the active layer, and the rate and depth of annual thaw are factors that determine whether the carapace (beam) will fail in a given year. Therefore, mud injection may be expected to occur on a less than annual basis.

In a given year the tensile strength of the carapace may be just greater than the applied force; loading the carapace (i.e., walking on it) may cause it to collapse. Similarly, digging into the centre of a mudboil late in the thaw season may weaken the carapace and cause an upwelling of mud, a phenomenon reported by Shilts (1978).

Stabilization

The importance of mudboil diameter in determining whether a carapace (beam) will fail or not has been discussed above. If the effective diameter (or length (L) in the model) of a mudboil can be made smaller over time, such as by the encroachment of vegetation along the borders, then the probability of carapace collapse and mud injection may be reduced. The converse is also true: the removal of vegetation from the borders, effectively increasing mudboil diameter, may promote mud injection. This may explain, in part, why formerly stable and vegetated mudboils at Henik Lake, District of Keewatin, remain highly active more than 13 years after the vegetation was removed from their borders (Egginton, 1981).

Summary

A simple two-dimensional model has been introduced to describe mudboil behaviour during the latter part of the thaw season. It relies upon a reverse density gradient. Although the data obtained from this model do not strictly apply to a three-dimensional field case, it does provide approximations. For mudboils to remain stable (i.e. no mud injection), the model requires critical thickness values for the carapace that are the same and/or substantially greater than the active layer thicknesses measured in the field. In other words, in some cases, field conditions appear to favour carapace collapse and mud injection by this mechanism.

References

Dyke, A.D. and Zoltai, S.C.
1980: Radiocarbon-dated mudboils, central Canadian Arctic; in Current Research, Part B; Geological Survey of Canada, Paper 80-1B, p. 272-275.

Egginton, P.A.
1979: Mudboil activity, central District of Keewatin; in Current Research, Part B; Geological Survey of Canada, Paper 79-1B, p. 349-356.

1981: The impact of disturbance on mudboil activity, North Henik Lake, District of Keewatin; in Current Research, Part A; Geological Survey of Canada, Paper 81-1A, p. 299-303.

Mackay, J.R.
1970: Disturbances to the tundra and forest environment of the Western Arctic; Canadian Geotechnical Journal, v. 7, p. 420-432.

Mackay, J.R. (cont.)
1980: The origin of hummocks, western Arctic coast, Canada; Canadian Journal of Earth Sciences, v. 17, p. 996-1006.

Parmuzina, O. Yu.
1978: The cryogenic structure and certain features of ice separation in a seasonally thawed layer; in Problems of Cryolithology, ed. A.I. Popov; Moscow University Press, Moscow, USSR, p. 141-164 (In Russian).

Shilts, W.W.
1978: Nature and genesis of mudboils, central Keewatin, Canada; Canadian Journal of Earth Sciences, v. 15, p. 1053-1068.

Veillette, J.J.
1980: Nonsorted circles in cohesionless fine silty sand, north-central District of Keewatin; in Current Research, Part B; Geological Survey of Canada, Paper 80-1B, p. 259-267.

Washburn, A.L.
1969: Weathering, frost action, and patterned ground in the Mesters Vig District, Northeast Greenland; Meddelelser om Gronland, v. 176, 303 p.

Zoltai, S.C. and Tarnocai, C.
1981: Some nonsorted patterned ground types in northern Canada; Arctic and Alpine Research, v. 13, no. 2, p. 139-151.

25. INVESTIGATION OF REGIONAL AIRBORNE GAMMA RAY SPECTROMETRIC PATTERNS IN NEW BRUNSWICK AND NOVA SCOTIA

Project 760045

K.L. Ford
Resource Geophysics and Geochemistry Division

Ford, K.L., Investigation of regional airborne gamma ray spectrometric patterns in New Brunswick and Nova Scotia; in Current Research, Part B, Geological Survey of Canada, Paper 82-1B, p. 177-194, 1982.

Abstract

Between 1976 and 1979 reconnaissance airborne gamma ray spectrometric surveys were flown over most of the Province of New Brunswick and all of Nova Scotia. Elevated regional radioelement contents were found to relate mainly to granitic rocks. Maximum concentrations of uranium and thorium in New Brunswick are associated with those phases of the Devonian granitic rocks which exhibit a higher differentiation index. New Brunswick granitoids exhibit a normal crustal ratio of uranium to thorium indicating a positive relationship between these two elements with increasing differentiation.

In contrast to granitoids located in New Brunswick, concentration patterns in Nova Scotia granitoids are characterized by high eU/eTh ratio values. Maximum concentrations of uranium, high eU/eTh ratio values as well as lowest thorium concentrations are associated with the more differentiated phases of the Devonian-Carboniferous peraluminous granitic suite. The high eU/eTh ratio is the result of a general increase in uranium and a decrease in thorium with increasing differentiation. Other lithophile elements (i.e. Sn) show increased levels in the more differentiated phases of the granitic rocks of Nova Scotia as well, and therefore, by association the radioelement patterns, determined by airborne surveying, appear usable in delineating potential areas for exploration of these elements.

Introduction

During 1976, airborne gamma ray spectrometric surveys, with 5 km line spacing, were flown over the non-Carboniferous areas of New Brunswick as part of the Uranium Reconnaissance Program (Geological Survey of Canada, Geophysical Series Maps 35 721G, 35 821G, 36 021G, 36 421G, 36 521G, and 36 621G) and the southern half of Nova Scotia (Geological Survey of Canada, Open File 429). The remainder of mainland Nova Scotia and Cape Breton Island were flown in 1978 and 1979 respectively (Geological Survey of Canada, Geophysical Series Maps 35 411G, 35 511G, 35 611G, and Open File 816). The extent of airborne gamma ray spectrometric coverage is shown on Figures 25.1A and 25.3A which are generalized geological maps of New Brunswick and Nova Scotia, compiled from Federal and Provincial geological maps published by the Department of Natural Resources, New Brunswick (Potter et al., 1968) and the Department of Mines and Energy, Nova Scotia (Keppie, 1979) respectively. In the case of Nova Scotia the entire province has been flown with 5 km line spaced surveys. Also indicated on Figures 25.1A and 25.3A are the limits of airborne surveys flown with a line spacing of 1 km to provide increased resolution of radioelement distribution patterns in selected areas. Additional 1 km surveys were flown in the fall of 1981 in Nova Scotia covering an area equal to six 1:50 000 scale N.T.S. map areas. Two of these cover the area around Aylesford Lake and Dalhousie East (Fig. 25.3A), the remainder complete the coverage between Sangster Lake and Fletcher Lake.

Field investigations of the airborne gamma ray spectrometric maps and profiles have been carried out during parts of the 1977 and 1980 field seasons to assess the significance of the regional radioelement patterns. These investigations included in situ gamma ray spectrometric measurements and sample collection for later petrographic and chemical analysis as well as neutron activation and gamma ray spectrometric laboratory analysis.

Regional Radiometric Patterns

The regional radioelement distribution patterns for equivalent thorium, equivalent uranium and the eU/eTh ratio for those portions of New Brunswick and Nova Scotia surveyed to date can be seen on Figures 25.1B, 25.2, 25.3B, and 25.4. Equivalent thorium concentrations (Fig. 25.1B, 25.3B) in excess of 10 ppm occur over portions of the Miramichi Highlands, the Pokiok Batholith and a major portion of the Charlotte Batholith of New Brunswick. Equivalent thorium levels in Nova Scotia are considerably lower with only a few isolated localities exceeding 10 ppm. Equivalent uranium patterns also show elevated levels over portions of the Miramichi Highlands, the Pokiok Batholith (P, Fig. 25.1A) and a major portion of the Charlotte Batholith (C(A) and C(B), Fig. 25.1A) in New Brunswick. Values in excess of 1 ppm eU appear to define regionally anomalous zones with only a small percentage of the total area in excess of 2 ppm. Equivalent uranium patterns in Nova Scotia show that a greater percentage of the survey area exceeds 2 ppm than in New Brunswick. Virtually all areas exceeding 2 ppm eU are confined to the Meguma Zone of central and southern Nova Scotia. In both New Brunswick and Nova Scotia, values in excess of 2 ppm eU relate mainly to the more differentiated phases of the Devonian-Carboniferous granitic rocks.

The eU/eTh ratio map for New Brunswick (Fig. 25.2B) shows that levels are at or generally below the normal crustal ratio of 0.25 (Clark et al., 1966); this map appears virtually featureless except for a small isolated high-ratio anomaly located at Beadle Mountain (BM, Fig. 25.1A) in central New Brunswick. This anomaly relates to a small pluton of strongly peraluminous biotite-muscovite granite (Table 25.2). The eU/eTh ratio map for Nova Scotia on the other hand (Fig. 25.4B) shows much higher levels than in New Brunswick. The higher ratios appear to relate to increased uranium and depleted thorium levels (compared to normal crustal abundances) in the more differentiated phases of the Devonian-Carboniferous peraluminous granitic rocks.

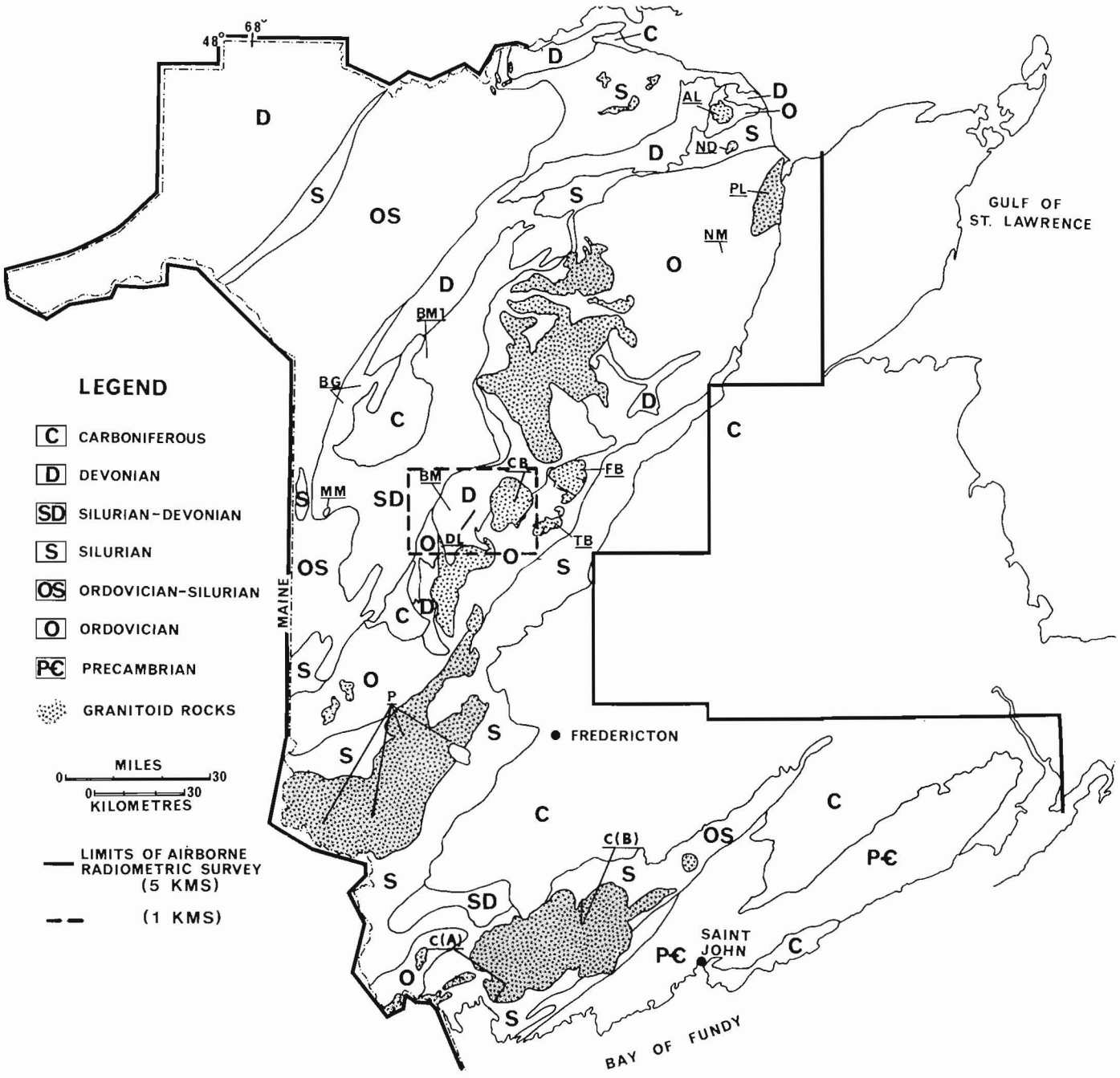

Figure 25.1A. Generalized geology of New Brunswick (adapted from Potter et al., 1968) showing limits of airborne gamma ray spectrometric coverage and localities where in situ gamma ray spectrometric studies were conducted.

The relationship of the contoured radioelement patterns and the distribution of the major anomalous lithologies has formed the basis for this investigation. Individual flight line profiles were not extensively investigated. These often have small, sharp features which may indicate mineralization which may be lost on contour maps because of the smoothing process used in their preparation.

The general locales where in situ spectrometric measurements were made are shown in Figures 25.1A (underlined letter symbols) and 25.3A (place names with arrows) and tabulated in Table 25.1. Twenty-four localities were investigated in New Brunswick and Nova Scotia and over 350 in situ gamma ray spectrometric measurements were made. The number of readings at some localities is small and larger variations than indicated would likely exist if a greater number of measurements were made. In Table 25.1 the in situ results are organized by province and listed by increasing eU/eTh ratio. The picture presented by these values correlates well with the patterns presented in the airborne radiometric maps. These data, along with some chemical analysis, and airborne maps form the basis of the following discussion of the radioelement distribution patterns.

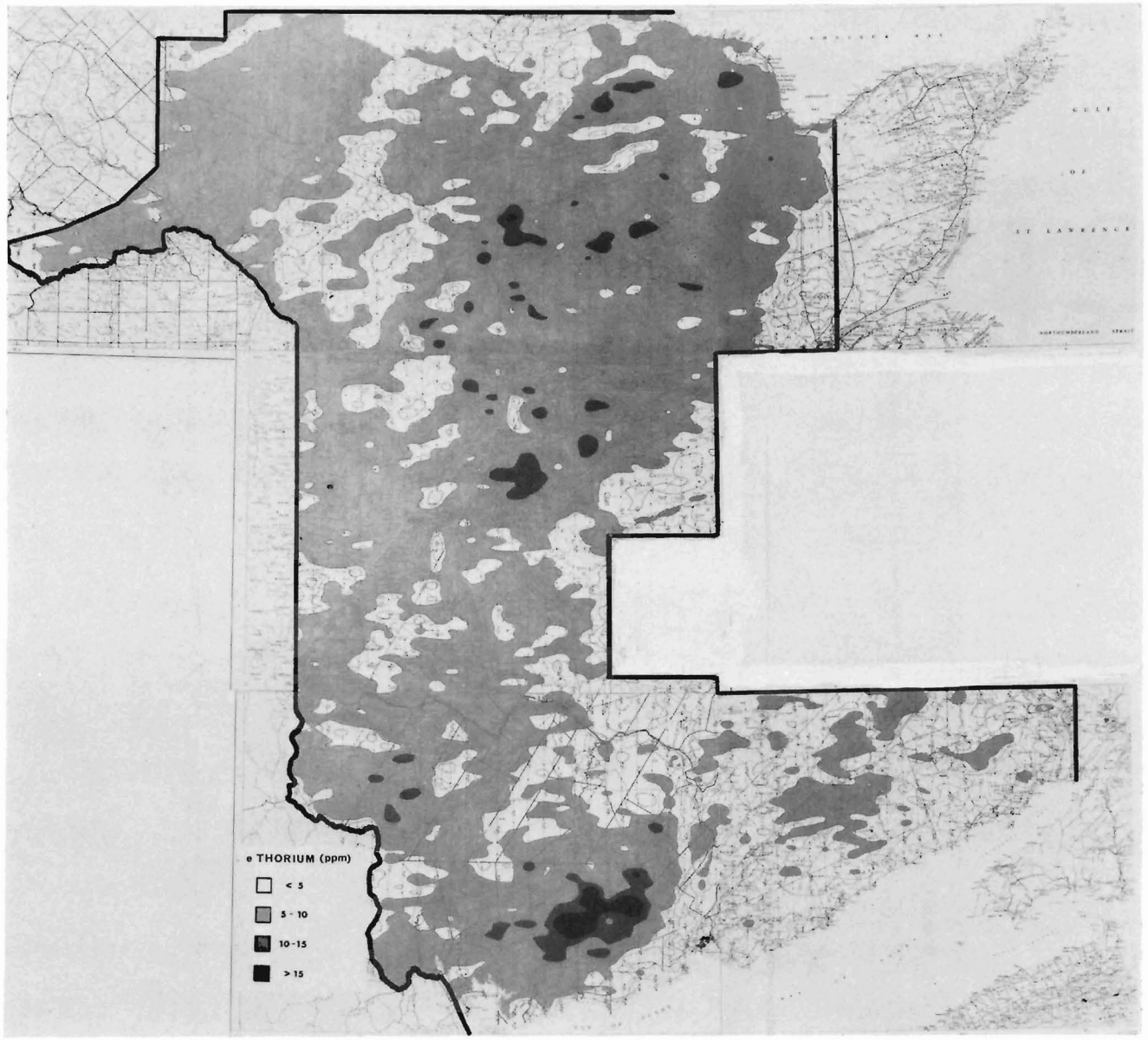

Figure 25.1B. *Equivalent thorium (ppm) map for part of New Brunswick compiled from 5 km line spaced airborne gamma ray spectrometric surveys.*

The general relationship between airborne radioelement levels and ground levels has been discussed by Charbonneau et al. (1976). The relationship between contoured airborne radioelement values, representing average surface concentrations over areas several square kilometres in size, and the concentration in bedrock depends on: the percentage of outcrop, the relation between overburden and bedrock radioelement content, percentage of marshland or surface water, soil moisture, and density of vegetation within the field of view of the airborne spectrometer. They concluded that airborne radioelement contour maps give a relative indication of the bedrock radioelement content, and that in general airborne measurements of 3 to 4 ppm eU in drift covered areas (e.g. Elliot Lake, Ontario and Mont Laurier, Quebec) relate to an overburden uranium content of 4 to 5 ppm and a concentration in the order of 8 to 10 ppm eU in the underlying bedrock. Similar relationships were found to be valid in general for the areas investigated in New Brunswick and Nova Scotia. For example, the eastern portion of the Charlotte Batholith has a contoured equivalent uranium value reaching 3 ppm eU with in situ values averaging about 8 ppm eU.

Because the radioactivity associated with granitic rocks dominates the anomalous radiometric patterns in the Maritimes, 21 of 24 sites investigated on the ground related to the granites. Increased levels of radioelement concentration are also associated with rhyolitic rocks. Consequently three areas where these lithologies are present were examined briefly.

New Brunswick Investigations

The three areas where rhyolitic rocks were examined are located in northern New Brunswick and include Blue Mountain (BM1), Nine Mile Fire Tower (NM) and Bell Grove (BG) indicated in Figure 25.1A. Radioelement concentrations measured by in situ gamma ray spectrometry are tabulated in

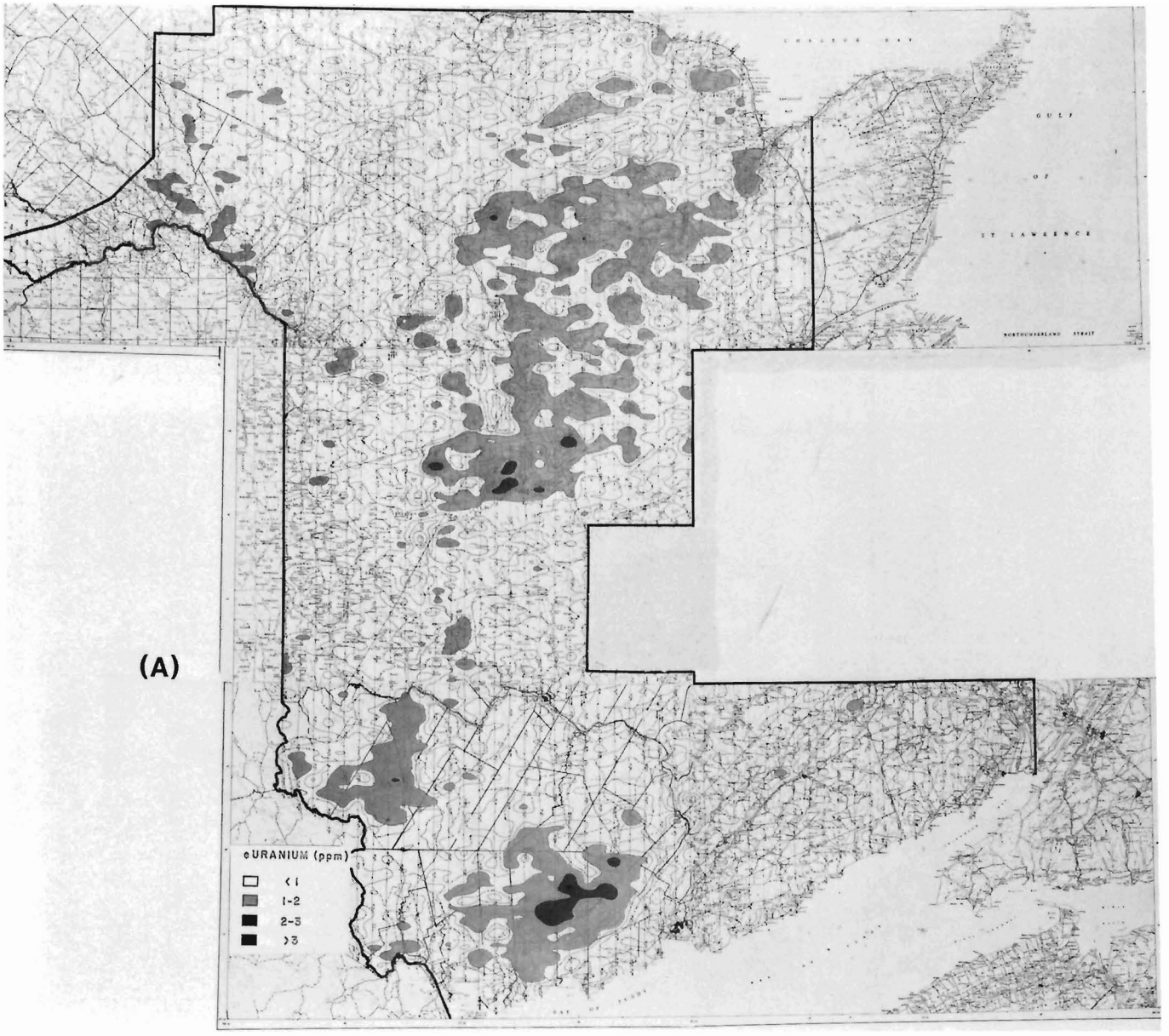

Figure 25.2. *Equivalent uranium (ppm) (A) and equivalent uranium/equivalent thorium ratio maps (B) for part of New Brunswick compiled from 5 km line spaced airborne gamma ray spectrometric surveys.*

Table 25.1. Average concentrations for these three areas are about 6% K, 4 ppm eU and 25 ppm eTh. Many of these rhyolitic units are distinguishable on profiles (NM, Fig. 25.7A) usually showing up as broad potassium peaks sometimes with smaller associated equivalent thorium and equivalent uranium peaks.

A major part of the ground investigations was concentrated on the granitic rocks of New Brunswick and Nova Scotia. In all, eleven granite localities were examined in New Brunswick and ten granite localities were examined in Nova Scotia. These investigations confirm the variation in radioelement content between the various granitic rocks as indicated on the airborne maps and also confirms a major radioelement difference, to be discussed, between those granites studied in New Brunswick and those studied in southern and central Nova Scotia.

Martin (1966) in a petrographic and chemical study of the granitic rocks of New Brunswick classified them chronologically into: (1) Precambrian, (2) Ordovician, and (3) Devonian classes. He further subdivided the Devonian granitic rocks into: (a) Main Belt (west and north of Fredericton) including the Pokiok Batholith, (b) Charlotte Batholith (west of St. John), and (c) Isolated Stocks. Variations of the differentiation indices between each type were noted. Martin stated that in general granodioritic and tonalitic rocks predominate within the Main Belt reflecting a lower differentiation index than rocks of the Stock and Charlotte Batholith types where granitic and adamellitic rocks predominate.

Radioelement contents reflect this variation with the highest radioelement concentrations occurring in those members of the Devonian granitic rocks which exhibit higher

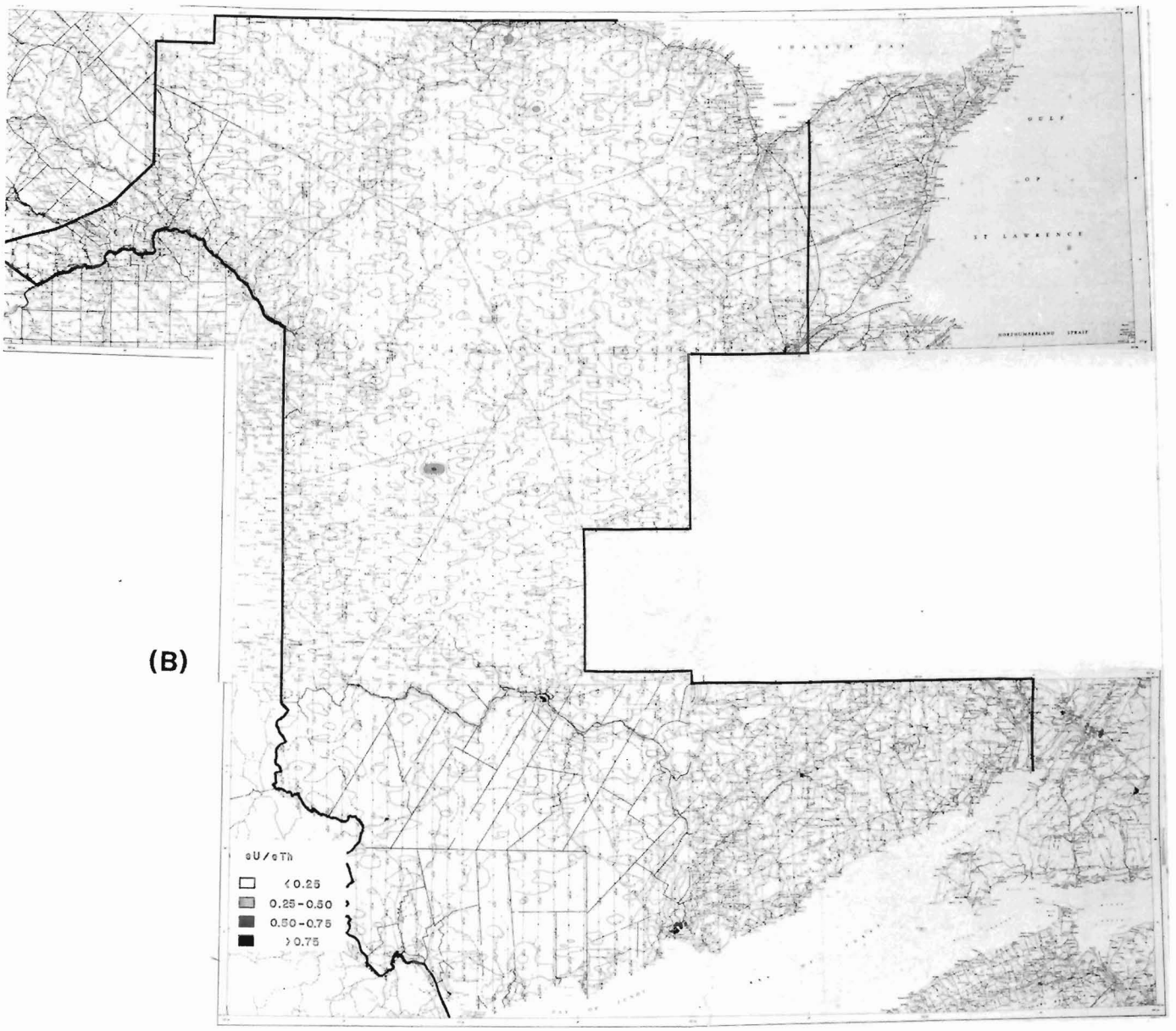

differentiation indices. This correlation is commonly observed in igneous rocks (Clark et al., 1966; Rogers and Adams, 1970). Table 25.2 summarizes the chemistry of some of the Maritime granites investigated. Results were obtained from samples collected in this study and from literature sources. Classification of the New Brunswick granites has been based on that of Martin (1966), and the Nova Scotia granites on McKenzie and Clarke (1975). The granitoid rocks of New Brunswick are predominantly biotite adamellite but range from biotite granodiorite to biotite granite. Table 25.2 shows the strongly peraluminous nature of the Beadle Mountain granite along with the low contents of TiO_2, Fe(TOT), MgO, CaO, Zr, and Ba. Comparable trace element data for other elements exists at this time only for the Nova Scotia granites (to be discussed later) and shows that Beadle Mountain has elevated contents of Cs, Nb and Sn to levels comparable to some of the minor more differentiated phases of the Nova Scotia granites. Beadle Mountain also differs from other New Brunswick granites examined in that it has an average eU/eTh ratio of 1.64 compared to other granites whose ratios range from 0.11 to 0.55. The high eU/eTh ratio in this granite is clearly evident on the airborne profile (Fig. 25.7B).

Other New Brunswick granitoids may exhibit elevated levels of similar lithophile elements as Beadle Mountain but without the associated high eU/eTh ratio. The lack of an associated high eU/eTh ratio should not eliminate the possibility that the more differentiated phases of these granitoids as indicated by high uranium and thorium values may also have associated lithophile element enrichments or deposits as pointed out by Strong (1981).

For New Brunswick granites in general, average equivalent uranium concentrations range from 2 ppm to greater than 14 ppm. Equivalent thorium concentrations range mainly between 20 and 40 ppm with the exception of Nicholas Denys (ND, Fig. 25.1A) which averages only 8 ppm eTh. Average concentrations for all New Brunswick granites sampled (with the exception of Beadle Mountain) average 6.9 ppm equivalent uranium and 25.4 ppm equivalent thorium with an eU/eTh ratio of approximately 0.27. These concentrations are considerably higher than normal crustal averages and slightly higher than average values for granites (Clark et al., 1966), while the average eU/eTh ratio of 0.27 is close to the crustal average. Of the eleven granite localities investigated in New Brunswick, six would be grouped in

Figure 25.3A. *Generalized geology of Nova Scotia (adapted from Keppie, 1979) showing limits of airborne gamma ray spectrometric coverage and localities where in situ gamma ray spectrometric studies were conducted. Total area covered with 5 km line spaced surveys, dashed lines indicate coverage with 1 km line spaced surveys.*

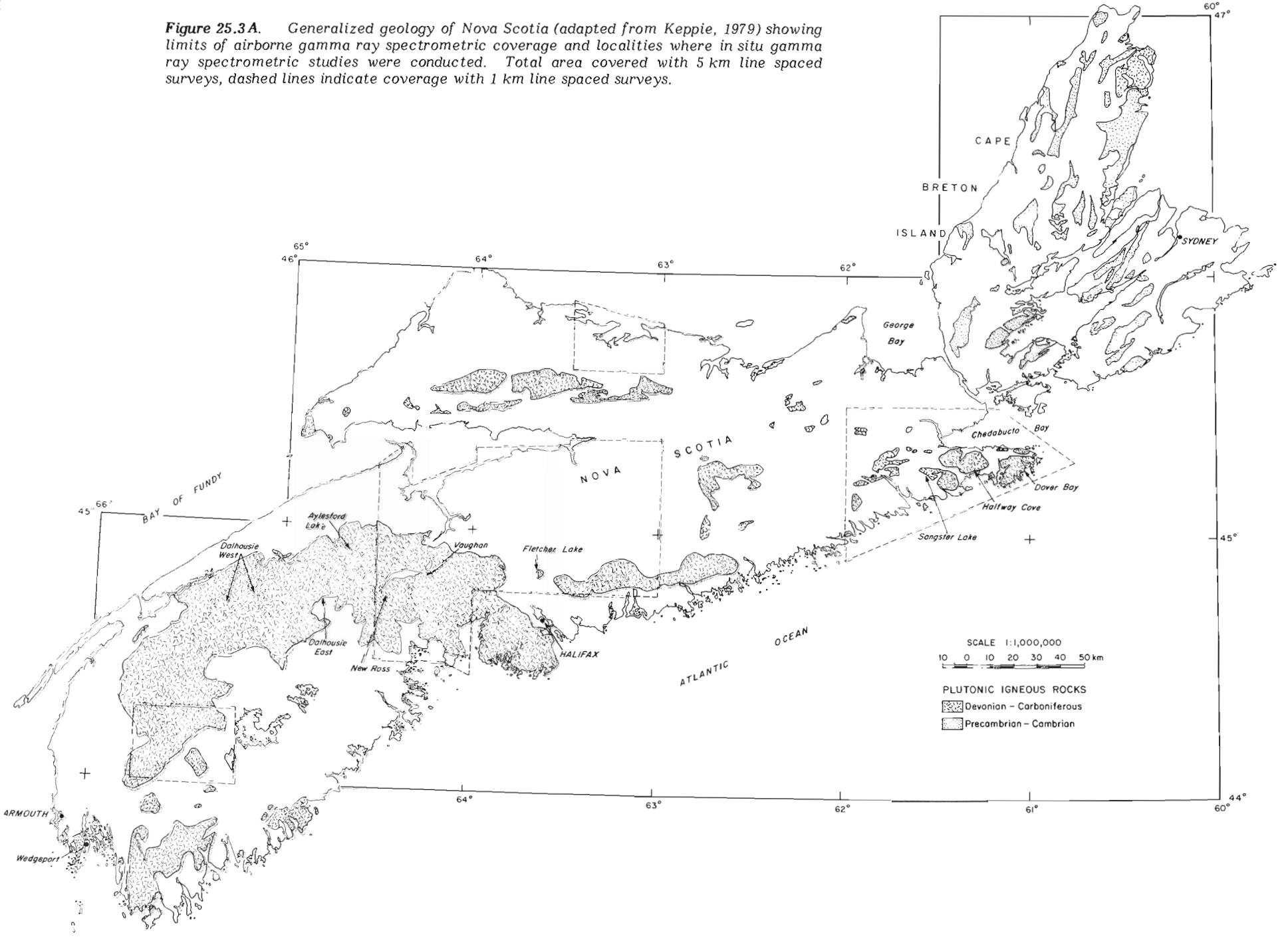

Figure 25.3B. *Equivalent thorium (ppm) map for Nova Scotia compiled from 5 km line spaced airborne gamma ray spectrometric surveys.*

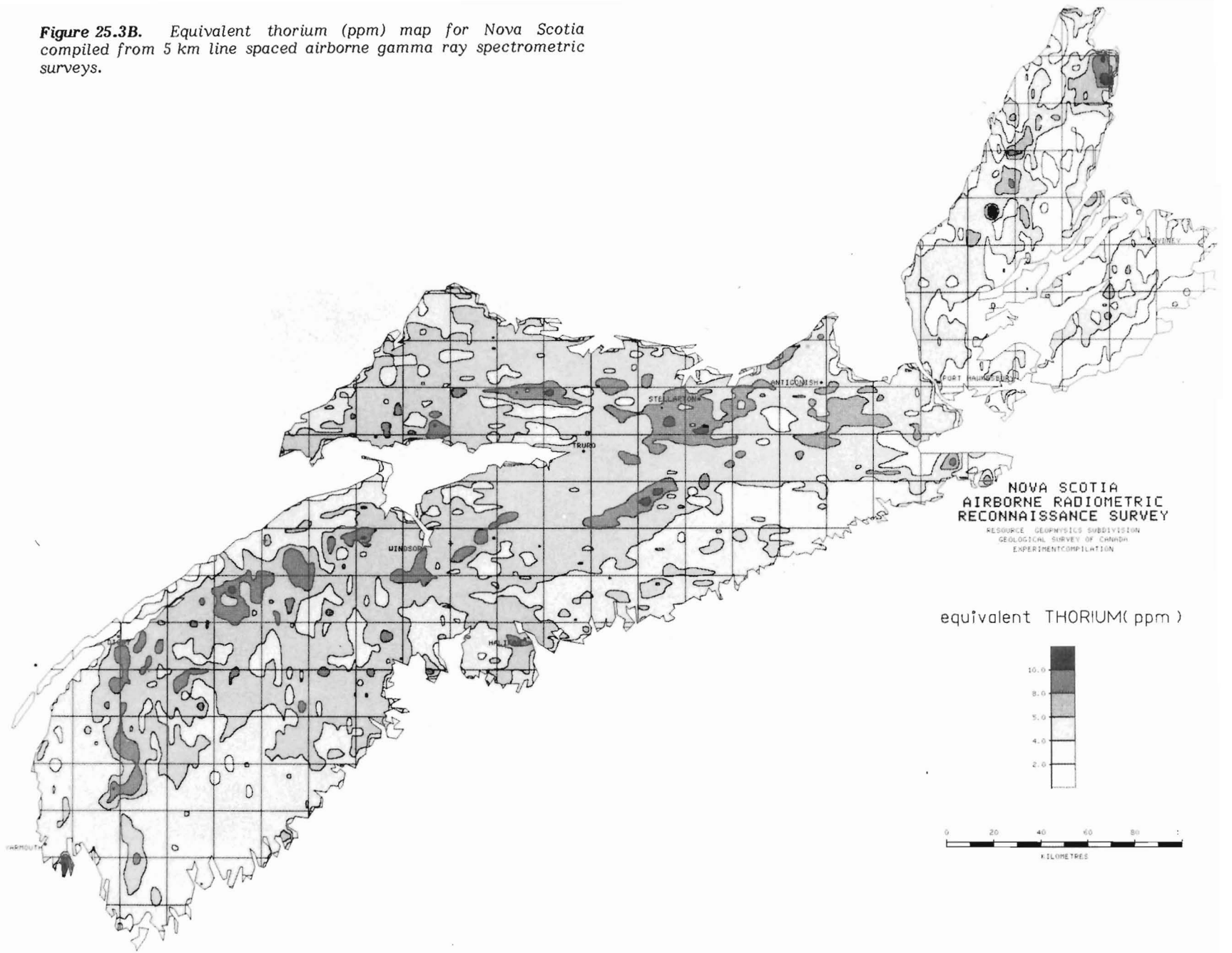

Figure 25.4A and 4B

Equivalent uranium (ppm) (A) and equivalent uranium/equivalent thorium maps (B) for Nova Scotia compiled from 5 km line spaced airborne gamma ray spectrometric surveys.

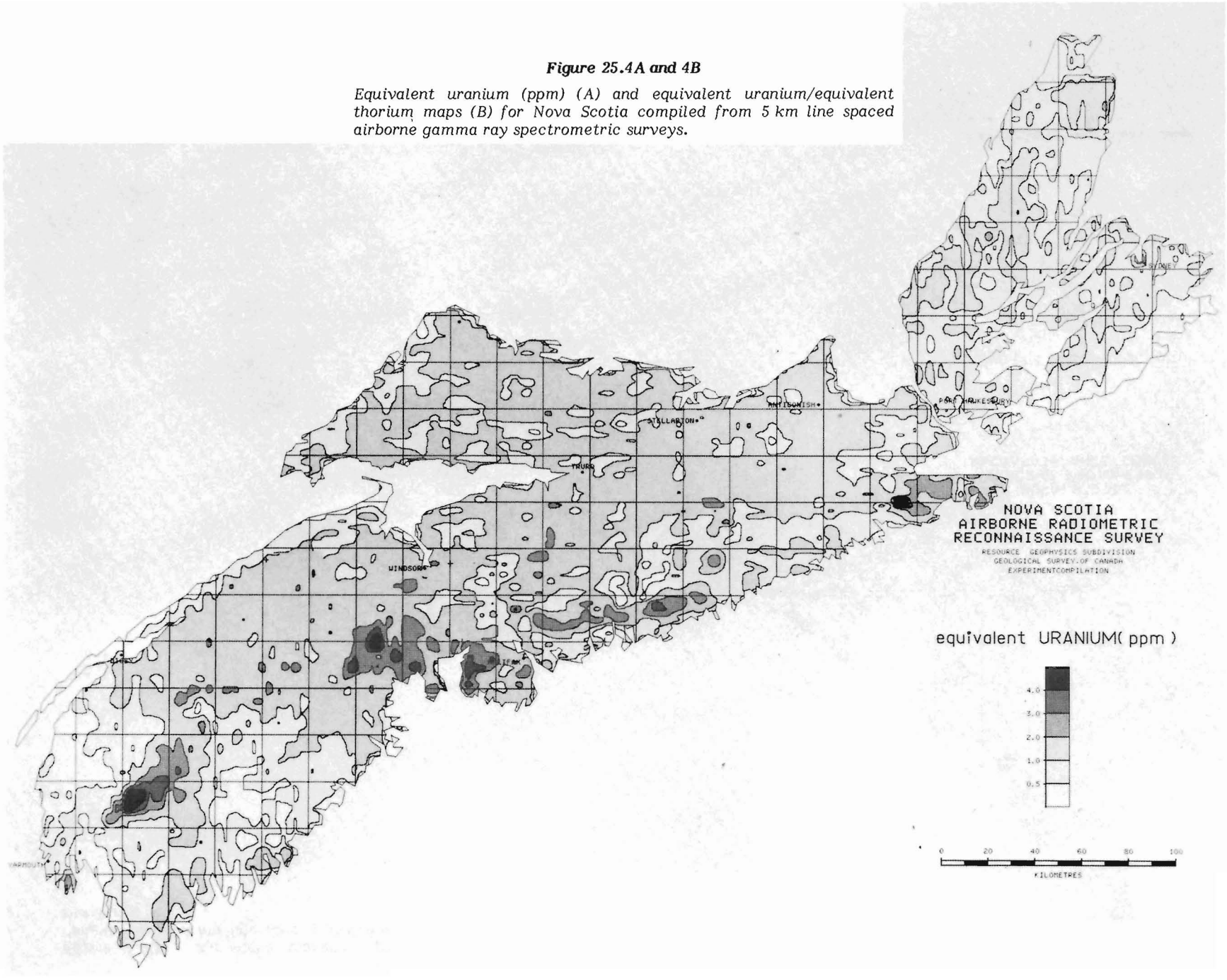

Figure 25.4B

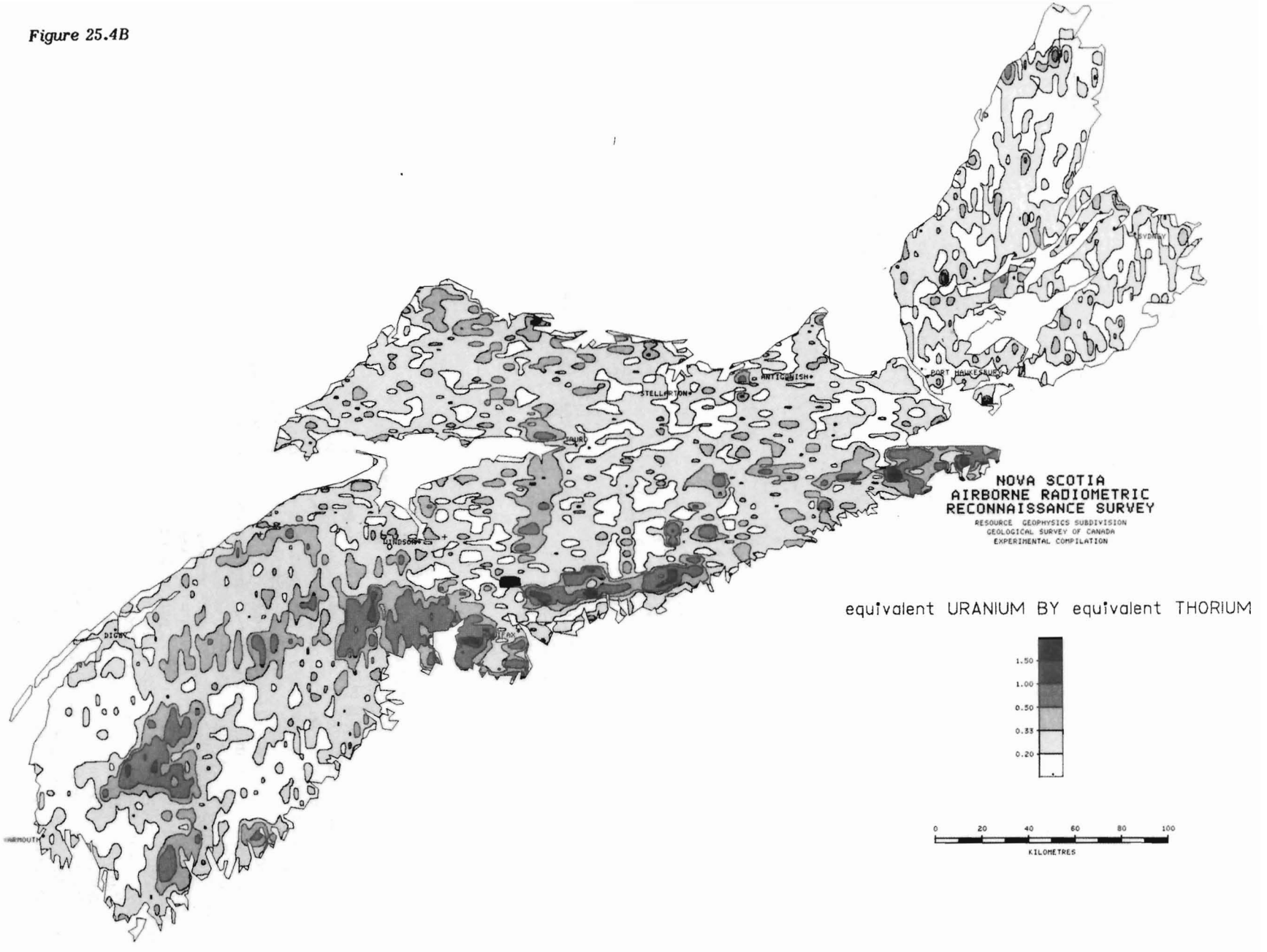
NOVA SCOTIA
AIRBORNE RADIOMETRIC
RECONNAISSANCE SURVEY
RESOURCE GEOPHYSICS SUBDIVISION
GEOLOGICAL SURVEY OF CANADA
EXPERIMENTAL COMPILATION
equivalent URANIUM BY equivalent THORIUM
1.50
1.00
0.50
0.33
0.20
0
20
40
60
80
100
KILOMETRES
PORT HAWKESBURY
ANTIGONISH
STELLARTON
TRURO
WINDSOR
DIGBY
YARMOUTH

Table 25.1

Radioelement content of various rhyolitic and granitic rocks of New Brunswick and Nova Scotia arranged by province and by increasing eU/eTh ratio

	Location	No. of Values	Arithmetic Mean eU (ppm)	Arithmetic Mean eTh (ppm)	Arithmetic Mean K (%)	Arithmetic Mean eU/eTh[3]	Range eU (ppm)	Range eTh (ppm)	Range K (%)	Predominate Rock Type[2]	Age & Source[4]
New Brunswick	Diamond Lake (DL)	4	4.5	37.9	4.1	0.11	1.1-8.7	32.9-45.9	3.4-4.6	Bio. Adamellite	Ord.-Sil.(A)
	Blue Mountain (BM1)	6	3.9	22.9	6.2	0.15	2.0-6.3	20.2-26.7	2.3-8.6	Acid Volcanics and Associated Tuffs	Sil.-Dev.(B)
	Nine Mile Fire Tower (NM)	4	4.2	28.7	7.3	0.15	2.9-5.4	24.9-37.2	5.9-10.0	Rhyolite	Ord.(B)
	Bell Grove (BG)	5	3.7	23.2	5.1	0.16	3.2-5.3	17.3-30.0	3.8-7.1	Rhyolite and Associated Tuffs	Sil.-Dev.(B)
	Pokiok Batholith (P)	31	2.8	17.2	3.4	0.18	1.0-7.7	7.7-28.2	1.9-4.6	Bio. Adamellite	Dev. 387 my (K-AR)(C)
	Charlotte Batholith (C) Group A	9	3.8	20.6	3.6	0.21	2.0-6.6	15.3-24.1	2.9-5.6	Bio. Granite	Dev. 381 my (K-AR)(C)
	Group B	8	8.2	43.2	3.5	0.19	5.9-10.7	38.9-47.6	2.6-5.0	Bio. Granite	
	Total AB	17	5.9	31.2	3.5	0.20	2.0-10.7	15.3-47.6	2.6-5.6		
	Moose Mountain (MM)	4	4.5	19.8	2.8	0.22	2.5-6.1	13.2-26.2	1.9-3.5	Granite	Dev.(A)
	Antinourri Lake (AL)	6	7.0	29.6	3.9	0.24	4.4-8.7	20.4-43.1	3.1-5.2	Bio. Granite	Dev.(C)
	Nicholas Denys (ND)	2	2.0	7.8	2.0	0.25	1.6-2.4	7.1-8.5	1.9-2.1	Bio. Granodiorite	Dev. 392 my (K-AR)(C)
	Fall Brook (FB)	24	9.3	28.4	3.4	0.34	3.4-16.2	17.2-44.1	2.4-4.2	Bio. Musc. Adamellite	Dev.(C)
	Papineau Lake (PL)	3	7.1	20.4	3.5	0.35	5.8-9.7	15.4-25.1	3.4-3.6	Bio. Adamellite	Dev. 398 my (K-AR)(C)
	Clearwater Brook (CB)	10	14.6	40.6	4.1	0.38	7.8-24.1	31.6-50.9	3.7-5.1	Bio. Adamellite	Dev. 339 my (K-AR)(C)
	Trout Brook (TB)	13	11.3	21.3	3.8	0.55	4.6-29.8	7.2-26.6	3.2-4.3	Bio. Adamellite	Dev. 392 my (K-AR)(C)
	Beadle Mountain (BM) Group A	8	2.1	5.8	3.6	0.43	1.5-3.0	3.2-10.2	3.2-3.9	Bio.-Musc. Adamellite	Dev.(D)
	Group B	9	13.6	5.8	3.3	2.29	5.6-21.0	4.6-7.8	2.8-3.7	Musc. Adamellite	
	Total AB	17	9.5	5.8	3.4	1.64	1.5-21.0	3.2-10.2	2.8-3.9		
Nova Scotia	Dalhousie West	11	5.2	21.8	4.2	0.25	4.5-6.6	15.9-27.6	3.9-4.8	Bio.-Musc. Monzo-Granite	Dev.-Carb.(E)
	Wedgeport	6	9.3	36.6	4.0	0.25	3.9-12.1	32.8-46.1	3.6-4.5	Bio. Granite	Dev.-Carb.(E)
	South Mountain	31	3.6	12.9	3.6	0.28	1.8-5.4	8.7-15.4	3.0-4.5	Bio. Granodiorite	Dev.-Carb. 371 my (Rb-Sr)(E)
	Aylesford Lake	9	5.7	11.6	4.1	0.52	3.0-8.8	8.7-16.1	3.6-4.7	Bio.-Musc. Monzo-Granite	Dev.-Carb.(E)
	Dover Bay Group A	5	5.3	17.6	4.3	0.33	4.5-6.5	12.7-22.5	4.2-4.3	Bio.-Musc. Granite	Dev.-Carb.(E)
	Group B	4	4.6	6.9	4.1	0.75	3.7-6.1	4.5-9.0	3.9-4.2	Bio.-Musc. Granite	
	Total AB	9	4.9	11.6	4.2	0.56	3.7-6.5	4.5-22.5	3.9-4.3		
	Halfway Cove	11	6.6	9.6	4.3	0.70	4.8-9.0	8.1-12.8	3.5-5.3	Bio.-Musc. Granite	Dev.-Carb.(E)
	New Ross Vaughn Group A	54	6.9	10.9	4.3	0.72	2.7-21.7	2.1-20.9	1.8-5.5	Bio.-Musc. Monzo-Granite	Dev.-Carb. 364 my (Rb-Sr) (E)
	Group B	20	8.5	6.4	4.1	1.72	2.5-21.7	2.3-10.9	3.1-7.0	Dike Rocks and Minor Intrusives	
	Total AB	74	7.4	9.7	4.2	0.99	2.5-21.7	2.1-20.9	1.8-7.0		
	Dalhousie East	15	6.6	6.7	3.4	1.24	3.6-13.0	1.9-11.8	1.5-4.3	Bio.-Musc. Monzo-Granite	Dev.-Carb.(E)
	Fletcher Lake	14	6.3	3.6	3.5	2.00	2.8-13.2	1.3-5.2	2.9-4.3	Musc.-Bio. Granite	Dev.-Carb.(E)
	Sangster Lake Group A	20	12.0	5.1	3.6	2.40	6.7-16.5	1.2-6.1	3.1-4.3	Musc.-Bio. Granite	Dev.-Carb.(E)
	Group B	5	24.1	2.6	4.1	9.00	9.0-51.7	1.2-4.6	2.9-5.7	Leucocratic Musc. Granite	
	Total AB	25	14.5	4.6	3.8	3.72	6.7-51.7	1.2-6.1	2.9-5.7		
	Average Granite		3.5	12.0							(F)
	Average Silicic Igneous Rock		4.7	20.0							(G)
	Average Granodiorite		2.6	9.3	2.55						(G)
	Typical Silicic Extrusive						2.0-7.0	2.0-25.0			(H)

[1]Measured by in-situ gamma-ray spectrometry. Arranged according to increasing eU/eTh ratio.

[2]Majority of rock type terminology taken from sources. Bio.=Biotite, Musc.=Muscovite.

[3]These values are the average of the ratio and not the ratio of the averages.

[4]Sources include: A-Poole, 1963; B-Potter, 1968; C-Martin, 1966, 1970; D-Skinner, 1972; E-Keppie, 1979; F-Whitfield et al, 1959; G-Clarke et al, 1966; H-Adams et al, 1959.

Martin's Stock class. These include Trout Brook, Clearwater Brook, Papineau Lake, Fall Brook, Nicholas Denys and Antinourri Lake. As a group these localities average 8.5 ppm equivalent uranium and 24.7 ppm equivalent thorium with an average eU/eTh ratio of 0.34. However considerable variation is indicated on Table 25.1 among these Stock class localities. Some of the variability for a few of these Stock class granites is indicated on Figure 25.5. Overall averages within the Charlotte Batholith are 5.9 ppm equivalent uranium and 31.2 ppm equivalent thorium with an average eU/eTh ratio of 0.20. The Pokiok Batholith, part of Martin's Main Belt class, averages 2.8 ppm equivalent uranium and 17.2 ppm equivalent thorium with an average eU/eTh ratio of 0.18. This limited sampling thus indicates that the average equivalent uranium and eU/eTh ratio tend to increase slightly from the Pokiok Batholith to the Charlotte Batholith to the Stock class granites in correspondence with Martin's differentiation increases.

Figure 25.5 illustrates diagrammatically that the eU/eTh ratio increases consistently with uranium but appears to be independent of thorium. In the upper panel of Figure 25.5, the individual in situ gamma ray spectrometric analysis for the Fall Brook, Clearwater Brook and Trout Brook localities are shown. The dashed lines around each grouping only isolate these groupings and have no statistical significance. There is no apparent correlation of equivalent uranium with equivalent thorium or the eU/eTh ratio with equivalent thorium however the eU/eTh ratio does appear to be positively correlated with equivalent uranium. The lower panel on Figure 25.5 illustrates in situ measurements within the Charlotte and Pokiok batholiths and the Beadle Mountain granite. Measurements for the Charlotte Batholith and Beadle Mountain localities appear to be bimodally distributed. In the case of the Beadle Mountain measurements, radioelement variation appears to be associated generally with muscovite-biotite variation. The Beadle Mountain 'B' grouping is composed mainly of measurements over phases where muscovite is dominant and in the case of the 'A' grouping biotite appeared dominant. In the case of the Charlotte Batholith measurements, the bimodal grouping appears to correspond to variations noted by other authors. Martin (1966, 1970) described the Charlotte Batholith as being composite in nature ranging from granodioritic (western portion) to granite.

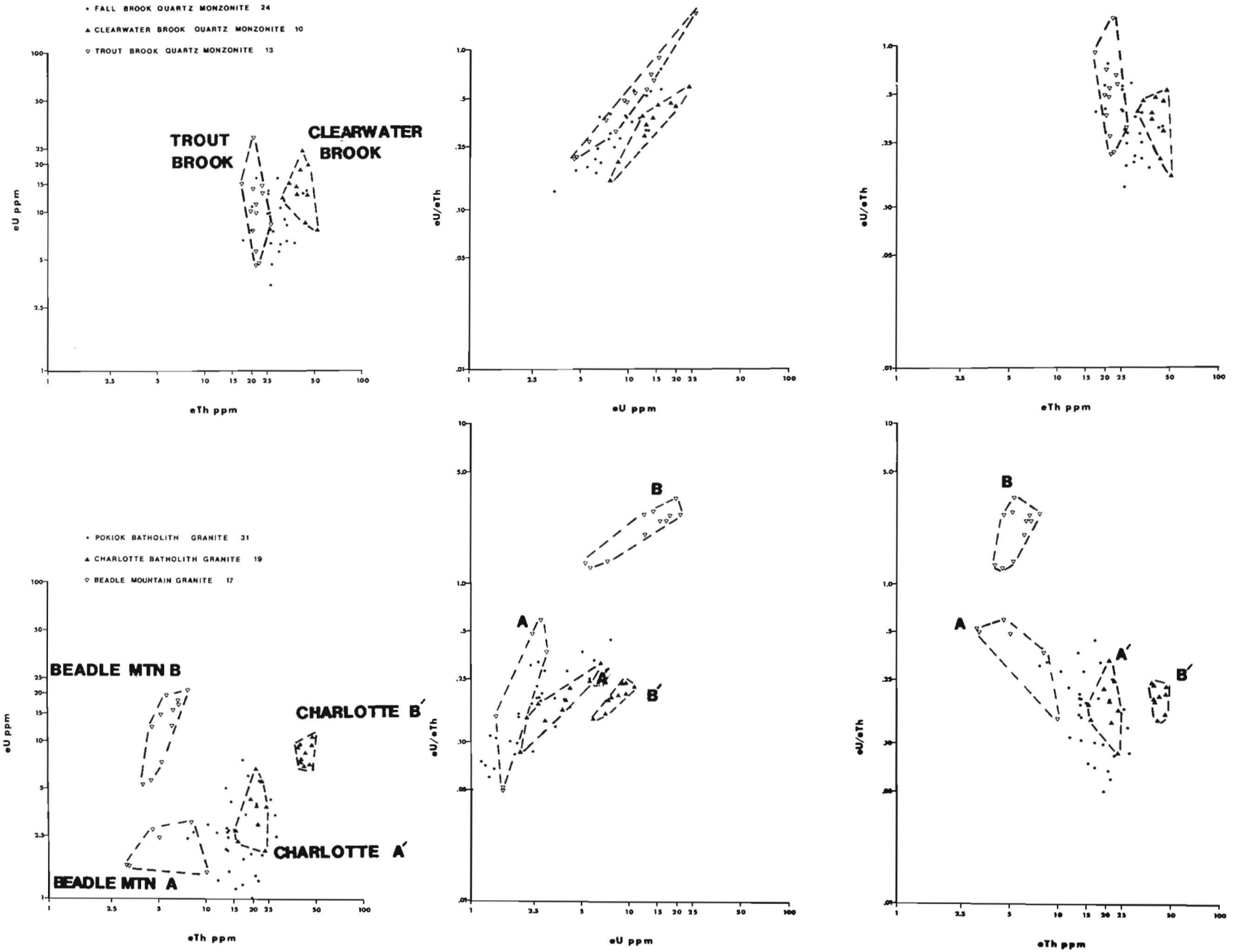

Figure 25.5. *Log – Log plots of individual in situ gamma ray spectrometric measurements showing the equivalent uranium vs equivalent thorium, the eU/eTh ratio vs equivalent uranium and the eU/eTh ratios vs equivalent thorium for six granite localities examined in New Brunswick.*

Table 25.2

Representative chemical analysis of some Maritime granites from Martin (1966), for the New Brunswick granites and McKenzie and Clarke (1975), for the Nova Scotia granites with additional analyses from this study

	New Brunswick					Nova Scotia						
	Main Belt Class		Stock Class Bodies	Charlotte Batholith	Beadle Mountain	South Mountain Batholith						Sangster Lake
	South	North				Granodiorites		Adamellites		Dike Rocks & Minor Intrusive Phases		
Predominate Rock Type[5]	Granodiorite	Adamellite	Adamellite	Granite								
Number of Analysis	43[1]	16[1]	23[1]	26[1]	5[3]	5[3]	11[2]	10[3]	10[2]	17[3]	10[2]	4[3]
SiO_2 (%)	70.10	72.00	72.30	72.30	73.50	69.30	69.40	73.60	73.40	74.20	74.40	72.00
TiO_2	.51	.33	.28	.26	.06	.58	.61	.22	.24	.08	.15	.11
Al_2O_3	15.10	14.80	14.30	13.50	15.70	14.80	14.40	14.40	13.80	14.50	13.70	16.70
Fe_2O_3	3.36	3.17	2.22	2.46	.70	.80	.44	.60	.20	.50	.30	.60
FeO					.20	3.10	3.50	1.00	1.70	.50	1.10	.70
MnO	.07	.05	.06	.05	.04	.09	.10	.03	.05	.03	.04	.09
MgO	1.14	.80	.71	.38	.10	.97	1.02	.31	.35	.11	.19	.26
CaO	2.28	1.77	1.45	1.25	.27	1.41	1.93	.52	.67	.36	.52	.30
Na_2O	3.30	3.44	3.60	3.60	3.80	3.00	3.30	3.10	3.40	3.50	3.60	3.90
K_2O	3.90	3.90	3.90	4.50	4.38	4.23	3.86	4.84	4.80	4.38	4.53	4.00
H_2O					.40	.50	.90	.40	.80	.40	.80	.90
CO_2					.40	.20		.30		.20		.20
P_2O_5					.28	.22	.10	.29	.12	.36	.16	.39
Sr (ppm)	41	50	54	67	50	142	138	76		53		58
Ba	443	486	220	267	34	884	667	281	254	99	132	45
Rb					448	174	147	321	334	504	452	490
Zr	75	105	56	110	18	190	206	79	85	25	35	25
F					860	560		960		1340		675
Cl					180	380		230		253		325
Li					95	89		140		185		213
Cs					25	8		17		24		44
Nb					28	9		11		19		25
Sn					30	7	11	12	16	24	24	34
A/CNK[4]					1.25	1.16		1.14		1.18		1.38

[1]Martin 1966. Total Fe expressed as Fe_2O_3.

[2]McKenzie and Clarke 1975.

[3]This study - major and minors, Sr, Rb, Ba, Zr, Sn, Nb analyzed by x-ray fluorescence, F by fusion and specific-ion electrode, Cl by colorimetric methods, Li and Cs by atomic absorption.

[4]Shand's Alumina Saturation Index from Hyndman 1972.

[5]Rock type terminology from sources.

McGrath (1970) also subdivided the batholith on the basis of magnetic characteristics into a magnetic northwestern unit and a nonmagnetic central and eastern unit. Atkinson et al. (1981) also described the composite nature of the Charlotte Batholith referring to an older, megacrystic western portion and a younger rapakivi textured eastern portion with ages ranging from 380 to 320 Ma. They also mentioned that greissen occurrences are generally found only in the eastern part of the granite. In situ measurements in the younger, northeastern portion of the batholith ('B' grouping, Fig. 25.5) indicate average equivalent uranium and equivalent thorium concentrations of 8.2 ppm and 43.2 ppm respectively whereas the older, western portion of the batholith ('A' grouping, Fig. 25.5) averages 3.8 ppm equivalent uranium and 20.6 ppm equivalent thorium. A recent more detailed study of radioelement variation within the Charlotte Batholith also indicated significant internal variation in the radioelement content of the Charlotte Batholith with general radioelement concentrations consistent with values reported here (Hassen et al., 1980).

Nova Scotia Investigations

Figures 25.3B, 25.4A, and 25.4B show the equivalent thorium, equivalent uranium, and the eU/eTh ratio distribution patterns for Nova Scotia. Figure 25.3B shows an equivalent thorium pattern that is much less intense than patterns over much of New Brunswick with virtually all the survey area having values less than 10 ppm eTh.

The equivalent uranium map (Fig. 25.4A) indicates a background level which is slightly higher than in New Brunswick and also indicates that a larger portion of the survey area in Nova Scotia exceeds 2 ppm eU compared with similar levels in New Brunswick. The most striking difference between the regional radioelement patterns of New Brunswick and Nova Scotia is shown in Figure 25.4B, a compilation of the eU/eTh ratio. This indicates that much of southern and central Nova Scotia exceeds the crustal average of 0.25 and a significant portion is shown to exceed 0.50. These high eU/eTh ratios and associated high equivalent uranium contents relate in general to the more differentiated phases of the Devonian-Carboniferous peraluminous granitic rocks of southern Nova Scotia. The geology of and differentiation trends within the Devonian-Carboniferous granitic rocks of southern Nova Scotia, dominated by the South Mountain Batholith, have been studied by Taylor (1967, 1969), McKenzie and Clarke (1975) and more recently by Chatterjee and Muecke (1982).

McKenzie and Clarke (1975) and Chatterjee and Muecke (1982) concluded that the South Mountain Batholith represents a cogenetic suite of granitoid rocks composed

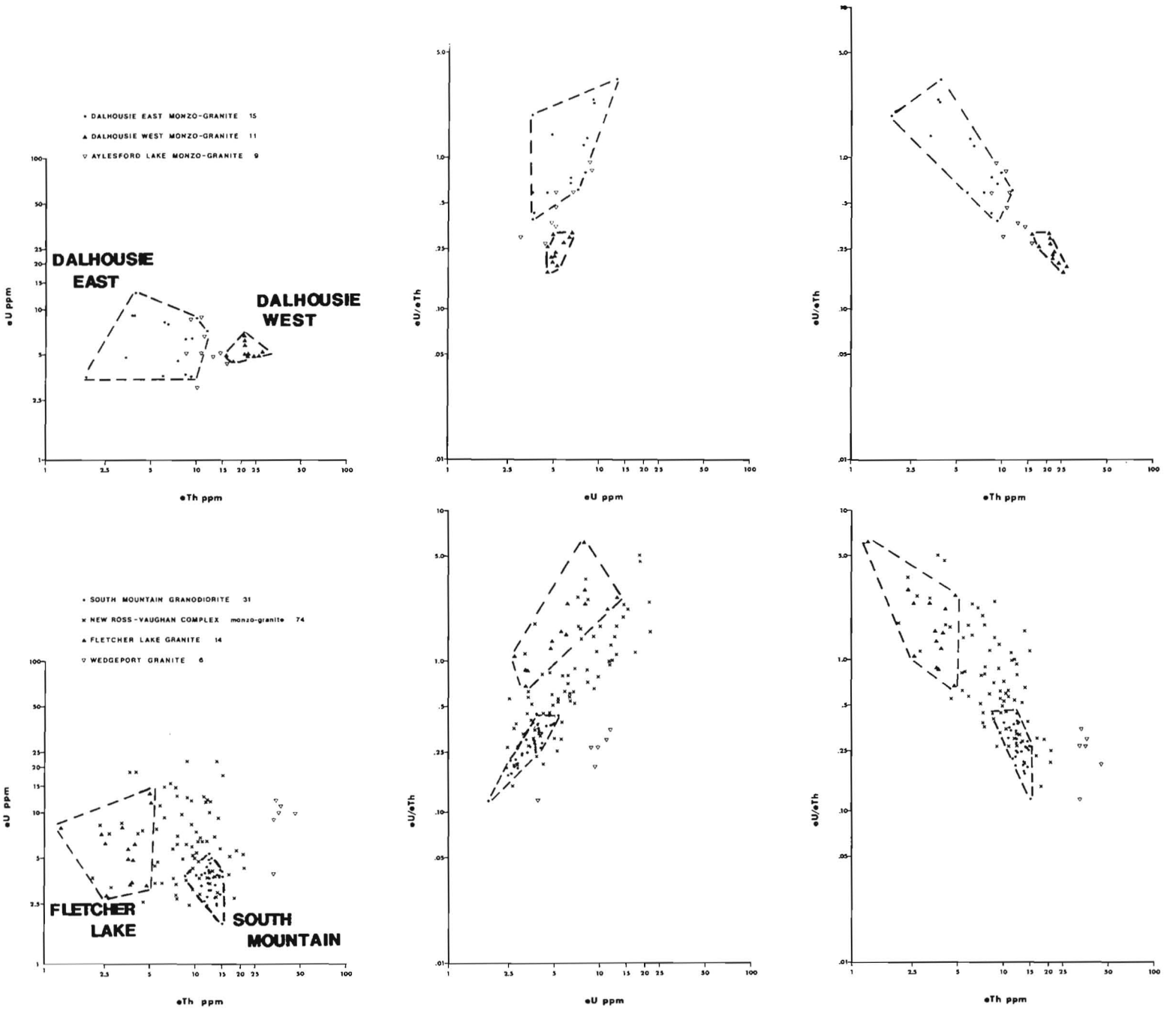

Figure 25.6. *Log – Log plots of individual in situ gamma ray spectrometric measurements showing the equivalent uranium vs equivalent thorium, eU/eTh ratio vs equivalent uranium and the eU/eTh ratios vs equivalent thorium for seven granite localities examined in Nova Scotia.*

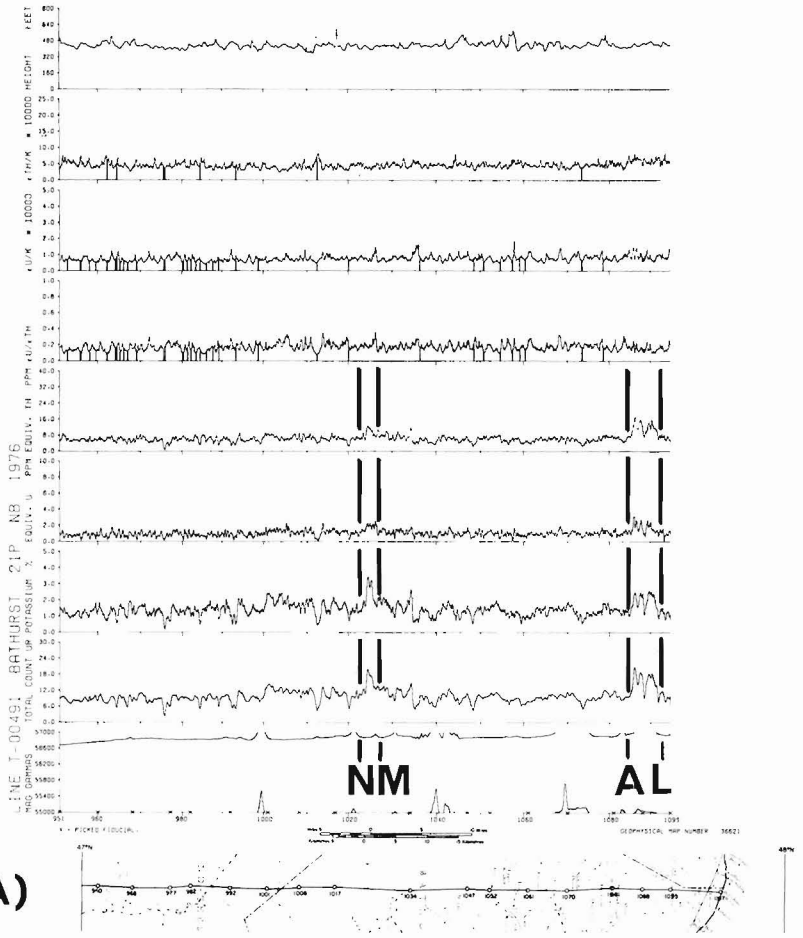

Figure 25.7A

Airborne gamma ray spectrometric profile showing typical profile form of rhyolitic (NM) and Stock class granite bodies (AL) in New Brunswick.

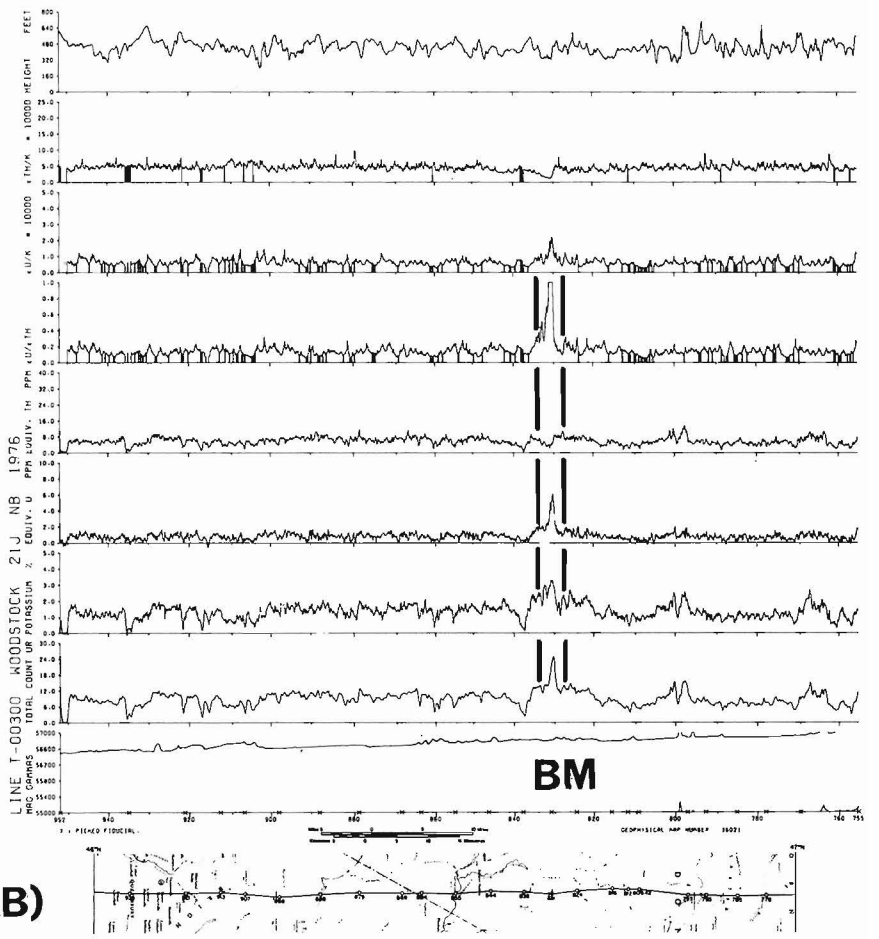

Figure 25.7B

Airborne gamma ray spectrometric profile showing the high equivalent uranium and eU/eTh nature of the Beadle Mountain granite.

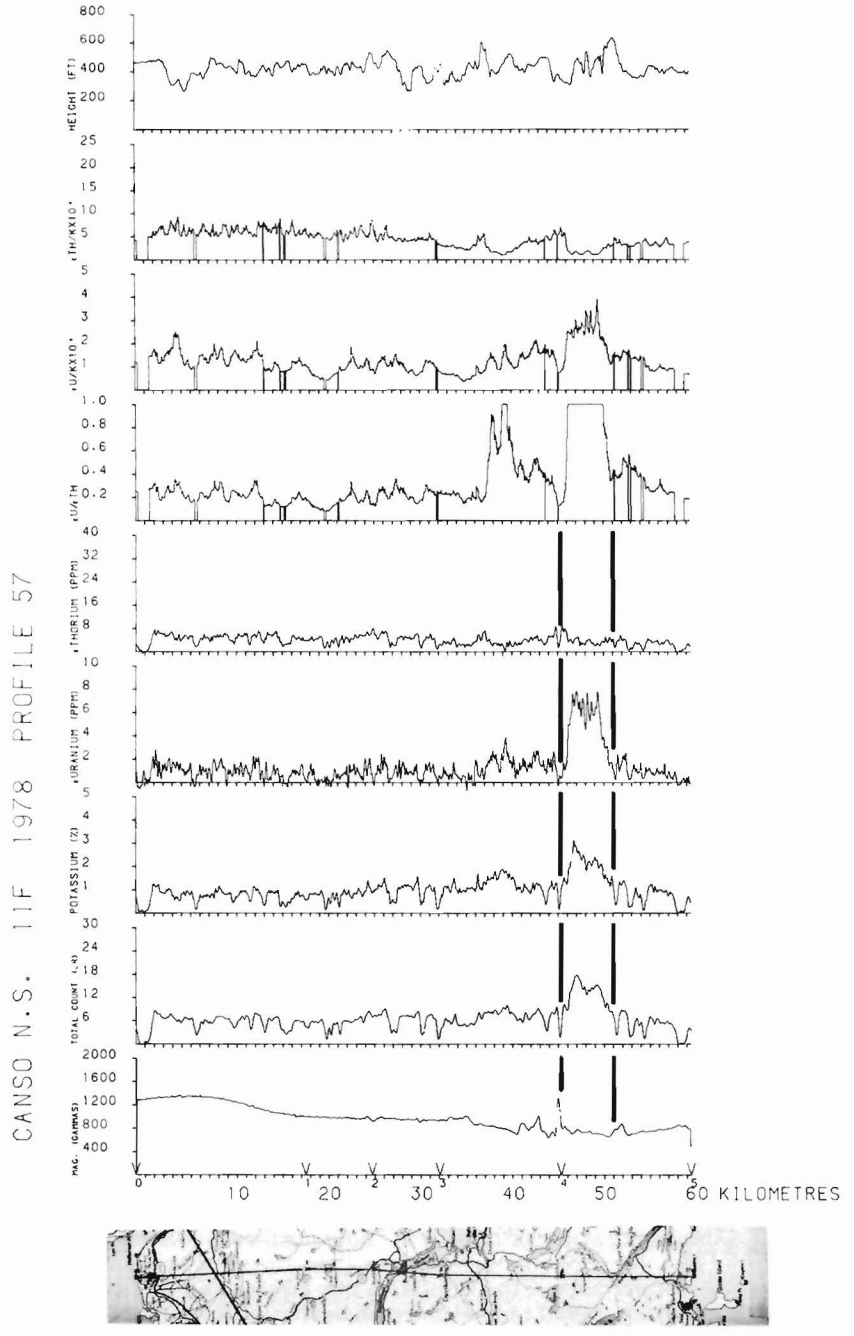

Figure 25.8. *Airborne gamma ray spectrometric profile over the Sangster Lake granite showing the typical high eU/eTh ratio profile response of many of the late phases of the Nova Scotia peraluminous granitic suite.*

predominantly of biotite granodiorite, followed by smaller discrete bodies of biotite-muscovite adamellite and leucocratic adamellite. Following these phases are small dykes and irregular bodies of aplite, pegmatite and porphyries. Chatterjee and Muecke (1982) also recognized a para-intrusive suite composed of a variety of argillitized, sericitized and albitized granites and greissens which they feel may be the result of the interaction of a late stage fluid phase with residual magma and/or the cogenetic crystalline rocks. They stated that the normal differentiation trends of the cogenetic suite tend to breakdown for some elements resulting in extreme enrichments (U, Sn, Li) or depletions (REE, Th). Some of their para-intrusives may be included in the averages of Table 25.2 but most analyses appear to be from the cogenetic suite.

Figure 25.3A shows the limits of reconnaissance airborne gamma ray spectrometric surveys in Nova Scotia; also indicated are the limits of additional surveys flown to investigate, in more detail, significant features from the reconnaissance surveys. Investigations of radiometric anomalies found on these detailed surveys led to the discovery of low-grade uranium mineralization at the base of the Mississippian Windsor Group (Charbonneau and Ford, 1978). These detailed surveys are also of particular use in outlining some of the small discrete bodies of adamellite, aplite, pegmatite and para-intrusive which may have dimensions smaller than the 5 km line spacing of reconnaissance surveys (see Geological Survey of Canada, Geophysical Series Maps 35 121(9)G, 35 121(16)G and 35 821(1)G).

In situ gamma ray spectrometric measurements over the granites of southern and central Nova Scotia (Table 25.1, Fig. 25.6) demonstrate the increased average equivalent uranium and high eU/eTh in these rocks along with equivalent thorium contents below the general crustal average. Average uranium concentrations of the Nova Scotia granites (Table 25.1) are about 7 ppm which is comparable to that for the New Brunswick granites (6.9 ppm). Average thorium concentrations are about one half that of the New Brunswick granites (12.9 ppm vs 25.4 ppm) and consequently the eU/eTh ratios are much higher on average.

The majority of in situ gamma ray spectrometric measurements in Nova Scotia relate to the various granitic phases of the South Mountain Batholith. Table 25.1 indicates that the earliest phase of this batholith, the granodiorite (South Mountain, Table 25.1), has a mean equivalent uranium content of 3.6 ppm and an equivalent thorium content of 12.9 ppm. With increasing differentiation the later adamellites show increased equivalent uranium and lower equivalent thorium contents. For example, Aylesford Lake has mean contents of 5.7 ppm eU and 11.6 ppm eTh, Dalhousie East has contents of 6.6 ppm eU and 6.7 ppm eTh and the New Ross-Vaughn Complex has contents of 6.9 ppm eU and 10.9 ppm eTh. Within the New Ross-Vaughn Complex the more differentiated phases of McKenzie and Clarke's cogenetic suite are represented by dykes of aplite, pegmatite and porphyry. These have mean contents of 8.5 ppm eU and 6.4 ppm eTh. This inverse relationship between uranium and thorium has also been described by Chatterjee and Muecke (1982). They mentioned, however, that a second trend, characterized by uranium and thorium increasing with differentiation, exists in the western extremities of the batholith. In situ measurements from two adamellite intrusives near the central and western portions of the batholith, Dalhousie West and Wedgeport, tend to support this second trend with both bodies having equivalent thorium contents greater than that for the granodiorites (21.8 and 36.6 ppm respectively).

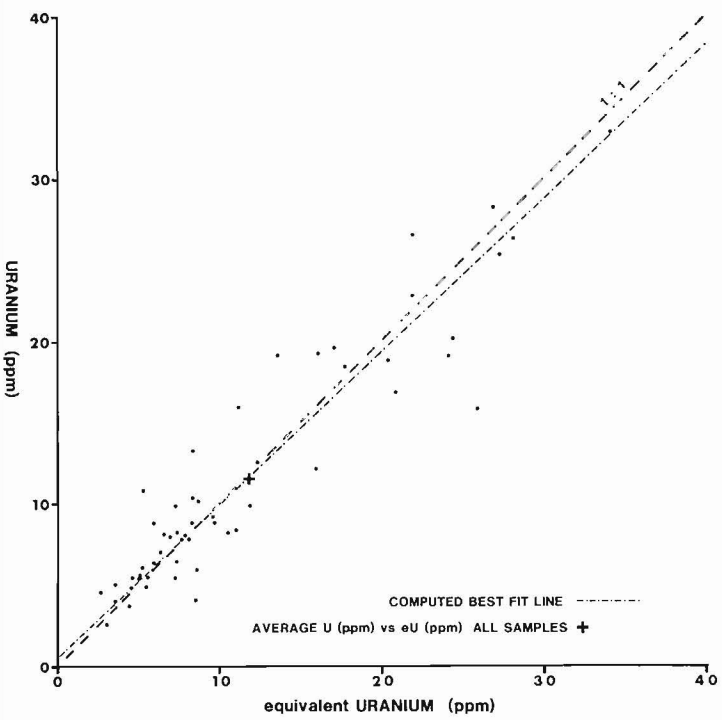

Figure 25.9. *Comparison of uranium analysis by laboratory gamma ray spectrometry (eU) with analysis by delay neutron counting (U) for granite samples from New Brunswick and Nova Scotia.*

Examples of extreme thorium depletion within the more differentiated phases of the Nova Scotia granites include the Sangster and Fletcher Lake plutons, and in particular the leucocratic muscovite-rich phases of the Sangster Lake pluton (Table 25.1, Group B) which has a mean eTh content of 2.6 ppm. The low equivalent thorium content of the Sangster Lake granite is particularly evident on the airborne profile over this body (Fig. 25.8). This is typical of many of the profiles over more differentiated phases of the Nova Scotia granites. Table 25.2 shows the strongly peraluminous nature of this pluton as it compares with different phases of the South Mountain Batholith.

Laboratory Investigations

Laboratory analyses by gamma ray spectrometry and delayed neutron counting were performed on samples collected from sites of in situ gamma ray measurements to test for the possibility of disequilibrium between elemental uranium and equivalent uranium (bismuth-214). Comparison of gamma ray spectrometric laboratory analysis and delayed neutron counting are shown in Figure 25.9. The slope of the computed best fit line is 0.94 with a Y-intercept of 0.53 and a correlation coefficient of 0.91.

For the 54 samples shown on Figure 25.9 the average equivalent uranium value is 11.8 ppm and the average elemental uranium value is 11.6 ppm. Individual samples can however show considerable variation (see Fig. 25.9). To estimate the effects of possible sample inhomogeneity for delayed neutron counting, duplicate and triplicate analyses were performed on 9 samples with uranium contents ranging from 4 to 900 ppm. In all but one case in-sample variation was under 5 per cent. V.R. Slaney (personal communication) found similar in-sample variation both for delayed neutron counting and for determinations made by laboratory gamma ray spectrometry. Taking into account these in-sample variations, the scatter from a 1:1 correlation between delayed neutron counting and laboratory gamma ray spectrometry would appear to indicate that there is in some cases considerable disequilibrium within the ^{238}U decay series. This disequilibrium however may only be local as some samples show excess ^{238}U whereas others show deficiency of ^{238}U with respect to ^{214}Bi. An extreme case of local disequilibrium was reported by Ostrihansky (1976) where he determined uranium deficiencies of up to 90 per cent and similar excesses over distances of a few centimetres in shallow drill core from sedimentary rocks of the Elliot Lake area.

A shallow (to depths of 12 cm) drilling program was conducted on a variety of phases of the South Mountain Batholith to assess the extent of local disequilibrium in this environment. The results, presented in Table 25.3, show some interesting aspects of this environment. The last three drill sites (DS-5, DS-6 and DS-7), which have relatively low uranium contents, show very good correlation between elemental uranium and equivalent uranium, implying that disequilibrium is not an important consideration in these phases. The lack of variation with depth, particularly sites 5 and 6 suggests that much of the uranium may be in a non-labile form. The first four drill sites however, show considerable variation, not only between elemental uranium and equivalent uranium but also with depth. These data imply that there can be considerable local disequilibrium, in some cases (DS-3) showing excessive elemental uranium compared to equivalent uranium and in other cases (DS-1) showing the opposite. It is also suggested that uranium is being removed from the surficial layers and being deposited locally at lower depths in the drill core (DS-2, 4). This however cannot be confirmed without drill core from greater depths than were obtained in this study. Rock type inhomogeneity (both textural and elemental) particularly in the higher concentrations, should be considered to explain some of the variability, but this probably should not alter the overall impression that these data present, i.e., that disequilibrium does exist. However it may only be of local significance (i.e. outcrop scale) and that on a regional basis equilibrium is maintained between elemental uranium and equivalent uranium (Charbonneau et al., 1981).

Summary

The main purpose of this investigation has been to provide an initial assessment of the regional radioelement concentration patterns over those portions of New Brunswick and Nova Scotia surveyed to date by airborne gamma ray spectrometry. The results of this investigation indicate that major regional radioelement anomalies in New Brunswick are relatable to granitic rocks with maximum concentrations of uranium and thorium associated with those phases of the Devonian granitic rocks exhibiting higher differentiation indices. The high eU/eTh ratio anomalies which characterize much of the surveyed area of Nova Scotia were found to be related to the more differentiated phases of the Devonian-Carboniferous peraluminous granitic rocks. Uranium and thorium contents generally increase and decrease, respectively, with differentiation. The reason for this unusual tendency has not been established but it appears that thorium is being removed early in the differentiation sequence. In some cases the high ratio character of a particular granite body is the result of an unusually low thorium content with only a marginal increase in uranium (i.e. Fletcher Lake).

Strong (1981) in a recent article on granitic rocks and their associated mineral deposits in Eastern Canada has referred to the typical association of lithophile elements with the muscovite biotite (2-mica) leucogranites thought to be

Table 25.3

Variation of radioelement concentrations in shallow drill core from the South Mountain Batholith illustrates the extent of local, small scale variation in uranium and thorium and between equivalent uranium measured indirectly as ^{214}Bi and elemental uranium to assess the magnitude of disequilibrium in this particular granitic environment

	In-Situ Analysis[1]					Geol. Surv. Can. Gamma-Ray Spectrometry Lab Analysis				Elemental Uranium and Thorium[3]			
Drill Site	eU ppm	eTh ppm	K %	eU/eTh	[2]	eU ppm	eTh ppm	K %	eU/eTh	U ppm	Th ppm	U/Th	Rock Type[4]
DS-1	11.2	3.2	3.3	3.58	A	13.2	0.5	3.2	---	7.5	1.0	7.50	M.G., Bio.-Musc. Granite
					B	15.5	0.0	3.4	---	11.2	2.0	5.60	
DS-2	11.9	9.3	3.9	1.28	A	13.0	5.7	3.7	2.28	12.6	6.7	1.87	C.G., Bio.-Musc. Monzo-Granite
					B	17.8	6.6	3.6	2.70	22.2	7.7	2.88	
DS-3	11.1	12.5	4.0	0.89	A	9.4	9.1	3.9	1.03	12.6	9.7	1.30	C.G., Bio.-Musc. Monzo-Granite
					B	13.7	9.4	3.6	1.46	17.4	10.0	1.74	
DS-4	19.1	8.5	2.8	2.31	A	24.8	4.3	2.6	5.77	18.3	5.0	3.66	C.G., Musc.-Bio. Granite-Pegmatite
					B	27.2	3.4	1.9	8.00	35.1	5.3	6.62	
DS-5	3.3	12.5	4.3	0.26	A	3.6	8.3	4.0	0.43	3.9	9.3	0.42	C.G., Bio.-Musc. Monzo-Granite
					B	4.1	7.9	4.1	0.52	4.1	7.7	0.53	
DS-6	2.5	11.4	3.4	0.22	A	2.6	9.2	3.2	0.28	2.8	10.3	0.27	Porphyritic Bio.-Granodiorite
					B	2.7	9.0	3.2	0.30	3.1	10.8	0.29	
DS-7	5.4	9.7	4.1	0.56	A	4.5	7.9	3.8	0.57	4.7	9.3	0.51	C.G., Bio. Musc. Monzo-Granite
					B	7.8	7.7	3.6	1.01	6.2	8.3	0.74	

[1]5 in-situ measurements were made, high and low were removed, remaining 3 averaged.

[2]A - Upper 6 cm of drill core.
B - Lower 6 cm of drill core.

[3]Uranium determined by delayed neutron counting.
Thorium determined by neutron activation.

[4]M.G. - Medium grained.
C.G. - Coarse grained.
Bio.-Biotite
Musc.-Muscovite

the result of extreme differentiation processes. The ability to be able to delimit individual granitic plutons or phases of larger granitic bodies which exhibit the characteristics of extreme differentiation is helpful in exploring for the associated elements mentioned above. From this investigation it appears that the airborne radiometric patterns presented here are useful in delineating the more differentiated granitic phases which exhibit elevated levels of other lithophile elements, in particular Sn and Nb along with uranium.

Acknowledgments

The author gratefully acknowledges the assistance of J.M. Carson, P.B. Holman and G.W. Cameron of the Geological Survey of Canada for airborne operations, map compilation and gamma ray spectrometry laboratory analysis; J. Chandra of the New Brunswick Department of Natural Resources and A.K. Chatterjee of the Nova Scotia Department of Mines and Energy for their assistance in the field and valuable discussions and R. Crosby of the Miramichi Lumber Company for providing access to company roads. The author was assisted in the field by I. Falconer and W. Sattlegger. The paper was critically read by W. Goodfellow, B.W. Charbonneau and R.L. Grasty.

References

Adams, J.A.S., Osmond, J.K., and Rogers, J.J.W.
1959: The geochemistry of uranium and thorium; Physics and Chemistry of the Earth, Ahrens, ed., v. 3, p. 298-348.

Atkinson, J.R., Koofman, G., and Coates, H.J.
1981: Mount Pleasant taps 3 types of breccia; The Northern Miner, Dec. 17, 1981.

Charbonneau, B.W. and Ford, K.L.
1978: Uranium mineralization at the base of the Windsor Group South Maitland, Nova Scotia; in Current Research, Part A, Geological Survey of Canada, Paper 78-1A, p. 429-425.

Charbonneau, B.W., Ford, K.L., and Cameron, G.W.
1981: Equilibrium between U and eU (Bi-214) in surface rocks of Canada; in Current Research, Part C, Geological Survey of Canada, Paper 81-1C.

Charbonneau, B.W., Killeen, P.G., Carson, J.M., Cameron, G.W., and Richardson, K.A.
1976: Significance of radioelement concentration measurements made by airborne gamma ray spectrometry over the Canadian Shield; IAEA Symposium on Exploration for Uranium Ore Deposits, Vienna, Austria, 1976, ST1/PUB/434, p. 35-53, IAEA-SM 208/3.

Chatterjee, A.K. and Muecke, G.K.
1982: Geochemistry and the distribution of uranium and thorium in the granitoid rocks of the South Mountain Batholith, Nova Scotia; Some genetic and exploration implications; in Uranium in Granites, ed. Y.T. Maurice, Geological Survey of Canada, Paper 81-23, p. 11-17.

Clark, S.P., Jr., Peterman, Z.E., and Heier, K.S.
1966: Abundances of uranium, thorium, and potassium; in Handbook of Physical Constants, Geological Society of America, Memoir 97, p. 521-541.

Hassen, H.H., Hale, W.E., and Pajari, G.E.
1980: Preliminary observations on the distribution of uranium and thorium in rocks of southwestern New Brunswick; in Abstracts, Uranium in Granites Workshop, Ottawa, November 25 and 26.

Keppie, J.D.
1979: The Geological Map of the Province of Nova Scotia; Department of Mines and Energy, Nova Scotia.

Martin, R.F.C.
1966: A chemical and petrographic study of the granitic rocks of New Brunswick, Canada; M.Sc. thesis, Pennsylvania State University.

1970: Petrogenetic and tectonic implications of two contrasting devonian batholithic associations in New Brunswick, Canada; American Journal of Science, v. 268, April 1970, p. 309-321.

McGrath, P.H.
1970: Magnetic investigations of the Charlotte and Pokiok intrusions, Southern New Brunswick; Geological Association of Canada, Proceedings, v. 21, 1970.

McKenzie, C.B. and Clarke, D.B.
1975: Petrology of the South Mountain batholith, Nova Scotia; Canadian Journal of Earth Sciences, v. 12, p. 1209-1218.

Ostrihansky, L.
1976: Part 2: Radioactive disequilibrium investigations, Elliot Lake area, Ontario; in Radioactive Disequilibrium Determinations, Geological Survey of Canada, Paper 75-38.

Poole, W.H.
1963: Hayesville, New Brunswick; Geological Survey of Canada, Map 6-1963.

Potter, R.R., Jackson, E.V., and Davis, J.L.
1968: Geological Map of New Brunswick; Department of Natural Resources, New Brunswick, Map Number N.R.-1.

Rogers, J.J.W. and Adams, J.A.S.
1963: Chapters 90B-90O and Chapters 92B-92O; in Handbook of Geochemistry, K.H. Wedepohl, ed., Volume II-5.

Skinner, R.
1972: Juniper (east half) map-area, New Brunswick (21J/11, E-1/2); Geological Survey of Canada, Paper 72-1, Part A, p. 11-14.

Strong, D.F.
1981: Granitoid rocks and associated mineral deposits of eastern Canada and western Europe; in The Continental Crust and Its Mineral Deposits, ed. D.W. Strangway, Geological Association of Canada Special Paper 20, p. 741-769.

Taylor, F.C.
1967: Reconnaissance geology of Shelburne map-area, Queens, Shelburne and Yarmouth Counties, Nova Scotia; Geological Survey of Canada, Memoir 349.

1969: Geology of the Annapolis-St. Marys Bay map area, Nova Scotia (21A, 21B east half); Geological Survey of Canada, Memoir 358.

Whitfield, J.M., Rogers, J.J.W., and Adams, J.A.S.
1959: The relationship between the petrology and the thorium and uranium contents of some granitic rocks; Geochimica et Cosmochimica Acta, v. 17, p. 248-271.

GEOLOGY OF THE GRAVENHURST REGION, GRENVILLE STRUCTURAL PROVINCE, ONTARIO

Project 760061

DSS Contract OSU 80-00033

W.M. Schwerdtner[1] and C.K. Mawer[1]
Precambrian Geology Division

Schwerdtner, W.M., and Mawer, C.K., Geology of the Gravenhurst region, Grenville Structural Province, Ontario; in Current Research, Part B, Geological Survey of Canada, Paper 82-1B, p. 195-207, 1982.

Abstract

The Gravenhurst region of central Ontario is underlain by strongly deformed high-grade gneisses whose regional structural grain delineates major folds, large lenticular structures and smaller oval structures (domes and basins). Other major structures are ductile shear zones that trend NNE, and WSW-trending brittle faults that appear to postdate the Grenville Orogeny.

Although the attitude of gneissosity is highly variable throughout the region, most dip values lie between 15 and 45 degrees. This range of gneissosity attitude and associated tight folds is compatible with large-scale simple shearing as well as mature diapirism, but neither mechanism is capable of explaining the large lenticular structures and the distribution of rock types as seen on various scales within the area.

Introduction

The Gravenhurst region, central Ontario, is defined for the present purposes as the region bounded to the north by latitude 45°N, to the west by the shore of Georgian Bay, to the east by Ontario Highway 35, and to the south by the edge of the Canadian Shield. Gravenhurst, the largest town of the region, is 140 km due north of Toronto.

Ontario Highway 11 divides the Gravenhurst region into two nearly equal areas, hereafter called the East Half and West Half. Most of the East Half was mapped by C.K. Mawer. Schwerdtner mapped large portions of the West Half prior to 1980 in detailed reconnaissance fashion. Following Lumbers (1975, 1978), he attempted to identify protoliths of all gneissic rocks. It was realized in 1980-81 that because numerous metaplutonic bodies and tight folds lie within the structural grain of gneissosity (Schwerdtner et al., 1981), only outcrop-by-outcrop mapping would provide a clear structural and lithological picture of the region. Time did not permit this type of coverage in many places. This is the final report of the area mapped under the terms of DSS Contract OSU 80-00033. Thanks go to M. Donnan for field assistance, and J. van Berkel for considerable help in drafting. We acknowledge many discussions with A. Davidson (Geological Survey of Canada) and S.B. Lumbers (Royal Ontario Museum), and National Scientific and Engineering Research Council support since 1979.

Major Structures

Most of the region is underlain by strongly deformed high-grade gneisses, whose regional structural grain is apparent on aerial photographs and 1:125 000 shaded topographic relief maps (Orillia and Bobcaygeon sheets, NTS 31D/NW and 31D/NE). Topographic ridges on these maps are generally parallel to gneissosity and transposed compositional layering, both of which dip gently throughout most of the region (Fig. 26.1).

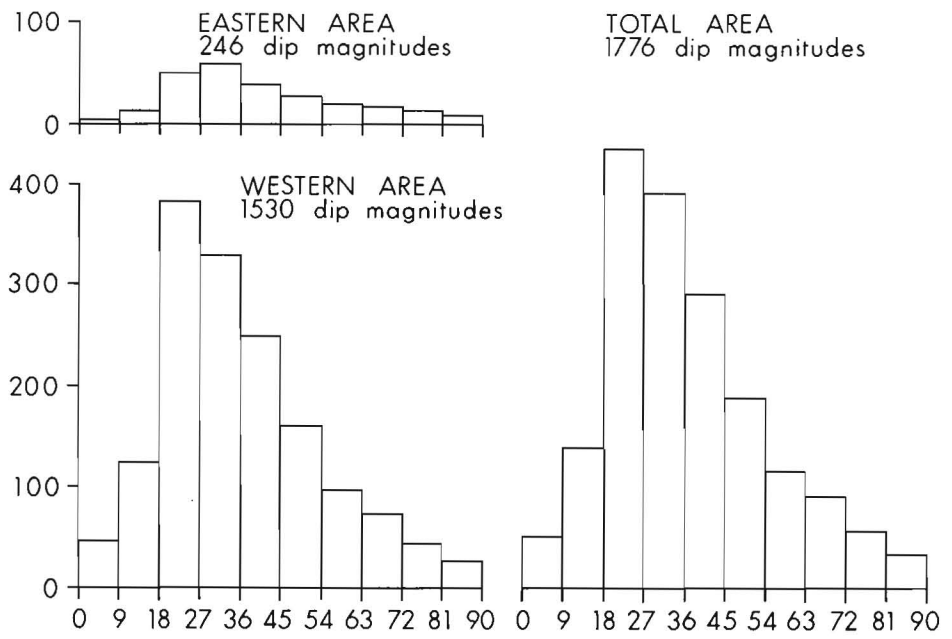

Figure 26.1

Histogram of average dip values determined at individual stations.

[1] Department of Geology, University of Toronto, Toronto, Ontario, M5S 1A1

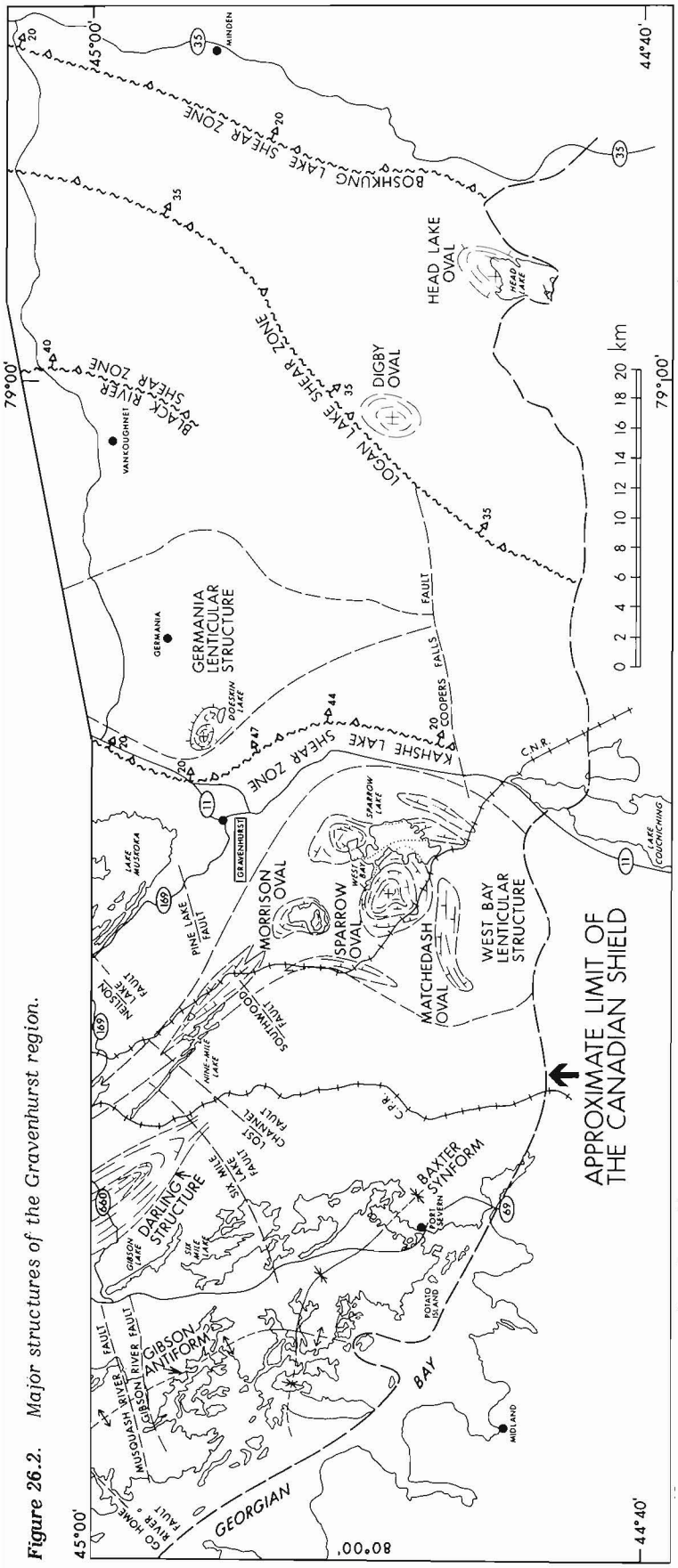

Figure 26.2. Major structures of the Gravenhurst region.

The gneissosity pattern of the central Gravenhurst region is dominated by two lenticular structures previously called granitoid domains (Schwerdtner et al., 1981). These lenticular structures are >20 km in major diameter, and are centred about West Bay of Sparrow Lake and the hamlet of Germania respectively (Fig. 26.2). Both lenticular structures are open ended, and largely made up of oval structures typically cored by orthogneiss with relict igneous texture and moderately high degrees of deformation. Gneissosity is subhorizontal in the centre of most oval structures, and generally displays a prominent stretching lineation (Schwerdtner et al., 1981). Oval structures are not confined to the central Muskoka region, but also occur in western Digby Township and near Head Lake, west of Ontario Highway 35 (Fig. 26.2).

These enigmatic lenticular and oval structures must be part of a regional tectonic framework that also incorporates the large folds outlined east of Georgian Bay (Fig. 26.2, 26.3). In western Gibson and Baxter Township, a zone of marble-bearing metasediments delineates two perpendicular fold structures whose crossing point lies within a region of subhorizontal gneissosity. Less severe undulations of local hinge lines characterize parts of the composite Gibson Antiform (Fig. 26.3).

The Gibson Antiform is transected by several faults that involve no significant strike separation (Fig. 26.3). The faults are part of a west-southwest-trending, post-Grenvillean system in central Ontario. Most faults of that system exhibit characteristic breccias.

In the East Half of the Gravenhurst region, several major ductile shear zones have been recognized (Fig. 26.3). Two of these zones of mylonitic rocks transect the entire East Half, and all zones trend roughly NNE and dip toward the east at shallow to moderate angles.

The Kahshe Lake Shear Zone (westernmost) effectively separates the East and West Halves of the Gravenhurst region, and may be taken as the boundary between the Muskoka and Algonquin domains of Davidson and Morgan (1981). The Logan Lake Shear Zone separates an area of mixed orthogneiss and paragneiss to the west from an area of mainly orthogneiss to the east, while the Boshkung Lake Shear Zone may be taken as the boundary between the Algonquin Domain (Davidson and Morgan, 1981) and the Central Metasedimentary Belt. The shear zones are on the order of 100 m thick with gradational boundaries, and are thought by one of us (C.K.M.) to represent major ductile thrusts. There is no evidence of a marked change in metamorphic grade across the shear zones as has been reported for the discontinuities bounding the Parry Sound Domain (Davidson and Morgan, 1981; Davidson et al., 1982).

Lithology and Structure of the West Half

A north-trending zone of metasediments follows Ontario Highway 11 and seems to bifurcate near Gravenhurst (Schwerdtner et al., 1981, Fig. 1). This zone separates the orthogneisses of the lenticular Germania structure from those of the lenticular West Bay structure, and is composed of (1) pink arkosic gneiss with mafic interlayers and (2) magmatitic garnet-biotite gneiss containing narrow units of calc-silicate marble. Similar metasedimentary gneisses occur on the western margin of the West Bay structure, although calc-silicate marble appears to be absent.

An assemblage of metaplutonic and metasedimentary gneisses, including many marble units, is well exposed in the western part of the map area. Exposures of this assemblage, which is highly folded on all scales, define the Gibson antiform and Baxter synform (Fig. 26.3).

Results of modal analyses of pink meta-arkosic rocks of the Moon River Synform, just north of the Gravenhurst region, were figured by Waddington (1973, p. 20-27). He found that the modal compositions plot into Krynine's (1948) arkose and impure arkose fields and into Pettijohn's (1944) arkose and greywacke fields. A feature linking all arkosic rocks is the common occurrence of calc-silicate layers containing small amounts of calcite.

Numerous units of metaplutonic rocks occur within the metasedimentary zones. Most conspicuous in the field are gabbroic units that tend to contain subunits of anorthositic gabbro, e.g. the unit northeast of Potato Island, southwest of Port Severn on Georgian Bay (Fig. 26.3). This northwest-trending unit, which is exposed on several small islands, has been folded on a small scale about NE-SW axes. It constitutes an excellent example of a lithological unit with transverse gneissosity (cf. Schwerdtner et al., 1981, Fig. 3).

A composite unit of metaplutonic rocks, referred to as the Gibson Lake unit, is well exposed on Ontario Highway 660 (northwest of Gibson Lake) and on Ontario Highway 69 (Fig. 26.3). Much of this unit is composed of metamorphosed gabbro, granodiorite and quartz diorite with small isolated xenoliths of calc-silicate gneiss (Jacques Martignole, personal communication, 1977; Schwerdtner and Waddington, 1978, p. 211). The metaplutonic unit is sandwiched between a pair of marble-bearing metasedimentary units, and extends southward along Ontario Highway 69, as well as into western Six Mile Lake, before being folded back toward the northeast (Fig. 26.3).

Two subunits of another metaplutonic unit form the core of the tight Darling structure, a well defined large fold within the gneissic grain (Fig. 26.3). A quartz dioritic subunit crosses Ontario Highway 660, but others have not been mapped in sufficient detail to help delineate the fold structure.

The West Bay lenticular structure is largely made up of orthogneisses that display characteristic augen structure and/or stretched mafic clots. Most of the augen gneisses have weakly deformed portions where one finds relict megacrysts of mesoperthite. The entire suite of rocks resembles that of the Brandy Lake Complex, between Bracebridge and Port Carling, which has been described previously (Janes, 1973; Bennett, 1974; Schwerdtner et al., 1977). Strained mafic clots are typical for gneissic quartz diorites and monzodiorites (Fig. 26.4).

The Sparrow Lake Oval owes its eccentricity to a highly strained northeastern segment in which relict igneous textures are virtually absent. Individual gneiss units can be traced around the structure and reveal the effect of increasing strain on the mineral fabric. Similarly, the Matchedash Lake Oval has a core of augen gneiss displaying variable degrees of preservation of plutonic textures.

The northwestern tail of the West Bay lenticular structure is made up of severely stretched migmatitic gneisses whose parent rocks are difficult to identify. In addition, a thick plutonic unit, largely composed of mafic orthogneiss and augen gneiss, extends from Southwood to the northwest, and is well exposed along the CNR tracks as well as between Bastedo and Nine Mile Lakes. The tectonic significance of the long northwestern tail of the West Bay structure is unknown.

Davidson and Morgan (1981) have identified several zones of "tectonoclastic" gneiss in which the level of strain is supposed to be abnormally high. Although these zones contain inclusion-rich gneisses that exhibit macroscopic evidence of severe destruction of a compositional layering, no quantitative data are available that the overall strain in the fragmented rocks exceeds that in quasi-homogeneous gneisses. It is equally plausible that the macroscopic destruction is caused by high ductility contrasts between layers of different composition and texture, without being accompanied by abnormal overall strain.

One "tectonoclastic" zone forms the southwestern boundary of the Moon River Subdomain (Davidson et al., 1982), enters the Gravenhurst region west of Bala, and crosses the CPR tracks near Nine Mile Lake. This fragmental-gneiss unit does not extend far along the structural grain to the southeast. Detailed mapping would be required to trace the unit across the grain. However, a wide zone of similar fragmental gneiss and migmatitic metasediments occurs to the east, between the CNR tracks and Ontario Highway 169, and continues northwestward to Long Lake, west of Bala. This zone forms the northeastern envelope of the West Bay lenticular structure, and follows Ontario Highway 169 east to Gravenhurst and then Highway 11 south toward Orillia.

Geology of the East Half

Macroscopic Structure and Distribution of Rock Types

Lineaments derived from aerial photographic analysis are shown in Figure 26.3. Only distinct major lineaments are drawn; many smaller or less distinct lineaments are observed upon close inspection of the photographs. Field work revealed that most of the weaker lineaments coincide with high-order structures or boundaries of narrow lithological units too small to be shown on a regional geological map. Examination of Figure 26.3 reveals the following features:

1. Lineaments in areas of paragneiss are gently curved, laterally extensive, and virtually parallel to lithological boundaries. They are approximately parallel to the boundaries of the major lithological zones in the East Half (Fig. 26.3). Folds outlined by arcuate lineaments are commonly tight to isoclinal and intrafolial.
2. Lineaments in areas of orthogneiss are usually short and moderately to severely curved. While coinciding with gneissosity they outline folds that are irregular to elliptical in plan. Lineaments are rarely parallel to lithological boundaries. The difference in lineament signature between paragneiss and orthogneiss is pronounced and corresponds to differences in scale and type of mesoscopic structures in the two types of gneiss.
3. A late-stage brittle fault trending ENE like those of the West Half and crosscutting the westernmost zone of paragneiss (Fig. 3) follows a well defined lineament.
4. Two regional ductile shear zones (thrusts) recognized by Mawer and discussed in the section on major structures are associated with well defined NNE-trending lineaments, which transect the entire East Half (Fig. 26.3). He mapped a third zone east of Gravenhurst, which is relatively short.

On the basis of the long shear zones, the East Half can be divided into three lithological zones numbered from west to east. Zone 1 is a mixed unit of migmatite, paragneiss and orthogneiss, zone 2 is predominantly orthogneiss, and zone 3 is an assemblage of paragneisses and calc-silicate marble, grading lithologically into the Central Metasedimentary Belt of the Grenville Province. The three zones exhibit differences in lithology, metamorphism and signature of lineaments.

A regional mineral lineation is ubiquitous throughout the East Half. The mineral elongation lineation is oriented down-dip on the NNE-trending and southeasterly dipping gneissosity (Fig. 26.1). This attitude is consistent with the tight folds, oval structures, etc. that are generally reclined toward the NW.

Figure 26.3. *Generalized geological map of the Gravenhurst region.*

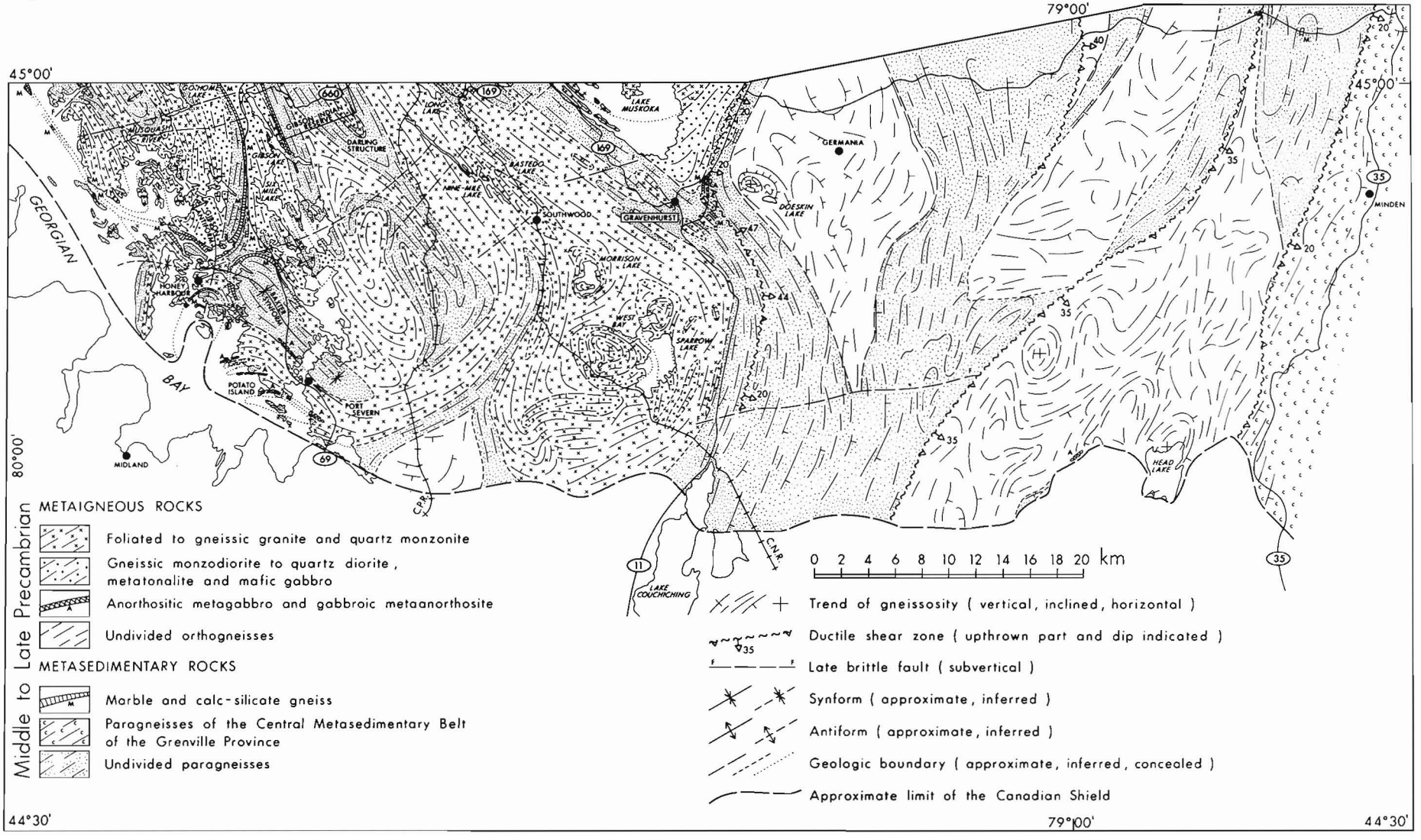

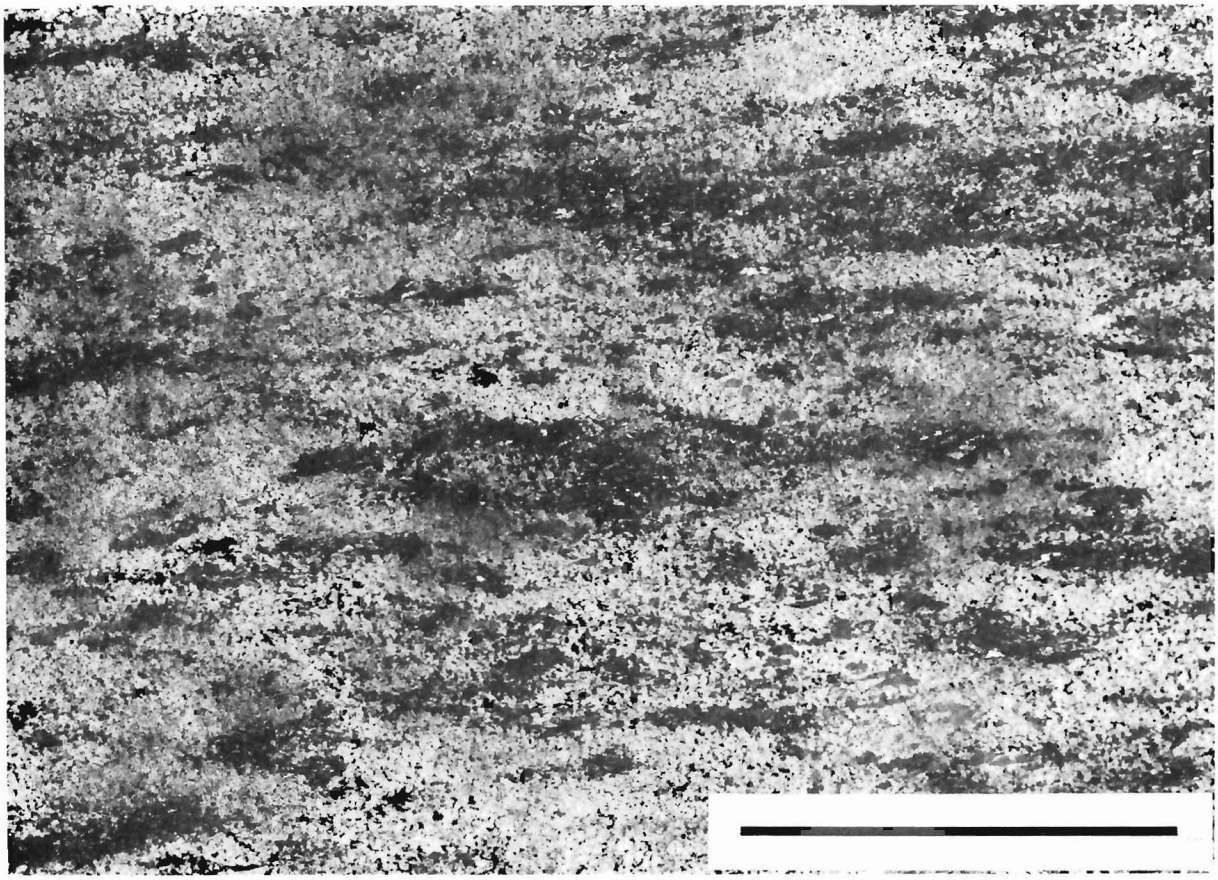

Figure 26.4. *Lineated quartz diorite orthogneiss, centre of Sparrow oval. Scale bar shown is 5 cm long.*

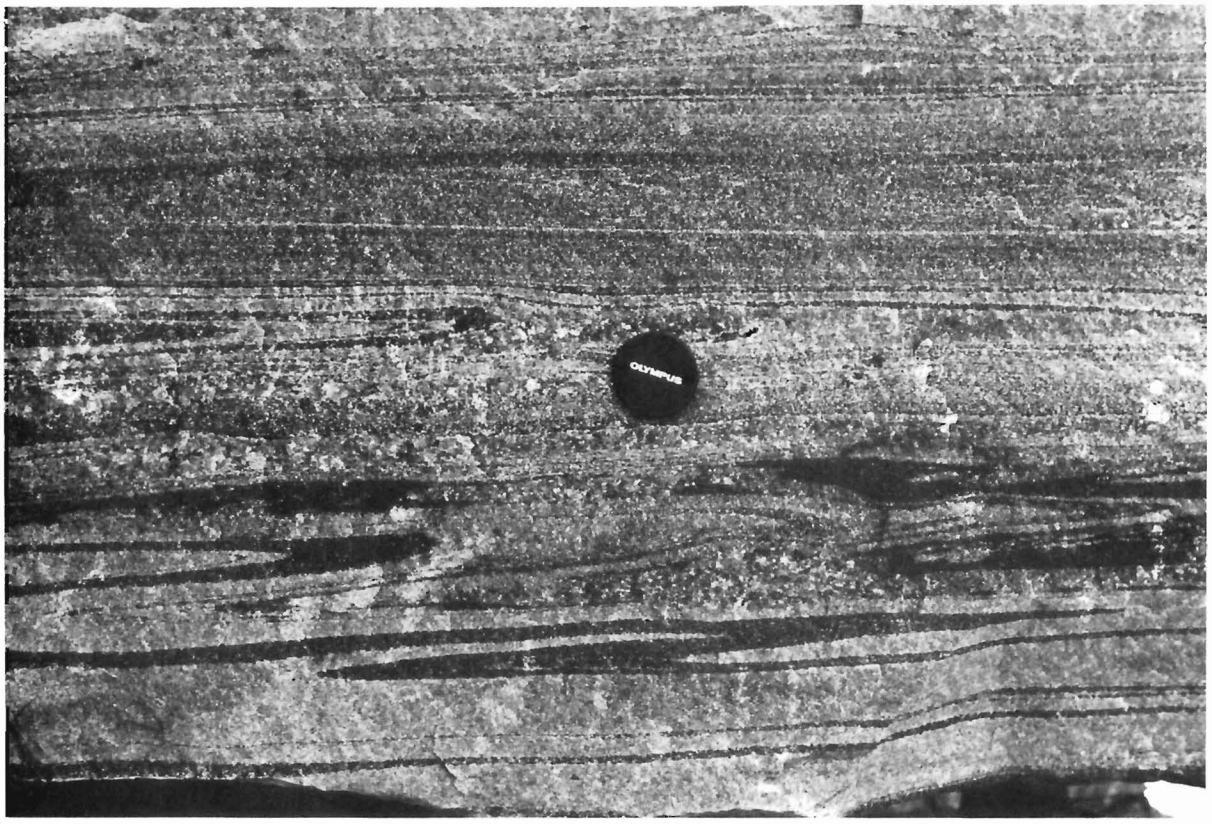

Figure 26.5. *Isoclinal intrafoliat folds in meta-arkosic gneiss. Lens cap is 5 cm diameter.*

Petrography and Metamorphism

Considerable difficulty was encountered in ascribing parentage to large tracts of gneiss in the East Half. Many outcrops of quartzofeldspathic gneiss possess no distinctive mineralogy or texture. These gneisses consist of equigranular quartz, feldspar, biotite and commonly amphibole. The gneisses are pink or grey, layering can be well developed or virtually absent, and foliation may be prominent or weak. Where paragneiss and orthogneiss can be identified with confidence, they are commonly interlayered and folded into one another, generally on a scale of metres or hundreds of metres. Details of lithology, mineral assemblages, texture, etc. of rocks of the East Half are provided in Tables 26.1 and 26.2.

The metamorphic grade of the East Half is largely middle to upper amphibolite facies as judged in the absence of distinctive mineral parageneses. However, the peak of metamorphism was at granulite facies, as shown by the following observations: 1. clinopyroxene-orthopyroxene-bearing assemblages, 2. charnockitic gneiss, 3. paragneiss with sillimanite-quartz-perthite and, 4. coronitic gabbros (Davidson et al., 1982). These features indicate high temperatures and pressures probably close to, or in excess of, 700°C and 8 kbar, apparently implying burial to depths of approximately 25-30 km.

Mylonites and blastomylonites of the main ductile shear zones of thrusts show retrogression of their parent gneisses to lower to middle amphibolite facies. Two types of tectonites are associated with the ductile shear zones, (1) schistose mylonite-blastomylonite and (2) migmatitic mylonite-blastomylonite.

Type 1 occurs along the regional shear zones (Fig. 26.3) and is derived from various parent gneisses, through deformation and retrogression. The mylonitic rocks are very well layered and mainly consist of fine grained quartz, feldspar and biotite. Porphyroblasts of plagioclase and microcline and rarely of amphibole are observed in many outcrops. In general, the rocks have undergone almost complete dynamic recrystallization, though some larger grains of feldspar, mica, amphibole and rarely quartz show significant internal strain.

Type 2 occurs east of Gravenhurst, along Ontario Highway 11, and differs from type 1 by having coarser grain size, lacking strained porphyroblasts, and exhibiting layer-parallel leucosomes.

Dominant Structural Elements

Among the various rock types of the East Half, meta-arkosic gneisses exhibit the most pronounced fold structures on all scales (Fig. 26.3, 26.5, 26.6). The most common structural style is tight to isoclinal folding of the compositional layering (Fig. 26.5). These folds can be very attenuated (Fig. 26.6) and are commonly rootless. The folds are of similar style and appear to have straight hinges that generally form angles of 5-25° with the prominent mineral elongation lineation. The isoclinal folds are commonly refolded (Fig. 26.7) within the gneissosity, giving rise to type 3 interference patterns (Ramsay, 1967, p. 531, Fig. 10-13). An axial surface schistosity is rarely developed, and generally restricted to mafic layers with inequant mineral grains.

Table 26.1

Paragneisses of East Half

Rock Type	Mineralogy (In Decreasing Order of Abundance)*	Texture	Grain Size (Average)	Colour	Scale of Layering
Arkosic Gneiss	feldspar, quartz, mafics (amphibole, biotite), garnet (pink-violet)	equigranular	0.5-2 mm	pink with black mafic interlayers	10-100 cm
Quartzofeld-spathic Gneiss	plagioclase, quartz, biotite, amphibole, garnet (pink-violet), clinopyroxene, sillimanite	equigranular	1-3 mm	pink to grey	1-100 cm
Pelitic Gneiss	plagioclase, quartz, sillimanite, amphibole, biotite, garnet (pink-violet), microcline or perthite, clinopyroxene	equigranular	1-3 mm	pink to grey	1-100 cm
Marble-Calc-silicate Gneiss	calcite, forsterite, diopside, plagioclase, tremolite, grossularite	equigranular	3-8 mm	pink, white or grey	5-100 cm
Quartzite	quartz, plagioclase, microcline, biotite	equigranular (sugary)	1-2 mm	white to grey	10-50 cm
Graphitic Sulphide-rich Gneiss	quartz, feldspar, pyrite, sillimanite, garnet, graphite	equigranular	0.5-2 mm	rusty brown	10-50 cm

*Not necessarily all coexisting.

Most highly deformed meta-arkosic gneiss possesses a prominent schistosity and lineation defined by inequant aggregates of quartz and feldspar.

The quartzofeldspathic (see Table 26.1) and pelitic gneisses have comparable fold structures. They show a marked schistosity and mineral lineation, defined by mafic minerals and occasionally by sillimanite. Axial-surface cleavage defining cleavage mullions is rare.

All paragneisses have been folded into broad open structures at a late stage of their structural evolution, and some enclose pegmatite dykes parallel to the late axial surfaces.

Most orthogneisses exhibit less evidence of severe deformation than the paragneisses. Arcuate gneissosity traces (Fig. 26.3) attest to the fact that folding has nonetheless occurred. In general, these macroscopic folds are not as tight as those in the paragneisses. The orthogneisses are rarely well layered and have but a weak schistosity and mineral lineation, whereas in the mafic dykes and sheets, a more pronounced schistosity and lineation are developed.

Examination of Figure 26.3 reveals numerous irregular folds and oval structures within the zones of orthogneiss. Many of the oval structures appear to be domes, reclined toward the northwest. In contrast to structures in the zones of paragneiss, the macroscopic folds in the orthogneisses fail to show consistency of pattern, shape or orientation. This fundamental difference is due in large part to the lack of compositional layering and other marked anisotropy in the orthogneisses. Presumably, the two families of gneiss have also experienced different structural histories, with the paragneisses being deformed prior to orthogneiss emplacement.

Mesoscopic Structures in Ductile Shear Zones

Three regional Shear Zones and one shorter shear zone, from west to east, the Kahshe Lake, Black River, Logan Lake and Boshkung Lake shear zones (Fig. 26.2), have been identified in the East Half. These shear zones are characterized by highly deformed marble-calc-silicate rocks, anorthositic metagabbros and mylonitic rocks of mixed parentage, referred to as tectonite types 1 and 2 (see below). A variety of characteristic mesoscopic features are found in the ductile shear zones. Most important are sheath folds (Cobbold and Quinquis, 1980), observed in the two easternmost shear zones.

Tectonite type 1 is highly foliated, and contains inclusions of less deformed gneisses, such as anorthositic and coronitic gabbros (Davidson et al., 1982), calc-silicate gneiss, and paragneiss. These inclusions locally have sigmoidal internal foliation that is discordant to the undulose mylonitic foliation of the rock matrix. Extensional features, such as rectangular boudinage, symmetric and asymmetric foliation boudinage (Platt and Vissers, 1980), and shear band cleavage (for example White et al., 1980) are commonly observed.

In addition, detachment surfaces or cutoffs (Fig. 26.8) occur. These are commonly subparallel to the mylonitic foliation, and probably represent an advanced stage of asymmetric foliation boudinage. Commonly, these surfaces are the site of late pegmatite dykes and veins. Most quartz and pegmatite dykes and veins are folded, boudinaged or partly disaggregated within the mylonitic matrix. A characteristic feature of the type 1 tectonite is isolated feldspar augen (porphyroblasts or porphyroclasts), apparently rotated with respect to foliation (Davidson et al., 1982), and showing a consistent sense of rotation indicating overthrusting towards the northwest. There is also a prominent mineral lineation defined by alignment of mafic minerals or elongated aggregates of quartz and/or feldspar. Both drag and sheath folds are commonly developed in the zones.

Tectonite type 2 is migmatitic and occurs mainly in the Kahshe Lake Shear Zone, along Ontario Highway 11. Structural features of this type are similar to those of type 1, but the matrix foliation is less undulose and tectonic inclusions are less common, though locally abundant. A mineral lineation is still present but considerably weakened by grain growth. This tectonite type has therefore a similar origin to that of type 1, but the grain size in the matrix has been coarsened subsequent to deformation.

Table 26.2

Orthogneisses of East Half

Rock Type	Mineralogy (In Decreasing Order of Abundance)	Texture	Grain Size (Average)	Colour	Scale of Layering
Granodioritic-Tonalitic Gneiss	plagioclase, quartz, microcline, and/or perthite, oxides, biotite, amphibole, clinopyroxene, myrmekite, garnet (brick-red)	equigranular (granitic)	5-10 mm	pink usually (can be greyish)	1-10 cm
Charnockitic Gneiss	plagioclase, green perthite, garnet (brownish-red), clinopyroxene, orthopyroxene, quartz	megacrystic to equigranular (granitic) frequently cut by syenitic veins	8-15 mm	olive green to buff green brown	10-100 cm
Coronitic Metagabbro	plagioclase, clinopyroxene, amphibole, oxides, garnet, olivine	relict ophitic to equigranular	ophitic-5-30 mm equigranular 1-2 mm	dark grey to greenish black	1-10 cm
Anorthositic Metagabbro	plagioclase, clinopyroxene, amphibole, biotite, orthopyroxene, oxides, garnet, olivine, microcline, quartz	relict megacrystic to equigranular; sugary to elongated grains	2-5 mm	white to light grey to dark grey	1-50 cm

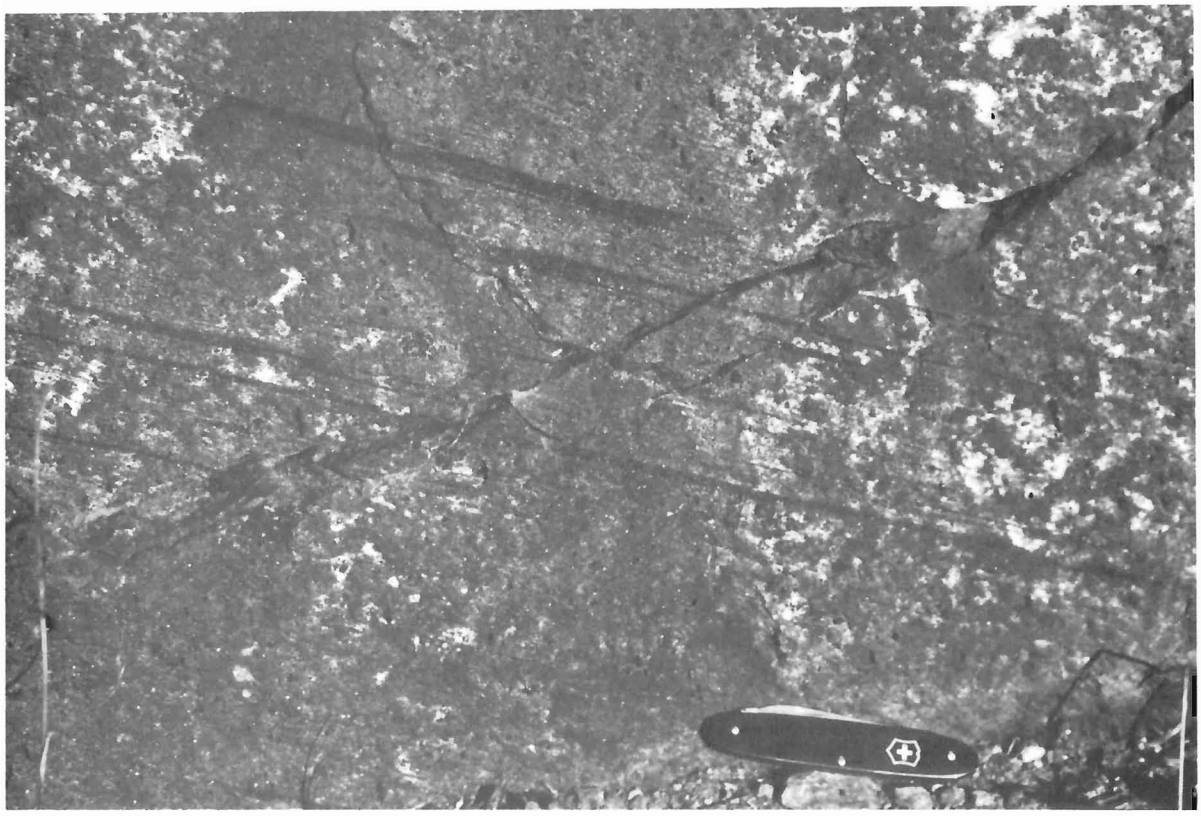

Figure 26.6. *Extremely attenuated rootless isoclinal intrafolial folds in meta-arkosic gneiss. Knife is 8 cm long.*

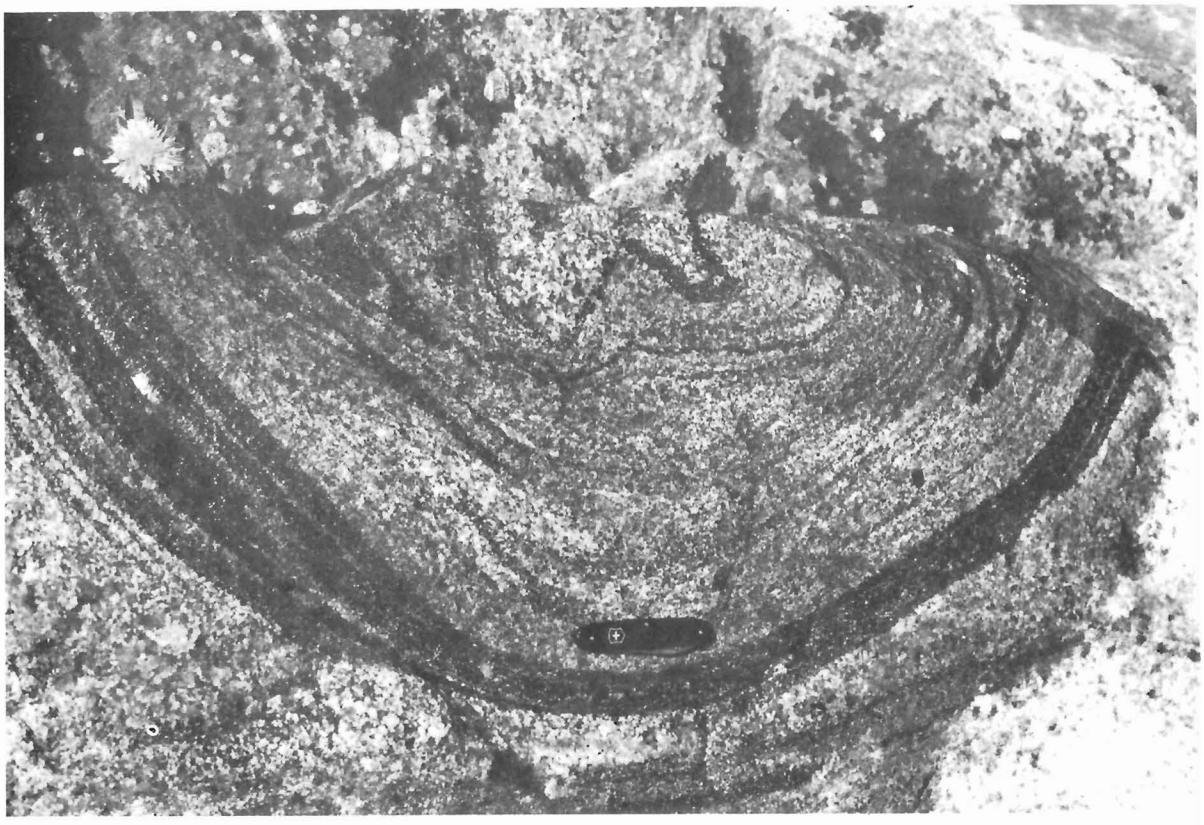

Figure 26.7. *Refolded isoclinal intrafolial folds in paragneiss. Knife is 8 cm long.*

Anorthositic metagabbro occurs in two of the ductile shear zones (Fig. 26.3). The structural behaviour of the metagabbro is similar in both cases. After initial plastic deformation leading to prominent foliation, lineation and folds, the gneissic rocks (Fig. 26.9) were broken up into blocks separated in places by pegmatitic material. Cutoffs, minor shear zones and rhombohedral blocks are most common in the leucocratic members. Sheath and drag folds are also observed, together with large rotated feldspar augen.

All of the marble-calc-silicate rocks observed in the East Half occur in proximity to major ductile shear zones and all outcrops show evidence of strong penetrative deformation (Fig. 26.10). In places, the marble-calc-silicate gneiss resembles a breccia that is due to a great ductility contrast between calcareous and siliceous layers. There are many mesoscopic folds with complicated geometry, including typical sheath folds and highly disharmonic structures. Partly or wholly disaggregated pegmatite dykes occur in places.

Unsolved Structural Problems

While the complex structural history and intricate deformation of the Muskoka gneisses cannot be comprehended on the basis of regional mapping alone, we have nonetheless succeeded in identifying a number of key problems. Three simple questions must be answered before the tectonic processes that produced the complicated internal structure of the Gravenhurst gneiss terrain can be understood:

1. What is the tectonic significance of the prevailing shallow attitudes of gneissosity and associated tight folds?
2. What was the original shape and position of the metaplutonic units that are now interleaved with other gneisses in the western Gravenhurst region?
3. What is the origin of the oval and lenticular structures which dominate the central Gravenhurst region?

Prevailing Gentle Dip of Gneissosity

The gneisses of the Gravenhurst region have a characteristic augen texture, mafic lamination, and/or compositional layering at a scale of millimetres to centimetres. Lithological layering at the scale of metres is common in some rock types. Collectively, these planar elements define a prominent gneissosity. Depending on the amount of euhedral mafic minerals, a crude schistosity can be developed together with, and generally parallel to, the prominent gneissosity.

In most areas of the Gravenhurst region, the average dip of gneissosity is less than 45 degrees (Fig. 26.1). Tight reclined or recumbent folds, whose hinge surfaces coincide with the structural grain conspicuous on air photographs, are ubiquitous on all scales of observation. Many minor recumbent folds are rootless because of severe attenuation of their limbs. Only a few recumbent folds at the scale of kilometres have been delineated to date by detailed mapping (Fig. 26.3). This folding is thought to be responsible for the common termination of prominent lithological units along the structural grain. There is abundant field evidence (stretched mineral aggregates, boudins, etc.) that the gneissosity and the tight to isoclinal folds have been extended severely, without coinciding everywhere with a principal plane of total strain.

Two simple tectonic processes are capable of producing the observed structural features,

i) mature diapirism and

ii) pervasive simple shear on subhorizontal to slightly inclined planes.

Theoretical and physical modelling with soft materials (Fletcher, 1972; Dixon, 1975) have shown that a pervasive subvertical foliation develops at an appropriate structural level (Schwerdtner et al., 1977, Fig. 8) in immature buoyant diapirs and adjacent interdiapiric depressions. This foliation is prone to refolding during the early stages of lateral spreading ("mushrooming") of mature diapirs and interdiapiric depressions (cf. Carey, 1979, Fig. 2.3 and 2.4). The result are tight reclined to recumbent folds in the original foliation at structural levels that pass through, or are near to, the inflection lines on the lithological interface between the light diapiric material and the heavier overlying rocks.

A further complication arises from the fact that natural diapirism tends to occur on different macroscopic scales resulting in structures of different orders (Schwerdtner, in press). Where parasitic "mushrooms" develop on immature first-order ridges, the intensity r of total strain (Watterson, 1968) can easily reach values between 50 and 100 (cf. data of Dixon, 1975). These figures can best be appreciated in comparison with those for shear zones. For instance, large simple shears of $\gamma = 10$ correspond to r-values of 20, and very large simple shears of $\gamma = 20$ to r-values of 40. One reason for the high maximum values of r in diapirs is their triaxial deformation, another the superposition of parasitic domes on diapiric ridges.

Whether the diapiric model is relevant to the Muskoka gneisses remains to be seen. Oval structures prevailing in the southern portion of the Gravenhurst region may be likely candidates for parasitic diapirs, but seem to involve no obvious change in density with respect to their metasedimentary envelopes. The possibility of diapirism is discussed further in the subsequent section.

Recent work by Cobbold and Quinquis (1980) allows one to make a test for large scale simple shear by means of passive minor folds. These authors demonstrated in simple experiments that sheath-like passive folds, with sheath axes close to the local direction of maximum extension, cannot be avoided in ductile shear zones. Therefore, the occurrence of properly oriented sheath folds is an important requirement for the identification of ductile shear regimes in metamorphic terranes.

Wherever possible, the geometry of tight or isoclinal folds has been studied throughout the Gravenhurst region. Several recumbent folds have been found that are perfectly exposed in road cuts (cf. Schwerdtner and Waddington, 1978, p. 211, Stop 2.2). None of these folds, few of which may be regarded as passive, has a sheath-like form. Because gneissosity is the folded surface, passive folds may be rare or confined to certain rock types. As mentioned above, one of us (C.K.M.) has identified minor sheath folds in narrow zones of mylonitic rocks in the East Half of the Gravenhurst region. Detailed work is required throughout the region on the geometry and origin of the minor folds.

There is widespread evidence (small scale boudinage, etc.) in many localities that the gneissosity has been stretched parallel to the regional NW trend while being sheared in the same direction (see above and cf. Davidson and Morgan, 1981; Davidson et al., 1982). The sense of shear is compatible with a component of overthrusting to the NW.

During ideal simple shear, often compared with the shear of a card deck, the shear surfaces (cards) are neither contracted nor extended. It is, therefore, impossible that the gneissosity planes themselves are surfaces of simple shear. In fact, there is no compelling reason for embracing the concept of large scale simple shearing at this stage of knowledge.

Figure 26.8. *Detachment surface or cutoff in tectonite type 1. Hammer is 30 cm long.*

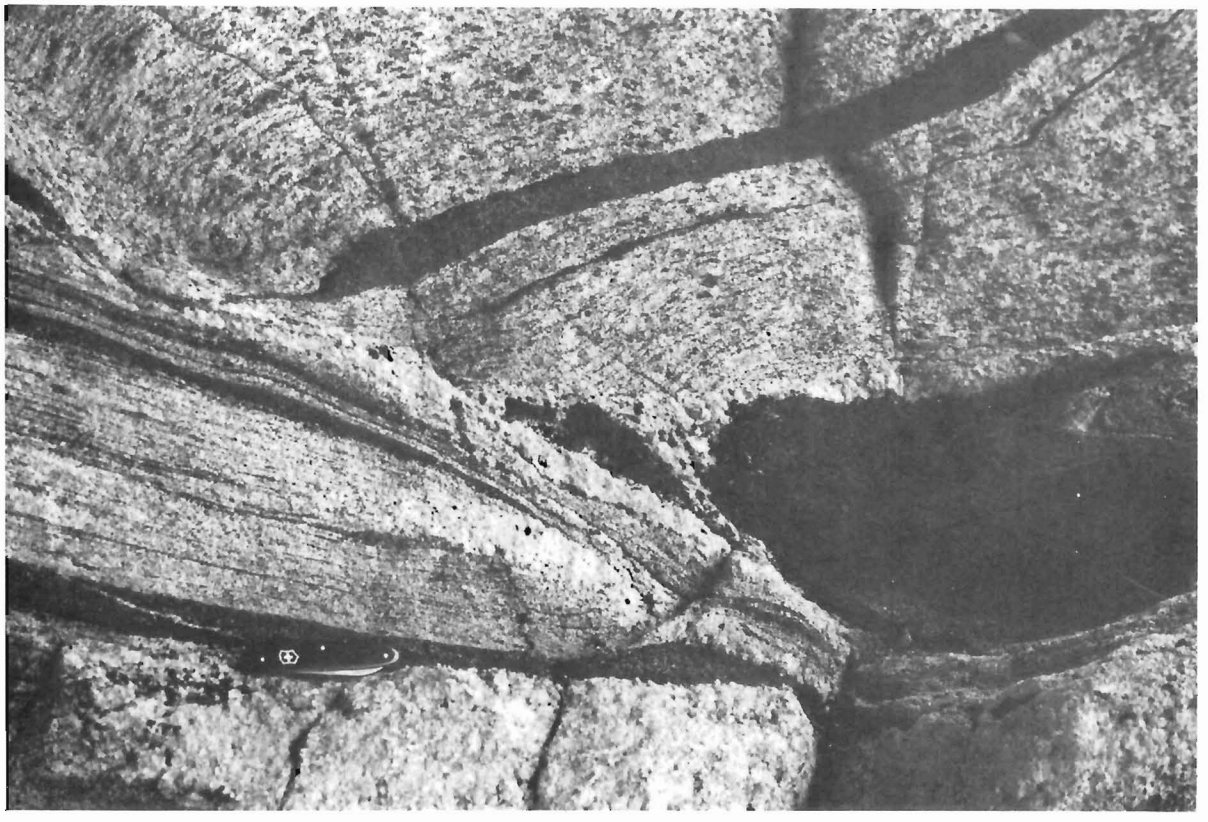

Figure 26.9. *Inhomogeneous deformation of anorthositic gabbro. Knife is 8 cm long.*

Figure 26.10. *Calc-silicate gneiss showing strong deformation (note folds). Scale bar is 1 m long.*

Original Shape and Position of Metaplutonic Units

In the western half of the Gravenhurst region, there are numerous units of orthogneiss which have been stretched severely and folded on the scale of kilometres. Were these units originally equant and subject to extreme ductile stretching during metamorphism, or have they been injected as concordant plutonic sheets along a pre-existing structural grain in the host gneisses? Alternatively, have some of the tabular units of orthogneiss been detached from a large pluton by dip-slip faulting and juxtaposed with other gneisses at a different structural level?

Convincing answers to these questions will only be found by detailed structural work. For example, Davidson (in press) made a quantitative study of the strain field within a narrow unit of deformed porphyritic granite on Go Home Lake, 3.5 kilometres north of the present map area. Although most of the central segment of this gneissic unit is weakly strained, it is nonetheless concordant to the surrounding metasedimentary units and appears to have been emplaced as a finite tabular body. Until more structural studies of this kind have been completed, one can only speculate as to the original geometry of deformed plutons.

Origin of Oval and Lenticular Structures

Large oval structures are conspicuous in the gneissosity pattern of the central and southeastern portions of the Muskoka region (Schwerdtner et al., 1981). Some oval structures (like those southwest of Gravenhurst) occur in tight aggregates bounded by lenticular envelopes, others (like the Head Lake oval) are surrounded by large folds. The oval structures may be parasitic diapirs, large sheath folds, or parts of fold interference patterns. As pointed out previously (Schwerdtner et al., 1981), the dip of major lithological contacts cannot be observed in the field. Although highly questionable, we have followed the common practice of equating the attitudes of lithological boundaries with those of gneissosity.

The Sparrow Lake oval is a well exposed "basin" that has been studied in detail. It is zoned lithologically, and the exposed eccentric core is made up of strongly lineated quartz diorite and monzodiorite orthogneiss (Fig. 26.3). The horizontal lineation is defined by mafic aggregates, and coincides with the axis of minor recumbent folds in gneissosity.

A key question is whether all of the minor structures and the associated finite strains predate the oval structure. While this question is difficult to answer at present, there is no doubt that the eccentricity of the core is caused by steeper dips of gneissosity and greater flattening of the various lithological units southwest of West Bay (Fig. 26.2 and 26.3).

As mentioned above, the gneissosity pattern of the central Gravenhurst region (Fig. 26.2 and 26.3) is dominated by major lenticular structures (Schwerdtner et al., 1981). The origin and tectonic significance of the lenticular structures are not known. At least the West Bay structure (Fig. 26.2) is enveloped by different assemblages of highly strained metasedimentary gneisses, i.e. by pink meta-arkosic rocks on the east side and by grey biotite-garnet gneiss, meta-arkose and migmatite on the west side. The conical axis of the gneissosity pattern of both structures plunges easterly to southeasterly. This need not be true for the axes of the major lithological interfaces.

If one assumes that the dip of gneissosity corresponds to that of lithological boundaries, then both lenticular structures as well as most of the "isolated" oval structures are reclined in a westerly direction. Are the lenticular structures part of a heterogeneous regional strain field in which the ductile deformation is concentrated in narrow zones that form a rhomboidal or lenticular mesh? Analogous strain fields are associated with the overall extension of competent amphibolitic members at an outcrop scale. Some of these foliated members lack internal layering, but develop lenticular deformation zones that lead to a type of boudinage structure.

What is the significance of the oval features within the lenticular structures? Are they earlier plutons or gneiss diapirs that have resisted the strain which shaped the large lenticular structures? Alternatively, are the lenticular structures major diapirs, or could they be related to thrust-and-nappe tectonics as envisaged by Davidson et al., (1982) for the area to the north?

It appears important, at this stage of knowledge, to formulate a host of tectonic hypotheses that can be tested by modern structural methods. Detailed lithological and structural mapping seems to be prerequisite to finding acceptable solutions to the tectonic puzzle in the Grenville gneiss terrane of Ontario.

Summary and Conclusions

Regional geology mapping in the Muskoka District is faced with two major problems:

1. the prevalence of (superficially) monotonous felsic gneisses, and
2. an abundance of tight large folds within the structural grain (regional gneissosity).

Lithological marker horizons do exist, but cannot be traced along the structural grain where they have been disrupted tectonically or doubled back in themselves. Enveloping surfaces to the noses of adjacent intra-gneissosity folds cannot be drawn without detailed lithological mapping. Such enveloping surfaces are generally oblique to gneissosity – a surface of strain rather than lithology.

Narrow units of marble-calc-silicate gneiss are common in the westernmost portion of the Gravenhurst region, but are difficult to trace over long distances. Rather than tracing individual marble units, we mapped an assemblage of metasedimentary biotite-garnet gneisses that includes all marble occurrences in the Georgian Bay subregion (Fig. 26.3). Using this method, the Gibson Antiform proved to be enveloped by a marble-bearing zone of metasediments (Fig. 26.3). The same assemblage seems to outline the Baxter Synform to the south, and follows the Musquash River from Gibson Reserve toward Go Home Lake.

Narrow units of anorthositic rocks are mapped more readily than individual marble horizons. One narrow unit of gabbroic meta-anorthosite and anorthositic metagabbro has been traced for many kilometres along the Georgian Bay shore, south of Honey Harbour (Fig. 26.3). In fact, many marker units utilized in the present project are metaplutonic and members of the anorthosite suite (Lumbers, 1975). Unfortunately, all metaplutonic units that have been transformed from equant plutons to long lenticular bodies are apt to be parallel to gneissosity rather than to major lithological boundaries. We do not know the original geometry of most orthogneiss units in the Gravenhurst region. A useful future study would be to analyze in detail the strain field of suitable units with a view to restoring their original shapes.

While most major structures making up the gneiss complex of the Gravenhurst region have now been delineated, we are far from understanding the tectonic significance of these structures and the deformation history of the region. We do not know the origin of the large lenticular structures south and east of Gravenhurst, or of the Gibson Antiform

near Georgian Bay. Neither do we know the significance of the prevailing shallow dips of gneissosity and associated recumbent folds.

These planar features define a number of large oval structures whose relative place in the structural succession of the region remains to be determined. The oval structures cannot be early, and must be coeval with, or younger than, the recumbent folds. Field evidence shows that the development of the oval structures led to severe ductile deformation. Although there was a strain fabric prior to their inception, the oval structures did not form merely by solid-body rotation of gneissosity and associated folds, coupled with small strains to retain macroscopic cohesion. Rather, the prior strain fabric was strongly modified during the growth of the oval structures. In spite of this new information, the geodynamic process responsible for these important structures remains unknown (Schwerdtner, in press).

Several prominent zones of mylonitic rocks traverse the East Half of the Gravenhurst region from NNE to SSW (Fig. 26.3). These ductile structures contain minor sheath folds and other evidence of simple shearing, but their age in the structural succession of the region is not certain. One of us (C.K.M.) regards these shear zones as probable major dislocations that separate large blocks of Proterozoic crust. He interprets the zones as ductile thrusts comparable to those recognized by Davidson and Morgan (1981) and Davidson et al. (1982) in the Parry Sound-Muskoka region.

References

Bennett, P.J.
1974: Deformation of the Northern Half of the Brandy Lake Complex, Port Carling, Ontario; unpublished M.Sc. thesis, University of Toronto, Toronto, Ontario.

Carey, P.D.
1979: Incremental strain in diapiric ridge structures; unpublished B.Sc. thesis, Queen's University, Kingston, Ontario.

Cobbold, P.R. and Quinquis, H.
1980: Development of sheath folds in shear regimes; Journal of Structural Geology, v. 2, p. 119-126.

Davidson, D.M.
Strain analysis in Helikian gneisses, Muskoka district, Ontario; Tectonophysics. (in press)

Davidson, A. and Morgan, W.C.
1981: Preliminary notes on the geology east of Georgian Bay, Grenville Structural Province, Ontario; in Current Research, Part A, Geological Survey of Canada, Paper 81-1A, p. 291-298.

Davidson, A., Culshaw, N.G., and Nadeau, L.
1982: A tectonometamorphic framework for part of the Grenville Province, Parry Sound Region, Ontario; in Current Research, Part A, Geological Survey of Canada, Paper 82-1A, p. 175-190.

Dixon, J.M.
1975: Finite strain and progressive deformation in models of diapiric structures; Tectonophysics, v. 28, p. 89-124.

Fletcher, R.
1972: A finite amplitude model for the emplacement of mantled gneiss domes; American Journal of Science, v. 272, p. 197-216.

Janes, T.W.
1973: Deformation of the Southern Half of the Brandy Lake Complex, Muskoka Region, Ontario; unpublished M.Sc. thesis, University of Toronto, Toronto, Ontario.

Krynine, P.D.
1948: The megascopic study and field classification of sedimentary rocks; Journal of Geology, v. 56, p. 130-165.

Lumbers, S.B.
1975: Geology of the Burwash Area, Districts of Nipissing, Parry Sound and Sudbury; Geological Report 116, Ontario Division of Mines.

1978: Geology of the Grenville Front tectonic zone; in Toronto '78, Field Trips Guidebook, ed. A.L. Currie and W.O. Mackasey; Geological Association of Canada, p. 347-351.

Pettijohn, F.J.
1944: Unpublished chart; in Krumbein, W.S. and Sloss, L.L. (1963), Stratigraphy and Sedimentation, 2nd ed. Freeman and Co., San Francisco, p. 157 ff.

Platt, J.P. and Vissers, R.L.M.
1980: Extensional structures in anisotropic rocks; Journal of Structural Geology, v. 2, p. 397-410.

Ramsay, J.C.
1967: Folding and Fracturing of Rocks; McGraw-Hill, New York, 568 p.

Schwerdtner, W.M.
Strain patterns of oval gneiss domes in the Superior and Grenville Provinces of Ontario (abstract); 1st Meeting, Canadian Tectonics Group; Journal of Structural Geology. (in press)

Schwerdtner, W.M. and Waddington, D.H.
1978: Structure and lithology of Muskoka-Southern Georgian Bay region, Central Ontario; in Toronto '78, Field Trips Guidebook, ed. A.L. Currie and W.O. Mackasey; Geological Association of Canada, p. 204-212.

Schwerdtner, W.M., Bennett, P.J., and Janes, T.W.
1977: Application of L-S fabric scheme to structural mapping and paleostrain analysis; Canadian Journal of Earth Sciences, v. 14, p. 1021-1032.

Schwerdtner, W.M., Mawer, C.K., and Hubbs, A.F.
1981: Geology of the Gravenhurst Region, Grenville Structural Province, Ontario: preliminary mapping results; in Current Research, Part B, Geological Survey of Canada, Paper 81-1B, p. 167-169.

Waddington, D.H.
1973: Foliation and mineral lineation in the Moon River Synform, Grenville Structural Province, Ontario; unpublished M.Sc. thesis, University of Toronto, Toronto, Ontario.

Watterson, J.
1968: Homogeneous deformation of the gneisses of Vesterland, south-west Greenland; Meddelelser om Grønland, Bd. 175, nr. 6.

White, J.H., Burrows, S.E., Carreras, J., Shaw, N.D., and Humphreys, F.J.
1980: On mylonites in ductile shear zones; Journal of Structural Geology, v. 2, p. 175-187.

27. SUBBOTTOM PROFILING OF CANADIAN SHIELD LAKES – IMPLICATIONS FOR INTERPRETING EFFECTS OF ACID RAIN

Project 800027

W.W. Shilts and L.E. Farrell
Terrain Sciences Division

Shilts, W.W. and Farrell, L.E., Subbottom profiling of Canadian Shield Lakes – implications for interpreting effects of acid rain; in Current Research, Part B, Geological Survey of Canada, Paper 82-1B, p. 209-221, 1982.

Abstract

Maps drawn from interpretations of acoustic subbottom profiles can show the distribution and physical characteristics of both modern lake sediments and unconsolidated sediments related to glacial processes. Examples from four lakes of the southern Canadian Shield indicate that 3 to 5 m of gyttja overlies bedrock and glacial sediments in all but the steepest parts of the lake basins. Laminated, fine grained sediments, till, and outwash gravels have been discerned beneath this sedimentary fill, and in Weslemkoon Lake the glacial sediments attain thicknesses of more than 30 m in buried preglacial valleys. The thickness of the clastic glacial fill and the anomalously high carbonate content of drift adjacent to Turkey lakes and Weslemkoon Lake may provide significant buffering capacity to surface and subsurface hydrologic systems carrying abnormally high proton loadings as a result of acid precipitation.

Introduction

This paper illustrates how subbottom profile records may be used to map morphologic and sedimentation features in small lakes. Although not presently supported by drilling, we feel that the interpretations of the acoustic records are sufficiently accurate to draw many inferences about the configuration and characteristics of lacustrine and glacial sedimentary fill. Maps and records such as these have many possible practical applications, but the principal ones discussed here relate to the possible influence of the unconsolidated fill on the potential effects on surface and subsurface waters acidified by acid rain or snow.

Klassen and Shilts (1982) presented preliminary results of subbottom profiling carried out in 1981 as well as several typical subbottom profiles of Canadian Shield lakes. Profiling was carried out with a Raytheon RTT-1000-A system which utilized two transducers generating 200 and 3.5 kHz acoustic signals. The system was mounted on a small inflatable boat. The basis for correlating the acoustic records with specific sediment types was discussed by Klassen and Shilts (1982) and the descriptive terminology of that paper is used here.

Although the bathymetric information has not been calibrated by sounding, depths calculated for the bathymetric maps of Turkey lakes correspond closely to those determined by Jeffries and Semkin (1982). The bathymetric map of Harrington Lake corresponds closely to an unpublished map provided by the National Capital Commission. The interpretations of subbottom records are based on knowledge of the local surficial geology and on sampling carried out in conjunction with similar programs elsewhere. These maps should be regarded as preliminary, showing the main bottom features and their geologic relationships. Navigation was done by eye between headlands, and many factors could combine to cause slight inaccuracies in positioning of boundaries or contacts. Where sufficient profiles were lacking, we have interpolated bathymetry or geology.

Surveys

Little Turkey Lake and Turkey Lake (Fig. 27.1) are the two principal lakes in the Department of Environment's calibrated drainage system located north of Sault Ste. Marie (Jeffries and Semkin, 1982). Twenty-one profiles were completed on these lakes in October of 1981 comprising approximately 2.2 line kilometres on Little Turkey Lake and 7.3 line kilometres on Turkey Lake. Several samples were taken of typical glacial sediments near these lakes, and trace element concentrations in the less than 2 μm fraction and $CaCO_3$ equivalent (Coker and Shilts, 1979) concentrations in the less than 64 μm fraction were determined to gain some insight into the chemical influence of drift on groundwaters and surface waters in their basins.

Weslemkoon Lake is a large, irregular lake situated southeast of Bancroft, Ontario. Forty-four profiles comprising approximately 18 line kilometres of traverse were completed on this lake. As at Turkey lakes, several samples were collected for trace element and $CaCO_3$ equivalent analyses.

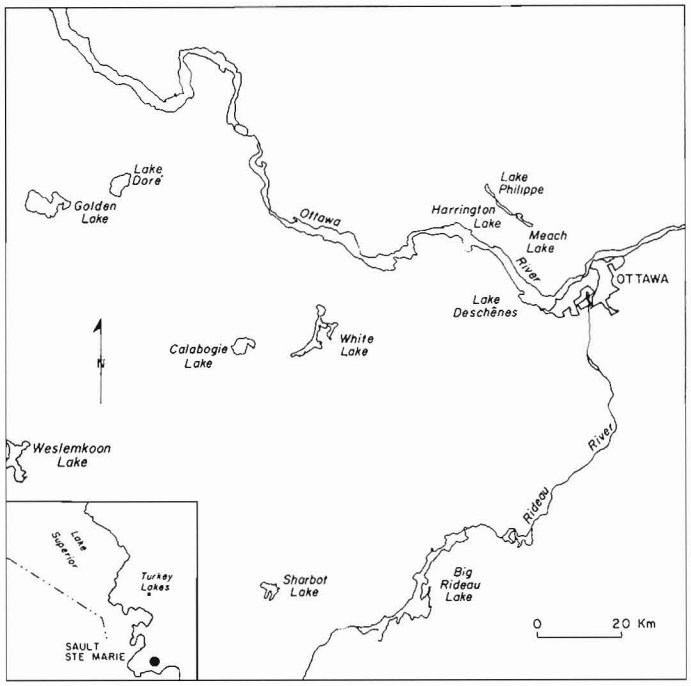

Figure 27.1. *Location of all lakes surveyed and mapped in 1981. Turkey Lake, Little Turkey Lake, Weslemkoon Lake, and Harrington Lake (Lac Mousseau) are discussed in this paper; the others are discussed in Klassen and Shilts (1982).*

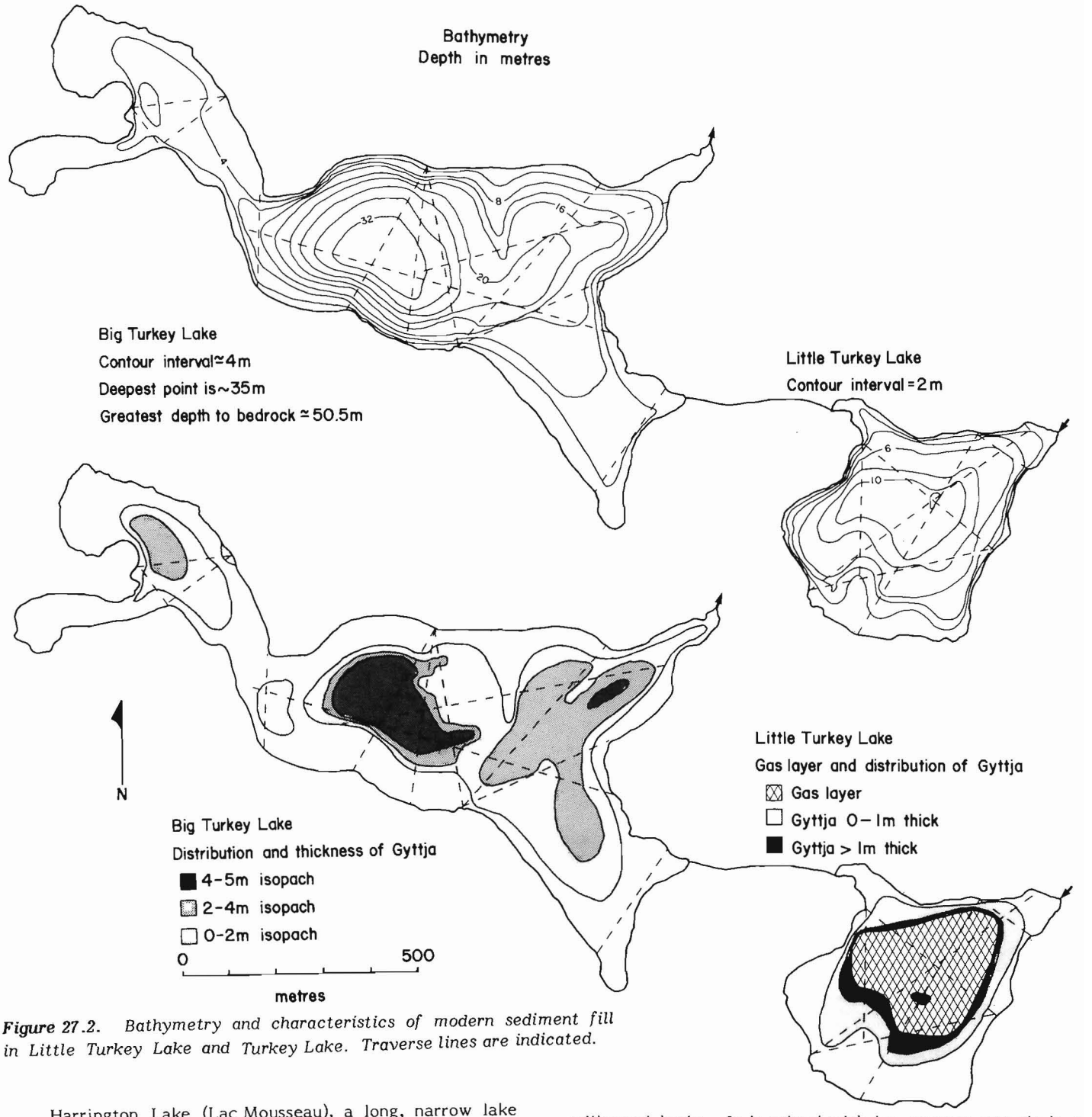

Figure 27.2. Bathymetry and characteristics of modern sediment fill in Little Turkey Lake and Turkey Lake. Traverse lines are indicated.

Harrington Lake (Lac Mousseau), a long, narrow lake located in Gatineau Park north of Ottawa, was profiled by 68 traverses totalling approximately 24 line kilometres. No sampling of drift was done adjacent to this lake.

Turkey Lake – Little Turkey Lake

Geology

The drainage basin of Turkey Lake and Little Turkey Lake is covered by a discontinuous layer of bouldery, sandy, compact olive grey till which is charged with debris from the local basic metavolcanic (greenstone) and granitic bedrock. Laminated silty clay with distinctive maroon clay (winter) layers lies on the till and occurs along the access road to the calibrated basin. It is mixed with ice-contact gravels in a borrow pit not far from Little Turkey Lake. The maximum elevation of the laminated silt was not determined and no search of literature on late-glacial history of the region has been carried out. The red colour of the finer part of the laminated sequence is probably derived from glacial erosion of Proterozoic redbeds that underlie parts of the Lake Superior Basin. Although the tills near Sault Ste. Marie were described as grey, Dell (1975) indicated that red tills occurred on the northwest shore of Lake Superior. The red laminated sediments of the Turkey lakes area were possibly derived from glacial ice lying to the west in the Lake Superior Basin. Proglacial lakes could have been dammed by that ice.

Geochemistry of Drift

Five samples were collected in or near the Turkey lakes basin – three of till and two of laminated silty clay (Table 27.1). The clay (less than 2μm) fraction of these samples was analyzed by atomic absorption, fluorometric (U), and colorimetric (As) techniques for Cu, Pb, Zn, Co, Ni, Ag, Cr, Mo, Mn, Fe, Cd, As, and U. The laminated sediments have no particular enrichment in any of the elements investigated, but the tills have high concentrations of some elements, particularly copper. In addition, the concentrations of Co, Zn, Ni, As, Cr, and possibly Ag are considered high for till, though not unduly so. The carbonate content of the sediments is surprisingly high. The till exposed in a borrow pit at the outlet of Turkey Lake contains 3.7% $CaCO_3$ equivalent in the less than 64μm fraction and unoxidized varves on the access road have about 3.0% $CaCO_3$. Although other samples, some of which may be leached, have less than 1% carbonate, the presence of 3% $CaCO_3$ equivalent in this noncalcareous bedrock terrane is considered anomalous and may have an important effect on the alkalinity of the lakes. The source of carbonate is not known, but calcareous debris could have been transported from the Hudson Bay Basin (Coker and Shilts, 1979) or from the Lake Superior Basin.

Little Turkey Lake

Results of Profiling. In general, both Turkey and Little Turkey lakes have bedrock shores covered with boulders. Little Turkey Lake lies in a bowl-shaped depression and has a maximum depth of about 12.5 m (Fig. 27.2). The bedrock surface beneath the lake is mantled with an average of 2 m of till which may be overlain by pockets 0.5 to 1 m deep of laminated, fine grained clastic sediment (Fig. 27.3). It is thought that the clastic sediment is similar to the varved sediment observed in exposures along the access roads.

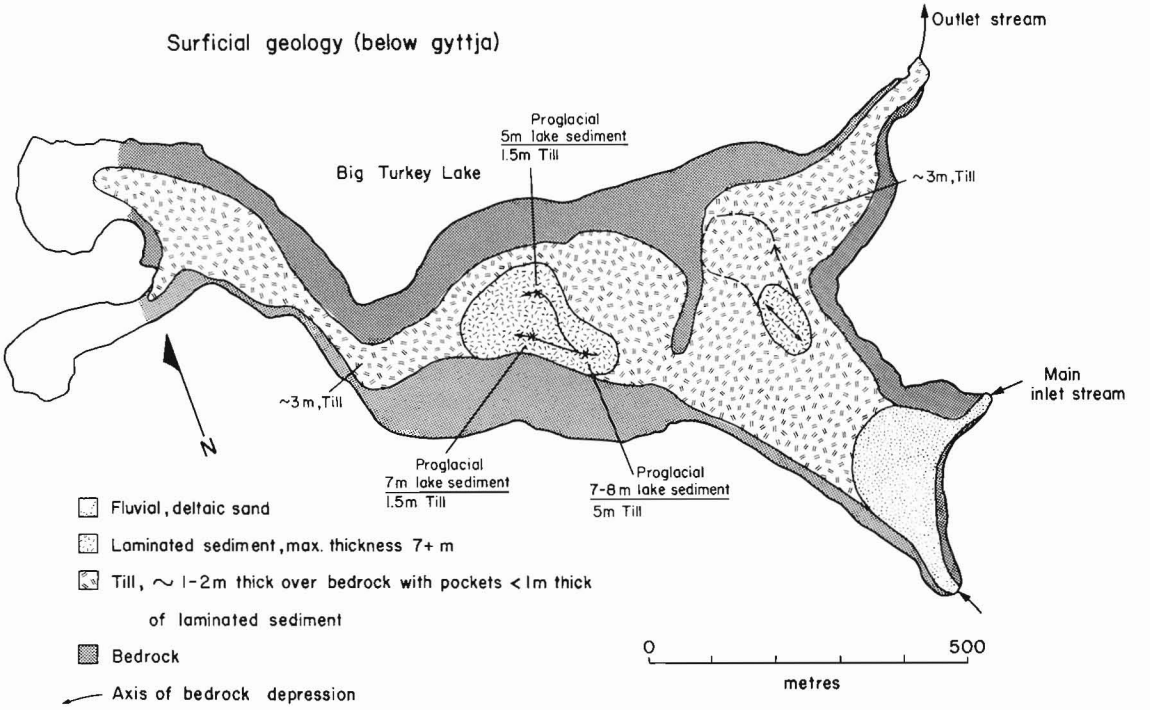

Figure 27.3. *Bedrock and glacial or proglacial sediments beneath the modern sediments of Turkey Lake.*

Table 27.1

Trace element chemistry and carbonate content ($CaCO_3$ equivalent) of drift samples collected around Weslemkoon and Turkey lakes

Sample	Location	Material	Trace elements*													Equivalent $CaCO_3$**
			Cu	Pb	Zn	Co	Ni	Ag	Cr	Mo	Mn	Fe	Cd	As	U	
S270	Outlet Turkey Lake	Till	184	17	40	38	45	0.4	98	3	920	3.0	0.2	16	3.1	3.67
S271	Near Little Turkey Lake	Till	520	14	140	46	120	0.1	104	2	980	4.7	N.D.	9	2.5	1.08
S274	Near Wishart Lake	Till	690	16	142	34	125	0.2	102	3	815	4.3	N.D.	11	1.8	0.33
S272	Access Road	Varves	76	7	88	16	43	0.1	96	2	520	4.3	N.D.	4	1.0	0.58
S273	Access Road	Varves	42	8	66	12	30	0.4	60	2	760	3.3	N.D.	4	1.0	3.00
S188	Weslemkoon Lake	Gravel	13	11	150	20	22	N.D.	43	4	720	6.0	N.D.	5	9	0.67
S189	Weslemkoon Lake	Gravel	152	33	112	36	52	N.D.	78	4	1650	9.4	N.D.	16	4.9	1.50
S190	Weslemkoon Lake	Gravel	112	48	132	34	56	N.D.	100	3	1900	7.4	0.5	14	10	3.42
S191	Weslemkoon Lake	Till	30	22	72	18	30	N.D.	64	N.D.	270	4.6	N.D.	9	7.2	3.08
S192	Weslemkoon Lake	Sand	31	32	136	24	36	0.3	92	N.D.	1900	5.0	0.5	N.D.	N.D.	3.08
K161	South end of Weslemkoon Lake	Gravel	-	-	-	-	-	-	-		-	-	-	-	-	4.50

* Concentrations in the less than 2μm fraction in ppm, except for iron which is in per cent; N.D. – not detected.
** Determined using Leco Carbon Analyzer; soluble carbon converted to equivalent weight of $CaCO_3$ (%).

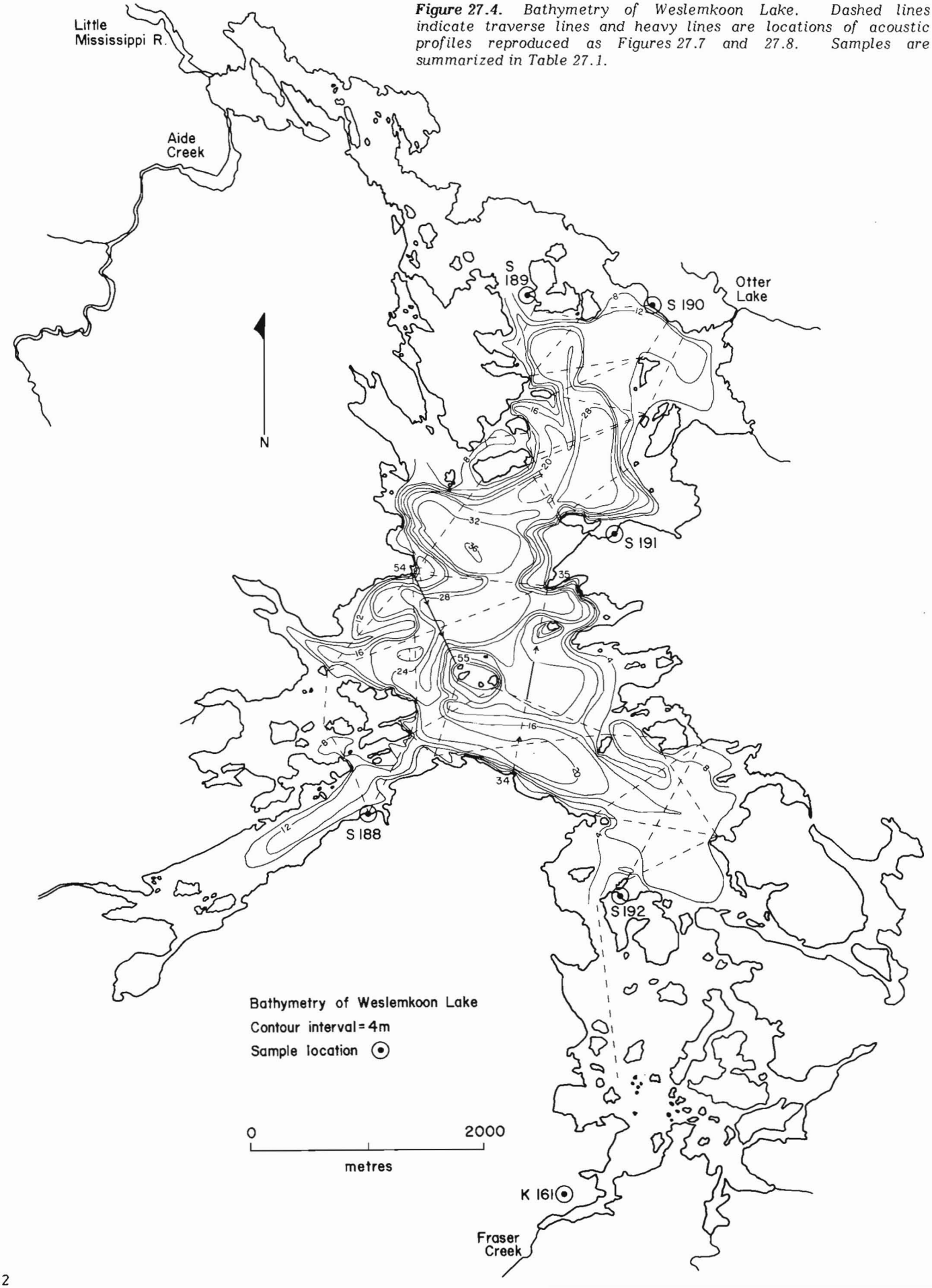

Figure 27.4. *Bathymetry of Weslemkoon Lake. Dashed lines indicate traverse lines and heavy lines are locations of acoustic profiles reproduced as Figures 27.7 and 27.8. Samples are summarized in Table 27.1.*

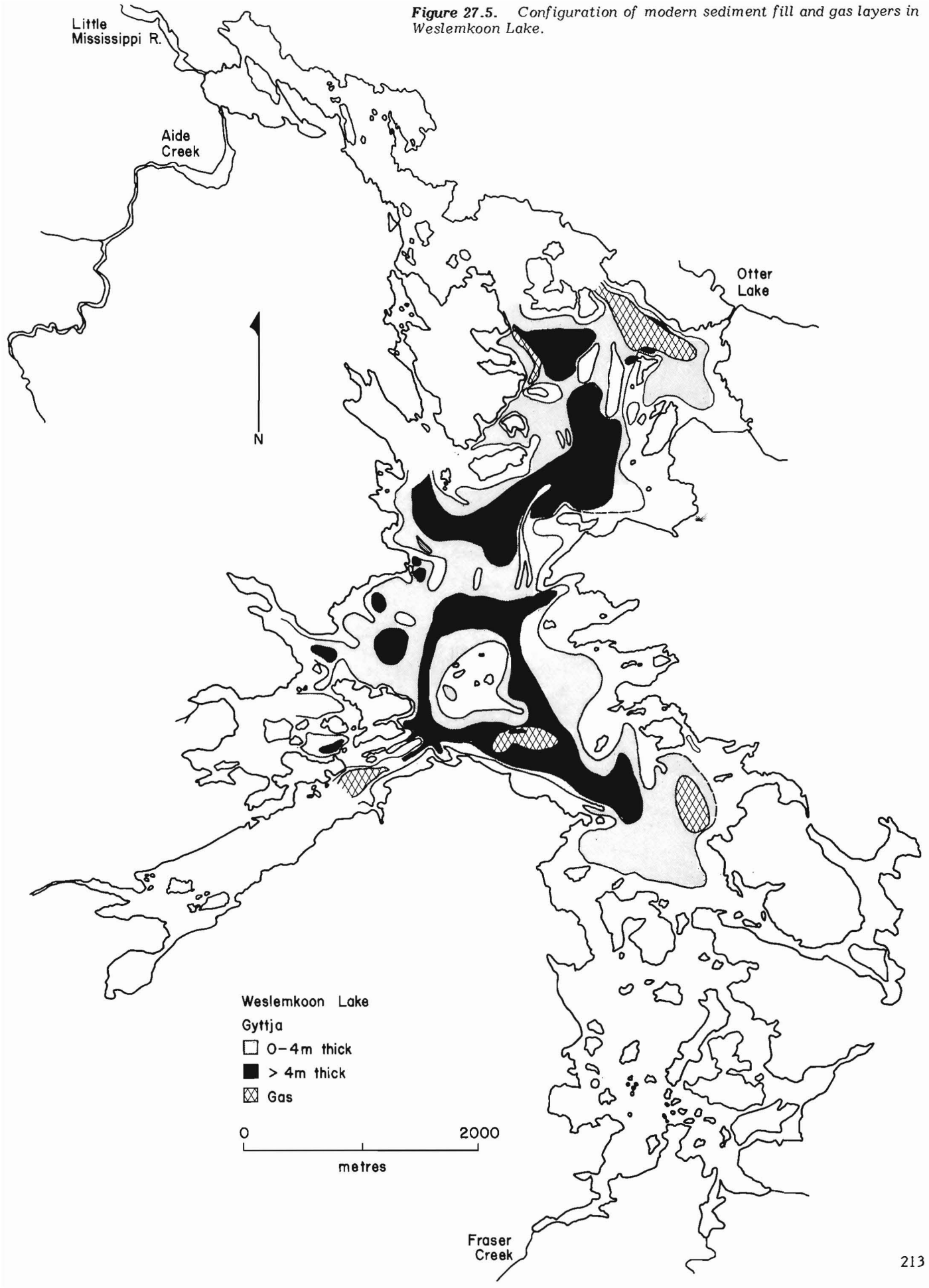

Figure 27.5. *Configuration of modern sediment fill and gas layers in Weslemkoon Lake.*

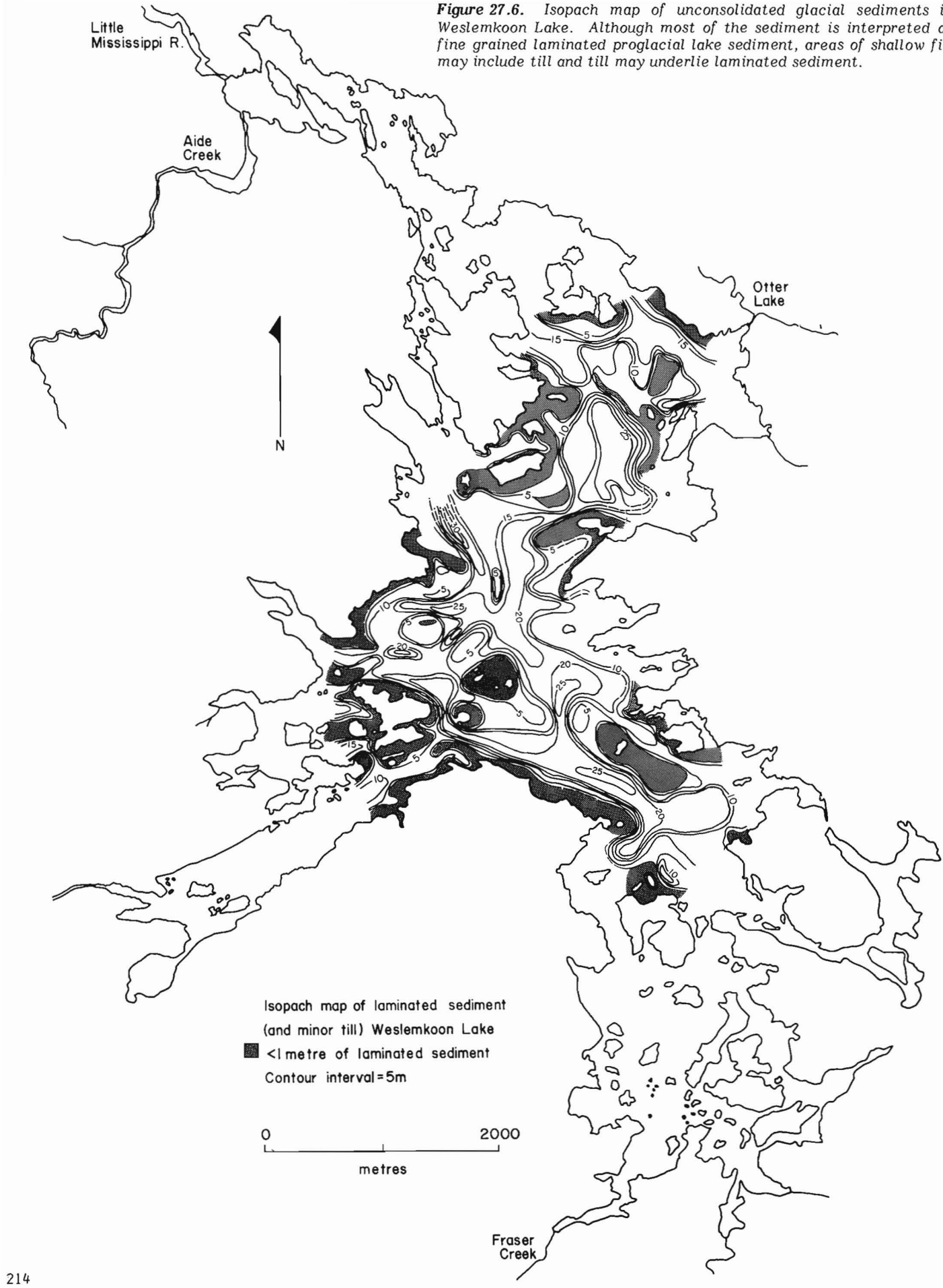

Figure 27.6. *Isopach map of unconsolidated glacial sediments in Weslemkoon Lake. Although most of the sediment is interpreted as fine grained laminated proglacial lake sediment, areas of shallow fill may include till and till may underlie laminated sediment.*

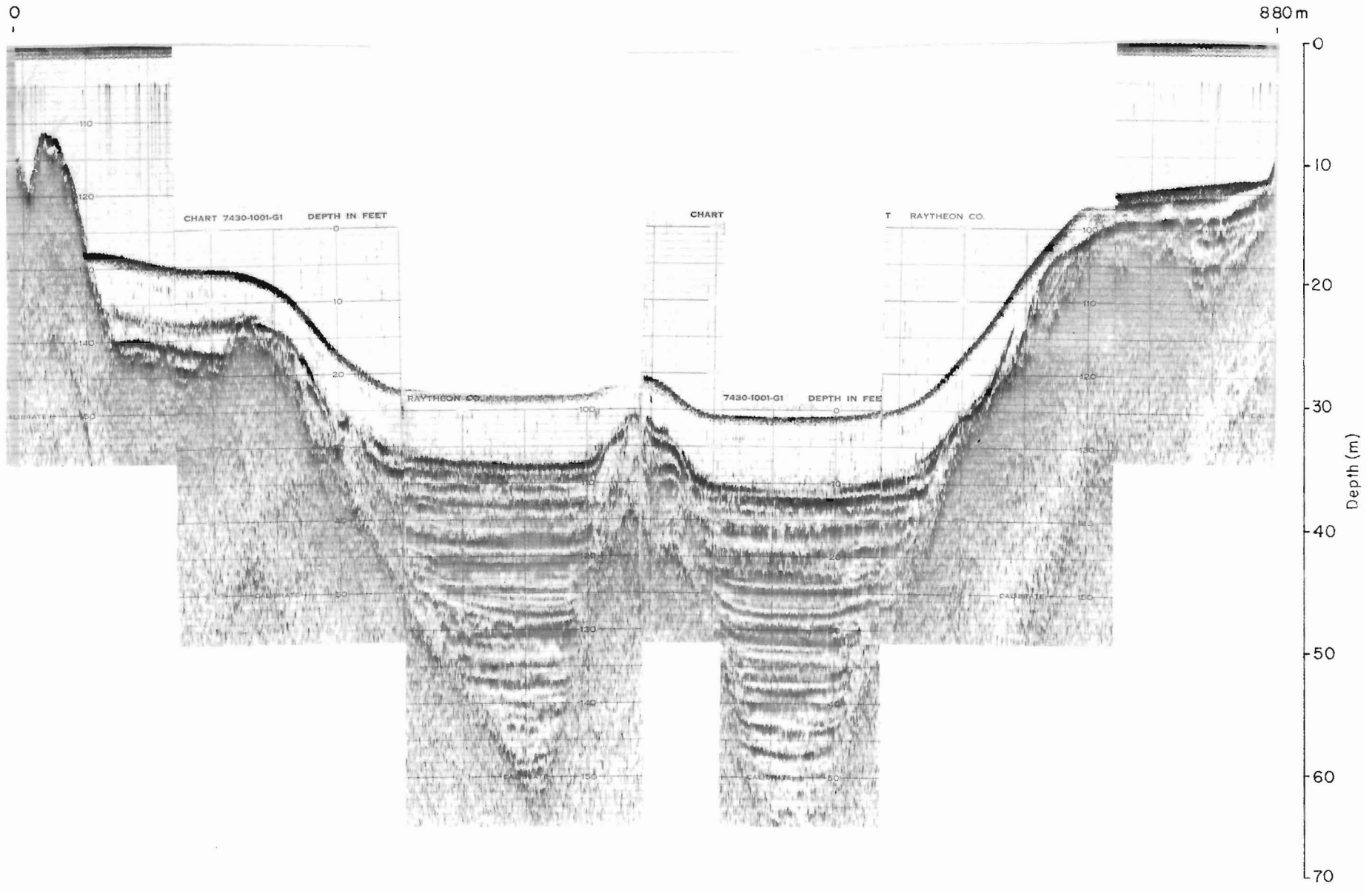

Figure 27.7. *Subbottom profile across two buried valleys in Weslemkoon Lake. Note that the sediment fill has completely obscured the original bedrock topography.*

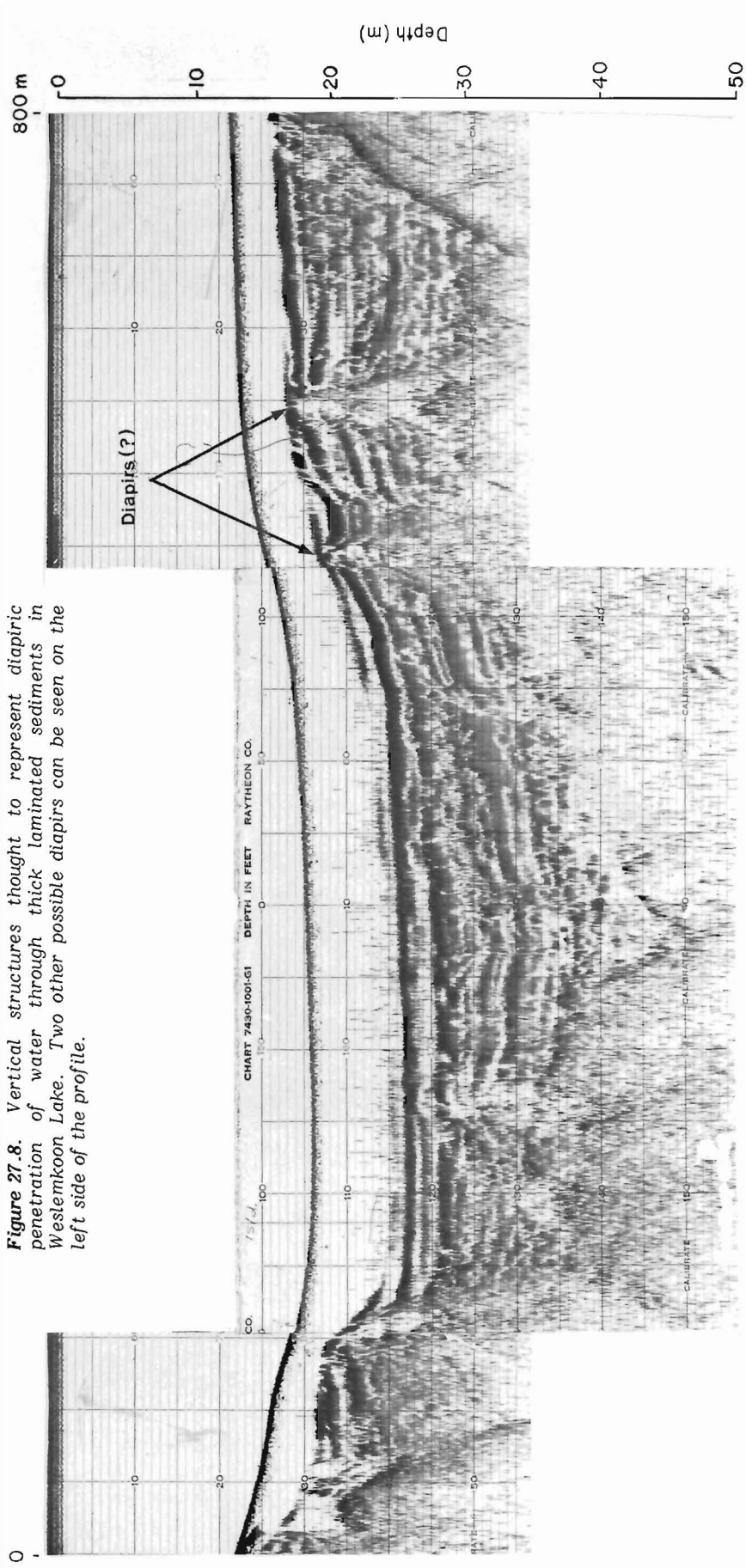

Figure 27.8. *Vertical structures thought to represent diapiric penetration of water through thick laminated sediments in Weslemkoon Lake. Two other possible diapirs can be seen on the left side of the profile.*

The till and clastic sediment are overlain by as much as 5 m of acoustically transparent gyttja which covers about 70 per cent of the bottom of the lake. One to two metres beneath the surface of the gyttja, a zone which is opaque to the 3.5 kHz signal at the power setting used obscures the underlying sediments and topography. Elsewhere, similar opaque zones lacking prominent multiple reflections have been interpreted to be caused by concentrations of gas (methane?) near the base of the gyttja (Keen and Piper, 1976; Müller, 1977; Klassen and Shilts, 1982), the interpretation we favour for this feature in Little Turkey Lake. The possibility that the gas is trapped near the base of the gyttja after being released from groundwater (Barker and Fritz, 1981) flowing into the lake through the bottom sediments should be investigated as should the possibility that the gas layer changes its extent through the ice-free season as anaerobic conditions develop (Müller, 1977). It should be noted that the much more deeply submerged sediments in Turkey Lake show no evidence of this opaque layer, although their stratigraphic succession and physical characteristics appear to be similar to those in Little Turkey Lake.

Turkey Lake

Results of Profiling. Turkey Lake is a deep, east-west oriented bedrock basin, the axis of which lies at approximately right angles to the regional direction of glacial flow. It may be part of the former drainage system. The sheltered (with respect to glaciation) position of Turkey Lake basin would seem to preclude significant overdeepening by glacial erosion. Overdeepening would have had to be on the order of 50 m, the maximum depth of bedrock below the present outlet stream.

Turkey Lake has three sedimentation basins, a deep central basin separated from shallower basins to the east and west by bedrock ridges (Fig. 27.2). Each basin is partially filled with gyttja, which attains a maximum thickness of about 5 m in the central basin. In both Turkey and Little Turkey lakes, gyttja represents most of the 'modern' (i.e. postglacial) sediment accumulation.

The sides of Turkey Lake are steep and appear to be bedrock. The bedrock of the less steep parts of the basins is mantled by an acoustic unit interpreted to represent a 1 to 3 m cover of till. On shore, the till is very stony and bouldery. Pockets of up to 2 m of laminated, fine grained clastic sediment are found on the till surface throughout the basins. In the deepest part of the central basin, 7 to 8 m of clastic sediment overlies about 5 m of till in a bedrock valley (the location of this sequence is directly beneath the Primary NWRI Lake Sampling site L5 as described by Jeffries and Semkin, 1982, p. 27).

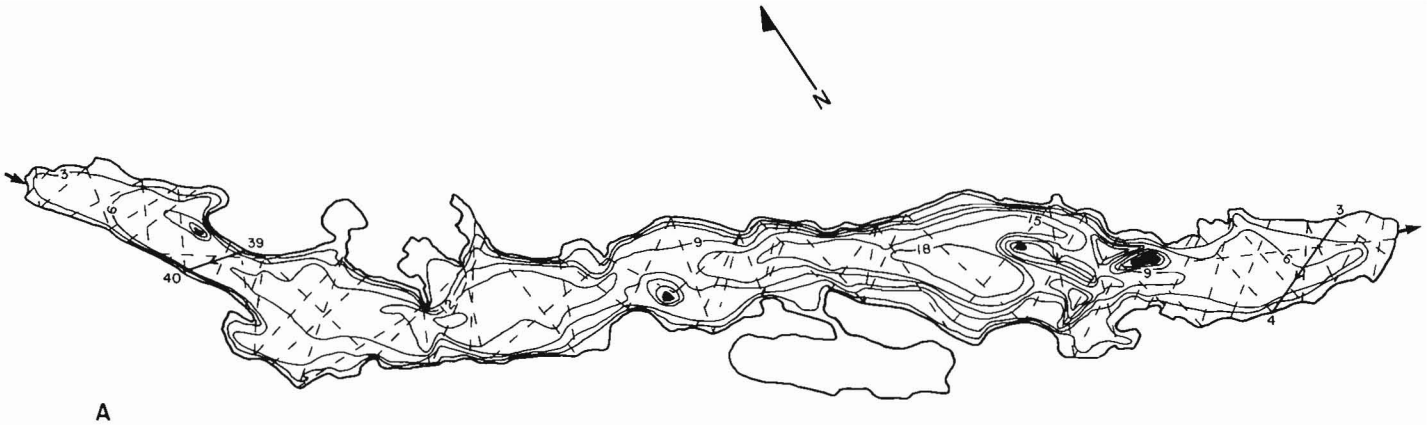

A

Bathymetry of Harrington Lake

Contour interval = 3m

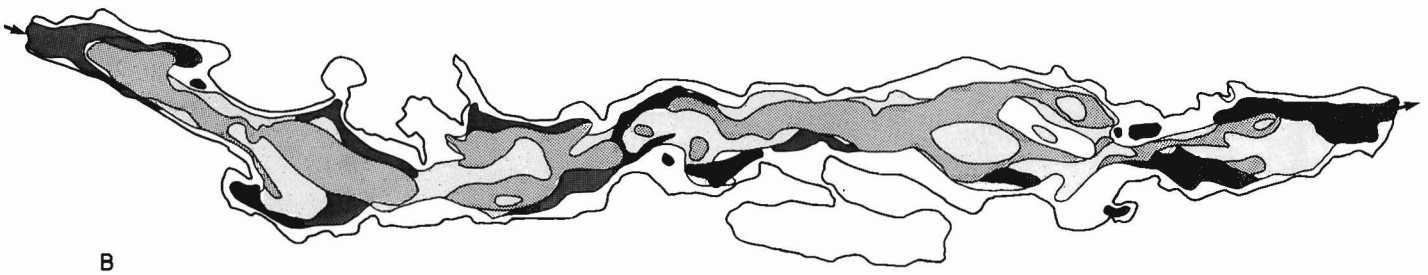

B

Modern sediment and acoustic mask(gas), Harrington Lake

- Acoustic mask probably gas(methane ?) layer near base of gyttja
- Gyttja ;watery organic lake sediment
- Gyttja with significant clastic (sand-silt) component

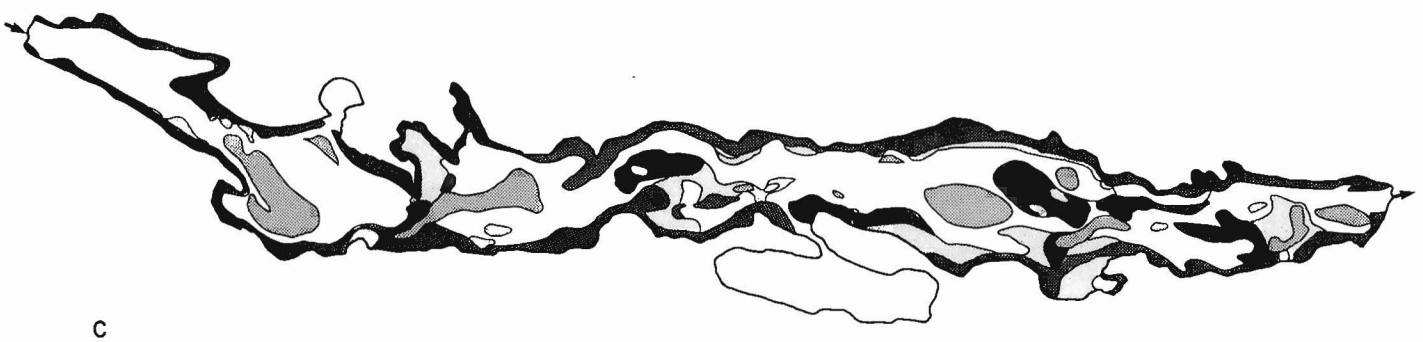

C

Bedrock, proglacial sediment, and till underlying modern sediment, Harrington Lake

- Laminated silty clay
- Outwash sand or gravel
- Till
- Bedrock
- Areas not traversed or obscured by acoustic masks in modern sediment

0 500 1000

metres

A. Bathymetry, traverse lines (dashed), and locations of acoustic profiles, (heavy lines) shown in Figure 27.10.

B. Distribution of modern sediment (gyttja) and gas layer.

C. Bedrock and surficial sediments beneath cover of modern sediment. Note that much of the subbottom record is obscured by acoustic masks (gas and gravel layers).

Figure 27.9. *Bathymetry and sediment fill in Harrington Lake (Lac Mousseau).*

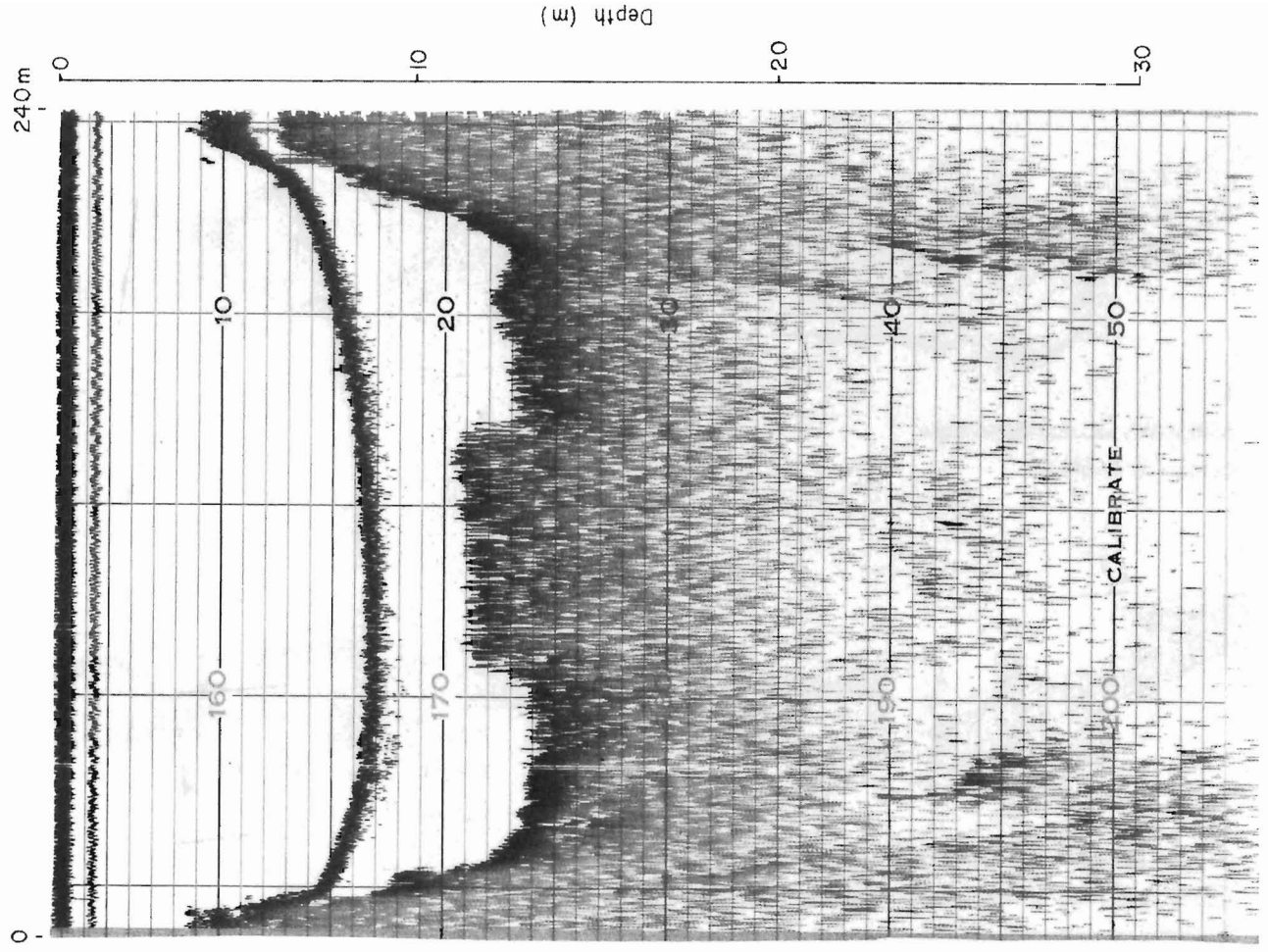

Figure 27.10A

The bay into which the principal inlet stream enters Turkey Lake from Little Turkey Lake is floored by sand with little or no cover of organic sediment. The bay of the outlet stream is floored with 1 m or more of gyttja and woody debris on and in which large (1 m diameter) erratic boulders rest.

Compared to lakes profiled in eastern Ontario, Turkey and Little Turkey lakes are quite deep for their size. This is partially a result of lack of infilling by glacial and late-glacial clastic sediments, which commonly attain thicknesses of 25 m or more in eastern Ontario lake basins (Klassen and Shilts, 1982).

Weslemkoon Lake

Geology

Weslemkoon Lake has numerous inlet streams, and its outlet stream is Little Mississippi River which flows northwestward from the north end of the lake. The lake lies completely within the outcrop area of a granitic batholith, and a significant part of the shoreline consists of glacially smoothed granite with little or no boulder or drift cover. Generally, drift is thin on the forested slopes surrounding the lake. Thick, ice-contact gravel and sand are exposed in pits at the south end of the lake, and many of the islands in its southernmost bay consist of gravel and sand, probably originating as outwash, lying on bedrock. The carbonate content of the less than 64 µm fraction of till and gravel collected at several places around the lake ranges from 0.7 to 4.5% $CaCO_3$ equivalent. Most of the carbonate is probably derived from marble and associated calcareous metasediments that encircle the batholith and outcrop within 8 to 10 km northeast of the north end of the lake.

The regional direction of glacial flow was approximately southwestward, and the marble erratics and accompanying fine grained calcareous debris were undoubtedly transported into the basin by glacial processes. Several pieces of Paleozoic limestone were also found in outwash gravels that form part of the northern shore of the lake. The nearest known source for these erratics lies more than 80 km northeast of the lake, but they may have been derived from closer, presently unmapped outliers of Paleozoic rock, similar to those that occur north of Madoc, 40 to 50 km south of Weslemkoon Lake. The common occurrence of calcareous erratics and calcareous glacial sediments along the shores of Weslemkoon Lake partially explains its anomalously high pH, which, according to the Ontario Ministry of Natural Resources, averages 7.0.

The trace element concentrations of glacial sediments surrounding Weslemkoon Lake are not unusual, copper and zinc being slightly higher than the regional background and arsenic being several times its regional background of about 1 ppm. Uranium, probably derived from pegmatitic phases in the granite, reaches 10 ppm, a fairly high concentration in relation to the local background of less than 1 ppm.

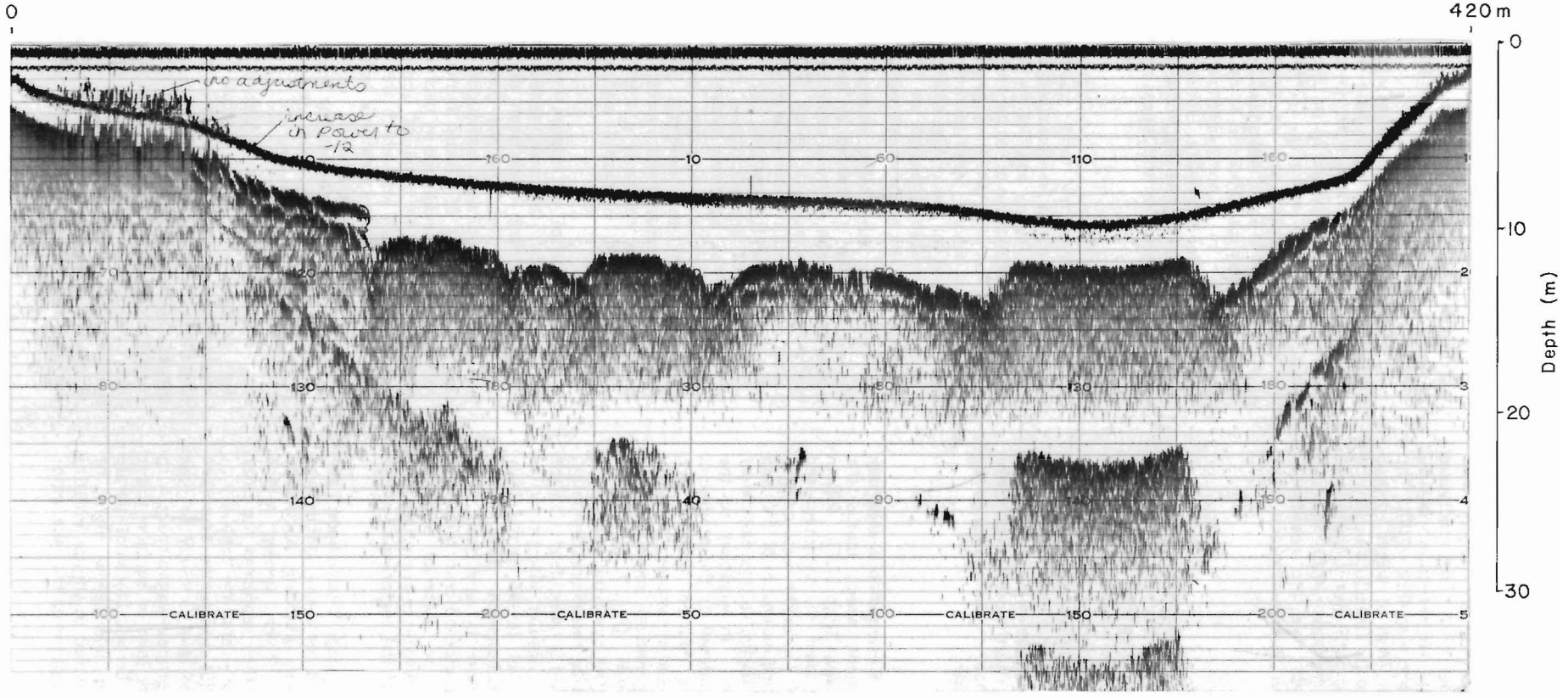

Figure 27.10B

Figure 27.10. *Profiles from Harrington Lake illustrating two types of 'raised' acoustic masks. The mask in Figure 27.10A creates a diffuse reflection with no apparent multiples and is interpreted as gas. The mask in Figure 27.10B produces a sharp reflection with strong multiples and is interpreted as a sand or gravel layer that originated as outwash in channels on glacier ice that was trapped in the basin.*

Results of Profiling

Weslemkoon Lake is unlike the other three lakes described here in that it is underlain by thick proglacial and postglacial sediments which in aggregate are thicker than 35 m over bedrock in places. The body of the lake (exclusive of its many arms) comprises several sedimentation basins, which are reflected by the bathymetric map (Fig. 27.4). The deepest of these basins lies in 30 to 36 m of water, depths considerably less than those depicted by Ontario Ministry of Natural Resources (1973). Since our bathymetric data from Turkey lakes and Harrington Lake correspond closely to those of other independently drawn maps, we are reasonably confident that our bathymetric data for Weslemkoon Lake are accurate.

Gyttja

As in the other lakes studied, gyttja forms a 3 to 5 m cover over significant parts of the lake bottom (Fig. 27.5). The cover of gyttja is probably more extensive than that shown in Figure 27.5, particularly in the numerous bays that were not surveyed. As in the other lakes, there are areas that are characterized by an acoustic mask which is interpreted to be methane trapped at the base of the gyttja. The areas of gas are minor compared to those in Harrington and Little Turkey lakes, and the most northwesterly of them occurs along a slope, suggesting that it was emplaced by groundwater issuing from the basin side.

Thick Laminated Sediment

Unlike the other lakes studied, Weslemkoon is underlain by thick laminated[1] clastic sediment which masks the considerable relief of the bedrock basin (Fig. 27.6). Fill in deep valleys which appear to be part of an integrated ancestral drainage system reaches 30 + m in the west-central part of the lake (Fig. 27.7). Landward extension of the axis of this fill suggests that one or more buried valleys exist west of the northern part of the lake. In addition to the glaciotectonic features formed by collapse of the proglacial laminated sediment over melting buried glacier ice (Klassen and Shilts, 1982) large vertical structures, presently interpreted to be of diapiric origin, penetrate and disrupt the bedding of over 20 m of sediment (Fig. 27.8). This disturbance appears to extend into the overlying gyttja, the surface of the laminated sediment being raised and disrupted. An acoustic discontinuity in the gyttja is coincident with the raised surface of the disturbance. Similar discontinuities have been interpreted elsewhere as layers particularly enriched in a clastic mineral component (Klassen and Shilts, 1982). If this interpretation is applicable, the discontinuity may represent material ejected onto the gyttja surface and subsequently buried, or material injected laterally into a thicker gyttja layer. Whatever the origin, the diapiric disturbance seems to postdate the beginning of gyttja accumulation.

The thick laminated sediments under Weslemkoon Lake were probably deposited while the last retreating glacier was still in the Weslemkoon watershed, blocking northward drainage through the Mississippi River system which presently drains the lake. As such, they represent the finer parts of the glacial load – rock flour – and are probably at least as calcareous as the surficial sediments described above. Groundwater inflow into the lake is likely to pass through these sediments and in the process would react with them and be buffered, as would any lake or surface water that comes into contact with them. Erratic blocks of marble and limestone around and in the lake show signs of considerable chemical abrasion compared to similar erratics observed elsewhere. The neutral character of the lake water in Weslemkoon may be as much a result of buffering by the thick laminated sediments as of buffering by the relatively thin glacial sediments that occur on the flanks of the lake.

Harrington Lake (Lac Mousseau)

Geology

Harrington Lake (Lac Mousseau) is a relatively shallow, narrow lake which is the middle link in a chain of three similar lakes in Gatineau Park north of Ottawa. It has two deep sedimentation basins in its central part and a shallow basin at its south end (Fig. 27.9A). It lies wholly within Precambrian syenite, and its present surface is near or slightly below the local postglacial marine limit. It and its associated lakes (Lac Philippe to the north and Lac Meach to the south) lie in a northwest-trending fault system that displaces hornblende syenite. Its surrounding forested slopes are steep and have little drift cover; bouldery, sandy till was noted in an exposure on the access road to the lake.

Results of Profiling

The bathymetry and sedimentation features in Harrington Lake can be described as intermediate between those of Little Turkey and Turkey lakes. Harrington Lake is about 20 m deep in one of its central basins but averages less than 15 m (Fig. 27.9A). It is generally steep-sided with a relatively flat floor. Some terrace-like benches occur here and there along its flanks, but whether these are remnants of a preglacial erosional surface or formed by glacial erosion and deposition has not been determined.

As in the other lakes studied, much of the bottom of Harrington Lake is covered by gyttja. Like Little Turkey Lake, much of the surficial sediment fill below the gyttja is obscured by an acoustic mask (Fig. 27.9B). Most of the acoustic mask is interpreted to be gas, accumulated as in the other lakes near the base of the gyttja. In several places another type of acoustic mask, interpreted by Klassen and Shilts (1982) as sand or gravel deposited in meltwater streams, lies on and obscures underlying sediment. The reflection from this material is sharp and is usually accompanied by equally sharp multiple reflections. The "gas" layer causes, in contrast, a characteristic diffuse, fuzzy reflection which is rarely accompanied by a multiple reflection.

The gyttja of Harrington Lake in many places passes into an apparently laminated sediment (Fig. 27.9B). Similar bodies of sediment have been noted in Lac Philippe and Lac Meach, but they are not common in the other lakes surveyed. This sediment is thought to be gyttja mixed with a significant amount of clastic mineral sediment transported into the lake by streams or by nearshore processes. The best development of this type of sediment is in the shallow sedimentation basin into which the inlet stream flows. The sediment also occurs commonly near the sides of the lake. The acoustic characteristics of the sediment and its distribution strongly support the hypothesis that it contains more clastic material than the acoustically transparent gyttja elsewhere in the lake.

Glacial and proglacial clastic sediments that underlie the postglacial sediments of Harrington Lake are considerably obscured by acoustic masks and by the clastic-rich facies (Fig. 27.9C). Till has been identified in many places, and its spotty occurrence may reflect its similarly patchy occurrence on the slopes of the region surrounding the lake. In spite of the location of the lake near or below marine limit, very little clastic sediment that might be attributed to marine or proglacial deposition was noted. It is possible, however, that if the acoustic masks could be

[1] The acoustic record of this sediment, as in other lakes surveyed, shows distinct laminations of uncertain origin; therefore, we use the term 'laminated' sediment to describe this distinctive, probably proglacial, lacustrine facies.

penetrated, much more clastic sediment would be found. The peculiar tabular appearance of the 'sand-gravel' layers has been discussed previously (Klassen and Shilts, 1982) (Fig. 27.10). If those masking sediments are truly sand and gravel and are not another form of gas layer, the presence of sediment indicating fluvial conditions in a lake basin presents an apparent paradox. It is suggested here that the (glacio) fluvial sediments observed in Harrington Lake and on islands in Weslemkoon Lake were deposited on glacier ice which was trapped in the lake basins and formed a temporary floor above the level of the present outlet of the lakes, allowing temporary free drainage. The outwash sediments, deposited in channels in the ice, would have been let down onto the bottom of the lake as the ice melted. The tabular morphology of these sediments in Harrington Lake (Klassen and Shilts, 1982) may mirror the configuration of the former ice channels.

Conclusions

Subbottom profiling can be used to map the glacial and lacustrine sediment facies that occur in lakes of the Canadian Shield. The profiles provide not only an inventory of the types and three-dimensional configuration of unconsolidated sediments in these lakes, but can yield insights into their late and postglacial history as well. The amount and nature of fill could be of critical importance in evaluating the effects of inflow of the increasingly acid surface water and groundwater expected to be generated by acid rain. The anomalously high pH of the water in Weslemkoon Lake is probably partially attributable to the presence beneath its bottom of thick, probably calcareous clastic sediments. Such features as gas layers have been shown to be continuous, mappable features and not instrumental abberations or sediment peculiarities on isolated profiles. Finally, it should be noted that no coring or drilling has yet been done in support of the conclusions drawn about these profiles. Only by deep coring can the interpretations of the sediment facies represented by these acoustic signals be confirmed.

Acknowledgments

The authors thank R.A. Klassen and J. Hornsby for their assistance in developing operational procedures for the profiling equipment. Dalton Cross and Mr. and Mrs. Walter McKinnon provided much help on Weslemkoon Lake, and Mr. Cross and Derek McDermolf brought the anomalously high pH of this lake to our attention on behalf of the Weslemkoon Lake Conservation Association. The National Capital Commission graciously allowed us access to Harrington Lake and Paul Kyer, Director of Gatineau Park, provided maps of the lake bathymetry. Laura Johnston of the Department of the Environment suggested the Turkey lakes project to us and provided valuable field support. R.N.W. DiLabio and T.W. Anderson provided helpful critical comments on the paper, but the authors assume full responsibility for the interpretations presented.

References

Barker, J.F. and Fritz, P.
1981: The occurrence and origin of methane in some groundwater flow systems; Canadian Journal of Earth Sciences, v. 18, p. 1802-1816.

Coker, W.B. and Shilts, W.W.
1979: Lacustrine geochemistry around the north shore of Lake Superior: implications for evaluation of the effects of acid precipitation; in Current Research, Part C; Geological Survey of Canada, Paper 79-1C, p. 1-15.

Dell, C.I.
1975: Relationships of till to bedrock in the Lake Superior region; Geology, v. 3, p. 563-564.

Jeffries, D.S. and Semkin, R.
1982: Basin description and information pertinent to mass-balance studies of the Turkey Lakes watershed; Environmental Contaminants Division, National Water Research Institute, Burlington, 34 p.

Keen, M.J. and Piper D.J.W.
1976: Kelp, methane, and an impenetrable reflector in a temperate bay; Canadian Journal of Earth Sciences, v. 13, p. 312-318.

Klassen, R.A. and Shilts, W.W.
1982: Subbottom profiling of lakes of the Canadian Shield; in Current Research, Part A; Geological Survey of Canada, Paper 82-1A, p. 375-384.

Müller, H.E.
1977: Observations of interactions between water and sediment with a 30-kHz-sediment echosounder; in Interactions between sediments and freshwater, ed. H.L. Golterman; Proceedings of International Symposium, Amsterdam, W. Junk, B.V., p. 448-452.

Ontario Ministry of Natural Resources
1973: Weslemkoon Lake; Ontario Ministry of Natural Resources, Map 52L2.

28.

AN OCCURRENCE OF THE SILURIAN OSTRACODE BEYRICHIA (BEYRICHIA) FROM ANTICOSTI ISLAND, QUEBEC

Project 720072

M.J. Copeland
Institute of Sedimentary and Petroleum Geology, Ottawa

*Copeland, M.J., An occurrence of the Silurian ostracode **Beyrichia (Beyrichia)** from Anticosti Island, Quebec; in Current Research, Part B, Geological Survey of Canada, Paper 82-1B, p. 223-224, 1982.*

Abstract

***Beyrichia (Beyrichia)**, an Euroarctic ostracode genus, is reported for the first time from the Silurian of eastern North America. Its discovery in late Anticosti strata of Anticosti Island, Quebec, questions the hypothesis of an essentially endemic late Early Silurian ostracode fauna in the northern Appalachian region.*

Introduction

Ulrich and Bassler (1923) proposed a zonal classification of eastern North American lower Silurian strata based on beyrichiacean Ostracoda. This zonation has been used extensively throughout the Appalachian region but is apparently of limited application in Anticosti strata of eastern Canada. Copeland (1974) showed that only zones 2 and 3 (**Zygobolba anticostiensis** and **Zygobolba decora**) of Ulrich and Bassler's "Lower Clinton" are represented on Anticosti Island by their nominal species. Zone 1 (**Zygobolba erecta**) has been replaced by up to four 'Sub-zones' (Copeland, 1974), the ostracode fauna of which have not been obtained elsewhere. The uppermost stratigraphic unit on Anticosti Island (Chicotte Formation) contains, only within its basal 30-60 cm, specimens of **Z. decora** (Billings); whether younger strata of this formation should be referred to zone 3 or 4 (Ulrich and Bassler's "Middle Clinton" zone of **Zygobolbina emaciata**) is unknown.

Associated with the youngest occurrence of **Z. decora** at "The Jumpers" on the south-central coast of the Island (Bolton, 1972) are specimens of a previously unreported ostracode **Beyrichia (Beyrichia)** sp., an ostracode that should not be expected to occur in the highly endemic Silurian ostracode assemblage of Appalachian North America (Copeland and Berdan, 1977). This occurrence, 30-60 cm above the base of the Chicotte Formation at the uppermost range of **Zygobolba decora** (Billings) known from the Island, indicates that, at least within Anticosti Basin, the late Anticosti ostracode fauna may not have been as endemic as that of the Appalachian region to the south. This appearance of **Beyrichia (Beyrichia)** may represent the interfingering of European and Appalachian ostracode faunas near the end of the Anticosti Series and permit future correlation between Ulrich and Bassler's ostracode zonation and that proposed by Martinsson (1967) for the Baltic region.

Strata of the basal Chicotte Formation contains numerous **Costistricklandia** sp. and underlie by ca. 15 m Chicotte strata containing the button coral **Palaeocyclus-Rhabdocyclus** (Bolton, 1981). This predicates the position of the present collection of **Beyrichia (Beyrichia)** sp. as near the Anticosti (Llandovery C5-C6) – Wenlock boundary (Martinsson, 1967). Martinsson (1962, 1967) and Siveter (1978) have indicated that the earliest known occurrences of **Beyrichia** from Gotland and Great Britain respectively are those of **Beyrichia (Beyrichia) halliana** Martinsson and **Beyrichia salopiensis** (Harper). These late Anticosti (=Late Llandovery (Lower Visby and Telychian) of European usage) beyrichiacean ostracodes occur in Lower Visby strata with species of **Apatobolbina, Leptobolbina, Barymetopon, Noviportia** and **Craspedobolbina** (Martinsson, 1962) and in the Telychian with **Craspedobolbina (Artiocraspedon)** and **Stroterobolbina** (Siveter, 1978, 1980). On Anticosti Island **Beyrichia (Beyrichia)** sp. occurs with species of the beyrichiacian genera **Bolbineossia (Brevibolbineossia), Craspedobolbina (Artiocraspedon), Apatobolbina, Noviportia, Zygobolba** and **Bolbibollia** (Copeland, 1974, 1981). The last two (**Zygobolba** and **Bolbibollia**) are apparently endemic eastern North American genera; **Bolbineossia** and **Apatobolbina** are recorded from elsewhere in North America, and **Craspedobolbina (Artiocraspedon)** and **Noviportia** are at present known only from Anticosti Island and Great Britain or the Baltic.

Strata of the Chicotte Formation are predominantly crinoidal calcarenite; they rest conformably on blue-grey calcareous shale of the upper Jupiter Formation. This Jupiter lithology recurs ca. 30-60 cm and ca. 3 m-3 m 15 cm above the initiation of crinoidal carenite deposition, which is mapped as the base of the Chicotte Formation. Numerous collections have been made over the past 15 years of both the Jupiter and Chicotte blue-grey calcareous shale units at "The Jumpers" but only in the 1981 collections have specimens (3 tecnomorphs) of **Beyrichia (Beyrichia)** sp. been found. Future collections may provide the additional heteromorphic specimens necessary for more adequate specific identification. The presence of specimens of **Beyrichia (Beyrichia)** sp. is, however, considered of sufficient importance to warrant this preliminary note.

Family BEYRICHIIDAE Matthew, 1886
Subfamily BEYRICHIINAE Matthew, 1886
Genus **Beyrichia (Beyrichia)** M'Coy, 1846
Type species: **Beyrichia (Beyrichia) kloedeni** M'Coy, 1846
Beyrichia (Beyrichia) sp.
Figures 28.1A, B, C

Diagnosis: Large, subamplete **Beyrichia (Beyrichia)** species with poorly differented tuberculation on the lobes, a row of tubercles anteroventrally on the tecnomorphic velar ridge, one cusp on the preadductorial lobe, two subequal cusps on the syllobium and an indistinct syllobial groove. Surface evenly granular with superimposed tuberculation.

Description: This is a very generalized **Beyrichia (Beyrichia)** species in that it combines most of the common features of the genus. The tuberculation is, however, more coarse than most species of the genus and the velar tubercles are well removed from the ventral margin of the valves. The syllobial tubercles may be arranged in four rows (Fig. 28.1A), two rows above and two below the shallow syllobial groove. The preadductorial and syllobial cusps protrude over the hingeline, the posterior syllobial cusp being lower than the others. There is a very low anteroventral depression beneath the prominent adductorial node.

Discussion: Without additional, well preserved and, in particular, heteromorphic specimens, comparison may be made with difficulty with other species of the genus. are some features in common with **Beyrichia (Beyrichia) halliana** Martinsson but that species is more

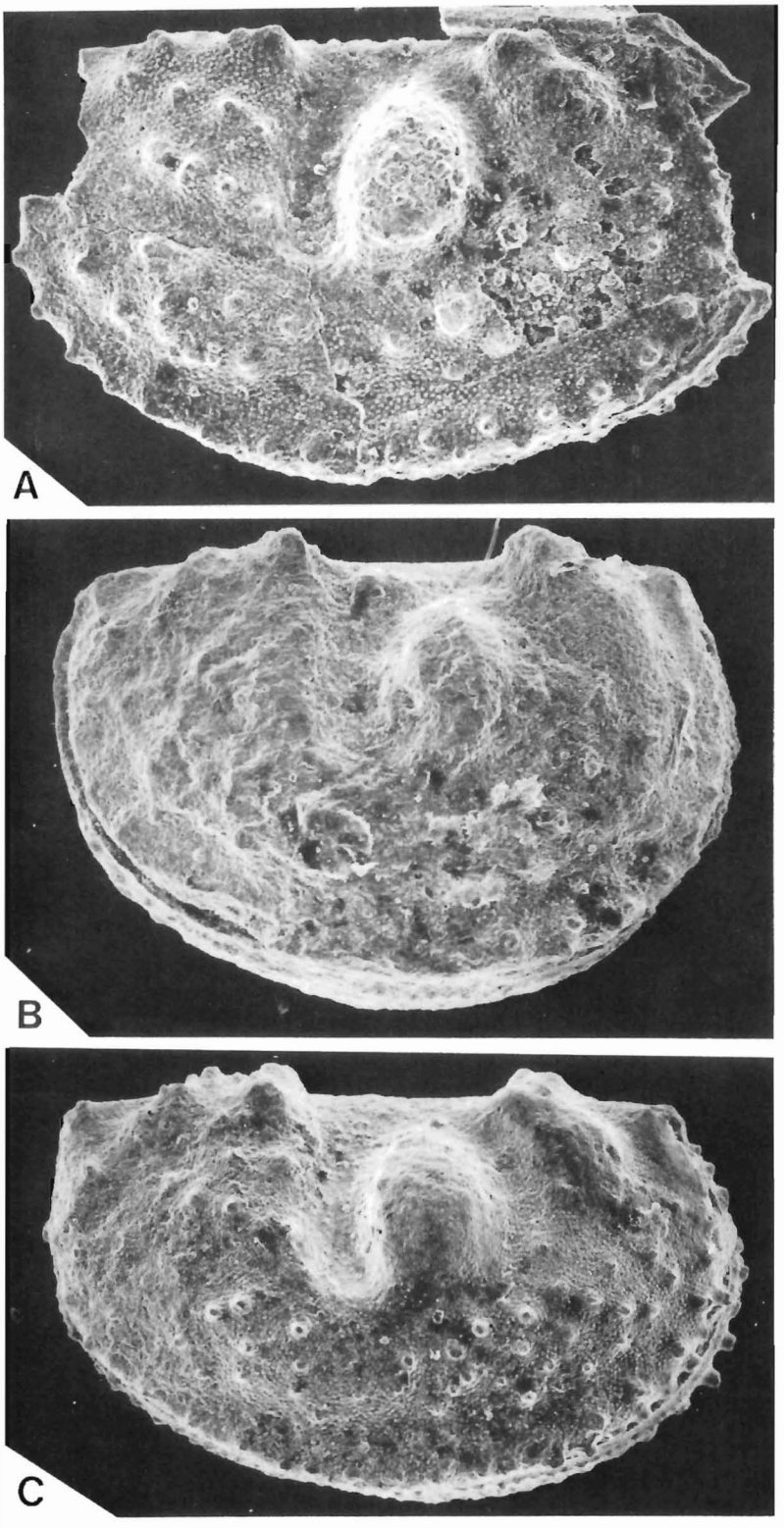

Figure 28.1. ***Beyrichia (Beyrichia)*** *sp. Lower Chicotte Formation, "The Jumpers", Anticosti Island, Quebec; (GSC loc. 76200); right lateral views of three tecnomorphic specimens, A, B-X60, C-X88. (GSC figured specimens 69488-69490)*

uniformly tuberculate and bears smaller tubercles (Martinsson, 1962, figs. 141, 144). **Beyrichia salopiensis** (Harper) is as coarsely tuberculate as **Beyrichia (Beyrichia)** sp. but the tubercles are evenly distributed on the broad preadductorial and syllobial lobes and the syllobial groove is barely discernible (Siveter, 1978, pl. 1, figs. 1, 2). Also, **Beyrichia salopiensis** (Harper) has acute tubercles instead of cusps protruding above the hingeline.

Measurements of the three tecnomorphic specimens are:

GSC 69488 – length 1.66 mm, height 1.0 mm
GSC 69489 – length 1.55 mm, height 1.1 mm
GSC 69490 – length 1.08 mm, height 0.69 mm

Occurrence: Ca. 30-60 cm above the base of the Chicotte Formation at "The Jumpers", south-central coast of Anticosti Island, Quebec, 5000 m east-southeast of Southwest Point lighthouse (GSC loc. 76200).

References

Bolton, T.E.
1972: Geological map and notes on the Ordovician and Silurian litho- and biostratigraphy, Anticosti Island, Quebec; Geological Survey of Canada, Paper 71-19.

1981: Ordovician and Silurian biostratigraphy, Anticosti Island, Quebec; Subcommission on Silurian Stratigraphy, Ordovician-Silurian Boundary Working Group, Field Meeting, Anticosti-Gaspé, Quebec 1981, v. II: Stratigraphy and Paleontology, p. 41-59.

Copeland, M.J.
1974: Silurian Ostracoda from Anticosti Island, Quebec; Geological Survey of Canada, Bulletin 241.

1981: Latest Ordovician and Silurian ostracode faunas from Anticosti Island, Quebec; Subcommission on Silurian Stratigraphy, Ordovician-Silurian Boundary Working Group, Field Meeting, Anticosti-Gaspé, Quebec 1981, v. II: Stratigraphy and Paleontology, p. 185-195.

Copeland, M.J. and Berdan, J.M.
1977: Silurian and early Devonian beyrichiacean ostracode provincialism in northeastern North America; in Report of Activities, Part B, Geological Survey of Canada, Paper 77-1B, p. 15-24.

Martinsson, A.
1962: Ostracodes of the Family Beyrichiidae from the Silurian of Gotland; Publications from the Palaeontological Institution of the University of Uppsala, No. 41.

1967: The succession and correlation of ostracode faunas in the Silurian of Gotland; Geologiska Föreningens i Stockholm Forhandlingar, v. 89, p. 350-386.

Siveter, D.
1978: The Silurian; in A Stratigraphical Index of British Ostracoda, R. Bate and E. Robinson ed., Geological Journal Special Issue No. 8, p. 57-100.

1980: British Silurian Beyrichiacea (Ostracoda). Part I; Palaeontographical Society Monographs, v. 133, p. 1-76, 27 plates.

Ulrich, E.O. and Bassler, R.S.
1923: Maryland Geological Survey, Silurian, Paleozoic Ostracoda: Their Morphology, classification and occurrence; p. 271-391. Systematic Paleontology of Silurian deposits (Ostracoda); p. 500-704, pls. 36-65.

29. QUELQUES DONNÉES NOUVELLES SUR LES DÉPÔTS QUATERNAIRES DU WISCONSINIEN ET DE L'HOLOCÈNE DANS LE PIEDMONT APPALACHIEN, GRANBY, QUÉBEC

Projet de recherche 210-4-78

Gilbert Prichonnet[1]
Division de la science des terrains

Prichonnet, Gilbert, Quelques données nouvelles sur les dépôts quaternaires du Wisconsinien et de l'Holocène dans le piedmont appalachien, Granby, Québec; dans Recherches en cours, partie B, Commission géologique du Canada, Etude 82-1B, p. 225-238, 1982.

Résumé

La région de Granby est située à 50 km à l'est-sud-est de Montréal. Elle inclut, à l'ouest, la bordure des basses-terres, et, vers l'est, les premières crêtes appalachiennes. Les dépôts quaternaires forment une mince couverture (0-50 m) en discordance angulaire sur les roches paléozoïques déformées. Une séquence basale comprend deux tills séparés par des dépôts non glaciaires: on attribue le till inférieur et les dépôts non glaciaires au Wisconsinien moyen. Le till supérieur s'est déposé lors de la dernière glaciation (Wisconsinien moyen à supérieur). Le premier till a été mis en place par des glaces venant du nord-est, et le second, principalement, par des glaces venant du nord-ouest et nord-nord-ouest. La déglaciation commence vers 13 000 ans B.P. (?). Un certain nombre d'accumulations fluvio-glaciaires de contact montrent un retrait par petites étapes, vers le nord-ouest, sans stabilisation de longue durée. Des lignes de rivage soulevées marquent un littoral glacio-lacustre, vers 240-245 m d'altitude. Le niveau marin maximum suggéré est de l'ordre de 190 m: la mer de Champlain a recouvert le territoire, entre 12 500 et 10 000 ans B.P. (80% lors du maximum). Des lacs peu profonds ont occupé les dépressions, entre les crêtes: ils ont été remplacés par des tourbières à partir de 8000 ans B.P.

Introduction

Les résultats préliminaires exposés dans ce bref rapport ont été obtenus à l'occasion de travaux de cartographie (à 1/50 000^{e}) sur un large secteur situé à l'est de Montréal (fig. 29.1).

Les principaux objectifs portaient sur l'identification des unités lithostratigraphiques, leur corrélation avec les séries régionales voisines et l'amélioration du schéma paléogéographique régional. Quelques remarques sur l'intérêt économique des dépôts quaternaires présents découlent du premier objectif.

La plupart des données présentées ici proviennent de la région de Granby (31 H/7, fig. 29.1B). Un rapport détaillé, incluant la carte des dépôts meubles, a été soumis à la Commission géologique du Canada.

Généralités

La carte topographique de Granby, à 1/50 000^{e}, est située à l'est-sud-est de Montréal. La région inclut la bordure de la plaine des basses-terres, à l'ouest, et les premières crêtes du piedmont appalachien, au centre et à l'est: la plaine est à environ 35 m d'altitude, tandis que les crêtes atteignent 175 m au centre, et 250 m à l'est. Trois collines montérégiennes culminent avec des sommets à environ 412, 520, 550 m, dominant le paysage: ce sont respectivement les monts Yamaska, Shefford et Brome. Le réseau hydrographique est partiellement adapté et partiellement inadapté aux structures géologiques NNE-SSW (soit parallèle ou orthogonal aux reliefs).

Les roches du substratum sont principalement d'âge cambro-ordovicien, tandis que des sédiments quaternaires, discordants sur ce socle, peuvent présenter une période allant du Wisconsinien moyen à nos jours.

Dans le substratum, la ligne Logan délimite deux catégories de roches très différentes:

1. à l'ouest, une étroite bande de formations ordoviciennes, incluant des roches carbonatés, appartient à la séquence des dépôts de la plate-forme cambro-ordovicienne de l'est du continent;

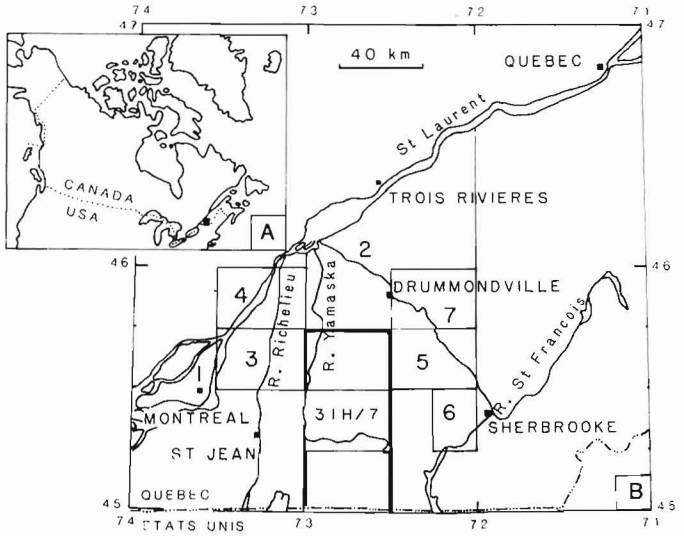

Figure 29.1. *(A) La carte de Granby (31 H/7) est au centre des 3 cartes objet d'un programme de cartographie dans le sud du Québec. (B) Les travaux de cartographie déjà publiés autour de la présente étude:*

1 – Prest et Hode-Keyser (1962, 1977)
2 – Gadd (voir historique in 1971)
3 – LaSalle et Elson (1962)
4 – LaSalle (1963)
5 – McDonald (1966)
6 – McDonald (1967)
7 – Warren et Bouchard (1976).

[1] Département des sciences de la Terre, université du Québec à Montréal, CP. 8888 – Succ. A. Montréal H3C 3P8

2. à l'est, des roches détritiques terrigènes, d'âge cambrien surtout, proviennent des séquences plus internes du miogéosynclinal appalachien, mises en place lors de l'orogénèse taconique (Ord. moy. à sup.). Les monts Yamaska (au nord-ouest) et Brome et Shefford (au sud-est) font partie de la série intrusive des Montérégiennes – d'âge crétacé inférieur.

Travaux antérieurs

Les principaux travaux de cartographie utiles à la connaissance du Quaternaire régional sont indiqués sur la figure 29.1B.

De Prest et Hode-Keyser (1962, 1977), on retiendra principalement l'identification de deux tills et d'une séquence intermédiaire complexe, à caractère glaciaire proximal mais correspondant à un recul de l'inlandsis; deux hypothèses sont présentées pour l'attribution stratigraphique de cette séquence: l'une "très courte", soit Wisconsinien supérieur, et l'autre "plus longue", soit de la base du Wisconsinien moyen au Wisconsinien supérieur (voir aussi Prest, 1977). Cette séquence est analogue à celle identifiée plus au sud-ouest, le long de la voie maritime dans l'état de New-York[1] (MacClintock et Stewart, 1965) et l'est ontarien[1], (Terasmae, 1965). Dans les événements postglaciaires, les auteurs étendent le lac Vermont (défini par Stewart et MacClintock, 1969) jusqu'au coeur des basses-terres.

Un mémoire de synthèse (Gadd, 1971) présente les résultats d'une large région, cartographiée quelques années plus tôt principalement par l'auteur (voir la bibliographie de l'auteur): le till de Bécancour y est attribué au Wisconsinien inférieur, ainsi que les sédiments de Saint-Pierre; les varves de Deschaillons (Karrow, 1957) et la base du till de Gentilly sont également rangés dans le Wisconsinien inférieur; une importante phase éolienne s'intercale dans les événements postglaciaires (comparables, par ailleurs, à ceux décrits par les auteurs précédents), après le retrait des eaux marines et/ou lacustres.

Vers la même époque, les recherches dans les Appalaches révèlent une stratigraphie avec trois unités de till (cf. McDonald et Shilts, 1971). Toutefois, la séquence glaciaire des cartes limitrophes à celle de Granby (McDonald, 1966, 1967), ne mentionne que le till supérieur: par contre, d'importants dépôts fluvio-glaciaires, essentiellement de contact, sont délimités. Sur trois autres cartes très proches (LaSalle et Elson, 1962; LaSalle, 1963; Warren et Bouchard, 1976), aucun site montrant deux tills superposés n'est signalé.

Les problèmes stratigraphiques majeurs de ces séquences wisconsiniennes ont été discutés récemment (Gadd, 1976; Hillaire-Marcel, 1979; Occhietti, 1980).

La région de Granby étant située sur la bordure des Appalaches, il conviendra de signaler les trois phases glaciaires du Vermont (Stewart et MacClintock, 1969): au cours d'importantes recherches (1956-66), les auteurs ont particulièrement analysé les phases lacustres postglaciaires tardiwisconsiniennes, qui couvrirent également la bordure sud du Québec jusqu'au territoire objet du présent rapport.

Certains auteurs (Gadd, 1964, 1971; Gadd et al., 1972) ont vulgarisé des concepts importants pour la déglaciation: deux grands fronts morainiques sont tracés sur le territoire de la carte de Granby (le Complexe morainique du front des hautes-terres, à l'est, et la moraine de Drummondville, à l'ouest). Ces concepts ont influencé des interprétations paléogéographiques récentes dans lesquelles ces moraines séparent des phases de la mer de Champlain (Hillaire-Marcel et Ochietti, 1977). En fait, l'idée de fronts recoupant partiellement ces grandes moraines était déjà suggérée (Prichonnet, 1977). La validité du concept même de fronts morainiques stables est discutée, et remise en cause (Prichonnet, en préparation; Prichonnet et al., 1982).

Les questions relatives à l'invasion et au recul de la mer de Champlain, qui a occupé environ 80% du territoire de Granby après la déglaciation, sont variées. Dans la région, en particulier sur les pentes des collines montérégiennes, des preuves littorales ont été identifiées depuis longtemps (Chalmers, 1899; Goldthwaith, 1911; Goldthwait et al., 1913): au mont Yamaska, l'altitude de 175 m est présentée comme un niveau possiblement atteint par la mer; mais l'hypothèse que les dépôts reconnus se soient déposés dans un "lac bordé de glace" (Goldthwait, 1911, p. 234) n'est pas écartée. Nous avons recherché, dans les faciès littoraux de cette colline, un modèle de la séquence régressive champlainienne (Prichonnet, 1973): celui-ci s'avère assez constant dans l'ensemble du bassin. Au cours de cette exondation lors d'un important niveau de stabilisation des eaux, la partie ouest de la carte aurait été marquée par le littoral de Rigaud – à quelque 55 m d'altitude (Brown MacPherson, 1967). Par ailleurs, de nombreuses remarques pertinentes, d'intérêt certain pour la région d'étude, ont été formulées par plusieurs auteurs. On pourra voir, par exemple: sur les faciès, Karrow (1961); sur le problème de fluctuations du niveau marin, Elson (1969); sur les reconstitutions environnementales à l'aide de microfaunes, Cronin (1977); enfin, pour les modèles paléo-océanographiques (salinité, température) – à partir de données paléo-écologiques et surtout de la géochimie isotopique –, Hillaire-Marcel (1979).

L'histoire de la végétation postglaciaire a pu être reconstituée grâce à des sites situés sur les collines montégériennes: l'enregistrement dans les sédiments des premiers restes organiques révèle un assez large écart pour deux collines relativement proches, soit le mont St-Hilaire, 15 km à l'ouest de la carte (LaSalle, 1966) et le mont Shefford, dans la partie est de la carte (Richard, 1978). Toujours est-il que les données du mont Shefford constituent, avec 10 dates ^{14}C de contrôle, une séquence assez rare: elle est donc proposée comme standard régional par l'auteur. Un fait marquant en est, sans doute, l'absence de preuve pour une oscillation climatique (vers un refroidissement) aux environs de 11 000 ans B.P.

Soulignons enfin que les cartes pédologiques de la région (Cann et al., 1948) signalaient déjà plusieurs zones de dépôts organiques et quelques kames et eskers (notamment entre le lac Brome et Waterloo).

Lithostratigraphie

La figure 29.2 montre la localisation et la succession sédimentaire de 7 coupes réparties sur le territoire. Neuf unités ont été identifiées: seuls les dépôts de plaine alluviale (unité 8) ne sont pas représentés ici.

Le fait stratigraphique majeur est l'identification d'un till inférieur séparé du till supérieur, habituellement identifié en surface, par des dépôts non glaciaires.

Le till inférieur (unité 1) a été identifié, avec certitude, en deux secteurs: au sud-ouest, près de l'Ange-Gardien, entre des ondulations du socle, découvertes pour en exploiter les calcaires, et, au nord-est, près de Roxton-Sud (ou Ste-Prudentienne), dans le fossé d'une route. Pour ce deuxième cas, on peut voir un till déformé, sans doute tronqué par le till supérieur, appartenant lui-même à une traînée de till. Dans ce même secteur nord-est de la carte, près de Martin Corner, le long d'une nouvelle route (rue Ingram), on a observé des interdigitations de till et de dépôts silto-argileux rythmiques, sous des dépôts graveleux et sableux; deux hypothèses sont proposées sur la figure 29.2D: l'une (A) considère qu'il s'agit du sommet du till inférieur, et l'autre (B) que toute la séquence est à rattacher au till supérieur.

[1] En fait, on a rangé, dans le till de Malone, deux unités de till séparées par des dépôts non glaciaires (varves, ...).

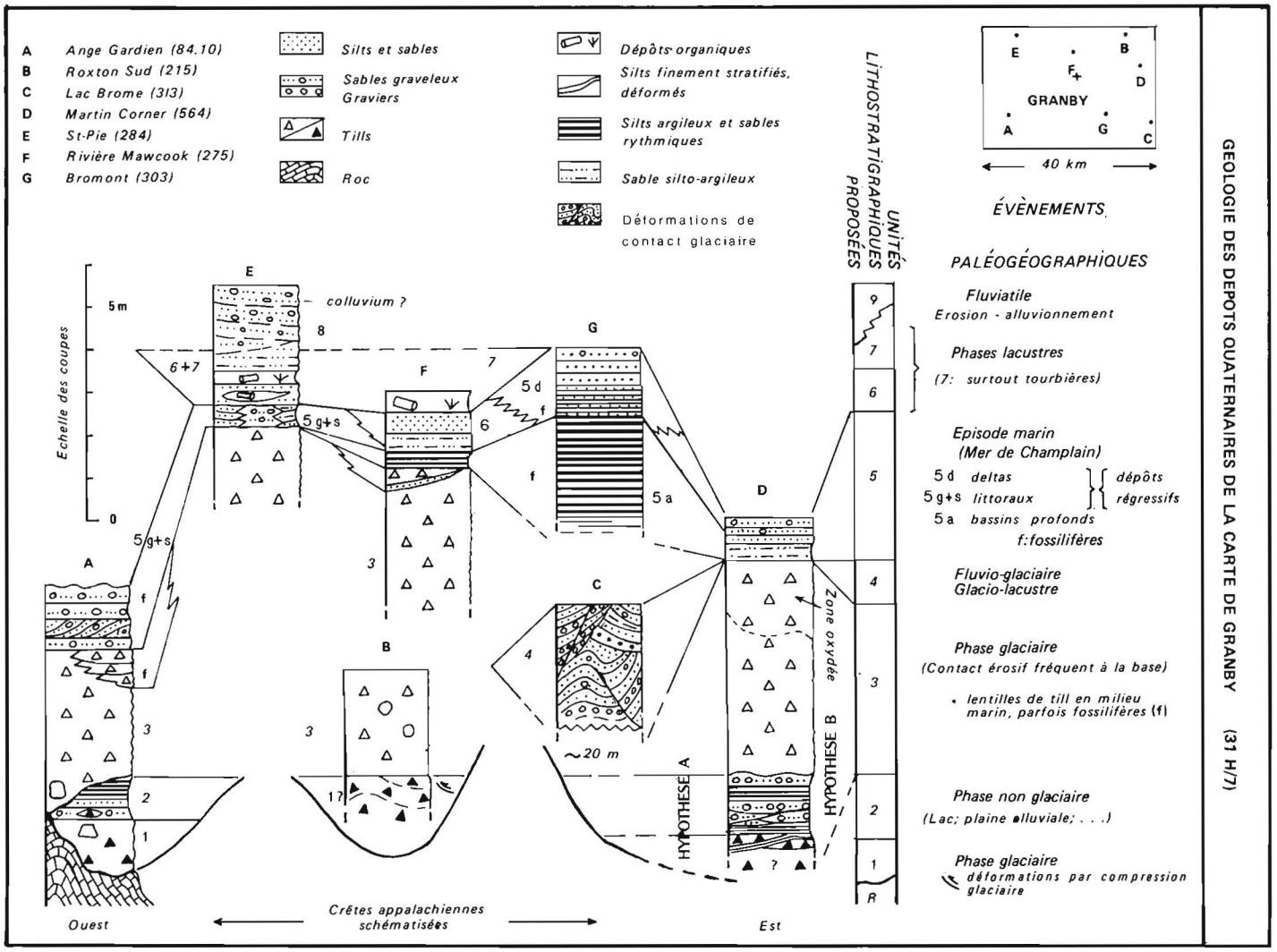

Figure 29.2. *Les unités lithostratigraphiques et les événements paléogéographiques majeurs.*

On propose de nommer ce till inférieur, Till de l'Ange-Gardien, puisqu'il affleure en plusieurs endroits sur les bordures d'une large exploitation à proximité du village du même nom (voir figure 29.5, pour la localisation).

À l'Ange-Gardien (fig. 29.2A, 29.3), le till atteint 1,4 m d'épaisseur, et repose sur le roc. Vers le sommet, il est caillouteux, lâche, grisâtre et carbonaté (3 à 4% dans la fraction inférieure à 0,210 mm). Sa matrice est constituée par 50% de sables moyens à très fins. Pour une coupure granulométrique à 8 mm, le till contient alors 71% d'arénite et 24% de lutite (silt et argile). La partie basale s'apparente à un till de fond, comme celui de Roxton Sud (fig. 29.2B).

À l'Ange-Gardien, la texture tridimentionnelle (fig. 29.3, 29.4) montre un pôle dominant à 040° (avec des concentrations à 0°, 25°, 35°, 45°, 175° et 225°). Pour 120 galets, 15% proviennent du klippe de Granby, situé à l'est de l'affleurement. Soulignons aussi que 59% des galets plongent vers le secteur nord-nord-est à nord-est. À Roxton Sud, dans les déformations, les galets s'orientent en îlots erratiques, autour du grand cercle: pour 118 galets, 85% proviennent du klippe de Granby sous-jacent. Près de Martin Corner, l'exiguité des affleurements et la texture très fine du till n'ont pas permis ce type d'analyse.

En conclusion, on peut retenir que le till inférieur doit exister, en placages fréquents, dans le fond des dépressions étroites, entre les crêtes du substratum. Il est probable que l'unité est constituée d'un till de base suivi d'un till d'ablation, ou de lentilles de till mises en place en milieu glacio-aquatique. L'analyse tridimensionnelle et la pétrographie sont en accord avec une origine orientale de la glace. Des dépôts non glaciaires (unité 2) stratifiés succèdent au till inférieur.

Parmi les trois coupes déjà citées, deux ont permis d'observer, chacune, 1 m de ces dépôts. À l'Ange-Gardien, l'altitude sommitale est de l'ordre de 80 m; le contact érosif du till supérieur est bien démontré, sur quelques centaines de mètres: celui-ci contient même des lambeaux de l'unité stratifiée, et repose parfois directement sur le till inférieur dont il incorpore également des débris. Les sédiments y sont stratifiés, sablonneux, silteux ou argileux (fig. 29.3). Plus fins vers le sommet, ils contiennent des galets striés, atteignant 10 cm de longueur. À la base, ils peuvent être déformées, avec présence de brèche de till. Le caractère rythmique de la séquence est suggéré par des lits d'argile de couleur marron. La teneur en carbonates (Ca + Mg) varie de 4 à 8%. Deux échantillons de 50 g, pris dans les sédiments fins sommitaux, ont été examinés: aucun microfossile n'a été identifié.

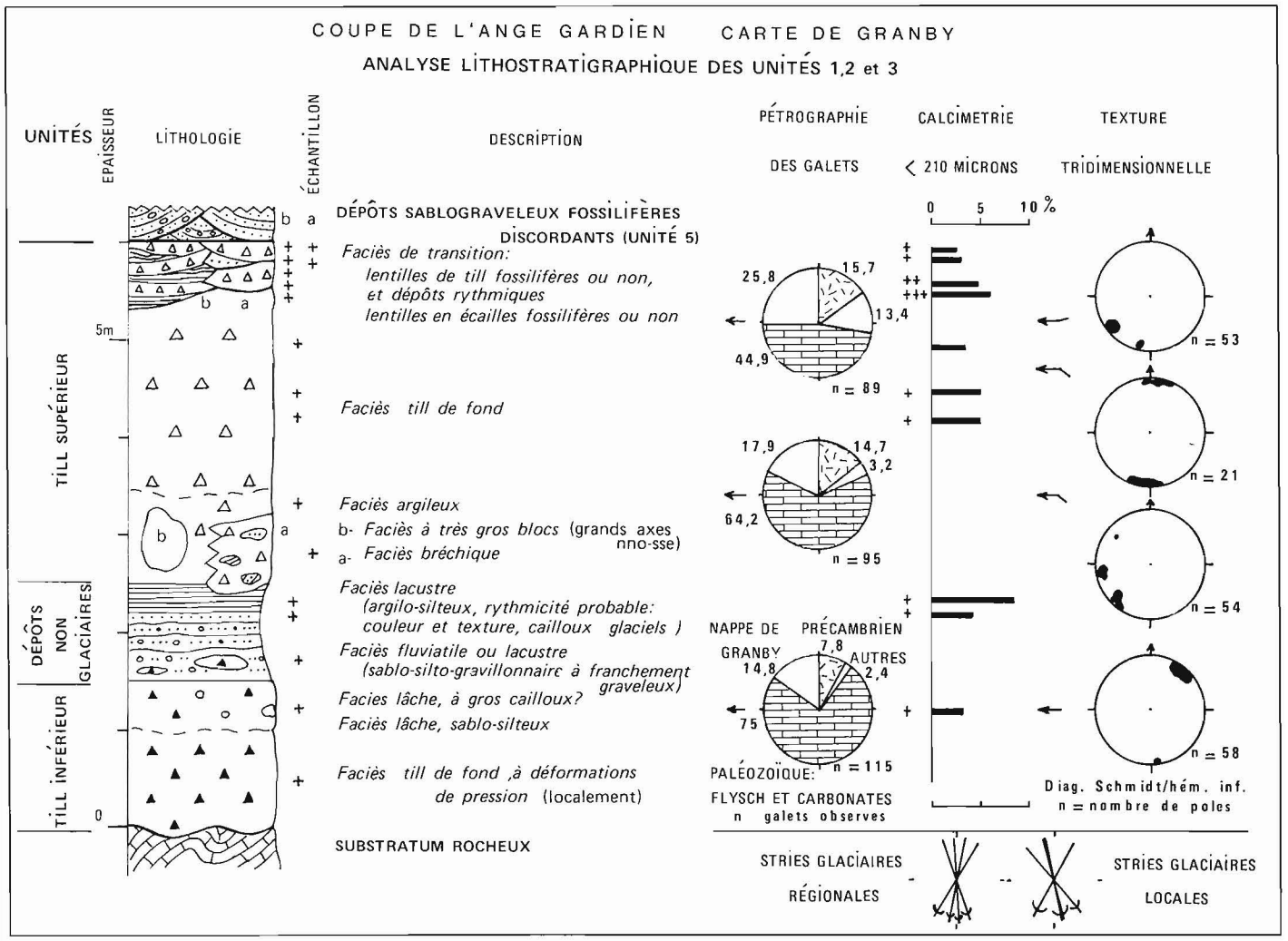

Figure 29.3. *Analyse lithostratigraphique des unités 1, 2, 3, à l'Ange-Gardien (n°. 84.10).*

À Martin Corner, ce sont des sables et graviers qui alternent en couches lenticulaires de 5 à 35 cm. Près du sommet de l'unité, on a relevé une couche diamictique, à galets striés, de 20 cm d'épaisseur. Ici, l'altitude du dépôt se situe à environ 168 m.

Des dépôts non glaciaires, graveleux, sont également identifiés sur la carte de Cowansville (Prichonnet, 1982) à 20 et 25 km au sud-est de l'Ange-Gardien: le sommet de ces dépôts se situe vers 103 et 108 m d'altitude.

Dans l'état actuel des recherches, on doit admettre que l'unité est, comme la précédente, présente dans toute la région du piedmont appalachien. Toutefois, la diversité des altitudes où se situent ces dépôts (80, 103, 108, 168 m) autorise de nombreuses spéculations sur la profondeur des bassins locaux, comme sur leur synchronisme. Seul, le site le plus bas (l'Ange-Gardien: 80 m) démontre l'existence de faciès très fins, de décantation, probablement rythmiques. Dans tous les cas, la proximité des reliefs – même de faible importance – favorise la reprise des matériaux grossiers glaciaires, antérieurs (par les vagues, le ruissellement et le transport glaciel).

Le till supérieur (unité 3) repose sur les unités précédentes en discordance d'érosion. Une nouvelle avancée glaciaire sur les unités antérieures a eu pour résultat le dépôt d'une variété de faciès, bien identifiés à la base de cette unité à l'Ange-Gardien (fig. 29.3): les crêtes rocheuses ont même été impliquées dans cette nouvelle troncature des dépôts antérieurs, comme en témoigne le faciès à blocs.

Cette unité occupe probablement près de la moitié du territoire.[1] Mais, en fait, ce sont des produits de remaniement (graviers et sables graveleux) qui sont souvent rencontrés en surface. Le till atteint fréquemment 3 à 4 m d'épaisseur tandis que dans quelques cas, les graviers de remaniement atteignent 1 à 2 m et sont occasionnellement exploités. Ce remaniement est en partie responsable de l'absence de till d'ablation, sauf pour quelques coupes.

Généralement, le till de fond est gris, compact en profondeur, et légèrement carbonaté (jusqu'à 5,5%). Ses galets reflètent les roches locales du substratum, et les galets précambriens diminuent sensiblement d'ouest en est (de 16 à 6%).

Signalons que ce till a subi un lessivage important des carbonates de sa matrice: le phénomène peut s'étendre à plus d'un mètre de profondeur. La zone d'oxydation pénètre plus profondément.

Dans la moitié est de la carte, de nombreuses formes fuselées marquent la surface du till (voir plus loin). Le till est alors plus épais (7 m).

[1] En surface cartographiée.

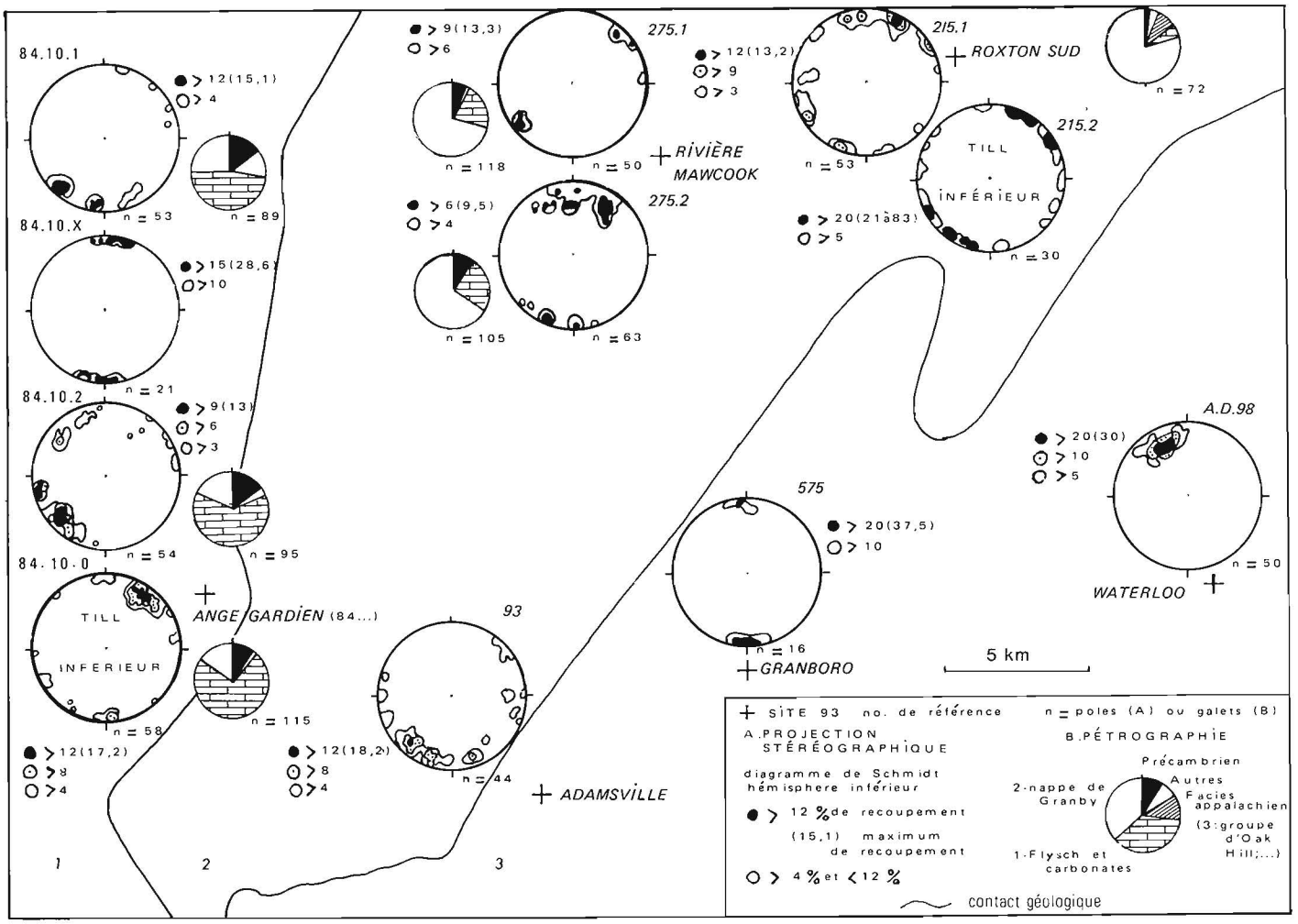

Figure 29.4. *Analyses de quelques tills. Les projections stéréographiques des textures tridimensionnelles (till fabric) indiquent les 2 ou 3 premières aires de recoupement. Classes de 10°. Les pétrographies sont exprimées en %.*

Ces accumulations constituent de bonnes réserves de ce matériau. On l'a utilisé lors de la construction du nouveau réservoir d'eau potable pour la ville de Granby, en 1976.

Quelques analyses tridimensionnelles (fig. 29.4) démontrent que plusieurs orientations sont présentes dans l'unité: l'orientation NW-SE à NNW-SSE des galets y est fréquente (voir aussi Doiron, 1981). On pense que celle-ci est reliée à l'écoulement glaciaire vers le nord-est et le sud-sud-est, lors du pléniglaciaire wisconsinien supérieur. Dans la partie supérieure du till, des orientations NNE-SSW à NE-SW sont décelées dans les faciès à lentilles, ou écailles de till (fig. 29.2A et F, 29.3, 29.4).

Ces faciès sommitaux marquent la transition aux dépôts rythmiques, soit d'origine glacio-lacustre (non cartographiables), soit d'origine glacio-marine, à la base de l'unité 5.

Les dépôts fluvio-glaciaires (unité 4.1 et 4.2)[1] sont présents sur environ 2% du territoire. Ils sont surtout de contact glaciaire: terrasses de kames, kames, moraines et eskers. Ce sont des graviers et sables, de granulométrie variable, avec déformation mineures (failles et plissements).

Les épaisseurs maximales enregistrées sont de l'ordre de 15 à 20 m en coupe et de 20 à 30 m en forage: le caractère lenticulaire de ces dépôts se trouve particulièrement affecté par la présence de noyaux rocheux.

Du point de vue chronologique, ces dépôts sont diachroniques puisqu'ils jouxtent, en général, le glacier en retrait (kames, moraines de kame,...); les eskers eux-mêmes correspondent à des chenaux de faible longueur dans la bordure glaciaire (cf. Shilts et McDonald, 1975).

Dans plusieurs cas, il est possible d'associer les moraines de kame à des positions glaciaires précises, tandis que les eskers s'ordonnent selon une direction grossièrement perpendiculaire aux précédents (Prichonnet et al., 1982). Les zones où ces dépôts sont les plus abondants sont localisées dans la moitié est de la carte (fig. 29.5). Mais, plusieurs eskers, localisés entre Granby et le mont Yamaska, sont encore exploités.

Signalons enfin que les analyses sédimentologiques dans plusieurs dépôts fluvio-glaciaires montrent que les eaux de fusion glaciaires s'écoulaient vers le sud-est ou le sud tant dans la zone sud-est de la carte (Doiron, 1981) que dans la zone ouest (Prichonnet, en préparation).

[1] 4.1 = de contact; 4.2 = d'épandage

Il ressort des observations de terrain que des dépôts fluvio-glaciaires de contact sont présents dans plusieurs secteurs (fig. 29.5) du territoire. Lorsque des séries de segments morainiques ou de moraines de kame sont cartographiés (région de Waterloo – voir fig. 29.5, 29.8), elles démontrent un recul progressif des glaces. À l'ouest de la carte, quelques eskers sont bien identifiées, mais aucun ne se situe sur le tracé de la moraine de Drummondville (Gadd, 1964; Gadd et al., 1972).

Du point de vue cartographique, les dépôts glacio-lacustres (unité 4.3) ne sont vraiment représentés que par des graviers littoraux à l'est de Shefford Vale (fig. 29.6A). Ils sont associés au lac proglaciaire qui ennoyait les vallées déglacées. Toutefois, certains dépôts de sables, à rides et lits entrecroisés, s'étalent autour des formes fluvio-glaciaires de contact ou les "ennoient". On n'a pas observé de dépôts rythmiques importants (voir unité suivante).

La limite lacustre à 244 m (fig. 29.5) est déduite des observations suivantes: zones de till délavé et champs de blocs associés, autour de quelques collines. On considère aussi que les dépôts fluvio-glaciaires de terrasses de kame (?), au sud-est du mont Shefford, pourraient correspondre à un plan d'eau temporaire, à 275 m: leur présence s'expliquerait par la création d'un lac local et éphémère, situé entre le mont Shefford et les glaces en fusion.

Une approche de type statistique (fig. 29.6) montre la répartion des phénomènes littoraux se rapportant à la phase glacio-lacustre, avant l'invasion marine.

La figure 29.4 permet de voir que les sédiments marins (unité 5) recouvrent presque autant de territoire que le till supérieur. Ils furent mis en place au cours de l'invasion de la mer de Champlain.

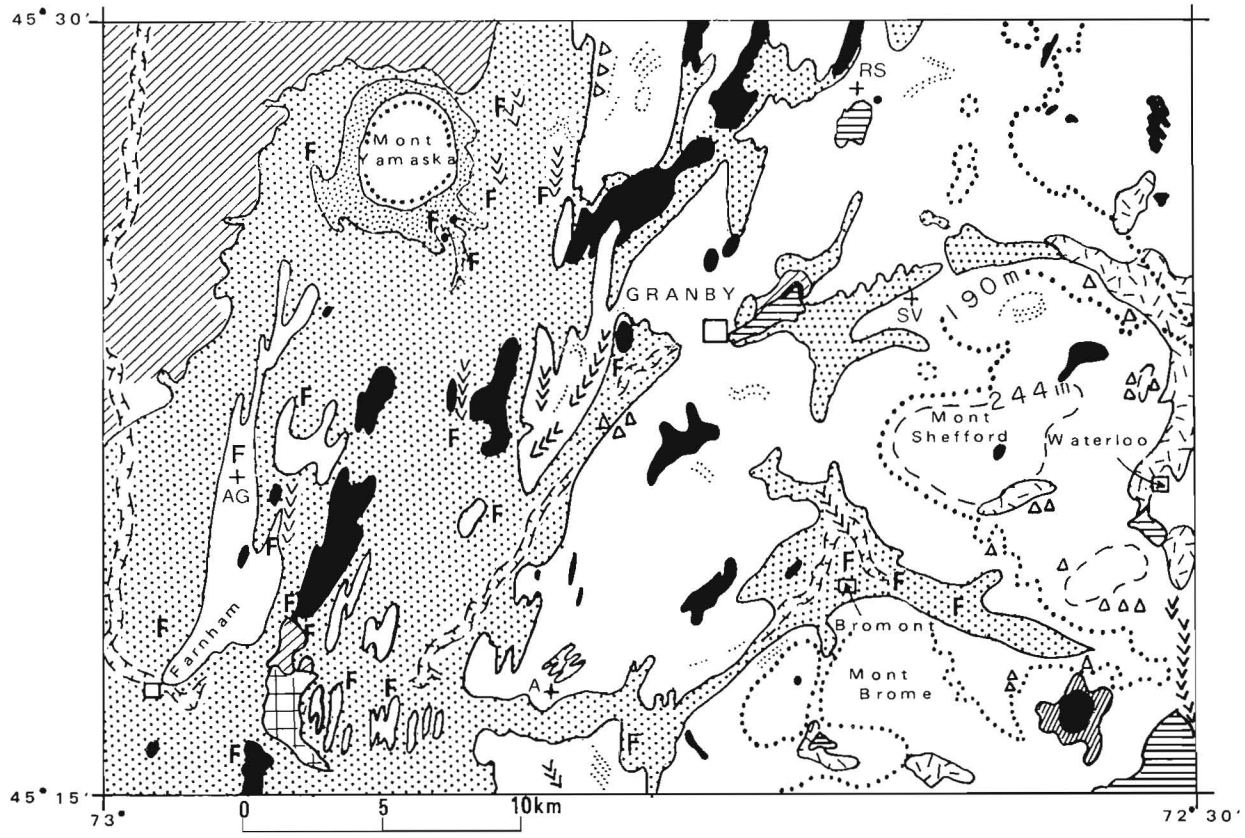

CARTE SIMPLIFIEE DE LA RÉPARTITION DES PRINCIPAUX DÉPÔTS ET DE QUELQUES FORMES D'ACCUMULATION

- *Dépôts organiques*
- *Sables et limons de plaine alluviale*
- *Dépôts lacustres*
- *Sédiments marins régressifs* (s-sables, g-graviers)
- *Sédiments marins de décantation*
- *Accumulations fluvioglaciaires*
- *Tills et tills remaniés* – *Roc*
- *Terrasse d'érosion alluviale*
- *Cordons littoraux*
- *Champs de blocs*
- F *Site fossilifère*
- *Limite d'invasion marine*
- *Littoral lacustre*
- *Esker*
- *Lac; Etang; Réservoir*

Figure 29.5. *Carte simplifiée des dépôts et des formes. Echelle originale à 1/250 000. La disposition des collines de till et les alignements des dépôts organiques reflètent les directions structurales des crêtes appalachiennes. Les principales vallées, à l'est, ont favorisé la mise en place de petits deltas, lors de la régression marine. A: Adamsville; AG: Ange-Gardien; RS: Roxton Sud; SV: Shefford Vale.*

Ils occupent surtout la moitié ouest de la carte et les fonds des vallées principales vers l'est. Ils sont fréquemment fossilifères, sauf au sommet des coupes à cause du lessivage. Deux grands types de faciès, inégalement répartis en surface, se superposent dans l'ordre ascendant:

a. les faciès de décantation et/ou sublittoraux;

b. les faciès de forte énergie (sables, graviers et leurs mélanges en proportions variables).

Les coupes observées montrent rarement plus de 7 à 8 m de dépôts, sauf dans la flèche littorale au sud-est du mont Yamaska (fig. 29.5), où les graviers régressifs peuvent atteindre plus de 15 m.

Quelques coupes montrent des laminations, à caractères rythmiques, associées à des lentilles (ou écailles) de till, ou des diamictons: dans un cas, la présence de fossiles marins (**Hiatella arctica**) suggère un passage rapide de la phase glacio-lacustre à l'environnement glacio-marin.

La séquence normale des sédiments marins montre un granoclassement vertical inverse; de plus, les dépôts graveleux forment des auréoles autour des reliefs, ou des nappes s'épaississant vers les zones d'apport. Des centaines de cordons littoraux affectent la surface des faciès grossiers, ou régressifs: on en trouve également sur les pentes des collines, où le till est subaffleurant. Ces cordons abondent en particulier autour du mont Yamaska (secteurs sud-ouest et sud-est), où, également, de très belles flèches littorales se sont développées: l'une atteint 3 km de long (fig. 29.5).

En fait, dans la zone couverte par la carte, peu de recherches systématiques ont été entreprises à propos des littoraux marquant les anciens plans d'eau. Pour deux secteurs, toutefois, on dispose de quelques données anciennes. Chalmers (1899) a signalé plusieurs phénomènes littoraux autour du mont Shefford, entre 270 et 198 m d'altitude. Près de Roxton Sud et Granby, la limite marine a été proposée à environ 167 et 171 m par plusieurs auteurs: voir, par exemple, Goldthwait et al (1913), Chapman (1937).

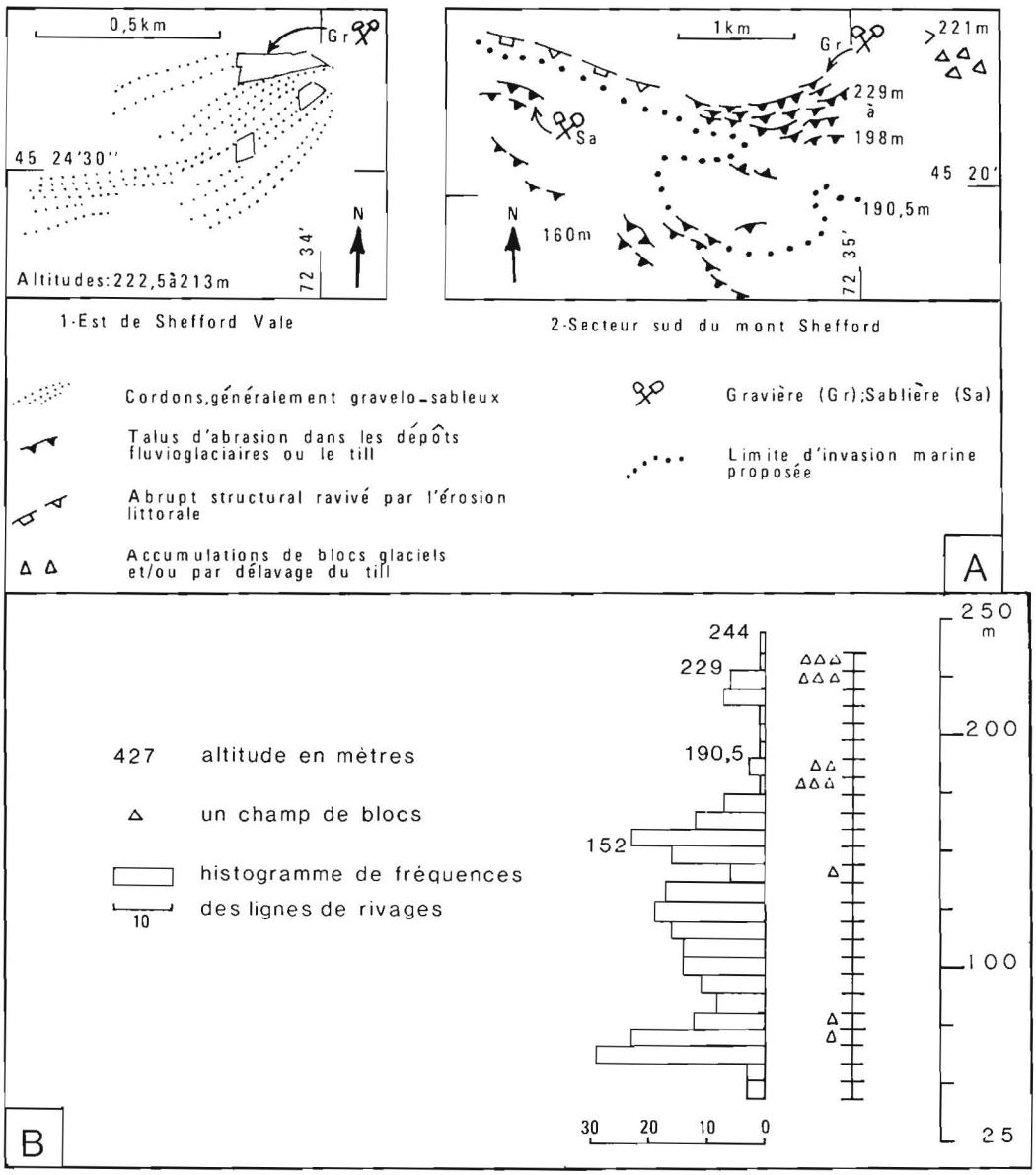

Figure 29.6. *Quelques aspects géomorphologiques des littoraux (A) et histogramme de fréquence des phénomènes littoraux (B).*

La limite marine se situe probablement vers 190 m (fig. 29.5, 29.6): à partir de cette altitude, les champs de blocs, les cordons littoraux, les placages de sables sur pentes et les talus d'érosion attribués à l'action littorale (fig. 29.6A) sont fréquents, et leur nombre s'accroît rapidement. En fait, la fig. 29.6B montre qu'il n'y a pas de lacune franche entre les phénomènes littoraux attribués au lac glaciaire et ceux, plus nombreux et plus répandus, que l'on associe au plan d'eau supérieur de l'invasion marine.

Notons qu'une date au ^{14}C, sur **Mya** sp. en thanatocénose, donne un âge relativement précoce pour l'invasion marine régionale: 12480 ± 240 ans B.P. (QC-475; Prichonnet, 1980). Le gisement est situé quelques kilomètres au nord du présent territoire, au sud-est de St-Dominique[1] (carte de St-Hyacinthe 31 H/10). À 2,5 km au sud-est d'Adamsville (fig. 29.5), une date à 11 360 ± 110 B.P. (UQ-29)[2] a été obtenue sur **Macoma balthica,** en thanatocénose. Enfin, à l'Ange-Gardien (fig. 29.5) des **Balanus crenatus** et **sp.** sont datés à 10 700 ± 120 ans B.P. (QC-473). Ces fossiles vivaient sur un haut fond à substratum de till: des phénomènes glaciels ont mélangé les fossiles aux sédiments, lorsque le plan d'eau s'abaissa. Vers 10 000 ans B.P., les collines basses de la partie ouest de la carte devaient être exondées (selon des datations obtenues sur faunes marines du territoire de St-Hyacinthe; exemple: à 84 m d'altitude, 10 400 ± 95 ans B.P., sur **Mya arenaria** (UQ-46)[3]; Prichonnet, en préparation). En considérant la limite marine à 190 m vers 12 500 ans B.P., et l'exondation des collines de 90 m vers 10 400 ans B.P., on obtient un taux d'émergence moyen de l'ordre de 5 cm/an.

Les argiles silteuses et silts argileux sont identifiés surtout au nord-ouest de la carte, en bordure de la plaine des basses-terres, tandis que les sables et graviers occupent 30% du territoire. Les dépôts grossiers, appartenant à une séquence régressive, reposent en concordance sur les dépôts argilo-silteux dans les zones basses, et tronquent les unités antérieures autour des reliefs en particulier. Deux deltas principaux sont cartographiés; l'un à l'est de Granby, l'autre à Bromont. Plus de 20 sites fossilifères marins sont identifiés (fig. 29.5). Parmi les macrorestes, signalons les espèces les plus abondantes: **Balanus crenatus** Bruguière et **sp.**, **Hiatella arctica** (Linné), **Macoma balthica** (Linné), **Mytilus edulis** (Linné).

Des unités suivantes, seuls les dépôts organiques (unité 7) occupent des surfaces importantes (3% du territoire). En fait, les dépôts lacustres (unité 6), organiques (unité 7) et fluviatiles (unité 9) se sont parfois déposés de façon synchrone, mais en des sites différents. L'ordre stratigraphique adopté traduit tout de même une succession normale générale. En effet, les dépôts organiques succèdent presque partout aux derniers sédiments lacustres détritiques, tandis que les plaines alluviales se comblent au fur et à mesure que l'érosion fluviatile transporte ses alluvions sur les terrasses d'incision et dans les zones en dépressions.

Les dépôts organiques forment des lentilles, dans les dépressions, atteignant 7 m d'épaisseur. Les autres unités dépassent rarement 1,5 m.

À titre d'illustration, signalons quelques datations sur bois:

1. près de Chapel Corner – carte de Cowansville, à 140 m d'altitude sous la limite marine – 8050 ± 190 ans B.P., UQ-347[4];
2. près de St-Dominique – carte de St-Hyacinthe, à 60 m d'altitude – 7650 ± 170 ans B.P., UQ-356[5]. Mais les accumulations organiques "in situ", ou dans les méandres morts de petites plaines alluviales, se poursuivent pendant tout l'Holocène, jusqu'à nos jours; exemple, au pied du versant nord-ouest du mont Yamaska, à Émileville (fig. 29.2E): bois daté à 2510 ± 90 ans B.P., UQ-342.

Corrélations et paléogéographie

Prises isolément, les trois premières unités décrites ci-dessus (fig. 29.2, 29.3) peuvent être interprétées de plusieurs manières. L'approche la plus simple consiste à considérer qu'elles représentent au moins deux événements glaciaires (stades ?) et une déglaciation dont la durée est indéterminée. Mais, en fait, outre les lacunes de sédimentation toujours possibles, et difficiles à identifier, dans l'unité 2, la surface d'érosion laissée par la dernière avancée glaciaire peut avoir supprimé plusieurs types de dépôts, y compris du till. Et, en l'absence de matériel organique, en particulier, l'interprétation paléo-écologique et les relations stratigraphiques doivent être prudentes. Un aspect positif, toutefois, semble ressortir des diverses données sédimentologiques, ce sont les changements de direction d'écoulement glaciaire.

Hypothèse d'une séquence du Wisconsinien moyen

Le site de l'Ange-Gardien n'est situé qu'à 40 km de l'île de Montréal. Il paraît assez probable que la séquence identifiée ici est équivalente à celle décrite par Prest et Hode-Keyser (1962, 1967) et , de ce fait, avec celle décrite par MacClintock et Stewart (1965) dans le nord de l'état de New York.

Les dépôts non glaciaires de l'Ange-Gardien (fig. 29.3) montrent des faciès influencés par des environnements "proglaciaires" au sens large. On peut y noter que les galets des graviers sont à facture glaciaire: ceux-ci peuvent donc provenir du remaniement du till inférieur ou d'un épandage proglaciaire. Grâce à leur présence, on démontre que les glaciers s'étaient retirés du secteur considéré. Par ailleurs, les dépôts fins, stratifiés et à caractère rythmique, au sommet des sables et graviers, s'expliquent par la présence d'un plan d'eau, en milieu froid.

Comme d'autres preuves de déglaciation existent sur la région de Granby, ainsi que dans le secteur ouest de la carte de Cowansville (Prichonnet, 1982), et que Montréal n'est situé qu'à quelques dizaines de kilomètres de tous ces sites, l'hypothèse d'un vaste secteur déglacé, au Québec méridional, est assez vraisemblable. On peut donc proposer de corréler les dépôts non glaciaires de l'unité 2 avec le complexe inter-till de Montréal. Or, pour ce complexe inter-till, Prest et Hode-Keyser (1977) et Prest (1977) semblent privilégier une corrélation stratigraphique avec les dépôts du Wisconsinien moyen du lac Ontario, plus précisément avec la Formation de Thorncliffe (Karrow, 1967). Et, le Till de Malone, à la base du complexe inter-till, est rangé également par ces auteurs dans le Wisconsinien moyen (basal), sans argument spécifique toutefois.

On sait que la Formation de Thorncliffe montre qu'il y eut des fluctuations de glaces: deux couches de till séparent "l'unité non glaciaire". Quant au Till de Malone (Terasmae, 1965, p. 14), il est composé de 3 sous unités, à savoir deux couches de till séparées par des matériaux stratifiés non glaciaires.

Il ressort de ces quelques remarques que l'attribution des unités 1 et 2 de la région de Granby au Wisconsinien moyen, est une hypothèse de travail raisonnable: elle est basée principalement sur l'idée que l'inlandsis a fluctué (avancées et reculs) dans cette sorte de grand couloir que constitue la dépression du St-Laurent et du lac Ontario.

---

[1] 45°31'48"N, 72°49'21"W
[2] Université du Québec à Montréal, Laboratoire de géochimie isotopique. (UQ-00)
[3] 45°34'5"N, 72°52'17"W.
[4] 45°9'10"N, 72°48'10"W
[5] 45°31'48"N, 72°49'21"W

De plus, l'origine orientale du till de l'Ange-Gardien (unité 1) permet de reposer le problème de l'extension vers l'ouest des glaciers appalachiens à la même époque. Rappelons en effet:

a. que dans les Appalaches du Québec – à l'est de la zone présentée ici – McDonald (1967) et McDonald et Shilts (1971) attribuent la base du Till de la Chaudière à des glaces appalachiennes s'écoulant vers le sud-ouest;

b. qu'au nord-est de Granby, Lortie (1975) corrèle avec ce mouvement, des érosions glaciaires anciennes vers le sud-ouest et l'ouest;

c. qu'au Vermont, lors du stade de Shelburne (till B), les glaces s'écoulaient aussi vers le sud-ouest (Stewart et MacClintock, 1969).

Enfin, récemment, on a mis en évidence l'existence de 3 épisodes glaciaires, à faible distance des basses-terres, dans la région de Thetford Mines (Chauvin, 1979; LaSalle et al., 1979): un ou deux tills (en partant de la base) sont présentés comme équivalent du Till de la Chaudière.

En conclusion de cette première hypothèse, le Till de l'Ange-Gardien est présenté comme un équivalent latéral du Till de la Chaudière et du till B de Vermont.

Hypothèse d'une séquence du Wisconsinien supérieur

Prest et Hode-Keyser (1977) n'ont pas écarté totalement l'idée que la séquence de Montréal ne représente que le Wisconsinien supérieur. C'est d'ailleurs la corrélation suggérée par Dreimanis (1977) qui s'appuie sur l'absence de dépôts clairement attribuables au Wisconsinien inférieur ou moyen. Notons, tout d'abord, que l'argumentation de Dreimanis n'est pas probante: l'absence de dépôts n'est pas un argument suffisant, surtout dans une séquence continentale, qui, rappelons-le, est tronquée par une ou plusieurs érosions glaciaires. Mais, par ailleurs, un argument plus général nous fait écarter cette corrélation "restreinte": la présence continue des glaces sur la région de Toronto, au Wisconsinien supérieur (voir, par exemple, Dreimanis, 1977, fig. 29.2), semblerait difficile à expliquer avec des fluctuations multiples dans la région de Montréal.

La corrélation avec les basses-terres centrales

La dernière possibilité discutés ici concerne les relations éventuelles de la séquence de Granby avec celle des basses-terres centrales décrites par Gadd (1971) et Occhietti (1980). La différence essentielle réside dans le fait que la série de dépôts entre le till de Bécancour et le till de Gentilly est beaucoup plus riche en faciès et données paléo-écologiques que celles connues au sud-ouest (Montréal et Granby). Actuellement, on possède deux informations chronologiques au sud et l'ouest-sud-ouest de la région du lac St-Pierre:

1. une date sur bois, transporté dans des dépôts fluvio-glaciaires, est signalée près de Sutton (environ 32 km au sud de Granby): >28 000 B.P. (GSC-655, dans Morasse et Barrette, 1981);

2. des débris de bois ont été trouvés sous le seul till local, à la frontière du Québec et de l'Ontario: ils sont plus vieux que 42 000 ans (GSC-2932, Gadd et al., 1981). Aucune de ces dates ne peut être utilisée pour préciser la chrono-stratigraphie des régions considérées, ni leur relation entre elles. Ces bois transportés démontrent que des vieux dépôts organiques ont existé dans le bassin des basses-terres (ce qui est déjà bien établi par des sédiments de l'intervalle St-Pierre) et qu'ils furent dispersés, en partie, à différents moments de l'histoire wisconsinienne. Mais, en théorie, les deux tills de la région de Granby pourraient toujours être corrélés avec les deux tills des basses-terres centrales: il ne s'agit là que d'une simple relation géométrique, de série à série. Une telle corrélation impliquerait une ou plusieurs longues lacunes dans les dépôts de la région décrite ici, comme dans celle de Montréal.

En résumé, nous retenons l'hypothèse que les unités 1 et 2 représentent des événements du Wisconsinien moyen.

La deuxième avancée glaciaire

Lors d'une avancée majeure, sans doute dès le Wisconsinien moyen (moyen à supérieur), la glace commença à déposer le till supérieur (unité 3), corrélatif du till de Fort Covington. Le till de la région de Granby, comme d'ailleurs celui de Fort Covington, doit représenter une assez longue glaciation au cours de laquelle les glaces s'écoulèrent selon des directions différentes: ceci est suggéré par plusieurs analyses tridimensionnelles (voir fig. 29.3, 29,4) en plusieurs sites de la région (Prichonnet, en préparation).

Les analyses des stries et formes orientées de till (fig. 29.7) apportent quelques informations sur le sujet. Selon les observations recueillies sur plus de 60 sites de surface glaciaire, plusieurs familles de stries sont décelables: la plus ancienne, NE-SW serait reliée à des glaces venant des Appalaches. Il semble que ces marques d'un "vieux" mouvement glaciaire soient présentes dans plusieurs zones de la région (Cloutier et Prichonnet, 1980; Doiron, 1981; Prichonnet, en préparation). Dans la présente étude, on a attribué à des glaces venant des Appalaches (au nord-est ou à l'est-nord-est) le till inférieur. Ce sont, bien sûr, les marques de la dernière glaciation qui sont les plus abondantes (fig. 29.7). Il semble bien que l'on puisse y déceler au moins trois mouvements successifs. Dans l'ordre ascendant (ancien à récent) on aurait les écoulements suivants:

1. du nord-ouest vers le sud-est;

2. du nord-nord-ouest vers le sud-sud-est;

3. du nord-nord-est vers le sud-sud-ouest.

Le mouvement n°2 serait dominant, correspondrait au pléniglaciaire du Wisconsinien supérieur, et serait responsable du façonnement du till (fig. 29.7C): parmi les 101 formes fuselées de till, le regroupement autour de la direction 340°-160° est particulièrement net. La famille de stries correspondante est connue à l'échelle régionale (Gadd et al., 1972; Prichonnet, en préparation). On retiendra aussi que l'étude des stries dans la zone du piedmont appalachien met en évidence le rôle de crêtes et chaînes plus élevées dans la canalisation des écoulements glaciaires: il n'est pas étonnant de voir les derniers mouvements, lorsque la glace devient moins épaisse, canalisés par les reliefs qui sont justement NNE-SSW.

Les évènements postglaciaires

Le retrait glaciaire de la région s'effectua rapidement vers la fin du Wisconsinien supérieur. Il a probablement commencé dans la zone sud-est de la carte quelques centaines d'années avant que ne se déposent les premiers sédiments marins, datés à environ 12 500 ans B.P., quelques kilomètres au nord du mont Yamaska (date citée précédemment). L'allure des fronts glaciaires présentés sur la figure 29.8 est basée sur la disposition des dépôts fluvio-glaciaires, les sens des écoulement des eaux de fusion et les derniers réseaux de stries observés.

Le modèle présenté est différent de celui de Gadd (1964) et Gadd et al. (1972). Les dépôts fluvio-glaciaires de la région de Waterloo (fig. 29.5, 29.8) correspondent à divers dépôts de contact glaciaire diachroniques (Prichonnet et al., 1982): on ne peut y tracer un front unique stable. Et, entre Farnham et le mont

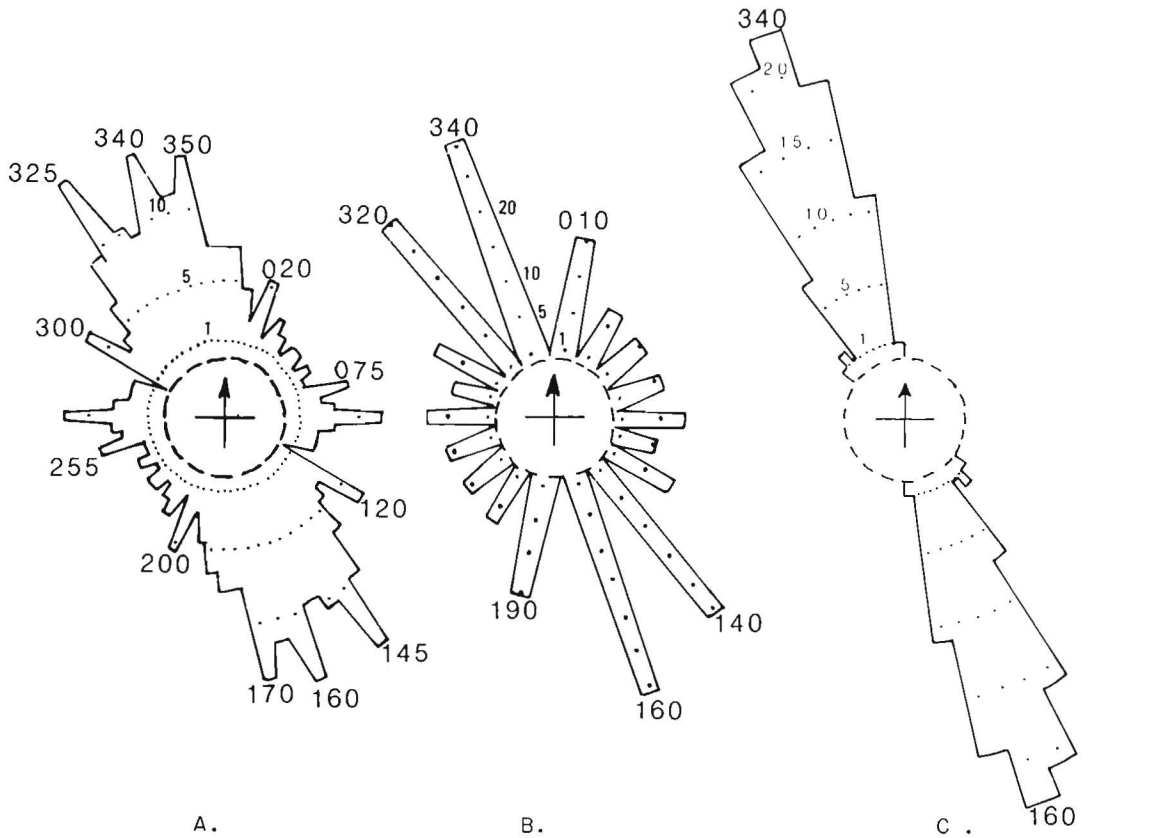

Figure 29.7. *Analyse des familles de stries et des formes orientées de till. Sur le diagramme A, les familles apparaissent moins clairement qu'en B. Le diagramme C illustre bien que la famille dominante des stries est contemporaine du modelage de la nappe de till supérieur.*

Yamaska, l'allure des fronts glaciaires, prenant en considération les eskers identifiés, ne justifie plus le maintien de la moraine de Drummondville (Prichonnet, en préparation).

Ce schéma paléogéographique tient compte aussi du fait que les preuves littorales les plus élevées, identifiées dans le quadrant sud-est de la carte, sont attribuées au prolongement nord du lac proglaciaire Vermont (Stewart et McClintock, 1969). On trouvera d'ailleurs dans Chapman (1937) une mise au point générale sur les plans d'eau postglaciaire de la vallée du lac Champlain, incluant la bordure sud du Québec adjacent. C'est peut-être les fronts glaciaires de cet auteur (ibid, fig. 29.2, 29.3) qui ont influencé des modèles plus récents sur les fronts glaciaires et les lacs postglaciaires du Vermont (Stewart et MacClintock, 1969). La compréhension de l'ennoyage postglaciaire dans la région de Granby dépend des données qui sont plus au sud: leur analyse sur le territoire de Cowansville (Prichonnet, 1982) n'est pas achevée, aussi nous ne tenterons pas de corrélations précises (d'ailleurs délicates étant donné la non continuité des preuves littorales: concentrations de blocs; cordons; deltas; terrasses).

Cette approche, de type statistique (fig. 29.6B), est basée sur l'identification du plus grand nombre de preuves littorales possible: 17 paléofalaises, 16 champs de blocs[1] (ou d'accumulations anormalement denses et présumées d'origine littorale) et environ 230 cordons (pour les zones en-dessous de 100 m, on n'a retenu que les plus grandes séries).

Il est possible que des plans d'eau limités se soient développés autour des hauts sommets du secteur sud-est de la carte, lorsque les massifs montérégiens émergèrent du terminus glaciaire en recul (cf. les littoraux élevés de Chalmers, 1899). Il est probable qu'un premier plan d'eau assez important a marqué le paysage, vers 240-250 m d'altitude (actuelle): talus d'abrasion et délavage du till sur les collines. Les preuves littorales les plus nettes commencent vers les altitudes actuelles de 230 m. Et, les preuves littorales plus abondantes, vers 190 m, marqueraient, croyons nous, la présence d'un plus large plan d'eau (la mer de Champlain) que celui du lac. Cette limite suggérée pour la limite marine doit correspondre au retrait des glaces du piedmont appalachien au nord-est de Granby (fig. 29.8); elle marquerait le début d'un accroissement des preuves d'action littorales (fig. 29.6B). Qu'elle que soit la limite choisie, l'histogramme de fréquence de la figure 29.6 montre qu'il n'y a pas de coupure dans la répartition des littoraux.

Suite au relèvement isostatique, les eaux de la mer de Champlain se retirèrent progressivement de la région. Les deltas dans les vallées appalachiennes à l'est, et les épandages sableux dans le secteur centre et ouest de la carte, se sont accumulés progressivement, à l'embouchure des rivières qui se déversaient dans la mer en régression.

Si l'on admet un retrait définitif des eaux marines vers 10 000 ou 9500 ans B.P. (Prichonnet, 1977), on constate qu'il s'écoulera environ 1500 à 2000 ans avant le développement de

[1] Plusieurs de ces phénomènes ont été examinés avec A. Doiron (1981).

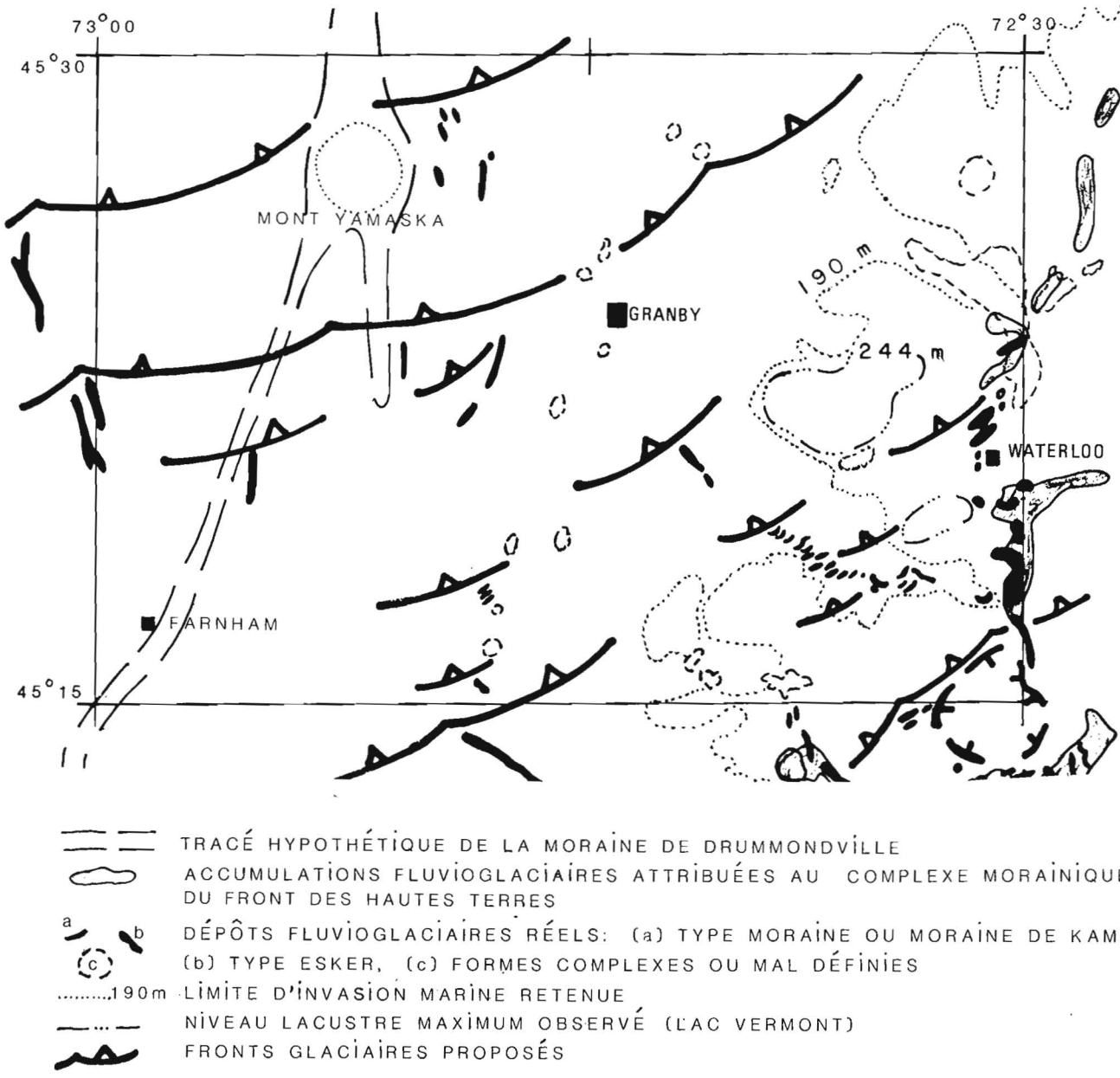

Figure 29.8. *Allure probable du retrait glaciaire régional.*

larges tourbières dans les dépressions intercrêtes (voir fig. 29.4). Cette période correspond certainement à la présence de lacs, piégés dans ces dépressions larges et peu profondes, maintenus en place grâce au ralentissement du relèvement isostatique. Il faut attendre la fin du lac à **Lampsilis** (cf. Elson, 1969) pour que l'érosion soit réactivée, en particulier dans les zones basses de la partie ouest de la carte. Au moins trois niveaux de terrasses se sont développés le long de la rivière Yamaska. Les dépôts organiques piégés dans certains méandres pourraient bien correspondre à des variations du niveau de base (mais aussi à des phénomènes plus aléatoires: crues exceptionnelles; glissement de terrain; feu de forêt provoquant des érosions et des sédimentations anormales (Gangloff et Richard, 1978), voire de simples barrages de castor.

Conclusion

Un certain nombre d'analyses tendent à prouver qu'un premier till fut déposé par des glaces d'origine appalachienne: stries anciennes NE-SW et ENE-SSW; pétrographie et texture tridimensionnelle du Till de l'Ange-Gardien. En l'absence de restes fossiles, il est difficile de proposer un âge certain pour les dépôts non glaciaires qui succèdent à ce till. L'attribution de ces deux premières unités au Wisconsinien moyen est donc une hypothèse de recherche, qui prend en considérations quelques données régionales. La dernière glaciation, du Wisconsinien moyen et supérieur n'a laissé que des lambeaux des dépôts antérieurs, déposant une couverture de till de quelques mètres d'épaisseur sur le territoire: mais de nombreuses crêtes rocheuses ne furent sans doute jamais recouvertes de till. Ce till supérieur a été profondément marqué (dans sa texture comme dans ses formes orientées) par les écoulements glaciaires en provenance du nord-nord-ouest.

Les événements paléogéographiques contemporains, ou postérieurs à la déglaciation s'étendent sur la fin du Pléistocène (Wisconsinien supérieur tardif) et l'Holocène. Ils sont enregistrés dans des accumulations sédimentaires parfois importantes: sables et graviers fluvio-glaciaires; graviers, sables et silts marins, fossilifères (mer de Champlain); dépôts organiques; silts et sables alluviaux. L'érosion fluviatile est encore active localement; les rivières coulent parfois sur le roc.

Des dépôts fluvio-glaciaires jalonnent les étapes de la phase de déglaciation (environ 13 000 à 12 500 ans B.P.). Ceux du secteur oriental, antérieurement attribués au Complexe morainique du front des hautes-terres, sont plus largement reconnus; ils correspondent plutôt à une série de positions glaciaires, diachroniques, sans signification climatique précise. D'autres formes, surtout des eskers, sont identifiées en divers secteurs de la carte. Un autre événement paléogéographique majeur de la déglaciation est remis en question: la moraine de Drummondville n'est pas représentée dans la région. La glace se retirait par petites étapes, difficiles à corréler, en direction nord-ouest et nord-nord-ouest.

Les eaux marines ont ennoyé une partie du piedmont appalachien vers la fin du Wisconsinien (12 500 ans B.P.). Vers 10 000 ans B.P., les petites collines en bordure des basses-terres, à l'ouest, devaient être exondées. Le taux moyen d'émergence est de l'ordre de 5 cm/an.

Les tourbières se sont développés surtout à partir de 8000 ans B.P.

L'érosion fluviatile a surtout été active à l'Holocène. Des tourbes ensevelies sous des dépôts détritiques (vers 2500 ans B.P., par exemple) pourraient marquer des variations du niveau de base.

Remerciements

Cette recherche a été possible grâce aux subventions de la Commission géologique du Canada (projet EMR 1978-82, n° 210.4.78 et p,). Les subventions d'appoint du Fonds Institutionnel de Recherche de l'université du Québec à Montréal nous ont également facilité le travail. Nous exprimons notre gratitude aux personnes responsables de ces aides. Plusieurs étudiants ont collaboré à ce projet: en particulier, MM. M. Cloutier et C. Marcotte (été 1978); Mlle F. Fortin et MM. G. Labelle, A. Doiron, K. Arroyo et N. Koné m'ont assisté dans certains aspects du projet; Mlle O. Mercier a patiemment préparé de nombreux échantillons et des lettrages. Nous avons apprécié l'aide du personnel technique du département.

Les datations sont l'oeuvre de plusieurs laboratoires dont nous remercions les responsables pour leur aide partielle (D. Pardi de Queen's University), ou totale (C. Hillaire-Marcel de l'UQAM.

Quelques chercheurs m'ont aidé à préciser bien des idées au cours de discussions scientifiques: MM. C. Hillaire-Marcel de l'université du Québec à Montréal et M.N. Gadd de la Commission géologique du Canada. Je tiens également à souligner la collaboration des mes étudiants de maîtrise MM. A.Doiron et M. Cloutier. Enfin, sans les suggestions et critiques de M. J.S. Vincent cette modeste contribution au Quaternaire du sud du Québec serait encore plus imparfaite.

Bibliographie

Brown MacPherson, J.
1967: Raised shorelines and drainage evolution in the Montreal Lowland: Cahiers de Géographie de Québec, vol. 23, p. 343-360.

Cann, D.B., Lajoie, P. et Stobbe, P.C.
1948: Étude des sols des Comtés de Shefford, Brome et Missisquoi dans la province de Québec; Service des fermes expérimentales, ministère Fédéral de l'Agriculture, en collaboration avec le ministère de l'Agriculture du Québec et du collège MacDonald, université McGill, 94 p., 3 cartes (1:63,360).

Chalmers, R.
1899: Surface geology and auriferous deposits of southeastern Quebec; Commission géologique du Canada, Rapport annuel, 1897, vol. 10, partie J., 160 p.

Chapman,
1937: Late-glacial and post-glacial history of the Champlain Valley; American Journal of Science, 5th Ser., vol. 34, n° 200, p. 89-124.

Chauvin, L.
1979: Géologie des dépôts meubles, région d'Asbestos-Disraeli; ministère Énergie et Ressources, Québec, DPB-176, 13 p.

Cloutier, M. et Prichonnet, G.
1980: Hiérarchie des stries glaciaires Wisconsiniennes du secteur montagneux de Cowansville-Knowlton-Sutton, Québec. Annales Association Canadienne Francaise pour l'Avancement des Sciences, vol. 47, n° 1, résumé p. 113.

Cronin, T.M.
1977: Champlain sea foraminifera and ostracoda: a systematic and paleoecological synthesis; Géographie Physique et Quaternaire, vol. XXXI, n° 1-2, p. 107-122.

Doiron, A.
1981: Les dépôts quaternaires de la région de Granby-Waterloo, Québec. Cartographie, sédimentologie et stratigraphie; thèse de M.Sc. non publiée, Département des sciences de la Terre, université du Québec à Montréal, 100 p.

Dreimanis, A.
1977: Correlation of Wisconsin glacial events between the Eastern Great Lakes and the St-Lawrence Lowlands; Géographie Physique et Quaternaire, 31 (1-2), p. 37-51.

Elson, J.A.
1969: Late Quaternary marine submergence of Quebec; Revue de Géographie de Montréal, vol. 23, n° 3, p. 247-258.

Gadd, N.R.
1964: Moraines in the Appalachian region of Quebec; Short notes; Geological Society of American Bulletin, vol. 75, p. 1249-1254, 1 fig.

Gadd, N.R.
1971: Pleistocene geology of the central St-Lawrence Lowland; Commission géologique du Canada, Mémoire 359, 153 p.

1976: Quaternary stratigraphy in southern Quebec; in Quaternary Stratigraphy of North America, ed. W.C. Mahaney; Dowden, Hutchinson and Ross Inc., Penn., p. 37-50.

Gadd, N.R., McDonald, B.C. et Shilts, W.W.
1972: Deglaciation of southern Quebec; Commission géologique du Canada, Étude 71-47, 19 p.

Gadd, N.R., Richard, S.H. et Grant, D.R.
1981: Pre-last-glacial organic remains in Ottawa valley; dans Recherches en cours, partie C; Commission géologique du Canada, Étude 81-1C, p. 65-66.

Gangloff, P. et Richard, P.
1978: Feu de Forêt et morphogénèse holocènes dans la cuvette du mont Brome, Québec; Annales Association Canadienne Française pour l'Avancement des Sciences, vol. 45, nº 1, Résumé p. 103.

Goldthwait, J.W.
1911: Plages soulevées du Sud du Québec; Rapport sommaire, Commission géologique du Canada, p. 228-242.

Goldthwait, J.W., Johnston, W.A. et Keele, J.
1913: Pleistocene, Montreal Covey Hill et Ottawa; Geological Survey of Canada, Fieldtrip Guidebook, A-10, p. 117-135.

Hillaire-Marcel, C. et Occhietti, S.
1977: Fréquence des datations au ^{14}C de faunes marines post-glaciaires de l'est du Canada et variations paléoclimatiques; Palaeogeography, Palaeoclimatology, Palaecology, vol. 21, nº 1, p. 17-54.

Karrow, P.
1957: Pleistocene geology of the Grondines map-area, Québec; unpublished Ph.D. Thesis, University of Illinois, Urbana.

1961: The Champlain Sea and its sediments; in Soils in Canada, ed. R.F. Leggett; Royal Society of Canada, Special publication no. 3, University of Toronto Press, p. 97-106.

1967: Pleistocene geology of Scarborough area; Ontario Department of Mines, Geological Report 46, 108 p.

LaSalle, P.
1963: Géologie des dépôts meubles de la région de Verchères; ministère Énergie et Ressources, Québec, RP 505, 9 p.

1966: Late Quaternary vegetation and glacial history in the St-Lawrence Lowlands, Canada; Leidse Geologische Mededelingen, vol. 38, p. 91-128.

LaSalle, P. et Elson, J.A.
1962: Région de Beloeil. Géologie des dépôts meubles; ministère Énergie et Ressources, Québec, RP 497, 10 p.

LaSalle, P., Martineau, G. et Chauvin, L.
1979: Géologie du Quaternaire au sud de la ville de Québec (Thetford Mines, Beauce, Monts Notre-Dame); Livret guide, excursion A. 11 A. Réunion annuelle, Association géologique et minéralogique du Canada, université Laval, Québec, 32 p.

Lortie, G.
1975: Direction d'écoulement des glaciers du Pléistocène des Cantons de l'Est, Québec; dans Report of Actitivies, partie A, Commission géologique du Canada, Étude 75-1A, p. 415-416.

MacClintock, P. et Stewart, D.P.
1965: Pleistocene geology of the St-Lawrence Lowland; New York State Museum and Science Services, University of the State of New York, The State Education Department, Bulletin 394, 152 p.

McDonald, B.C.
1966: Géologie des dépôts meubles: Richmond, Dudswell, Québec; Commission géologique du Canada, carte 4-1966 (1:63,360).

1967: Géologie des dépôts meubles: Sherbrooke, Ordord, Memphrémagog, Québec; Commission géologique du Canada, carte 5-1966 (1:63,360).

McDonald, B.C. et Shilts, W.W.
1971: Quaternary stratigraphy and events in southeastern Quebec; Geological Society of America Bulletin, vol. 82, p. 683-698.

Morasse, R. et Barrette, L.
1981: Répertoire des datations par le ^{14}C au Québec; ministère Énergie et Ressources, Centre de Recherche minérale, Québec, 65 p.

Occhietti, S.
1980: Le quaternaire de la région de Trois-Rivières – Shawinigan, Québec; Contribution à la paléogéographie de la vallée moyenne du St-Laurent et corrélations stratigraphiques, PaléoQuébec, vol. 10, 227 p.

Prest, V.K.
1977: General stratigraphic framework of the Quaternary in Eastern Canada; Géographie Physique et Quaternaire, vol. XXXI, no 1-2, p. 7-14.

Prest, V.K. et Hode Keyser, J.
1962: Géologie des dépôts meubles et sols de la région de Montréal, Québec; Cité de Montréal, Service des travaux publics, 35 p. (Surficial Geology and Soils – Montreal Area).

Prest, V.K. et Hode-Keyser, J.
1977: Geology of engineering characteristics of surficial deposits, Montreal Island and vicinity, Quebec; Commission géologique du Canada, Étude 75-27, 29 p.

Prichonnet, G.
1973: Intérêt des reliefs de basses-terres dans l'interprétation de la transgression et de la régression de la mer de Champlain; 2e Colloque sur le Quaternaire du Québec. Montréal. Résumé des communications, p. 18.

1977: La déglaciation de la vallée du St-Laurent et l'invasion marine contemporaine; Géographie Physique et Quaternaire, 1977, vol XXXI, nº 3-4, p. 323-345.

1980: La mer de Champlain et les lacs proglaciaires au Wisconsinien supérieur dans le piedmont appalachien (Québec); Annales, Association Canadienne Française pour l'Avancement des Sciences, vol. 47, nº 1, p. 113.

1982: Résultats préliminaires sur la géologie quaternaire de la région de Cowansville (31 H/2), Québec; dans Recherches en cours, partie B, Commission géologique du Canada, Étude 82-1B.

Prichonnet, G., Doiron, A. et Cloutier, M.
1982: Le mode de retrait glaciaire tardiwisconsinien de la bordure appalachienne, au sud du Québec; Géographie Physique et Quaternaire, vol. XXXVI, nº 1-2, p. 125-137.

Richard, P.
1978: Histoire tardiglaciaire et post-glaciaire de la végétation au mont Shefford, Québec; Géographie Physique et Quaternaire, vol. XXXII, nº 1, p. 81-93.

Shilts, W.W. et McDonald, B.C.
1975: Dispersal of clasts and trace elements in the Windsor eskers, Southern Quebec; in Report of Actitivies, partie A, Commission géologique du Canada, Étude 75-1A, p. 495-499.

Stewart, D.P. et MacClintock, P.
1969: The surficial geology and Pleistocene history of Vermont; Vermont Geological Survey Department of Water Resources, Bulletin 31, 251 p.

Terasmae, J.
1965: Surficial geology of the Cornwall and St-Lawrence seaway project areas, Ontario; Commission géologique du Canada, Bulletin 121, 54 p.

Warren, B. et Bouchard, M.
1976: Carte des dépôts meubles; Drummondville, ministère Énergie et Ressources, Québec, DP 347.

30. # A SUMMARY OF WATER CHEMISTRY DATA FOR UNDISTURBED COAL-BEARING WATERSHEDS AND A SYNOPTIC SURVEY OF OPEN PIT MINE LEACHATES, SOUTHERN ROCKY MOUNTAINS, ALBERTA AND BRITISH COLUMBIA

Project 770060

Lionel E. Jackson, Jr.
Terrain Sciences Division, Calgary

Jackson, L.E. Jr., A summary of water chemistry data for undisturbed coal-bearing watersheds and a synoptic survey of open pit mine leachates, southern Rocky Mountains, Alberta and British Columbia; in Current Research, Part B, Geological Survey of Canada, Paper 82-1B, p. 239-251, 1982.

Abstract

Surface water chemistry data were assembled from undisturbed coal-bearing watersheds located in the Rocky Mountain Foothills and Front Ranges of Alberta and British Columbia. Basins underlain by all three of the coal producing formations were represented in the compilation. Stream water chemistries reflect the abundance of carbonate minerals in bedrock and overburden. Waters are alkaline and are dominated by calcium, magnesium, and bicarbonate ions; sulphate may also be an important constituent. Toxic trace elements are well within acceptable limits for drinking water except for local occurrences during winter months. Phenols may regularly and naturally exceed Environment Canada water quality guidelines for the protection of aquatic life.

The chemistries of leachates emanating from orphaned coal mine wastes were determined for twelve sites representing the three coal-bearing formations found in the Foothills and Front Ranges of Alberta and British Columbia. Leachates were generally alkaline. Those sites with slightly acidic leachates drained wastes predominantly coal wastes. Calcium and magnesium were the dominant cations and bicarbonate was the dominant anion at all sites. Luscar Formation and "Coalspur Beds" leachates were richer in sodium with respect to Kootenay Formation leachates. Conversely, Kootenay Formation leachates were richer in sulphate content with respect to the leachates of the other two formations. Only the concentrations of iron and manganese regularly exceeded permissible guidelines set by Environment Canada for drinking water and the protection of aquatic life. No harmful organic compounds were detected.

Introduction

Water pollution has been and still is one of the most chronic problems associated with coal mining and overburden waste disposal over much of eastern North America and western Europe. Much of the pollution problem in these areas has been the direct or indirect result of the weathering of sulphide-rich shales, carbonaceous shales, and coal. The iron-rich, acidic solutions that result damage receiving streams or lakes by direct acidification, depletion of dissolved oxygen due to the oxidation of dissolved ferrous iron, and the resulting precipitation of ferric hydroxides. In addition, acid solutions within the piles of rock waste often produce toxic trace elements in greater quantities than would be released during normal weathering of similar undisturbed rocks. These dissolved substances further exacerbate water quality problems. Bibliographies containing extensive references to water pollution and water quality problems related to both underground and surface coal mining may be found in Downs and Stocks (1978) and Torrey (1978).

With increasing production of coal in the Foothills and Front Ranges of the Rocky Mountains of Alberta and British Columbia by open pit methods in late 1960s and early 1970s, public concern was directed to the possibility of widespread water pollution in these areas. Little hard evidence existed at that time to determine if this fear was well founded.

Coal mining had previously flourished in the Rocky Mountain Foothills and Front Ranges from the turn of the century until the early to late 1950s. The conversion of railroad locomotives from steam to diesel power largely caused the industry's near demise. The overburden and preparation plant dumps from these pre-1960 workings were almost always left unreclaimed.

In examining the environmental impact of coal resources development in this region, I have had the opportunity both to assemble available water chemistry data for undisturbed coal bearing areas and to carry out a synoptic sampling of leachates emanating from orphaned open pit workings.

Acknowledgments

I wish to acknowledge the following individuals, firms, and agencies for their support and access to their lands: Tim Godfrey and Union Oil Ltd.; Martin Bik, Elco Mining Ltd.; Jim Lant, Coleman Collieries; Doug MacFarlane and Meadowlark Farms Ltd.; Scurry Rainbow Oil Ltd.; Tony Milligan and Kaiser Resources Ltd.; Consolidated Coal Ltd.; Denison Mines Ltd.; The British Columbia Water Resources Service; Howard Block and Merle Korchinsky of Environment Canada; Mike Youso and Western Alpine Surveys; John Harrision of the Ministry of State for Science and Technology; Doug Hackbarth and Dominic Borneff of the Research Council of Alberta; McIntyre Mines Ltd.; and Dr. S.A. Teland of the Kananaskis Centre for Environment Research. Special thanks go to Dr. K.U. Weyer of Environment Canada and J.A. Heginbottom of the Geological Survey of Canada for critically reviewing parts of this paper. Any omissions or errors are entirely the responsibility of the author.

Physical and Geologic Setting

The Canadian Rocky Mountain Foothills and Front Ranges form a long narrow belt stretching from southwestern Alberta and southeastern British Columbia, northwest to northeastern British Columbia (Fig. 30.1). The Foothills are composed of northwest-trending folds and thrust faults of Mesozoic and lower Cenozoic clastics. Surface elevations range from about 1000 m in the Foothills to almost 3000 m in the Front Ranges. The region is characterized by short cool summers and long severe winters (Table 30.1), which are sporadically moderated by chinook winds bringing warmer air

Table 30.1

Climatic data for selected locations in the Canadian Rocky Mountain Foothills and Front Ranges[1]

Period 1941-1970

Location	Elevation (m)	Position	Mean daily temperature (°C)		No. days w/frost	Mean total Precipitation (cm)	Total rain (cm)	Total snow (cm)
			Jan.	July				
Fernie	1011	49°31'N, 115°03'W	-8.3	16.4	185	108.0	71.1	368
Coleman	1341	49°38'N, 114°35'W	-8.1	14.5	198	53.7	31.6	222
Kananaskis	1390	51°02'N, 115°03'W	-9.7	14.1	220	64.7	37.7	266
Hinton	1014	53°24'N, 117°33'W	-11.8	15.2	218		-No data-	
Jasper	1061	52°53'N, 118°04'W	-12.2	15.1	213	40.2	27.4	137

[1] Data from Environment Canada, 1973.

from the Pacific coast. Precipitation generally increases with elevation and with distance westward into the Foothills and Front Ranges. Mean annual temperature generally decreases with increasing elevation and latitude.

Two distinct structural belts have yielded coal within the area. From west to east they are the inner Foothills and outer Foothills (Latour, 1972). In the outer Foothills coal production has been principally from the Upper Cretaceous "Coalspur Beds" (MacKay, 1949) in the Coal Valley and Saunders areas (Fig. 30.1). This unit outcrops in a narrow belt between the North Saskatchewan and Athabasca rivers. The coal produced from this area is typically high volatile bituminous in rank. Although the coal-bearing units within this belt have been folded and faulted, relative relief is low, generally less than 200 m. The inner Foothills belt extends westward to the mountains and includes parts of the Front Ranges. Within the belt are major folded and faulted structures which are expressed as high ridges and which can commonly be traced many kilometres. Relative relief generally ranges between 500 and 1000 m. Coal producing formations are Lower Cretaceous in age. South of Red Deer River, the Kootenay Formation produces coal, whereas to the north of it, the Luscar Formation is productive. Coal from the inner Foothills belt is low to medium volatile bituminous in rank.

Bedrock and Regolith Chemistry

The inorganic water chemistry of the streams draining the coal belts of the Canadian Rocky Mountain Foothills is largely dictated by the chemistry of the bedrock and overburden materials. Equally important, the chemistry of these rocks and overburden materials determines changes in water chemistry when they are disturbed and exposed as rock wastes during and after the mining process. Analysis of bedrock chemistry has only been carried out at a few sites within the coal belt, typically as a part of environmental baseline studies. Values for samples from representative cores from the Kootenay and Luscar formations, and "Coalspur Beds" are presented in Table 30.2A; the table is not intended to be a complete summary of bedrock chemistry data but rather an indication of the ranges of values found within a single section or a cluster of closely spaced sections or mine dumps.

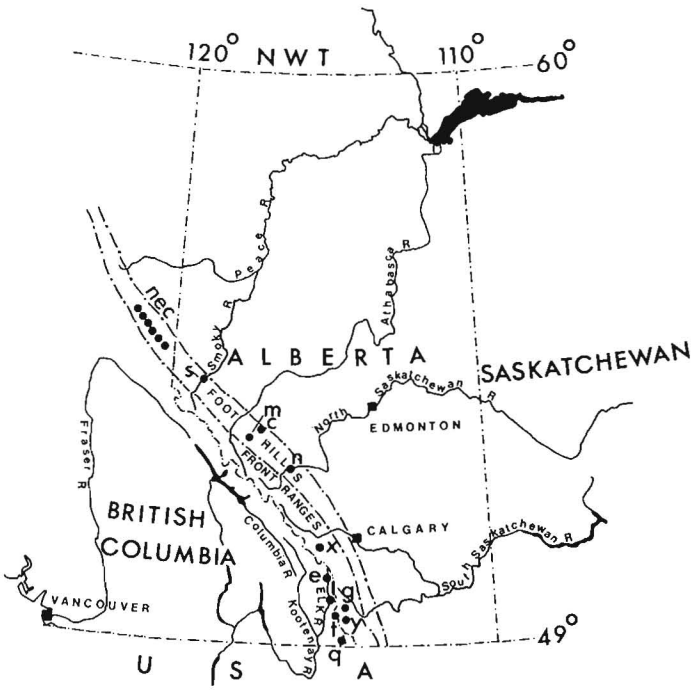

nec – *Water chemistry stations operated by the British Columbia Ministry of Environment (BCME) in the northeastern coal block*

s – *Grande Cache area studied by Hackbarth (1979)*

m – *Tri Creek Basin, Cadomin, and Mountain park area*

x – *Marmot Creek Experimental Watershed*

e – *Upper Elk River basin*

q – *Cabin and Howell Creeks BCME water chemistry sites*

c – *Coal valley area*

n – *Nordegg area*

g – *Grassy Mountain Mine*

t – *Tent Mountain Mine*

y – *York Creek Mine, Crowsnest River.*

Figure 30.1. *Reference map showing locations of the orphaned mine sites studied as well as locations of stations monitored for pristine water chemistry.*

Table 30.2

A. Soluble major cations and anions and miscellaneous chemical parameters of crushed rocks from coal-bearing sections, Rocky Mountain Front Ranges and Foothills, Alberta

Formation	Sample section thickness (m)	Number of samples	pH	Conductivity (millimhos/cm)	H_2O Soluble (meq/L)* Ca	Mg	Na	K	HCO_3^-	SO_4^{-2}	Sodium absorption ratio	Total sulphur (ppm)
Luscar[1]	160	41	9.6 6.4	2.0 0.27	7.02 0.16	7.02 0.12	20.49 1.49	3.21 0.10	17.2 0.0	12.13 0.53	53.9 0.7	8415 237
Coalspur[2,3]	10	7	7.6 4.0	1.50 0.14	1.91 0.21	0.37 0.08	22.4 4.13	0.38 0.09	10.5 2.5	30.2 2.25	39.3 7.3	534 149
Kootenay[4]	Not Available	6	8.2 7.5	2.3 0.87	23.21 1.50	2.36 0.21	0.28 0.05	1.73 0.03	3.06 1.14	28.12 0.15	1.18 0.36	<10 000[5]

B. Soluble major cations and anions and miscellaneous chemical parameters of inorganic regolith materials from coal-bearing areas of the Rocky Mountain Foothills and Front Ranges, Alberta and British Columbia

Location (coal-bearing formation)	Number of samples	pH	Conductivity (millimhos/cm)	Ca	Mg	Na	K	HCO_3^-	SO_4^{-2}	Sodium absorption ratio
Luscar and Coal Valley (Luscar Formation[2,6] and "Coalspur Beds")	24	6.5 4.3	0.12 0.6	3.27 0.27	1.83 0.12	0.53 0.18	0.57 0.06	2.4 < 0.2	9.75 0.55	0.72 0.21
Crowsnest Pass and Elk Valley[5] Alberta and British Columbia (Kootenay)	9	8.2 5.1	1.95 0.08	18.46 0.25	10.20 0.04	1.04 0.05	0.18 0.02	3.06 1.14	28.12 0.15	0.64 0.07

*Where two values are given, they represent maximum and minimum

[1] Devenny and Ryder, 1977

[2] Luscar Sterco Ltd., unpublished data

[3] Samples obtained from three separate cores

[4] Unpublished data collected for this study from abandoned open pit dumps Crowsnest Pass area, Alberta and British Columbia

[5] Consolidation Coal, personal communication, 1978

[6] Luscal Ltd., unpublished data

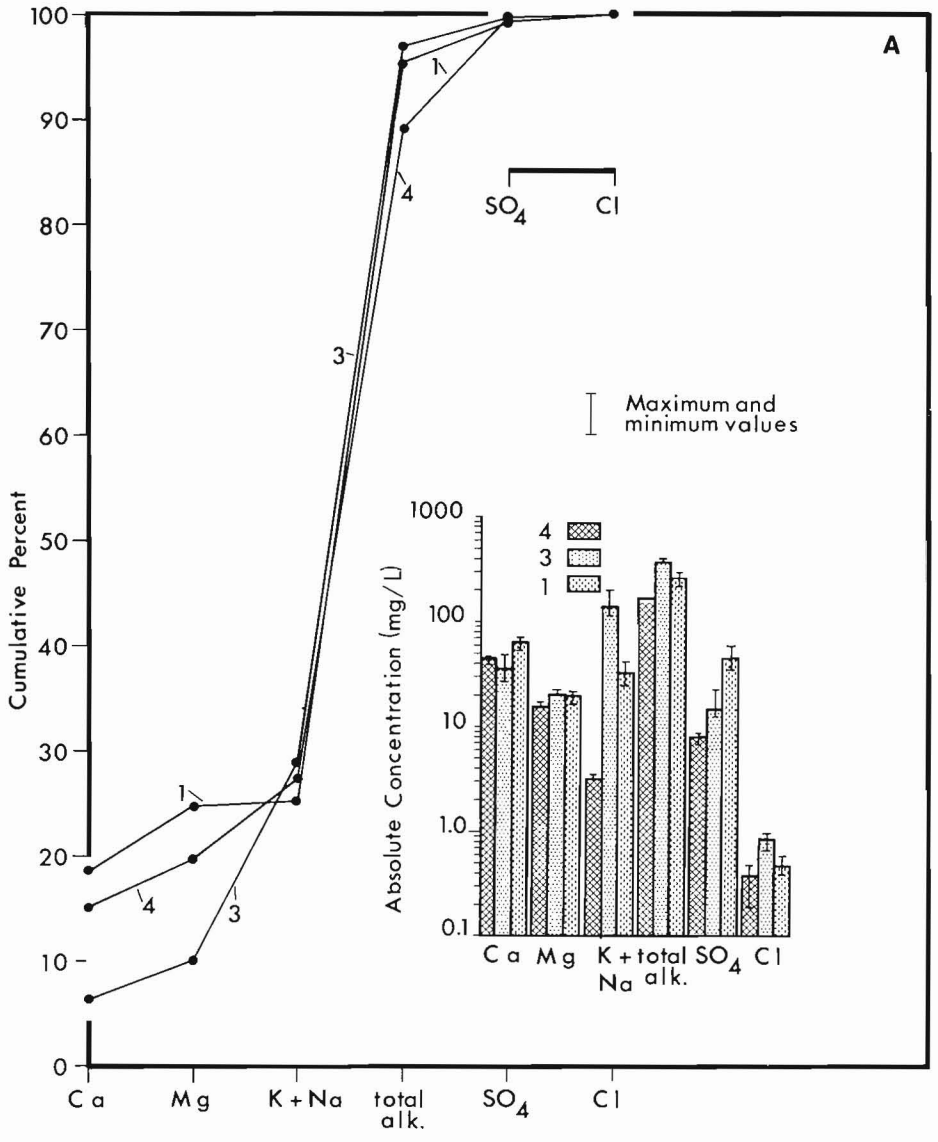

A. Luscar Formation overburden dumps and coal wastes in the Mountain Park-Cadomin area: 1 - Mountain Park north pit seep, 3 – Mountain Park plant dump spring, 4 Mannix south pit spring near Cadomin.

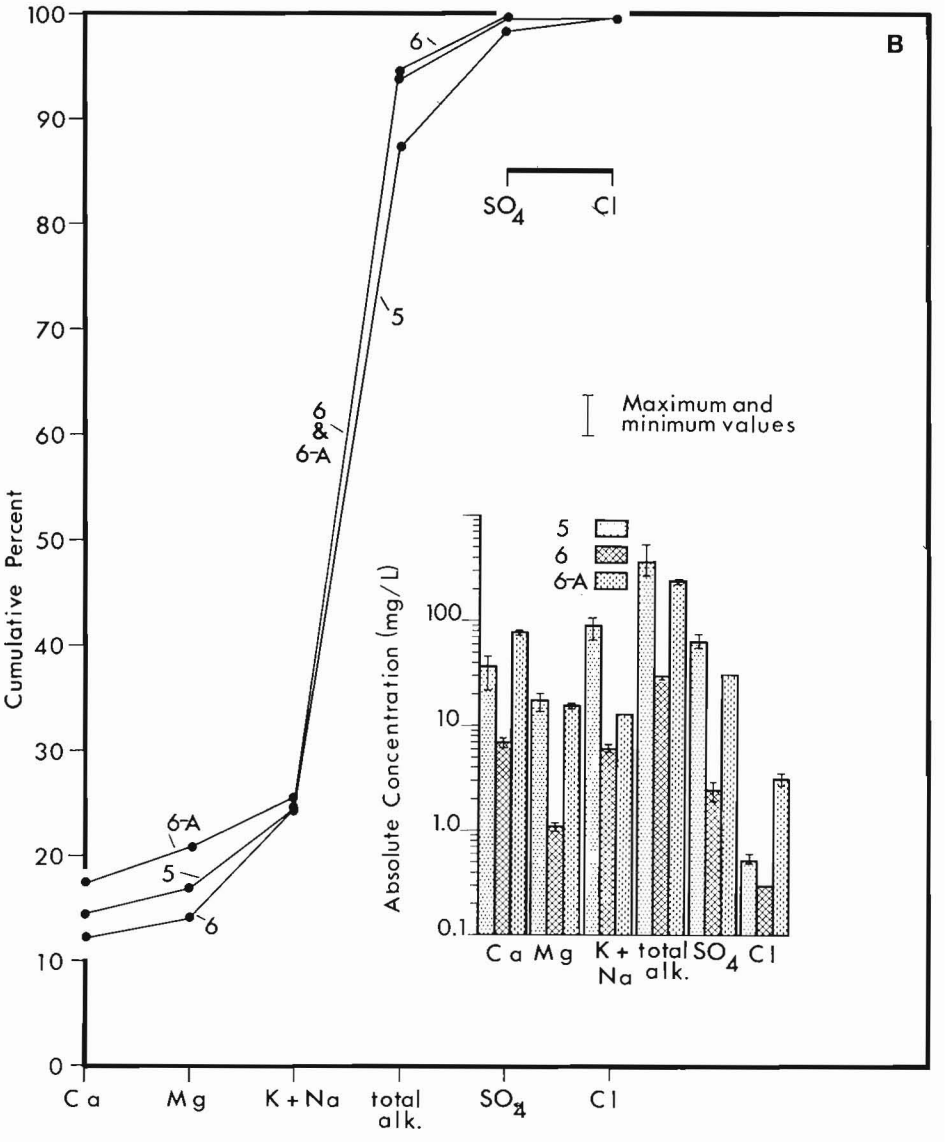

B. "Coalspur Beds" overburden waste dumps, Coal valley: 5 - Coal valley catch pond between north and south pits, 6 - Stream flowing into north pit pond, Coal valley, 6A - Spring at Sterco siding.

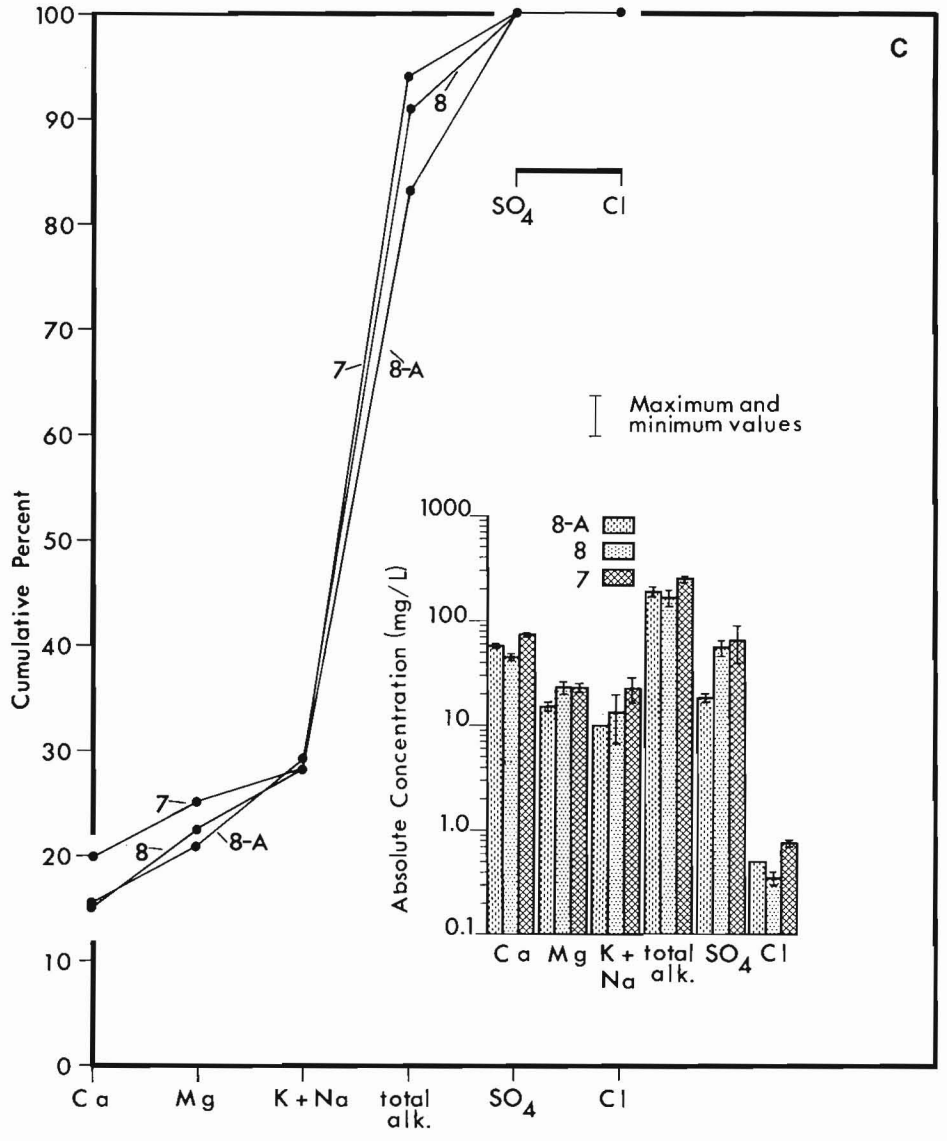

C. Luscar Formation overburden dumps and coal wastes in the Nordegg area: 7 - Nordegg stop pond, 8 - Stream outflow at south pit, 8A - Stream at toe of mine plant dump.

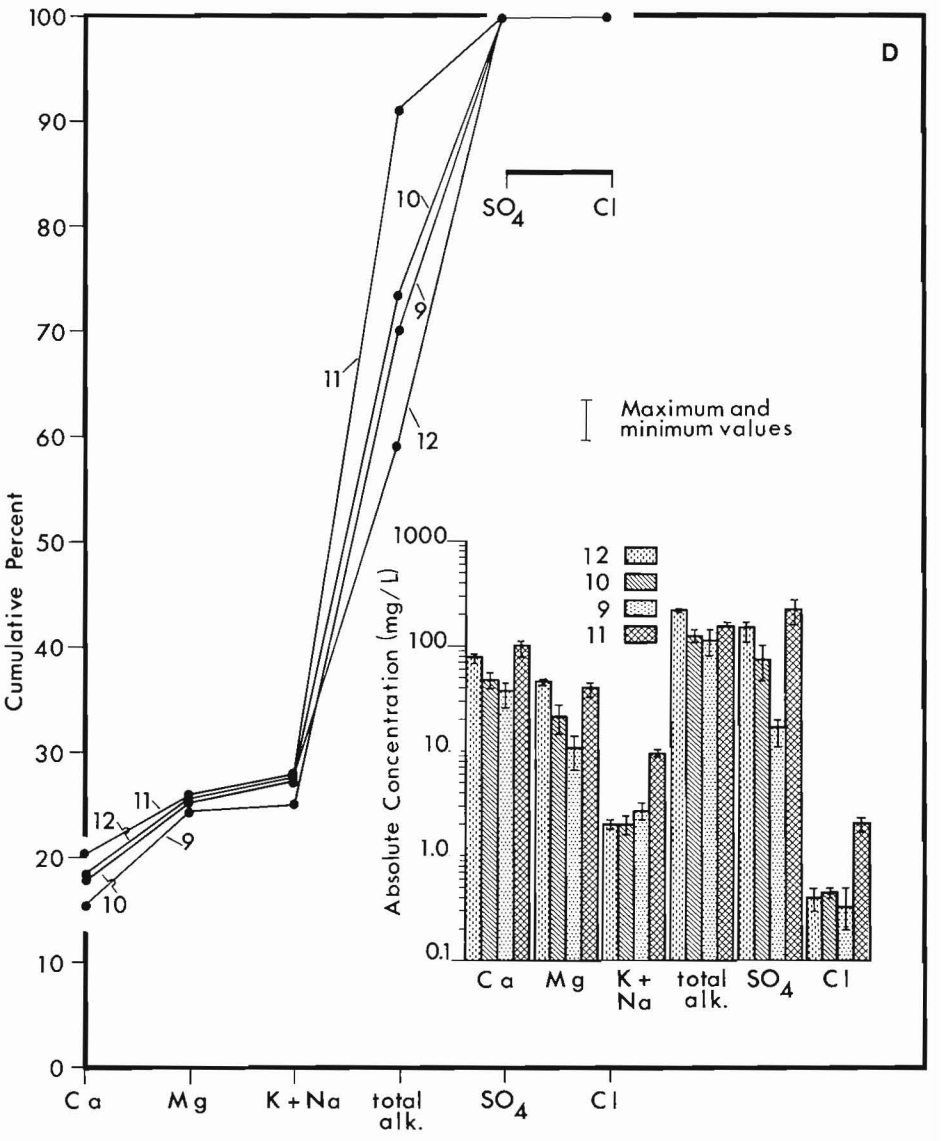

D. Kootenay Formation overburden dumps and coal wastes: 9 - Grassy Mountain Mine, spring above Lake #4, 10 - Grassy Mountain Mine, pond below Lake #4, 11 - Spring below north pit pond York Creek Mine, 12 - Stream below overburden dump, Tent Mountain Mine.

Figure 30.2. *Major cation and anion chemistries in leachates from coal overburden waste dumps (for site descriptions cf. Table 30.4).*

General observations can be made based upon the data in Table 30.2A. First, the Luscar Formation and the "Coalspur Beds" contain significant sources of soluble sodium whereas the Kootenay Formation does not. The sources of this sodium are sodic shale beds which represent a significant thickness of the "Coalspur Beds" but are thinner and of less significance in the Luscar Formation. Secondly, soluble carbonate is present in all three formations; the sources of the carbonate are carbonate minerals which form the cementing media in associated sandstones. Thirdly, all the units are low in sulphur; sulphur is in the form of pyrites in the Kootenay Formation and is present in organic compounds in the Luscar Formation (Weyer and Vonhof, 1980). The form of sulphur in the "Coalspur Beds" has not been established.

Inorganic regolith materials can be subdivided into two general classifications: colluvium, which encompasses disaggregated sediment formed in place or transported only a short distance from its parent bedrock, and glacial till. Unlike colluvium, the composition of till is influenced to varying degrees by all the rock that the glacial ice traversed. Table 30.2B details the chemistries of till and colluvial sediments from coal producing areas of the Foothills and Front Ranges. High pH values and relatively large values for soluble calcium, magnesium, and bicarbonate reflect the chemistry of tills in areas adjacent to the carbonate-rich Front Ranges. Those with acidic pH values and relatively low values for soluble calcium, magnesium, and bicarbonate reflect colluvial sediments developed upon noncalcareous shales and older tills that have been leached of carbonates. In general, glacial sediments containing calcite and dolomite are present in most valleys of the Foothills and Front Ranges as a consequence of former valley glaciers which advanced from the carbonate-rich Front Ranges during the ice ages.

Previous Work

Water Chemistry of Undisturbed Coal-bearing Areas

Although numerous streams are monitored for water chemistry in Alberta and British Columbia by federal, provincial, and municipal agencies and industrial firms, detailed water chemistry sampling of streams draining essentially unaltered basins predominantly underlain by coal-bearing formations is rare. Those basins for which data are available are typically either experimental watersheds or watersheds monitored by coal companies during the course of environmental baseline studies prior to mining operations.

Table 30.3 describes these basins. Their locations are plotted on Figure 30.1. Of these, only the upper Elk River basin, Flathead River basin, Marmot Creek experimental watershed, Tri Creek experimental watershed, and streams sampled by Hackbarth (1979) in the Grande Cache area provided significant enough quantities of data to merit compilation[1].

Water Chemistry of Disturbed Coal-bearing Areas

Few past studies have dealt with changes in surface water chemistry specifically due to dumping of bedrock or overburden material in conjunction with open pit coal mining in the Foothills and Front Ranges of the Canadian Rockies. Etter (1971) analyzed water chemistry in three streams near the Cardinal River Mine. All streams sampled drained coal overburden dumps or areas disturbed by coal exploration activities. Measured concentrations of iron, dissolved solids, and alkalinity were well within the guidelines for drinking water. No values were available for nearby pristine streams for comparison. Root (1976) analyzed water from a variety of sites ranging from flooded pits to springs flowing from waste dumps at an abandoned open pit coal mine south of Cadomin, Alberta. One sample was obtained from each of six sites, including undisturbed drainage where it entered the waste dumps. Root found the chemistry of water in the ponds and springs to fall within the same range as water entering the dump. Concentrations of all cations and anions in the samples were within the standards for drinking water set by the Alberta Government. Harrison (1977) sampled underground mine effluent, pond water in flooded open pits, and springs below waste dumps in the Crowsnest Pass area of southwestern Alberta and southeastern British Columbia. Samples were analyzed for a number of physical parameters and major dissolved cations and anions. No attempt was made to compare analyzed values with surface streams except qualitative comparisons of suspended sediment content. Samples were not filtered in the field so that the values he reported for samples fixed with acid in the field measured extractable rather than dissolved concentrations. Harrison generally found little difference between pond, dump spring, and adit drainage in the area. Hackbarth (1979) monitored water chemistry changes in springs emanating from dumps at the McIntyre Mine near Grande Cache over a seven year period. He found that the yield of total dissolved solids progressively increased to a factor of four during the period of observation but that the ratios of cations to one another remained the same. However, some changes in the ratios of anions occurred: sulphate increased at the expense of bicarbonate, and nitrate increased dramatically to levels well beyond those set for drinking water as the result of explosives residues. Nitrate values dropped rapidly, however, following the cessation of the dumping of recently blasted rock. The pH remained in the range of 7.6 to 8.2, which is normal for the streams in the Grande Cache area.

The Present Study

Field work carried out around orphaned open pit coal mines during the summers of 1977 and 1978 provided an opportunity to locate and sample leachates emanating from waste rock of a variety of lithologies. These materials had been weathering for twenty years or longer. The goal of this sampling and analysis was to determine if any major or minor trace elements or compounds were present in quantities that might prove to be a water pollution hazard. The sampling was not intended to be a year-round continuous monitoring program but rather a synoptic survey which "prospected" for possible sources of water pollution. These sources, if found, could then be concentrated on in future studies.

Chemistry of Leachates from Open Pit Mine Dumps

The descriptions of the open pit mine dumps and spoil areas where leachate samples and pond waters were collected are summarized in Table 30.4. Figures 30.2A-D present the results of analyses for major cations and anions[2].

Field Methodology. At each sampling site, weather conditions, estimated flow rate, water temperature, and pH were routinely recorded (Fig. 30.3). Samples were then collected for all or part of the following: physical chemistry (dissolved oxygen, specific conductance, alkalinity, turbidity, nonfilterable residue), total organic/inorganic carbon, extractable metals, dissolved metals, cyanide, nitrates, mercury, and organic compounds (hydrocarbons, organic sulphur compounds). Samples taken for dissolved metals analysis were filtered through a Satorius SM165-11 filtration apparatus containing a 0.45 micron membrane filter under a vacuum created by a Nalgene 6130 hand vacuum pump (Fig. 30.3). Prior to filtering each sample, the filtration apparatus was rinsed with 0.5 L distilled water. The rinse water was collected and bottled for analysis, and a fresh filter was placed within the apparatus. Following filtrations, the filter was removed and the apparatus rinsed with

[1] As of December 1979 when this compilation was made.

[2] Compiled tables of data for leachate physical characteristics and concentrations of minor and toxic trace elements and organic compounds may be obtained from the author upon request.

Figure 30.3

a) Water chemistry sampling at the Grassy Mountain Mine.

b) Field water chemistry sample preparation lab.

1:1 HNO_3 solution and then given a second rinse with distilled water. One half litre of the dissolved metal sample was acidized with 1 ml concentrated HNO_3. Extractable metal samples were acidized in the same proportions without filtration. Samples obtained for mercury analysis were filtered and 0.25 L of the filtrate was placed in the Teflon bottle and preserved with 2 ml concentrated HNO_3 followed by 2 ml of 5% of $K_2Cr_2O_7$. Cyanide samples were filtered and 0.25 L of the filtrate was combined with 2 ml of a 50% NaOH solution. Water samples of 40 L each were obtained for analysis of organic compounds. The organic content of the water sample was extracted in the field by agitating hexane in the Squibb separatory funnel filled with sampled water.

All samples were packed in an insulated box and chilled during transport to the laboratory.

Laboratory Methodology. Analysis of the samples, except those for analysis of organic compounds, was carried out by the Water Quality Branch of Inland Waters Directorate, Calgary, Alberta, following Environment Canada standard methodologies (Inland Waters Directorate, 1979). The samples for analysis for hydrocarbons and organic sulphur compounds were analyzed by Dr. S.A. Telang, of the Kananaskis Centre for Environmental Research of the University of Calgary, using gas chromatography.

Physical Characteristics. Samples were usually clear with generally small nonfilterable residues and low turbidities. The pH of leachates from the "Coalspur Beds" and the Luscar Formation wastes was generally less alkaline than that from Kootenay wastes. The few values that were slightly acidic were invariably associated with wastes that contained a large percentage of coal and coaly shales.

Dissolved oxygen levels were usually adequate to support fish, except for station 3 at Mountain Park which was responsible for the low mean and low minimum values for the Cadomin-Mountain Park area. The low dissolved oxygen values at this site are apparently the result of the dump burning. The significant dissolved oxygen contents of the leachates in most dumps indicate that the chemical weathering of the dumps is taking place under well oxygenated conditions.

Water Chemistry of Undisturbed Coal-bearing Areas

Major Cations and Anions. The chemistries of streams in the Rocky Mountains reflect the presence of abundant carbonate minerals in the bedrock and glacial regolith. They are naturally alkaline with all pH values falling between 7.2 and 8.9. Total dissolved solids always fall well within acceptable drinking water standards. These concentrations range between 80 and 300 mg/L. Figure 30.4 shows cumulative per cent and absolute values for major cations and anions (concentrations $\geq$0.1 mg/L) from pristine basins. It can be seen from these figures that water chemistry is relatively uniform within the coal-bearing belts of the Rockies. The alkalinity of the surface waters is almost entirely due to bicarbonate ion which is the dominant anion (carbonate concentration is almost zero over this pH range). Sulphate concentration varies greatly with values from less than 1.0 to 100 mg/L, as does chloride concentration from less than 1.0 to 10 mg/L. Calcium and magnesium are the dominant cations. The sum of the concentrations of calcium and magnesium expressed as equivalents is approximately equal to the concentrations of bicarbonate expressed as equivalents. Potassium concentration is usually less than 1 mg/L whereas sodium concentration ranges from less than 1 to 10 mg/L. Sodium concentration is usually greater in streams draining terrain underlain by the Luscar Formation and the "Coalspur Beds" than for terrain underlain by the Kootenay Formation.

Sulphate concentrations are independent of calcium concentrations; therefore the sulphate does not originate from gypsum in the bedrock but rather from the oxidation of sulphide minerals or sulphur-containing organic compounds present in shales.

Table 30.3

Sources of inorganic water quality data for coal-bearing terrain undisturbed by coal resources development

Location (cf. Fig. 30.1)	Stream Basin	Monitoring Agency	Station number or reference	Period of record and record quality
q	Flathead River basin, B.C.	B.C. Pollution Control Branch	B.C. Ministry of Environment, 1976a.	1971-1974; major and minor nutrients, toxic trace elements; 6-8 samples per parameter.
l	Elk River basin, B.C.	As above	B.C. Ministry of Environment, 1976b.	1972-1974; upper Elk River, sporadic sampling of total N, TDS, alkalinity, total P. 1973-1974; upper Fording River, sporadic sampling of major ions and trace elements. 6-21 samples per parameter.
e	Upper Elk River basin	Elco Mining Ltd.	Elco Mining Ltd. 1978 (unpublished)	1976-1977; major and minor nutrients, trace elements on a regular basis from Elk River, site specific sampling from smaller streams in the area.
x	Marmot Creek experimental watershed, Alberta	Environment Canada	00AL05BF0001 00AL05BF0002 00AL05BF0003 00AL05BF0004 00AL05BF0005	1963-present; major and minor nutrients; >200 samples per parameter.
m	Tri Creek experimental watershed, Alberta	As above	00AL07AF0001 00AL07AF0002 00AL07AF0003	1971-1975; major and minor nutrients; 20-25 samples per parameter.
s	Smoky River above Hells Creek	As above	00AL07GA0001	1970-1975; major nutrients; 43-48 samples per parameter.
s	Sheep Creek – Smoky River, Alberta	Meadowlark Farms Ltd. (1976), unpublished data	Numerous sites	1974; major and minor nutrients, toxic trace elements; about 10 samples per parameter.
s	McIntyre Mine area, Grande Cache, Alberta	Alberta Research Council	Hackbarth, 1979	1972-1978; major and minor nutrients, toxic trace elements; >12 samples per parameter.
nec	Peace River Coal Block, B.C. (Murray, Wolverine, Sukunka, Narraway, Belcourt, and Wapiti River, and Pine River basins)	B.C. Pollution Control Branch	Stations 1177701-1177748	1976-present; major and minor nutrients, toxic trace elements; 2-21 or more samples per parameter.

Total dissolved solids (TDS) and major cations and anions follow general seasonal cycles in concentration. TDS and major ion concentrations are usually lowest in the spring and early summer when snowmelt and precipitation are at their maximum and greatest in fall and winter when groundwater seepage becomes the most significant source of water supplying streams. TDS range from values as low as 60 to almost 300 mg/L. Silica is present in quantities ranging from less than 1 to about 16 mg/L. Dissolved oxygen levels are usually in the 10 to 12 mg/L range, typical of well oxygenated mountain streams. Exceptions exist locally where bogs feed oxygen-poor water to streams.

Minor and Toxic Trace Elements. Although numerous gaps exist in the available data, concentrations of toxic or problem trace elements or compounds[1] are within Environment Canada drinking water standards (McNeely et al., 1979) for pristine streams in coal-bearing areas[2]. Occasionally, however, high values do exceed these limits. The high values shown in Table 30.5 were confined entirely to the winter months when stream waters are largely sustained by groundwater seepage.

Dissolved trace elements, which are likely to be present in surface waters in detectable or excessive concentrations during low flow periods due to groundwater discharge, can possibly be predicted in some of the areas studied by analysis of groundwater chemistries. For example, high values of cadmium, lead, mercury, and total phosphorous were found in groundwaters sampled from exploratory wells drilled for the proposed Elco Mine in upper Elk Valley, British Columbia (Elco Mining Ltd., 1978, unpublished report). High concentrations of cadmium and mercury were recorded during winter sampling of streams in this area (Table 30.5).

Organic Compounds. Naturally occurring organic compounds and constituents that are commonly analyzed for in stream waters of the Rocky Mountains and Foothills include total organic carbon (TOC), phenols, ammonia, and oxides of nitrogen.

[1] These include: dissolved and extractable iron, manganese, arsenic, copper, chromium, nickel, lead, zinc; dissolved fluoride, aluminum, cadmium, boron, selenium; extractable mercury and vanadium; and total inorganic phosphate and total phosphate.

[2] A tabular data summary is available from the author upon request.

Table 30.4

Description of Leachate Sampling Sites at Open Pit Coal Mine Dumps

Site No.	Site Name	Location (UTM)	Production Formation[1]	Dates Sampled (1978)	Parameters Sampled[2]	No. Years of Dump Weathering	Description
X-1	McIntyre #9 mine dump	354500E 5989100N	L	7 Sept.	OC	0-4	Stream 0-2 of Hackbarth (1979). Stream fed by drainage from the #9 mine dump. Flow rate ~20 L/minute.
X-2	McIntyre #8 dump	360800E 5989400N	L	7 Sept.	OC	3-7	Spring at base of #8 mine. Sampled by Hackbarth (1979). Flow rate ~1L/minute.
1	Mountain Park north pit seep	479250EL 5864600N	L	14 June, 23 July, 8 Sept., 28 Oct.	PC, EM, DM, NFR, TOC TIC, Hg, HCN, N, DO	22	A series of seeps on the slopes of a shale and sandstone overburden dump. Flow rate ~1 to 0.5 L/minute.
3	Mountain Park plant dump spring	481850E 5863400N	L	as above	as above	22	Spring at base of a burning coal and coaly shale-rich waste dump. Spring decreased in flow rate from ~10 to ~0.5 L/minute during period of sampling.
4	Mannix south pit spring near Cadomin	480240E 5873850N	L	14 June, 22 July, 8 Sept., 28 Oct.	DO, PC, EM DM, NFR, TOC, TIC, Hg, HCN	26	Spring flowing from base of dump filling the original valley. Flow rate ranged from ~12 to ~4 L/minute during period of sampling.
5	Coal valley catch pond between north and south pits	513000E 5882150N	C	15 June, 22 July, 7 Sept., 27 Oct.	as above	20	Shallow catch pond draining both shale-rich and coal-rich waste dumps. Flow rate from ponds varied between 3 to 10 L/minute during sampling period.
6	Stream flowing into north pit pond, Coal valley	512000E 5883000N	C	15 June, 22 July	DO, PC, EM, DM, NFR, TOC, TIC	20	Stream originating in muskeg and flowing through coal-rich spoil pile. Stream flow rate >15 L/minute.
6A	Spring at Sterco siding #47	511400E 5883400N	C	7 Sept., 27 Oct.	DO, PC, EM, DM, NFR, TOC, TIC, Hg, HCN, N	20	Spring at base of a mine dump containing coaly waste, clinkers, and iron debris. Flow rate decreased from ~2 to 1 L/minute during sampling period.
7	Nordegg stop pond	561950E 5812700N	L	15 June, 21 July	DO, PC, EM, DM, NFR, TOC, IC	22	Pond in coaly waste material fed by adit drainage.
8	Stream outflow at south pit	564650E 5809450N	L	15, 20 July	as above	22	Confluence of two small streams draining open pit mine. Flow rate ~1 to 2 L/minute.
8A	Stream at toe of mine plant dump	562100E 5812900M	L	9 Sept., 27 Oct.	DO, PC, EM, DM, NFR,TOC, TIC, Hg, HCN	22	Stream at toe of spoil piles containing coaly waste and ash debris. Flow rate >50 L/minute during sampling.
9	Grassy Mountain Mine, spring above Lake #4	685800E 5505050N	K	22 June, 25 July, 25 Aug., 29 Oct.	DO, DC, EM DM, NFR, TOC, TIC, OC, Hg HCN	16	Area of springs at the base of a spoil pile above Lake #4 at Grassy Mountain Mine. Flow rate decreased from 4 to 1 L/minute during sampling period.
10	Grassy Mountain Mine, pond below Lake #4	685700E 550435ON	K	22 June, 25 July	DO, PC, EM, DM, NFR, TOC, TIC	16	Pond occupying part of pit at Grassy Mountain Mine.
11	York Creek Mine, spring below north pit pond	680850E 5496950N	K	22 June, 25 July 25 Aug., 29 Oct.	DO, PC, EM, DM, NFR, TOC, TIC, OC, Hg, HCN	22	Spring at base of spoil pile of sandstone and shale overburden waste. Flow rate ranged from >30 to <20 L/minute during sampling period.
12	Tent Mountain Mine, stream below overburden	665600E 5489150N	K	as above	as above	0-29	Stream sampled ~1 km below active dumps of Tent Mountain Mine. Flow rate ranged from >50 to 20 L/minute during sampling period.

[1] L–Luscar, C–Coalspur, K-Kootenay

[2] OC – organic compounds
PC – physical chemistry
EM – extractable metals
DM – dissolved metals
NFR – nonfilterable residue
TOC – total organic carbon
TIC – inorganic carbon
Hg – mercury
HCN – cyanide
N – nitrogen oxide compounds
DO – dissolved oxygen

Organic compounds in the stream waters of the Marmot Creek experimental watershed were studied in detail by researchers of the Kananaskis Centre for Environmental Research at the University of Calgary. The absolute concentrations of TOC averaged 4 mg/L during the five year study period. Only about 25 per cent of the organic compounds present could be identified. About 80 per cent of the identified compounds were humic and fulvic acids. The balance of the identified compounds consisted of tannins, lignins, carbohydrates, hydrocarbons, phenols, fatty acids, and amino acids. None of these compounds occurred in concentrations which exceed acceptable limits for drinking water where limits for these compounds have been established. However, the maximum acceptable concentration of phenolic compounds for the protection of freshwater aquatic life of 0.001 mg/L was exceeded naturally by concentrations of phenols up to 0.090 mg/L. It appears likely on the basis of the Marmot Basin data that phenol concentrations probably exceed guideline concentrations elsewhere within similar coal-bearing areas in the Rocky Mountain Foothills and Front Ranges.

The organic substances found in pristine stream waters are almost entirely derived from soil leachates or biological processes within the stream themselves (B.L. Baker, personal communication, 1979). Nitrogen oxides are all of low concentration and well within drinking water standards of 10 mg/L. Data on ammonia are available only for the Marmot Creek basin and the upper Elk River basin; concentrations are within the 0.5 mg/L acceptable limit in Marmot basin but are greatly exceeded in the Elk basin. The presence of extensive bogs in Elk valley may provide the ammonia through seepage of anaerobic waters during the winter months when the high ammonia values are recorded. More work on this phenomenon would be required, however, for a definite explanation.

Water Chemistry of Leachates from Orphaned Open Pit Mines

Major Cations and Anions. The range of variations of mean, maximum, and minimum concentrations of major cations and anions was found to be generally similar from one coal producing formation to the next (Fig. 30.2). Individual values, however, range widely from site to site. Only two apparent systematic variations between leachates on a formation to formation basis were found. A higher relative per cent concentration of sodium was found in leachates from the "Coalspur Beds" and Luscar Formation relative to the Kootenay Formation leachates. Conversely, a higher relative content of sulphate was found in Kootenay leachates relative to the contents of Luscar and "Coalspur beds" leachates (Fig. 30.2). The relatively higher contents of sodium in the Luscar Formation and the "Coalspur beds" are undoubtedly due to the presence of sodic shales in these units and their absence from the Kootenay Formation (Table 30.2A). The higher sulphate content, apparently at the relative expense of alkalinity, is probably the result of more rapid oxidation and/or higher concentrations of sulphur compounds in the Kootenay Formation than in the other two. This relationship would be expected where iron sulphide minerals are present. This high sulphate content relative to alkalinity persisted in both station 12 samples (Table 30.4), which were obtained below the still active Tent Mountain Mine dump, and the Grassy Mountain Mine site (stations 9, 10) which has been inactive for approximately 20 years. By contrast, leachates from the York Creek dump (site 11), which consists mostly of coal and coaly shale fragments, contain the lowest relative sulphate content.

All values for the concentrations of major cations and anions measured in waste dump effluents and ponds are acceptable for drinking water (McNeely et al., 1979).

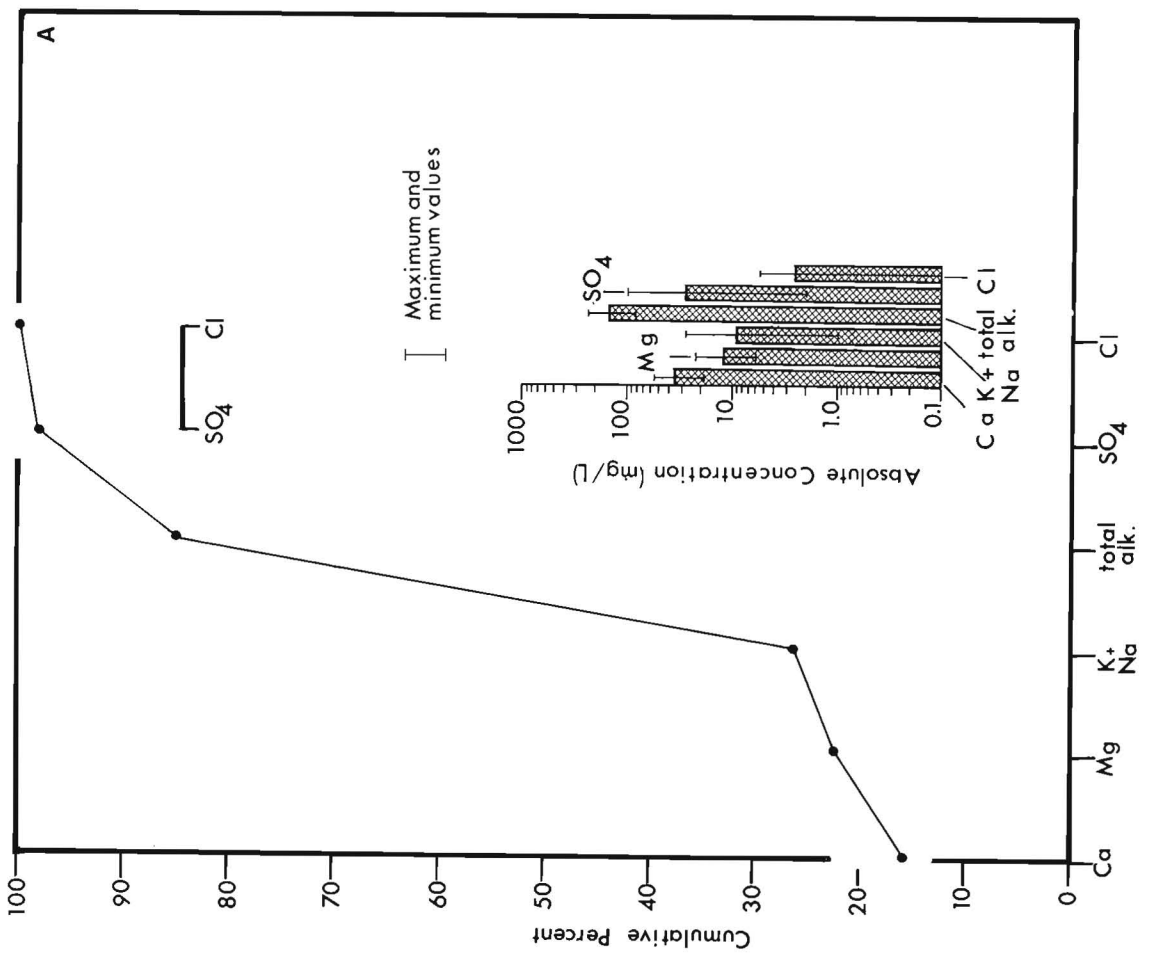

A. Streams flowing over terrain underlain by the Luscar Formation in the Grande Cache area (from Hackbarth, 1979).

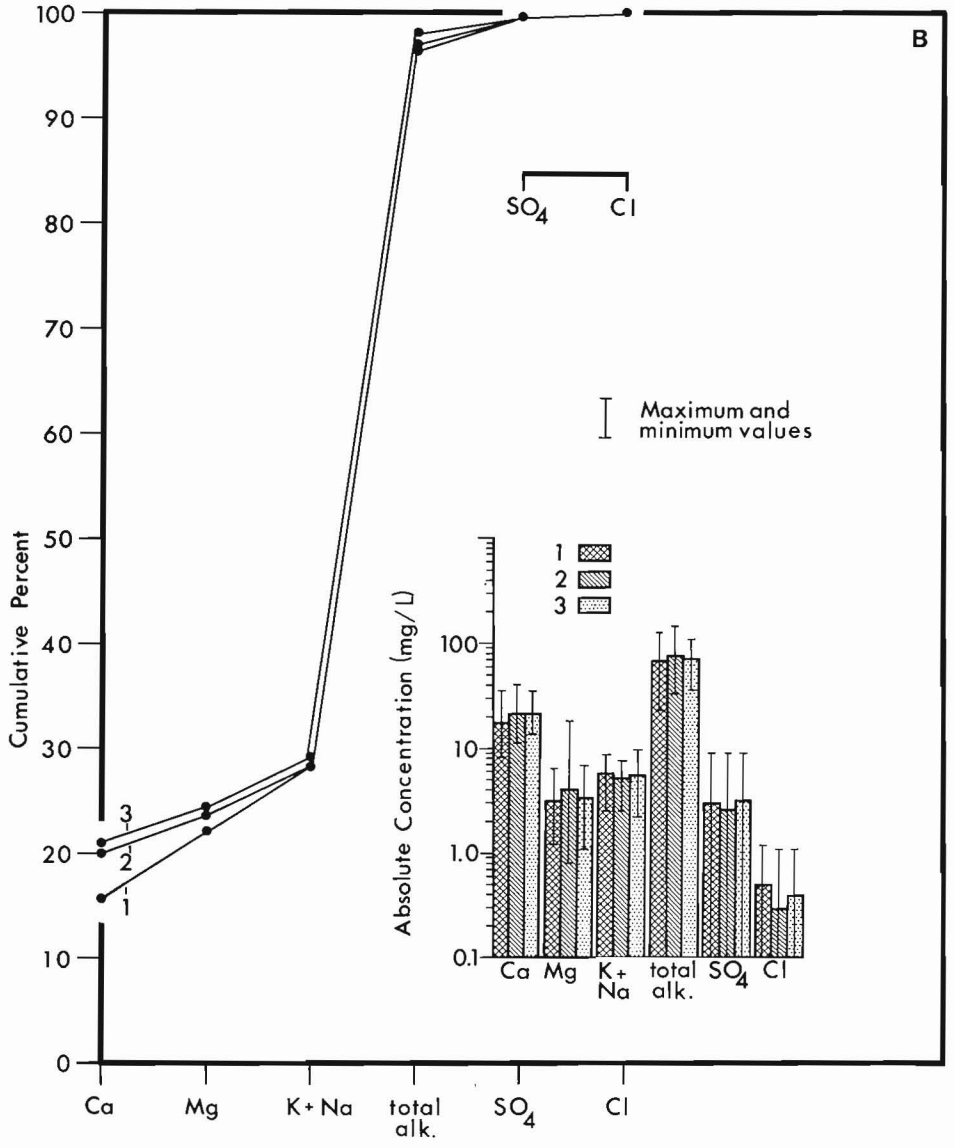

B. Tri Creek basin (predominantly underlain by the Brazeau Formation which is composed of sediments similar to the "Coalspur Beds"): 1 - Wampus Creek, 2 - Eunice Creek, 3 - Deerlick Creek.

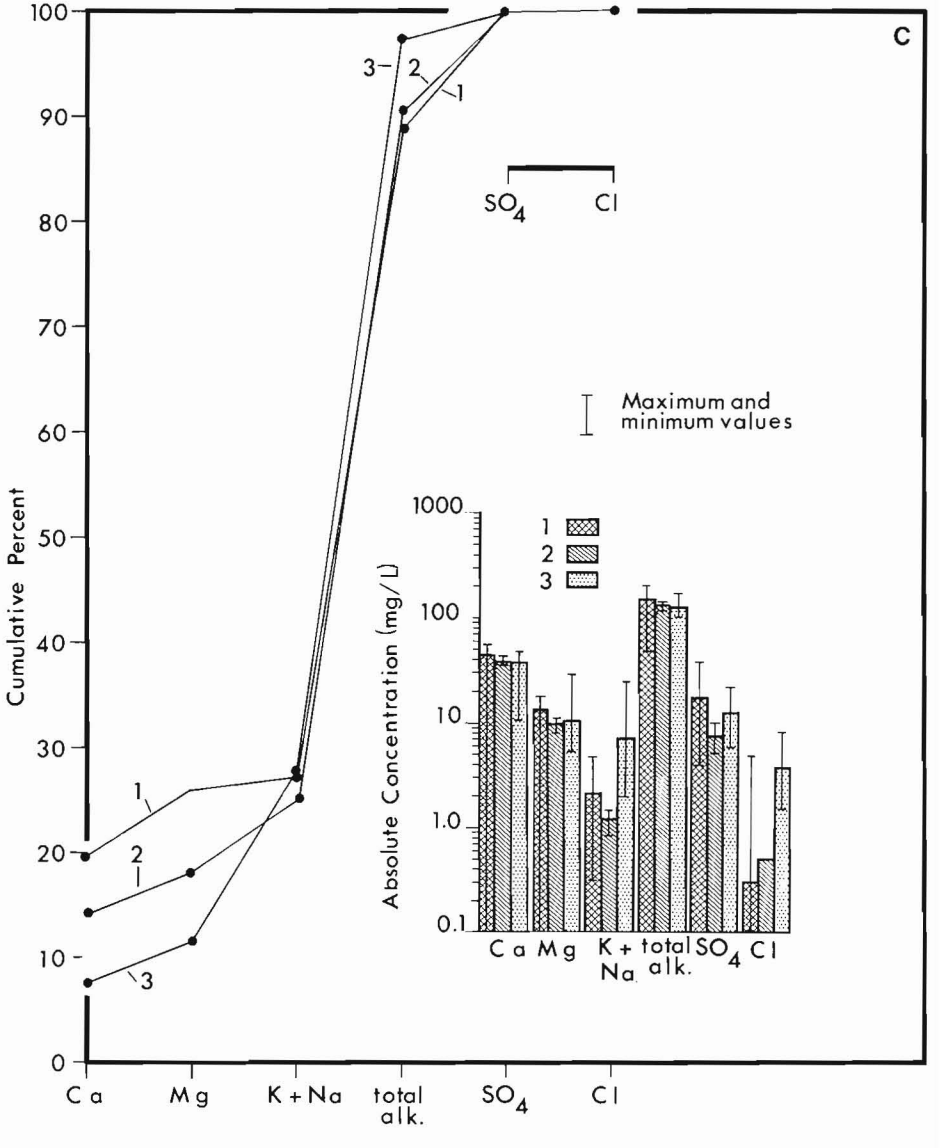

C. Streams flowing over terrain underlain by the Kootenay Formation and stratigraphically adjacent rocks:

1 - Middle Fork Creek, Marmot Creek experimental watershed
2 - Cabin and Howell creeks
3 - Upper Elk River.

Figure 30.4. *Major cation and anion chemistries for pristine streams in coal producing areas.*

Table 30.5

Elements and compounds exceeding permissible concentrations in streams largely or entirely originating from undisturbed coal-bearing drainage basins in the Rocky Mountain Foothills and Front Ranges of Alberta and British Columbia

Parameter	Location	Maximum Value	Range of means from available basins	No. Samples	Environment Canada maximum permissible concentration for	
					drinking water	protection of freshwater aquatic life
Dissolved Manganese	Marmot Creek experimental watershed	2.60 mg/L	≤0.01-0.013 mg/L	704	0.05 mg/L	not determined
Dissolved Fluoride	as above	1.6 mg/L	0.07-0.17 mg/L	910	≤1.5 mg/L	as above
Dissolved Cadmium	Upper Elk River Valley	0.050 mg/L	≤0.005 mg/L	32	≤0.005 mg/L	≤0.002 mg/L
Dissolved Lead	Marmot Creek experimental watershed	0.034 mg/L	≤0.001-0.002 mg/L	302	≤0.05 mg/L	≤0.03 mg/L
Extractable Mercury	Smoky River above Hills Creek (Grande Cache area)	0.13 µg/L	not detected to 0.07 µg/L	49	≤1.0 µg/L	≤0.1 µg/L
	Upper Elk River valley	0.8 µg/L	not determined	43		
Total Phosphates	Marmot Creek experimental watershed	0.228 mg/L	≤0.005-0.022 mg/L	551	≤0.100 mg/L	≤0.025 mg/L

Minor and Toxic Trace Elements. Thirteen minor and toxic trace elements were sampled in the mine dump leachates[1]. Of these, only dissolved iron and manganese exceeded Environment Canada permissible guidelines (McNeely et al., 1979) for drinking water (≤0.3 mg/L and ≤0.05 mg/L, respectively) and the protection of aquatic life (≤0.3 mg/L) for iron only. No levels have yet been set for manganese by Environment Canada. In only one case, copper exceeded Environment Canada guidelines for the protection of aquatic life (≤0.005 mg/L). With respect to the elevated iron and manganese values, it can be noted that the permissible standards are frequently exceeded in natural surface waters within coal-bearing areas of the Rocky Mountain Foothills and Front Ranges (Table 30.5). The elevated level of copper is anomalous and requires further investigation. This value was associated with the Kootenay Formation and may be the result of local leaching of shales by sulphuric acid generated by the weathering of pyrites.

The general absence of excessive levels of toxic trace elements in the leachates probably reflects chemical conditions in the dump sediments which cause minerals containing these elements to remain almost insoluble. If toxic trace elements are released they must be quickly immobilized.

Organic Compounds. Total organic carbon, total nitrogen, cyanide, total inorganic and total organic phosphate contents were determined for dump leachates. In addition five samples were collected for analysis of organic sulphur compounds and hydrocarbon compounds. Phenols were inadvertently omitted during field sampling. Ammonia was not sampled since blasting had long since ceased at all sites except Tent Mountain. All values were well within drinking water standards. The values for total nitrogen and total inorganic phosphorus and total phosphorus included one sample from each established station plus some synoptic sampling from flooded pits nearby. The phosphorus present in the waters was found to be of inorganic origin. The additional five samples of leachates were obtained from stations X-1 and X-2 near Grande Cache, station 3 at Mountain Park, and stations 9 and 11 in the Crowsnest Pass area. Detection limits for these hydrocarbons and organic sulphur deposits using gas chromatography is approximately 10 ng/L (10^{-9} g/L). None of these substances were detected. Collection sites ranged from active dumps to burning coaly waste piles which have been abandoned for almost 30 years.

Discussions and Conclusions

Although it is tempting to make a comparison between the chemistries of pristine waters and leachates based upon the data reported in this paper alone, none will be made. The synoptic nature of the sampling and the limited size of the leachate data base prohibits such a comparison. The ranges of concentrations of major cations and anions in the leachates, however, fall into the same range as those reported by Hackbarth (1979) after seven years of spoil weathering in the Grande Cache area. This may indicate that leachate chemistry shows a progressive increase in major cation and anion concentrations for the first decade and then levels out with concentrations of each parameter at two to four times the values found in pristine streams. Further monitoring will be required to confirm this.

[1] These include: dissolved and extractable iron, manganese, aluminum, arsenic, cadmium, chromium, copper, lead, vanadium; dissolved boron, fluoride, selenium; extractable nickel and mercury.

References

British Columbia Ministry of Environment
1976a: Kootenay air and water quality study, Phase 1. Water quality in Region 1, the Flathead River Basin; Water Resources Service, British Columbia Department of Environment, 19 p.

1976b: Kootenay air and water quality study, Phase 1. Water quality in Region 2, the Elk River Basin; Water Resources Service, British Columbia Department of Environment, 139 p.

Devenny, D.W. and Ryder, D.E.
1977: Weathering of coal mine waste: assessing potential side effects of Luscar, Alberta; Proceedings Canadian Land Reclamation Association Second Annual Meeting, Paper 15, 9 p.

Downs, C.G. and Stocks, J.
1978: Environmental Impact of Mining; Applied Science Publishers, London, England, 371 p.

Environment Canada
1973: Canadian Normal 1941-1970, Volume 1 and 2; Environment Canada, Atmosphere Environment.

Etter, H.M.
1971: Preliminary report of water quality measurements and revegetation trails on mined land at Luscar, Alberta; Canadian Forestry Service, Northern Forest Research Centre, Internal Report NOR-3.

Hackbarth, D.A.
1979: The effects of surface mining of coal on water quality near Grande Cache, Alberta; Canadian Journal of Earth Sciences, v. 16, n. 6, p. 1242-1253.

Harrison, J.E.
1977: Coal mining surface water quality: Crowsnest Pass, Alberta and British Columbia - preliminary data; in Report of Activities, Part A, Geological Survey of Canada, Paper 77-1A, p. 319-322.

Inland Waters Directorate
1979: Analytical Methods Manual: Environment Canada.

Latour, B.A.
1972: Coal deposits of western and northern Canada; in Proceedings, First Geological Conference on Western Coal, ed. G.B. Mellon, J.W. Kramers, and E.J. Segal; Research Council of Alberta, Information series no. 60, p. 1-8.

MacKay, B.R.
1949: Atlas - coal areas of Alberta to accompany estimate of coal reserves; prepared for the Royal Commission on Coal, 1949; Canada Department of Mines and Resources, Geological Survey of Canada.

McNeely, R.N., Neismanis, V.P., and Dwyer, L.
1979: Water quality sourcebook. A guide to water quality parameters; Inland Waters Directorate, Water Quality Branch, Environment Canada.

Root, J.D.
1976: Physical environment of an abandoned strip mine near Cadomin, Alberta; Alberta Research Council, Bulletin 34, 33 p.

Torrey, S.
1978: Trace contaminants from coal; Pollution Technology Review, no. 50, Noyes Data Corporation, 294 p.

Weyer, K.U. and Vonhof, J.A.
1980: Water quality? - a discussion of "The effects of surface mining on water quality near Grande Cache, Alberta" by D.A. Hackbarth; Canadian Journal of Earth Sciences, v. 17, p. 952-955.

31.

THE LEACHING OF RADIONUCLIDES AND OTHER IONS DURING ALTERATION AND REPLACEMENT OF ACCESSORY MINERALS IN RADIOACTIVE ROCKS

Project 770061

J. Rimsaite
Economic Geology Division

Rimsaite, J., The leaching of radionuclides and other ions during alteration and replacement of accessory minerals in radioactive rocks; in Current Research, Part B, Geological Survey of Canada, Paper 82-1B, p. 253-266, 1982.

Abstract

Atomic proportions of radionuclides and other ions released during natural alteration and partial to complete replacement of the following minerals are presented and discussed in relation to the type and degree of their alteration:

1. *uraninite and secondary hydrated uranium oxides, silicates, phosphates, carbonates and sulphates;*
2. *uranothorite, uranoanthorianite, thorite, thorianite and thorogummite;*
3. *apatite, monazite, xenotime, bastnaesite and secondary radioactive phosphates;*
4. *allanite and alteration products;*
5. *ilmenite, rutile, anatase, brookite, titanite and chlorite;*
6. *pyrochlore, samarskite, fergusonite and metamict Nb-U and U-Y-Si, REE minerals;*
7. *pyrite, marcasite, chalcopyrite, molybdenite, galena and iron oxides;*
8. *Fe-Mg-tourmaline, Al-tourmaline and phyllosilicates;*
9. *zircon;*
10. *radionuclides and REE in fractures and crusts.*

Introduction

Cameron-Schimann (1978) determined chemical compositions of radioactive ore and accessory minerals and calculated average weight percentages of U, Th and rare-earth elements (REE) contained in minerals from radioactive occurrences in the Baie-Johan-Beetz area, Quebec. According to her calculations, uraninite is the main source of uranium, 75 per cent; thorogummite of thorium, 42 per cent; and monazite of REE, 40 per cent (Cameron-Schimann, 1978, Table 42). High power scanning electron micrographs, however, revealed the fractured and heterogeneous nature of ore and accessory minerals, implying that between 10 and 80 per cent of the uranium and other original radionuclides and nonradioactive ions have been leached from the minerals during alteration and replacement (Fig. 31.1; Rimsaite, 1981a). Fracturing and shattering of minerals result in part from radiation damage. The heterogeneity of the accessory minerals is due to subsequent alteration along fractures, to inclusions and to intergrowths of various mineral phases. Primary minerals either alter to secondary oxides, hydroxides, carbonates, silicates and phosphates, whereby part of the chemical constituents can remain in the altered host, or they are replaced by phyllosilicates, oxides and other constituents, all introduced from outside, and thus lose most or all the original constituents (Fig. 31.1).

Mineral inclusions can be older than, contemporaneous with, or younger than, the host, introduced after fracturing (Rimsaite, 1981b).

Some of the mineral phases can be identified using conventional optical and/or X-ray diffraction (XRD) procedures. However, most of REE- and Nb-bearing phases, secondary phyllosilicates and other hydrated and irradiated minerals are heterogeneous, too fine grained for optical identification (submicroscopic) and amorphous to X-rays (Rimsaite, 1979a). Some minerals produce unidentified X-ray patterns which may resemble, but are not identical with, known mineral species. Others, such as metamict minerals, yield X-ray patterns after heating. Such mineral phases which could not be positively identified by XRD are marked with a question mark preceding the number of their XRD patterns, e.g. fergusonite-polycrase (? XRD-65254). Scanning electron microscopy (SEM) coupled with energy dispersive spectrometry (EDS) have been used to determine chemical compositions of these fine grained and amorphous compounds.

This paper provides illustrated examples of the most common alterations and replacements, and in Tables 31.1 and 31.2, calculated atomic proportions of radionuclides and other constituents in primary and secondary minerals. Leached and added elements can be determined by comparing elemental contents of the primary, secondary and replacing (introduced from outside) minerals in Tables 31.1 and 31.2.

Acknowledgments

My sincere thanks are due to: A.C. Roberts for X-ray identification of minerals; D.A. Walker for the microbeam data, and the staff of the Photographic Section for preparation of photographic plates. I also thank I.R. Jonasson for the critical review of the manuscript and his valuable suggestions.

Examples

1. Alteration of Uraninite and of Secondary Hydrated Uranium Oxides, Silicates, Phosphates, Carbonates and Sulphates

Uraninite and pitchblende of Precambrian age consist of uranium oxides and of radiogenic lead. The proportion of uranium and lead in a mineral is a function of mineral age and of diffusion, losses and/or additions of uranium and lead. Additions and losses of radioactive and radiogenic constituents commonly result in marked variations in the Pb/U ratio within and between radioactive grains and in discordant Pb/U, Pb/Th and $^{207}Pb/^{206}Pb$ apparent isotopic ages (Rimsaite, 1982c).

Several varieties of Pb-rich mineral phases pseudomorphously replace uraninite grains. These include hydrated oxides and silicates.

Uraninite crystals replaced by a Pb-rich unnamed $PbUO_4$-like phase (? XRD-65225) occur in radioactive pegmatite in Baie-Johan-Beetz area, Quebec. Such uraninite grains, partly replaced by Pb-rich phases, crystallized within a biotite flake that grades to muscovite. A uraninite crystal replaced in part by the Pb-rich phase, has lost about 30 atomic percentage uranium and gained radiogenic lead (Rimsaite, 1981a, Fig. 17.3A,B; Rimsaite, 1982c, Fig. 3.5b). Other Pb-rich phases replacing uraninite and pitchblende include triuranium heptaoxide; curite and unnamed $Pb_2U_5O_{17}{\cdot}3H_2O$ (? XRD-65288); metastudtite (? XRD-65099); kasolite; vandendriesscheite; woelsendorfite and rarely anglesite. The pseudomorphous replacement of uraninite by anglesite results in the complete removal of uranium from the replaced part (Table 31.1, minerals 1a to 1i; Rimsaite, 1981a, Fig. 17.4).

Other secondary hydrated uranium oxides, such as masuyite, and silicates may contain variable quantities of radiogenic lead which replaces uranium, but in a hydrous environment, they usually grade to Pb-poor mineral aggregates, such as metastudtite (? XRD-65096).

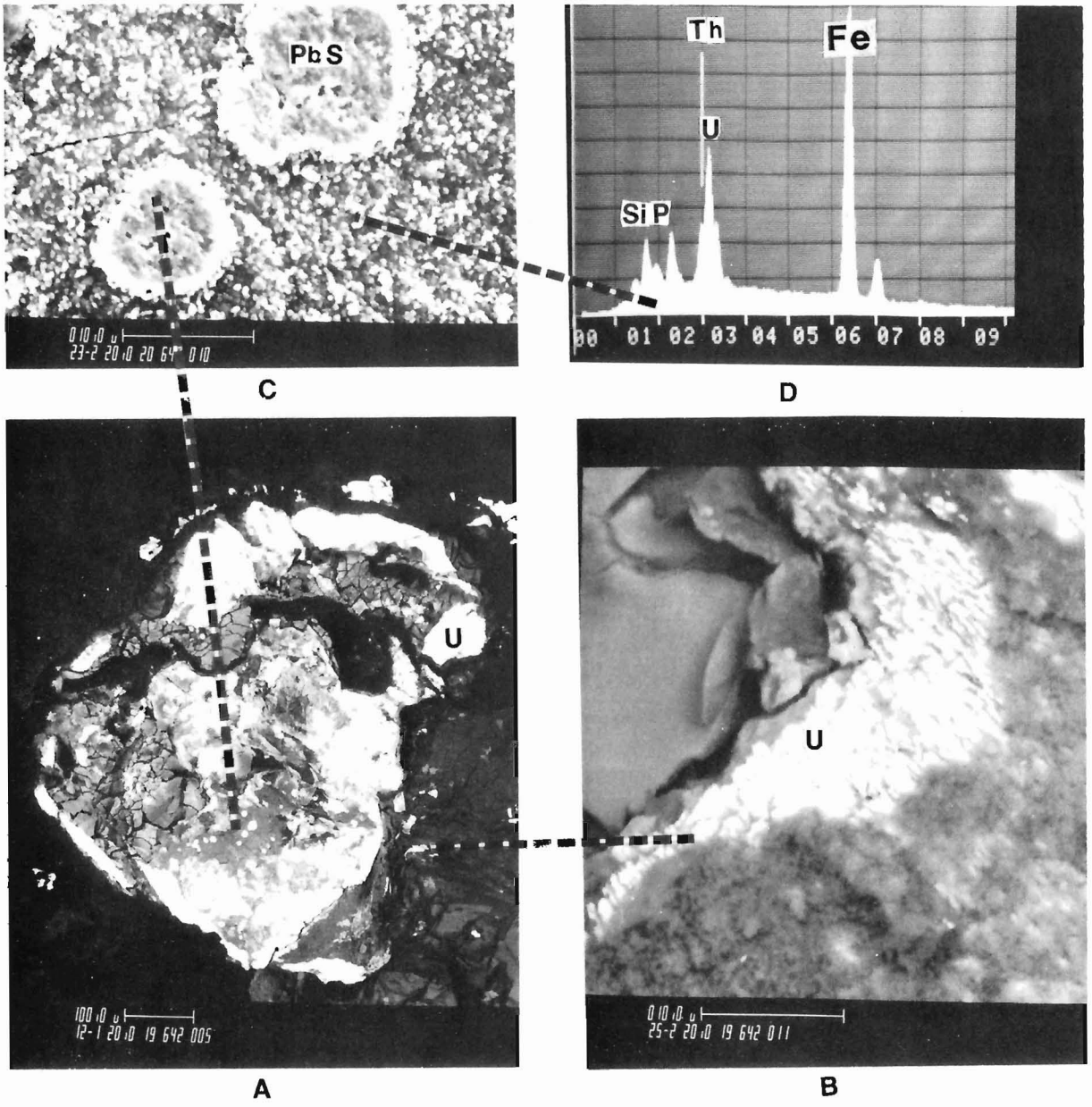

A. BEI of remnant uraninite (U, white) in Fe-rich gummite-like aggregates. Most of the replacing constituents were introduced from outside.*

B. BEI of fractured remnants of uraninite (U, white) partly replaced by phyllosilicates.

C. BEI of specked Fe-rich mineral aggregates with globules of secondary galena (PbS), enlarged from (A).

*D. ED spectrum of Fe-rich material replacing uraninite in (A,C): Fe>U>Th>Pb>Si>P**.*

Figure 31.1. *Fractured uraninite pseudomorphously replaced by fine grained Fe-rich aggregates and by phyllosilicates. GSC 203577-G*

* Backscattered electron images.

** The symbology U>Pb means that the U peak on the spectrum is higher than the Pb peak. It does not refer to the concentrations of these elements.

Table 31.1

Atomic percentages of elements in primary radioactive minerals and in their alteration products

Mineral	Atomic percentages										Elemental changes during replacements	
	O	U	Pb (Th)	H	Si (Cu)	Ca (Al)	S (K)	Mg (Fe)	C	P	Losses	Additions
1a. Uraninite	67	33										
1b. Unnamed $PbUO_4$	67	16	17								U	Pb
1c. Pb-triuraniumheptaoxide	54	14	6	26							U,O	Pb,H
1d. Curite	62	16	6	16							U,O	Pb,H
1e. Unnamed $Pb_2U_5O_{17}\cdot 3H_2O$	60	15	7	18							U,O	Pb,H
1f. Vandendriesscheite	57	16	5	22							U,O	Pb,H
1g. Kasolite	60	8	8	16	8						U,O	Pb,H,Si
1h. Woelsendorfite	58	12	3	24		3					U,O	Pb,H,Ca
1i. Anglesite	66		17				17				U	Pb,S
1j. Masuyite	50	10		40							U,O	H
1k. Metastudtite	55	9		36							U,O	H
1l. Coffinite	66	17			17						U	Si
1m. Sklodowskite	48	6		37	6			3			U,O	H,Si,Mg
1n. Uranophane	50	6		35	6	3					U,O	H,Si,Ca
1o. Boltwoodite	49	4		33	7		(7)				U,O	H,Si,K
1p. Halloysite	48			34	9	(9)					U,O	H,Si,Al
1q. Rutherfordine	72	14							14		U	O,C
1r. Liebigite	45	5		42		2			6		U,O	H,C,Ca
1s. Bayleyite	40	2		50				3	5		U,O	H,C,Mg
1t. Calcite	60					20			20		U,O	C,Ca
1u. Phosphuranylite	51	8		35		2				4	U,O	H,Ca,P
1v. Autunite	46	5		42		2				5	U,O	H,Ca,P
1w. Torbernite	46	5		42	(2)					5	U,O	H,Cu,P
1x. Zippeite	56	6		36			3				U,O	H,S
2a. Thorite	67		(16)		17							
2b. Uranothorite	67	8	(8)		17							
2c. Thorianite	66		(34)									
2d. Uranothorianite	66	17	(17)									
2e. Thorogummite	52	6	(6)	30	6						Th,O(U)	H,Si
2f. Goethite	50			25				(25)			Th,O(U)	H,Fe

Uranium silicates: coffinite, sklodowskite, uranophane and boltwoodite contain only small quantities of, or no detectable lead as determined by EDS, and are ultimately replaced by phyllosilicates (Table 31.1, minerals 1j to 1p).

Uranium carbonates commonly occur in altered radioactive rocks in association with calcite and/or fluorite and gypsum. Rutherfordine (XRD-65280) associated with kasolite, woelsendorfite and vandendriesscheite replaces radioactive minerals in fluorite-bearing U-Th-pegmatites in the Bancroft area. Other carbonates, liebigite and bayleyite, occur on wet walls of the open pit in the Rabbit Lake U-deposit, Saskatchewan (Rimsaite, 1977).

Fractured uraninite crystals replaced by coffinite which grades to zippeite-like aggregates (U,S) occur in mylonitized and partly oxidized pyrite-rich rocks in the Bancroft area (Fig. 31.2). Secondary calcite and phyllosilicates ultimately replace these hydrated uraniferous carbonates and sulphates (Table 31.1, minerals 1q to 1t, 1x).

Surface exposures of radioactive pegmatites in Baie-Johan-Beetz area, Quebec, locally contain patches of brightly coloured uranyl phosphates: phosphuranylite, autunite and torbernite. They form around uraninite, uranothorite, xenotime and altered monazite crystals (Table 31.1, minerals 1u, 1v, 1w; Rimsaite, 1982b, Fig. 3A-F).

2. Uranothorite, Uranoan Thorianite, Thorite, Thorianite and Thorogummite

In all granitoid rocks studied, thorium oxides and silicates are intergrown or closely associated with uranium and zirconium minerals. Uranothorite and uranoan thorianite grains contain varied quantities of uranium; U-free thorite and thorianite grains are very rare in radioactive rocks and were found only in oxidation zones where the original uranium was leached by oxidizing solutions. Uranothorite crystals are commonly speckled and zoned. They contain various inclusions and round aggregates of radiating chlorite enclosed in fluorite rims, representing the late pegmatitic liquids in the Bancroft area.

Uranothorite phases with and without Y and light REE, surround and replace uraninite grains along fractures, thus indicating that liquid residues containing U, Th, and REE were present after solidification of the pure U-Pb-uraninite. Thorian phases replacing shattered and fractured uraninite grains contain various proportions of uranium which may be derived from the partly replaced uraninite, thus part of the uranium leached from the host may be retained in the replacing phase (Table 31.1; Rimsaite, 1982c, Table 3.2, analyses 1, 6, 7).

Table 31.2

Atomic percentages of REE, P, Ti, Nb, B, Zr and other constituents in accessory minerals and in their alteration products

Mineral	Atomic percentages														Elemental changes during replacements	
	O	H (S)	P (B)	U (C)	Th (F)	Ce (Cl)	La (Ti)	Y (Zr)	Pb (Nb)	Si (Ta)	Al (Cu)	Fe (Mo)	Mg	Ca (K)	Losses	Additions
3a. Apatite	54		14		(6)	(6)								20		
3b. Xenotime	66		17					17								
3c. Monazite	66		17			10	7									
3d. Hydroxyl bastnaesite	58	14		(14)		9	5								P	H(C)
3e. Chlorite	50	22								6	11	3	8		O,P,Ce,La	H,Si,Al,Fe,Mg
4a. Allanite	59	5			2	2	1			13	9	2	2	5		
4b. Hydroxyl bastnaesite	58	14		(14)		9	5								Th,Si,Al,Mg,Ca	H(C)Ce,La
4c. REE-P-silicate	50	8	12	1	1	4	1	2		12	1	3	3	2	O,La,Al,Ca	H,U,Ce,Y,P
4d. Chlorite	50	22								6	11	7	4		O,Si,Th,Ce,La,Ca	H,Al,Fe,Mg
4e. K-feldspar	61									23	8			8	Th,Ce,La,Fe,Mg,Ca	Si,K
4f. Gummite-like	56	25		6	7					6					Ce,La,Si,Al,Fe,Mg,Ca	H,U,Th
4g. Galena		(50)							50						O,Th,Ce,La,Si,Al,Fe,Mg,Ca	Pb,S
5a. Ilmenite	60						(20)					20				
5b. Rutile, anatase, brookite	66						(34)									
5c. Titanite	61						(13)			13				13	Ti	Si,Ca
5d. U-Ti-silicate	54			16			(15)			15					O,Ca	U
5e. Chlorite	50	22								6	11	9	2		O,Ti,Si	H,Al,Fe,Mg
6a. Pyrochlore	50	5				(5)	(12)	2	(12)	(12)						
6b. Fergusonite	66							17	(17)							
7a. Pyrite		(66)										34				
7b. Chalcopyrite		(66)									(17)	17			Fe	Cu
7c. Molybdenite		(66)										(34)			Fe,Cu	Mo
7d. Galena		(50)							50						Mo,S	Pb
7e. Anglesite	66	(17)							17						S,Pb	O
8a. Zircon	66							(17)		17						
8b. Fe-gummite	56	25		3	3					6		7			O,Zr,Si	H,U,Th,Fe
9a. Fe-Mg-tourmaline	57	7	(6)							11	9	4	4	4		
9b. Al-tourmaline	57	7	(6)							11	18			1	Fe,Mg,Ca	Al

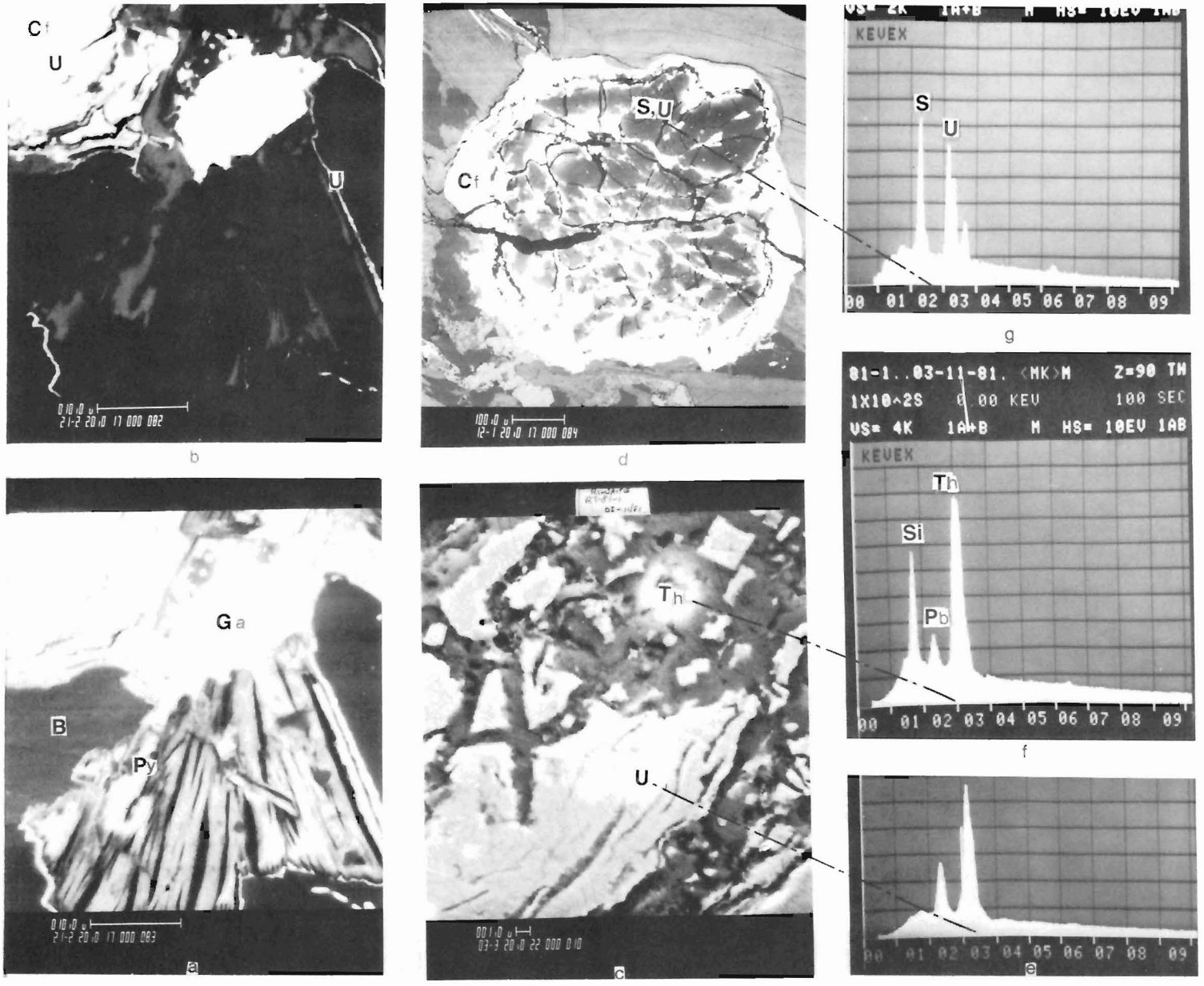

a,b. BEI of uraninite (U), partly replaced by coffinite (Cf) and surrounded by pyrite rim (Py) and grains of galena (Ga) in biotite (B). Pyrite blades are rimmed by U-bearing bands (U in Fig. b). Figures a and b are the same, but (a) is overexposed and (b) is underexposed to show various shades of grey produced by the minerals having extreme differences in their mass number.

c. BEI of uraninite (U) that is partly replaced by thorite (Th).

d. BEI of uraninite that is replaced by coffinite (Cf) and zippeite-like S-U-phase.

e. ED spectrum of uraninite in (c): U>Pb.

f. ED spectrum of thorite in (c): Th>Si>Pb.

g. ED spectrum of S-U-phase in (d): S>U>Ca.

Figure 31.2. *Uraninite in various stages of replacement by coffinite, Si-Th-phase and zippeite-like S-U phase. GSC 203724-G*

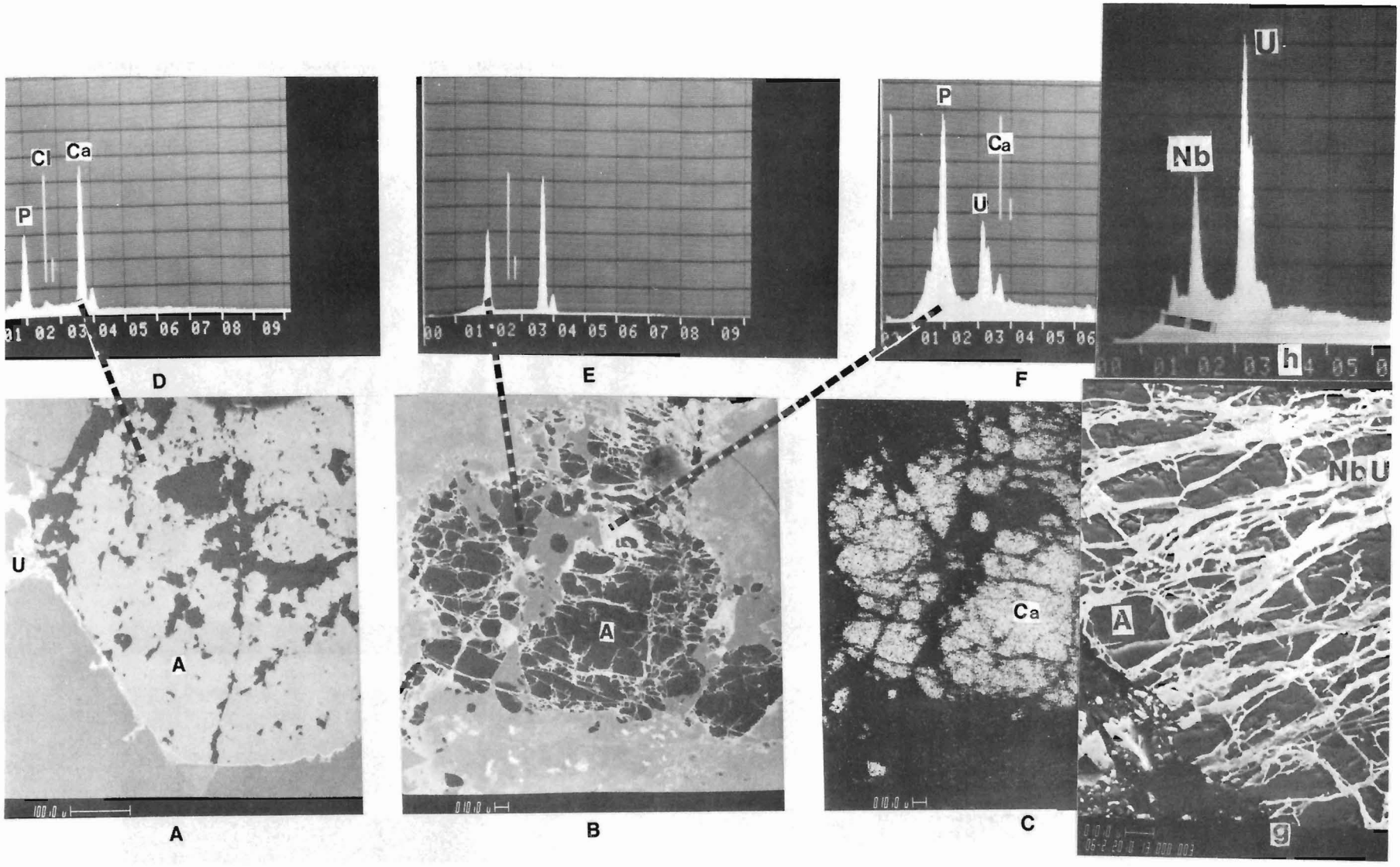

a. *BEI of fractured apatite (A) surrounded by U-bearing rims (U, white).*

b. *BEI of fractured apatite (A, black) that contains uraniferous phases in fractures (pale grey).*

c. *Electron scanning image (map) for Ca, showing distribution of Ca in the fractured apatite in (B).*

d. *ED spectrum of Cl-bearing apatite in (A): Ca>P>Cl.*

e. *ED spectrum of apatite in (B): Ca>Si (Cl concentration is below the limit of detection).*

f. *ED spectrum of autunite-like uraniferous phase in fractures of apatite grain in (B): P>U>Ca>Si.*

g. *BEI of shattered apatite (A) that is traversed by fractures filled with Nb-U-phase.*

h. *ED spectrum of Nb-U-phase in apatite in (g): U>Nb>Si.*

Figure 31.3. *Shattered and partly replaced apatite crystals. GSC 203532-I*

Thorite and uranoanthorianite occur in contact zones between pyroxenite, granite pegmatite and fluorite-carbonate veins, common in the Bancroft area.

In oxidation zones of U-Th deposits, uranothorite alters either to unidentified Pb-rich phases or to Fe-rich gummite. Such alteration and replacements cause losses of Th and U (50 to 70 per cent) and additions of Pb, Fe and Si (Rimsaite, 1982c, Table 3.2, analyses 8, 13). Thorogummite grains ultimately alter to siliceous iron oxides or to limonite. Losses and gains during replacement and alteration of Th minerals are summarized in Table 31.1, minerals 2a to 2d.

3. Apatite, Monazite, Xenotime, Bastnaesite and Secondary Radioactive Phosphates

In radioactive occurrences, apatite, monazite and xenotime grains contain inclusions and radionuclide-bearing crusts, and crystallize in groups with micas, uraninite, uranothorite, zircon, allanite and pyrochlore (Rimsaite, 1981a, Fig. 17.5). Apatite grains are abundant in granitoid rocks adjacent to, or contaminated with xenoliths of mafic and calcic rocks. Although apatite is relatively stable in hydrothermal and in weathering environments, shattered crystals partly replaced by an unidentified U, Nb-bearing phase were found in relatively fresh pyrochlore pegmatite from the Bancroft area (Fig. 31.3). Phosphate ion and calcium leached from the fractured apatite can react with uranium and other ions to form secondary uraniferous phosphates (Table 31.1, minerals 1u, 1v, 1w).

Monazite and xenotime are important ore minerals of Ce, La, Th, Y and of other REE. Monazite is associated with, and can alter to, REE carbonate (a member of hydroxyl bastnaesite series, XRD-65148). Association of monazite, xenotime, apatite, zircon and U-Th minerals alters and is replaced by fine grained poorly crystallized glauconite-chlorite (? XRD-65175), chlorite (XRD-65176), amorphous phyllosilicates (XRD-65157), and patches of anatase, kasolite, uranophane and secondary REE-carbonates and U-phosphates (Rimsaite, 1981b, Fig. 4.3). Unidentified REE aggregates, overgrown on monazite, resemble bastnaesite in their ED spectrum (Fig. 31.4). Compared to the monazite host, these overgrowths contain a higher concentration of REE and a higher proportion of La, implying that REE-rich phases have been added to the host monazite as crusts during late deuteric or hydrothermal stages.

Table 31.2, minerals 3a, to 3e, illustrate chemical changes during replacements of primary phosphates by REE-rich and REE-poor phases, such as carbonates and phyllosilicates.

4. Allanite and Alteration Products

Allanite-rich pegmatites occur in the Bancroft area, Ontario, and allanite-zircon-biotite bands are common in radioactive metaquartzites and in pegmatites associated with basic rocks in the Mont-Laurier area, Quebec (Rimsaite, 1978). As a result of inclusions, alteration and replacements, allanite crystals are very heterogeneous. Some grains are partly replaced by patches of microcline, chlorite and amorphous phyllosilicates and contain inclusions of thorite, uraninite, micas, zircon, baddeleyite (? XRD-65363), REE-bearing phosphates, specks and crusts of galena, unidentified (metamict) Y, Ce, La-silicates and allanite (Fig. 31.5; XRD-65364, 65365; Rimsaite, 1982a, Fig. 38.6c,d). In radioactive rocks from the Mont-Laurier area, Quebec, U-, Th-bearing allanites are metamict, fractured and contain higher concentrations of REE along fractures, rims and around radioactive inclusions. The late crystallized REE mineral aggregates in fractures and rims of a relatively fresh allanite grain from the Madawaska Mine, Bancroft area, contain higher La/Ce ratios than the unaltered host, thus confirming relative increase of La with the sequence of crystallization (Van Wambeke, 1977). The unaltered grain of allanite yielded an XRD pattern of allanite, whereas REE-rich material along fractures was identified as a mixture of allanite and a member of hydroxyl bastnaesite series (XRD-65367), and U-, Th-bearing rims were poorly crystallized or amorphous (unidentified, XRD-65386 to 65389).

Partly altered allanite has a mottled appearance and consists of several phases, including small specks of galena and of uranothorite, identified in their ED spectra (Fig. 31.5, 31.6). General chemical trends during common alterations and replacements of allanite are given in Table 31.2, minerals 4a to 4g. However, some elements, such as U, Th and REE are present in the allanite structure and in inclusions and fractures of the host allanite. With an exception of REE carbonate, most of the secondary REE-rich mineral aggregates are amorphous or produced weak unidentified X-ray patterns (XRD-65386). In a hydrous oxidizing environment, inclusions alter with the allanite host, and leached elements reprecipitate in secondary minerals and crusts. Table 31.2 presents theoretical chemical compositions of the replacing mineral phases, whereas natural secondary mineral phases are more complex (Rimsaite, 1982c, Table 3.2, allanite and alterations, analyses 5, 19-24).

5. Ilmenite, Rutile, Anatase, Brookite, Titanite and Chlorite

Ilmenite grains intergrown with uraninite crystallize in epidote veins that fill fractures in feldspar (Rimsaite, 1982c, Fig. 3.3a,b). At high magnification, the ilmenite appears fractured and altered to titanium and iron oxides. At the contact with uraninite, fragments of shattered rutile and anatase alter and are partly replaced by chlorite-like groundmass (XRD-65231).

In metamorphic and tectonically deformed rocks, ilmenite alters to titanite. Titanite and associated allanite are major constituents of the high grade U-Th-REE ore in the Bancroft area. Abundant titanite occurs at the contact between granite pegmatite and mafic metamorphic rocks and their xenoliths. In quartz mylonites, Bancroft area, titanite grains are deformed, partly replaced by chlorite and locally recrystallized to anatase, brookite and calcite aggregates. The remnant titanite grains and recrystallized Ti-oxides locally contain coatings and patches of REE mineral aggregates and disseminated uraninite grains (Fig. 31.8). Because uraninite grains in titanite are surrounded by La-rich REE rims, the reaction between the uraninite and titanite did not take place. However, in mylonitic rocks containing massive pyrite, remnants of titanite in direct contact with uraninite reacted to form unidentified U, Ti, Si compounds (Fig. 31.7b,c,f). Losses and gains of various elements during transition from titanite to oxides and during replacements of Ti-minerals by phyllosilicates are summarized in Table 31.2, minerals 5a to 5e.

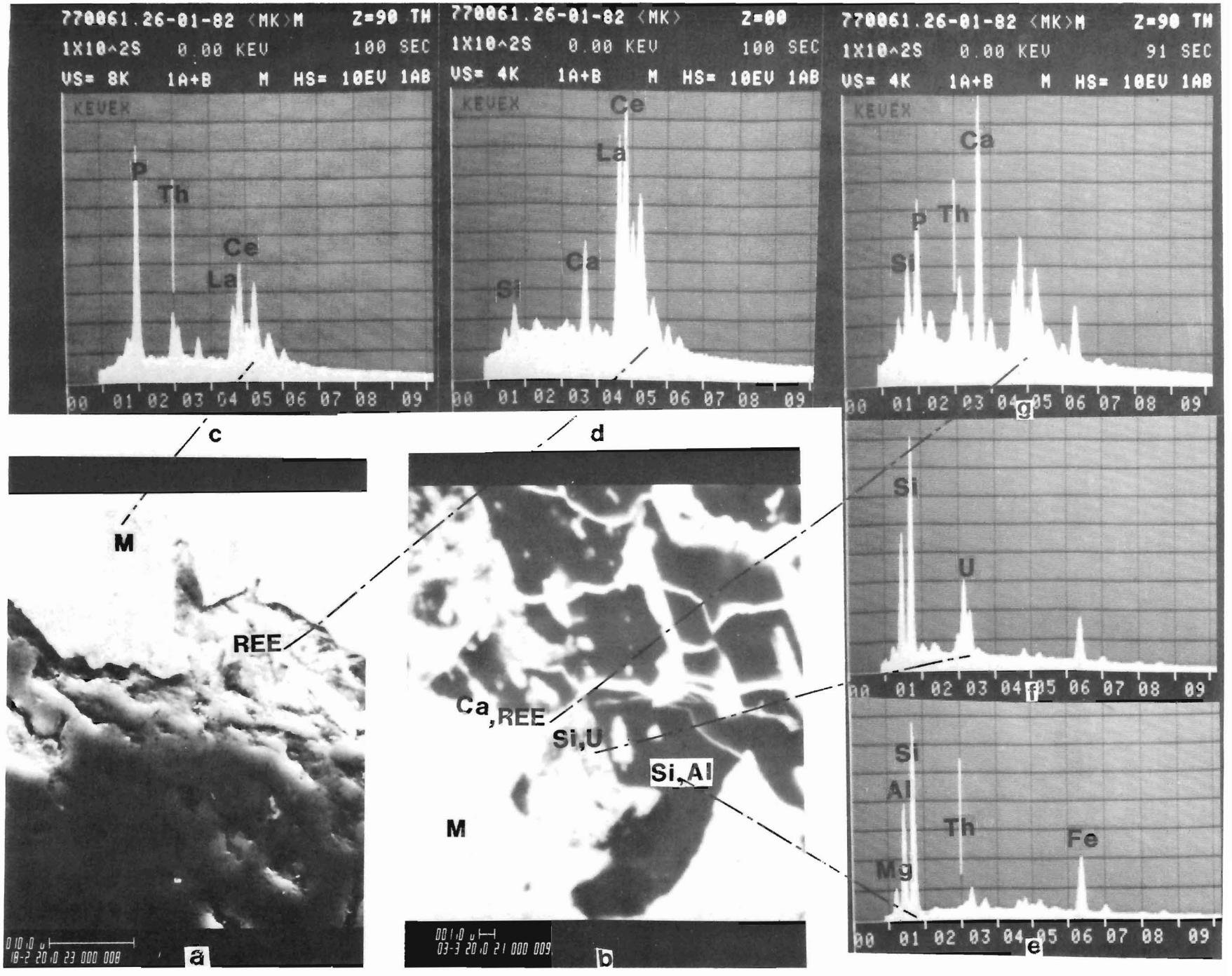
770061.26-01-82 (MK)M Z=90 TH
1X10^2S 0.00 KEV 100 SEC
VS= 8K 1A+B M HS= 10EV 1AB
KEVEX
P
Th
Ce
La
00 01 02 03 04 05 06 07 08 09
770061.26-01-82 (MK) Z=00
1X10^2S 0.00 KEV 100 SEC
VS= 4K 1A+B M HS= 10EV 1AB
KEVEX
Ce
La
Ca
Si
00 01 02 03 04 05 06 07 08 09
770061.26-01-82 (MK)M Z=90 TH
1X10^2S 0.00 KEV 91 SEC
VS= 4K 1A+B M HS= 10EV 1AB
KEVEX
Ca
P Th
Si
00 01 02 03 04 05 06 07 08 09
g
c
d
M
REE
a
Ca,REE
Si,U
Si,Al
M
b
Si
U
00 01 02 03 04 05 06 07 08 09
f
Si
Al
Th
Fe
Mg
00 01 02 03 04 05 06 07 08 09
e

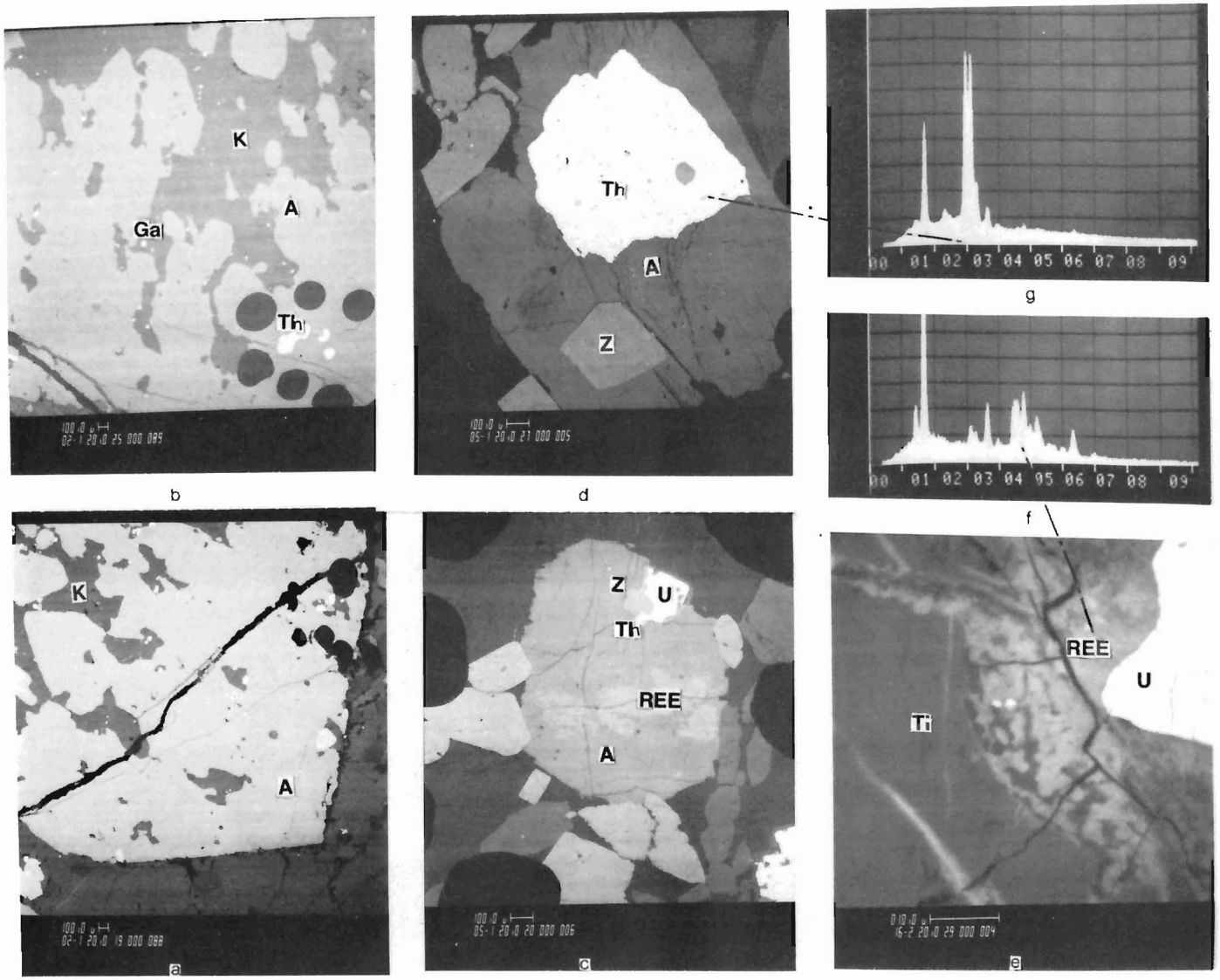

Figure 31.4 *(opposite). Monazite surrounded by REE-rich crusts and by fractured rims filled with radioactive REE-bearing phases. GSC 203724-M*

a. BEI of monazite (M) with resorbed edges, replaced by REE-rich phase (REE).

b. BEI of monazite (M) surrounded by fractured rims. The fractures are filled with REE and radioactive phases.

c. ED spectrum of thorian monazite in (a): P>Ce>La>Th>Ca.

d. ED spectrum of REE-rich rim on monazite in (a): Ce>La>Ca>Si. Note a relatively higher intensity of La in the rim than that in the monazite spectrum in (c).

e. ED spectrum of REE-bearing phyllosilicates surrounding monazite in (b): Si>Al>Fe>Mg>K>Ca>Ce.

f. ED spectrum of radioactive phases in fractures surrounding monazite in (b): Si>Al>U>Fe>Th>Y = Pb = Ce = Al.

g. ED spectrum of Ca-rich edges of monazite in (b): Ca>P>Si = Ce>La>U>Th = Pb>Al.

Figure 31.5 *(above). Mineral inclusions in, and intergrowths and replacements of, allanite and titanite. GSC 203724-J*

a. BEI of fractured allanite crystal (A) and patches of microcline (K, grey).

b. BEI of allanite-microcline intergrowths (A, K) that contain disseminated specks of galena and inclusions of uranothorite (Th) marked for a microbeam analysis with black ink dots (in lower part, right).

c. BEI of fresh allanite (A, XRD-65365) with inclusions of zircon (Z), uraninite (U) and uranothorite (Th), and a REE-rich patch of hydroxyl bastnaesite (XRD-65367) along a horizontal fracture.

d. BEI of fresh allanite (A) with inclusions of zoned zircon (Z) and of uranothorite (Th).

e. BEI of titanite (Ti) and uraninite (U). The uraninite in titanite is overgrown by REE-bearing rim (REE).

f. ED spectrum of REE-bearing rim on uraninite in (e): Si>Ca = Ti = La>Ce = Al>U.

g. ED spectrum of uranothorite in (d): Th = U>Si>Ca = Pb.

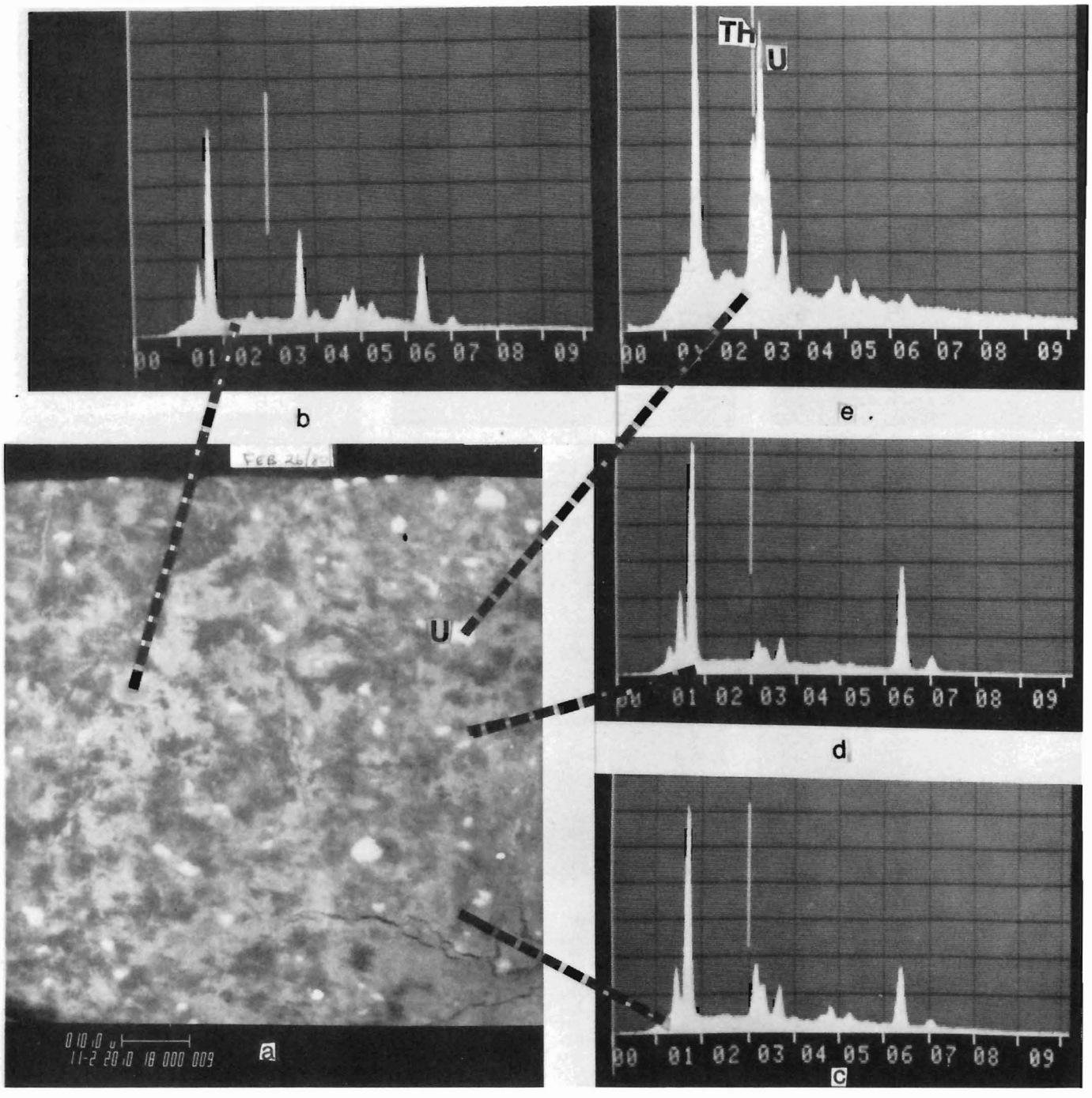

a. *BEI of mottled allanite that consists of irregular relatively unaltered patches (light grey), uraniferous patches (medium grey), Fe-rich patches (dark grey <5 µm in size) and small specks of uranothorite (U, white 1-3 µm in size).*

b. *ED spectrum of remnant allanite patches in (a): Si>Ca>Fe>Al>Ce>La.*

c. *ED spectrum of altered uraniferous patches in (a): Si>Fe = U = Al>Ca>Ce>La.*

d. *ED spectrum of Fe-rich patches in altered allanite in (a): Si>Fe>Al>U = Ca>Mg.*

e. *ED spectrum of uranothorite in altered allanite in (a): Si>U>Th>Ca>Ce>La.*

Figure 31.6. *Mottled appearance of an altered allanite. GSC 203755-A*

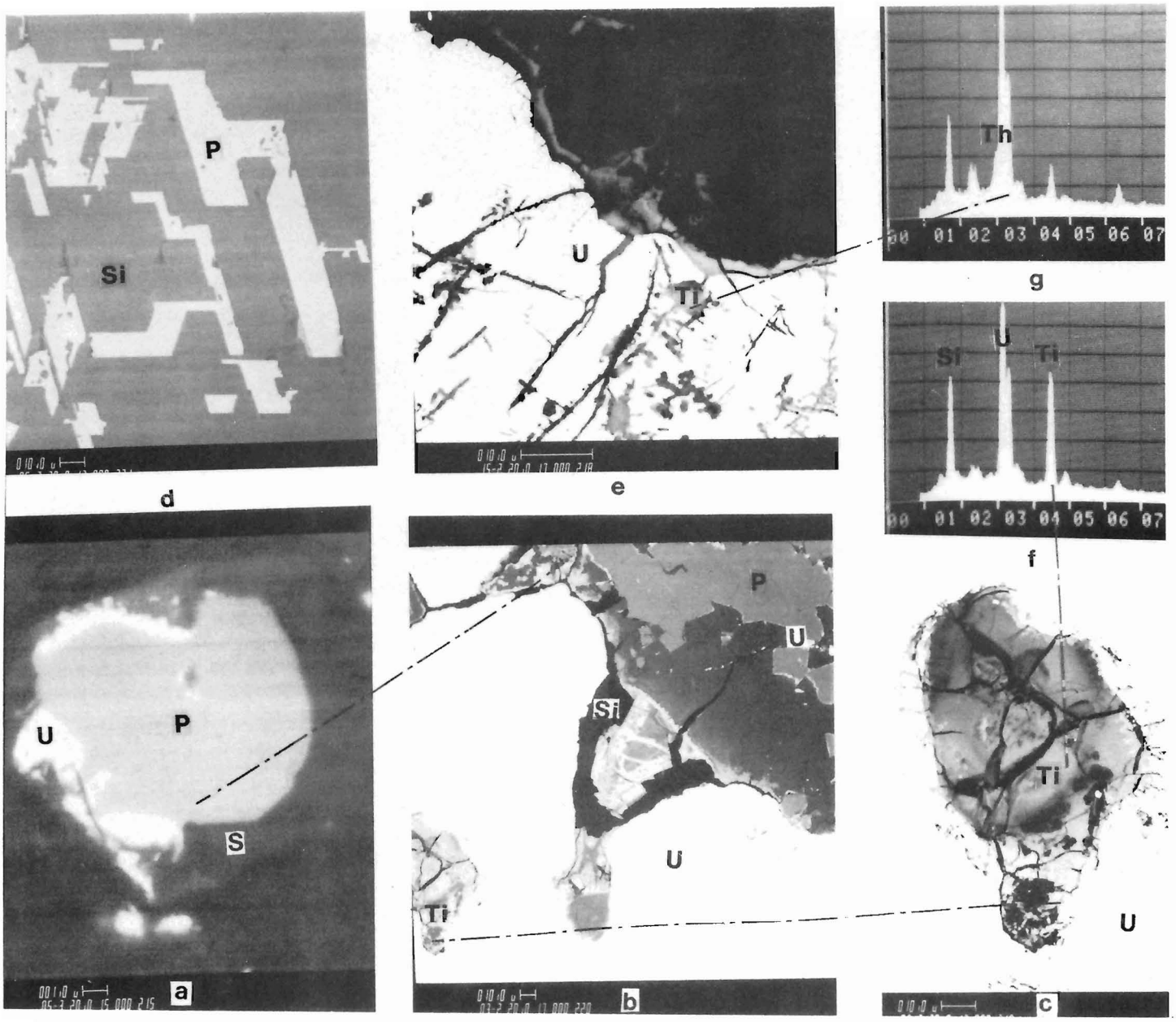

a. BEI of pyrite (P) that is surrounded by uraniferous rims (U) in a groundmass of phyllosilicates and disseminated sulphides (S) at the edge of massive pyrite in (b).

b. BEI of uraninite (U) with enclosed grains of altered titanite (Ti) in massive pyrite (P). The massive pyrite has recrystallized to small pyrite cubes and is partly replaced by chlorite with U-bearing specks at the contact with uraninite.

c. BEI of altered titanite (Ti) in uraninite (U), enlarged from (b). The titanite reacted with the host uraninite to form U-Si-Ti compounds that contain variable proportions of U and Si.

d. BEI of pyrite blades (P) in mylonitic quartz (Si).

e. BEI of fractured uraninite (U, white) that is partly replaced by Th-Ti-bearing phase (Ti-grey).

f. ED spectrum of U-Si-Ti grains in (c): U>Si = Ti.

g. ED spectrum of Ti-bearing phase that replaces and coats uraninite in (e): U>Si>Th = Pb = Ti>Fe.

Figure 31.7. *Three generations of pyrite in radioactive mylonites and reactions between uraninite and enclosed titanite. GSC 203724-L*

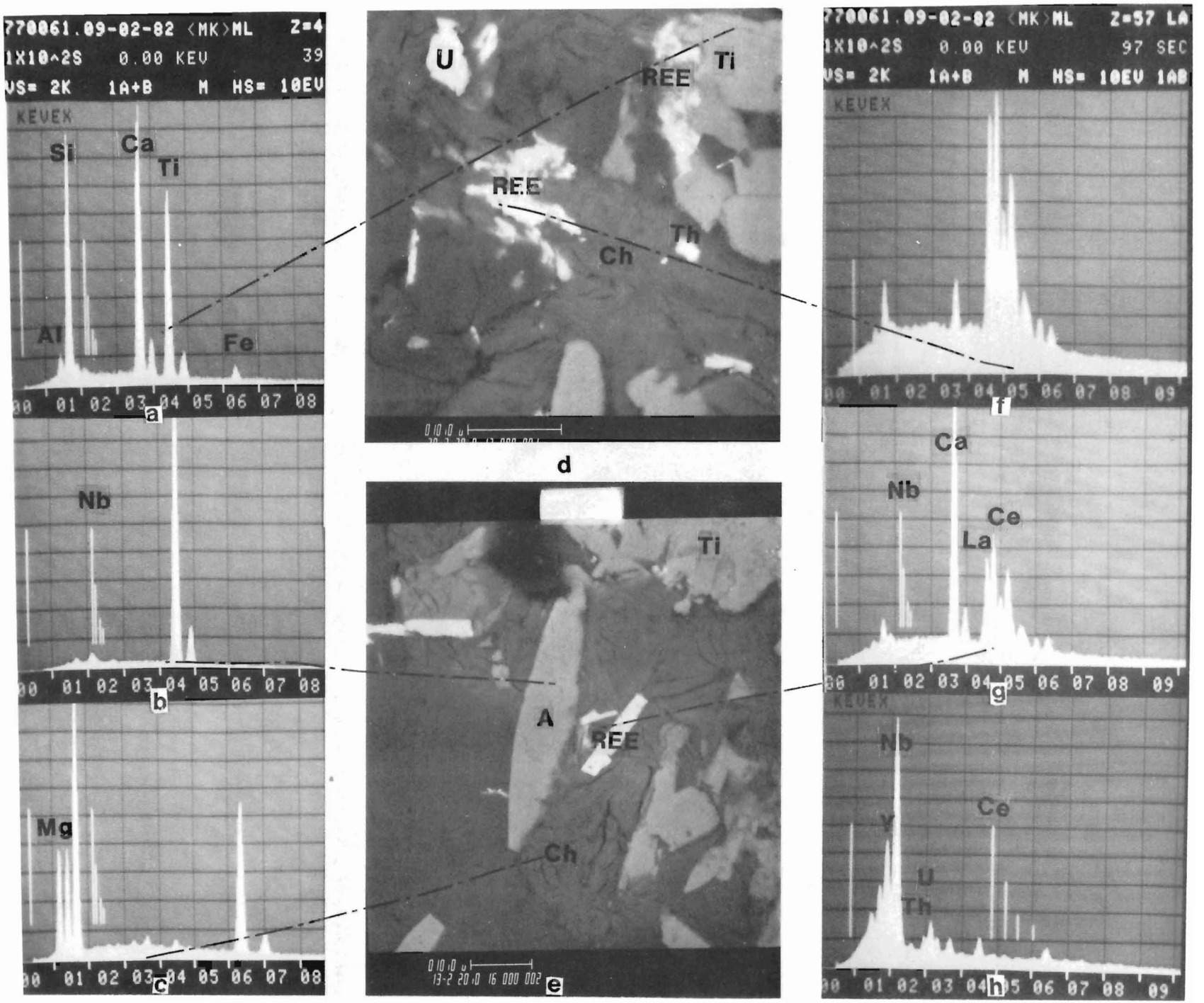
770061.09-02-82 (MK)ML Z=4
1X10^2S 0.00 KEV 39
VS= 2K 1A+B M HS= 10EV
KEVEX
Si
Ca
Ti
Al
Fe
00 01 02 03 04 05 06 07 08
a
Nb
00 01 02 03 04 05 06 07 08
b
Mg
00 01 02 03 04 05 06 07 08
c
U
REE
Ti
REE
Th
Ch
d
Ti
A
REE
Ch
e
770061.09-02-82 (MK)ML Z=57 LA
1X10^2S 0.00 KEV 97 SEC
VS= 2K 1A+B M HS= 10EV 1AB
KEVEX
00 01 02 03 04 05 06 07 08 09
f
Ca
Nb
Ce
La
00 01 02 03 04 05 06 07 08 09
g
KEVEX
Nb
Ce
Y
U
Th
00 01 02 03 04 05 06 07 08 09
h

6. Pyrochlore, Samarskite, Fergusonite and Metamict Nb-U and U-Y-Si, REE Minerals

Pyrochlore, samarskite, fergusonite-polycrase and unidentified Nb-U and U-Y-Si minerals are metamict and contain varied proportions of Ti, Nb, Ta, U and REE as determined in their ED spectra. After heating, one glassy chip yielded an X-ray pattern similar to, but no identical with, samarskite and fergusonite-polycrase (XRD-65245, 65254).

A pyrochlore studied from the Bancroft area contains 21 weight per cent U and 32 weight per cent Nb. It alters to mottled U-rich and Ta-rich phases (Rimsaite, 1982c, Fig. 3.4d, Table 3.2, analyses 3, 15-17). Pyrochlore from the Baie-Johan-Beetz area, Quebec, is associated with pseudorutile (XRD-65205) and contains more Ti, Th and Y, and less U, Nb and Ta than the pyrochlore from the Bancroft area (Rimsaite, 1982c, Table 3.2). Pyrochlore from the Bancroft area occurs in intergrowths with uraninite and commonly contains Ti minerals and Ti-bearing mineral aggregates in surrounding rims. The mobile U, Nb-rich phase enters fractures in shattered apatite adjacent to altered pyrochlore (Fig. 31.3).

Metamict U-Y-Si grains, associated with anatase, brannerite-like mineral and uranothorite in the Baie-Johan-Beetz area produced a weak X-ray pattern of uraninite and coffinite-like structures (XRD-65213; Rimsaite, 1981a, Fig. 17.5A). In high grade U, Th, REE ore from the Bancroft area, unidentified metamict yellow grains and patches contain disseminated specks of galena and yielded an X-ray pattern for galena only (XRD-65406). These unidentified metamict minerals consist of Si, Y, Ce, La and varied proportions of U, Th, Fe and Ca. Because such metamict minerals are very heterogeneous, contain numerous inclusions, and grade to amorphous chlorite or vermiculite-like aggregates (XRD-65255), it is technically impossible to separate homogeneous domains for a meaningful X-ray identification of heated fragments. Thus, large proportions of REE and Nb minerals which are an important source of REE can be overlooked using the conventional XRD procedures, but they can be identified and studied using EDS and SEM.

Poorly crystallized chlorite, serpentine and vermiculite-like mineral aggregates ultimately replace the metamict U-Nb, U-Y-Si and U-Th-Ce-La-Si minerals (XRD-65201). The calculated atomic proportions of various constituents that can be leached during replacement of the metamict Nb-Ta-REE minerals are given in Table 31.2, minerals 6a to 6d, and their elemental contents determined by semiquantitative EDS analyses, by Rimsaite, 1982c, Table 3.2, analyses 3, 15-18.

7. Pyrite, Marcasite, Chalcopyrite, Molybdenite, Galena and Iron Oxides

In uranium occurrences studied, sulphides occur in several generations and commonly alter to carbonates, iron oxides and sulphates, thus liberating sulphur. Figure 31.7 illustrates three generations of pyrite in quartz mylonite from the Bancroft area. Massive pyrite of the first generation crystallizes along fractures of deformed granitoid rock and bands of quartz mylonite and engulfs uraninite and titanite. Microscopic studies of the sequence of crystallization indicate that the massive pyrite recrystallizes around the edges to euhedral pyrite crystals which are coated with U-bearing films (Fig. 31.7b); the last generation of pyrite crystallizes as narrow blades in interstices of mylonitized quartz (Fig. 31.7d). In surface exposures, some pyrite grains recrystallize to fine grained marcasite aggregates (XRD-65058). Pyrite commonly crystallizes in a groundmass of Fe-rich phyllosilicates. It can alter to jarosite (XRD-65525).

Sulphides crystallized in the following sequence: pyrite, chalcopyrite and molybdenite -2H (XRD-65057). Molybdenite is one of the latest sulphides. It crystallizes in fractures after solidification of the host rock and locally can be replaced by galena along the basal fractures (Rimsaite, 1982c, Fig. 3.3e). In radioactive rocks, much of the galena is radiogenic and forms from the lead liberated from altered radioactive minerals during metamorphism and tectonic activity. In an oxidizing environment, galena alters to anglesite, chalcopyrite to malachite, and other sulphides are replaced by hematite and goethite (XRD-65072), brightly coloured gummite and phyllosilicates (optical SEM and EDS determination). Red pegmatites commonly contain remnants of oxidized sulphides. The calculated atomic proportions of Fe, Cu, Mo, Pb and S that can be leached during oxidation and during replacement of sulphides by phyllosilicates are given in Table 31.2, minerals 7a to 7e.

8. Fe-Mg-Tourmaline, Al-Tourmaline and Phyllosilicates

In radioactive granitoid rocks from the Madawaska Mine, Bancroft area, tourmaline followed by amorphous chlorite crystallized from residual liquids. The tourmaline and associated amorphous radioactive REE-bearing chlorite-like aggregates engulfed numerous radioactive and accessory minerals. During alteration of radioactive rocks the chemically complex Fe-Mg-tourmaline recrystallizes to secondary Al-rich radiating tourmaline needles and is gradually replaced by phyllosilicates (Rimsaite, 1979b, Table 32.1, analyses II-3 and II-8). Compared to the original Fe-Mg-tourmaline, the white secondary Al-tourmaline has a relatively simple chemical composition, implying that many constituents have been leached during the transition. Calculated atomic proportions of chemical constituents in Fe-Mg- and Al-tourmalines and eventual losses of various constituents can be seen by comparing minerals 9a, 9b, in Table 31.2 and analyses II-3, II-8, II-9, II-11 and IX-1 in Table 32.1 of Rimsaite (1979b).

9. Zircon

Cyrtolite is a common companion of uraninite and uranothorite. Among various mineral inclusions, zircon grains contain iron sulphide blades and apatite. In spite of relative resistance to weathering, zircons can alter in an oxidizing environment, such as Fe-rich thorogummite, and release zirconium and other ions (Table 31.2, minerals 8a, 8b).

Heterogeneous zircons, their application for isotopic age dating and to petrology have been discussed in some detail by Rimsaite (1981b).

Figure 31.8 *(opposite). Illustrations of titanite, altered to secondary Ti-oxides, that is partly replaced by chlorite containing disseminated REE, U and Th minerals. GSC 203724-N*

a. ED spectrum of titanite in (d): Ca>Si>Ti.

b. ED spectrum of Nb-bearing anatase in (e): Ti>Nb.

c. ED spectrum of chloritic groundmass in (e): Si>Fe>Al = Mg.

d. BEI of altered titanite (Ti) which is partly replaced by chlorite (Ch) with disseminated REE-bearing patches and specks of uraninite (U), and thorite (Th).

e. BEI of altered titanite that is in part recrystallized to anatase blades (A) and replaced by chlorite (Ch) containing disseminated Ca-rich REE minerals.

f. ED spectrum of REE-rich mineral aggregates in (d): Ce>La>Ca>Si. It is important to note that the chlorite and REE minerals were not detected in XRD patterns of these altered titanites.

g. ED spectrum of REE-rich mineral aggregates in (e): Ca>Ce>La>Si>Y.

h. ED spectrum of metamict Nb-Y mineral that after heating produced fergusonite-polycrase XRD pattern (XRD-65254).

10. Radionuclides and REE in Mineral Fractures and Crusts

Some minerals, such as allanite, monazite, xenotime and zircon, can contain radionuclides and REE in their structure and in inclusions, whereas other rock-forming and accessory minerals have no radionuclides and REE detectable in their energy dispersive spectra, but may have radioactive mineral inclusions and crusts. In radioactive occurrences studies, crusts, coatings and rims may have varied and very complex chemical compositions (Rimsaite, 1982c, Table 3.2, analyses 25 to 28; Rimsaite, 1982b, Table 2). These crusts and inclusions can alter with the host and thus liberate various radionuclides and REE and contribute U, Th, REE, Mn, Ti, Zr and Pb for the formation of secondary deposits. Lead is usually radiogenic. It precipitates in the form of galena or a Pb-rich uranium compound in fractures in pyrite, feldspar and mica thus altering the isotopic composition of the rock lead. Feldspar and biotite containing U-Pb-rich coatings on fractures yielded old apparent isotopic ages (Rimsaite, 1982c, Table 3.3).

Summary and Conclusions

This study of ore and accessory minerals in high power electron micrographs provides data on the nature and extent of alteration and replacements of radioactive and REE minerals under natural environmental conditions in uranium occurrences. Examples of common alterations are illustrated in electron micrographs and in energy dispersive spectra, and atomic proportions of major constituents in primary, secondary and replacing phases introduced from outside are summarized in Table 31.1 and 31.2 for the following minerals:

1. Uraninite, the principal source of uranium in radioactive occurrences examined, alters to secondary hydrated oxides, silicates, carbonates, phosphates, sulphates and eventually can be replaced by oxides and phyllosilicates. Depending on the physicochemical environment and on availability of P, C, Si, S and other entities that can capture liberated uranium and form secondary U minerals, losses of uranium range from 20 to 100 per cent.

2. Thorium minerals replace uraninite and alter to thorogummite, Fe-rich thorites, and can be replaced by siliceous goethite and/or phyllosilicates. Uranium and Th minerals enclosed in micas, commonly alter to Pb-rich mineral aggregates.

3. Allanite, monazite, xenotime and zircon contain radionuclides and REE in their crystal structure and in inclusions. The inclusions alter with the host and released ions can reprecipitate within the altered mineral, thus retaining all or part of the original constituents in secondary mineral aggregates, or the released ions can be leached out.

4. Many primary REE, Nb-U and U-Y-Si minerals are metamict. Altered pyrochlore is heterogeneous and breaks down to Nb-U, Ta-, and Y-rich phases. The Nb-U phase seems to be very mobile and fills fractures in adjacent apatite.

5. Titanite, apatite, pyrite, micas and feldspar may contain radionuclides and REE in fractures, rims and mineral inclusions. The concentration level of radionuclides and REE is below detection limits in ED spectra of these minerals. The new data on U- and Pb-bearing crusts in overgrowths on pyrite and in fractures of rock-forming minerals are important for the interpretation of isotopic ages and for determination of isotopic composition of the "rock lead" in Pb isotope studies.

6. Transformation of chemically complex Fe-Mg-tourmaline to relatively simple Al-tourmaline accompanied by leaching of various ions provides data that may be useful for studies on the behaviour of various constituents in boron glasses under comparable conditions of alteration.

7. In addition, this study provides basic data on quantities of radionuclides and REE that can be leached from accessory minerals in natural radioactive occurrences. Depending on environmental conditions, the leached constituents can be fixed in metastable secondary minerals and crusts along fractures, or they dissolve in aqueous solutions and migrate out from the host rock. The dissolved radionuclides and REE can reprecipitate under favourable conditions thus contributing to the formation of secondary mineralizations.

References

Cameron-Schimann, M.
1978: Electron microprobe study of uranium minerals and its application to some Canadian deposits; unpublished Ph.D. thesis, University of Alberta, Edmonton, Canada, 337 p.

Rimsaite, J.
1977: Occurrences of rare secondary U- and Pb-bearing mineral aggregates in uranium deposits, Northern Saskatchewan: a progress report; in Current Research, Part C, Geological Survey of Canada, Paper 77-1C, p. 95-97.

1978: Mineralogy of radioactive occurrences in the Grenville Structural Province Ontario and Quebec: a preliminary report; in Current Research, Part B, Geological Survey of Canada, Paper 78-1B, p. 49-58.

1979a: Natural amorphous materials, their origin and identification procedures; in Development in Sedimentology 27, ed. M.M. Mortland and V.C. Farmer; International Clay Conference, 1978, p. 567-576.

1979b: Petrology of basement rocks at the Rabbit Lake deposit and progressive alteration of pitchblende in an oxidation zone of uranium deposits in Saskatchewan; in Current Research, Part B, Geological Survey of Canada, Paper 79-1B, p. 281-299.

1981a: Petrochemical and mineralogical evolution of radioactive rocks in the Baie-Johan-Beetz area, Québec: a preliminary report; in Current Research, Part A, Geological Survey of Canada, Paper 81-1A, p. 115-131.

1981b: Isotope, scanning electron microscope, and energy dispersive spectrometer studies of heterogeneous zircons from radioactive granites in the Grenville Structural Province, Québec and Ontario; in Current Research, Part B, Geological Survey of Canada, Paper 81-1B, p. 25-35.

1982a: Mode of occurrence of secondary radionuclide-bearing minerals in natural argillized rocks: a preliminary report related to a barrier clay in nuclear waste disposal; in Current Research, Part A, Geological Survey of Canada, Paper 82-1A, p. 247-259.

1982b: Alteration of radioactive minerals in granite and related secondary uranium mineralizations; in Ore Genesis – The State of the Art, ed. G.C. Amstutz, A. El Goresy, G. Frenzel, C. Kluth, G. Moh, A. Wauschkuhn, and R.A. Zimmermann; Springer-Verlag, Berlin, Heidelberg, New York, p. 269-280.

1982c: Mineralogical and petrochemical properties of heterogeneous granitoid rocks from radioactive occurrences in the Grenville Structural Province, Ontario and Quebec; in Uranium in Granites, ed. Y.T. Maurice, Geological Survey of Canada, Paper 81-23, p. 19-30.

Van Wambeke, L.
1977: The Karonge rare-earth deposits, Republic of Burundi; Mineralium Deposita, v. 3, p. 373-380.

GEOLOGY OF REDCAP MOUNTAIN AREA, BRITISH COLUMBIA

Project 800028

M.L. Hill[1]
Cordilleran Geology Division, Vancouver

Detailed mapping in the vicinity of Redcap Mountain, about 60 km northeast of Prince Rupert, was started late July through August 1980 and continued July through August 1981. The area lies within Prince Rupert-Skeena map area, originally mapped by Hutchison (1967, 1982). This report presents observations and interpretations based on field studies and preliminary petrographic work.

In the Redcap Mountain area, rusty weathering metasedimentary schists with interbedded amphibolites overlie leucogneisses of the Central Gneiss Complex. Late granodiorite plutons intrude the section (Fig. 1).

The metasedimentary sequence in the upper part of the section reaches a maximum thickness of 700 m. True sedimentary thickness is obscured by deformation. The section includes impure quartzite and feldspathic schist, hornblende-biotite schist, marble, amphibolite, and minor pelitic schist. Thin marble units increase in abundance towards the top of the section. A 10 m thick unit of relatively pure white marble with pyrite and chalcopyrite is exposed on one ridge.

The metasedimentary section includes at least two distinctive black amphibolite units. Field relations, petrography, and whole-rock geochemical analyses suggest a sedimentary protolith for these amphibolites (i.e. a limy shale rather than a mafic igneous rock).

The age and affinity of these metasediments are not known. Unfortunately, the rocks are too highly metamorphosed to preserve any trace of fossils.

Underlying the rusty weathering metasediments is a thick sequence of mainly granitoid gneisses which has been mapped as part of the Central Gneiss Complex. These gneisses are stratified on a scale of metres, and include some clearly metasedimentary units. For example, Figure 2 shows a conglomerate unit found within the Central Gneiss. Clasts, up to 20 cm across, are mainly felsic and resemble the

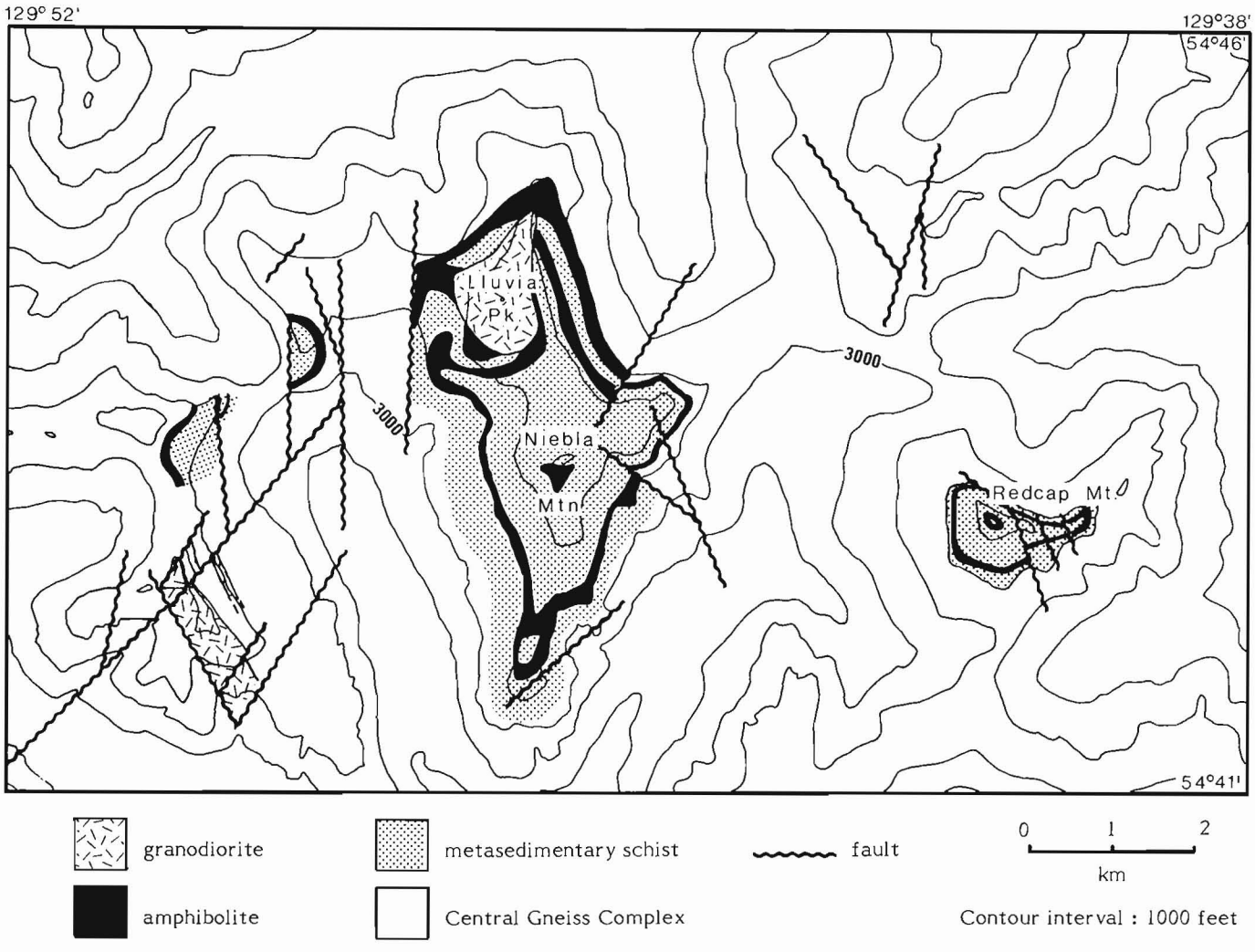

Figure 1. *Lithological map of Redcap Mountain area.*

[1] Department of Geological and Geophysical Sciences, Princeton University, Princeton, New Jersey, U.S.A. 08544

From: Scientific and Technical Notes in Current Research, Part B; Geol. Surv. Can., Paper 82-1B.

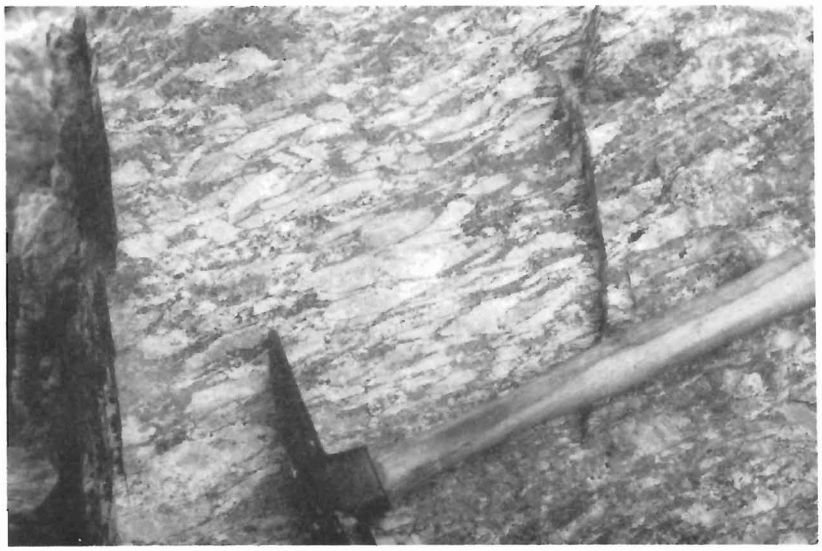

Figure 2

Conglomerate unit from Central Gneiss Complex.

underlying leucogneisses. The matrix is pelitic, containing biotite and garnet at this grade of metamorphism. Primary structures in most other strata in the gneisses have been obscured by metamorphism, partial melting, and deformation. A felsic to intermediate volcanic or volcaniclastic protolith for many of the leucogneisses is likely but has not yet been demonstrated.

The contact between the felsic gneisses and the overlying metasediments is locally conformable. However, on the scale of the map area, the relationship is unconformable. In the eastern half of the area, the top few hundred metres of the gneiss section is missing beneath the base of the metasediments. This contact could be either a low angle thrust or a sedimentary unconformity. There is no direct evidence for either. The contact predates metamorphism and penetrative deformation.

Both the rusty weathering metasedimentary section and the underlying Central Gneiss have been metamorphosed to upper amphibolite facies and deformed by at least two generations of folding. The main structure on the ridge west of Redcap Mountain is a tight recumbent fold closing to the northwest with nearly horizontal axial plane and southwest-trending fold axis. This event folded the contact between the metasediments and the underlying gneisses. Foliation in both the metasediments and the gneisses is axial planar to this folding.

These early tight folds (F1) are deformed by later more open and upright folds (F2). Fold axes to these folds are approximately horizontal and trend east. Most minor fold axes and mineral lineations in the area have this orientation. There was no development of a cleavage axial planar to second phase folds.

Peak metamorphism appears to have been synchronous with the first phase of folding, since metamorphic minerals define the axial planar foliation of these folds. Metamorphic assemblages and preliminary biotite-garnet geothermometry indicate that conditions of metamorphism reached a maximum of about 650 to 700°C and 5 to 6 kbars. Due to the scarcity of pelitic units, isograds are not clearly defined. Isotherms are apparently subhorizontal, dipping gently to the southeast. The lowest grade rocks in the area occur on top of Redcap Mountain, which is the area's highest topographic point. These rocks include muscovite-and staurolite-bearing schists. Elsewhere in the area, the stability field of staurolite has been exceeded and staurolite occurs mainly as inclusions in garnet. The amount of igneous material apparently derived by in situ partial melting of the rocks also increases as one descends topographically or goes northwest in the area. The southeast-dipping isothermal surfaces are not parallel to stratigraphic or structural horizons.

A discordant granodiorite pluton caps Lluvia Peak in the centre of the study area. The contact with the metasediments is sharp, but there is no contact aureole. K-Ar ages were determined for both biotite and hornblende separates by the Geochronology Section (sample no. WV-ML-103, laboratory nos. K-Ar 3383(2), K-Ar 3428). The hornblende date is 53.7 ± 3.0 Ma, the biotite date is 51.9 ± 1.3 Ma.

The latest event in the area was brittle faulting and fracturing and emplacement of porphyritic mafic dykes. Nearly vertical conjugate shears strike about north and northeast. The north-south shears have right-lateral displacement, the northeast-southwest shears have left-lateral offset. Blocks between shears were downdropped as much as 100 m. This block faulting is probably responsible for preservation of this outlier of metasediments; surrounding peaks of the same height are leucogneiss. Along each fault is a zone of cataclasis up to a few metres wide with associated retrograde metamorphism. Late dykes fill tensile fractures that were apparently associated with this brittle faulting. These mafic dykes are usually less than a metre wide, are commonly amygdaloidal, and display chill margins and columnar jointing which indicate rapid cooling. These dykes intrude the dated granodiorite on Lluvia Peak, and therefore have a maximum Eocene age.

References

Hutchison, W.W.

1967: Prince Rupert and Skeena map-area, British Columbia; Geological Survey of Canada, Paper 66-33, 27 p.

1982: Geology of the Prince Rupert-Skeena map area, British Columbia; Geological Survey of Canada, Memoir 394, 116 p.

PRELIMINARY RESULTS OF SUBMERSIBLE OBSERVATIONS ON THE LABRADOR SHELF

Project 790018

H.W. Josenhans and J.V. Barrie[1]
Atlantic Geoscience Centre, Dartmouth

Introduction

Iceberg scour marks are the most dominant surface features on the Labrador Shelf and have until recently been described only on the basis of acoustic data. Regional acoustic mapping and sediment sampling on the Labrador Shelf as well as a detailed study on Makkovik Bank in the area of the Bjarni wells (Lewis and Barrie, 1980) have increased our understanding of the frequency and morphological characteristics of iceberg scour marks but lack detailed definition that can only be obtained by submersible observations. Side-scan sonar and high resolution Huntec profiles suggest a relationship between iceberg scour mark morphology and sediment properties that warrants more detailed investigation by submersible. Also submersible observations of the local seabed dynamics are necessary to determine the degradation rate of scour marks in order to ultimately establish their recurrence interval. In October 1981 the use of the Pisces IV manned submersible provided visual and photographic documentation of the seabed within the Bjarni area (Fig. 1) and provided a vehicle for precise surficial sampling in iceberg-scoured terrain and over areas of bedrock outcrop. Our three main objectives were to: 1) investigate areas of the seafloor that have been actively disrupted by the grounding keels of icebergs and to note the degradation of these scour marks by the superimposed current regime and benthic biological activity; 2) provide ground truth for the acoustic data and note the modern sedimentary environment in terms of erosion or deposition; and 3) describe and sample a section of Tertiary (?) outcrop. (An 18 minute video program of these results is also available; see Josenhans and Barrie, 1982).

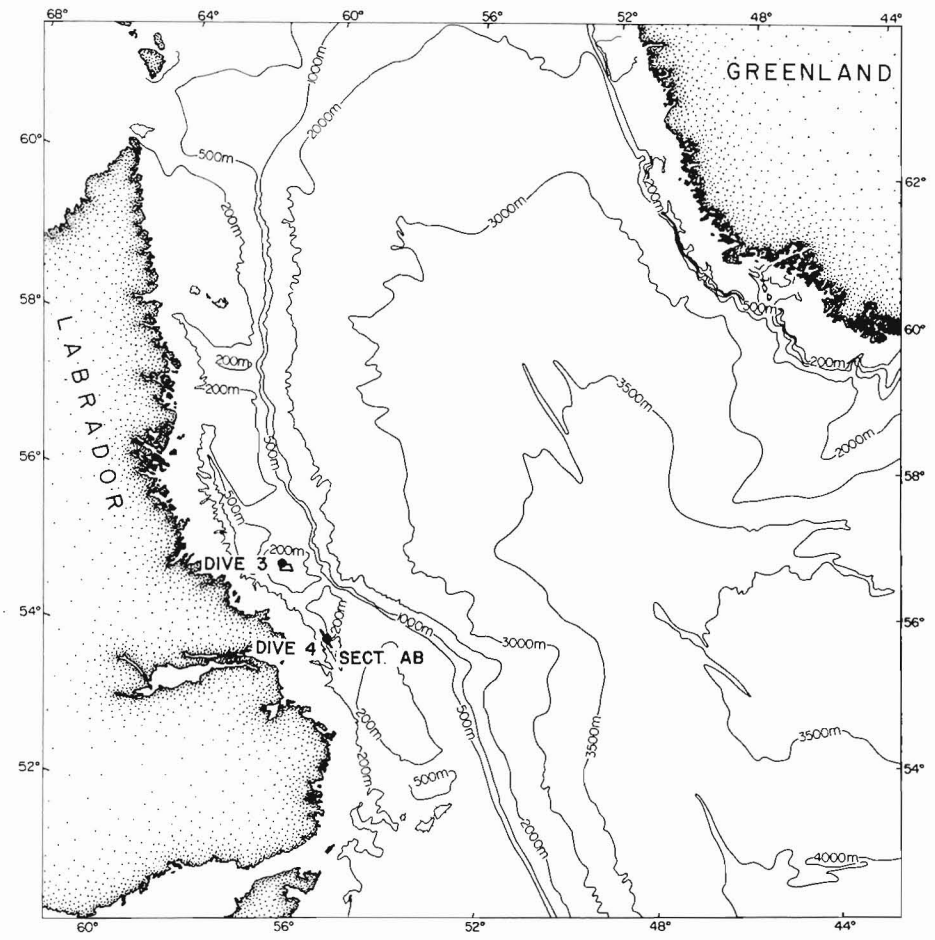

Figure 1. Index map showing location of dive sites. Small box (dive 3) indicates area of side-scan mosaic. Line through dive 4 indicates acoustic section AB.

Description of Dive Sites

Makkovik Bank

Dive 3, position 55°32.4'N, 57°45.9'W, on Makkovik Bank was over the Bjarni well site study area (Fig. 2) previously investigated by Lewis and Barrie (1980). Base line information included a complete scale corrected seabed mosaic obtained with the Bedford Institute of Oceanography 70 kHz side-scan sonar mosaic, sample texture and mineralogical analysis, bottom current data and Huntec DTS high resolution seismic coverage. The side-scan mosaic shows a matrix of scour marks of various age, size and degree of preservation as well as the presence of numerous iceberg crater marks or pits which are thought to have developed by the grinding action of a stationary or oscillating berg. A thin mobile sediment cover is indicated by the acoustic data and consists of well-sorted fine sand lying over a stiff clay and in places directly on the Tertiary (?) substrate.

The dive began at a depth of 140 m at the north end of the side-scan mosaic (Fig. 2) in an area of linear scour marks and potential sand migration. The dive transect was farther north than the desired track due to navigational inaccuracy at the time of submersible launching. Throughout the transect the seabed was essentially flat except for a high density of fresher and older looking scour marks and areas of cobble and boulder mounds. Scour marks all trended NNW-SSE with widths averaging 30 m and penetration depths of 1 to 2 m; these results compare to the acoustic data seen in the side-scan mosaic (Fig. 2). The current throughout the dive was from 090° at an estimated 10 - 15 cm/s.

Southwest Harrison Bank

Huntec DTS high resolution seismic and 40 inch air gun data show the presence of Tertiary (?) beds very near or at the seabed between a depth of 300 - 400 m at the base of Harrison Bank (Fig. 3a, b). The Huntec DTS data show a lack of recent stratified sediments and indicate two areas of bedrock near surface. Dive 4, (position 54°46.1'N, 56°33.4'W; Fig. 1), began at a depth of 459 m over an area of large exposed boulders, and no fine sediment. Current velocity was estimated at 25 cm/s flowing northwesterly. The dive track began at the base of the slope leading up to the southwestern corner of Harrison Bank. At the base, large accumulations of boulders having the appearance of a talus slope were found. These mainly igneous and metamorphic boulders are thought to have been ice rafted to the area, deposited on the steep slope of the bank and rolled to

[1] Ci-Core, Memorial University, St. John's Nfld.

From: Scientific and Technical Notes in Current Research, Part B; Geol. Surv. Can., Paper 82-1B.

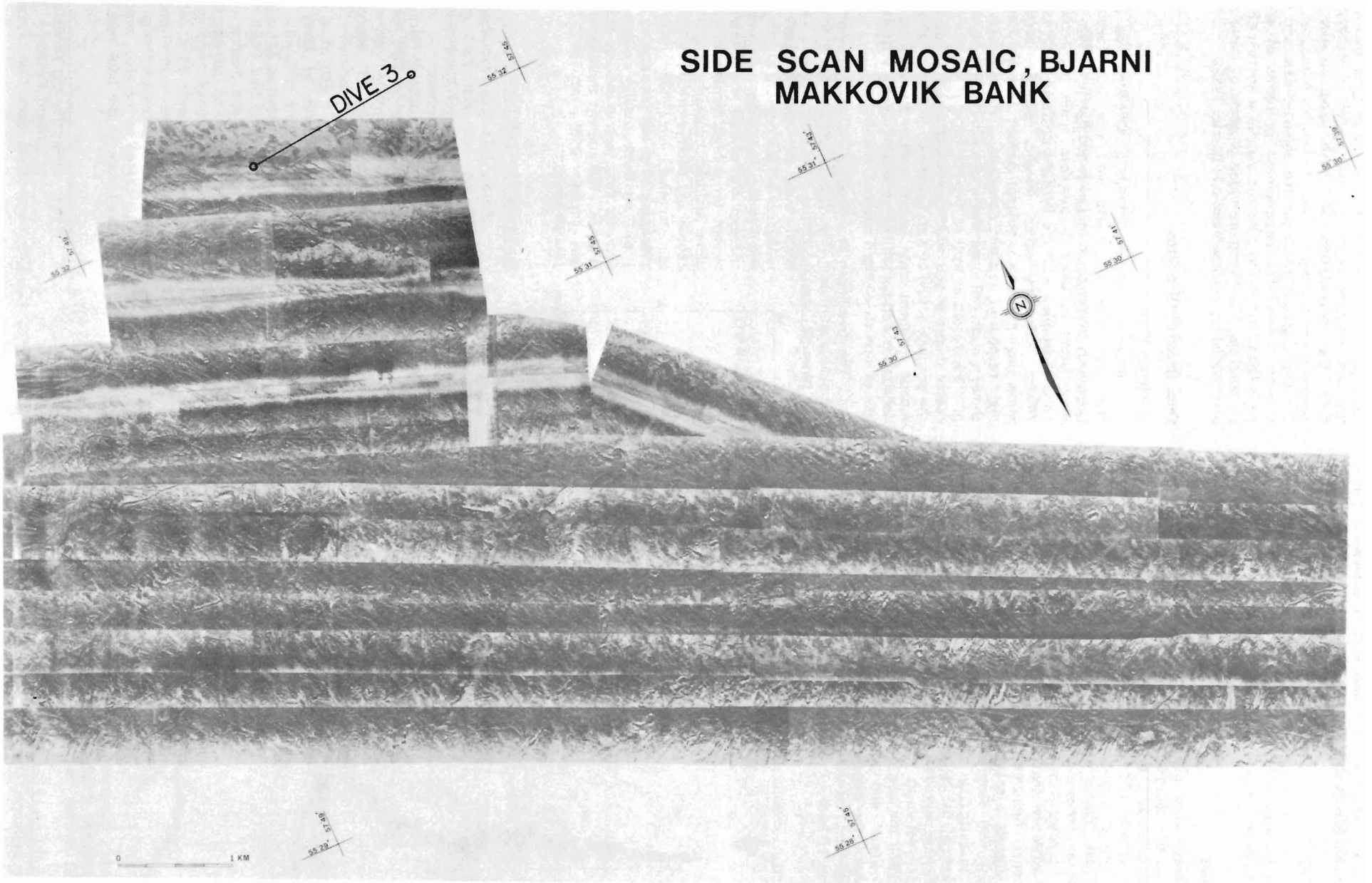

Figure 2. *A 70 kHz side-scan sonar mosaic of Bjarni well site area showing the position of dive 3. The traverse was displaced north of the mosaic through navigational error.*

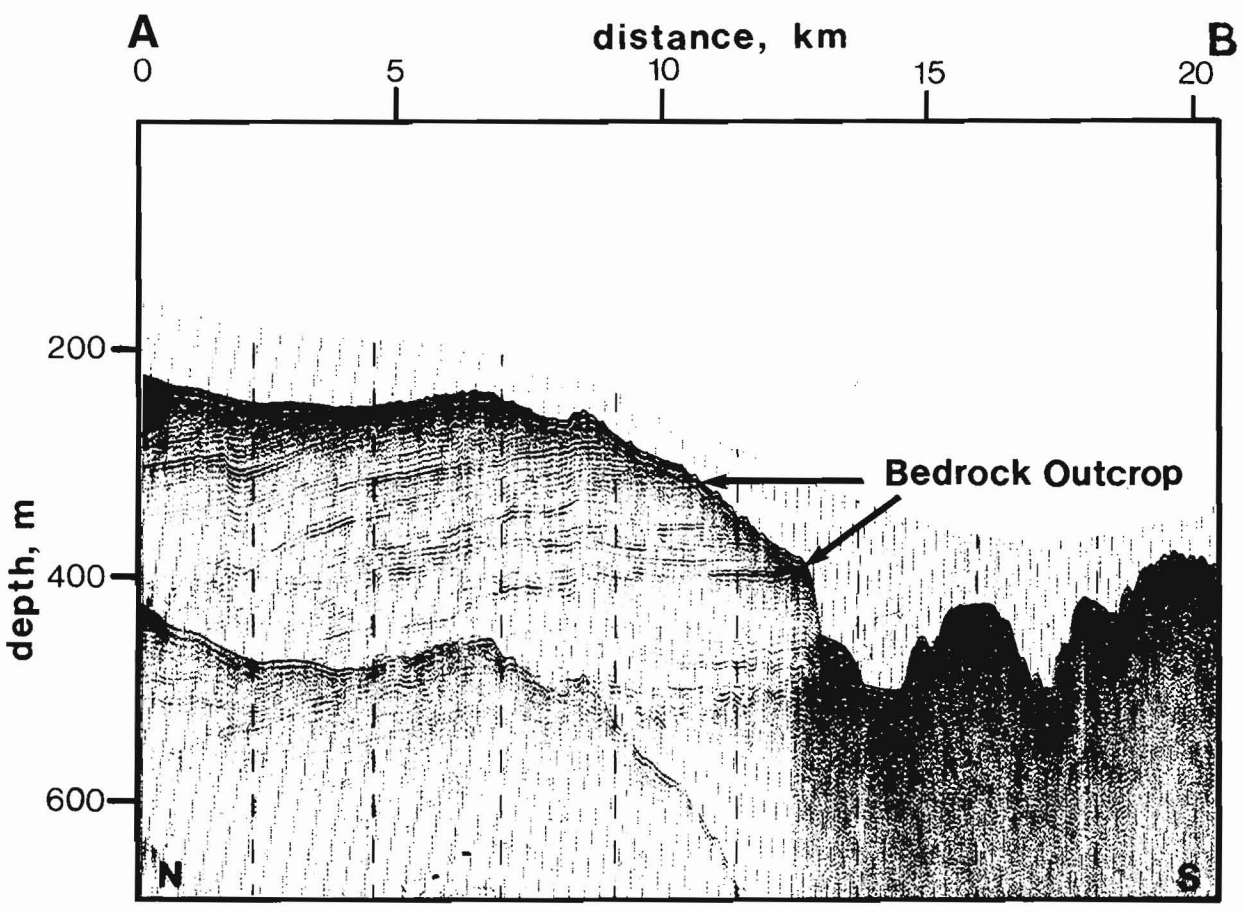

Figure 3a

Airgun profile (40 cubic inch) showing Tertiary (?) beds near surface. Depth is based on a water velocity of 1480 m/s.

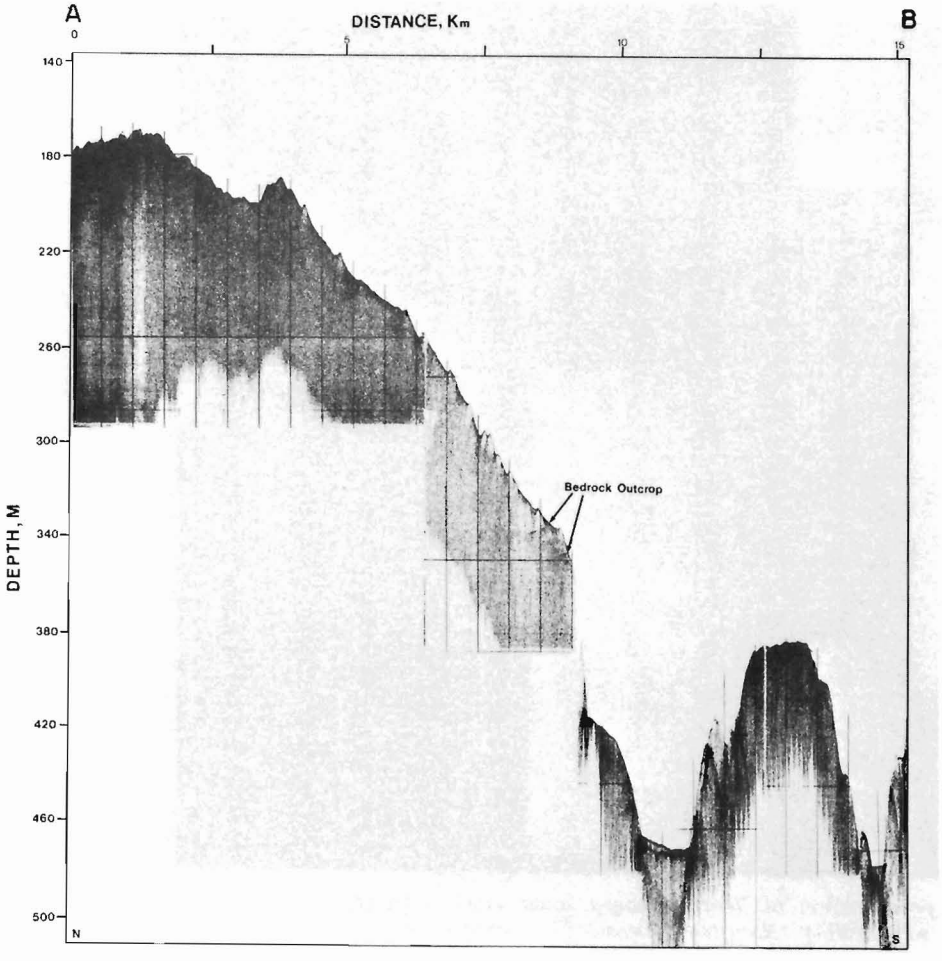

Figure 3b

Huntec DTS high resolution profile over same area showing outcropping beds exposed at the seabed. Depth is based on a water velocity of 1480 m/s.

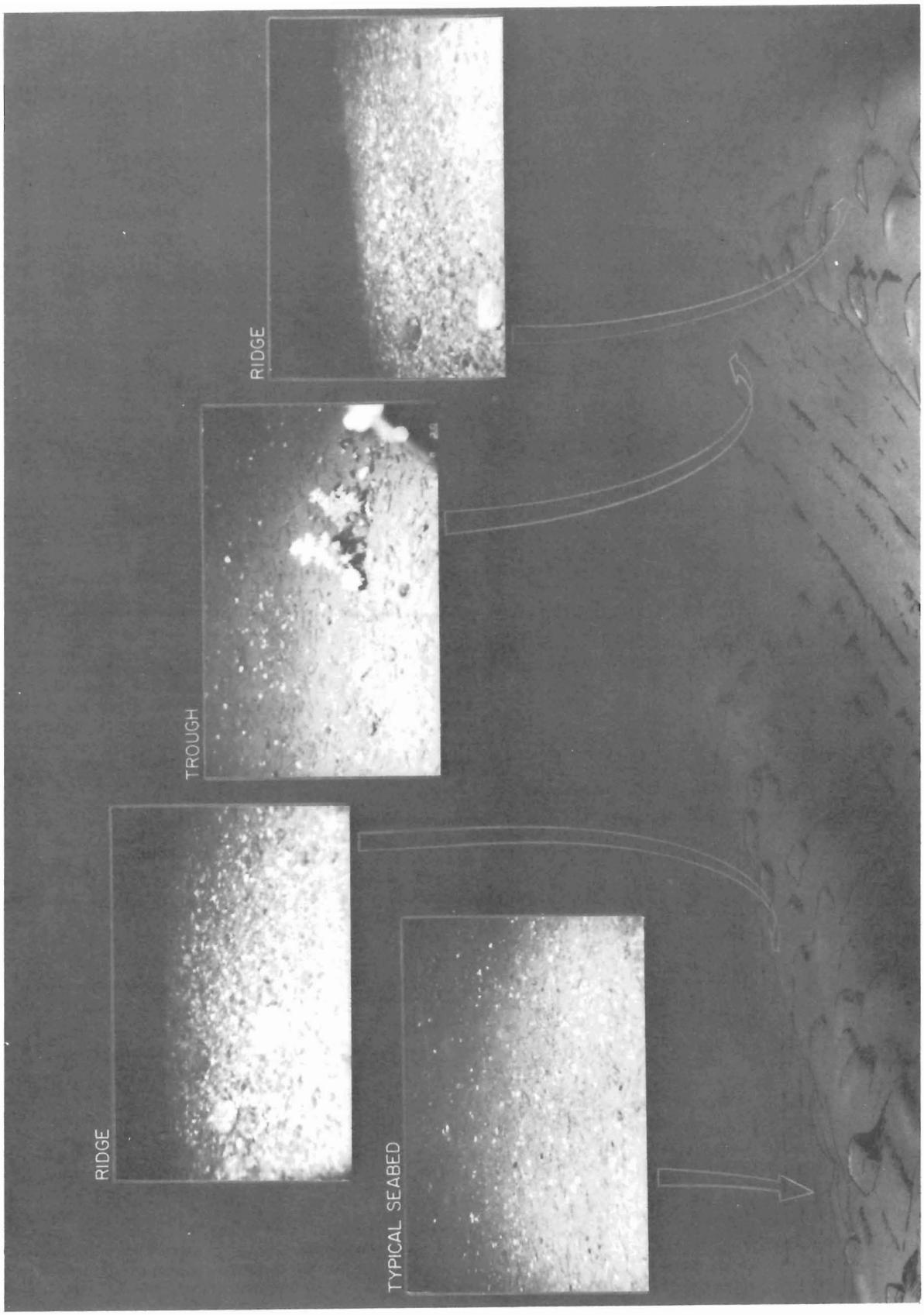

Figure 4. *Diagrammatic presentation of 'fresh' iceberg scour mark with representative bottom photographs taken from the submersible. Note the generally fine texture.*

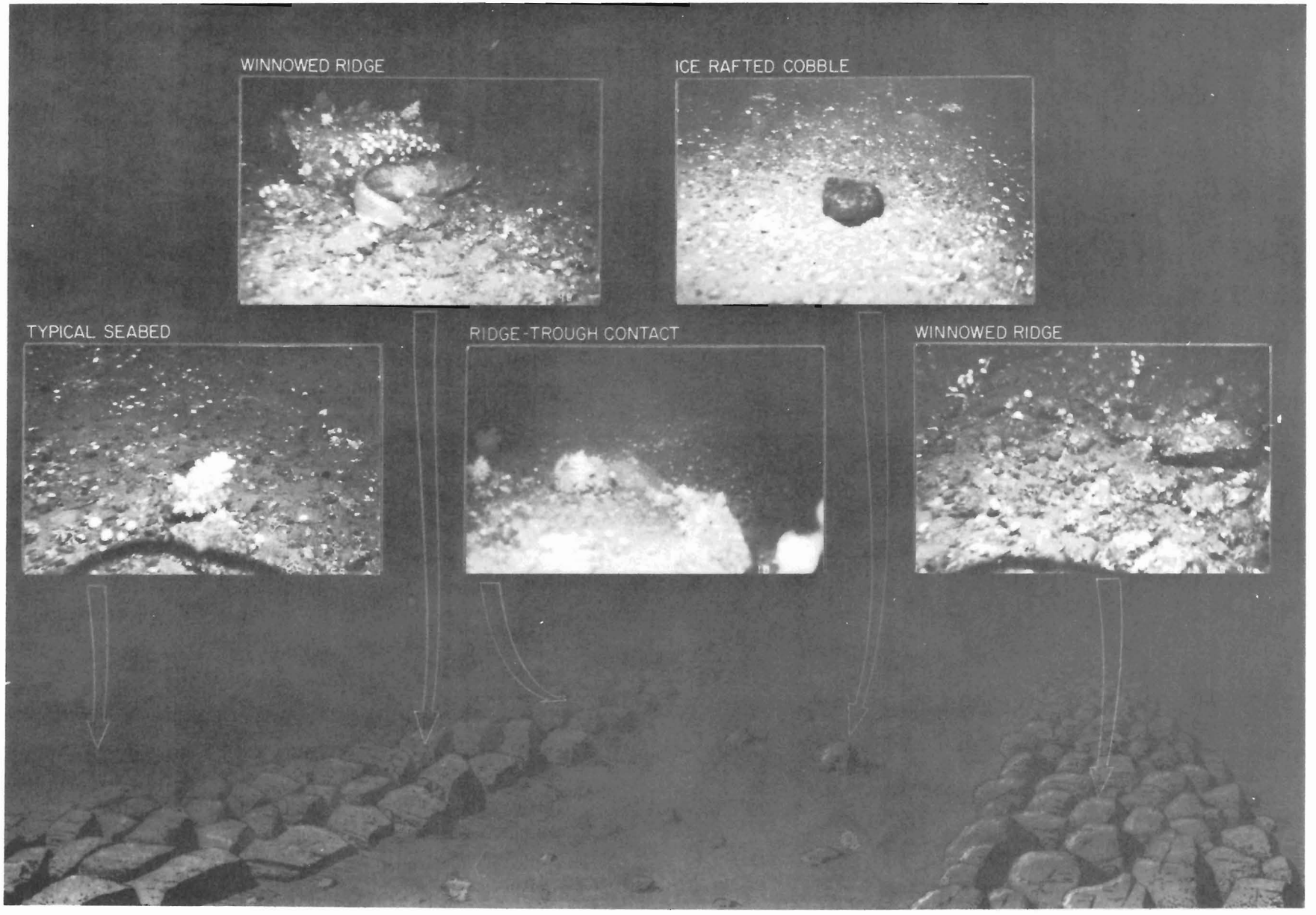

Figure 5. *Diagrammatic presentation of 'relict' iceberg scour mark with photographic examples. We suggest the lack of fine matrix is the result of gradual winnowing by bottom currents.*

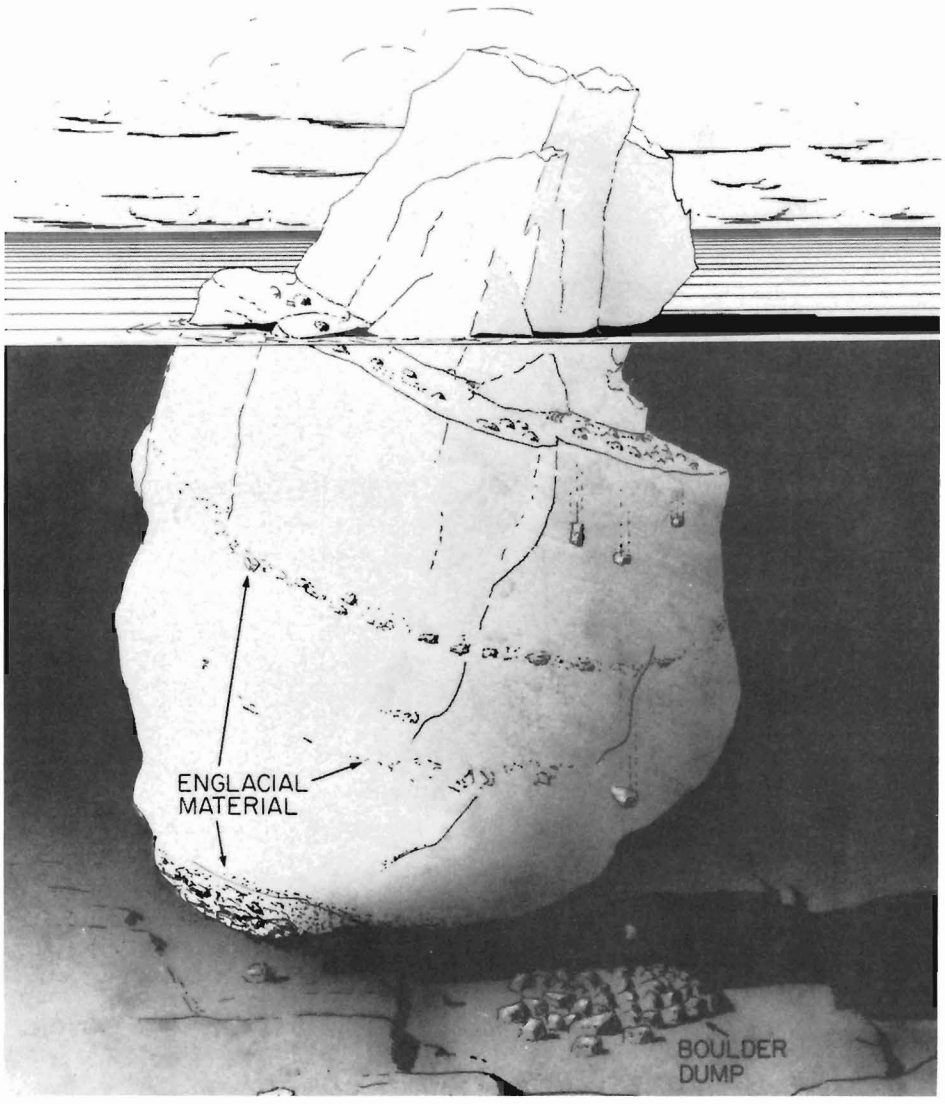

Figure 6. Diagrammatic presentation of ice rafting which produces concentrations of material on the seabed in the form of a boulder dump or as isolated fragments. Ice rafting is the primary form of deposition in this area.

the talus base. The significant accumulation of boulders observed illustrates the amount of ice rafted material. Lack of fine soft sediment and the noticeable current demonstrate that this is an area of nondeposition and possibly erosion.

Traversing upslope onto the bank between 450 m and 300 m several changes in slope of 10 - 30° were noticed which are thought to be associated with resistant Tertiary (?) beds. Two bedrock outcrops of similar orientation and appearance were found at depths of 366 and 340 m respectively. The lithology of the outcrop could not be clearly identified visually due to the organic cover and could not be sampled by the manipulator arm on the Pisces IV. However, the bedrock outcrop sites were surveyed for loose rocks of similar appearance and samples were taken at each site. These are presently being analyzed.

Iceberg Scour Marks

A large variation in the shape and textural character of scour marks was observed from the submersible. Direct observations have also led to an understanding of the local current regime which appears to be strong enough to modify the scour marks through time. Two distinctly different types were seen and are interpreted to represent fresh or relict scour marks.

Fresh Scour Marks

Fresh scour marks in this area have well developed levees or ridges of up to 2 m height with slopes of 3 - 6° (Fig. 4) rising above the surrounding seabed. The ridges are composed of cobbles and boulders protruding slightly from a matrix of silty sand. The floor or trough of the fresh scour mark was blanketed with fine well-sorted sediment and broken shell debris (Fig. 4). The trough was exceptionally smooth compared with the roughness of the scour mark rims, and appears to channel the winnowed fine sand and shell hash. Typical width of the trough between ridges is approximately 30 m. Occasional ice rafted boulders with a dense organic coating were noted scattered about the seabed outside the scour marks and an occasional boulder could be seen within the scour trough. Three angular cobbles with fresh surfaces were noted and the lack of organic cover shows that these have been deposited (ice rafted) recently. Numerous attempts at penetrating the scour mark trough and rims with the 30 cm corer were successful only in obtaining the surface veneer. The subsurface is too coarse in the rims and too compacted within the trough for submersible coring.

Relict Scour Marks

We suggest older scour marks can be readily distinguished from the fresh ones by the lack of fine matrix within their ridges and the lack of significant relief (Fig. 5) within this current regime. They are characterized by a concentration of boulders, cobbles and pebbles which make a linear ridge protruding above the seabed. Occasional lenses of fines and shell hash can be recognized on both sides of the boulder ridge and do not necessarily indicate the former scour mark trough. These older features are difficult to distinguish between the former trough and the surrounding seabed. Biogenic growth on the boulders consists mainly of sponges, Lithothamnion sp., bryozoans, and various brachiopods. Our observations have shown that within this current regime one can determine the relative age of the features based on the degree of winnowing, but absolute dating is not possible. One approach for the short term dating is to establish the rate of biogenic colonization on the ice rafted and exhumed boulders.

Boulder Dumps

Isolated mounds of large cobbles and boulders were observed throughout the dives. These mounds were typically 15 by 15 m in areal extent and had relief generally equivalent to the highest boulder, approximately 1 m (Fig. 6). These features are thought to have formed in one of the following ways. Icebergs, transported into a more temperate climate, melt down and concentrate their englacial material on the surface (see Fig. 7). At some point the bergs roll, possibly

Figure 7. *Labrador iceberg with examples of englacial material.*

due to contacting the seabed, and the englacial material is dumped off the bergs (Fig. 6). More importantly, according to White et al. (1980) most iceberg melting takes place below the waterline by convective heat transfer along the ice-water interface. This process is enhanced particularly when a berg becomes grounded and the prevailing currents are forced to flow rapidly past the stationary berg resulting in increased meltout of englacial material. The fines incorporated in the material are separated out during settling, or later through seabed winnowing, to produce a concentration of boulders and cobbles on the seabed in the form of a boulder dump. These areas appear as more reflective patches on the side-scan sonograms. A glacial origin for these patches is ruled out because of a lack of glacial morphological features within the area. At least two of these isolated boulder dumps were observed on dive 3.

Seabed Dynamics

The seabed has a surface veneer of very fine sand with a lag of pebbles and cobbles as well as ice rafted debris. Pebbles are subangular to subrounded and do not display evidence of having been subjected to marine transgression. Bottom currents measured during the dive are thought to be adequate to produce the sediment lag observed. The fact that the fine matrix has been completely removed from the scour mark ridges suggests that bottom winnowing is a significant agent acting on the seabed. In isolated areas, current winnowing is significant even at depths greater than 400 m, where the bottom currents are flowing adjacent to the bathymetry. Further investigation of bottom currents is needed to determine the rates of winnowing and the driving mechanisms for the icebergs.

Summary

1. On the Labrador shelf banks present day sedimentation is primarily by ice rafting; in some cases this results in isolated boulder dumps.
2. Within this current regime fresher (more recent) iceberg scour marks can be differentiated from older scour marks by: 1) lack of fines within the older scour mark rims; and 2) the extent of ice rafted deposition and biological activity that has overtaken the scour mark troughs.
3. Evidence suggests that surficial sediments on Makkovik and Harrison banks are winnowed by the present current regime. Localized sediment winnowing is occurring to a depth of at least 450 m at the base of Harrison Bank.
4. Submersible observations confirm the seismic interpretation of bedrock outcropping along the southwestern side of Harrison Bank.

Acknowledgments

We sincerely thank Capt. Robin Jones and officers of Pandora II, and Frank Chambers and his diving team for their enthusiastic support and a job well done. T. Atkinson and D. Beaver provided helpful technical support. We thank J.P. Syvitski and K. Moran for critical review.

References

Lewis, C.F.M. and Barrie, J.V.
1980: Ice scour studies on the Labrador Shelf; in Workshop on Research in the Labrador Coastal and Offshore Region, September 4 - 6. Published by Memorial University of Newfoundland, p. 264-265.

Josenhans, H.W. and Barrie, J.V.
1982: The effect of icebergs on the Labrador shelf as seen by submersible Pisces IV; Geological Survey of Canada, Open File 843 (18 minute 3/4 inch video program).

White, F.M., Spaulding, M.L., and Gominho, L.
1980: Theoretical estimates of the various mechanisms involved in iceberg deterioration in the open ocean environment; Coast Guard Research and Development Center, Groton, Connecticut 06340, Report Number CG R and D C 7/80.

GRANITE CLASTS IN LATE PROTEROZOIC CONGLOMERATE, SOUTHEASTERN BRITISH COLUMBIA

Project 700003

Andrew V. Okulitch
Institute of Sedimentary and Petroleum Geology, Calgary

Loveridge et al. (1981) have reported valuable data on the probable age of granitic clasts in conglomerate in the Late Proterozoic Toby Formation, Windermere Supergroup. They are to be particularly complimented on developing techniques to analyze minute quantities of zircon and monazite; techniques which will be of great value in subsequent radiometric studies. Their favoured hypothesis for the source of the clasts, the Shuswap Metamorphic Complex, seems improbable, however, and requires some comment.

The Shuswap Metamorphic Complex (Fig. 1) is formed of three terranes (Okulitch, 1981): the Monashee Terrane, composed of ortho- and paragneiss which has yielded radiometric dates of 3000, 2000 and 935 Ma (Duncan, 1978), 1960 Ma (Wanless and Reesor, 1975) and 770 Ma (Okulitch et al., 1981); the Shuswap Terrane, containing late Proterozoic to Triassic metasediments and Devonian and Mesozoic plutonic rocks; and the Okanagan Terrane, a highly heterogeneous assemblage of late Paleozoic and Mesozoic 'oceanic' rocks, Mesozoic and Tertiary granitoids and gneissic rocks of unknown age. The Shuswap Complex contains no granitoids known to be the same age as the clasts in the Toby Formation, although it is possible that undated rocks in the Monashee or Okanagan terranes could be of suitable age.

Evaluation of the likelihood that undated granitoids in the Shuswap Complex served as sources of the Toby clasts requires understanding of the position of such rocks relative to the basin of Windermere deposition. It is important to note that in any restoration of a predominantly compressional tectonic regime, any two localities end up farther apart than they are at present. Palinspastic reconstruction of the fold and thrust belt at about the latitude of the Monashee Terrane (measured from Price, 1981, Fig. 2) places Windermere strata on strike with the granite clast locality, southeast of Vernon (Fig. 1). Reconstruction of the position of the Monashee Terrane is less certain as it is tectonically isolated from the fold and thrust belt by the Monashee Décollement (Read and Brown, 1981) and must therefore be evaluated independently. Recent hypotheses treat the terrane as either a continental fragment separated from the North American craton by oceanic crust (Brown, 1981) or as a para-autochthonous, rifted part of North America that served as a basement of transitional crust to Purcell and Windermere sediments (Okulitch, 1981). The first hypothesis places the Monashee Terrane on the far side of the Windermere basin (or perhaps even farther west), well removed from the depositional site of the granitic clasts. The second hypothesis has the terrane nearer to the site of clast deposition, at least 200 km west of it, but implies that at the time of their derivation, the terrane was covered by Purcell strata of platformal or possibly greater thickness. In either case, it seems unlikely that the Monashee Terrane could have been a source for the Toby clasts.

The late Proterozoic location of hypothetical 1800 Ma-old parts of the Okanagan Terrane is even more problematical. Paleontologically dated successions in this terrane are allochthonous relative to strata of the pericratonic prism. Much of the gneissic part of the terrane formed as a consequence of Mesozoic plutonism and regional metamorphism. Possible remnants of the craton, such as the pre-Carboniferous Trail Gneiss and its northward extensions in Valhalla Dome (Simony, 1979) are presently interthrust

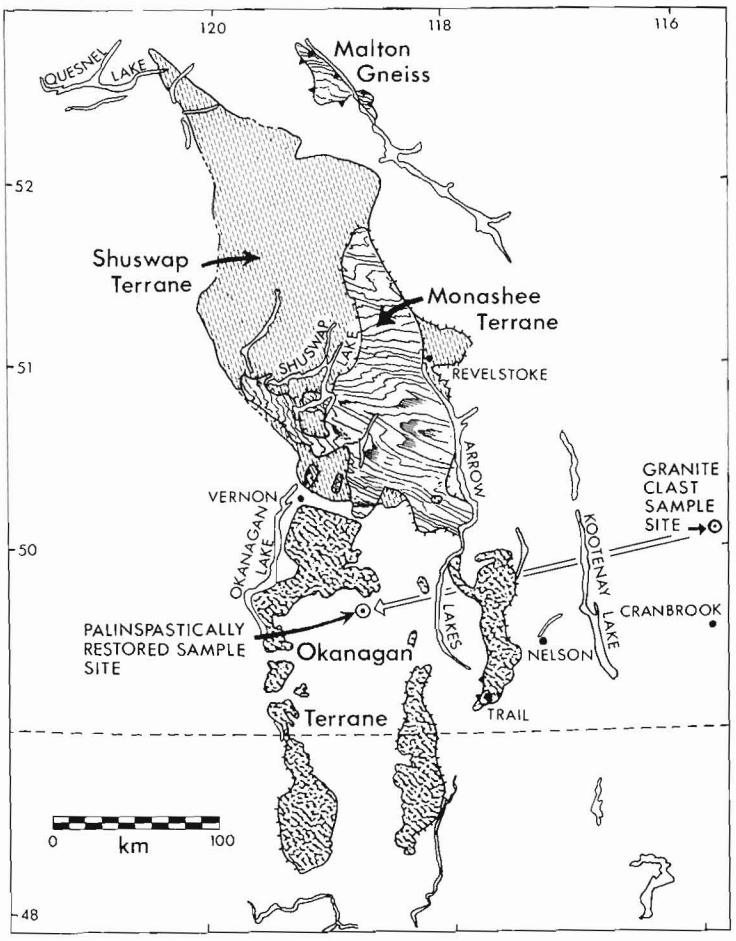

Figure 1. Major elements of the Shuswap Metamorphic Complex relative to granitic clasts in the Toby Formation.

with allochthonous Paleozoic and Mesozoic rocks. Their former position can only be loosely inferred to be well west of the Okanagan Valley and no direct link with Proterozoic pericratonic strata can be presently established.

North of the main body of the Shuswap Complex, basal late Proterozoic strata have been shown to lie directly upon a thrust slice of crystalline basement (Oke, 1981) known as the Malton Gneiss (Fig. 1). Ortho- and paragneiss have yielded radiometric dates of 3200, 1200-1300 and 890 Ma (Chamberlain et al., 1979), none of which, however, are the same as that obtained from the Toby clast. Palinspastic repositioning places the gneiss and its late Proterozoic cover about 200 km or more southwest of its present position, likely as part of the distal edge of the North American craton, and northwest of the restored position of the granite clast site (Fig. 1). Paleocurrent studies of late Proterozoic strata younger than the Toby Formation northwest of but approximately on strike with the Malton Gneiss (Young, 1978) indicated northeastern (cratonic) sources for these. Southwesterly flowing currents were therefore active northwest of and presumably at the clast site, albeit after Toby sedimentation and suggest that western sources for the clasts are improbable.

Additional provenance and paleocurrent studies (Young et al., 1973, p. 197) also indicated a predominant Shield derivation for the bulk of Windermere sediments. The proximity of the Shield, exposed at the time of Toby deposition 100 to 150 km to the east (derived from Price, 1981, Fig. 2), supports this interpretation. The absence of granitic clasts in western exposures of the Toby Formation also militates against a western source, as does

From: Scientific and Technical Notes in Current Research, Part B; Geol. Surv. Can., Paper 82-1B.

the presence of the Purcell Arch, which would block west-derived sediment flow from reaching eastern parts of the basin. The apparently limited quantity of granitic clasts in eastern exposures must be a function of the existing drainage system or perhaps the effects of glaciation.

If it can be shown that portions of the Windermere Supergroup had a major western source – apart from the local, fault-block provenance from Purcell strata (Lis and Price, 1976) – this would have significant effects upon regional models of late Proterozoic tectonism. Until this can be demonstrated, however, it seems more reasonable to accept the penultimate statement of Loveridge et al.: "The age of the granite from which the Toby pebble was derived is compatible with its origin in a Hudsonian Shield terrane. Furthermore, the granitic debris is in the easternmost Toby exposures, closest to the Shield. If the Toby Formation has glacial affinities the presence of granitic boulders and large cobbles could be accounted for by ice-rafting from the Shield".

Acknowledgment

The assistance of M.E. McMechan in stimulating discussions and incisive critical reading is greatly appreciated.

References

Brown, R.L.
1981: Metamorphic complex of southeastern Canadian Cordillera and relationship to foreland thrusting; in Thrust and Nappe Tectonics, The Geological Society of London, Special Publication 9, p. 463-474.

Chamberlain, V.E., Lambert, R.StJ., Baadsgaard, H., and Gale, N.H.
1979: Geochronology of the Malton Gneiss Complex of British Columbia; in Current Research, Part B, Geological Survey of Canada, Paper 79-1B, p. 45-50.

Duncan, I.J.
1978: Rb/Sr whole rock evidence for three Precambrian events in the Shuswap Complex, southeastern British Columbia; in Geological Association of Canada, Geological Society of America and Mineralogical Association of Canada, Abstracts with Program, v. 10, p. 392-393.

Lis, M.G. and Price, R.A.
1976: Large-scale block faulting during deposition of the Windermere Supergroup (Hadrynian) in southeastern British Columbia; in Report of Activities, Part A, Geological Survey of Canada, Paper 76-1A, p. 135-136.

Loveridge, W.D., Leech, G.B., Stevens, R.D., and Sullivan, R.W.
1981: Zircon and monazite age of a granitic clast in Toby conglomerate (Windermere Supergroup), Canal Flats, British Columbia; in Rb-Sr and U-Pb Isotopic Age Studies, Report 4, in Current Research, Part C, Geological Survey of Canada, Paper 81-1C, p. 131-134.

Oke, C.
1981: Structure and metamorphism of the Mount Blackman area, British Columbia; in Geological Association of Canada, Abstracts, v. 6, p. A-44.

Okulitch, A.V.
1981: The Shuswap Metamorphic Complex: its role in Cordilleran tectonism; in Geological Association of Canada, Abstracts, v. 6, p. A-44.

Okulitch, A.V., Loveridge, W.D., and Sullivan, R.W.
1981: Preliminary radiometric analyses of zircons from the Mount Copeland syenite gneiss, Shuswap Metamorphic Complex, British Columbia; in Current Research, Part A, Geological Survey of Canada, Paper 81-1A, p. 33-36.

Price, R.A.
1981: The Cordilleran foreland and fold and thrust belt in the southern Canadian Rocky Mountains; in Thrust and Nappe Tectonics, The Geological Society of London, Special Publication 9, p. 427-448.

Read, P.B. and Brown, R.L.
1981: Columbia River fault zone: southeastern margin of the Shuswap and Monashee Complexes, southern British Columbia; Canadian Journal of Earth Sciences, v. 18, p. 1127-1146.

Simony, P.S.
1979: Pre-Carboniferous basement near Trail, British Columbia; Canadian Journal of Earth Sciences, v. 16, p. 1-11.

Wanless, R.K. and Reesor, J.E.
1975: Precambrian zircon age of orthogneiss in the Shuswap Metamorphic Complex, British Columbia; Canadian Journal of Earth Sciences, v. 12, p. 326-331.

Young, F.G.
1978: The lowermost Paleozoic McNaughton Formation and equivalent Cariboo Group of eastern British Columbia: piedmont and tidal complex; Geological Survey of Canada, Bulletin 288.

Young, F.G., Campbell, R.G., and Poulton, T.P.
1973: The Windermere Supergroup of the southeastern Canadian Cordillera; in Belt Symposium, University of Idaho, Idaho Bureau of Mines and Geology, v. 1, p. 181-203.

COMMENTS ON THE GEOLOGY AND URANIFEROUS MINERAL OCCURRENCES OF THE WERNECKE MOUNTAINS, YUKON AND DISTRICT OF MACKENZIE

Project 750069

R.T. Bell
Economic Geology Division

Introduction

Proterozoic sedimentary rocks with local volcanics are well exposed in the Ogilvie, Wernecke and Mackenzie mountains which extend eastward about latitudes 64 and 65° from the Alaska boundary through northern Yukon Territory into District of Mackenzie and thence southeastward, a distance of over 600 km. The stratigraphy has gross consistencies but significant differences along this chain of mountains. Uranium-bearing breccia occurrences of the Wernecke Mountains are similar in many respects to the major breccia occurrence in the Adelaidean terrane in South Australia.

This note is submitted with the view of encouraging discussion of the possible metallogenetic similarities of the Precambrian terranes of the Wernecke and Ogilvie mountains to the Adelaidean terrane of South Australia. The first part focuses on some of the uncertainties concerning the stratigraphy, unconformities and "orogenies" and proposes that dextral transcurrent faulting be considered as an underlying factor in the Precambrian evolution of the Wernecke-Ogilvie area. The second part briefly summarizes the uranium occurrences and settings in the Wernecke Mountains. The final part summarizes a comparison with the Adelaidean terrane. References list relevant literature. I would particularly draw attention to the guidebook on the Adelaidean terrane by Thomson et al. (1976).

Stratigraphic Uncertainties and Structural Considerations

Excellent studies on two of the three identified Precambrian successions in the Wernecke and Mackenzie mountains have recently been published. These successions are schematically illustrated in Figure 1. The lowest succession, the Wernecke Supergroup (Delaney, 1978, 1981), is well defined and documented, including uncertainties of stratigraphic relationships within the supergroup. For example, Delaney (1981) has observed one probable unconformity above the Fairchild Lake Group near Dolores Creek. I would add that the Fairchild Lake Group southwest of Fairchild Lake and at Bond Creek is strongly overturned to

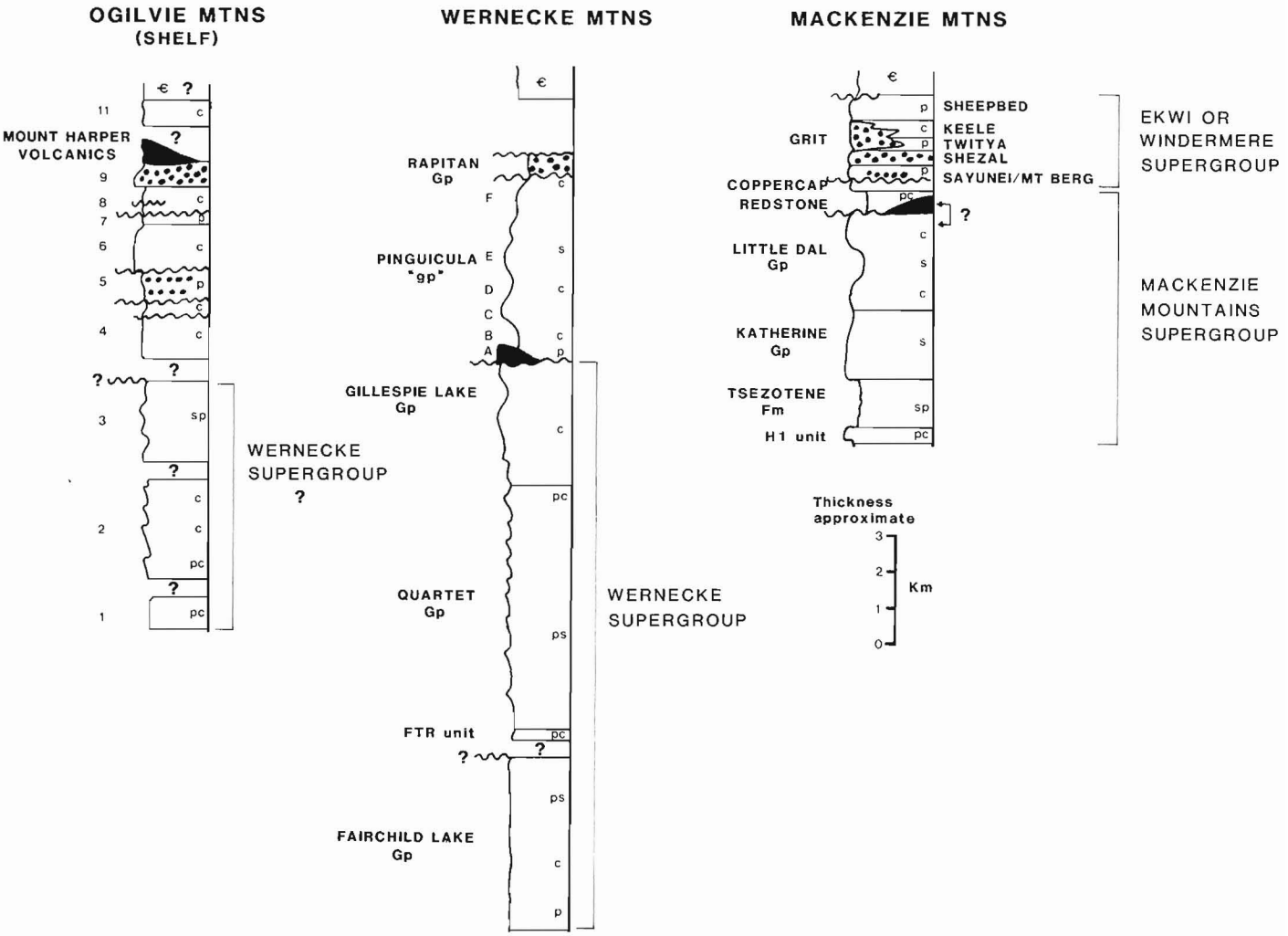

Figure 1. *Schematic representation of Proterozoic stratigraphic units of Ogilvie, Wernecke and Mackenzie mountains illustrating stratigraphic uncertainties (?), unconformities (~~), diamictites (), volcanic units (black) and dominant lithologies (s-sandstones, p-pelites, c-carbonates). Modified after Young et al. (1979a), Eisbacher (1979, 1981) and Thompson and Roots (1982). For distribution of major units see Figure 1.1, Delaney (1981).*

From: Scientific and Technical Notes in Current Research, Part B; Geol. Surv. Can., Paper 82-1B.

the southeast on northeast-trending structures, in contrast to upright structures in the overlying Quartet Group. This, together with a higher metamorphic grade in the lower group, suggests a regional unconformity, perhaps of great significance, or a hitherto unrecognized flat thrust fault or both.

The uppermost succession, the Windermere Supergroup (Eisbacher, 1978b, 1981) or Ekwi Supergroup (Yeo, 1981; Young, 1981) has been studied in detail and interpretations of its setting have been well documented in Mackenzie Mountains.

Unfortunately in the Wernecke and Ogilvie mountains the middle succession, the Pinguicula "group" has not been properly defined or described and accordingly there is some controversy (for example, see Eisbacher, 1978a, 1979). Eisbacher (1981) has published a thumbnail sketch of the group. In contrast the Mackenzie Mountains Supergroup (for example see Aitken, 1981; Jefferson, 1978a), in part correlative with the Pinguicula, has been well studied in the Mackenzie Mountains. A fault along the Snake River, at the south end of the Richardson Fault array, separates the Pinguicula group and Mackenzie Mountains Supergroup.

Thompson and Roots (1982) have published a detailed map of the southwestern Ogilvie Mountains and some reconnaissance sections that differ substantially from the Wernecke Mountains section, enough so that a single generalized stratigraphic section representing both Wernecke Mountains and Ogilvie Mountains is misleading (Young et al., 1979a,b; Eisbacher, 1979, 1981). Interestingly, Thompson and Roots show two horizons of diamictites (mixtites, tillites?) and six unconformities (plus stratigraphic uncertainties suggesting at least three more). Wisely they refrained from using Wernecke and Mackenzie stratigraphic terms until their studies are more complete. It appears that if the Pinguicula sequence is present in the western Ogilvie Mountains its lithology and stratigraphy there differ sufficiently from those in the Wernecke Mountains mentioned by Eisbacher (1981) to merit a separate formal nomenclature. My preference is to abandon the term Pinguicula altogether.

I suggest that the pre-Mesozoic tectonics of the Wernecke area were largely dominated by dextral transcurrent faulting rather than (orthogonal) rift opening and closure as envisioned by others (i.e. Stewart, 1972; Tempelman-Kluit, 1979, 1981a, p. 229-230).

In a broad area of dominantly transcurrent faulting one can expect strong tensional or strong compressional strain locally in the supracrustal rocks depending on how the transcurrent faults interact (Fig. 2). There would be sharp variations in the style and intensity of deformation from place to place and consequently interpretations of the strength of "orogenies" based on distinctions between "profound angular unconformities" and mere "angular unconformities" may be misleading. Thus, if the regional nature of the sub-Quartet Group unconformity within the Wernecke Supergroup is proved, there are at least three "major" unconformities to contend with, rather than two, and the argument is not simply over two "orogenies" (Yeo et al., 1978; Eisbacher, 1978a).

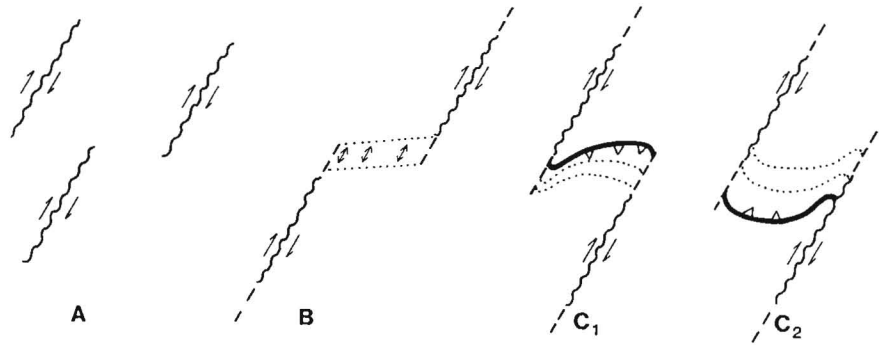

Figure 2. *Interaction between transcurrent faults.*

I propose the following model for the Wernecke-Ogilvie area for consideration:

1. The Proterozoic rocks of this terrane represent an original progradation of the North American craton, although they may very well have been deposited in the eastern side of a large intracratonic basin, the western side of which has drifted elsewhere (Siberia?: Sears and Price, 1978; Australia?: Jefferson, 1978b).
2. This sequence lay largely in the area now occupied by the Selwyn fold belt. Eisbacher (1977, see Fig. 46.9) provided a germinal suggestion on a smaller scale for this.
3. Sometime during Rapitan time (probably starting earlier) this terrane moved northward on a series of dextral transcurrent faults and in part rotated approximately 30 degrees counterclockwise.
4. Further movements probably occurred in Paleozoic time, perhaps in response to the northeasterly trending Kaltag fault system which could mean a further increase in counterclockwise movement of the southern Ogilvies. Late movements on the Kaltag Fault and Richardson Fault array in the late Mesozoic and Cenozoic have been documented (Norris and Hopkins, 1977).

Some features of the Wernecke terrane are consistent with this model. First, the Paleozoic rocks of the Wernecke and Ogilvie terranes show high freeboard (carbonate platform) sediments in contrast to surrounding shale basins (e.g. Road River) which suggests differing crustal response. Secondly, the restoration by translation and rotation of the Wernecke Mountains back to the Selwyn fold belt area would make Wernecke Supergroup paleocurrents (Delaney, 1981) consistent with a North American cratonic progradation. Thirdly, radiometric dates (Archer and Schmidt, 1978) in mineralized breccias suggest initial emplacement of uranium before 1.2 Ga and several reactivations until at least 0.3 Ga.

The above proposal can be tested by paleomagnetic techniques but must await improved documentation and refinement of the stratigraphy.

Wernecke Mineral Occurrences

Mineral occurrences and deposits in the Wernecke area have been discussed (Carrière et al., 1981; Laznicka, 1977a,b; Laznicka and Edwards, 1979; Bell, 1978; Bell and Delaney, 1977; Goodfellow, 1979; Delaney et al., in press; Archer and Schmidt, 1978; Morin, 1977). The following is a condensed summary, mainly of the U, U-Cu-Au and U-Co occurrences and their host rocks.

Observations:

1. More than 80 large breccia bodies cut the Wernecke Supergroup in eastern Wernecke Mountains. At least as many occur in Proterozoic terranes elsewhere as far west as Coal Creek Dome (Bell, 1978; Lefebvre, 1980). The breccia bodies are commonly in the order of a kilometre across; some are several kilometres across.

2. All uranium occurrences are in or within 20 m of breccias.

3. Uranium mineralized breccia zones are in the lowest group and lower part of the middle group of the threefold Wernecke Supergroup (Delaney, 1978).

4. Practically all uranium occurrences are in the eastern half of Wernecke Mountains; one other is in southern Richardson Mountains (NOR; Tempelman-Kluit, 1981b) and another occurrence is in the Coal Creek Dome (ROB; Morin et al., 1979) associated with Cu mineralization.

5. Most uranium occurrences in the eastern part of Wernecke Mountains are associated with the most intensely altered rocks (bleached, chloritized, K and Na metasomatized, hematitized, silicified and carbonatized).

6. Cu (Carrière et al., 1981) and to a lesser extent Co occur in virtually all breccias throughout the area. Fe, most commonly as intense hematitization (rarely as siderite), is present in all breccias (for example, see Norris, 1974).

7. Mafic (diabase?) dykes cut and are cut by breccias. In the Coal Creek Dome dykes appear to be coeval with some breccias. Lamprophyric dykes are found in three places; at one, they appear to cement breccia. Laznicka (1977a,b) and Laznicka and Edwards (1979) presented evidence that the syenite at Cobalt Cirque is of metasomatic origin.

8. Breccias are distributed in a regional pattern parallel with the Richardson Fault array that separates the distinct Proterozoic rocks of the Mackenzie Mountains from those of the Wernecke Mountains. The breccia zones themselves appear to be mechanically related to a kink in the otherwise northerly trending Richardson Fault array, perhaps through transition from en echelon, northerly trending transcurrent faults through northwesterly trending reverse faults.

9. The major deformation of the Wernecke Supergroup predates deposition of the Pinguicula sequence. Brecciation in the main breccia bodies is certainly pre-Middle Cambrian. However, there are no compelling reasons to conclude that all breccias are roughly the same age, or of the same origin. Indeed the apparent association of the breccias with the Richardson Fault array suggests development over a long time.

10. A single K-Ar age (Archer et al., 1977) suggests brecciation may be as early as 1.5 Ga. U-Pb ages are later, ranging from about 1.2 to 0.3 Ga (Archer and Schmidt, 1978). Delaney (1981) reports the K-Ar age of two of the lamprophyres to be 613 ± 15 Ma and 552 ± 13 Ma.

11. Preliminary stratigraphic geochemical data demonstrate that U and Cu anomalies are present in the lower two groups of the Wernecke Supergroup (Bell, 1978).

Some breccias are undoubtedly related to crush zones along faults (see Fig. 2 in Bell, 1978). A majority of breccias are monotonously homolithic, comprising weakly and uniformly metasomatized material; others are heterolithic, consisting of a mélange of fragments that exhibit different stages, degrees and combinations of metasomatism. The homolithic breccias are interpreted as chimney or stope breccias produced by gradual as opposed to explosive processes. The accompanying hydrothermal fluids may have been of deep-seated origin or have been expelled from deeply buried evaporites or both. Only a few heterolithic breccias are likely true diatremes (Bell and Delaney, 1977). Some breccias contain anastomosing mafic dykes. Some of the breccias, especially those showing very little alteration, show soft or semiplastic deformation (for example near Cobalt Cirque, also see Laznicka, 1977a) and almost certainly were formed soon after deposition of the wall rock sediments. Some may be diapirs, like those of South Australia (Dalgarno and Johnson, 1968).

Finally, most of the known uranium occurrences appear to be within about 300 m of the pre-Phanerozoic unconformity, and consequently some may be partly supergene. If the sub-Quartet Group unconformity is confirmed this possibility is further enhanced (see point 3 above).

Styles of uranium occurrences in the Wernecke terrane are summarized below:

a. brannerite crystals in crosscutting quartz veins in breccias

b. brannerite and pitchblende on margins of pinch-and-swell concordant quartz veins

c. brannerite and uraninite in matrix of heterolithic breccias

d. brannerite ± chalcopyrite ± native gold in matrix of homolithic (siliceous, feldspathic and hematitic) breccia

e. brannerite in and around barite-magnetite veins

f. brannerite and monazite in matrix and in veins in carbonatized, feldspathized and chloritized homolithic breccias that, in places, resemble syenite, accompanied by anomalous REE ± Au ± Th

g. pitchblende ± cobaltite ± chalcopyrite in matrix and in thin veins in slightly chloritized and slightly carbonatized homolithic breccia which show soft sediment deformational features

h. strongly radioactive, hematitic-altered lamellae in dark pelite, both as clasts in breccia and in wallrocks to breccia; also hematite-stained radioactive lamellae in micaceous phyllite

i. masuyite-curite-kasolite ± uranophane in nodules 1 to 10 cm in diameter within soils on creep-talus developed in unglaciated terrain underlain by mineralized breccia and lying 50 m below the projected pre-Middle Cambrian unconformity.

No molybdenum-bearing minerals other than irrigenite are known, although some breccias have anomalous Mo content.

The main concentration phase(s) of the majority of occurrences is clearly hypogene, dominated by brannerite and by uraninite or pitchblende. Intensive local metasomatism as hematitization is impressive in some breccias (e.g. PAGISTEEL, Green, 1972). Perhaps the suggestion by Gross (1965; Bell, 1978) that these are the sites of exhalations for the Rapitan iron formation bears closer scrutiny.

The relative importance of preconcentration of U in black shales (item h above), deposition by fluids from deep-seated sources (item f), and supergene reworking (item i) is not known.

Comparison with South Australia

Two other areas in the world are noted for huge breccia complexes, the Adelaide geosyncline in South Australia and the Copperbelt in Zaire. These areas show similarities with respect to dominant lithologies, age of the sedimentary successions, and types and styles of mineralization. The following notes and Table 1 compare aspects of the Wernecke-Ogilvie-Mackenzie area with South Australia, with a focus on uranium-bearing breccias. Other writers (for example, Rowlands, 1974) have compared the Adelaidean and the African Copperbelt, emphasizing copper deposits.

Table 1

Comparison between Adelaidean (A) and Wernecke-Ogilvie-Mackenzie (WOM) areas

	A	WOM
GENERAL		
SEDIMENTS	-INTRACRATONIC, BASINAL AND PLATFORM SEDIMENTS WITH MANY UNCONFORMITIES AND DISCONFORMITIES; GENERALLY LACKING EXTENSIVE TURBIDITE FACIES OF "TYPICAL" GEOSYNCLINES; 4 MAJOR CYCLES OF SEDIMENTATION.	-NOT DEMONSTRATED TO BE INTRACRATONIC, OTHERWISE SEDIMENTARY FACIES SIMILAR; FEW UNCONFORMITIES YET IDENTIFIED; 3 MAJOR CYCLES OF SEDIMENTATION IDENTIFIED.
TILLITES	-TWO SUCCESSIONS, ONE WITH Fe Fm	-SIMILAR
THICKNESS	-MAXIMUM THE ORDER OF 14 KM	-MAY EXCEED 14 KM
AGE OF SUCCESSION	-ROUGHLY BETWEEN 1400 Ma AND CAMBRIAN	-SIMILAR
METAMORPHISM	-UNDEFORMED TO DEFORMED, NON-METAMORPHOSED TO AMPHIBOLITE FACIES	-DEFORMED THROUGHOUT; LOCALLY METAMORPHOSED TO GREENSCHIST FACIES
BASEMENT	-IDENTIFIED, OLDER THAN 1600 Ma	-NOT IDENTIFIED
MINERAL DEPOSITS/ OCCURRENCES		
Fe Fm ASSOC. WITH TILLITES	-BRAEMAR, MALDORKY HILL	-SNAKE RIVER (RAPITAN)
Fe ASSOC. WITH BRECCIA	-DIAPIRS (e.g. WORUMBA); MOUNT PAINTER BRECCIAS (TILLITES?); LAYERED BRECCIA ROXBY DOWNS; SIDERITE VEINS; HEMATITE-LIMONITE ZONES IN FAULTS (NEW DAM, SE OF ROXBY)	-VARIOUS BRECCIAS, e.g. PAGISTEEL SIDERITE VEINS, e.g. COBALT CIRQUE JASPEROIDS IN BRECCIAS
SEDIMENT HOSTED Cu	-THROUGHOUT ADELAIDEAN, e.g. MT. GUNSON, KAPUNDA, YUDNAMATANA	-SCATTERED; NOTABLY REDSTONE-COPPERCAP; SEE ALSO GOODFELLOW 1979
VOLCANIC HOSTED Cu	-WOOLTANA	-UNKNOWN
BRECCIA HOSTED Cu	-NUMEROUS IN DIAPIRS BEDDED BRECCIA AT ROXBY DOWNS	-NUMEROUS IN BRECCIAS; SEE LAZNICKA 1977 a AND b
BARITE	-IN BRECCIAS AND ASSOCIATED VEINS	-BARITE-MAGNETITE VEINS WITH BRECCIA
Co/Ag	-IN DIAPIRS, e.g. YOUNG COBALT MINE	-NUMEROUS IN BRECCIAS, e.g. COBALT CIRQUE, FAIRCHILD LAKE
Au	-ASSOCIATED WITH Cu, ESPECIALLY IN STURTIAN BEDS, ALSO IN ROXBY BRECCIAS	-ASSOCIATED WITH BRANNERITE BEARING BRECCIAS
Mo	-ASSOCIATED WITH Cu	-GEOCHEMICAL ANOMALY WITH BRECCIAS
REE	-ROXBY AND MOUNT PAINTER	-ASSOCIATED WITH SOME BRANNERITE BEARING BRECCIAS
U	-ASSOCIATED WITH HEMATITIC Cu-BEARING BRECCIAS, ROXBY DOWNS AND MOUNT PAINTER	-ASSOCIATED WITH HEMATITIC Cu-BEARING BRECCIAS (SEE TEXT)

Table derived from references cited, notably Thomson et al.(1976), Coats and Blissett (1971), Knight (1975), McAndrew (1965), and Rowlands (1974.)

There are various proposals for the origins of the breccias in the Adelaide geosyncline, although most of the Adelaidean breccias appear to be related to diapirism through as much as 12 km of the Adelaidean geosynclinal succession. The proposals include:

1. diapiric, passive intrusion, perhaps driven by evaporites
2. explosive emplacement (magma derived gases)
3. tillites
4. coarse sediment aprons along active faults, perhaps including large slide blocks
5. crush zones associated with faults
6. crush zones in synclinal folds and upwards injection
7. magmatic and volcanic emplacement

These breccias may have been modified by various hypogene and supergene processes. The ferruginous Cu-U breccias in the Mount Painter region have been reinterpreted as sedimentary (tillite?) in origin (Thomson et al., 1976).

The layering of the Roxby Downs breccias, which are in the shelf sequence of the Adelaidean, suggests some form of rapid sedimentation (4 above) although they too may be modified by supergene or hypogene processes.

The uranium deposits in the Adelaidean terrane discovered prior to Roxby Downs are relatively small. The recent disclosure that the Olympic Dam deposit at Roxby Downs contains in the order of 750 000 000 tons of ore with 1.5 per cent Cu and approximately 0.05 per cent U_3O_8 (as interpreted by the author from Lyons, 1981) clearly indicates a new spectacular class of deposit. The broad geological similarities between the Wernecke and the Adelaidean areas is encouraging.

Finally, Lefebvre (1980) drew parallels between the Wernecke breccias and those of the Zairean Copperbelt. He also provided evidence for brecciation of Proterozoic rocks younger than the Wernecke Supergroup. His volcanic rocks are perhaps part of the lower Rapitan (unit 4 of Green, 1972; Payne and Allison, 1981; Thompson and Roots, 1982) but they may be lower "Pinguicula" (Fig. 1). It is important to underline that there are many uncertainties concerning Proterozoic stratigraphy in Yukon as mentioned earlier (e.g. Eisbacher, 1979).

The eastern Wernecke Mountains are rated very high potential for U-Cu-Au-Fe deposits in breccias but require much more study. It is instructive to note that South Australia has been intensively explored since the mid-1800s, particularly since the start of economic interest in uranium, but that the large intriguing and enigmatic Cu-U ± Au deposits were only confirmed within the last six years.

Acknowledgments

J-J. Lefebvre persuaded me that there are metallogenic similarities between the Ogilvie-Wernecke-Mackenzie mountains area and the Copperbelt in Zaire. G.M. Yeo informed me of the Adelaidean tillites and associated iron formations. This in turn led me to the newer interpretations of the Mount Painter breccias by other geologists and to the knowledge that the breccias are hematitic. Further reading on the geology of South Australia convinced me that the area is a major Cu-U province as well as a major Cu province, and that the Wernecke terrane is also a Cu-U province. L. Curtis drew my attention to the impressive hematite in the Olympic Dam deposit. Subsequently a talk by D. Roberts introduced me to the geology of Roxby Downs.

I wish to thank those mentioned above as well as my colleagues at the Geological Survey of Canada, too numerous to list here, for many fruitful discussions.

References

Aitken, J.D.
1981: Stratigraphy and sedimentology of the Upper Proterozoic Little Dal Group, Mackenzie Mountains, Northwest Territories; in Proterozoic Basins of Canada, ed. F.H.A. Campbell, Geological Survey of Canada, Paper 81-10, p. 47-71.

Archer, A.R. and Schmidt, U.
1978: Mineralized breccias of Early Proterozoic age, Bonnet Plume River district, Yukon Territory; Canadian Institute of Mining and Metallurgy Bulletin, v. 71, no. 796, p. 53-58.

Archer, A.R., Bell, R.T., Delaney, G.D., and Godwin, C.
1977: Mineralized breccias of Wernecke Mountains, Yukon; Geological Association of Canada, Program with Abstracts, v. 2, p. 5.

Bell, R.T.
1978: Breccias and uranium mineralization in the Wernecke Mountains, Yukon – a progress report; in Current Research, Part A, Geological Survey of Canada, Paper 78-1A, p. 317-322.

Bell, R.T. and Delaney, G.D.
1977: Geology of some uranium occurrences in Yukon Territory; in Current Research, Part A, Geological Survey of Canada, Paper 77-1A, p. 33-37.

Carrière, J.J., Sinclair, W.D., and Kirkham, R.V.
1981: Copper deposits and occurrences in Yukon Territory; Geological Survey of Canada, Paper 81-12, 62 p., 2 maps.

Coats, R.P. and Blissett, A.H.
1971: Regional and economic geology of the Mount Painter province; Department of Mines, Geological Survey of South Australia, Bulletin 43, 426 p.

Dalgarno, C.R. and Johnson, J.E.
1968: Diapiric structures and Late Precambrian – Early Cambrian sedimentation in Flinders Ranges, South Australia; in Diaprisim and Diapirs, a Symposium, ed. J. Braunstein and G.D. O'Brian; American Association of Petroleum Geologists, Memoir 8, p. 301-314.

Delaney, G.D.
1978: A progress report on stratigraphic investigations of the lowermost succession of Proterozoic rocks, northern Wernecke Mountains, Yukon Territory; Department of Indian and Northern Affairs, Open File EGS 1978-10, 12 p., plus 3 figures.

1981: The mid-Proterozoic Wernecke Supergroup, Wernecke Mountains, Yukon Territory; in Proterozoic Basins of Canada, ed. F.H.A. Campbell, Geological Survey of Canada, Paper 81-10, p. 1-23.

Delaney, G.D., Jefferson, C.W., Yeo, G.M., McLennan, S.M., Aitken, J.D., and Bell, R.T.
Some Proterozoic sediment-hosted metal occurrences of the northeastern Canadian Cordillera; Idaho Bureau of Mines. (in press)

Eisbacher, G.H.
1977: Tectono-stratigraphic framework of the Redstone Copper Belt, District of Mackenzie; in Report of Activities, Part A, Geological Survey of Canada, Paper 77-1A, p. 229-234.

1978a: Two major Proterozoic unconformities, northern Cordillera; in Current Research, Part A, Geological Survey of Canada, Paper 78-1A, p. 53-58.

1978b: Redefinition and subdivision of the Rapitan Group, Mackenzie Mountains; Geological Survey of Canada, Paper 77-35, 22 p.

1979: Comment 'Middle and late Proterozoic evolution of the northern Canadian Cordillera and Shield'; Geology, v. 7, p. 329.

1981: Sedimentary tectonics and glacial record in the Windermere Supergroup, Mackenzie Mountains, northwestern Canada; Geological Survey of Canada, Paper 80-27, 40 p.

Goodfellow, W.D.
1979: Geochemistry of copper, lead, and zinc mineralization in Proterozoic rocks near Gillespie Lake, Yukon; in Current Research, Part A, Geological Survey of Canada, Paper 79-1A, p. 333-348.

Green, L.H.
1972: Geology of Nash Creek, Larsen Creek and Dawson map-areas, Yukon Territory; Geological Survey of Canada, Memoir 364, 157 p.

Gross, G.A.
1965: Geology of iron ore deposits and iron-formations of Canada; in Report of Activities, Field 1964, Geological Survey of Canada, Paper 65-1, p. 142-143.

Jefferson, C.W.
1978a: Stratigraphy and sedimentology, Upper Proterozoic Redstone Copper Belt, Mackenzie Mountains, N.W.T. – a preliminary report; in Mineral Industry Report 1975, Northwest Territories, Department of Indian and Northern Affairs, EGS 1978-5, p. 157-169.

1978b: Correlation of middle and upper Proterozoic strata between northwestern Canada and south and central Australia; Geological Association of Canada, Program with Abstracts, v. 3, p. 429.

Knight, C.L., ed.
1975: Economic Geology of Australia and Papua New Guinea; The Australasian Institute of Mining and Metallurgy, Monograph Series no. 5, 1126 p. with Map Supplement.

Laznicka, P.
1977a: Geology and mineralization in the Dolores Creek area, Bonnet Plume Range, Yukon; in Current Research, Part A, Geological Survey of Canada, Paper 77-1A, p. 435-439.

1977b: Geology and mineralization in the Dolores Creek area, Yukon; Department of Indian and Northern Affairs, Open File, May 1977, 87 p.

Laznicka, P. and Edwards, R.J.
1979: Dolores Creek, Yukon – a disseminated copper mineralization in sodic metasomatites; Economic Geology, v. 74, p. 1352-1370.

Lefebvre, J-J.
1980: A propos de l'existence d'un "Wildflysch Katangien"; Annales de la Société géologique de Belgique, T. 103, p. 1-13.

Lyons, L.A.
1981: Australia's big copper-uranium deposit; World Mining, July 1981, p. 28-32.

McAndrew, John, ed.
1965: Geology of Australian Ore Deposits, Second Edition; Eighth Commonwealth Mining and Metallurgical Congress, Australia and New Zealand, 1965; The Australasian Institute of Mining and Metallurgy Publications, v. 1, 530 p.

Morin, J.A.
1977: Uranium-copper mineralization and associated breccia bodies in the Wind-Bonnet Plume River area, Yukon; in Mineral Industry Report for Yukon Territory 1976, Department of Indian Affairs and Northern Development, p. 101-107.

Morin, J.A., Marchand, M., Craig, D.B., and Debicki, R.L.
1979: Mineral Industry Report 1977, Yukon Territory; Department of Indian and Northern Affairs, EGS 1978-9, 124 p.

Norris, D.K.
1974: Structural and stratigraphic studies in the northern Canadian Cordillera; in Report of Activities, Part A, Geological Survey of Canada, Paper 74-1A, p. 343-349.

Norris, D.K. and Hopkins, W.S.
1977: The geology of the Bonnet Plume Basin, Yukon Territory; Geological Survey of Canada, Paper 76-8, 20 p.

Payne, M.W. and Allison, C.W.
1981: Paleozoic continental-margin sedimentation in east-central Alaska; Geology, v. 9, p. 274-279.

Rowlands, N.J.
1974: The gitology of some Adelaidean stratiform copper occurrences; in Gisements stratiformes et provinces cuprifères, ed. P. Bartholomé; Société géologique de Belgique, p. 419-427.

Sears, J.W. and Price, R.A.
1978: The Siberian connection: a case for Precambrian separation of the North American and Siberian cratons; Geology, v. 6, p. 267-270.

Stewart, J.H.
1972: Initial deposits in the Cordilleran geosyncline: evidence of a late Precambrian (<850 m.y.) continental separation; Geological Society of America Bulletin, v. 83, p. 1345-1360.

Tempelman-Kluit, D.J.
1979: Transported cataclasite, ophiolite and granodiorite in Yukon: evidence of arc-continental collision; Geological Survey of Canada, Paper 79-14, 27 p.

1981a: CRAIG, summary of assessment work and description of mineral properties; in Yukon, Geology and Exploration 1979-80, Geology Section, Department of Indian and Northern Affairs, p. 225-230.

1981b: NOR, summary of assessment work and description of mineral properties; in Yukon, Geology and Exploration 1979-80, Geology Section, Department of Indian and Northern Affairs, p. 300-301.

Thompson, R.I. and Roots, C.F.
1982: Ogilvie Mountains project, Yukon; Part A: a new regional mapping program; in Current Research, Part A, Geological Survey of Canada, Paper 82-1A, p. 403-411.

Thompson, B.P., Barley, B., Coats, R.P., and Forbes, B.G.
1976: Late Precambrian and Cambrian geology of the Adelaide 'Geosyncline' and Stuart Shelf, South Australia; Excursion Guide 33A, 25th International Geological Congress, Canberra, Australia, 53 p.

Yeo, G.M.
1981: The late Proterozoic Rapitan glaciation in the northern Cordillera; in Proterozoic Basins of Canada, ed. F.H.A. Campbell, Geological Survey of Canada, Paper 81-10, p. 25-46.

Yeo, G.M., Delaney, G.D., and Jefferson, C.W.
1978: Two Proterozoic unconformities, northern Cordillera: discussion; in Current Research, Part B, Geological Survey of Canada, Paper 78-1B, p. 225-230.

Young, G.M.
1981: Upper Proterozoic supracrustal rocks of North America: a brief review; Precambrian Research, v. 15, p. 309-330.

Young, G.M., Jefferson, C.W., Delaney, G.D., and Yeo, G.M.
1979a: Middle and late Proterozoic evolution of the northern Cordillera and Shield; Geology, v. 7, p. 125-128.

1979b: Reply – 'Middle and late Proterozoic evolution of the northern Canadian Cordillera and Shield'; Geology, v. 7, p. 329-330.

MAPPING SUB-SEABOTTOM PERMAFROST IN THE TUKTOYAKTUK AREA, NORTHWEST TERRITORIES

Project 730006

R.L. Good and J.A. Hunter
Resource Geophysics and Geochemistry Division

Introduction

From 1972 to 1978 the offshore area near Tuktoyaktuk, Northwest Territories, was used by the Geological Survey of Canada as a test site for marine shallow refraction systems used in the offshore Mackenzie Delta area in sub-seabottom permafrost mapping. Over the years a number of traverse lines were run with differing types of seismic refraction equipment as "shake-down" cruises prior to deployment of these systems in other areas.

Sufficient information has been acquired in the Tuktoyaktuk area to enable us to determine, in a reconnaissance manner, the general structure of the upper surface of sub-seabottom ice-bonded permafrost.

The survey was carried out in Kugmallit Bay in the near offshore area west and north of the hamlet of Tuktoyaktuk (see Fig. 1). The area surveyed was approximately 12 x 6 km and represents 91 line-km of coverage.

Survey Procedure

A 12 channel buoyed hydrophone cable with 15 m spacings was used throughout the survey. The cable was towed in a near surface configuration from a small boat at slow speeds and at intervals seismic shots were detonated astern the boat and in-line with the cable. The initial surveys used small charges (0.3 kg) of explosives, however, later surveys employed a small airgun as a seismic source. Positioning was done from shore ranges, radar, and portable radio transmitting positioning systems. Various types of seismic recording systems were used over the years with continual improvement in timing accuracy and record quality.

First arrival refraction events were interpreted for most records and velocity and depth computations were made in a manner similar to that given by Hunter and Hobson (1975). In some shot locations where first arrival refractions were too low in amplitude to be determined, the wide-angle reflection from the top of ice-bonded permafrost was interpreted.

Most refraction interpretations yielded a two layer case for sub-seabottom sediments: an upper non-ice-bonded sediment velocity of 1500 m/sec and an ice-bonded sediment velocity with an average of 3500 m/sec. The ice-bonded permafrost velocity is indicative of ice-bonded sands. The accuracy of depth estimates from refraction interpretation depends largely on the record quality. An average depth error may be 10 per cent with local zones where error may occasionally exceed that estimate.

Results

The depth from sea surface to ice-bonded permafrost is shown in the form of a contoured map in Figure 1. Water depths throughout the map area did not exceed 4 m. West of the hamlet the top of ice-bonding drops abruptly from surface at the shore to depths in excess of 30 m within a few hundred metres offshore and gradually achieves a depth of 60 m within 2 km offshore.

Northwest of Flagpole Point the ice-bonded zone is only 20 m below sea surface corresponding to a bathymetric shoal area. Photographs taken early in the century showed this shoal area to be land (Father R. Lemeur, Tuktoyaktuk, personal communication) which has subsequently been eroded by thermal degradation of permafrost and wave action. Since this is a shoal area, (1 to 2 m water depth), sea ice freezes to the bottom and the mean annual seabottom temperatures, although positive, are probably much lower than adjacent areas. Hence, thermal degradation of permafrost may be lower in this area.

A similar shoal area southwest of Topkak Pt. (1 m water depth) also freezes to bottom in winter. Beneath this shoal, the top of ice-bonded permafrost is similarly only 20 m below sea surface.

North of Tuktoyaktuk Island a depression in the top of ice-bonded permafrost strikes northwest. The shape of this depression resembles the topographic expression of a river valley. Tuktoyaktuk harbour is thought to be a drowned river system; and this depression in the top of permafrost may be an expression of the relict river channel outflow at lower sea level.

In summary, the depth to the top of ice-bonded permafrost in the offshore area near Tuktoyaktuk varies from 20 to 70 m below sea surface. This variation in depth results from coastal erosion, location of bathymetric shoals and the influence of river "outflow" at lower sea level.

Reference

Hunter, J.A. and Hobson, G.D.
1975: A seismic refraction method to detect sub-seabottom permafrost; in Proceedings of Beaufort Sea Symposium, San Francisco, Arctic Institute of North America, p. 401-416.

From: Scientific and Technical Notes in Current Research, Part B; Geol. Surv. Can., Paper 82-1B.

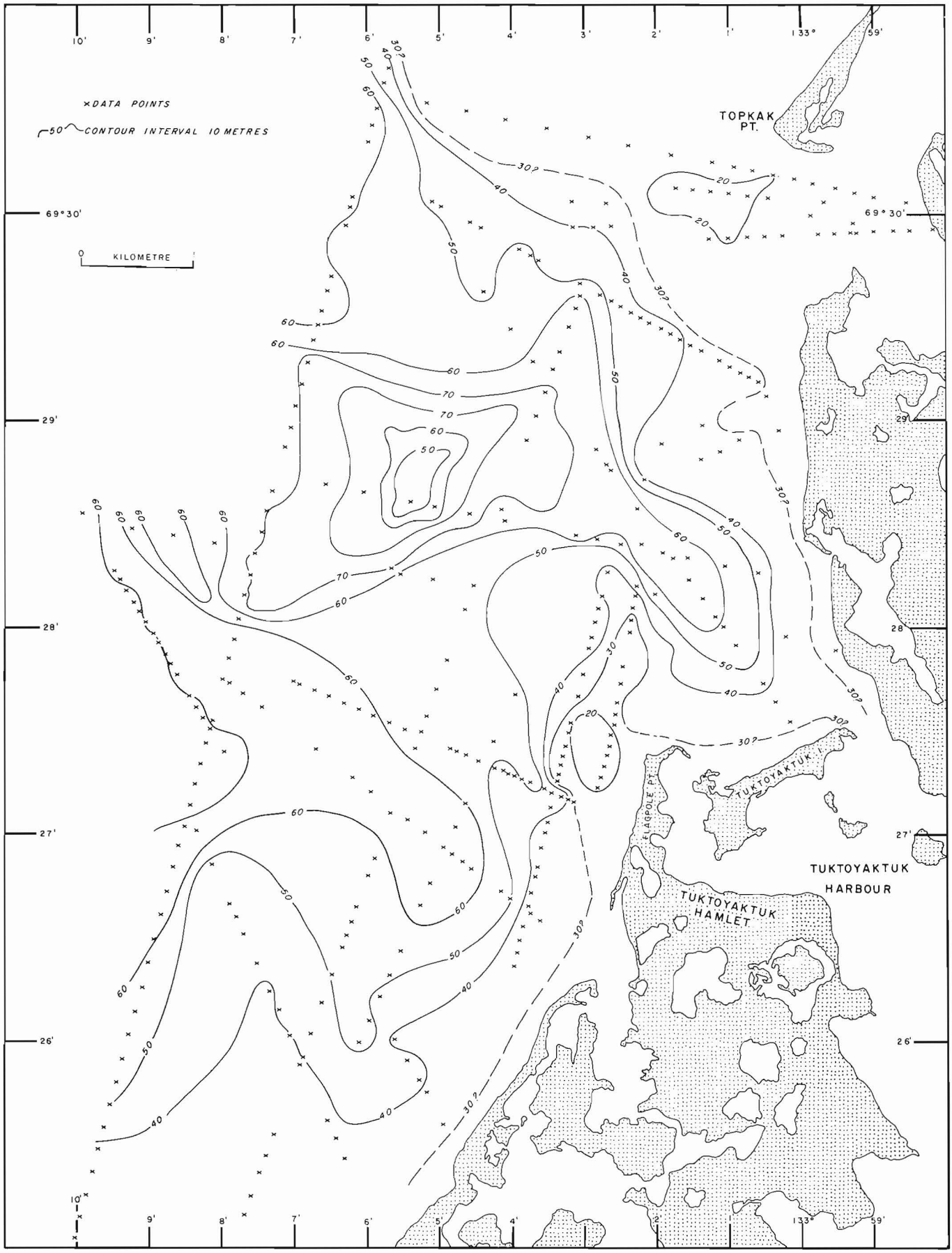

Figure 1. *Depth from sea surface to the top of ice-bonded permafrost from seismic results.*

SOME OBSERVATIONS OF UP-HOLE SEISMIC VELOCITIES AND PERMAFROST TEMPERATURES IN MACKENZIE DELTA SEDIMENTS

Project 730006

J.A. Hunter and H.A. MacAulay
Resource Geophysics and Geochemistry Division

Introduction

During the 1978 and 1979 field seasons, a series of shallow holes were drilled in sediments of the modern Mackenzie River delta in co-operation with C.P. Lewis (Department of Indian and Northern Affairs) who was carrying out delta sedimentation studies. Many of these holes presented an excellent opportunity to obtain comparisons of in situ velocities, sediment types and temperatures of permafrost materials.

The locations of the holes shown in Figure 1 were chosen to obtain a broad areal coverage of the delta and, for this study, they were positioned as far as possible away from the thermal influence of delta channels.

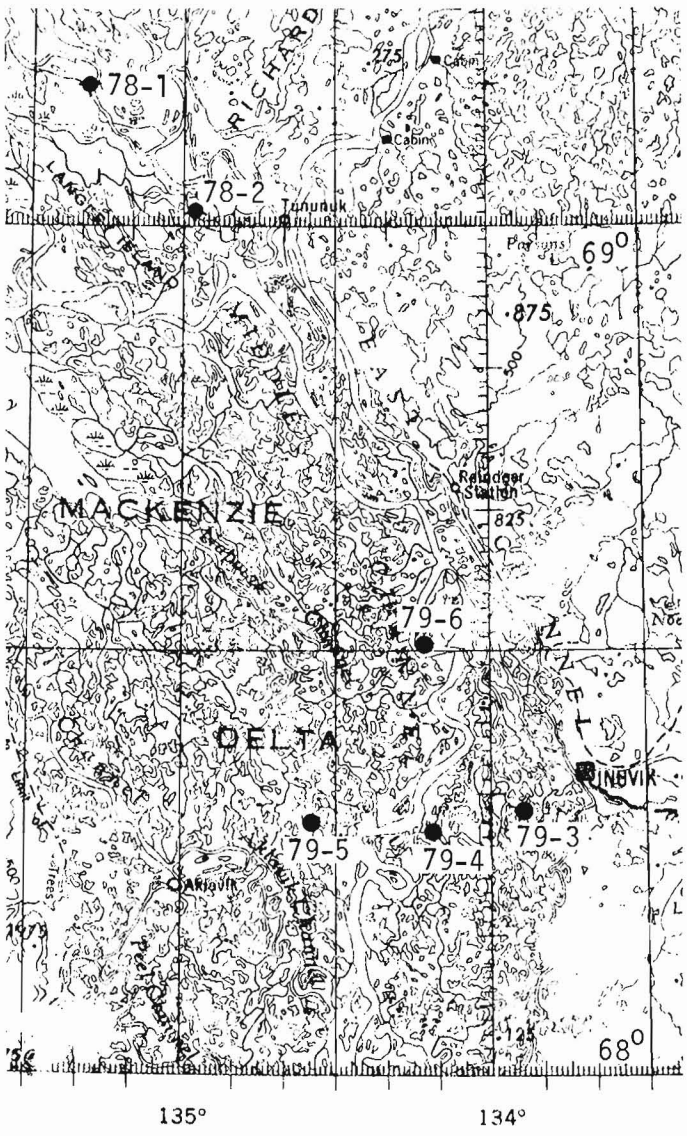

Figure 1. *Location of drillholes in the "modern" Mackenzie delta.*

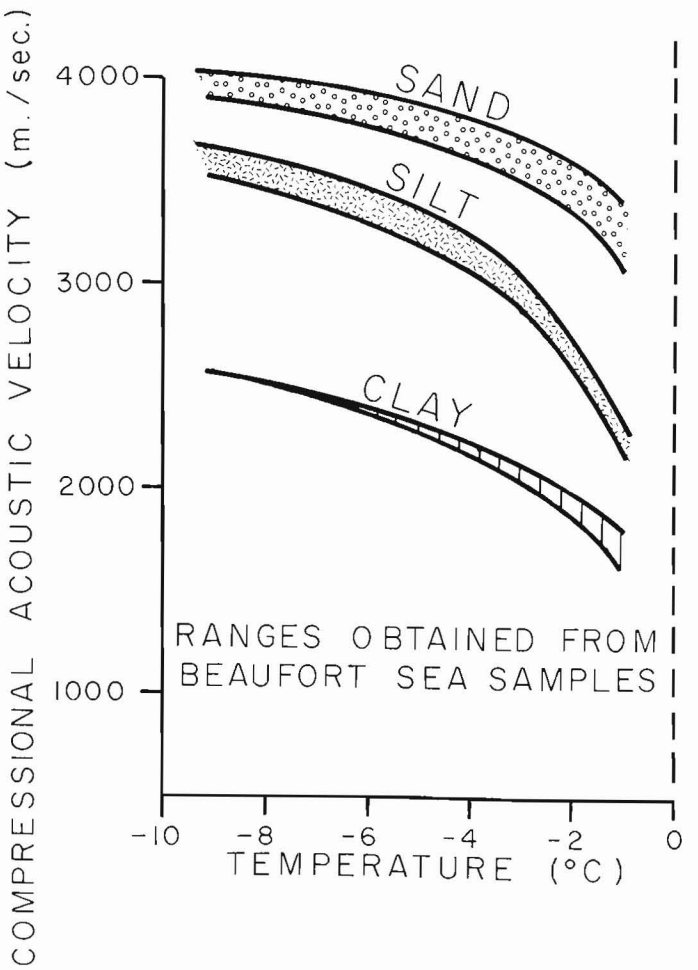

Figure 2. *Variation of acoustic velocities with permafrost temperatures for Beaufort Sea subbottom samples after King et al. (1982).*

All holes were drilled using the hydraulic jetting method described by MacAulay (1979). Most holes were drilled to 40 m depth or more and washed sediment samples were recovered on surface. ABS casing was installed as deeply as possible in each hole so that a single hydrophone could be lowered for seismic measurements. Composite first arrival travel time-depth record suites were obtained by repeatedly shooting with a small explosive charge on surface and moving the hydrophone down the hole in 0.76 m intervals. Time-distance plots of first-arrival refracted P waves were constructed for each hole, and least-squares velocity segments were interpreted. Multithermistor cables were installed in the holes and temperature readings were taken 4 to 6 weeks after installation to insure near-equilibrium measurements.

The results are shown in Figures 3 to 8 in the form of velocity, geology and temperature logs. Correlations between parameters are quite complex. From numerous laboratory velocity-temperature measurements of ice-bonded sediments (Aptikaev, 1964; Dzhurick and Leshchikov, 1973; Frolov and Zykov, 1971; Kurfurst and Hunter, 1976; Nakano et al., 1971, 1972; Nakano and Froula, 1973; Nakano and Arnold, 1973; King et al., 1982), a correlation between seismic velocity and lithology should be recognizable for isothermal conditions. That is, at any fixed temperature below 0°C seismic velocities should increase with increasing grain size for freshwater saturated unconsolidated sediments.

From: Scientific and Technical Notes in Current Research, Part B; Geol. Surv. Can., Paper 82-1B.

Figures 3-8

Seismic velocity, lithology and temperature logs for Mackenzie delta drillholes.

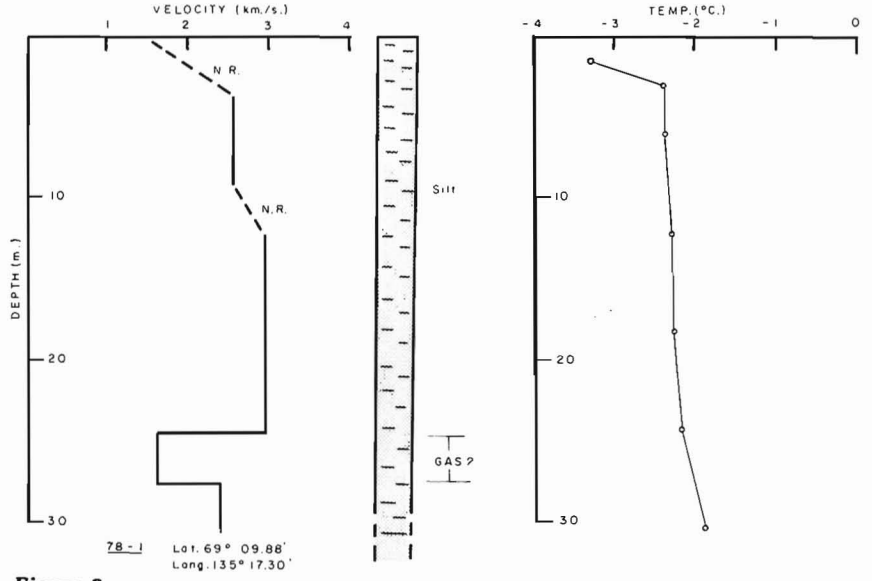

Figure 3

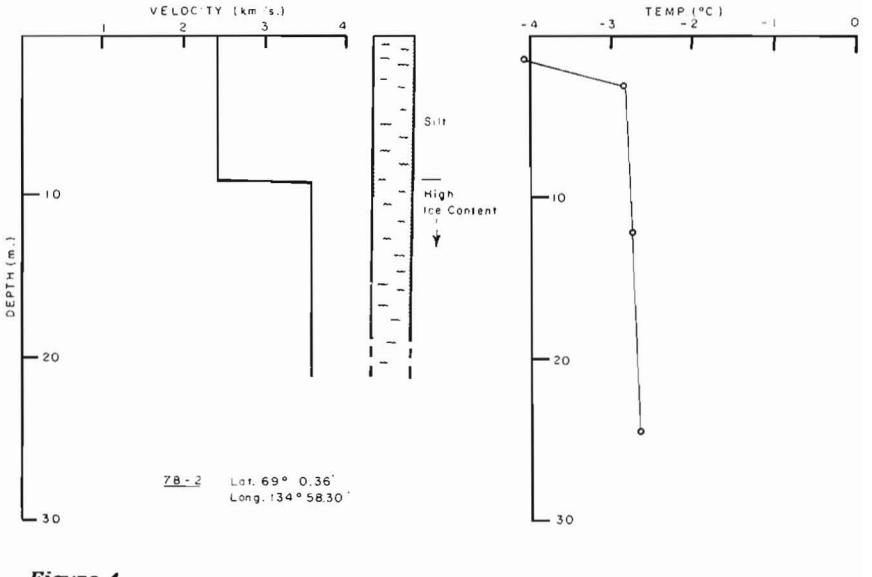

Figure 4

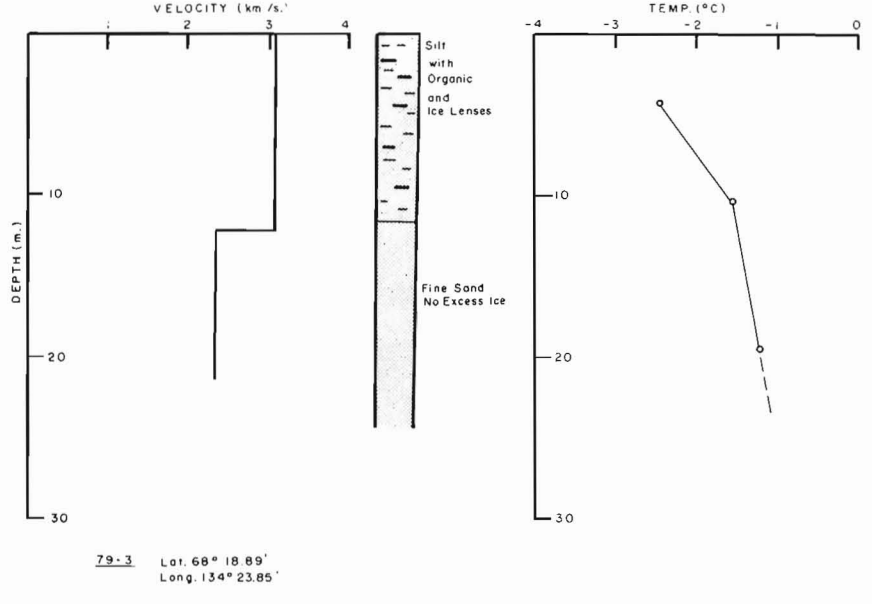

Figure 5

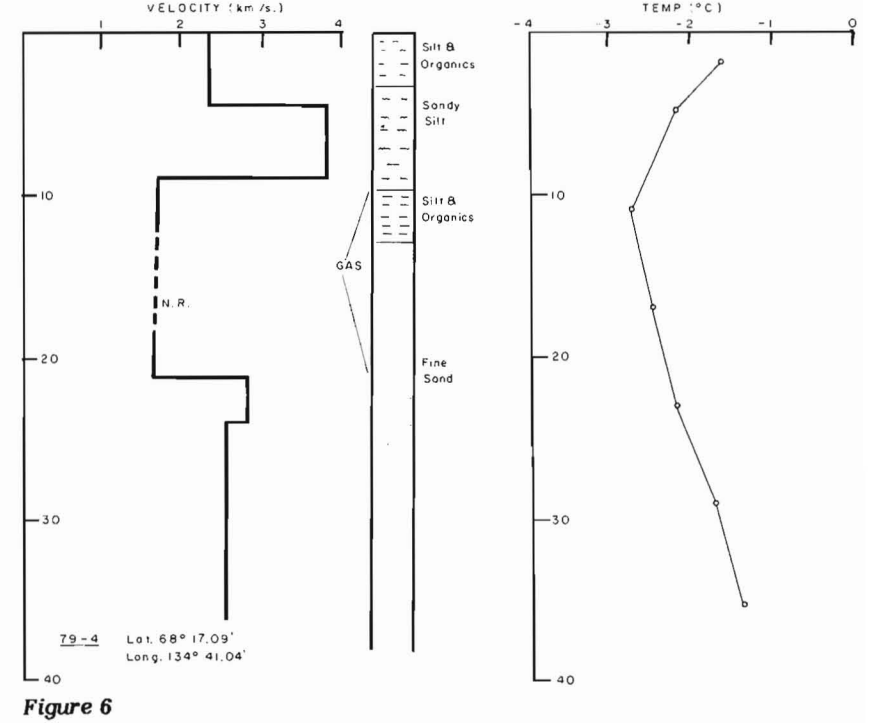

Figure 6

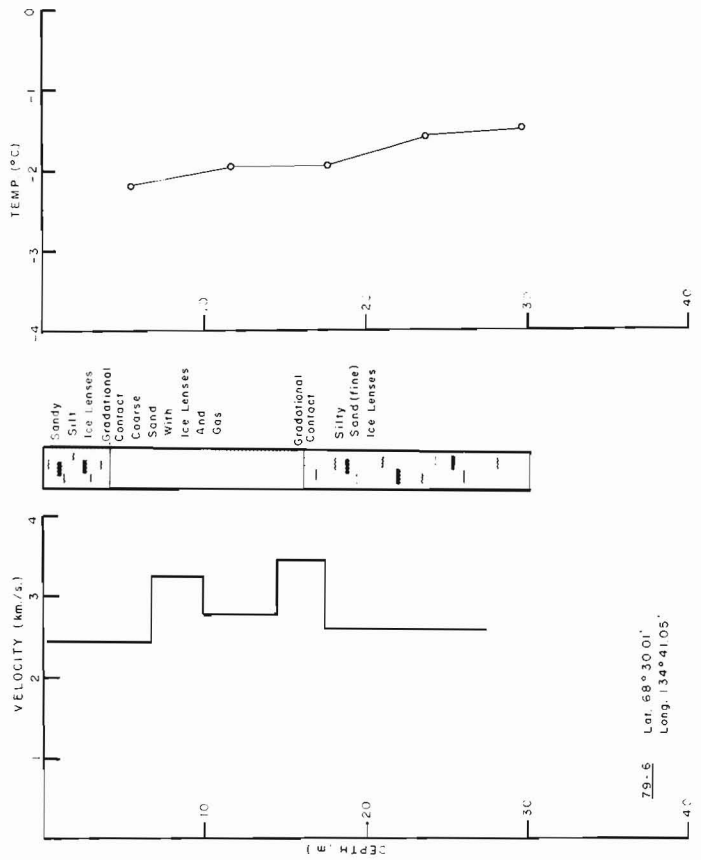

Figure 8

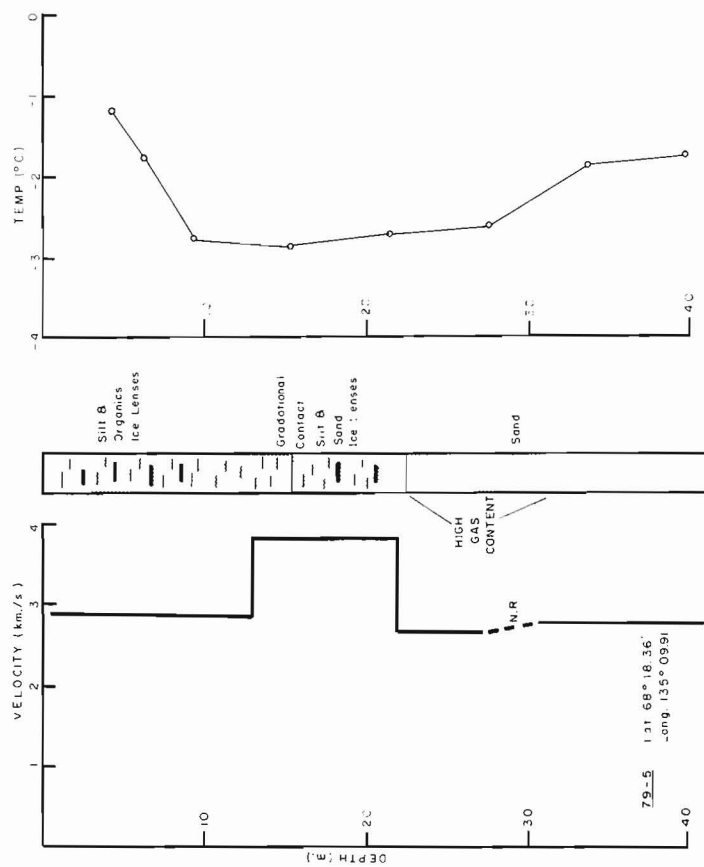

Figure 7

Figure 2 from King et al. (1982) shows velocity-temperature curves for Beaufort Sea core samples of various grain sizes and is a useful guide for comparison with present in situ data discussed here. The data discussed here indicate that other factors control the observed in situ velocities; that is, both excess ice and gas were logged in many of the holes drilled. Unfortunately, with the hydraulic jet drilling technique, it is not possible to obtain quantitative estimates of these parameters.

Holes 78-1 and 78-2 (Fig. 3, 4)

Drillholes 78-1 and 78-2 indicate silt throughout the sections. Although near surface temperatures in the top 5 m are low, the observed velocities are also low, yet are in the range expected for silts at these temperatures (from laboratory results). In both holes, higher velocities are observed below 10 m depth indicating higher ice content. A zone of low velocity (1600 m/sec) in DH 78-1 at a depth of 27.5 m suggests the presence of gas or possibly saline pore water, since temperatures are less than -2°C.

Hole 79-3 (Fig. 5)

In hole 79-3 a 12 m thick layer of silt overlies fine sand. Although the silt temperature is in the range of -1.5° to -2.5°C, its velocity might be expected to be less than that of fine sand at -1.2°C. However, excess ice in the silt layer results in an observed velocity of 3000 m/sec, substantially higher than the fine sand at 2300 m/sec, an anomalously low velocity.

Hole 79-4 (Fig. 6)

The logs from hole 79-4 show a wide variety of velocities associated with a narrow range of sediment types. The surface layer of silts and organics at an average temperature of -2°C gives a velocity of 2300 m/sec which might be expected from laboratory data. However, the velocity of the underlying sandy silt (3800 m/sec) at a temperature of -2.5°C is somewhat high. For such a velocity to occur, grain-to-grain contact must be maintained with most of the pore water in the form of ice; further, the sand content must predominate.

From 9 to 21.5 m depth, gas was logged in association with silt, organics and fine sand. The observed velocity of 1700 m/sec is anomalously low for temperatures in the range of -2.5°C. It is well known that small quantities of gas in pore spaces of nonpermafrost material result in dramatic lowering of velocities (Domenico, 1976). In the depth zone of 15 m, refraction signals were so strongly attenuated (probably as a result of gas content) that compressional wave velocities could not be accurately interpreted.

At depths below 25 m the observed velocity of fine sand (2500 m/sec) at 1.5° to -2°C is somewhat lower than might be expected from laboratory results. Here again, a small quantity of gas may be responsible for the lower velocities.

Hole 79-5 (Fig. 7)

The effect of excess ice is noticeable on seismic velocities in hole 79-5. The top 13 m of silt and organics shows an anomalously high velocity of 2850 m/sec.

The 3800 m/sec velocity associated with the silt and sand layer is also anomalously high. Although ice-bonded sands (without excess ice) in the temperature range -2.5°C to -3.0°C should exhibit velocities in the range of 4000 m/sec, the effect of excess ice or high silt content should result in a much lower velocity (3000 m/sec).

The unit (fine sand) occurring below 22.5 m yielded an observed velocity of 2750 m/sec which is somewhat lower than expected for temperatures of -2° to -2.5°C. In the upper portion of the layer, gas was noted on the drilling log. A small gas content may have contributed to the low velocity and resulted in the anomalous loss of refraction signal in the region 27.5 to 30 m depth.

Hole 79-6 (Fig. 8)

The upper layer of drillhole 79-6 was logged as sandy silt with ice lenses and the observed velocity is in the range expected. The coarse sand layer shows velocities in the range of 2200-3500 m/sec which are typical of ice-saturated sand at -2°C. However, the zone from 10 m to 14.5 m depth shows a somewhat lower velocity which is probably associated with the gas concentration noted in the log. The lowest unit of silty sand occurring below 27.5 m depth yielded an observed velocity of 2550 m/sec which is slightly lower than expected for temperatures in the range of -1.5°C when excess ice is present.

Conclusions

It is apparent that for permafrost sediments in the range -1° to -3°C, the seismic velocity grain size relationship can be strongly altered by the presence of excess ice and gas. The presence of gas can strongly lower the observed velocity of coarse grained, ice-rich sediments into the same range as that of fine grained, low ice-content sediments. The presence of large amounts of excess ice can either increase the velocity of fine grained sediments into the range of that of coarse grained ones, or lower the velocity of coarse grained ones towards the velocity of ice (approximately 3000 m/sec).

Without borehole control, seismic velocities cannot be used to determine accurately the grain size of materials. Observed velocities alone, however, can be used as a relative indication of ice content only if gas is absent. Velocities above 2500 m/sec suggest high ice-content materials. Velocities in excess of 3500 m/sec indicate coarse grained materials in grain-to-grain contact (little excess ice). Velocities in the range of 3000 m/sec may either indicate silts or fine sands with interstitial ice or any grain size material with a considerable amount of excess ice (where grain-to-grain contact is broken). Velocities less than 2000 m/sec may not necessarily indicate low ice-content materials but may result from high ice-content materials having minor amounts of gas in pore spaces.

References

Aptikaev, F.F.
1964: Temperature field effect on the distribution of seismic velocities in the permafrost zone; Akademiya Nauk SSSR Sibirskoye otd-ie. Institut Merzlotovedeniia. Teplovye portesessy v merzlykh porod.

Domenico, S.N.
1976: Effect of brine-gas mixture on velocity in an unconsolidated sand reservoir; Geophysics, v. 41, no. 5, p. 882-894.

Dzhurick, V.I. and Leshchikov, F.N.
1973: Experimental studies of seismic properties of frozen ground; IInd International Conference on Permafrost, Yakutsk, v. 6, p. 64-68.

Frolov, A.D. and Zykov, Y.D.
1971: Peculiarities of the propagation of elastic waves in frozen rocks; Izv. Vysh. Ucheb. Zaved., Geol. Razvedka, no. 10, p. 89-97.

King. M.S., Pandit, B., Hunter, J.A., and Gajtani, M.
1982: Some seismic, electrical and thermal properties of sub-seabottom permafrost from the Beaufort Sea; in Proc. of IVth Canadian Permafrost Conference, National Research Council of Canada. (in press)

Kurfurst, P.M. and Hunter, J.A.
1976: Field and laboratory measurements of seismic properties of permafrost; Proceedings of a Symposium on Permafrost Geophysics, National Research Council of Canada, Technical Memoir no. 119, p. 1-15.

MacAulay, H.A.
1979: The use of hydraulic drilling methods to study offshore bottom permafrost; in Proceedings of a Symposium on Permafrost Field Methods, National Research Council of Canada, Technical Memoir no. 124, p. 25-30.

Nakano, Y. and Arnold, R.
1973: Acoustic properties of frozen Ottawa sands; Water Resources Research, v. 9, no. 1, p. 178-184.

Nakano, Y. and Froula, N.H.
1973: Sound and shock transmission in frozen soils; Proceedings of the IInd International Conference on Permafrost, North American Contribution, National Academy of Sciences, Washington, p. 359-368.

Nakano, Y., Martin, R.J., and Smith, M.
1972: Ultrasonic velocities of the dilatational and shear waves in frozen soils; Water Resources Research, v. 8, no. 4, p. 1024-1030.

Nakano, Y., Smith, M., Martin, R., Stevens, H., and Knuth, K.
1971: Determination of the acoustic properties of frozen soils; Prepared for Advanced Research Projects Agency ARPA order 1525, by Cold Regions Research and Engineering Laboratory, U.S. Army.

FEASIBILITY TESTS ON THE USE OF A QUADRUPOLE MASS SPECTROMETER FOR SULPHUR ISOTOPE DETERMINATIONS

Project 780015

W. Dyck and J.C. Pelchat
Resource Geophysics and Geochemistry Division

Introduction

The need for sulphur isotope analyses in the Geochemistry Subdivision and the presence of a quadrupole mass spectrometer, recently acquired for dissolved gas studies, prompted a series of tests to determine if the quadrupole could be used for sulphur isotope analyses. Mass spectrometer experts at McMaster University (Clarke, Rees), in the Geological Survey of Canada (Stevens, Van Breemen), and at UTI (manufacturers of the precision quadrupole mass analyser 100C) indicated that, to the best of their knowledge, no one has tried to use a quadrupole instrument for isotope work. Double collector, magnetic deflection type mass spectrometers allegedly give much higher precision than quadrupoles hence established laboratories have simply not deemed it useful to test the latter for isotope work.

The UTI 100C quadrupole mass analyser has a mass range of 1-300, a resolution of unit mass using the peak width at one half of peak height criterion and a sensitivity of 0.001 A/Torr with a Faraday cup.

In this study the first series of tests with the UTI 100C were carried out with instrument purity (99.99%) sulphur hexafluoride using a single inlet system. The isotopic composition and isotope ratios of the three sulphur isotopes ^{32}S, ^{33}S, and ^{34}S from ten runs on ten different days, using a single inlet system, are given in Table 1. Each run consists of the average of 10 scans of the mass peaks 127, 128, 129 corresponding to the main ionization products of SF_6 in the analyser, namely $(^{32}S^{19}F_5)^+$, $(^{33}S^{19}F_5)^+$, and $(^{34}S^{19}F_5)^+$. An inlet pressure of 2 mm Hg was used. This resulted in a Faraday cup ion current of about 60 pico-amperes at the mass peak of 129 (^{34}S peak).

The results in Table 1 show that a single determination of ten scans results in a 2 per cent precision for the $^{34}S/^{32}S$ ratio. Futhermore, this ratio is also dependent on the partial pressure in the analyser as evident from the ion current-isotope ration results shown in Table 2. Obviously, a single inlet system will not give accurate absolute isotope ratio results.

The dual inlet system permits close comparison of an unknown sample to a standard or reference sample by recording isotope peak currents alternately from sample and standard many times in succession and averaging the results. In this study the same gas was used in both sides of the dual inlet system under as similar conditions of pressure and leak rate as possible. The values in the last two columns of Table 2 should therefore have been zero had all conditions been perfect. This zero enrichment correction, column 6, Table 2, can be kept to 0.05‰ according to one manufacturer of double collector instruments. Similarly internal reproducibility, represented by $2\sigma_{10}$, should approach zero as noise and bias is reduced. It is calculated using the expression

$$2\sigma_{10} = 2\sqrt{\sum_{i=1}^{10} \frac{(\bar{X} - X_i)^2}{10 \times 9}}$$

Table 1

Isotopic composition of SF_6 determined on a UTI 100C quadrupole mass spectrometer using a single inlet system (each run constitutes ten scans of the mass peaks)

	%									
RUN	^{32}S		^{33}S		^{34}S		$(^{33}S/^{32}S)\times10^5$		$(^{34}S/^{32}S)\times10^4$	
N	$\bar{X}$	SD*	$\bar{X}$	SD	$\bar{X}$	SD	$\bar{X}$	SD	$\bar{X}$	SD
1	94.74	0.042	0.766	0.0062	4.482	0.039	809	6.6	478	4.1
2	94.83	0.018	0.768	0.0065	4.399	0.015	810	6.9	464	1.6
3	94.80	0.050	0.770	0.0118	4.433	0.048	812	12.5	468	5.1
4	94.82	0.023	0.768	0.0076	4.412	0.025	810	8.0	465	2.7
5	94.58	0.030	0.769	0.0061	4.639	0.025	813	6.5	490	2.7
6	94.75	0.035	0.770	0.0089	4.486	0.026	813	9.4	473	2.8
7	94.83	0.026	0.760	0.0045	4.413	0.026	802	4.8	465	2.8
8	94.83	0.034	0.759	0.0094	4.415	0.028	800	10.0	466	3.0
9	94.87	0.019	0.753	0.0068	4.369	0.026	793	7.2	460	2.8
10	94.83	0.042	0.761	0.0033	4.409	0.042	802	3.5	465	4.5
$\bar{X}$ SD	94.79	0.083	0.764	0.0058	4.446	0.077	806	6.8	469	8.4
$SD/\sqrt{N}$		0.026		0.0018		0.024		2.2		2.7

$$*SD = \sqrt{\sum_{i=1}^{N} \frac{(Xi - \bar{X})2}{N - 1}}$$

From: Scientific and Technical Notes in Current Research, Part B; Geol. Surv. Can., Paper 82-1B.

Table 2

Isotope ratios of SF_6 determined on a UTI 100C, quadrupole mass spectrometer using a dual inlet system (each run constitutes 12 alternate (6 from each side) isotope measurements of the same gas in both sides of the dual inlet system)

RUN	^{34}S ion current amps x 10^{12}	Left Side $(^{34}S/^{32}S)x10^5$ = L	Right Side $(^{34}S/^{32}S)x10^5$ = R	$2\sigma_{10}/R$ ‰	$\frac{L-R}{R}$ ‰
1	69	4646	4684	4.1	-8.2
2	68	4617	4630	6.3	-2.8
3	67	4625	4658	1.5	-7.1
4	37	4283	4299	1.3	-3.7
5	37	4411	4421	2.7	-2.3
6	29	4221	4203	3.5	+4.3
7	22	4346	4355	1.4	-2.1
8	22	4387	4386	2.1	+0.1
9	14	4539	4532	1.4	+1.5
10	12	4320	4313	1.9	+1.6
11	11	4330	4334	1.2	-0.9

$\bar{X}$ and X_i are derived from a series of twelve alternate isotope ratio measurements of the sample and reference gases. Adjacent pairs of readings are used to give eleven values for the difference in isotopic ratios between the sample and reference. Pairs of these are then averaged to derive ten values, X_i, that are effectively corrected for any linear drift. The average of these ten X_i values is represented by $\bar{X}$ in the above expression.

Obviously precision improves considerably using the dual inlet system but is still about a factor of ten away from the 0.2 ‰ precision claimed by dual inlet-dual collector type systems. Nonetheless these experiments show that where 1‰ precision is acceptable quadrupole mass spectrometers may be used. For some mineral exploration applications a precision of 1‰ on $\delta^{34}S$ should be quite adequate (E.M. Cameron, Geological Survey of Canada, personal communication). Furthermore, sampling precision is often of the same order of magnitude and, therefore, there may seldom be a need for much higher precision. The results in Table 2 also indicate that the precision increases as the ion current or partial pressure in the analyser is lowered. We are confident that procedures such as greater gain-, power-, and room temperature stabilization, automatic computer controlled peak scanning, and a more sophisticated dual inlet system, would improve precision further.

One of the main advantages of a quadrupole is its considerably lower purchase price. Its lower weight and higher portability could also prove advantageous under certain circumstances.

SOME MEASUREMENTS OF SEABOTTOM SEDIMENT VELOCITIES ON THE SCOTIAN SHELF

Project 790034

J.A. Hunter, H.A. MacAulay, R.A. Burns, and R.L. Good
Resource Geophysics and Geochemistry Division

Introduction

In co-operation with the Shallow Water Acoustics Group of Defence Research Establishment Atlantic, an experiment was conducted in December 1980 on the Scotian Shelf area of the Atlantic continental shelf to measure the compressional wave velocities of seabottom surficial sediments. Fourteen sites (Fig. 1) were investigated encompassing a variety of seabottom sediment types described by King (1970). Two types of seabottom refraction arrays, similar to those described by Hunter et al. (1979) were deployed from **CFAV Quest** during a two-day operational period. An attempt has been made to correlate observed velocities with sediment-type occurring both on the seabottom and within the immediate subseabottom zone.

Arrays and Recording Equipment

The two types of arrays are denoted as the 'fixed' and 'long' arrays. The fixed array consisted of 12 Interocean T-111 hydrophones affixed at 1.52 m intervals along a 6 cm diameter hollow teflon tube. Steel plates holding 4 seismocaps each were affixed at each end of the tube also at a distance of 1.52 m from the end hydrophone. Two shielded multiconductor cables were attached to the seismocaps and the hydrophones and were taped together and wound on a reel on deck. Each seismocap was fired independently giving a maximum of 4 shots for each end of the array yielding a reversed refraction profile.

The 'long' array consisted of 12 Mark products P-38 hydrophones connected by 'pigtails' to a double-jacketed multiconductor 'bay' seismic cable. Spacing between hydrophones was 15.2 m. A separate two-conductor shielded shot line was taped along the 'bay' cable extending (initially) 15.2 m beyond the outboard hydrophone to which a small dynamite charge (with seismocap priming) was connected. The extension cables for both shot line and hydrophone line were wound on a small reel on deck.

Shooting was done via a seismic electric blaster on deck which also provided shot instance for the recording equipment.

Amplification and recording of the hydrophone signals was done with a Nimbus model 1210F engineering seismograph and G-724S digital tape recorder. Record analysis was done with an Apple II mini-computer and periferal devices utilizing an RS-232C serial interface link with the tape recorder.

Field Procedures

The fixed array was deployed by dropping it over the side while the ship was stationary. Because of the water depths involved it was decided to hold ship's position rather than anchor. This technique worked well in normal sea state conditions. However, on the second day of the operation high winds and heavy seas curtailed deployment of this array. Hence, only sites 1 to 6 were done with the fixed array.

The fixed array, despite being deployed end-on over the side, appears to sink in a horizontal position yet is flexible enough to conform to rough seabottom topography. Only at one site (site 2) was there evidence that the array was bent. Maximum shooting time with the array on bottom was 10 minutes.

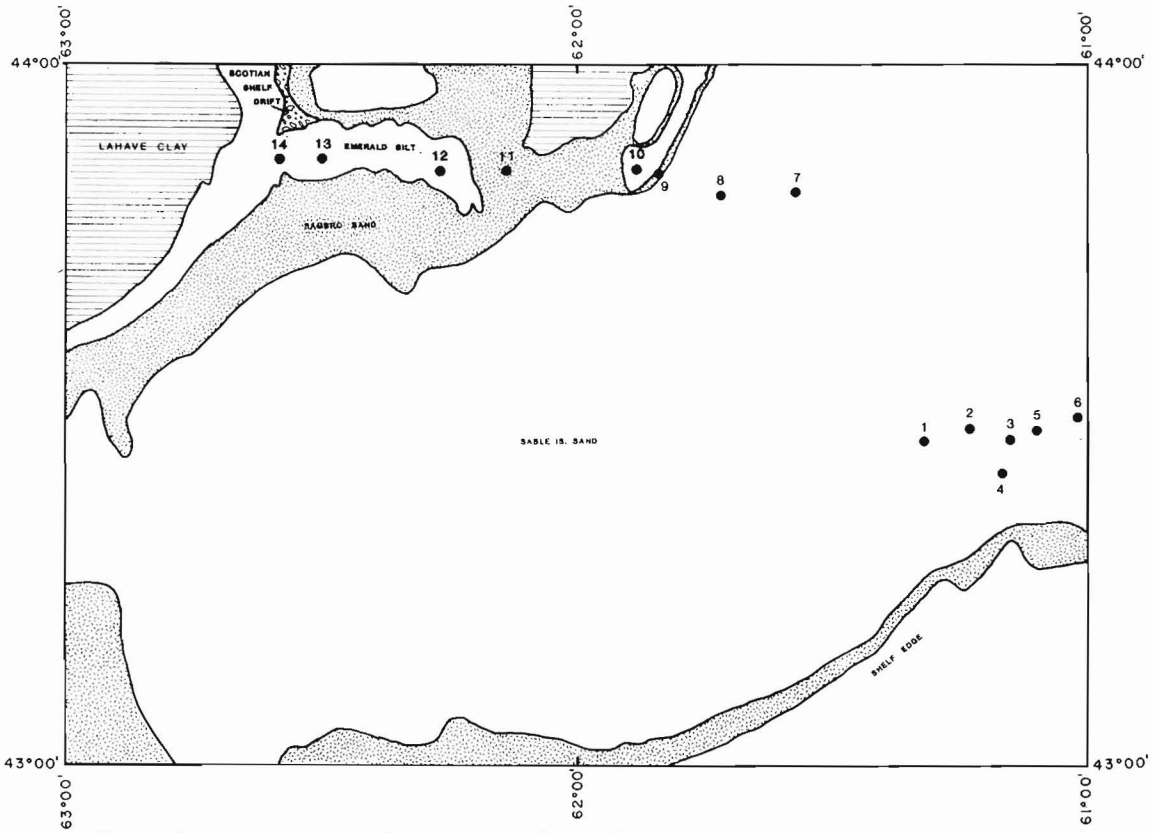

Figure 1. *Site locations for the seabottom refraction measurements on the Scotian Shelf.*

From: Scientific and Technical Notes in Current Research, Part B; Geol. Surv. Can., Paper 82-1B.

The long array was deployed with the ship in drift mode. For some sites, when wind velocities were low, the array was deployed with the ship underway at slow speed downwind. With the array deployed on bottom extra slack line was reeled off before connecting the seismograph to the reel to remove tension (hence noise) from the hydrophone spread while shooting. Shooting time was less than 1 minute.

To deploy and recover either of the two arrays in water depths between 70 m and 180 m took 40 to 60 minutes.

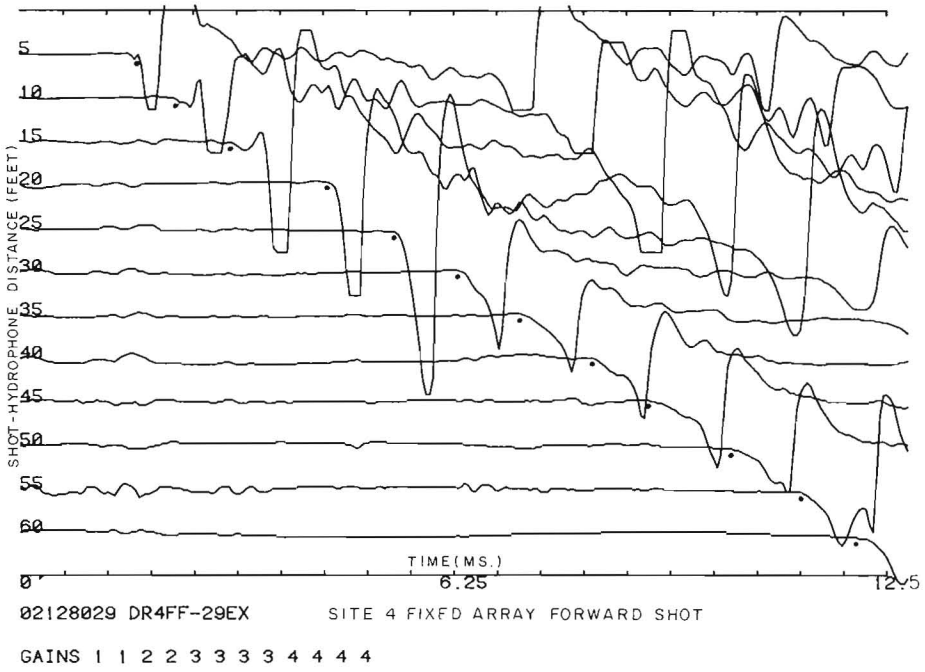

Figure 2. *Example record from the 'fixed' array.*

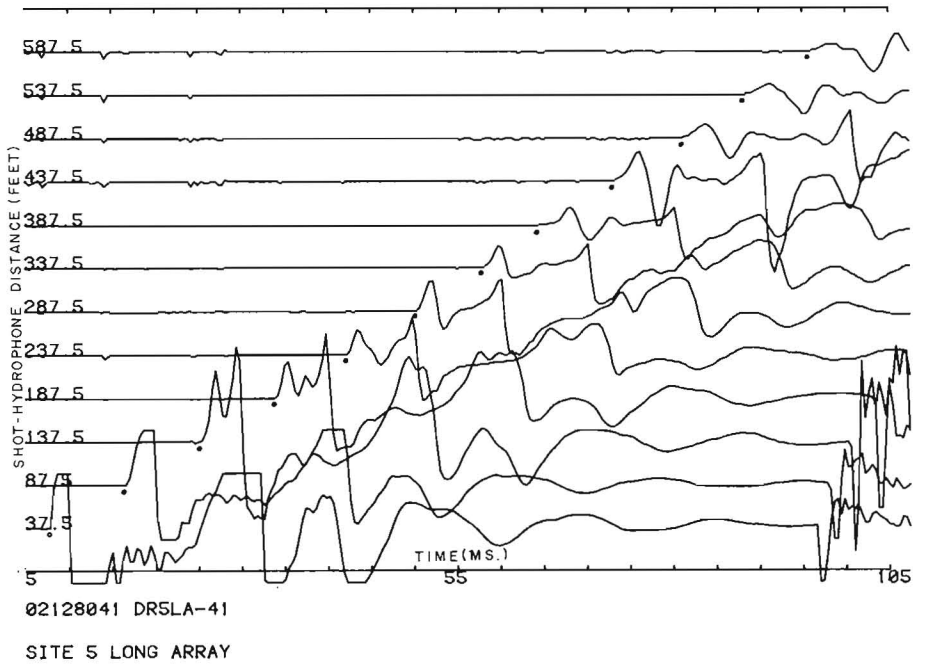

Figure 3. *Example record from the 'long' array.*

Data Quality

An example record shot with the fixed array is shown in Figure 2. Water arrivals are the highest amplitude events on the records. The energy transmitted through the sediment is generally 1 order of magnitude less than the water pulse with amplitudes decreasing with distance from the source. At site 2 the array was severely bent on the bottom and the water-break pulse was used to obtain relative shot-hydrophone distances. Shot pulse timing errors are estimated to be less than ±0.5 ms.

An example record shot with the long array is shown in Figure 3. At most sites a distinct sediment arrival can be seen of ten having lower frequency content than the water arrival. In sites 10 to 14 where sediment velocities were only slightly higher than water velocity, the sediment and water arrivals interfere within the first half-cycle of the pulse. Shot pulse timing errors are also estimated to be less than ±0.5 ms. No record was obtained for site 1 where the array had been improperly deployed (bunched) and water-break pulses could not be accurately determined to compute relative distances.

Interpretation Techniques

Fixed Array Records

The records obtained from the fixed array were replotted via the computer and gain adjusted where necessary to enhance the first breaks. Travel times were manually picked and computer plotted on a time-distance presentation. The time-distance plots were visually inspected; none of the plots indicated strong evidence for more than one sediment velocity. Hence, least squares fits were applied to the data from each site to obtain sediment velocities and standard errors.

Long Array Records

The first arrival times from the long array records were manually picked from the seismograph monitor records and were computer plotted in the form of a time-distance plot. The plots were visually inspected and velocity segments were identified. Least squares velocity fits with associated standard errors were computed for all velocity segments.

Intercept times for the upper layer (the first velocity segments) gave an indication of the shot pulse timing error and were generally less than ±0.5 ms.

By combining the fixed array velocities (where the data were available) with the velocity-intercept time data from the long array, a layered refraction model was computed for each site. Errors associated with the layer thickness calculations are those computed from the standard error of estimate of the least squares fit for the intercept time of each velocity segment. These errors do not include the cumulative errors on layer thicknesses lying above a particular layer,

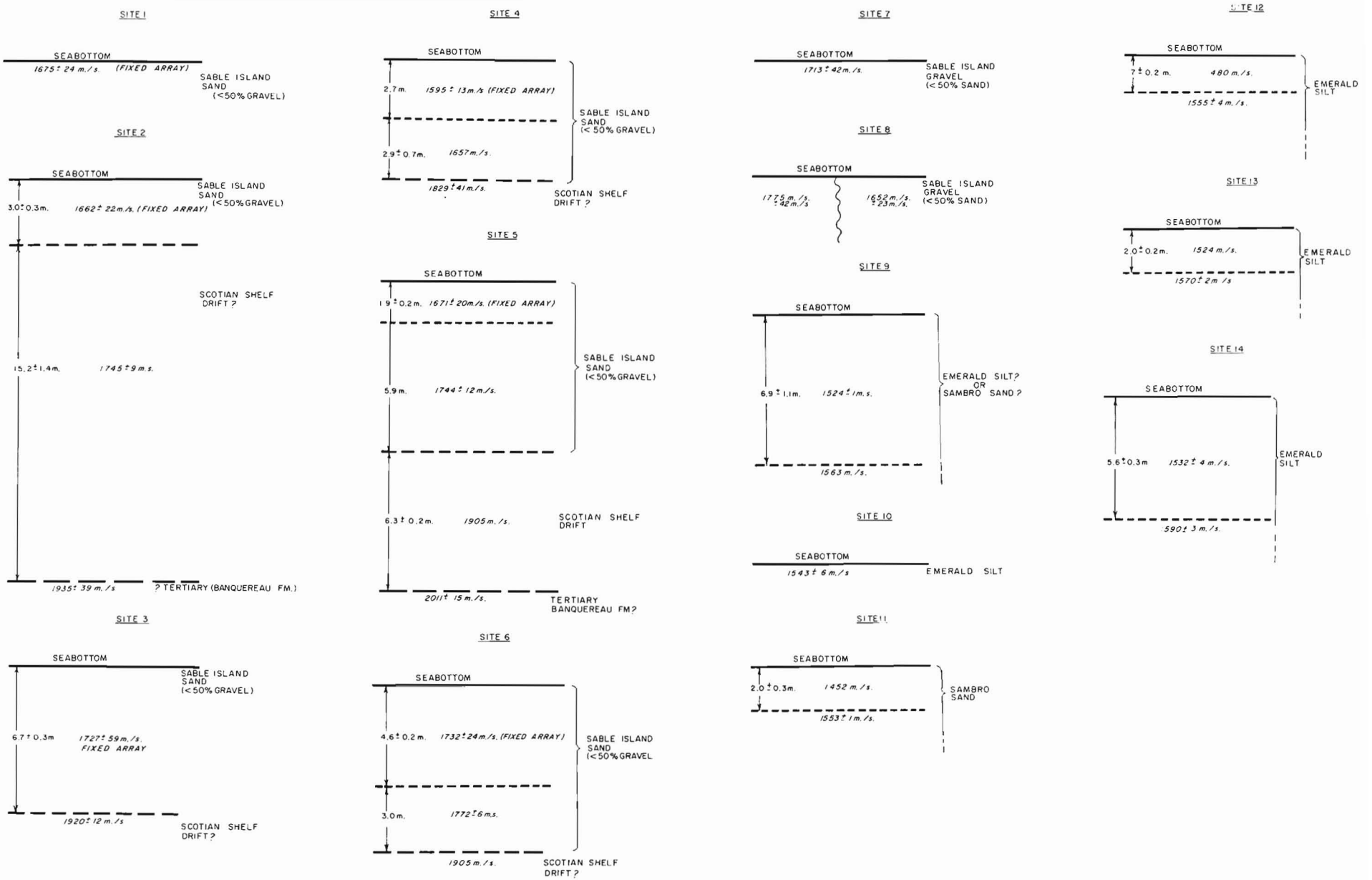

Figure 4. *Interpreted velocity layering for the seabottom sites.*

the possible error associated with shot pulse timing error, or the possible error of the arrival time picked. For the velocity contrasts observed it is estimated that timing errors in the order of 0.5 ms might yield additional layer thickness errors in the order of ± 1 m.

Results

The velocities computed from forward and reverse profiles of the fixed array correlate well in that the error ranges overlap for both directions of shooting. Only at one site (site 3) were the forward and reverse velocities significantly different suggesting low reliability.

The velocity models computed for each site are shown in Figure 4 and are discussed individually as follows:

Site 1. Since only fixed array data were available for this site only the bottom sediment velocity was determined. From King's (1970) map the sediment is Sable Island sand with less than 50 per cent gravel.

Site 2. The seabottom velocity of 1662 m/s is correlated with the Sable Island sand. A thick layer of 1745 m/s is suggested to be that of the Scotian Shelf Drift based on King (1970). A deep layer (depth 18.2 m below bottom) with a velocity of 1935 m/s may be the top of the Banquereau Formation (Tertiary).

Site 3. A thick layer (6.7 m) of Sable Island sand (1727 m/s) is interpreted to overlie Scotian Shelf Drift (1920 m/s).

Site 4. Two seismic layers (1595 and 1657 m/s) are interpreted to be correlated with the Sable Island sand. The higher velocity zone may result from either increased gravel content or greater compaction of sand with depth. The Scotian Shelf drift (1829 m/s) is interpreted to underlie the sand at a depth of 5.6 m below seabottom.

Site 5. Sable Island sand is interpreted to consist of two seismic layers of 1671 and 1744 m/s with a total thickness of 7.8 m overlying a 6.3 m layer of Scotian Shelf Drift (1905 m/s). The deepest layer observed (14.1 m below seabottom) is interpreted to be the Banquereau Formation (Tertiary).

Site 6. Sable Island sand is interpreted to consist of two seismic layers of 1732 and 1772 m/s with a total thickness of 7.6 m overlying Scotian Shelf Drift (1905 m/s).

Site 7. Only one velocity was observed for the Sable Island gravel (1713 m/s), suggesting a thick layer overlying the Scotian Shelf drift. Using a drift velocity of 1905 m/s a minimum depth estimation for the top of the Scotian Shelf drift would be 20.5 m.

Site 8. An apparent velocity reversal was observed on the travel-time distance plot for this site. After checking the water break arrivals which suggested that the cable had been correctly positioned on bottom a lateral velocity variation from 1775 to 1652 m/s was interpreted. Hence, a probable sediment grain size change may have occurred over the length of the refraction array, from high gravel content (1775 m/s) to high sand content (1652 m/s). This occurrence is extremely fortuitous but geologically possible (King, 1970).

Site 9. Two seismic layers were encountered; a 6.9 m layer of 1524 m/s and a lower layer of 1563 m/s. Because of the approximate site location it is not possible to determine precisely whether the site was situated on Sable Island sand, Sambro sand or Emerald silt. From examining the results of all sites it is highly probable that the low velocities observed indicate either of the last two sediment types.

Site 10. This site situated on Emerald silt (silty and clayey sand) gave a single velocity of 1543 m/s. Using a velocity of 1905 m/s for the Scotian Shelf Drift a minimum depth computation to that horizon would be 29 m.

Site 11. A thin layer of 1452 m/s overlies a layer of 1553 m/s. The site is in Sambro sand, however, the low velocity seabottom layer suggests that a thin veneer of clay may overlie the sand. Since the upper layer velocity is determined by only two data points, the reliability of the determination is suspect.

Site 12. In a manner similar to site 11 an upper low velocity layer (1480 m/s) has been determined based on two data points. The site is in Emerald silt (well sorted silt).

Site 13. Two seismic layers were interpreted for the Emerald silt (well sorted silt). An upper layer of 1524 m/s with a thickness of 2 m overlies a more competent layer of 1570 m/s.

Site 14. This site, similar to site 13, indicated two seismic layers. A 1532 m/s layer with thickness of 6.5 m overlies a lower more competent layer of 1590 m/s.

Table 1

Velocity Ranges

Sable Island sand	1595-1775 m/s
Sambro sand	1452-1563 m/s
Emerald silt	1480-1590 m/s
Scotian Shelf Drift	1745-1920 m/s
Tertiary Banquereau Fm.	1935-2011 m/s

Discussion

The range of velocities associated with the bottom sediment types and interpreted subbottom layering is given in Table 1. Sable Island sand, Sambro sand, and Emerald silt often form a thin veneer (less than 1 m thick) overlying LaHave clay (L. King, personal communication). Hence, the lower portions of the velocity ranges shown for these materials may result from velocity averaging of more than one formation, for the array geometry used. Shorter hydrophone spacings may be required to obtain reliable velocities from a thin high velocity layer.

It is unfortunate that no sites were occupied where the Scotian Shelf Drift or LaHave clay outcropped on the seabottom.

It must be cautioned that the limited sampling from the 14 sites occupied cannot yield statistically reliable ranges of velocities for Scotian Shelf sediment types. Because of the variability of grain size and texture indicated within each sediment type (King, 1970) several hundred measurements may be needed within the various geologic formations to provide meaningful velocity-grainsize-age relationships.

References

Hunter, J.A., Burns, R.A., Good, R.L., and Harrison, T.E.
1979: Seabottom seismic refraction array designs; in Current Research, Part C, Geological Survey of Canada, Paper 79-1C.

King, L.H.
1970: Surficial geology of the Halifax-Sable Island map area; Marine Science Paper 1.

RÉSULTATS PRÉLIMINAIRES SUR LA GÉOLOGIE QUATERNAIRE DE LA RÉGION DE COWANSVILLE, QUÉBEC

Convention de recherche 237-4-79

G. Prichonnet[1]
Division de la science des terrains

Introduction

La région est située au sud-est de Montréal, à la frontière du Vermont. Le feuillet topographique à 1:50 000 de Cowansville s'appelait encore récemment Sutton. Dès la bordure ouest de la carte (zone de Bedford) quelques petites collines atteignent 80 m d'altitude: elles correspondent souvent à des lambeaux de roches paléozoïques résistantes. Vers l'est, les déformations appalachiennes majeures (failles et plis) sont orientées ENE-SSW et NE-SW: les crêtes et chainons montagneux s'alignent selon les mêmes directions. Dans le quadrant sud-est de la carte, les montagnes de Sutton culminent à 960 m environ. Mais à leurs pieds, côté ouest, dans le val de Sutton, une étroite plaine alluviale n'est qu'à 135 m d'altitude: le réseau hydrographique, adapté ou inadapté aux structures, entaille donc profondément le piedmont appalachien (fig. 1).

J'ai étudié les quadrants nord-ouest, sud-ouest, et sud-est (plus de 300 points d'observations). Le quadrant nord-est fut étudié par L.M. Cloutier et moi-même.

Lithostratigraphie

On n'a pas retrouvé le till inférieur observé sur le territoire de Granby (Prichonnet, 1982). Par contre des graviers grossiers et stratifiés précèdent le till supérieur. Ils ont été identifiés au nord de Pearceton dans une tranchée artificielle (fig. 2; nº 367). Entre Pearceton et Dunham, un forage a traversé environ 18 m de graviers aquifères sous le till supérieur de 8 m d'épaisseur (fig. 2; nº 413). Plus au sud-est, à East Dunham (fig. 2; nº 442) près de 6 m de till sont divisés en deux sous unités par 0,4 m de sables gravillonnaires. Les variations granulométriques de cette couche non diamictique suggèrent une stratification fruste. Quelques lits sableux sont également présents au sommet de la sous unité inférieure: seul ce "niveau" inférieur du till est carbonaté. Un certain nombre d'analyses ont été effectués par Cloutier (en préparation) sur les sédiments de cette coupe: il en ressort que la sous unité de base pourrait bien avoir été mise en place par une glace en provenance du nord-est. Sachant que le till régional supérieur peut atteindre 8 à 10 m d'épaisseur (et sans doute le double dans certains drumlins du lac Selby), il serait hasardeux, pour le moment,

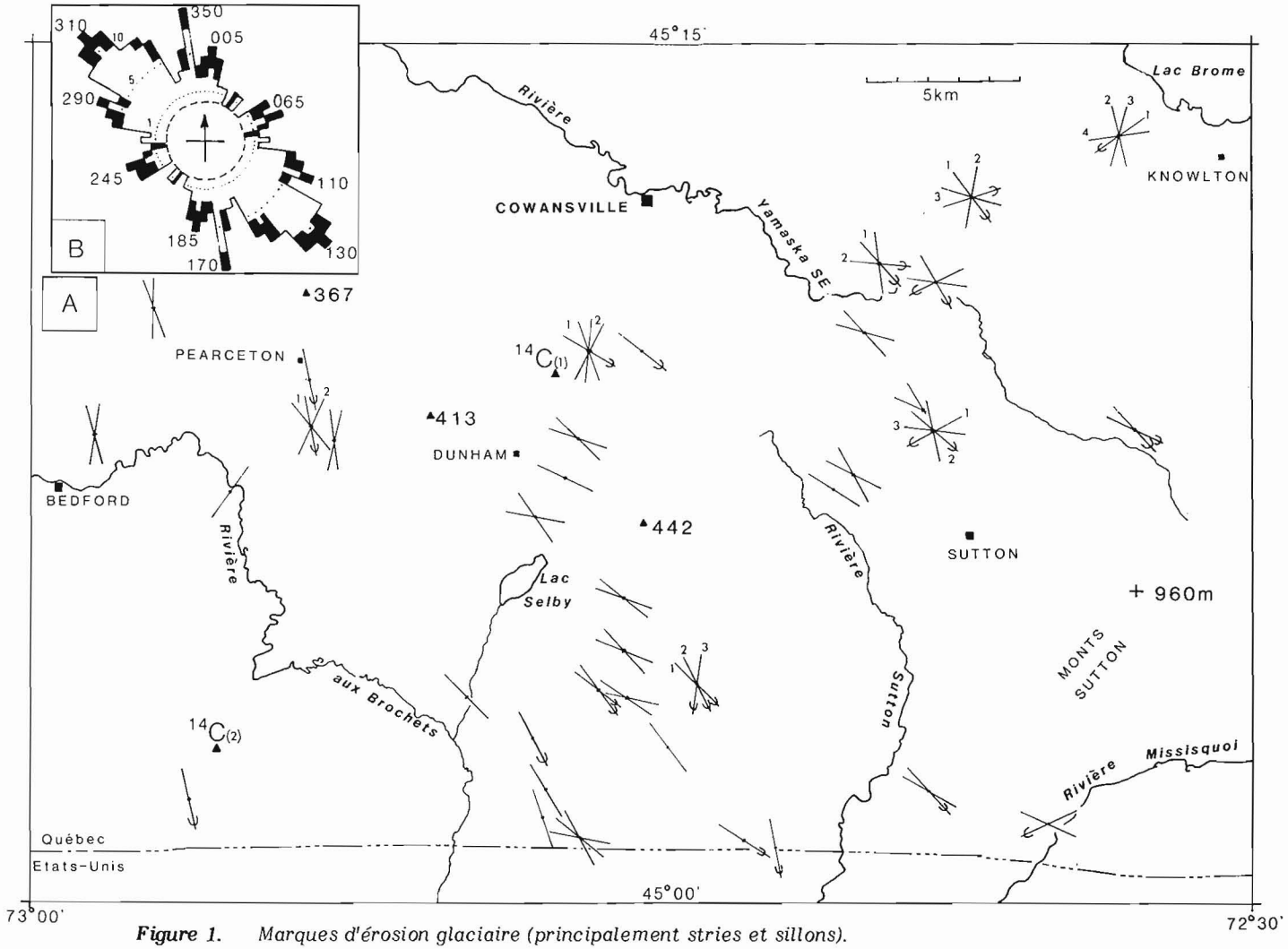

Figure 1. *Marques d'érosion glaciaire (principalement stries et sillons).*

A – Carte de localisation: pour la hiérarchie, voir texte;
B – Histogramme des orientations: 34 sites, 142 mesures. En noir, données du quadrant nord-est: la famille ENE-SSW est plus nette. Les sites de datations au ^{14}C correspondent aux dates discutées dans le texte: (1) UQ 347; (2) UQ 349.

[1] Département des sciences de la Terre, université du Québec à Montréal, C.P. 8888 – Succ., A, Montréal, Québec H3C 3P8

From: Scientific and Technical Notes in Current Research, Part B; Geol. Surv. Can., Paper 82-1B.

de corréler la couche inter-till avec les épais graviers identifiés à quelques kilomètres au nord-ouest. Si l'on attribue le till supérieur régional à la fin du Wisconsinien moyen et au Wisconsinien supérieur (Prichonnet, 1982), les graviers sous jacents pourraient représenter l'une des phases non glaciaires du Wisconsinien moyen. Il faut encore démontrer la relation qui peut exister entre les mouvements glaciaires anciens (NE-SW) et cette séquence stratigraphique. Sur le territoire de Granby, Prichonnet (1982) attribue le till inférieur – appelé Till de l'Ange-Gardien – à des glaces appalachiennes, d'âge Wisconsinien moyen, et compare la séquence globale avec celle de la région montréalaise (Prest et Hode-Keyser, 1977; Prest, 1977).

Les dépôts postglaciaires présentent une suite d'unités classiques. Les dépôts fluvio-glaciaires de contact sont abondants, surtout dans la moitié est du territoire. Ils illustrent bien un mode de retrait influencé, au moins partiellement, par la topographie locale (Cadwell, 1978); les formes d'accumulation sont donc variées: moraines de kame sur les pentes des monts Sutton; segments morainiques dans la vallée de la rivière Sutton; nombreux trains d'eskers de direction SE-NW à nord-sud. Dans la moitié est du territoire, plusieurs deltas sablo-graveleux et des placages de silts sableux sont reliés aux plans d'eau successifs du lac proglaciaire qui ennoyait les vallées, surtout à partir de 320 m.

Vers l'ouest, ce sont les dépôts marins, – silts et sables –, qui occupent dépressions et fonds de vallée. Sur les interfluves et autour des noyaux rocheux, les graviers littoraux, mal triés et mal stratifiés, dominent. L'analyse détaillée des phénomènes littoraux n'étant pas achevée, on étend à la région de Cowansville la limite marine suggérée pour le territoire de Granby, soit 190 m (Prichonnet, 1982). Les dépôts organiques occupent quelques surfaces de faible étendue. Au nord-est de Dunham (fig. 1) une date sur bois marque sans doute l'extension des premières tourbières régionales: 8050 ± 190 ans B.P. (UQ-347)[1]. L'échantillon est pris à la base d'une accumulation organique vers 140 m d'altitude. Les dépôts alluviaux sont limités aux étroites zones où l'action fluviatile s'est manifestée, le long des vallées principales. Dans un cas ils fossilisent des dépôts organiques, au sud-sud-est de Bedford (fig. 1). L'événement s'est produit, d'après une date sur bois, après 3920 ± 80 ans B.P. (UQ-349)[2].

Paléogéographie

Après avoir discuté brièvement les différents mouvements glaciaires identifiés, on présentera les principaux faits marquant la déglaciation et les événements post-glaciaires.

a. Les marques d'érosion glaciaire

Environ 40 sites de surface rocheuse érodée par les glaces ont été analysés. Ils sont répartis sur l'ensemble du territoire (fig. 1,A), et permettent de distinguer plusieurs mouvements érosifs successifs. Dans l'ordre chronologique normal (ancien à récent), il est probable que l'on a eu: 1) un écoulement de glaces venant des Appalaches (soit de l'est-nord-est vers le sud-sud-ouest). Un bel exemple de ces stries anciennes, conservées à l'abri de nodules décimétriques de roches résistantes, est observable de part et d'autre de la tranchée de la route 139, à 3,5 km au nord-nord-ouest de Sutton; 2) des écoulements (successifs?) en provenance du secteur nord-ouest: le diagramme cumulatif de la fig. 1,B semble indiquer que ce sont ces mouvements de glace, orthogonaux aux reliefs, qui ont laissé le plus grand nombre d'empreintes (comparer avec fig. 1,A); les marques NNW-SSE correspondent, sans doute, au pléniglaciaire du Wisconsinien supérieur; 3) des écoulements plus récents, surtout NNE-SSW, semblent correspondre à des influences topographiques sur le terminus glaciaire lors de son recul. Mais on a aussi identifié des écoulements vers l'est et l'est-sud-est attribuables à la même période: quadrant nord-est de la carte (Cloutier et Prichonnet, 1980). Le mouvement vers le sud-sud-ouest (Prichonnet, 1977) est bien représenté sur les territoires limitrophes, au nord (Granby 31 H/7 et St-Hyacinthe 31 H/10). Le mouvement ancien "vers le sud-ouest", laissé par des glaces appalachiennes, serait surtout observable dans les régions à plus fort relief (Cloutier et Prichonnet, 1980; Doiron, 1981, Prichonnet, en préparation).

Sur le territoire de Granby (Prichonnet, 1982) on peut relier les premiers mouvements glaciaires, en provenance du nord-est, avec le Till de l'Ange-Gardien. Ici, il est difficile de dire si ces mouvements sont responsables de la mise en place d'une partie du seul till identifié (fig. 1, n° 442), ou d'un autre till non identifié et sous-jacent aux dépôts non glaciaires de base. Par contre, les divers mouvements en provenance du secteur nord-ouest ont mis en place le till sus-jacent identifié; ils ont façonné, en particulier, plusieurs groupes de formes fuselées de till: des trainées de till dans la région de Cowansville et de Bedford, et des drumlins épais dans la région du lac Selby.

b. La déglaciation et les lacs glaciaires

De nombreux dépôts de contact glaciaire marquent les étapes de la déglaciation. Celle-ci commence sans doute sur les versants nord-ouest des monts Sutton: on peut identifier plusieurs exemples de terrasses de kame et des segments morainiques parallèles aux pentes. Dans certaines vallées (de la rivière Sutton, ...) des moraines arquées démontrent, elles aussi, que le recul glaciaire se faisait par petites étapes difficiles à corréler entre elles[2]. Enfin, des trains d'eskers s'ordonnent plus ou moins perpendiculairement aux "moraines", selon un axe SE-NW.

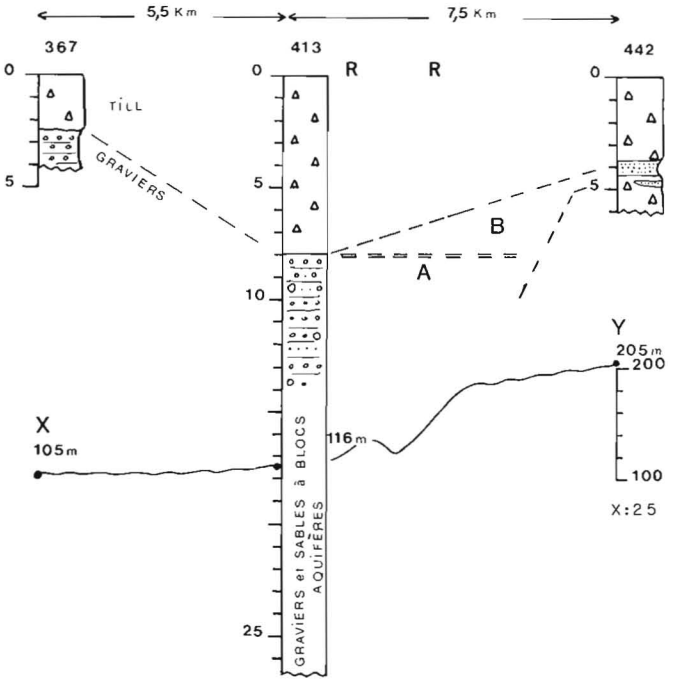

Figure 2. Le till "supérieur" et les graviers non glaciaires (?) dans le secteur Dunham-Pearceton. 367: n° de référence R: crêtes rocheuses affleurantes entre les coupes. XY: topographie simplifiée. Corrélations: A, probable; B, douteuse.

[1] Université du Québec à Montréal, Laboratoire de géochimie isotopique

[2] Ce mode de recul est comparable à celui décrit par Shilts (1981).

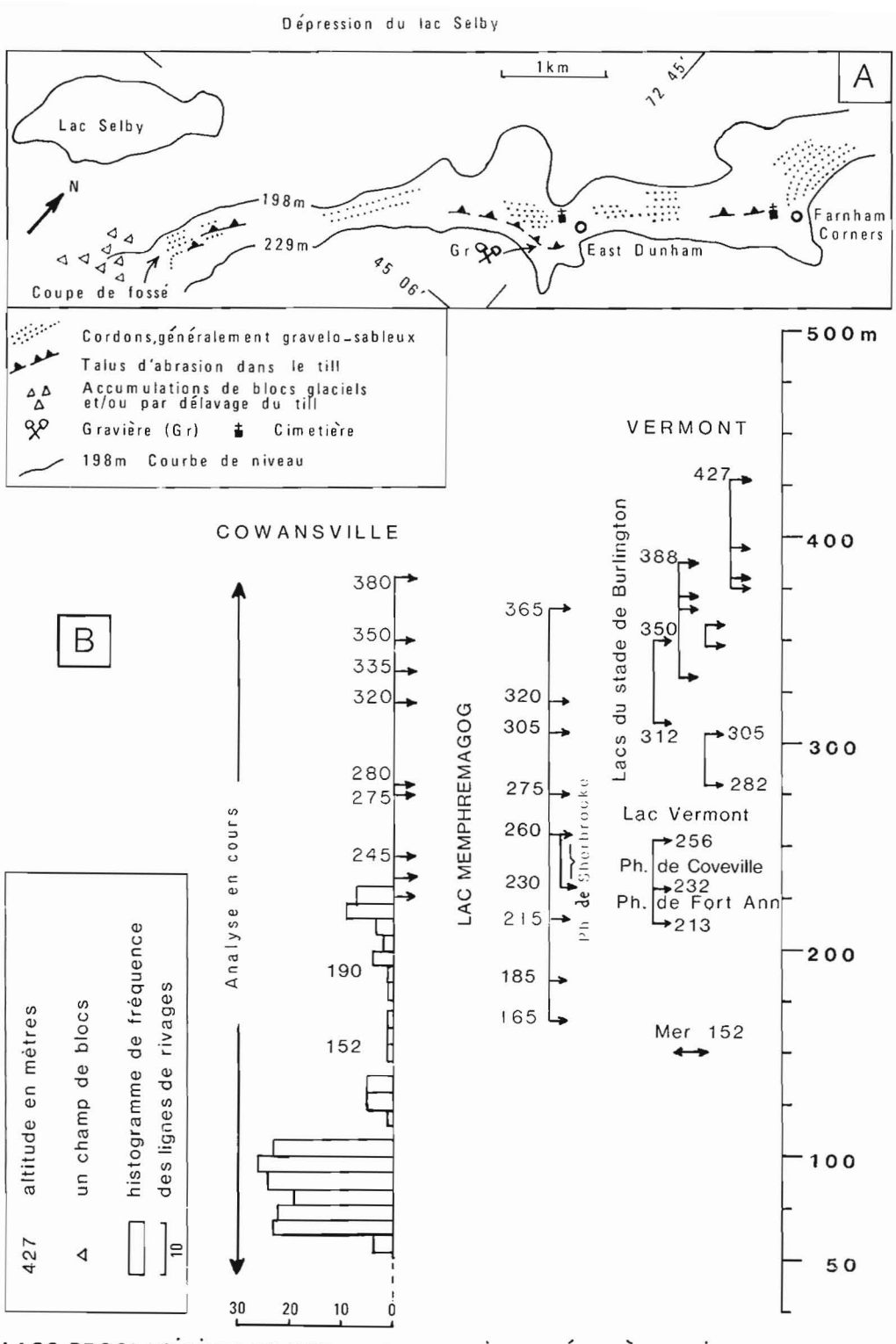

Figure 3. *Exemples de phénomènes littoraux (A) et comparaison de niveaux littoraux régionaux (B). Données: du Vermont, Stewart et MacClintock (1969); du lac Memphrémagog, Boissonnault et al. (1981) (voir aussi McDonald, 1967); de Cowansville, analyse en cours. Des corrélations sont très probables entre Cowansville et Memphrémagog (sens ouest-est), mais non proposées dans le sens nord-sud (Québec-Vermont).*

Tous ces faits permettent de définir un mode de retrait glaciaire, proposé par Prichonnet et al. (1982) pour le secteur oriental de ce territoire, qui s'oppose à celui de Gadd (1964) et Gadd et al. (1972). Dans la partie ouest du territoire, les quelques eskers identifiés nous conduisent à tracer des fronts glaciaires très obliques (Prichonnet, en préparation) au tracé présumé de la moraine de Drummondville (voir aussi le même problème sur Granby; Prichonnet, 1982).

Les eaux de fusion inondaient les vallées au fur et à mesure que le glacier reculait.

Au Vermont, Stewart et MacClintock (1969) ont étudié en détail les hauts niveaux lacustres qui accompagnèrent le recul de l'inlandsis du Stade de Burlington (phases I à V et 3 phases du lac Vermont – fig. 3B). Les eaux proglaciaires ennoyèrent aussi de larges secteurs au sud-est du territoire considéré ici. Plusieurs deltas sablo-graveleux ont déjà été identifiés par Elson (1962), surtout entre Sutton et Knowlton (à partie de 245 m). Nous avons identifié un certain nombre de dépôts lacustres et de formes littorales à partir de 380 m environ (fig. 3B). Les terrasses deltaïques s'étagent surtout à partir de 320 m.

Les eaux proglaciaires du Lac Memphrémagog et celles qui ennoyaient le secteur sud-est du territoire d'étude devaient communiquer par la vallée de la rivière Missisquoi. Certains niveaux sont comparables dans les 2 dépressions (voir fig. 3B, données de Boissonnault et al., 1981).

Signalons d'autres niveaux importants: 280 – 275 m au sud du mont Pinacle: 245 m de part et d'autre de la vallée de Sutton; 235 à 225 en maints sites du secteur est du territoire.

Une série de cordons littoraux (fig. 3A), des champs de blocs et des petits deltas étagés marquent les abaissements successifs de ce plan d'eau, sur le versant est de la dépression du lac Selby, entre Farnham Corners et Abbott Corners: à partir de 240 – 235 m.

En conclusion, notons que plusieurs des phases lacustres postglaciaires identifiées au nord du Vermont sont présentes au Québec, de part et d'autre des monts Sutton. La continuité de niveau repère dans les deux états reste à démontrer.

Remerciements

Les personnes suivantes nous ont assisté sur le terrain: MM. P. Corbeil, G. Lévesque, G. Lapierre et N. Togola.

Les datations mentionnées ont été réalisées par le Laboratoire de géochimie isotopique de M.C. Hillaire-Marcel, M. N.R. Gadd a bien voulu nous accompagner sur le terrain, et nous faire part de ses idées sur les sites visités. La lecture critique a été assurée par M. J-S. Vincent.

Que chacun soit assuré de notre gratitude.

Projet réalisé grâce au support financier de la Commission géologique du Canada et du Fonds Institutionnel de Recherche – UQAM.

Bibliographie

Boissonnault, P., Gwyn, Q.H.J. et Morin, B.
1981: Le lac proglaciaire Memphrémagog: Géologie, Géomorphologie Archéologie; Excursion Association Canadienne Française pour l'Avancement des Sciences. 49e Congrès. Bulletin de Recherche; université de Sherbrooke, Département de géographie, nº 55, 40 p.

Cadwell, D.H.
1978: Bedrock control of ice marginal positions in central New York; Geology, v. 6, p. 278-280.

Cloutier, M. et Prichonnet, G.
1980: Hiérarchie des stries glaciaires Wisconsiniennes du secteur montagneux de Cowansville-Knowlton-Sutton, Québec; Annales Association Canadienne Française pour l'Avancement des Sciences, vol. 47, nº 1, résumé p. 113.

Doiron, A.
1981: Les dépôts quaternaires de la région de Granby-Waterloo, Québec. Cartographie, sédimentologie et stratigraphie; thèse de M.Sc. non publiée, Université du Québec à Montréal, Département des sciences de la Terre, 100 p.

Elson, J.A.
1962: Geomorphology and Pleistocene geology of the Sutton area; McGill University, Department of Geological Sciences, unpublished report, 8 p.

Gadd, N.R.
1964: Moraines in the Appalachian region of Quebec; Short notes; Geological Society of America Bulletin, v. 75, p. 1249-1254, 1 fig.

Gadd, N.R., McDonald, B.C. et Shilts, W.W.
1972: Deglaciation of southern Quebec; Commission géologique du Canada, Étude 71-47, 19 p.

McDonald, B.C.
1967: Pleistocene events and chronology in the Appalachian region of southeastern Quebec, Canada; Unpublished Ph.D. dissertation, Department of Geology, Yale University, 161 p.

Prest, V.K.
1977: General stratigraphy framework of the Quaternary in Eastern Canada; Géographie Physique et Quaternaire, vol. XXXI, nº 1-2, p. 7-14.

Prest, V.K. et Hode-Keyser, J.
1977: Geology and engineering characteristics of surficial deposits, Montreal Island and vicinity, Quebec; Commission géologique du Canada, Étude 72-27, 29 p.

Prichonnet, G.
1977: La déglaciation de la vallée du Saint-Laurent et l'invasion marine contemporaine; Géographie Physique et Quaternaire, vol. XXXI, nº 3-4, p. 323-345.

1982: Quelques données nouvelles sur les dépôts quaternaires du Wisconsinien et de l'Holocène, dans le piedmont appalachien. Granby 31 H/7. Québec; Recherches en cours, partie B; Commission géologique du Canada, Étude 82-1B.

Prichonnet, G., Doiron, A. et Cloutier, M.
1982: Le mode de retrait glaciaire tardiwisconsinien de la bordure appalachienne, au sud du Québec; Géographie Physique et Quaternaire, vol. 36, nº 1-2.

Shilts, W.W.
1981: Surficial geology of the Mégantic area, Québec; Geological Survey of Canada, Memoir 397, 102 p.

Stewart, D.P. et MacClintock, P.
1969: The surficial geology and Pleistocene History of Vermont; Vermont Geological Survey, Department of Water Resources, Bulletin 31, 251 p.

ACIDES AMINÉS ET INTERSTADES DU WISCONSINIEN DE LA VALLÉE DU SAINT-LAURENT ET DE L'ÎLE DU CAP-BRETON

Conventions de recherche: 244-4-80 et 238-4-81; 207-4-80 et 145-4-81

S. Occhietti[1] et N. Rutter[2]
Division de la science des terrains

La stratigraphie du Quaternaire de l'île du Cap-Breton, notamment des unités non glaciaires (conventions 244-4-80 et 238-4-81 de S. Occhietti) est limitée par l'absence d'une échelle chronologique. En raison du type de matériel disponible, essentiellement de la matière végétale fossile, de rares ossements ou des coquilles marines en faible quantité, seule la méthode au ^{14}C a pu être utilisée jusqu'à présent. Compte-tenu de la gamme d'âges que peut donner cette méthode jusqu'à 40 000 ans B.P. ou exceptionnellement 75 000 ans B.P. si l'on utilise la méthode par enrichissement, le ou les intervalles antérieurs au milieu du Wisconsinien moyen de l'île du Cap-Breton n'ont pas encore d'âge connu significatif. Pour cette raison, seules les corrélations provisoires entre le principal intervalle de l'île, daté au-delà de la limite de la méthode du ^{14}C, et l'Interstade de Saint-Pierre, daté de $74\,700 \pm {}^{2800}_{2000}$ ans (QL-198, Stuiver et al. 1978) ont été proposées par Mott et Prest (1967), Prest (1977), et Grant (1975, 1977). Dans cette situation, la méthode de datation par le taux de racémisation des acides aminés offre une alternative prometteuse, en raison des faibles quantités de matériel organique nécessaire et de la gamme d'âges théoriquement étendue au moins à tout le Quaternaire. Elle a été appliquée en particulier au bois fossile par N. Rutter (conventions 207-4-80 et 145-4-81), dans des régions à pergélisol (Rutter et al., 1980).

Ce document présente les premiers résultats d'un projet comprenant les objectifs suivants:

1. tenter de mettre en corrélation chronologique les unités organiques antérieures au Wisconsinien supérieur de l'île du Cap-Breton et du Québec méridional,
2. continuer à développer la méthode des acides aminés sur le bois et
3. tester la méthode dans des régions actuellement tempérées et d'histoire thermique mal connue.

Les échantillons de bois ont été prélevés (S. Occhietti) sur quatre des sites datés les plus significatifs de l'île du Cap-Breton, en Nouvelle-Écosse, et aux Vieilles-Forges, dans la vallée du Saint-Laurent (fig. 1). Ce dernier site daté a été choisi en raison de la très grande abondance du matériel organique, en affleurement discontinu sur 1 km de long. Les taux de racémisation des acides aminés de quatorze échantillons (tableaux 1 et 2, fig. 2) ont été mesurés par N. Rutter. L'interprétation proposée tient compte du contexte stratigraphique et des dates ^{14}C connues.

Contexte stratigraphique des échantillons

Vallée du Saint-Laurent, Québec: les Vieilles-Forges

Sur la rive nord du Saint-Laurent, à 5 km au nord-ouest de Trois-Rivières, le site des Vieilles-Forges est localisé sur la rive droite du Saint-Maurice, immédiatement en aval du site historique. Gadd et Karrow (1960) ont établi la corrélation du lit de silt argileux contenant deux lits de tourbe et bois compactés avec les sédiments de Saint-Pierre. Le lit de silt repose sur le till de Bécancour et est recouvert par les varves de la formation de Deschaillons (Gadd, 1971; Occhietti, 1980). Les échantillons de bois (VF.1, VF.2A, VF.3, VF.4) ont été prélevés dans le lit organique inférieur,

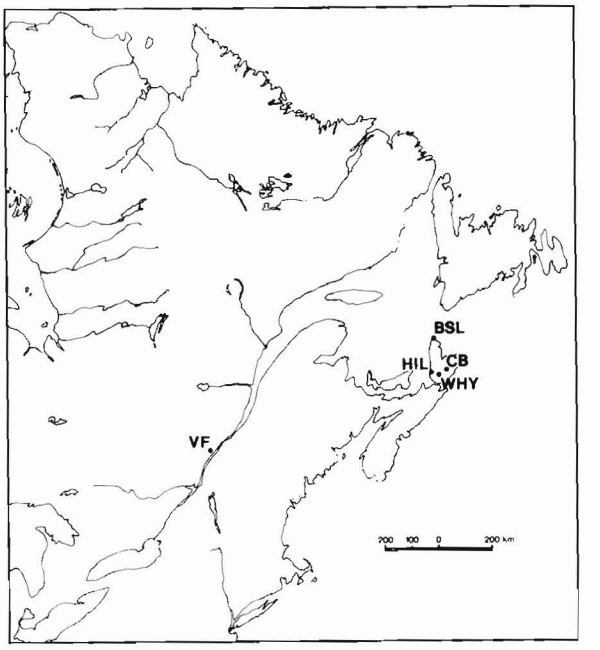

VF = Vieilles-Forges *CB = Castle Bay*
HIL = Hillsborough *WHY = Whycocomagh*
BSL = Baie Saint-Laurent

Figure 1. *Localisation des sites interstadiaires échantillonnés.*

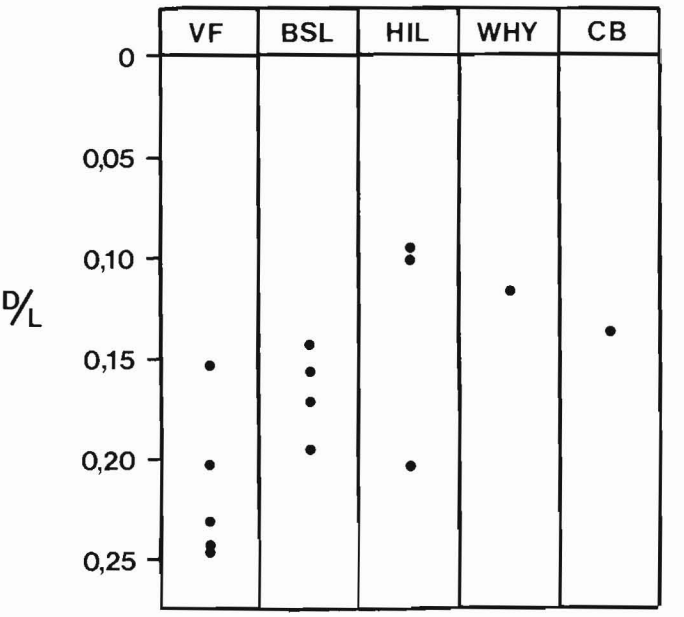

Figure 2. *Taux de racémisation de l'acide aspartique des échantillons de bois interstadiaires.*

[1] Département de géographie, UQAM, C.P. 8888, succ. "A", Montréal, Québec
[2] Department of Geology, University of Alberta, Edmonton, Alberta

From: Scientific and Technical Notes in Current Research, Part B; Geol. Surv. Can., Paper 82-1B.

Tableau 1

Radiodatations au ^{14}C et taux de racémisation de l'acide aspartique des échantillons de bois interstadiaires

VALLÉE DU SAINT-LAURENT	ÎLE DU CAP-BRETON			
Vieilles-Forges	Baie Saint-Laurent	Hillsborough	Whycocomagh	Castle Bay
>30 840 (Y-255, Gadd, 1971)	>38 270 (GSC-283, Mott et Prest, 1967)	>51 000 (GSC-570, Mott et Prest, 1967)	>44 000 (GSC-290, Mott et Prest, 1967)	>52 000 (GSC-1577, Grant, 1972)
		HIL.1P 0,0949 HIL.1R 0,1001		
			WHY.1 0,1162	
	BSL.9 (branche) 0,1438			CB.2 0,1358
VF.2B (lit organique supérieur) 0,1534				
	BSL.8 (tronc) 0,1565 BSL.9 (tronc) 0,1722 BSL.8 (branche) 0,1956			
VF.4 0,2026				
		HIL.1L 0,2038		
VF.3 0,2323 VF.1 0,2429 VF.2A 0,2450				

Tableau 2

Taux de racémisation des différents acides aminés des échantillons de bois interstadiaires

nº de laboratoire	nº d'échantillon	Rapports D/L des acides aminés						
		acide aspartique	alanine	glutamine	leucine	phénylaline	proline	valine
UA-752	VF.1	0,2429	0,1702	0,0773	0,0436	0,0548	0,0257	0,0224
UA-753	VF.2a	0,2450	---	0,0839	0,0237	0,0256	0,0256	---
UA-754	VF.2b	0,1534	---	0,0997	0,0199	0,0398	0,0252	---
UA-755	VF.3	0,2323	0,1661	0,0845	0,0347	0,0360	0,0278	0,0188
UA-756	VF.4	0,2026	0,1292	0,0680	0,0232	0,0301	0,0293	---
UA-757	CB.2	0,1358	---	0,0605	0,0252	0,0333	0,0261	---
UA-758	WHY.1	0,1162	0,1075	0,0789	0,0197	0,0294	0,0210	---
UA-759	HIL.1P	0,0949	---	0,0924	0,0192	0,0396	0,0205	0,0176
UA-760	HIL.1R	0,1001	---	0,0731	0,0166	0,0319	0,0196	---
UA-761	HIL.1L	0,2038	0,1392	0,0695	0,0194	0,0236	0,0219	---
UA-763	BSL.8 Branche	0,1956	0,1513	0,0526	0,0184	0,0438	0,0292	---
UA-764	BSL.8 Tronc	0,1565	0,1198	0,1013	0,0262	0,0884	0,0264	---
UA-765	BSL.9 Branche	0,1438	0,1407	0,0576	0,0210	0,0388	0,0180	---
UA-766	BSL.9 Tronc	0,1722	0,0995	0,1004	0,0363	0,0586	0,0292	---

sur quatre sites répartis sur 500 m en aval du site historique. L'altitude varie entre 0 et 1,5 m au-dessus du niveau moyen du Saint-Maurice. Un seul échantillon (VF.2B) a pu être prélevé dans le lit organique supérieur, à 1,5 m au-dessus du lit inférieur. L'âge d'un échantillon de bois du lit inférieur dépasse la limite de la méthode au ^{14}C: >29 630 ans (Y-254, Preston et al., 1955). L'âge significatif d'environ 75 000 ans B.P. déjà cité provient du site de Pierreville, à 42 km au sud-sud-ouest des Vieilles-Forges.

Île du Cap-Breton, Nouvelle-Écosse

Baie Saint-Laurent. Un lit de débris végétaux affleure sur environ 400 m de long, à 7 m et plus d'altitude, dans la moitié nord-est de la coupe de la baie Saint-Laurent (Mott et Prest, 1967; Grant, 1975, 1977) au nord de l'île. Il contient de la tourbe, des troncs, racines et branches compactés. Son épaisseur varie de 1 à 45 cm, incluant des lits de silts intercalés. Il repose sur un cailloutis de 4 à 5,5 m d'épaisseur, d'origine continentale (gélifraction sur les versants + gravité + ruissellement + eaux de fonte nivales) qui recouvre une plate-forme rocheuse d'érosion marine attribuée au Sangamonien ou une lentille de dépôts littoraux de 0,1 à 1,50 m d'épaisseur, d'âge non connu. Le lit organique est surmonté par une rudite de versant d'origine complexe, dont l'épaisseur atteint 35 m et qui contient une lentille de silts apparemment marins de 0,1 à 3,5 m d'épaisseur intercalée entre 14 et 21 m d'altitude. Le bois, **Larix**, est daté: >38 270 ans (GSC-283, Mott et Prest, 1967). Les 4 échantillons de bois analysés par les acides aminés proviennent de deux sites distants d'environ 30 m, où le lit organique est le plus épais.

Hillsborough et Whycocomagh. Le lit de matière organique des deux sites (Mott et Prest, 1967), distants de 20 km au centre ouest de l'île, a une épaisseur variable de 1 à 3 m, avec des lits intercalés silteux. Il repose sur un lit de silt de 0,5 à 1,5 m d'épaisseur qui recouvre lui-même une unité sablo-graveleuse ou un cailloutis très altéré. Un diamicton mal identifié recouvre les deux coupes. La base du lit à matière organique est disposée à environ 7 m au-dessus de la rivière Mabou à marée haute, à Hillsborough, et à environ 8 m au-dessus du lac Bras d'Or, à Whycocomagh. Le bois est daté (Mott et Prest, 1967): >51 000 ans (GSC-570), **Abies**, à Hillsborough et >44 000 ans (GSC-290), **Larix**, à Whycocomagh.

Castle Bay. Le site est localisé sur la rive nord de la baie Orientale du lac Bras d'Or (Mott et Prest, 1967; Grant, 1972). La série stratigraphique a été réanalysée dans le cadre de ce projet. Elle comprend les unités suivantes, de haut en bas:

		Épaisseur maximale (m)
4	Silt sableux, sable silteux avec brindilles et matière organique (13 030 ± 1270 ans, UQ-246)	5
3	Till gris brun rouge, quelques fragments de coquilles marines	6
2	Dépôts lacustres et deltaïques:	
	f) varves avec matière organique disséminée	4,5
	e) silt et sable fin finement stratifiés	6
	d) silt noir en apparence massif, avec fines stratifications, riche en matière organique et sulfures(?). Au sommet, lit avec fragments de bois flotté d'où provient probablement **Larix** ou **Picea**, >52 000 ans (GSC-1577, Grant, 1972)	5
	c) lentille de gravier sableux et caillouteux	4
	b) lentille de sable moyen à structure deltaïque	10
	a) silt inférieur noir, riche en matière organique et sulfures (?); fragments de bois: >42 000 ans (GSC-1577, Grant, 1972)	0,6
1	Cailloutis inférieur composé de gélifracts peu transportés	4

Le bois dont les taux de racémisation ont été mesurés provient du sommet de l'unité 2d. Cette unité fait partie de la séquence non glaciaire des unités 2 à 7 (lacustre-deltaïque-lacustre-glaciolacustre) qui succède à une phase très froide, apparemment périglaciaire. Elle précède l'englaciation majeure de l'île, comme à baie Saint-Laurent, Hillsborough et Whycocomagh.

En conclusion, les bois analysés par les acides aminés proviennent d'unités organiques antérieures au Wisconsinien supérieur et postérieures au Sangamonien, d'après la nature interstadiaire de la flore et la position lithostratigraphique (Terasmae, 1958; Gadd, 1971; Occhietti, 1980; Mott et Prest, 1967; Grant, 1977). D'après l'analyse pollinique, Mott et Prest (1967) mettent en corrélation les unités organiques d'Hillsborough et de Whycocomagh. Ils proposent, à titre d'hypothèse provisoire, de corréler les unités organiques d'Hillsborough, Whycocomagh et baie Saint-Laurent avec l'interstade de Saint-Pierre défini au Québec méridional.

Méthode d'analyse

Les échantillons ont été analysés au laboratoire de géochronologie par les acides aminés du Département de géologie de l'université d'Alberta, à Edmonton, par N. Rutter (Rutter et al., 1979). Les échantillons sont nettoyés au HCL (2N) froid et à l'eau distillée par sonification. Les acides aminés sont ensuite extraits par dissolution dans HCL (5,5N) en ébullition constante (108°C) pendant 24 h. Les carbonates et autres sels inorganiques sont séparés dans des colonnes échangeuses d'ions (résine AG 50W-X8 (H^+)). La solution est finalement évaporée sous vide. Les acides aminés qui composent le résidu solide sont alors chauffés en présence d'un réactif anhydre, l'alcool acide isopropanol. Les esters d'acides aminés obtenus sont acylés en ajoutant de l'anhydride pentafluoroproprionique (PFPA, 0,1 mL) et du chlorure de méthylène, puis en chauffant à 100° pendant 5 mn. Le mélange volatil des acides aminés est enfin séparé par chromatographie en phase gazeuse (Hewlett-Packard 5840, colonne capillaire CHIRASIL-VAL de 25 m), en employant l'hélium comme gaz porteur.

Taux de racémisation de l'acide aspartique et interprétation

À cette étape du projet, l'interprétation chronologique sera limitée à l'acide aspartique (tableau 1 et fig. 2). Cet acide à racémisation rapide (Rutter et al, 1979) est adapté au laps de temps étudié relativement court, à l'environnement froid qui caractérise l'est du Canada pendant le Wisconsinien et à la racémisation du bois ralentie par les propriétés hydrophobes de la lignine (Dunand et al., 1979). De plus, l'acide aspartique a déjà servi pour comparer des taux de

racémisation de bois, d'os et de coquilles de mollusques d'eau douce (Rutter et al., 1980). Les autres acides aminés séparés, alanine, glutamine, leucine, phénylaline, proline et valine (tableau 2), à vitesse de racémisation plus lente, sont indiqués à titre de comparaison.

L'analyse des résultats révèle que le premier objectif de corrélation entre les différentes unités n'est pas atteint. Les taux de racémisation de l'acide aspartique obtenus varient considérablement, à l'intérieur de chaque site et d'un site à l'autre (fig. 2). Ces écarts sont contradictoires avec la relation stratigraphique des échantillons prélevés dans le même lit organique et les âges ^{14}C. Quelques conclusions et interprétations peuvent néanmoins être formulées:

1. Les résultats les plus cohérents concernent les Vieilles-Forges où les valeurs de VF.2A (D/L = 0,2450), VF.1 (D/L = 0,2429) et VF.3 (D/L = 0,2323) sont proches et correspondent assez bien à l'âge de 75 000 ans B.P.
2. Étant donné l'âge apparent du bois de chaque site, au-delà de la limite de la méthode au ^{14}C, les faibles taux de racémisation de Castle Bay (CB.2, D/L = 0,1358) et de Whycocomagh (WHY.1, D/L = 0,1162), attribuables normalement à la fin du Wisconsinien et au début de l'Holocène, peuvent être considérés comme dépourvus de valeur chronologique. Cette conclusion s'applique aux deux faibles valeurs d'Hillsborough (HIL.1P, D/L = 0,0949 et HIL.1R, D/L = 0,1001).
3. Inversement, compte-tenu de nouveau des âges ^{14}C, il est probable que les taux les plus élevés mesurés à Hillsborough (HIL.1L, D/L = 0,2038), baie Saint-Laurent (BSL.8 sur branche, D/L = 0,1956) et les Vieilles-Forges (VF.2A, D/L = 0,2450) sont des valeurs minimales ou significatives par rapport aux autres valeurs plus faibles.
4. Le chevauchement des valeurs maximales d'un site à l'autre montre qu'il n'est pas possible actuellement d'affirmer que les unités datent du même interstade ou de deux, voire trois, interstades différents du Wisconsinien. Apparemment, les Vieilles-Forges dateraient du Wisconsinien inférieur, Hillsborough et baie Saint-Laurent dateraient du même interstade ou d'un ou deux interstades du Wisconsinien moyen.
5. La durée et l'âge de l'interstade de Saint-Pierre sont en cours de réexamen (Occhietti, 1980; Lamothe et al., 1982) à la suite notamment des datations au ^{14}C de l'ordre de 35 000-40 000 ans B.P. obtenus à partir de concrétions calcaires de la formation de Deschaillons (Hillaire-Marcel, 1979; Hillaire-Marcel et Pagé, 1981). Cette formation succède en concordance aux sédiments de Saint-Pierre et donnerait un âge minimal de la fin de l'interstade de Saint-Pierre. Même en tenant compte de ce réajustement chronologique à confirmer, où l'interstade de Saint-Pierre s'étendrait de 80 000 à 35 000 ans B.P., le taux de racémisation du lit organique supérieur des sédiments de Saint-Pierre, aux Vieilles-Forges (VF.2B, D/L = 0,1534) est nettement trop faible. Il indique un âge par racémisaton attribuable d'après les connaissances actuelles au Wisconsinien supérieur.
6. La variabilité des taux de racémisation d'une seule unité, au site de Hillsborough où les échantillons ont été prélevés verticalement à moins de 30 cm l'un de l'autre, est supérieure à la variabilité des taux entre les sites (fig. 2). De plus, comme les unités datent au moins du Wisconsinien moyen et qu'elles sont toutes constituées en majeure partie de tourbe, on ne peut donc invoquer des variations thermiques ou de Ph différentes pour expliquer la variabilité des résultats ni surtout les faibles taux de racémisation. Le rajeunissement apparent indiqué par ces derniers est attribué à d'autres facteurs, en particulier à l'action de bactéries et autres microorganismes organolytiques qui dénaturent le bois et peuvent éliminer ou recombiner une partie des acides aminés. L'action des microorganismes semble dépendre des conditions thermiques et aérobies. Elle est annulée dans un pergélisol, d'après les résultats observés au Yukon (Rutter et al., 1980).

Conclusion

Une analyse préliminaire des acides aminés du bois d'unités interstadiaires sans pergélisol actuel montre une grande variabilité des taux de racémisation. Les taux varient au sein de la même unité et entre les différents sites et unités. Les taux les plus élevés des sites des Vieilles-Forges, de Hillsborough et de baie Saint-Laurent, indiquent des valeurs significatives ou minimales pouvant être attribuées au Wisconsinien inférieur et/ou au Wisconsinien moyen. Les taux à valeur faible indiquent un âge apparent jeune en contradiction avec les données stratigraphiques. Ce rajeunissement ne peut être attribué à l'histoire thermique ou l'évolution du Ph dans le temps mais plutôt à des processus indépendants, notamment aux processus de dénaturation du bois dans des conditions thermiques favorables. La méthode de géochronologie par les acides aminés du bois de régions tempérées nécessite par conséquent une analyse très serrée du contexte des échantillons et de leur état actuel.

Bibliographie

Dunand, M., Amouroux, R., et Chastrette, M.
1979: La réaction de racémisation des aminoacides et quelques applications en géochimie; Bulletin de l'Association française pour l'étude du Quaternaire, nº 58-59, 1-2, p. 53-64.

Hillaire-Marcel, C.
1979: Les mers post-glaciaires du Québec, quelques aspects; thèse D. Sc. non publiée, université de Paris VI, Paris, 600 p.

Hillaire-Marcel, C. et Pagé, P.
1981: Paléotempératures isotopiques du Lac glaciaire de Deschaillons; in Quaternary Paleoclimate, ed. W.C. Mahaney, Geo Books, University of East Anglia, Norwich, England, p. 273-298.

Gadd, N.R.
1971: Pleistocene geology of the central St. Lawrence Lowlands, with selected passages from an unpublished manuscript: The St. Lawrence Lowlands, by J.W. Goldthwaith; Commission géologique du Canada, Mémoir 359, 153 p.

Gadd, N.R. et Karrow, P.F.
1960: Surficial geology Trois-Rivières; St. Maurice, Champlain, Maskinongé and Nicolet Counties, Quebec; Commission géologique du Canada, carte 54-1959.

Grant, D.R.
1972: Surficial geology of southeast Cape Breton Island, Nova Scotia; in Report of Activities, Étude 72-1, partie A, Commission géologique du Canada, p. 161-163.

1975: Surficial geology of northern Cape Breton Island; in Report of Activities, Étude 75-1, partie A, p. 407-408.

1977: Glacial style and ice limits, the Quaternary stratigraphic record, and changes of land and ocean level in the Atlantic Provinces, Canada; Géographie physique et Quaternaire, vol. 31, p. 247-260.

Lamothe, M., Hillaire-Marcel, C., Occhietti, S. et Pagé, P.
1982: Englacement tardif (40 000 – 28 000 BP) des basses-terres du Saint-Laurent au Wisconsinien moyen; Résumé, Congrès de l'Association géologique du Canada, Winnipeg.

Mott, R.J. et Prest, V.K.
1967: Stratigraphy and palynology of buried organic deposits from Cape Breton Island, Nova Scotia; Canadian Journal of Earth Sciences; vol. 4, p. 709-724.

Occhietti, S.
1980: Le Quaternaire de la région de Trois-Rivières-Shawinigan, Québec. Contribution à la paléogéographie de la vallée moyenne du Saint-Laurent et corrélations stratigraphiques; Paléo-Québec, université du Québec à Trois-Rivières, vol. 10, 227 p.

Prest, V.K.
1977: General stratigraphic framework of the Quaternary in eastern Canada; Géographie physique et Quaternaire, vol. 31, p. 7-14.

Preston, N.W., Person, E. et Deevey, E.S.
1955: Yale natural radiocarbon measurement II; Science, v. 122, p. 954-960.

Rutter, N.W., Crawford, R.J. et Hamilton, R.D.
1979: Dating methods of Pleistocene deposits and their problems: IV. Amino acid racemization dating; Geoscience Canada, v. 6, no. 3, p. 122-128.

1980: Correlation and relative age dating of Quaternary strata in the continuous permafrost zone of Northern Yukon with D/L ratios of aspartic acid of wood, freshwater molluscs, and bone; Biogeochemistry of Amino Acids, P.E. Hare, John Wiley, p. 463-475.

Stuiver, M., Heusser, C.J. et Yang, I.C.
1978: North American glacial history extended to 75,000 years ago; Science, v. 200, p. 16-21.

Terasmae, J.
1958: Contribution to Canadian palynology, pt. 2; Non-glacial deposits in the St. Lawrence Lowlands, Québec; Commission géologique du Canada, Bulletin 46, p. 13-28.

APPLICATIONS OF SPECTROCHEMICAL METHODS TO TRACE ELEMENT DETERMINATIONS IN GEOLOGICAL MATERIALS

Project 690090

W.H. Champ, K.A. Church, and G.P. Bender
Central Laboratories and Technical Services Division

In December 1981 the first of several spectrochemical analytical methods planned for our new 3.4 Metre Ebert Spectrograph was put into operation. This method is intended for determinations of trace elements in common silicate rocks and minerals only.

A prepared portion of powered sample plus buffer-diluent is volatilized from a graphite electrode by means of gas-jet stabilized DC arc excitation in an argon-oxygen atmosphere. The resulting radiation is dispersed by a 590 grooves per millimetre grating and recorded photographically. Spectra are measured and data obtained are processed by a minicomputer to produce concentrations of elements desired.

Sensitivities have been improved over previous methods. At present the method is calibrated for 21 elements over the ranges of concentration following:

Element	Range in ppm	Element	Range in ppm
Ag	0.5 - 300	Nd	20 - 10 000
B	20 - 5 000	Ni	3 - 2 000
Ba	1 - 10 000	Pb	30 - 10 000
Be	0.5 - 3 000	Sc	0.7 - 500
Ce	50 - 10 000	Sr	0.5 - 10 000
Co	3 - 10 000	V	3 - 3 000
Cr	3 - 5 000	Y	2 - 2 000
Cu	0.5 - 200	Yb	0.5 - 700
Ga	5 - 3 000	Zn	50 - 10 000
La	7 - 10 000	Zr	3 - 5 000
Mo	20 - 3 000		

For samples containing more than 20 per cent Ca. 15 per cent Mg or 20 per cent Fe, alternate methods may be required because of interference by these elements. As Ca. Mg and Fe approach these levels the sensitivity of determination of some of the listed traces may be reduced because of resulting background and spectral line interferences.

From: Scientific and Technical Notes in Current Research, Part B; Geol. Surv. Can., Paper 82-1B.

CORRELATIONS BETWEEN THE SUNBLOOD, ESBATAOTTINE AND WHITTAKER FORMATIONS IN THE LOWER PALEOZOIC SEQUENCE OF THE SOUTHERN MACKENZIE MOUNTAINS: DISCUSSION

Rolf Ludvigsen
Department of Geology, University of Toronto,
Toronto, Ontario M5S 1A1

In his recent report on Ordovician formations of the southern Mackenzie Mountains, Morrow (1982) presented some correlations of the Esbataottine and Whittaker formations (Middle and Upper Ordovician) that are at variance with those of Ludvigsen (1975, 1979). Morrow suggested that the entire lower Whittaker Formation at its type area in the Whittaker Range is correlative with the entire Esbataottine Formation at its type section in the Sunblood Range. Morrow's evidence for this "lithostratigraphic correlation" is three-fold:

1. The type Esbataottine Formation and the type lower Whittaker Formation are "strikingly similar faunally and lithologically" (Morrow, 1982, p. 98). Both comprise argillaceous, thin and irregularly bedded, and bioturbated lime wackestones with bryozoans, brachiopods, trilobites, gastropods, and crinoids.
2. The presence of a middle resistant cliff-forming division in both the Esbataottine and lower Whittaker formations (Morrow, 1982, Fig. 16.2, 16.3).
3. The dolostones which overlie the Esbataottine Formation in the Sunblood Range and overlie the lower Whittaker Formation in the Whittaker Range are similar. Morrow (1982, p. 98) placed particular emphasis on a shared basal unit of "light grey skeletal or intraclast packstone with abraided [sic] crinoid and dolomitized lime mudstone fragments".

Morrow's correlations of the Sunblood, Esbataottine, and Whittaker formations were displayed in a stratigraphic cross-section of Ordovician rocks from the Whittaker Range to the Third Canyon of the South Nahanni River.

Insofar as these correlations do no more than indicate rocks of similar facies, I have little argument with Morrow; indeed; I had earlier (Ludvigsen, 1978, Fig. 2, 14) documented this cratonward displacement of both lithofacies and biofacies belts in the Esbataottine and lower Whittaker intervals during the late Middle and early Late Ordovician. From the context of Morrow's paper, however, it is clear that he is treating lines of facies change as if they were lines of correlation. His Figure 16.1 indicates that the Whittaker dolostones in the Sunblood Range and the Whittaker Range are equivalent and that the Esbataottine and lower Whittaker in the same areas are equivalent. Neither correlation is correct.

Morrow noted the "faunal similarity" (or, more correctly, biofacies similarity) of the Esbataottine and lower Whittaker, but unexplicably omitted any mention of the published biostratigraphic studies of the trilobites (Ludvigsen, 1979), ostracodes (Copeland, 1974), or conodonts (Tipnis et al., 1978) of these formations. Correlations based on these faunal groups vary somewhat, but all three are unanimous on one point: the upper half of the limestone succession lying between the Sunblood and the middle Whittaker in the Whittaker Range (Morrow's lower member of Whittaker; Ludvigsen's Esbataottine plus lower Whittaker) is

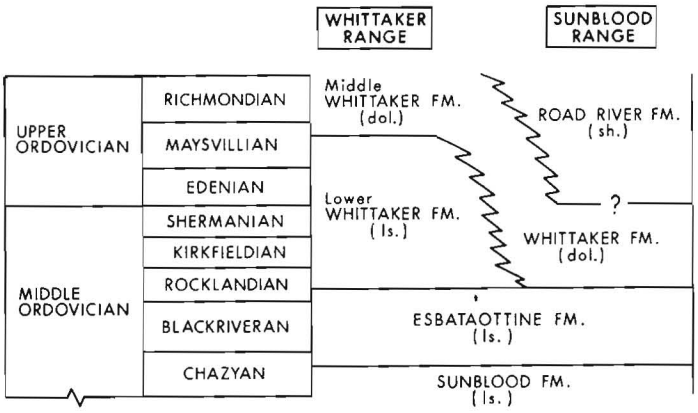

Figure 1. *Correlation of Middle and Upper Ordovician rocks of the Whittaker Range and the Sunblood Range, southern Mackenzie Mountains based on trilobite, conodont, and brachiopod biostratigraphy (compare with Morrow, 1982, Fig. 16.1).*

entirely younger than the Esbataottine in the Sunblood Range or elsewhere. The Esbataottine has now been recognized at six sections in the southern Mackenzie Mountains; at none of these sections is it demonstrably younger than Blackriveran/Rocklandian (**Ceraurinella longispina** Zone, conodont Fauna 8). The lower Whittaker Formation is largely confined to the Whittaker and Funeral ranges where it is Rocklandian to Edenian (or younger) in age (**Ceraurinella necra, Ceraurus mackenziensis,** and **Whittakerites planatus** zones; conodont Faunas 9 and/or 10 or younger; Ludvigsen, 1979; Tipnis et al., 1978). Moreover, unpublished work on the brachiopod faunas of the Whittaker Formation (Wigington, 1977; Mitchell, 1978) and re-assessment of some of the conodont faunas strongly suggest that the higher zones are even younger than indicated by Ludvigsen. Mitchell (1981) reports that, in a section of the Whittaker in the Thundercloud Range, the evolutionary transition of **Sowerbyella** to **Thaerodonta** occurs in the upper part of the **C. mackenziensis** Zone and that the base of the **Culumbodina penna** conodont assemblage (mid-Edenian to mid-Maysvillian) occurs in the lower **W. planatus** Zone. In the mid-continent, the first occurrence of **Thaerodonta** is early Maysvillian. These data suggest that the **W. planatus** Zone is Maysvillian in age.

Correlation by means of lithology in an area such as the Mackenzie Mountains is, by its very nature, incapable of resolving facies relationships. Morrow (1982) noted the lithological similarity of the dolostone units which overlie the Esbataottine Formation in the Sunblood Range and the lower Whittaker Formation in the Whittaker Range and correlated these units. The biostratigraphers mentioned above demonstrated that the base of these dolostones is actually markedly diachronous between the Sunblood Range, where it is Rocklandian (late Middle Ordovician), and the Whittaker Range, where it is Maysvillian or Richmondian (late Late Ordovician). This significant facies change (Fig. 1) is obliterated according to the simplistic lithological correlations of Morrow (1982, Fig. 16.1).

Cautious lithological correlation without support of fossil data is occasionally necessary in poorly known areas, but it is folly to attempt correlation by lithology alone when biostratigraphic data are readily available.

From: Discussions and Communications in Current Research, Part B; Geol. Surv. Can., Paper 82-1B.

References

Copeland, J.J.
1974: Middle Ordovician Ostracoda from southwestern District of Mackenzie; Geological Survey of Canada, Bulletin 244.

Ludvigsen, R.
1975: Ordovician formations and faunas, southern Mackenzie Mountains; Canadian Journal of Earth Sciences, v. 12, p. 663-697.

1978: Middle Ordovician trilobite biofacies, southern Mackenzie Mountains; in Western and Arctic Canadian Biostratigraphy, ed. C.R. Stelck and B.D.E. Chatterton; Geological Association of Canada, Special Paper 18, p. 1-38.

1979: A trilobite zonation of Middle Ordovician rocks, southwestern District of Mackenzie; Geological Survey of Canada, Bulletin 312.

Mitchell, C.E.
1978: Middle and Upper Ordovician strophomenids (Brachiopoda) from the central Mackenzie Mountains, Northwest Territories; unpublished M.Sc. thesis, University of Western Ontario, London, 305 p.

1981: An Upper Ordovician age for the "Arctic Ordovician fauna" of the lower Whittaker Formation, Northwest Territories; Abstracts, Geological Association of Canada Annual Meeting, Calgary, p. 40.

Morrow, D.W.
1982: Correlations between the Sunblood, Esbataottine and Whittaker formations in the Lower Paleozoic sequence of the southern Mackenzie Mountains; in Current Research, Part A, Geological Survey of Canada, Paper 82-1A, p. 95-98.

Tipnis, R.S., Chatterton, B.D.E., and Ludvigsen, R.
1978: Ordovician conodont biostratigraphy of the southern District of Mackenzie, Canada; in Western and Arctic Canadian Biostratigraphy, ed. C.R. Stelck and B.D.E. Chatterton; Geological Association of Canada, Special Paper 18, p. 39-91.

Wigington, R.J.S.
1977: The age and orthid fauna of the lower Whittaker Formation in the southern Mackenzie Mountains, Northwest Territories; unpublished M.Sc. thesis, University of Western Ontario, London, 148 p.

CORRELATIONS BETWEEN THE SUNBLOOD, ESBATAOTTINE AND WHITTAKER FORMATIONS IN THE LOWER PALEOZOIC SEQUENCE OF THE SOUTHERN MACKENZIE MOUNTAINS: REPLY

D.W. Morrow
Institute of Sedimentary and Petroleum Geology, Calgary

In the preceding discussion, Ludvigsen (1982) has criticized my conclusion that the lower part or member of the Whittaker Formation at its type section is lithostratigraphically the same as the Esbataottine Formation (Morrow, 1982). The reader should be aware that the Whittaker Formation at its type section was redefined by Ludvigsen (1975, p. 670) who assigned the basal part of the lower member of the Whittaker Formation to the Esbataottine Formation. This choice for the upper contact of the Esbataottine Formation within the lower part of the Whittaker Formation is not a lithologically distinctive boundary exhibiting mappability (Morrow, 1982) and I am not even certain that I have correctly identified the top of the Esbataottine at the Whittaker type section in accord with Ludvigsen (1975) because of the absence of lithological and mapping criteria necessary for the identification of this contact. The most readily identifiable mappable contact at the Whittaker type section is the contact between the argillaceous dark limestones of the lower member of the Whittaker Formation and the overlying dolostones of the middle part. Any other choice is insupportable. In this context, the faunal data cited by Ludvigsen (1982) are not relevant, although they are of course, very interesting and informative in their own right. My use of the word "correlation" (Morrow, 1982) was intended in a purely lithostratigraphic sense, divorced from any biostratigraphic or temporal considerations. I offer my apologies to any person who has been misled by my use of the word "correlation" but this should not be allowed to obscure the main point of my article (Morrow, 1982) concerning the lithostratigraphic continuity of the Esbataottine Formation (i.e. lithological composition and extent) and that of the Whittaker Formation.

References

Ludvigsen, R.
1975: Ordovician formations and faunas, southern Mackenzie Mountains; Canadian Journal of Earth Sciences, v. 12, p. 663-697.

1982: Correlations between the Sunblood, Esbataottine and Whittaker formations in the Lower Paleozoic sequence of the southern Mackenzie Mountains: discussion; in Current Research, Part B, Geological Survey of Canada, Paper 82-1B.

Morrow, D.W.
1982: Correlations between the Sunblood, Esbataottine and Whittaker formations in the Lower Paleozoic sequence of the southern Mackenzie Mountains; in Current Research, Part A, Geological Survey of Canada, Paper 82-1A, p. 95-98.

A PROVISIONAL STANDARD FOR CORRELATING THE PRECAMBRIAN ROCKS OF THE CANADIAN SHIELD: DISCUSSION

C.H. Stockwell
577 Gainsborough Avenue, Ottawa, Ontario K2A 2Y6

The above paper by Douglas (1980) has already been discussed in detail by Frarey (1981) and, although the present writer agrees with Frarey's remarks, except in the use of basic intrusion to define time units, a few additional comments might be helpful in reaching our objective of establishing the best possible scheme for the best classification and correlation of Precambrian rocks in Canada. The following comments emphasize some of the more important differences between the proposals by Douglas (1980) and those by Stockwell (1982). But first it should be noted that both of us agree in the need to define time units by actual rock ages rather than by purely absolute time as once proposed by Goldich (1968) or by non-events (boundaries of convenience) as proposed by James (1972, 1979). Both Douglas and I also agree that time units should be defined at type localities to serve as standards for reference.

General Remarks

Stockwell (1982) uses orogeny to define virtually all of his time units whether they be of era or subera rank or their minor subdivisions. Each unit spans the time from the close of one orogeny to the close of the next and the rock that terminated the orogeny serves as the standard. Non-orogenic assemblages such as sedimentary or volcanic sequences or basic sills and dykes are placed in their appropriate time unit by their geological relationships to the orogenies and to other dated events or by their isotopic age. The non-orogenic events are arranged in chronological order as far as possible in the text but only to a limited extent in a table. The scheme is consistent throughout and very simple.

On the other hand, the Douglas scheme, although retaining Stockwell's orogenies for defining most of the major time units, becomes quite complex by defining many of the minor subdivisions by time of deposition of stratigraphic sequences, by time of emplacement of non-orogenic, mainly basic intrusions, or by paleomagnetic characteristics. Isotopic ages and paleomagnetic results are used as standards or fixes for these subdivisions. Although the methods are different, the Douglas and Stockwell schemes, when based on the same data, give much the same chronological ordering and correlation of rocks and events.

In the writer's opinion the orogenic scheme has several advantages. Orogenies mark revolutionary changes in earth history. Each is followed by a period of erosion and then, based on the law of superposition on a grand scale, by the deposition of new sedimentary and volcanic sequences. The boundaries are major, high-angle unconformities which must be shown on geological and tectonic maps. The dating and mapping of orogenies should prove to be very helpful in studies of plate tectonics. Also, the cooling history of epi-orogenic events involving uplift and erosion can be determined by isotopic age studies on orogenic minerals, thus contributing to a better understanding of these important but commonly neglected intervals. In contrast, the basic dykes and sills used in the Douglas scheme were emplaced under relatively quiet conditions, do not mark unconformities and do not bring about any noticeable change in environment of deposition of sediments and volcanics. Another great advantage of the orogenic scheme is that orogenic materials are readily dated isotopically whereas the time of deposition of sediments is very difficult or impossible to date directly and generally can only be bracketed by their relationship to other events. Because of these difficulties it has not been possible to date a succession of sedimentary rocks from its beginning to ending. Volcanics are dated most reliably by zircon but this mineral commonly cannot be found in basic volcanics. Most available isotopic age determinations on basic intrusions are thought to be unreliable especially by the K-Ar method on whole-rock, but other methods have given reliable dates such as for the Nipissing Diabase and Sudbury Norite. Paleomagnetism does not give the age of rock which can be determined only by isotopic methods.

A very disturbing feature of the Douglas paper is its redefinition of well established terms such as Hudsonian, Aphebian, Huronian, Keewatin and Timiskaming. Instead of confusing established nomenclature it would have been better to introduce new names for new concepts.

Hudsonian Orogeny

The Hudsonian Orogeny was defined many years ago (Stockwell, 1961) in much the same terms as used today: as the last widespread period of important folding generally accompanied by regional metamorphism and virtually contemporaneous granitic intrusions in the Churchill Province which is the type region. The termination of the Hudsonian Orogeny in its type region defines the end of the Aphebian Era. Douglas objected to the use of such a large region as the type area claiming that existing isotopic dates are too meagre for dating the end of the orogeny. He speculated that the orogeny might extend into the Paleohelikian apparently having misunderstood that the Aphebian-Paleohelikian boundary is defined by the true (geological) age of the termination of the orogeny and that any change in its isotopic age does not change the definition. It is true that existing reliable U-Pb and Rb-Sr whole-rock isochron dates are meagre but it should be pointed out that there are numerous K-Ar mineral dates throughout the Churchill Province that give minimum ages for the orogeny and these indicate that the time of closing is unlikely to be significantly younger than the present estimate of 1750 Ma by the U-Pb method and 1755 Ma by the Rb-Sr method.

Douglas redefined the end of the Hudsonian Orogeny in a small type area which was selected because isotopic dates were available for both basement and nearby unconformably overlying rocks (the Dubawnt Group) to fix the end of the Hudsonian and consequently the end of the Aphebian at 1800 Ma. This age for the boundary was determined mainly by splitting the differences between a basement age of 1834 Ma and a Dubawnt age of 1786 Ma.

One objection to the 1800 Ma boundary is that, beyond the type area of Douglas, it splits the original Hudsonian along an unnatural boundary virtually impossible to map. This difficulty of course, is avoided by drawing the boundary at the end of the orogeny in the whole of the Churchill Province as Stockwell has done. Thus, available Hudsonian ages for the whole of the Churchill Province comprise one in the Taltson Fold Belt at 1750 Ma, three in the Wollaston Fold Belt at 1762, 1762 ± 60, and 1816 ± 62 Ma, one from the Flin Flon Belt at 1767 ± 14 Ma, one from the Thompson Belt at 1767 ± 190 Ma and the previously mentioned age of 1834 ± 22 Ma (for details see Appendix in Stockwell, 1982). As can be seen almost all are younger than the 1800 Ma horizon excluding the greater part of the original Hudsonian area and leaving the greater part unnamed and not even considered.

The 1800 Ma age is only slightly older than the original estimates of 1750 and 1755 Ma but nevertheless leads to undesirable changes in time classification and geological interpretations. First, available isotopic age determinations indicate that the basement to the Dubawnt very probably belongs to the Moranian Orogeny rather than to the Hudsonian as assumed by Douglas who did not recognize the

From: Discussions and Communications in Current Research, Part B; Geol. Surv. Can., Paper 82-1B.

Moranian. Although one age in the basement (the Rb-Sr whole-rock isochron at 1834 ± 22 Ma) if taken at face value would be very early Hudsonian, it is a borderline case and if allowance is made for the analytical error it could belong to the Moranian Orogeny which closed at about 1850 Ma in its type locality in the Beaverlodge area. Other dates in the basement support the conclusion that it is Moranian rather than Hudsonian. Thus a Rb-Sr whole-rock isochron gave 1900 ± 25 Ma and four K-Ar dates on orogenic biotites from localities very close to Dubawnt outcrops gave epi-Moranian cooling ages of 1810 ± 100, 1810 ± 100, 1785 ± 90 and 1770 ± 90 Ma which could hardly have survived a superimposed Hudsonian Orogeny. They average 1794 Ma which is close to the biotite average of 1787 Ma for the epi-Moranian of the type area and is appreciably older than that for the epi-Hudsonian at 1700 Ma.

The unwarranted assumption that the basement is Hudsonian led Douglas to the conclusion that the overlying flat-lying Dubawnt was early Paleohelikian. But, using the original definition, of the Hudsonian it falls within the late Aphebian as indicated by two isotopic dates on middle Dubawnt volcanics, the one being a Rb-Sr whole-rock isochron at 1786 ± 4 Ma and the other being a K-Ar date of 1770 ± 90 Ma on primary biotite. It is noted that these two ages fall within the range of the original Hudsonian Orogeny. But, as the middle Dubawnt is unfolded, this leads to the interesting conclusions that the Dubawnt escaped deformation by the orogeny, was being deposited while the orogeny was active elsewhere, and that the Hudsonian Orogeny of Stockwell may have been the source of the Dubawnt sediments.

Huronian

The Huronian series was originally named over a century ago by Logan and Hunt (1855) to designate sequences of mainly sedimentary rocks along and near the north shore of Lake Huron and in places along the shores of Lake Superior where such rocks have now been given other names. Since then the Lake Huron area has become known as the type locality and the name Huronian has been adopted worldwide. Its definition has most recently been clarified by Robertson et al. (1969) who used the name Huronian Supergroup instead of the earlier Huronian Series, the rock-stratigraphic term being appropriate because the time of its beginning and ending was and still is unknown. Should the time span ever be determined it would then be appropriate to again use the term Huronian Series. But Douglas would change all this by including in his Huronian Subera several other rocks and events both younger and older than the original Huronian. This drastic change in the widely understood meaning of Huronian is unacceptable to the present writer and disagrees with the carefully considered recommendation of the American Commission on Stratigraphic Nomenclature (1961) which states, in effect, that a mere change in rank of a unit or a change in classification from a rock unit to a time unit should not change its original content. The Huronian Subera of Douglas spans the time from the close of the Kenoran Orogeny to the time just after the intrusion of the Nipissing Diabase and so includes the epi-Kenoran period of cooling and erosion, the original Huronian, and its subsequent folding and granitic intrusions of the Blezardian Orogeny as well as the subsequent epi-Blezardian cooling period and the Nipissing Diabase. This redefines Stockwell's boundary between his early and late Aphebian which was defined by the termination of the Blezardian Orogeny.

Keewatin

The redefinition of the Keewatin is unjustified and can only lead to confusion. It was originally defined many years ago by Lawson (1885) to designate an assemblage of volcanic rocks that are older than the Laurentian Granite and are exposed in the Lake of the Woods area in Ontario which is the type locality. Subsequently the term became firmly established by widespread acceptance of the original definition and by its application to many other assemblages of relatively old volcanic rocks although in those days time correlation with the type was questionable because it relied solely on similarity in lithology and structural relationships. Even with modern isotopic dating techniques, the determination of the time at the beginning and at the ending of the type Keewatin has not been accomplished. For that reason the original Keewatin, which had been called a series, has recently been changed to Keewatin group without changing the rock content of the original Keewatin. Should the time span of the type Keewatin be determined eventually a return to the designation Keewatin Series would then be appropriate.

Instead, Douglas has redefined the Keewatin (calling it the Keewatian Subera) to include much more than the volcanics. It replaced Stockwell's late middle Archean which spans the time from the close of the Wanipigowan Orogeny to the close of the Laurentian Orogeny. Accordingly, the Keewatian Subera would include all rocks and events within that time interval such as the epi-Wanipigowan cooling and erosional period, deposition of volcanics whether Keewatin or not, their folding, metamorphism, and granitic intrusions of the Laurentian Orogeny. The Laurentian Granite would become a Keewatian Granite. Such a drastic redefinition of the widely understood meaning of Keewatin is clearly unjustified and is contrary to the generally accepted principles of time classification.

Timiskaming

Similarly, the drastic redefinition of the Timiskaming is unacceptable. The original Timiskaming Series comprised a sequence of mainly sedimentary rocks unconformably overlying the Blake River volcanics (formerly correlated with the Keewatin) and unconformably overlain by the Huronian. The Kirkland Lake-Noranda area of Ontario and Quebec has long been regarded as the type locality. The original designation as a series has now been changed to group because the time from the beginning to the end of its deposition has not yet been determined. If ever determined a return to the original series designation would be appropriate.

However, Douglas has redefined the widely accepted meaning of Timiskaming to include all rocks formed during the interval from the close of the Laurentian Orogeny to the close of the Kenoran Orogeny and so would include, for example, the epi-Laurentian period of cooling and erosion, the Timiskaming Group and all other late Archean events such as the widespread regional metamorphism and granitic intrusions of the Kenoran Orogeny. Douglas named this time unit the Timiscamian Subera, equivalent to Stockwell's late Archean.

References

American Commission on Stratigraphic Nomenclature
1961: Code of stratigraphic nomenclature; American Association of Petroleum Geologists, Bulletin, v. 45 no. 5 p. 645-665.

Douglas, R.J.W.
1980: Proposals for the time classification and correlation of Precambrian rocks and events in Canada and adjacent areas of the Canadian Shield, Part 2: a provisional standard for correlating Precambrian rocks of the Canadian Shield; Geological Survey of Canada, Paper 80-24, 19 p.

Frarey, M.J.
1981: A Provisional standard for correlating the Precambrian rocks of the Canadian Shield: Discussion; in Current Research, Part C, Geological Survey of Canada, Paper 81-1C, p. 83-88.

Goldich, S.S.
1968: Geochronology in the Lake Superior region; Canadian Journal of Earth Science, v. 5, p. 715-724.

James, H.L.
1972: Stratigraphic Commission, Note 40. Subdivision of Precambrian: an interim scheme to be used by the U.S. Geological Survey; American Association of Petroleum Geologists, Bulletin, v. 56, p. 1128-1133.

1979: Precambrian Subdivided. IUGS Subcommission on Precambrian Stratigraphy; fifth meeting. September 15-19, Minnesota, U.S.A. Episodes, v. 1979, no. 4, p. 34.

Lawson, A.C.
1885: Lake of the Woods Region; Geological and Natural History Survey of Canada, annual report, vol. 1, p. 5cc-151cc.

Logan, W.E. and Hunt, T.S.
1855: Esquisse géologique du Canada; Hector Rossange et Fils, Paris.

Robertson, J.A., Frarey, M.J., and Card, K.D.
1969: The Federal-Provincial Committee on Huronian Stratigraphy: progress report; Canadian Journal of Earth Sciences, v. 6, p. 335-336.

Stockwell, C.H.
1961: Structural provinces, orogenies, and time classification of rocks of the Canadian Precambrian Shield; in Geological Survey of Canada, Paper 61-17, p. 108-118.

1982: Proposals for time classification and correlation of Precambrian rocks and events in Canada and adjacent areas of the Canadian Shield, Part 1: a time classification of Precambrian rocks and events; Geological Survey of Canada, Paper 80-19, p. 1-135.

U-PB AGES OF ZIRCONS FROM THE FOOT BAY GNEISS AND THE DONALDSON LAKE GNEISS, BEAVERLODGE AREA, NORTHERN SASKATCHEWAN: DISCUSSION

R.I. Thorpe
Economic Geology Division

The recent paper by Tremblay et al. (1981) was published without reference to the geochronological (Rb-Sr) results of Sassano et al. (1972) on the same rocks and without any discussion of how the present results relate to the sequence of geological events proposed by the latter authors.

The pegmatite age of 1933 ± 20 Ma obtained by Sassano et al. (1972) established a minimum possible age for the rocks in question. Data for the Donaldson Lake gneiss yielded only a rough errorchron, but are compatible with the results of Tremblay et al. (1981). Results for the Foot Bay gneiss reported by Sassano et al. (1972) were inconclusive, but suggested that the rocks could be older than the Donaldson Lake gneiss.

References

Sassano, G.P., Baadsgaard, H., and Morton, R.D.
1972: Rb-Sr isotopic systematics of the Foot Bay gneiss, Donaldson Lake gneiss, and pegmatite dikes from the Fay Mine, NW Saskatchewan; Canadian Journal of Earth Sciences, v. 9, no. 11, p. 1368-1381.

Tremblay, L.P., Loveridge, W.D., and Sullivan, R.W.
1981: U-Pb ages of zircons from the Foot Bay gneiss and the Donaldson Lake gneiss, Beaverlodge area, northern Saskatchewan; in Rb-Sr and U-Pb Isotopic Age Studies, Report 4, in Current Research, Part C, Geological Survey of Canada, Paper 81-1C, p. 123-126.

U-PB AGES OF ZIRCONS FROM THE FOOT BAY GNEISS AND THE DONALDSON LAKE GNEISS, BEAVERLODGE AREA, NORTHERN SASKATCHEWAN: REPLY

L.P. Tremblay,[1] W.D. Loveridge[2] and R.W. Sullivan[2]

The authors regret that they omitted reference to this paper by Sassano et al. (1972) on attempts to date the Foot Bay gneiss and the Donaldson Lake gneiss by the Rb-Sr method, and thank R.I. Thorpe for bringing the omission to their attention. The senior author was familiar with this paper and his referred to it previously (Tremblay, 1978). However, due to the inconclusive nature of the Rb-Sr results we inadvertently did not refer to them in our presentation of U-Pb results on zircon from similar units (Tremblay et al., 1981).

References

Sassano, G.P. Baadsgaard, H., and Morton, R.D.
1972: Rb-Sr isotopic systematics of the Foot Bay gneiss, Donaldson Lake gneiss, and pegmatite dikes from the Fay Mine, NW Saskatchewan; Canadian Journal of Earth Sciences, v. 9, no. 11, p. 1368-1381.

Tremblay, L.P.
1978: Geologic setting of the Beaverlodge-type of vein-uranium deposit and its comparison to that of the unconformity-type; in Uranium Deposits: their Mineralogy and Origin, ed. M.M. Kimberley; Short Course, Mineralogical Association of Canada, University of Toronto, p. 431-456.

Tremblay, L.P., Loveridge, W.D., and Sullivan, R.W.
1981: U-Pb ages of zircon from the Foot Bay gneiss and the Donaldson Lke gneiss, Beaverlodge area, northern Saskatchewan; in Rb-Sr and U-Pb Isotopic Age Studies, Report 4, in Current Research, Part C, Geological Survey of Canada, Paper 81-1C, p. 123-126.

[1] Economic Geology Division
[2] Precambrian Geology Division

From: Discussions and Communications in Current Research, Part B; Geol. Surv. Can., Paper 82-1B.

ERRATA

Current Research, Part A

Geological Survey of Canada, Paper 82-1A

Report 37: Chromite occurrences in ultramafic rocks in the Mitchell Range, central British Columbia; Peter J. Whittaker; Paper 82-1A, p. 239-245.

p. 244 Captions for Figure 37.4 should read:

a) *lensoid fluid inclusions, some with shadowed ends and bright cores indicative of fluid and vapour phases present;*

b) *necked tubular fluid inclusions in intersecting planar swarms, some with bright cores;*

c) *euhedral to anhedral Ni-Fe sulphide (pentlandite) inclusion train;*

d) *euhedral Ni-Fe sulphide with irregular and darker exsolution patches possibly of NiS. Field of view in all photos is 0.3 mm.*

Figure 37.4

Report 57: Late Triassic (Upper Norian) and earliest Jurassic (Hettangian) rocks and ammonoid faunas, Halfway River and Pine Pass map areas, British Columbia; E.T. Tozer; Paper 82-1A, p. 385-391.

p. 387, right column, 1st paragraph under Section 4 should read:

This section is on the north side of Williston Lake 3.7 km northeast of the mouth of Nabesche River (56°05'00"N, 123°02'00"W). Description of the old exposures are in Beach and Spivak (1944, p. 3), McLearn and Kindle (1950, p. 61), Irish (1970, p. 141), McLearn (1960, p. 12) and Tozer (1967, p. 59). The Triassic rocks are exposed on a relatively small topographic feature east of Black Bear Ridge as identified on published maps (e.g. Ne-Parle-Pas Rapids, NTS 94 B/3E). McLearn (1960, p. 12) used the name for a small feature separated from the main ridge by a watercourse following the Pardonet-Fernie contact. In the old days the contact was not exposed. The new exposures provide nearly continuous coverage for the Pardonet Formation and about 11 m of overlying Jurassic strata. The **Monotis** beds, brown siltstone, 27 m thick, have provided ammonoids from two levels. The lower level, 19 m from the top, has **Paraguembelites ludingtoni** Tozer (GSC loc. 98534). The upper level, 1.2 m from the top, has **Placites** sp. associated with poorly preserved small ammonoids, probably **Lissonites canadensis** Tozer (GSC loc. 98545). **Monotis** shells from the uppermost Pardonet Formation are generally packed together and crushed, making specific determination uncertain but the specimens from the two ammonoid beds appear to be **Monotis ochotica** (Keyserling) rather than **M. subcircularis** (Gabb).

AUTHOR INDEX

NOTE TO CONTRIBUTORS

Submissions to the *Discussion* section of *Current Research* are welcome from both the staff of the Geological Survey and from the public. Discussions are limited to 6 double-spaced typewritten pages (about 1500 words) and are subject to review by the Chief Scientific Editor. Discussions are restricted to the scientific content of Geological Survey reports. General discussions concerning branch or government policy will not be accepted. Illustrations will be accepted only if, in the opinion of the editor, they are considered essential. In any case no redrafting will be undertaken and reproducible copy must accompany the original submissions. Discussion is limited to recent reports (not more than 2 years old) and may be in either English or French. Every effort is made to include both *Discussion* and *Reply* in the same issue. *Current Research* is published in January, June and November. Submissions for these issues should be received not later than November 1, April 1, and September 1 respectively. Submissions should be sent to the Chief Scientific Editor, Geological Survey of Canada, 601 Booth Street, Ottawa, Canada, K1A 0E8.

AVIS AUX AUTEURS D'ARTICLES

Nous encourageons tant le personnel de la Commission géologique que le grand public à nous faire parvenir des articles destinés à la section discussion *de la publication* Recherches en cours. *Le texte doit comprendre au plus six pages dactylographiées à double interligne (environ 1500 mots), texte qui peut faire l'objet d'un réexamen par le rédacteur en chef scientifique. Les discussions doivent se limiter au contenu scientifique des rapports de la Commission géologique. Les discussions générales sur la Direction ou les politiques gouvernementales ne seront pas acceptées. Les illustrations ne seront acceptées que dans la mesure où, selon l'opinion du rédacteur, elles seront considérées comme essentielles. Aucune retouche ne sera faite aux textes et dans tous les cas, une copie qui puisse être reproduite doit accompagner les textes originaux. Les discussions en français ou en anglais doivent se limiter aux rapports récents (au plus de 2 ans). On s'efforcera de faire coincider les articles destinés aux rubriques* discussions *et* réponses *dans le même numéro. La publication* Recherches en cours *paraît en janvier, en juin et en novembre. Les articles pour ces numéros doivent être reçus au plus tard le 1er novembre, le 1er avril et le 1er septembre respectivement. Les articles doivent être renvoyés au rédacteur en chef scientifique: Commission géologique du Canada, 601, rue Booth, Ottawa, Canada, K1A 0E8.*

Energy, Mines and Resources Canada

Énergie, Mines et Ressources Canada